1997

High-resolution sequence stratigraphy and diagenesis of mixed carbonate/siliciclastic successions.

Oliver, Guy Mark

HIGH-RESOLUTION SEQUENCE STRATIGRAPHY AND DIAGENESIS OF MIXED CARBONATE/SILICICLASTIC SUCCESSIONS

by

GUY MARK OLIVER

A thesis submitted to the University of Plymouth
in partial fulfilment for the degree of

DOCTOR OF PHILOSOPHY

Department of Geological Sciences
Faculty of Science

1997

To my fiancée Lian
and to my parents Pat and Graham Oliver,
all of whom have encouraged and supported me throughout.

In memory of
Beau and Belle -
happiness and companionship
was always with them

GUY MARK OLIVER

HIGH-RESOLUTION SEQUENCE STRATIGRAPHY AND DIAGENESIS OF MIXED CARBONATE/SILICICLASTIC SUCCESSIONS

The aims of this thesis are to evaluate whether the distribution of diagenetic features in nearshore successions can be explained within a sequence stratigraphic concept; to assess whether the identification and analysis of these features can be used to aid in making sequence stratigraphic interpretations; and to evaluate whether sequence stratigraphy can be used to predict the distribution of diagenetic heterogeneities at the field and inter-well scale.

High resolution sequence stratigraphic frameworks have been established for two nearshore mixed carbonate/siliciclastic successions, using facies and early diagenetic analyses. These are the Upper Jurassic Corallian Group of south Dorset and the Lower Cretaceous lower to middle Ericeira Group of west central Portugal. Early diagenetic analyses (including petrographic, CL, XRD and stable isotope work), was performed on 143 samples extracted from concretions and cemented beds at key horizons within these two successions. The early diagenetic results from within the majority of these cemented bodies generally supports the proposed facies-based sequence stratigraphic interpretation of parasequences, systems tracts and sequences.

At a parasequence scale, early diagenetic analyses indicate that concretionary growth is controlled by an initial phase of rapid burial, equating to the period of parasequence progradation, followed by a period of prolonged residence time within a single diagenetic zone. This equates to a period of non-deposition/marine flooding at a parasequence boundary. The results also indicate that the application of sequence stratigraphic theory can be used to predict the presence and location of early diagenetic concretions within similar successions. Analysis of early diagenetic features within carbonate cemented beds (such as marine hard-ground surfaces) also supports the facies-based identification of parasequences. Such features are closely associated with parasequence boundary formation and the available data indicates that it is possible to predict their distribution within systems tracts of similar successions.

At the systems tract scale, analysis of upward increasing or decreasing trends in the volume of pore-filling authigenic phases relates to subtle changes in the rate of sedimentation versus the rate of accommodation creation. A general upward increase in the volume of early diagenetic products (particularly dolomite) is seen to occur within highstand systems tracts, which is attributed to an increase in residence time within early diagenetic zones as the rate of progradation/burial increases and the rate of non-deposition/marine flooding at parasquence boundaries remains constant. Similarly, an upward increase in the $\delta^{18}O$ isotope values of carbonate cements (to a more marine value) occurs within shelf-margin or lowstand systems tracts where rates of relative sea-level are rising increasingly quickly and, a dominance of marine cements occurs within coarser grained beds of transgressive systems tracts.

At the sequence scale, early diagenesis is controlled by the degree of relative sea-level fall and subsequent sub-aerial exposure at the end of the highstand systems tract. If a sequence is bounded above by a type-1 sequence boundary and there is evidence of a period of sub-aerial exposure then the effects of surface related diagenesis (dissolution, replacement and further cementation) can be identified. However, if a sequence is bounded above by a type-2 sequence boundary, the effects of any meteoric diagenesis are likely to be confined to in-extensive fresh-water lenses originating from an up-dip/sub-aerially exposed area of the basin. Consequently, primary early diagenetic cements contained within pore spaces of the existing systems tracts will be preserved.

The approach taken in this research has demonstrated that early diagenesis is a useful tool in refining high resolution sequence stratigraphic interpretations and in the prediction of the distribution of early diagenetic heterogeneities within reservoir units. It also shows that for nearshore successions the distribution of diagenetic heterogeneities can be predicted at a range of scales.

CONTENTS

Chapter 7: Conclusions

LIST OF FIGURES[1]

[1] all figures are placed in order at the end of each chapter.

LIST OF TABLES[2]

[2] all tables are placed in order after the figures, at the end of each chapter.

ACKNOWLEDGEMENT

I wish to thank my supervisors Dr Matthew Watkinson and Professor Malcolm Hart for endless discussions, guidance, support and encouragement over the duration of this study.

Sincere thanks go to my fellow colleagues, Mike Caroll, Paul Castignetti, Andy Henderson and Cath Manley known through-out the world as "the geo-bunglers". Endless discussions concerning the finer points of life (and geology) enlightened my stay at Plymouth.

Thanks go to Mike Ashton for battling against all of the unforeseen elements and making my endless batches of thin-sections; to John Abraham for help and advice with "Adobe Illustrator"; to Pete Davis for help with the XRD analysis; to Marylin Tucker for encouragement, and to Mike Isaacs of Reading University for the isotope analysis.

Thanks go to Dr Roland Goldring, Dr Jim Hendry, Dr Duncan Pirrie, Prof. Mike Talbot and Dr Kevin Taylor for helpful advice and suggestions.

Thanks to Dr Mark Anderson for providing me with additional funds to help me complete my work.

Thanks to Dr Lian Blake and Mr Richard Thomas for assistance with fieldwork in Dorset.

Sincere thanks go to Mr George McCready, who while "working abroad" during the summer of 1996, leant me his P.C. Writing a PhD thesis during "the summer of sport" was hard enough, but without the use of his P.C., it would never have been completed.

Thanks to all my friends for understanding, support and encouragement.

Finally, the most thanks must go to my fiancée Lian, my parents Pat and Graham Oliver and my brother Warren Oliver. All put up with me, supported me, encouraged me, helped me and provided me with the financial support that is so necessary when producing a modern day thesis. Without their support, this thesis would never have been completed.

The author wishes to acknowledge the receipt of a University of Plymouth, Faculty of Science studentship.

AUTHOR'S DECLARATION

This is to certify that the work submitted for the degree of Doctor of Philosophy under the title "High-Resolution Sequence Stratigraphy and Diagenesis of Mixed Carbonate/Siliciclastic Successions", is the result of original investigation.

All authors and works quoted are fully acknowledged

At no time during the registration for the degree of Doctor of Philosophy has the author been registered for any other University award.

Signed: ..... (Candidate)

Date: .....

Signed: ..... (Supervisor)

Date: 6/2/93

1: Introduction

1.1: *Aims, objectives, methodology & concepts*

Since the early 1990's, sequence stratigraphy has become an increasingly high resolution tool and is now routinely applied in outcrop and well studies. At the commencement of this project (1993) field based high resolution sequence stratigraphy was in its relative infancy and had only just begun to be applied to the processes and products of early diagenesis (refer to Horbury & Robinson, 1993; Taylor *et al.*, 1994).

The application of high resolution sequence stratigraphy to outcrop and well studies has led to a re-evaluation of many stratigraphic successions, causing a major re-interpretation of stratigraphic evolution. This has brought sequence stratigraphy into the realm of production and reservoir geology, resulting in more geologically realistic descriptions of reservoir units and so reducing the stochastic requirement that was always a necessity within early reservoir models. Jennette & Riley (1996) and Wehr & Brasher (1996) demonstrate how a high resolution sequence stratigraphic approach can improve reservoir management (i.e. prediction of reservoir sands, heterogeneities and reservoir response).

A key aspect of reservoir characterisation is the identification of diagenetic processes and products which may increase or decrease reservoir quality and may influence fluid flow patterns in a field. The distribution of early diagenetic products are difficult to predict between well control points and across fields. High resolution sequence stratigraphy

provides (i) the conceptual framework; and (ii) the stratigraphic framework (coupled with good biostratigraphic control) to be able to perform such a study.

1.1.1: Aims

The aims of this thesis are to evaluate whether;

1. the distribution of diagenetic features in nearshore successions can be explained within a sequence stratigraphic concept;
2. can the identification and analysis of these features therefore be used to aid in making sequence stratigraphic interpretations, and;
3. can sequence stratigraphy be used to predict the distribution of diagenetic heterogeneities at the field and inter-well scale.

The approach taken within this project is that of a reconnaissance study of two nearshore successions - the Corallian Group of south Dorset and the lower to middle Ericeira Group of west central Portugal. The results of this analysis will be linked with previous studies to produce generalised models which will be of use in the petroleum industry (e.g. reservoir geology) and in high resolution basin analysis.

1.1.2: Objectives

The principal objectives of this study were to;

1. establish sequence stratigraphic interpretations at as high a resolution as is practically possible;
2. incorporate regional data from published literature to further constrain the models;
3. describe the distribution of diagenetic features within a high resolution sequence stratigraphic context;
4. evaluate if there are any clear correlations and weigh-up the relative importance of sequence stratigraphy and especially sea-level change in controlling this distribution;
5. attempt to explain the causes of diagenesis using analytical and petrographic techniques; and
6. use sequence stratigraphic theory to account for the relationship between facies, stratal surfaces and early diagenetic products.

This study focused particularly on the identification of diagenetic products which formed early after the deposition of each unit and can be related to changes in relative sea-level.

To test these objectives, two successions were chosen;

1. the Upper Jurassic Corallian Group exposed along the south Dorset coast; and
2. a section of the Lower Cretaceous Ericeira Group exposed along the coastal sections to the north of the town of Ericeira, west-central Portugal.

The two successions were chosen primarily because of the dominance of cyclically arranged shallow carbonate and siliciclastic lithologies. The Corallian Group is a well studied succession with a number of previous sedimentological and stratigraphic interpretations along with well constrained biostratigraphy and, as such, appeared to be an ideal succession in which to test the objectives. Although sequence stratigraphic models have already been published for this succession (see Chapter 2) none have utilised a high resolution sequence stratigraphic approach (*sensu* Van Wagoner *et al.*, 1990). The less well studied Ericeira Group was chosen because of its superficial similarity to the Corallian Group in that it is a mixed siliciclastic/carbonate shallow marine to nearshore succession (Hiscott *et al.*, 1990a). The study of two successions was thought necessary to highlight any local sequence stratigraphic or diagenetic responses from those that can be applied on a more general scale.

For logistical reasons, the study was conducted on a local rather than basin-wide scale, so that the validity of analysing diagenetic heterogeneities on an interwell/reservoir scale could be evaluated. However, within the Corallian Group succession, regional data were incorporated where possible from pre-existing studies. Due to the limited number of previous studies of the Ericeira Group, this was less possible.

1.1.3: Methodology

Figure 1.i sets out the analytical procedure which has been implemented throughout this project in order to answer the aims and objectives. The methodology is discussed in more

detail in the following sub-sections (1.1.3a-1.1.3e)

1.1.3a: *Facies Analysis*

Initially, detailed field logging of the two successions was undertaken in order to record the facies, facies successions, vertical grain-size changes, detrital mineralogy, sedimentological and palaeontological variations and hiatuses. Grain-size changes were analysed in the field by using a hand-lens and grain-size comparator and checked using thin section petrography where coincident with sample. The collected data were then combined with previously published data (sedimentary and biostratigraphic data), to construct graphic logs and to recognise and interpret the depositional environments. An estimation of palaeo-water depth (i.e. shallowing, deepening, maximum flooding) was made as a result of the palaeoenvironmental interpretations.

Field work for the Corallian Group of south Dorset was limited to five week-long field sessions conducted throughout the Autumn of 1993, Spring of 1994, Summer of 1994, Autumn of 1994 and Spring of 1995. Available funds meant that only one week-long field session was available for studying the Ericeira Group of west-central Portugal, and this was conducted during the Summer of 1995.

1.1.3b: *Construction of high resolution sequence stratigraphic framework*

Once the facies and depositional environments were interpreted, the next step was the subdivision of these strata into the hierarchical units of sequence stratigraphy (see Section

1.2.4) along with the recognition of the different types (and scales) of stratal surfaces. It is of vital importance to accurately identify the type of parasequence, stratal surfaces and style of parasequence stacking in order to be able to determine the type of parasequence set (aggradational, retrogradational or progradational). However, a lack of diagnostic features at some sedimentary horizons within the two successions, meant that parasequence identification was not possible. The parasequence set and facies associations were used to determine the type of system tract, stratal surfaces and ultimately the type of sequence. In some circumstances, stratal surfaces at different hierarchical scales coincide (e.g. parasequence boundary and sequence boundary).

1.1.3c: *Data collection & thin-section microscopy*

Sampling restrictions meant that only a low resolution strategy was implemented. Such restrictions included;

1. Logistics, particularly available time and funds. This was also a major factor when conducting further analytical work (see sub-section 1.1.3d);
2. Sampling was focused on stratal surfaces of key importance and samples were selected with the aim of resolving key sequence stratigraphic interpretations; and
3. Certain lithologies (such as siliciclastic and carbonate mudstones, which account for approximately 32% of the Corallian Group and approximately 24% of the Ericeira Group) were not sampled because it was felt that any evidence of early diagenesis (by standard petrographic or analytical techniques) was either unobtainable, or would have been contaminated/over-printed by later diagenetic reactions (particularly clay authigenesis or organic reactions).

Individual sampling schemes are discussed in the relevant chapters (Chapter 3 for the Corallian Group; Chapter 5 for the Ericeira Group) and in Appendix 1. Oriented samples were cut to 30μm, bonded to glass slides and stained for carbonates, using the method outlined by Dickson (1966). Individual cement phases are identified, described and photographed with a view to the interpretation of their paragenetic histories.

1.1.3d: *Further geochemical analysis*

Additional geochemical analysis was performed on selected samples (selection procedures are outlined in the Chapters 2 and 4) to further constrain diagenetic environments. Methods employed were x-ray diffraction (XRD), stable isotope analysis and cathodoluminescence (CL), details of which can be found within Chapters 3 and 4 and Appendices 2 to 4. Cathodoluminescence and stable isotope analysis were used to provide further evidence for geochemical changes in pore-waters which led to the crystallisation of various carbonate cements. X-ray diffraction was used to assess the purity of the sample used for stable isotope analysis.

It should be noted that for cost, practical reasons and, as this study is primarily concerned with early diagenetic and facies related processes within a high resolution sequence stratigraphic framework, fine-scale analytical procedures (e.g. microprobe work) were not implemented. However, it is realised that such studies could complement the results offered in this thesis and are outlined in Chapter 7, "recommendations for further work".

1.1.3e: *Construction of models to predict early diagenesis within high resolution sequence stratigraphy*

The data were collated (sedimentological, sequence stratigraphic and diagenetic) with the aim of constructing models which can aid in the prediction of stratal surfaces and units. These models indicate that the identification of early diagenetic products can be a useful tool in the construction of high resolution sequence stratigraphic models. However as this study is based on a low resolution sampling scheme, further diagenetic and analytical work is necessary before unequivocal support or rebuttal of models relating early diagenesis to changes in relative sea-level can be given.

1.1.4: Conceptual framework

1.1.4a: *Concepts & history of sequence stratigraphy*

Sequence stratigraphy (for a definition of sequence stratigraphy, refer to Table 1.i) was developed from seismic stratigraphy during the late 1970's and 1980's particularly by workers from the Exxon Production and Research Company. During this period, the controlling emphasis on the development of stratigraphic sequences and unconformities switched from local tectonic events to changes in global sea-level (eustacy, see Vail *et al.*, 1977).

Early sequence stratigraphic and seismic stratigraphic studies resulted in the construction of global sea-level curves consisting of 1 to 3 million year (third order) sea-level cycles, superimposed upon lower frequency (first and second order) cycles This "seismic-based stratigraphy" (Emery & Myers, 1996) has been termed "low-resolution sequence stratigraphy" by Posamentier & Weimer (1993) due to its coarse resolution. In the petroleum industry its uses are confined to hydrocarbon exploration.

Erskine & Vail (1988) observed that higher frequency unconformities were often present within previously recognised third-order cycles (1-10m.y.) suggesting that sea-level changes occurred at even higher frequencies (e.g. fourth and fifth order or 10^5-10^4 years). During the same year, the book "Sea-level Changes, an Integrated Approach" (Wilgus *et al.*, 1988) was published, providing geologists with the first real conceptual framework for sedimentology within a sequence stratigraphic framework. As a result of these new concepts, high resolution sequence stratigraphy evolved, allowing analysis at a scale below that of seismic resolution. The emphasis of sequence stratigraphy thus began to change from age-model predictions based on previous sea-level cycle charts, to lithological predictions (Posamentier *et al.* 1993).

In the late 1980's and early 1990's, sequence stratigraphy began to be used in the analysis of field successions and borehole core. An early publication outlining this high resolution approach was the book "Siliciclastic Sequence Stratigraphy in Well Logs, Cores, and Outcrops" (Van Wagoner *et al.*, 1990). Since then, several key publications (e.g. Posamentier *et al.*, 1993 and Howell & Aitken, 1996) have developed these original concepts, resulting in a re-evaluation of sedimentary successions in a range of depositional

settings (e.g. Walker, 1992).

The new concepts and higher resolution now allow for an improved understanding of facies geometry, reservoir architecture, stratal stacking patterns and particularly the importance of small scale cyclic changes in sedimentary rock successions that are a result of high frequency changes in sea-level. A greater emphasis is now placed on the predictable and repetitive nature of such successions, particularly when constructing a high resolution sequence stratigraphic framework (Posamentier *et al.*, 1993). Thus, high resolution sequence stratigraphy has developed into a powerful and predictive tool in facies analysis (Howell & Aitken, 1996) allowing stratal geometries to be linked with internal facies assemblages (Emery & Myers, 1996). High resolution sequence stratigraphy is of particular use to reservoir and production geologists because it can provide more realistic reservoir models away from well control points.

1.1.4b: *Concepts & importance of diagenetic prediction within a sequence stratigraphic framework*

The construction of diagenetic models could result in the accurate prediction of porosity and permeability within a basin or stratigraphic unit - information that is of the up-most importance to the petroleum industry in exploration and more particularly, production. A key aim of reservoir characterisation is to be able to predict the nature and distribution of diagenetic products and their effect on fluid flow within a gross reservoir unit. Diagenetic components are moved in and out of sedimentary strata by diffusion or advection involving moving pore-waters (Horbury & Robinson, 1993). This pore-water movement

occurs as a response to basin evolution including, amongst many other things, changes in relative sea-level.

As a result of the recent rapid development of high resolution sequence stratigraphy, the analytical approach now exists to interpret early diagenetic processes within patterns of high frequency relative sea-level change. Such studies could predict the type and extent of diagenetic products within a basin. As well as changes in relative sea-level; petrophysical properties within differing facies units, depositional environments, composition of pore-water, climate and carbonate sediment mineralogy (particularly within carbonate facies), are of importance to early diagenesis (Tucker, 1993). All of these criteria are controlled by, or are related to, changes in relative (and eustatic) sea-level.

Previous research relating diagenetic processes to sequence stratigraphy within clastic successions includes Bjørkum *et al.* (1993) and Taylor *et al.* (1994); and within carbonate successions includes, Tucker (1993), Read & Horbury (1993), Stemmerik & Larssen (1993) and Hendry (1993a).

1.2: *Introduction to high resolution sequence stratigraphy within shallow marine nearshore successions*

1.2.1: Introduction

Sequence stratigraphy is the study of "genetically related facies within a framework of chronostratigraphically significant surfaces, wherein the study of rocks is cyclic and is composed of genetically related stratal units" (Posamentier *et al.*, 1988; Van Wagoner *et al.*, 1990). Sequence stratigraphy relates the formation of stratal surfaces to relative changes in sea-level and places them within a chronostratigraphic context of parasequence and sequence boundaries (Van Wagoner *et al.*, 1990). It is the balance between the rate of accommodation creation (which provides the "space") and the rate of sedimentation (which provides the "fill") that is the driving force behind the principals of sequence stratigraphy.

The sequence stratigraphic terminology used throughout this thesis is that defined by Mitchum (1977), Posamentier *et al.* (1988), Posamentier & Vail (1988), Van Wagoner *et al.* (1988, 1990) and Posamentier *et al.* (1992) and is summarised in Table 1.i.

1.2.2: Basic theory

1.2.2a: *Eustacy*

Eustacy is measured between the sea-surface and a fixed datum, usually the centre of the Earth (Fig.1.ii). Eustacy can vary by changing ocean-basin volume or by varying ocean-water volume (Posamentier *et al.*, 1988; Emery & Myers, 1996) allowing it to rise and fall.

1.2.2b: *Relative sea-level*

Relative sea-level is a function of eustacy and subsidence (sediment compaction and tectonics) which control the amount of space made available for sediment accumulation (accommodation space) in a marine environment. It is measured between the sea-surface and a local datum, such as a surface within the sedimentary pile (Posamentier *et al.*, 1988) (Fig.1.ii). Relative sea-level "rises" due to subsidence, compaction and/or eustatic sea-level rise, and "falls" due to tectonic uplift and/or eustatic sea-level fall (Emery & Myers, 1996). The equilibrium point (Table 1.i) separates the zone at the basin margin where relative sea-level is falling, from the zone where relative sea-level is rising (Emery & Myers, 1996).

Within carbonate successions, changes in relative sea-level are also one of the primary controls on carbonate productivity (Schlager, 1992) and thus on the resultant facies distribution. Two other factors are also important - the depositional setting and climate. Unrestricted basins with normal, well circulated marine pore-waters provide a favourable

habitat for a more varied biota, whereas restricted basins with higher salinities have a specialised or reduced biota. Climate is important, not only in determining the depositional facies of carbonates, but also in controlling the extent of early post-depositional diagenesis associated with sub-aerial exposure.

1.2.2c: *Accommodation space*

Stratal packages and facies associations rely strongly on the amount of space available for sediment to accumulate in and the rate at which new space is added or taken away (Posamentier *et al.*, 1988). The space available is termed the "accommodation space" (see definition in Table 1.i) and in a marine environment is the space between the sea floor and the sea surface (Fig.1.iii). Accommodation space represents the accumulation potential of any clastic or carbonate sequence. The rate at which new space is made available for sediment to fill is determined by the rate of relative sea-level change. Swift & Thorne (1991) also include processes such as marine erosion and redistribution of material to create accommodation space. Their accommodation space is defined by a surface of dynamic equilibrium above which sediment cannot accumulate and is reworked.

Changes in relative sea-level control the amount of space made available for sediment accumulation (i.e. a rise in relative sea-level results in an addition of space, whereas a fall results in a loss of space). Water depth (relative sea-level minus accumulated sediment) is independent of relative sea-level, and dependent on the rate of sediment accumulation with respect to the rate of sea-level rise or fall. Thus, relative sea-level may rise creating more accommodation space, but if sediment accumulation occurs at a faster rate, then water

depth will decrease. Similarly, if relative sea-level falls at a slower rate than the sea floor subsides, the net effect will be a relative sea-level rise, and consequently, new space will be added. If sedimentation rates are lower than the rate of relative sea-level rise, then the water depth will increase. If rates of subsidence are greater than rates of relative sea-level change, new space will be created. The accommodation space available for sediment accumulation will thus be the addition of the new space created plus the "left-over", unfilled space (Posamentier *et al.*, 1988).

Detrital carbonate production, much of which is a by-product of photosynthesis, is highest in water depths of 10m, and drops off dramatically in deeper water (Sarg, 1988). Thus changes in relative sea-level are an important factor in the ability of carbonate production to keep pace with changing water depth (Fig.1.iv).

1.2.2d: *Accommodation fill*

The rate of sediment supply controls the degree to which accommodation space is filled spatially. The balance between sediment supply and relative sea-level rise controls whether siliciclastic facies belts prograde basinward or transgress landward (Emery & Meyers, 1996). Carbonate is generally produced in platform-top environments and (depending on environmental conditions) can keep pace with rising sea-level (Emery & Meyers, 1996). This contrasts with the siliciclastic system by accreting vertically, rather than backstepping during a transgressive period (Emery & Meyers, 1996).

The amount of sediment supplied to the basin is a function of both the general rate of sediment supply and the location of sedimentary entry points (Emery & Meyers, 1996). Figure 1.va-c (from Jervey, 1988) shows the relationship of facies, relative sea-level and rates of sediment accumulation at three points within a basin. All points have identical relative sea-level curves but differing rates of sediment supply. In Figure 1.va, which represents a point with a low sediment input, the rate of accommodation creation will always exceed the rate of sediment accumulation. The net affect of this will be a landward migrating shoreline and a transgression develops. In Figure 1.vb, which represents a location characterised by a moderate sediment input, the initial rate of accommodation creation exceeds the rate of sediment accumulation and a transgression begins. However, as the rate of relative sea-level rise diminishes, shoreline regression will begin and the rate of sediment supply exceeds the rate of accommodation creation. Excess sediment which cannot be accommodated will be transported basinwards. When relative sea-level falls, previously deposited sediment will be subject to erosion. Finally, in Figure 1.vc, which represents a point with a rapid sediment input, the rate of sediment supply will always exceed the rate of accommodation creation and shoreline regression will be continuous. However, the rate of sediment accumulation will be limited by the rate of accommodation creation.

1.2.3: Sequences and systems tracts

1.2.3a: *The sequence and sequence boundary*

A sequence (see Table 1.i for original definition) represents one cycle of deposition bounded by unconformities or correlative conformities and deposited during one "significant" cycle of fall and rise of relative sea-level (Emery & Myers, 1996). Sequences can be of two types, type-1 and type-2, which can be bounded by either type-1 or type-2 sequence boundaries.

The formation of a type-1 or type-2 sequence boundary will depend on whether the rate of relative sea-level fall exceeds, or is less than, the rate of subsidence at the offlap break (previously called the depositional shoreline break, see Table 1.ii for definition). Criteria for identifying sequence boundaries include a basinward shift in facies for a type-1 sequence boundary and a vertical change in parasequence stacking patterns for either a type-1 or a type-2 sequence boundary (Van Wagoner *et al.*, 1990).

If the rate of relative sea-level fall is greater than the rate of subsidence, a type-1 sequence boundary will develop (Table 1.i). Landward of the offlap break in siliciclastic successions the most pronounced features of a type-1 sequence boundary are truncation, a basinward shift in facies and subaerial exposure. If a type-1 sequence boundary develops in a basin or portion of a basin with numerous rivers, then valley incision will occur across the now exposed shelf (Fig.1.vi) with interfluves occurring between incised valleys. Depositional environments within the distal parts of these valleys vary and include

lowstand deltas, tidal-flats, estuaries and beaches. In proximal settings, these facies types typically grade into fluvial depositional environments, while laterally (on the exposed shelf) soils or rooted horizons are dominant (Van Wagoner *et al.*, 1990). However, if fluvial deposition is limited, then widespread evidence of subaerial exposure will be dominant.

Within carbonate dominated successions, two major processes occur during the formation of a type-1 sequence boundary (Sarg, 1988). Slope front erosion is one process, but will not be discussed further because the depositional environment is not within the realms of this review. Basinward movement of pore-water diagenetic zones also occur (Sarg, 1988; Tucker, 1993). Hunt & Tucker (1993) state that exposure of carbonate surfaces during a fall in relative sea-level will lead to chemical reworking (early meteoric diagenesis) rather than mechanical reworking. This feature will be discussed in more detail in Section 1.3. Therefore exposure of a carbonate shelf does not result in an increased sediment supply to the adjacent basin.

A type-1 sequence boundary that develops during a falling relative sea-level on a ramp margin will do so in response to a forced regression (Posamentier *et al.*, 1992) (Fig.1.vii). Forced regressions are defined as a seaward translation of a shoreline occurring in response to a relative sea-level fall and independent of sediment input variations (Posamentier *et al.*, 1992). The shoreface deposits associated with a forced regression are typically detached from the underlying highstand shoreline, associated with a zone of sedimentary by-pass and subaerial erosion and commonly characterised by a sharp base defining a sequence boundary (Posamentier *et al.*, 1992). Hunt & Tucker (1993) have re-

named these deposits "stranded parasequences".

Conversely, if the rate of relative sea-level fall is similar to the rate of subsidence across a shelf margin, then a type-2 sequence boundary will develop (Table 1.i). This will result in little or no basinward shift in coastal onlap (Posamentier & Vail, 1988) and limited or no subaerial erosion (depending on whether the shelfal area becomes exposed). As a result, there is no fluvial incision, stream rejuvenation or sediment bypassing on the shelf (Fig.1.viii).

A type-1 sequence is bounded at its base by a type-1 sequence boundary and at its top by either a type-1 or type-2 sequence boundary. It is composed of lowstand (LST), transgressive (TST) and highstand (HST) systems tracts (Posamentier & Vail, 1988). These are characteristically equivalent to progradational/weakly aggradational, retrogradational and progradational parasequence sets (Van Wagoner *et al.*, 1990) (Fig.1.vi).

A type-2 sequence is bounded at its base by a type-2 unconformity and at its top by either a type-1 or type-2 sequence boundary. It is composed of shelf-margin (SMW), transgressive (TST) and highstand (HST) systems tracts (Posamentier & Vail, 1988). These are characteristically equivalent to aggradational/weakly progradational, retrogradational and progradational parasequence sets (Van Wagoner *et al.*, 1990) (Fig.1.viii).

1.2.3b: *Systems tracts*

The systems tract (Table 1.i) generally represents the fundamental mapping unit for stratigraphic prediction, because it may contain a set of depositional systems with consistent palaeogeography and depositional polarity, and for which a single palaeogeographic map can be drawn (Emery & Myers, 1996). However, it should be stated that depositional systems can change at the parasequence scale within individual systems tracts.

Lowstand systems tract (LST):

The lowstand systems tract is deposited during intervals of relative sea-level fall and subsequent slow relative sea-level rise. A relative sea-level fall will occur when the rate of sea-level fall exceeds the rate of subsidence at the offlap break (Posamentier & Vail, 1988). Within clastic successions representing shelf-break margin profiles, the lowstand systems tract typically consists of a lowstand submarine fan and a lowstand wedge. As the lowstand submarine fan occurs predominantly within the basin, seaward of the shelf/slope break, it is not relevant to the successions discussed in this thesis. Only the lowstand wedge (Fig.1.ix) will be discussed here.

The lowstand wedge is commonly characterised by one or more progradational parasequence sets (Van Wagoner *et al.*, 1990) and is initiated during the latter part of a rapid relative sea-level fall during the sea-level lowstand (Posamentier & Vail, 1988) (Fig.1.ix). During this time, the rate of subsidence will exceed the rate of relative sea-

level fall at the offshore break, creating a slow rise of relative sea-level and an increase in accommodation space.

The proximal part of the wedge will consist of incised valley fills if the basin, or portion of the basin, contains rivers (caused by the cessation of stream downcutting and subsequent increase in deposition) and correlative shoreline deposits on the shelf and shoreface (Fig.1.ix). The distal part of the lowstand wedge will generally be composed of thick shale rich facies downlapping onto the underlying lowstand fan (Van Wagoner *et al.*, 1990).

Throughout the period of lowstand wedge formation, the rate of accommodation creation increases as the rate of relative sea-level rises more rapidly (Posamentier & Vail, 1988). Eventually, the rate of sedimentation will become less than the rate of accommodation creation and the beginnings of a marine transgression will occur. This is marked by the transgressive surface, which marks the first major flooding event of the shelf area within the new sequence. The transgressive surface is initiated because up to this point in time (from sequence boundary formation to transgressive surface formation) deposition on the shelf has been restricted to incised valley fills. As the rate of relative sea-level begins to rise, new accommodation space is initially added in the incised valleys alone. The old shelf is subaerially exposed because base level has yet to reach this height. Thus, sedimentation rates are able to "keep up" with rates of accommodation space creation. However, as soon as base level reaches the height of the shelf (i.e. as soon as the shelf becomes flooded) a large increase in the space available for accommodation occurs. The rapid increase in rates of accommodation addition drastically outpace existing rates of

sedimentation. Hence, on the shelf, a rapid marine transgression will occur. The timing of marine transgression is a function of eustacy, subsidence, sedimentation rates and the area available for sediment accumulation (Emery & Myers, 1996).

Within carbonate successions, Sarg (1988) suggests that lowstand systems tracts can be divided into two types: allochthonous deposits derived from erosion of the bank margin and slope and characterised by channelled megabreccia deposition, and autochthonous wedges deposited on the upper slope during either type-1 or type-2 sea-level lowstands. Sarg (1988) also points out that with the correct climatic and depositional conditions, evaporite and/or clastic lowstand deposition can occur.

Hunt & Tucker (1993) have suggested revisions for these models of lowstand deposition. In their model, they suggest that the current lowstand systems tract be subdivided into two newly named systems tracts - the forced regressive wedge systems tract and the lowstand prograding wedge systems tract. They also suggest that the positioning of the sequence boundary should be moved to coincide with the lowest point of relative sea-level. This would then place parasequences that stack to form at least the slope wedge component of the forced regressive wedge systems tract below the sequence boundary. The succeeding lowstand prograding wedge then behaves in a similar way to that described earlier. Thus, Hunt & Tucker's (1993) model effectively splits the original lowstand systems tract into two components occurring above and below a sequence boundary.

Shelf-margin systems tract (SMW):

The shelf-margin systems tract overlies a highstand systems tract and type-2 sequence boundary and is characterised by a decreasingly progradational to increasingly aggradational parasequence stacking pattern, passing eventually into a retrogradational transgressive system tract (Posamentier & Vail, 1988, my Fig.1.x).

The lower boundary of the shelf-margin systems tracts forms a type-2 sequence boundary separating coastal, paralic or deltaic sediments above, from highstand deposits below. The upper boundary of the shelf-margin systems tract is marked by a transgressive surface separating the dominantly aggradational parasequence stacking pattern of the upper shelf-margin systems tract below from the retrogradational parasequence stacking pattern of the transgressive systems tract above. The transgressive surface marks the first major flooding event to occur within the sequence (Posamentier & Vail, 1988).

Throughout the deposition of the shelf margin systems tract a progressive increase in the rate of relative sea-level rise will occur resulting in deposition of sediment on the outer part of the shelf (Posamentier & Vail, 1988). An increasing rate of relative sea-level rise may initially be accompanied by the deposition of a progradational parasequence set, as sedimentation rates will be greater than rates of accommodation creation. With time, the rates of progradation will slow in response to the increasing rate of new shelf space added. This will allow sedimentation rates and rates of accommodation creation to equilibrate, resulting in the deposition of a vertically stacked, or aggradational parasequence set.

Type-2 sequence boundaries beneath shelf-margin wedges are notoriously difficult to recognise in outcrop (Posamentier & James, 1993). This is because no overall relative sea-level fall occurs across a type-2 sequence boundary in a marginal marine setting. In a depositional succession spanning late highstand to early shelf-margin systems tracts, the deceleration and then acceleration of relative sea-level rise results in an increasingly progradational to decreasing progradational and then aggradational parasequence stacking pattern (Posamentier & James, 1993).

Transgressive systems tract (TST):

The transgressive systems tract occurs in both type-1 and type-2 sequences and is characterised by a retrogradational parasequence stacking pattern (Fig1.xi). It is deposited during a time of relative sea-level rise when the rate of accommodation creation is greater than the rate of sedimentation. Its base is the transgressive surface which represents the time of first significant flooding event within the new sequence (Posamentier & Vail, 1988). The maximum rate of relative sea-level rise occurs some-time within the transgressive systems tract (Emery & Myers, 1996). The end of the systems tract occurs when the rate of accommodation creation decreases to a point where it is equal to the rate of sedimentation, and then progradation begins. This point is known as the maximum flooding surface and is controlled by eustacy, subsidence, sedimentation rates and the area available for sediment accumulation (Emery & Myers, 1996).

In outcrop studies, positioning of a maximum flooding surface is based primarily on identification of changes in parasequence stacking patterns. In many cases, such as

condensed sections, or muddy shelfal depositional environments for example, it is difficult to recognise a single discrete surface in the field and so a "zone of maximum flooding" is recognised. Within this zone, a number of discrete surfaces may be candidates for a maximum flooding surface. Basinward of the shoreline, maximum flooding zones are represented by shelfal siltstones and mudstones (Emery & Meyers, 1996).

The retrogradational pattern associated with transgressive systems tracts varies depending on whether the sequence described is type-1 or type-2. Posamentier & Vail (1988) suggest that transgressive deposits following a lowstand wedge systems tract (i.e. a type-1 sequence) will be contained within incised valleys due to a rapidly rising relative sea-level flooding the shelf area quickly. This will result in limited transgressive deposition outside the incised valleys at that time. However, following a type-2 sequence boundary, flooding of the shelf occurs more gradually. As incised valleys are absent and the majority of the shelf area was probably not subaerially exposed, the extent of transgressive deposition will be greater both vertically and laterally.

In carbonate systems, rates of sediment production are commonly sufficiently high enough to outpace rates of relative sea-level rise (Schlager, 1981). Hunt & Tucker (1993) have distinguished between two types of stacking pattern that can develop during a transgressive systems tract and reflect the ratio of rates of sea-level rise to sedimentation rate. In their model, when rates of relative sea-level rise are greater than sedimentation, type-1 geometries are developed. If rates of relative sea-level rise are less than or equal to sedimentation rates (at the shelf margin) type-2 geometries are developed (although the rate of sea-level rise may be greater than sedimentation rates for inner-shelf facies). Hunt

& Tucker (1993) also note that, unlike clastic systems, carbonate sedimentation rates cannot always be assumed to be constant due to the strong environmental control on sedimentation. Thus changes in parasequence stacking patterns do not always reflect changes in the rates of relative sea-level rise, as carbonate production is affected by a number of other factors.

Highstand systems tract (HST):

The highstand systems tract is the youngest systems tract in either a type-1 or type-2 sequence, and is deposited after maximum transgression and before a sequence boundary when the rate of accommodation creation is less than the rate of sediment supply (Fig.1.xii). It is characterised by a decelerating rate of relative sea-level rise through time, resulting in an aggradational to progradational parasequence stacking pattern. When succeeded by a type-1 sequence boundary, the highstand systems tract may be significantly truncated or removed altogether.

Sarg (1988) suggests that carbonate highstand systems tracts can be characterised by early and late stages that reflect different rates of accommodation, water mass conditions, associated carbonate productivity and fundamentally different depositional histories. In his model, Sarg modifies the "keep-up" and "catch-up" terminology of Kendall & Schlager (1981). The keep-up carbonate systems tract displays a relatively rapid rate of accumulation and is able to keep up with rises in relative sea-level. In comparison, the catch-up carbonate systems tract displays a relatively slow rate of accumulation, which initially will always be less than the rate of accommodation creation. Only during the

latest portion of the highstand, when accommodation is reduced because of falling sea-level will a catch-up carbonate system display keep-up characteristics (Sarg, 1988). During highstand systems tracts, carbonate production usually exceeds the rate of accommodation creation, and excess carbonate will by-pass the carbonate platform top and be discharged into adjacent basins by a process known as "highstand shedding" (Schlager, 1992). Highstand shedding in carbonate systems provides a major contrast to siliciclastic sequence stratigraphy which predicts that most sediment is shed into the basin during a lowstand systems tract (Schlager, 1992; Emery & Myers, 1996).

1.2.3d: *Other systems tracts*

Emery & Myers (1996) describe two other possible systems tracts that can occur within a relative sea-level cycle. These are "the midstand systems tract" and "the regressive systems tract". The midstand systems tract (or forced regressive wedge of Hunt & Tucker, 1993) represents an entire sequence where at no time was subsidence sufficiently high enough to outpace sediment supply and allow transgression (Emery & Myers, 1996). The regressive systems tract consists of a prograding wedge that is bounded below by a maximum flooding surface and above by a maximum progradation surface (Emery & Myers, 1996).

1.2.3e: *Sequence stratigraphic models for carbonate ramps*

During the deposition of the transgressive systems tract, rising sea-level will commonly cause a ramp to retrograde due to its low carbonate productivity. With an increase in

water depth, the deeper parts of the ramp will become increasingly sediment starved, increasing the likely-hood of organic matter accumulation (Emery & Myers, 1996).

As the rate of sea-level rise decreases during the development of the highstand systems tract, the carbonate ramp will prograde. During the early highstand, when accommodation space is still being created, intertidal and lagoonal deposits may accumulate, but during the late highstand when very little accommodation space is being created strand-plain deposits may result (Tucker & Wright, 1990; Emery & Myers, 1996). Burchette *et al.* (1990) have written a review of carbonate ramp sequence stratigraphy, with particular implications for petroleum exploration.

1.2.3f: *Mixed carbonate/siliciclastic successions*

Hunt & Tucker (1993) state that mixed carbonate/siliciclastic depositional systems respond in a similar manner to purely siliciclastic depositional systems. During a falling sea-level, the landward portion of a carbonate ramp will be exposed. If the siliciclastic sediment supply is significant, it may overwhelm carbonate production and a siliciclastic lowstand systems tract may be established across the old carbonate ramp surface (Emery & Myers, 1996). This may also incise the underlying carbonate highstand (Hunt & Tucker, 1993). Partitioning of carbonates into transgressive/highstand systems tracts and siliciclastics into lowstand systems tracts, has also been identified by Cant (1995).

Examples of mixed siliciclastic-carbonate cyclic sedimentation are from the Lower Permian of New Mexico (Mack & James, 1986), the Albian of Lunda and Soba, Northern

Spain (García-Mondéjar & Fernández-Mendiola, 1993) and the Middle Cambrian of the southern Great Basin, USA (Osleger & Montañez, 1996). In the first example, allocyclic glacio-eustatic sea-level changes have been used to explain the siliciclastic-carbonate facies partitioning within symmetrical and asymmetrical sedimentary cycles. In the second example, type-1 sequence boundaries result in the emergence of carbonate platforms, which are then subjected to small periods of karstification and erosion. The overlying lowstand deposits include turbiditic, estuarine or fluvial sandstones. Type-1 sequence boundaries are produced by sea-level falls that are related to tectonic pulses. These produced angular unconformities in the basin margin or the inner platform, changes in palaeoslope of the basin floor and the sudden arrivals of sandstones into the basin. In the third example, siliciclastic sedimentation is controlled by relative sea-level with major sediment inputs occurring during inferred lowstand and highstand systems tracts.

Finally, Emery & Myers (1996) provide a review of sequence stratigraphic models for other types of carbonate platforms (rimmed shelves, escarpment margins and isolated platforms) and the reader is referred to their book for further details.

1.2.4: High resolution sequence stratigraphy

As outlined in sub-section 1.1.4a, high resolution sequence stratigraphy integrates information obtained from detailed data sets (from the log, core or outcrop scale) allowing gross stratal geometries to be linked with the internal facies assemblages. Table 1.ii (after Van Wagoner *et al.*, 1990) introduces the concepts of hierarchy within a high resolution

sequence stratigraphic framework. Van Wagoner *et al.* (1990) begin their hierarchical classification at the smallest unit - the lamina scale, although this scale is more likely to be the result of "events" rather than changes in relative sea-level. Within this brief review, I will begin at the parasequence scale.

1.2.4a: *The parasequence & parasequence boundary*

The parasequence:

Parasequences (see Tables 1.i & 1.ii for definition) are the building blocks of parasequence sets and ultimately sequences (Van Wagoner *et al.*, 1990). They are predominantly progradational packages of sediment, resulting in a typically shallowing-upward facies succession in which younger bedsets are deposited in progressively shallower water. Carbonate parasequences can also be composed of aggradational packages of sediment and shallow-up into shoal or reefal facies (Van Wagoner *et al.*, 1990; Tucker, 1993; Emery & Myers, 1996). Parasequences are separated by thinner units, representing an upwards-deepening facies succession. Occasionally, this upwards-deepening component is represented only by a hardground or omission surface marking a transition from shallower to significantly deeper water facies (Emery & Myers, 1996).

Parasequences can coarsen-upwards or fine-upwards depending on the depositional environment. In an upwards-coarsening parasequence representing a shallow marine, wave or storm dominated setting (Fig.1.xiiia) bedsets thicken, facies units coarsen and the ratio of coarser grained sediment to finer grained sediment increases upwards. In an

upwards-fining parasequence representing a channel, estuarine or tidal flat setting (Fig.1.xiiib) the opposite is true, with the parasequence commonly culminating in mudstones, heterolithic units or even coal beds (Van Wagoner *et al.*, 1990). In both types of parasequence, the vertical facies sequence usually suggests a gradual decrease in water depth.

Facies types within a parasequence will change laterally in a predictable manner (Van Wagoner *et al.*, 1990) as the depositional setting changes. In a basinward direction, (Fig.1.xiv) stratal characteristics may change from dominantly seaward dipping planar beds representing a foreshore or non-marine environment, through increasingly thinning and finer grained facies types representing a lower shoreface to shallow marine environment, to finally shelfal mudstones. The parasequence will be terminated updip (landward) by fluvial erosion/incision, or onlap onto a sequence boundary (Van Wagoner *et al.*, 1990) and downdip (basinward) by thinning and/or downlap onto an underlying boundary (parasequence, parasequence set or sequence, Van Wagoner *et al.*, 1990).

Trace fossil assemblages (ichnofacies assemblages) can reflect high frequency cyclic palaeoenvironmental changes, and therefore are of importance in interpreting parasequences (Savrda, 1991). Generally, the degree of bioturbation will increase upwards, reflecting the increase in energy as the parasequence progrades. However, the type of trace fossil assemblage will change laterally in a predictable manner depending on the depositional setting within the overall land-shore-shelf profile. For a review of the conceptual framework of ichnological assemblages the reader is referred to Pemberton (1992).

Carbonate parasequences may include a significant siliciclastic component and in this respect, contain all the elements of mixed siliciclastic-carbonate sequences that were described in sub-section 1.2.3e, but on a much smaller scale. Autocyclic mechanisms such as eustacy and tidal-flat progradation (after James, 1984) have been used to explain the origin of such cycles (Emery & Myers, 1996).

The parasequence boundary:

Parasequences are separated from one another by a parasequence boundary which represents a marine flooding surface (Van Wagoner *et al.*, 1990) (Figs.1.xiii & 1.xiv). The marine flooding surface in this definition is a surface separating younger from older strata, across which there is evidence of an upward increase in water depth (Emery & Myers, 1996). In coarsening-up parasequences, a marine flooding surface might, for example, separate deeper water siltstones or claystones above (representing the more distal part of the parasequence) from shallow water sandstones or oolitic/bioclastic grainstones below (representing the more proximal part of the parasequence). The flooding surface is characterised by minor submarine erosion with a minor hiatus indicated, although major erosion may indicate the formation of a ravinement surface (refer to Table 1.i). Ravinement surfaces are the result of transgressive erosion by shoreface retreat and are particularly well developed when; (i) a parasequence boundary corresponds to a major transgressive surface (i.e. the top surface of the lowstand or shelf-margin wedge systems tracts) or (ii) a facies unit was shallower than the shoreface prior to transgression.

Tucker (1993) states that carbonate parasequences may have an upper surface recording emergence that represents a relatively short period of time. Occasionally transgressive-lag deposits (see Table 1.i for definition) are associated with parasequence boundaries/ravinement surfaces, but are more common when a parasequence boundary coincides with a major transgressive surface. The transgressive lag is composed of material derived from underlying strata during shoreface erosion.

Parasequence thickness trends:

The thickness of a parasequence is a product of (i) the rate of rise in relative sea-level after the "drowning" of the previous parasequence and (ii) the periodicity of parasequence formation (Emery & Myers, 1996). For example, if parasequence periodicity is relatively constant, then a slow rate of rise of relative sea-level will result in thin parasequences and a rapid rate of rise will result in thick parasequences (Emery & Myers, 1996).

1.2.4b: *Parasequence sets*

For carbonate and siliciclastic dominated successions, parasequences commonly stack to form parasequence sets (see definition in Tables 1.i and 1.ii) which may be progradational, retrogradational or aggradational (Van Wagoner *et al.*, 1990). The type of stacking pattern refers to the architecture of a vertical succession of parasequences and depends on the ratio of sedimentation rates to rates of accommodation creation at the scale of the parasequence set. The terms "systems tracts" (refer back to Section 1.2.3) and "parasequence set" are not always synonymous (Posamentier & James, 1993). The use of the term "systems

tract" involves an interpretation regarding sea-level change, vertical and lateral relationships between facies successions and the nature and significance of any bounding surfaces (Posamentier & James, 1993). However, the use of the term "parasequence set" is purely descriptive and does not infer any interpretation of sea-level change (Posamentier & James, 1993). In areas of high subsidence and sediment input, it is possible that more than one parasequence set can exist in a systems tract (Emery & Myers, 1996).

Progradational parasequence set:

During the deposition of progradational parasequence sets, the rate of deposition or sedimentation becomes greater than the rate of accommodation space creation, over time (Fig.1.xva). Thus, successively younger parasequences become generally thicker, contain coarser grained facies and are deposited in successively basinward positions.

Retrogradational parasequence set:

During the deposition of retrogradational parasequence sets, the rate of sedimentation is less than the rate of accommodation creation (Fig.1.xvb). Thus, successively younger parasequences become generally thinner, contain finer grained facies and are deposited further landward. The youngest parasequence in the set may be composed entirely of sediment deposited on the shelf (Van Wagoner *et al.*, 1990).

Aggradational parasequence set:

During the deposition of aggradational parasequence sets the rate of sedimentation is equal to the rate of accommodation creation (Fig.1.xvc). Thus parameters such as facies types and thickness do not change significantly with time (at the time scale of the parasequence set).

The parasequence set boundary:

Parasequence sets are separated by parasequence set boundaries which are similar to parasequence marine flooding surfaces and their correlative surfaces (Van Wagoner *et al.*, 1990). They therefore separate distinctive parasequence stacking patterns and can coincide with systems tract boundaries - transgressive surfaces, maximum flooding surfaces (see sub-section 1.2.3c) or sequence boundaries (see sub-section 1.2.3a).

1.3: *Early diagenesis within a high resolution sequence stratigraphic framework*

1.3.1: Introduction

Within the context of this thesis, early diagenesis is considered to include those processes between the time of deposition and the early stages of lithification, at relatively low temperatures within a shallow burial environment (Friedman, 1964; McKay *et al.*, 1995).

Early diagenetic processes and products are strongly influenced by depositional environment (Berner, 1981; Curtis, 1987), relative sea-level changes (Taylor *et al.*, 1994; Tucker, 1993; McKay *et al.*, 1995), sedimentation rate (Curtis, 1987) and climate (Tucker, 1993). Early diagenetic processes encompass three major diagenetic environments - the marine, mixing zone and meteoric zones all of which are influenced by the features listed above (Tucker & Wright, 1990; Tucker, 1991, 1993). Inorganic/organic diagenesis and organic matter degradation, also occurs within each diagenetic environment as a series of depth related, microbially induced zones (Irwin *et al.*, 1977; Curtis, 1978, 1980, 1987; Berner, 1981; Curtis & Coleman, 1986). In these zones, the concentrations of oxygen and sulphate primarily control the degradation of organic matter (along with rates of reactivity, amount of organic matter, Fe content and temperature). These diagenetic reactions are all strongly influenced by pore fluids within each of the diagenetic environments.

This section provides a brief review of, (i) early diagenetic reactions, products and environments of siliciclastic and carbonate successions; and, (ii) previous work that has linked sequence stratigraphy (or high frequency changes in relative sea-level) with early diagenesis. For more comprehensive reviews, please refer to Curtis (1987), Tucker & Wright (1990), Tucker (1991 & 1993) and Read & Horbury (1993).

1.3.2: Review of early diagenetic processes

1.3.2a: *Inorganic/organic diagenesis of sediments*

Curtis (1987) provides a summary of depth related inorganic/organic diagenesis. During normal marine conditions (i.e. oxygenated bottom waters), three main diagenetic zones are encountered from the sediment/water interface downwards (Fig.1.xvi). These are the respiration or oxic zone (Ox), the sulphate reduction zone (incorporating the sub-oxic zone) (Sr) and the microbial methane zone (Me). Figure 1.xvi shows three other examples with varying zonation patterns depending on changes in environment and bottom-water oxygen conditions.

Within each of the diagenetic zones, different chemical reactions take place which are dependant on a number of factors including amount of organic matter and type of organisms present. Each of these chemical reactions produces important products which directly lead to mineral authigenesis. Simple chemical equations can be written to approximate these chemical reactions (after Curtis, 1987):-

$$\text{Ox:} \quad CH_2O + O_2 \rightarrow H^+ + HCO_3^- \quad \text{[Eq. 1]}$$

$$\text{Sr:} \quad 2CH_2O + SO_4^{2-} \rightarrow H^+ + 2HCO_3^- + HS^- \quad \text{[Eq. 2]}$$

$$\text{Me:} \quad 2CH_2O + H_2O \rightarrow H^+ + HCO_3^- + CH_4 \quad \text{[Eq. 3]}$$

Mineral authigenesis within the Sr zone is particularly important because approximately

double the quantity of HCO_3^- is produced compared to H^+. This raises the pH of the pore fluid and thus ultimately favours carbonate precipitation (Curtis, 1987).

Iron reduction is also an important process occurring within the Sr zone. *Fe(III)* will be reduced to Fe^{2+} with organic matter acting as a reducing agent. Curtis (1987) offers a simple equation to describe this reaction:-

$$2Fe_2O_3 + CH_2O + 3H_2O \rightarrow 4Fe^{2+} + HCO_3^- + 7OH^- \quad \text{[Eq. 4]}$$

This reaction (Equation 4) will favour carbonate precipitation by increasing bicarbonate activity and raising pH. Iron reduction is also important in the precipitation of pyrite within the Sr zone. Simultaneous reduction of *Fe(III)* compounds and SO_4^{2-} yields Fe^{2+} and HS^- which quantitatively precipitate as pyrite. A simple equation to describe this reaction (Curtis, 1987) is:-

$$15CH_2O + 2Fe_2O_3 + 8SO_4^{2-} \rightarrow 4FeS_2 + 7H_2O + 15HCO_3^- + OH^- \quad \text{[Eq. 5]}$$

The reaction outlined in Equation 5 will also favour carbonate production by significantly increasing bicarbonate activity and raising pH. The composition of the carbonate phase will reflect the relative rates of *Fe(III)* and sulphate reduction. If the sulphate reduction rate balances or exceeds *Fe(III)* reduction, the carbonate phase will be iron poor (either calcite or dolomite), whereas iron-rich carbonates (ferroan calcite, ferroan dolomite, siderite) will co-precipitate with pyrite if the opposite is true.

The importance of sedimentation rate on the production of mineralising fluids within each of the microbial zones has also been discussed by Curtis (1987) (Fig.1.xvii). Curtis states that authigenic precipitation is dependant on the rate of organic matter degradation and the time for which the particular zonal reaction operates (a function of zone thickness and rate of burial). Thus, slow rates of sedimentation would favour massive degradation of organic matter within the Ox zone (from sediments beneath oxygenated waters). By contrast, rapid sedimentation allows sediment to by-pass the Ox zone, thus preserving organic matter and transporting it rapidly into the deeper microbial zones where degradation is less intensive.

Thus, authigenic phases precipitated from pore-waters prior to any significant burial (or compaction) are an important product of early diagenesis. In clastic sediments the effects of early diagenetic precipitation are often found in the form of concretions. Concretions are often demonstrably early diagenetic features, often containing intact bioclastic material, sedimentary laminae that originated from within the host sediment and depositional fabrics that are devoid of compactional features.

1.3.2b: *Early diagenetic environments*

The three major early diagenetic environments (the marine, meteoric and mixing zone) pass vertically and laterally into one another (Fig.1.xviii). Sediments can therefore pass from one environment to another with time, deposition and relative sea-level changes. The following sub-section offers brief introductions to each of these environments, with particular reference to the main controlling factors. For a more detailed discussion

(especially of different carbonate cement types) refer to Leeder (1982), Tucker & Wright (1990) and Tucker (1991).

The marine diagenetic environment:

Within the marine realm of siliciclastic and carbonate successions, pore space is entirely filled by waters of marine composition and pressures and temperatures do not substantially differ from those at the Earth's surface. Sediment in contact with marine water is affected by oxidising conditions (refer back to sub-section 1.3.2a) while lower down, pore-waters are usually reducing and early diagenesis is strongly influenced by bacterial oxidation and reduction (Leeder, 1982).

Common products of marine diagenesis are calcium carbonate cements that precipitate within intergranular and intragranular porosity. The dominant controls on marine cementation within carbonate sediments are the degree of sea-water circulation through the sediments, the climate and the sedimentation/carbonate production rate (Tucker, 1991).

Above wave base, sea-water circulation is most active in unrestricted shallow marine environments and it is here where marine cementation is most pronounced. However, in restricted/stagnant shelfal or lagoonal environments, marine cementation is less important because pore-water movement is considerably slower (Tucker, 1991). If the climate is dominantly arid, then sea-water is subject to evaporation promoting precipitation of cements on the shallow sea-floor. The rate of carbonate production will also affect the degree of sea-floor sedimentation. Tucker (1991) states that where production rates are

low, marine cementation is more common.

Ancient marine calcite cements are dominantly of the fibrous type forming isopachous layers around detrital allochems, although Wilkinson *et al.* (1982b) and Wilkinson *et al.* (1985) provide evidence that for some of the geological past (e.g. the Jurassic) equant sparry calcite and syntaxial calcite overgrowths are common marine cements. All of these cements are closely associated with all the characteristic features of marine hard-grounds including truncation by endolithic borings and lithoclasts. The reason for this is that the composition of the marine carbonate cements has varied through geological time, with periods when aragonite and high-Mg calcite were dominant and periods when calcite with low-Mg content were dominant (e.g. the Jurassic and Cretaceous periods, Sandberg, 1983, 1985; Wilkinson *et al.*, 1985; Tucker & Wright, 1990 and Tucker, 1993). Sandberg (1983, 1985) states that the pattern of marine cement composition ties in with the first order sea-level curve (100-1000 million year fluctuations) with low-Mg calcite being dominant during global sea-level highstands. As the global position of sea-level is determined largely by plate tectonic processes, these trends have been related to periods of marine global tectonic activity (Wilkinson *et al.*, 1985). Similar trends have been observed in the occurrence of dolomite through-out geological time, with abundances coinciding with the periods of low-Mg calcite precipitation (first order sea-level highstands, Given & Wilkinson, 1987).

The meteoric diagenetic environment:

Within the meteoric realm of siliciclastic and carbonate successions, pore spaces are either entirely or partially filled with atmospheric gases resulting in oxidising conditions, or partially or totally filled with pore-water resulting in reducing conditions (refer back to sub-section 1.3.2a). In either situation, pressures and temperatures are similar to those at the Earth's surface. Any pore-water movement will occur in response to fluid potential gradients (Leeder, 1982). Tucker & Wright (1990) note the effect of a fall in sea-level on the development of meteoric lenses by discussing the Ghyben-Herzberg model (for a review of this model, see Tucker & Wright, 1990 page 338). Of importance to this review, Tucker & Wright state that small drops in sea-level can lead to the development of relatively large meteoric lenses

There are three important controls on the degree of meteoric diagenesis within carbonate sediments:- climate, amplitude and duration of sea-level fluctuations and original sediment mineralogy (Tucker, 1993). Under humid climatic conditions, the effects of meteoric diagenesis are more marked with grain leaching, karstification and extensive cementation by equant sparry calcite, all major processes. The magnitude of a relative sea-level fall controls the depth to which meteoric processes develop. The original sediment mineralogy controls the degree of leaching and cementation that can take place (Tucker, 1993).

The mixing zone diagenetic environment:

Mixing zone diagenesis occurs in the shallow subsurface where the marine and meteoric zones overlap. The geometry of the mixing zone varies along a shoreline and is dependant on the hydrostatic head, the petrophysical properties of the rock and relative sea-level or climatic fluctuations. Dolomite is a carbonate mineral often associated with this zone, primarily due to its distinct geochemical properties. Dissolution is an important process associated with this zone.

1.3.3: Early diagenesis and high resolution sequence stratigraphy

In the previous sub-sections, early diagenesis has been related to changes in relative sea-level, climate, sedimentation rate, organic content and many other factors. Basic principals of early diagenesis can now be related to the concepts and hierarchical classification of high resolution sequence stratigraphy that were discussed in Section 1.2. This section is a review of key papers by Sarg (1988), Hendry (1993a), Read & Horbury (1993), Tucker (1993) and Taylor *et al.* (1994).

1.3.3a: *The parasequence scale*

Within shallowing-up carbonate parasequences, Tucker (1993) suggests that the transgressive parts of a parasequence would be expected to show marine diagenetic textures, whereas the regressive part might show the effects of surface related diagenesis,

such as palaeokarstic surfaces (assuming a humid climate) or at least the effects of meteoric/mixing-zone diagenesis.

Carbonate parasequences that stack within a transgressive systems tract, would be expected to show more evidence of marine cementation, than those of a highstand systems tract that is capped by a type-1 sequence boundary. Similarly in the latter, meteoric cementation would be expected to be dominant (Tucker, 1993).

Read & Horbury (1993) make similar observations to those of Tucker (1993). In their model, they suggest that carbonate depositional environments that are a result of small, high frequency sea-level fluctuations are related to intracyclic diagenesis. Again, the importance of climate is stressed, with arid climates resulting in early dolomitisation and shallow leaching of parasequences (or parasequence tops). Under more humid conditions, Read & Horbury (1993) suggest that any dolomitisation will be negligible and parasequence tops may undergo some microkarstification, leaching and sparry calcite cementation associated with small fresh-water lenses.

Increasing the amplitude of the high frequency sea-level fluctuations can lead to intercyclic diagenesis, particularly in humid conditions (Read & Horbury, 1993). Cycles (or parasequences) can be capped by karstic disconformities and carbonate cements can extend down through several previous cycles (parasequences) because of repeated establishment of successive, relatively thick pore-water zones (Read & Horbury, 1993). Arid climates will result in small amounts of calcite cementation and relatively little leaching (Read & Horbury, 1993). Pedogenic and dissolution processes will occur during

a prolonged period of sub-aerial exposure, particularly under humid conditions (Tucker & Wright, 1990). Pedogenic processes may also modify the sediment and under suitable conditions result in the formation of calcretes (Tucker & Wright, 1990).

The importance of marine flooding surfaces (relating to parasequence boundaries) and their relationship to microbial diagenetic zones has been discussed by Taylor *et al.* (1994). Their model states that during periods of marine flooding (which result in an increase in the rate of accommodation development) sedimentation rates are very low and as a consequence, sediment has a longer residence time within early diagenetic (microbial) zones. Consequently, intensification of early diagenetic reactions allows the build-up of solutes within the sediment and the precipitation of early diagenetic cements in the form of concretions or laterally cemented beds. A lowering of sedimentation rates coincident with the marine flooding may be due to a cut-off in sediment supply rate.

1.3.3b: *The systems tract and sequence boundary scale*

The time scale of systems tract development is an order of magnitude greater than the parasequence scale (Table 1.ii). Consequently, early diagenesis will have a longer time to develop and will be more extensive.

During a lowstand systems tract, there is a basinward shift in the diagenetic environments in response to a fall in relative sea-level (Fig.1.xixa). In a humid climate, the exposed highstand sediments of the previous sequence will be subject to meteoric diagenesis with possible grain dissolution and calcite cementation. Karstic surfaces are also likely to form

in response to relative sea-level falls. In an arid climate, hypersaline waters are likely to develop in restricted lagoons or lakes. The descent of these fluids into the subsurface may lead to the precipitation of dolomite within earlier systems tracts.

During a transgressive systems tract, there is a landward shift in the diagenetic environments in response to a rise in relative sea-level (Fig.1.xixb). Carbonate sediments deposited during the transgressive systems tract will be subject to marine diagenetic processes on the sea-floor.

During a highstand systems tract the main diagenetic pattern may result in initial marine diagenesis being replaced by meteoric dissolution and cementation, supratidal diagenesis and evaporation (Fig.1.xixc). Alternatively a continuation of marine diagenetic processes could occur, depending on the climate and magnitude of relative sea-level fall (i.e. the formation of either a type-1 or type-2 sequence boundary). Sarg (1988) states that the basinward movement of the meteoric pore-water zone [or freshwater lens] is controlled by the rate and duration of any relative sea-level fall. Similarly, Read & Horbury (1993) suggest that large scale sea-level fluctuations (4^{th} order systems tract scale) are responsible for large, rapid vertical (and lateral) movements of diagenetic environments through many cycles. Thus diagenesis on this scale is markedly intercyclic.

Long term sea-level changes, associated with sequence boundary formation, may generate large scale regional aquifers if associated with a humid climate (Read & Horbury, 1993). Read & Horbury's model suggests that sediments in up-dip areas may be prone to leaching and are succeeded by cementation from dominantly oxidising meteoric pore-waters.

Again, time is an important consideration. Large falls in relative sea-level, will lead to prolonged sub-aerial exposure and a larger time scale for surface related diagenetic processes to occur. Consequently they will be extensive and well developed.

Finally, Hendry (1993a) illustrates the importance of identifying different scales of unconformity, and relating their genesis to particular patterns of cementation. In his model, unconformities associated with significant sea-level falls (e.g. type-1 sequence boundaries) provide prolonged exposure, an elevation head for deep penetration by surface meteoric waters, extensive karstification and cement production - all resulting in large scale regional cementation. However smaller scale unconformities that are a result of shallowing and progradation without any significant sea-level fall (i.e. parasequence boundaries) do not allow for hydraulic head development and thus no meteoric cementation occurs.

1.4: *Organisation of thesis*

The main body of the thesis is divided into four chapters. Chapters 2 and 3 are concerned with the Corallian Group succession, and describe and interpret the high resolution sequence stratigraphy and early diagenesis respectively. Chapters 4 and 5 relate to the studied Ericeira Group succession. Chapter 6 incorporates the observations and interpretation of the previous chapters and demonstrates how early diagenetic processes and products can be modelled for each of the sequence stratigraphic hierarchical units previously defined. Finally, Chapter 7 summarises the findings and key points of the

thesis and provides recommendations for further work.

The results of petrographic analyses for all samples are summarised in Appendix 1, while Appendices 2, 3 and 4 outline the procedure and detailed results of the XRD, CL and stable isotope analysis. Figures and Tables relating to the text are to found at the end of each chapter.

Figure 1.xx provides a key to all symbols and ornaments used in other Figures (unless otherwise stated).

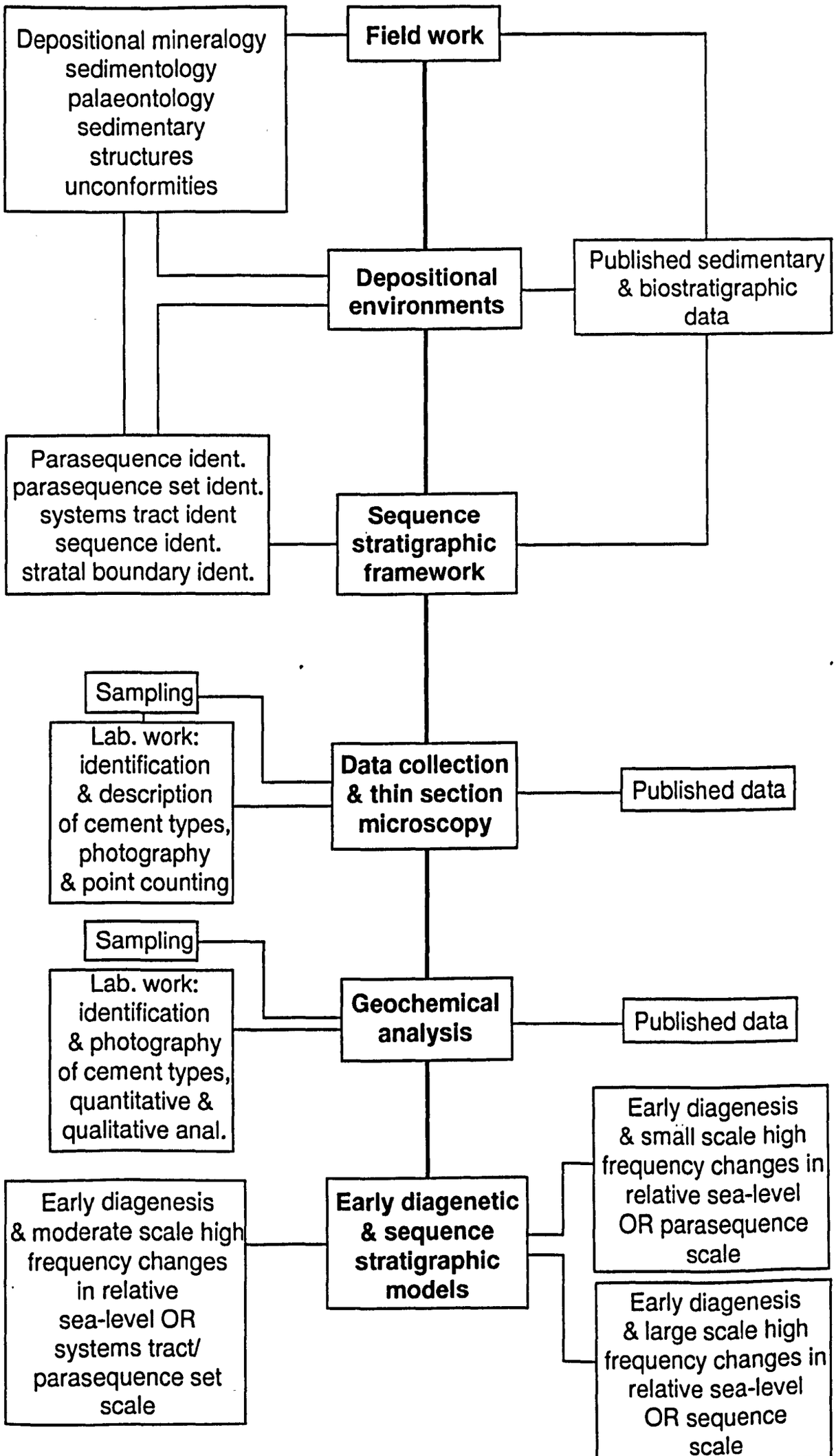

Fig.1.i: Methodology & procedure of thesis

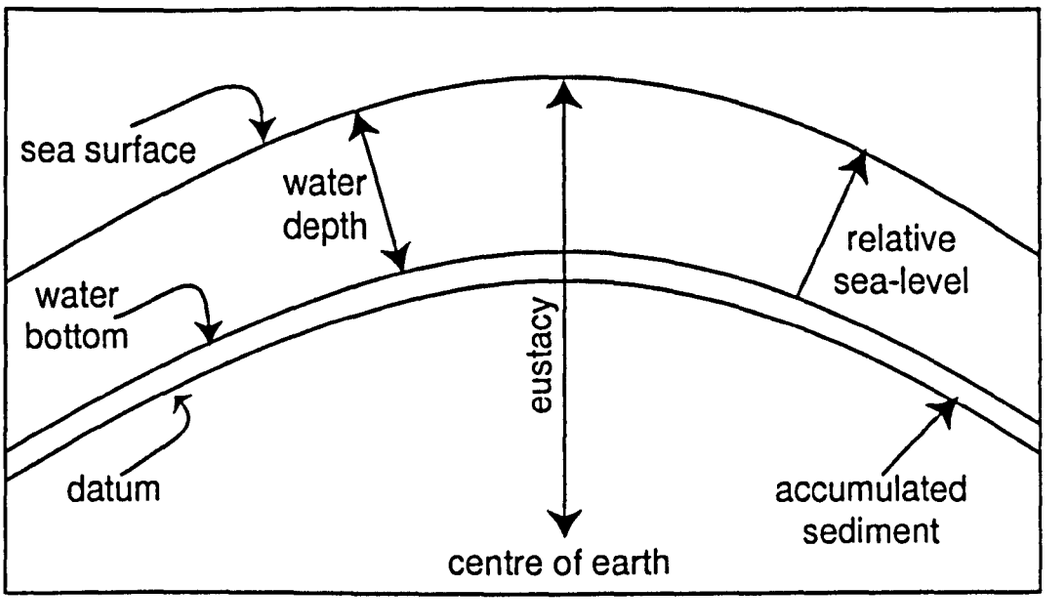

Fig. 1.ii: Eustacy, relative sea-level and water depth as a function of sea surface, water bottom and datum position (after Posamentier *et al.*, 1988)

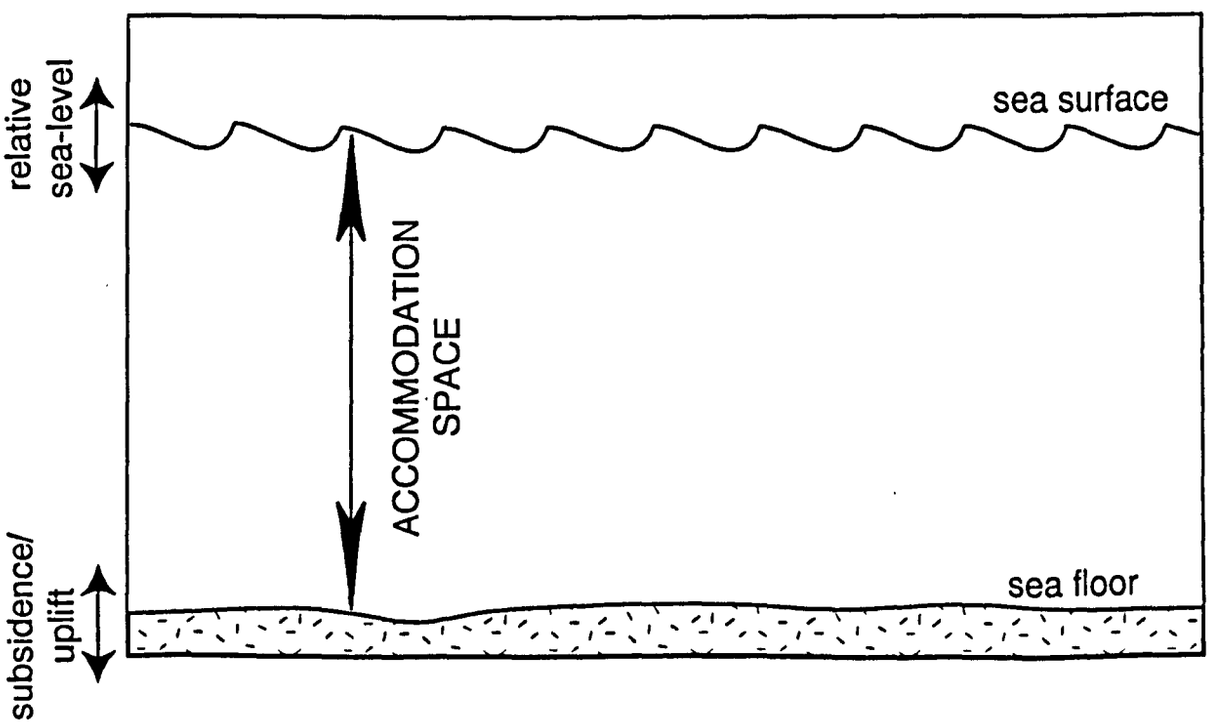

Fig.1.iii: Accommodation space as a function of relative sea-level and subsidence (modified from Posamentier *et al.*, 1988)

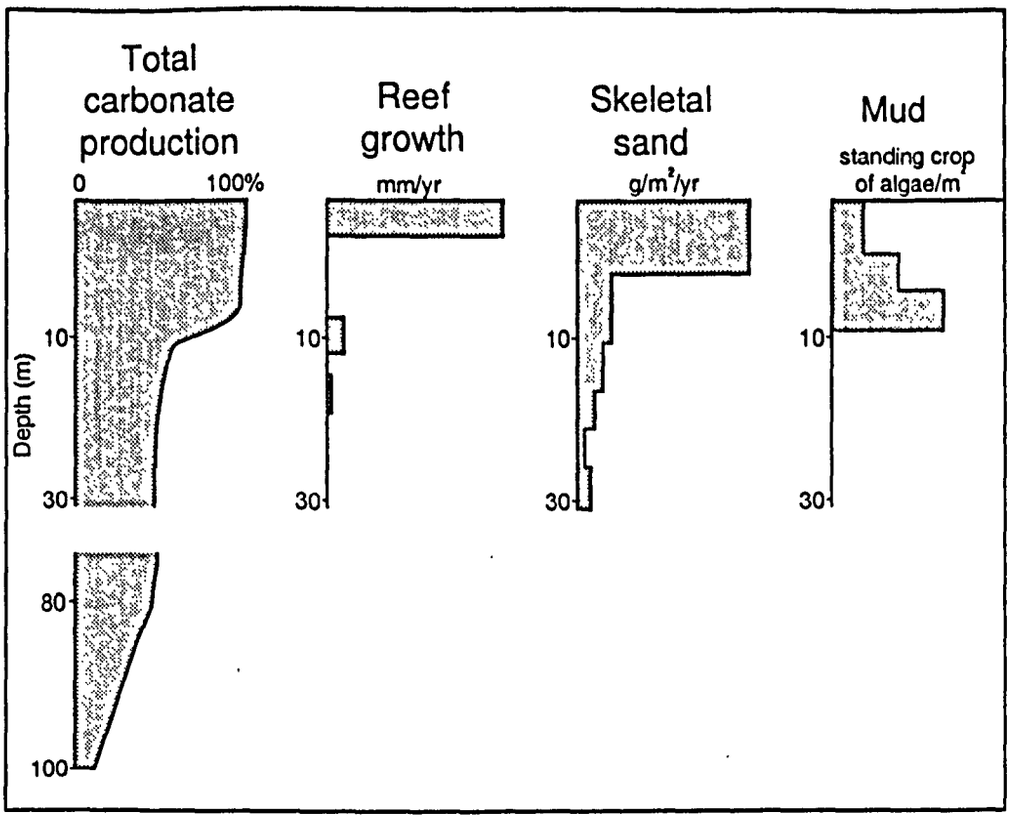

Fig.1.iv: Carbonate production versus water depth, demonstrating high-carbonate productivity in shallow water and an abrupt, dramatic fall-off at a water depth of about 10m (modified from Schlager, 1981)

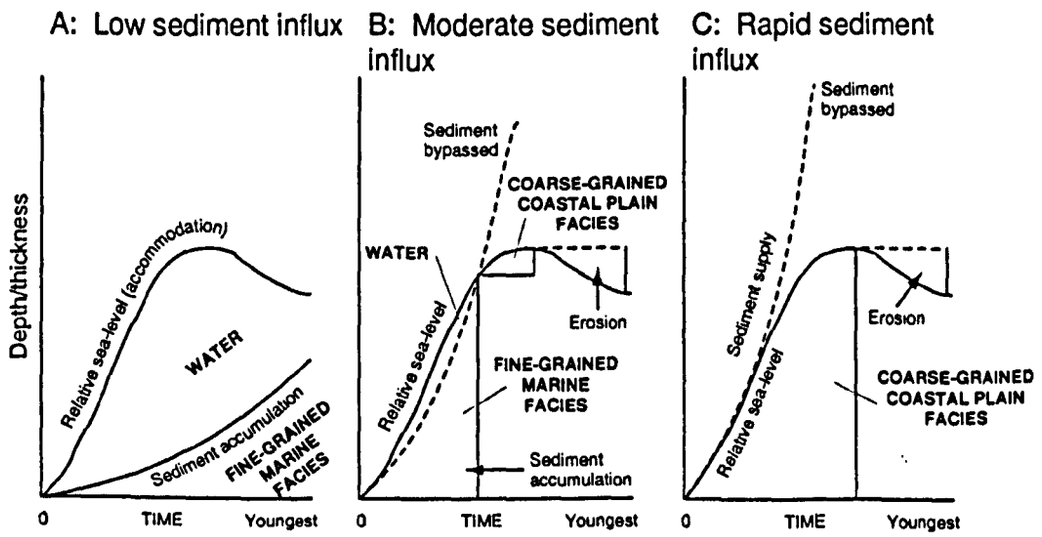

Fig.1.v: Water depth and facies relationships with varying sediment supply rates (from Jervey, 1988; Emery & Myers, 1996)

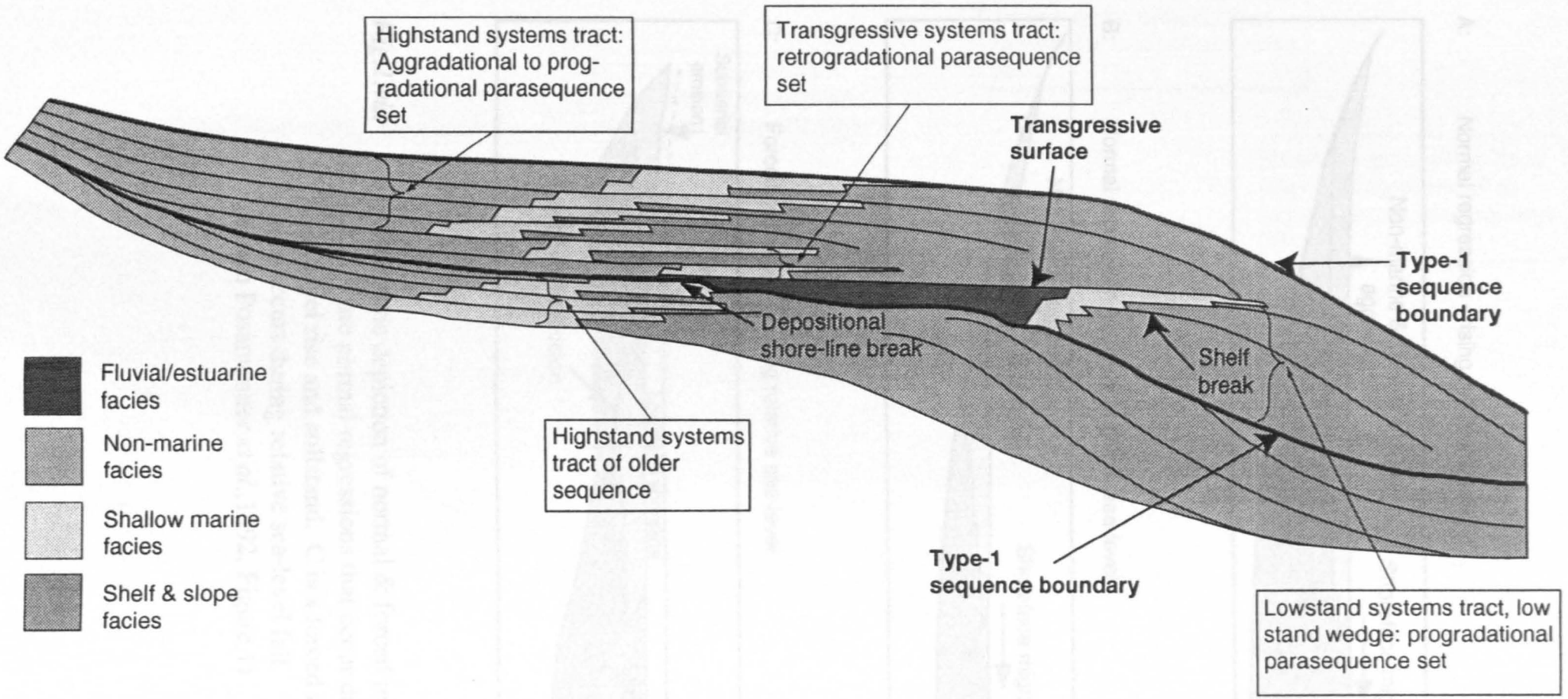

Fig.1.vi: Stratal patterns in a Type-1 sequence (from Van Wagoner *et al.*, 1990, Figure 19)

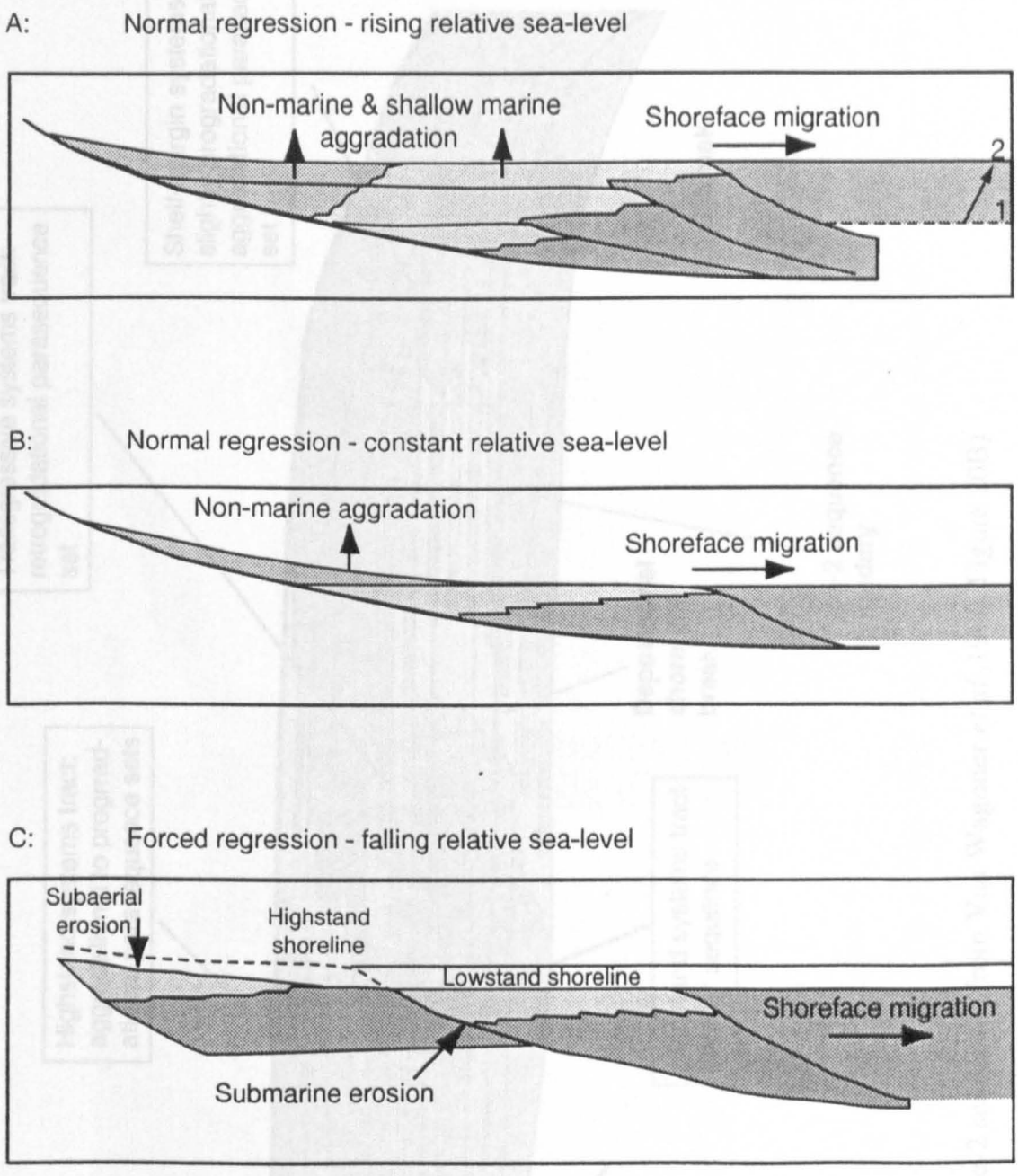

Fig.1.vii: Schematic depiction of normal & forced regressions A & B are normal regressions that occur during rel. sea-level rise and stillstand. C is a forced regression that occurs during relative sea-level fall (from Posamentier *et al.*,1992, Figure 1)

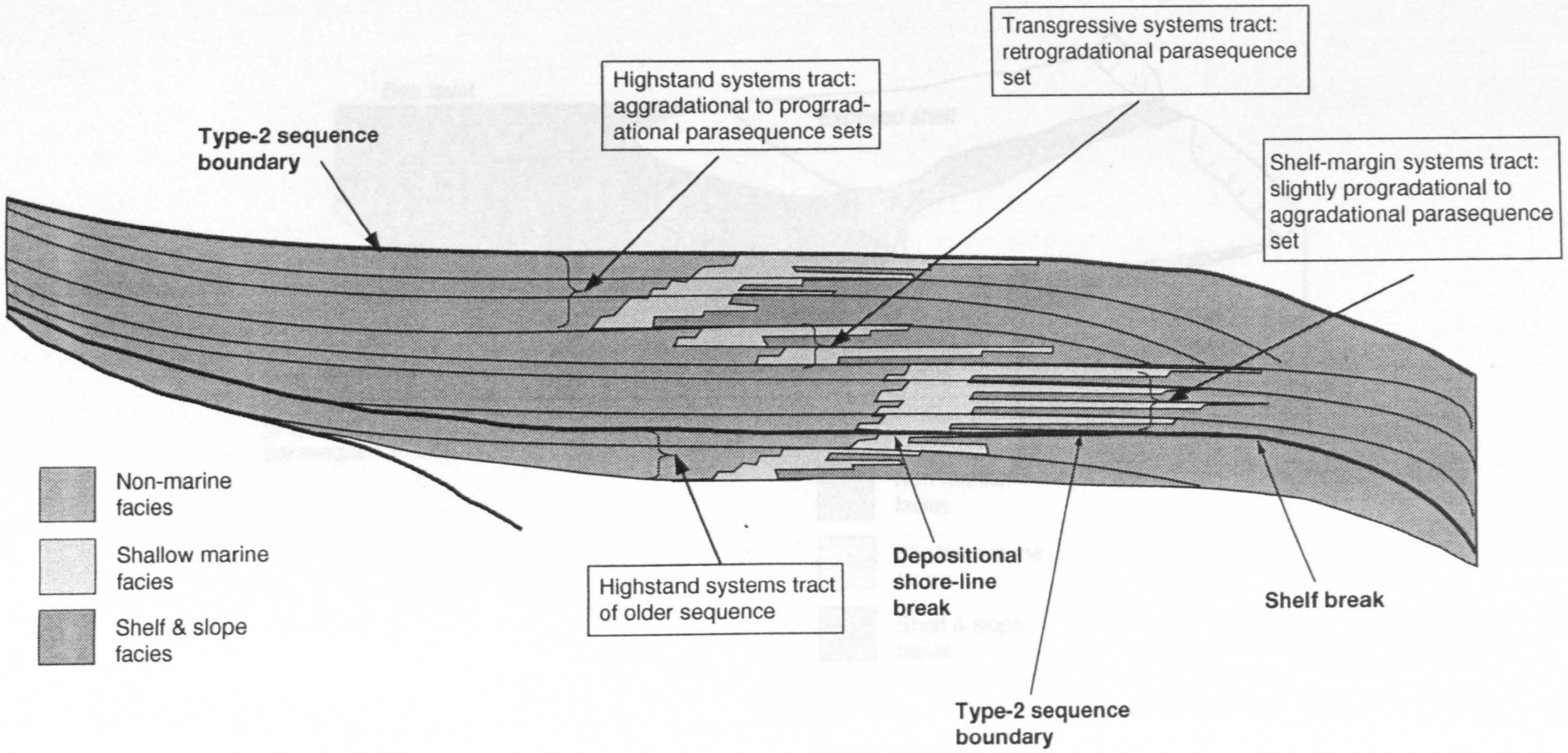

Fig.1.viii: Stratal patterns in a Type-2 sequence (from Van Wagoner *et al.*,1990, Figure 20B)

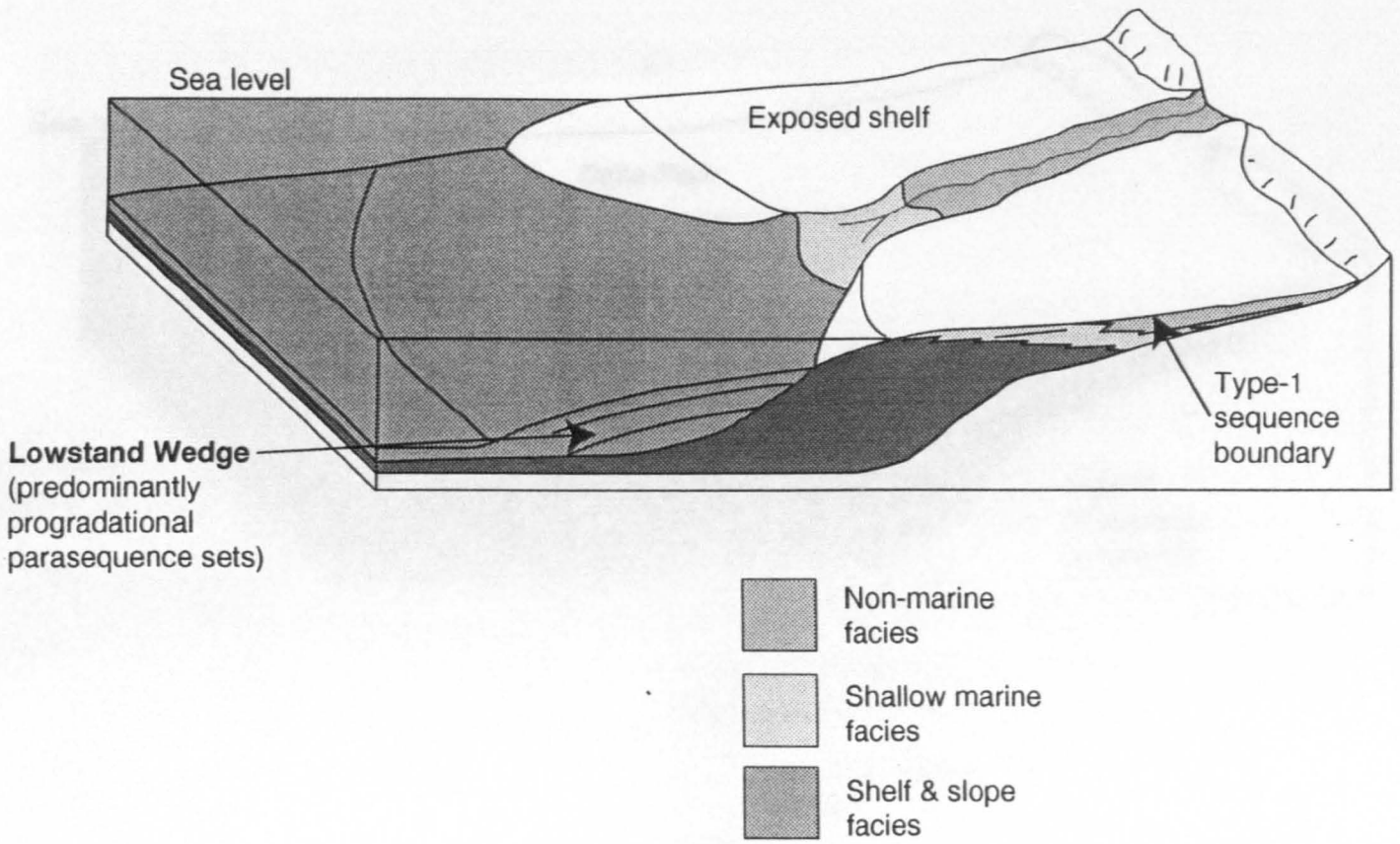

Fig.1.ix: Lowstand systems tract: lowstand wedge (from Posamentier & Vail, 1988 Figure 3)

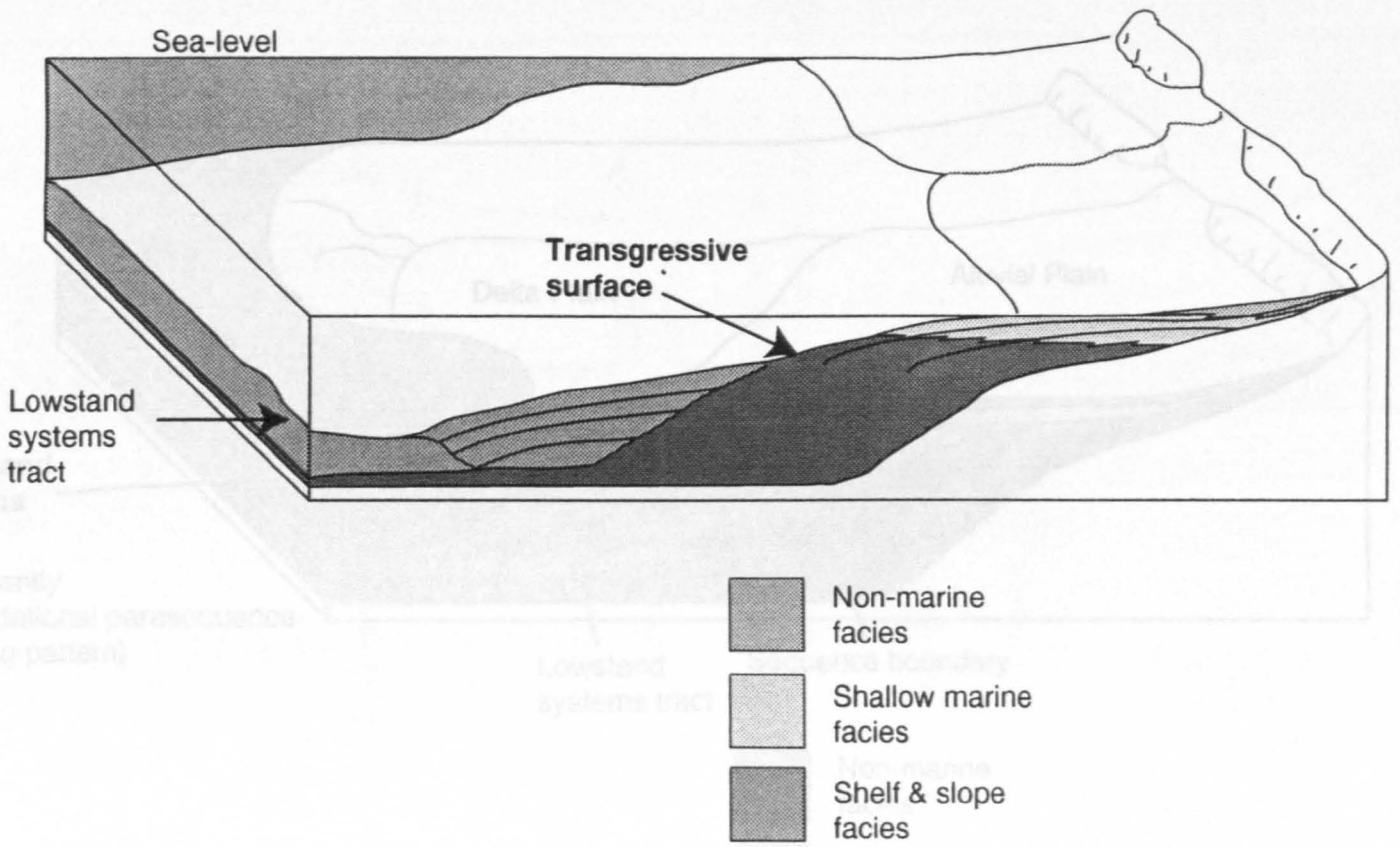

Fig.1.xi: Transgressive systems tract (from Posamentier & Vail, 1988 Figure 6)

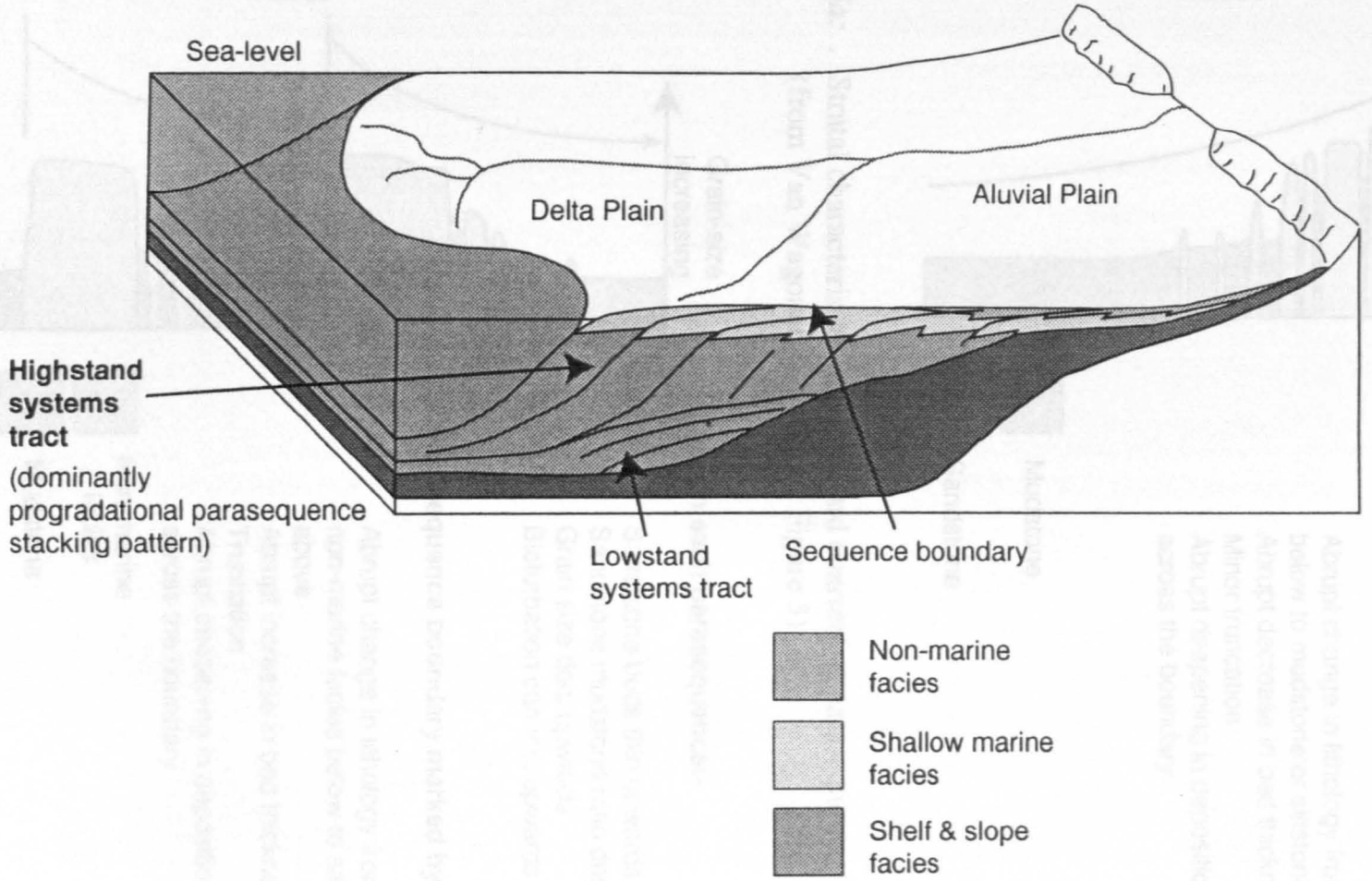

Fig.1.xii: Highstand systems tract (from Posamentier & Vail, 1988 Figure 5)

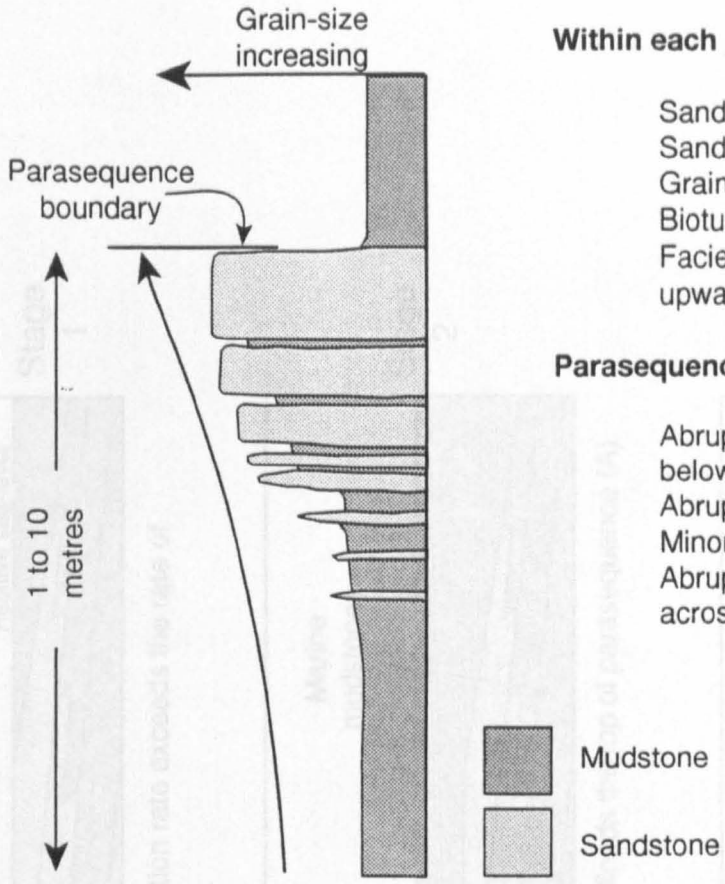

Within each parasequence:-

Sandstone beds thicken upwards
Sandstone mudstone ratio inc. upwards
Grain size inc. upwards
Bioturbation can inc. upwards
Facies within each parasequence shoal upwards

Parasequence boundary marked by:-

Abrupt change in lithology from sandstone below to mudstone or siltstone above
Abrupt decrease in bed thickness
Minor truncation
Abrupt deepening in depositional env. across the boundary

Fig.1 xiiia: . Stratal characteristics of an upward coarsening parasequence (from Van Wagoner *et al.*, 1990, Figure 3)

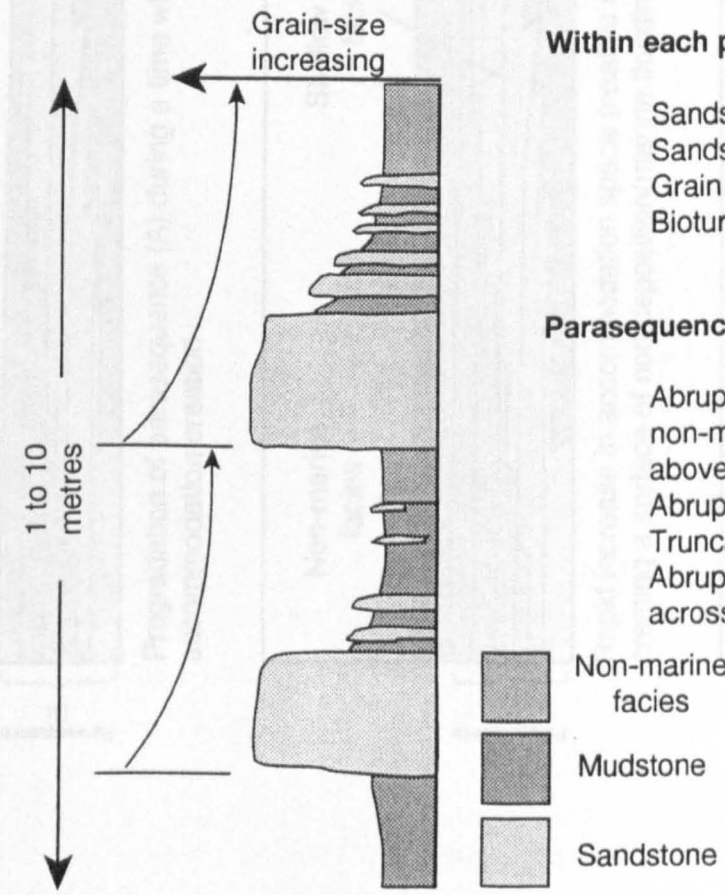

Within each parasequence:-

Sandstone beds thin upwards
Sandstone mudstone ratio dec. upwards
Grain size dec. upwards
Bioturbation can inc. upwards

Parasequence boundary marked by:-

Abrupt change in lithology from mudstone/ non-marine facies below to sandstone above
Abrupt increase in bed thickness
Truncation
Abrupt deepening in depositional env. across the boundary

Fig.1 xiiib: Stratal characteristics of an upward fining parasequence (from Van Wagoner *et al.*, 1990, Figure 3)

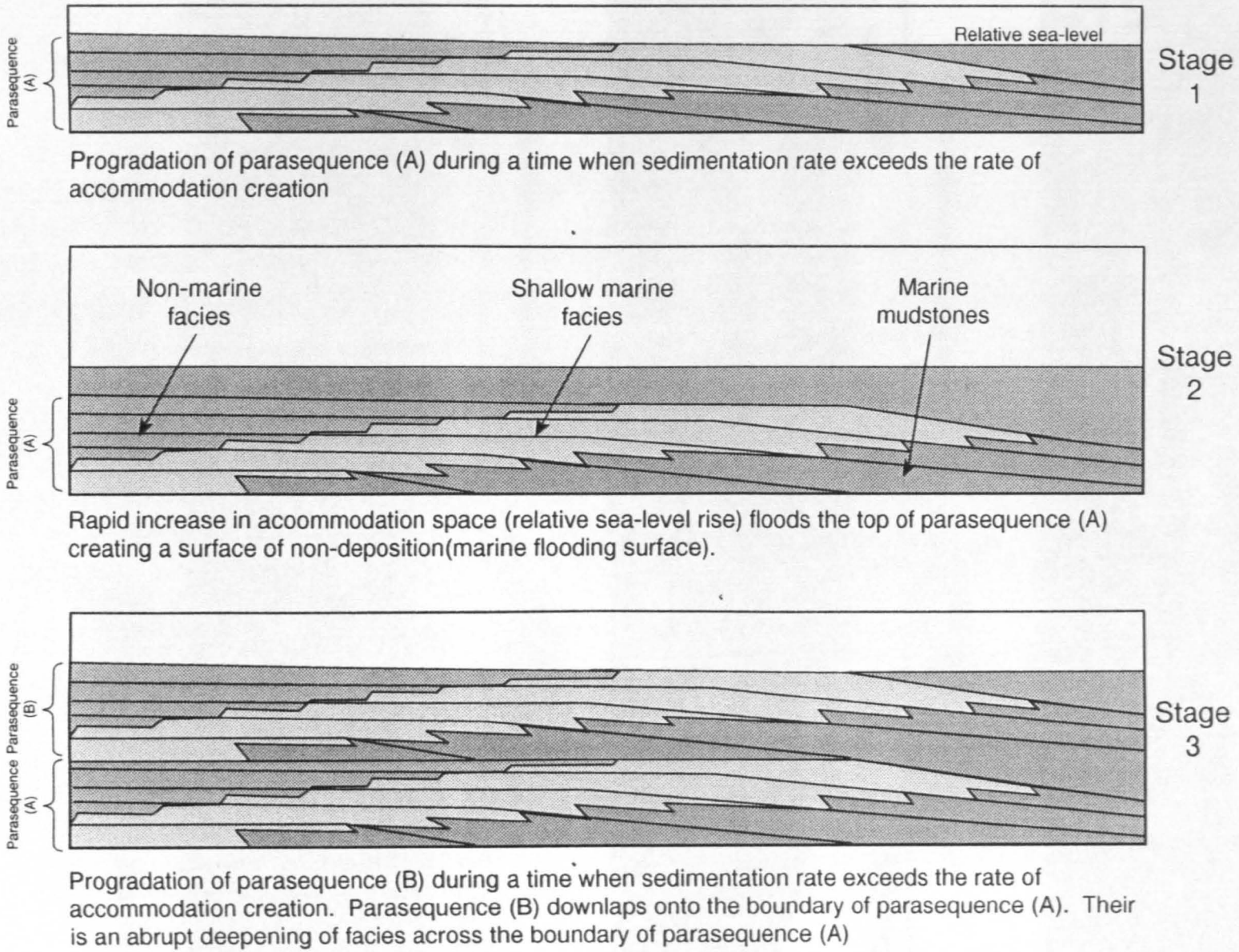

Fig.1.xiv: Development of a parasequence boundary (coarsening-up parasequence) (from Van Wagoner *et al.*,1990 Figure 4)

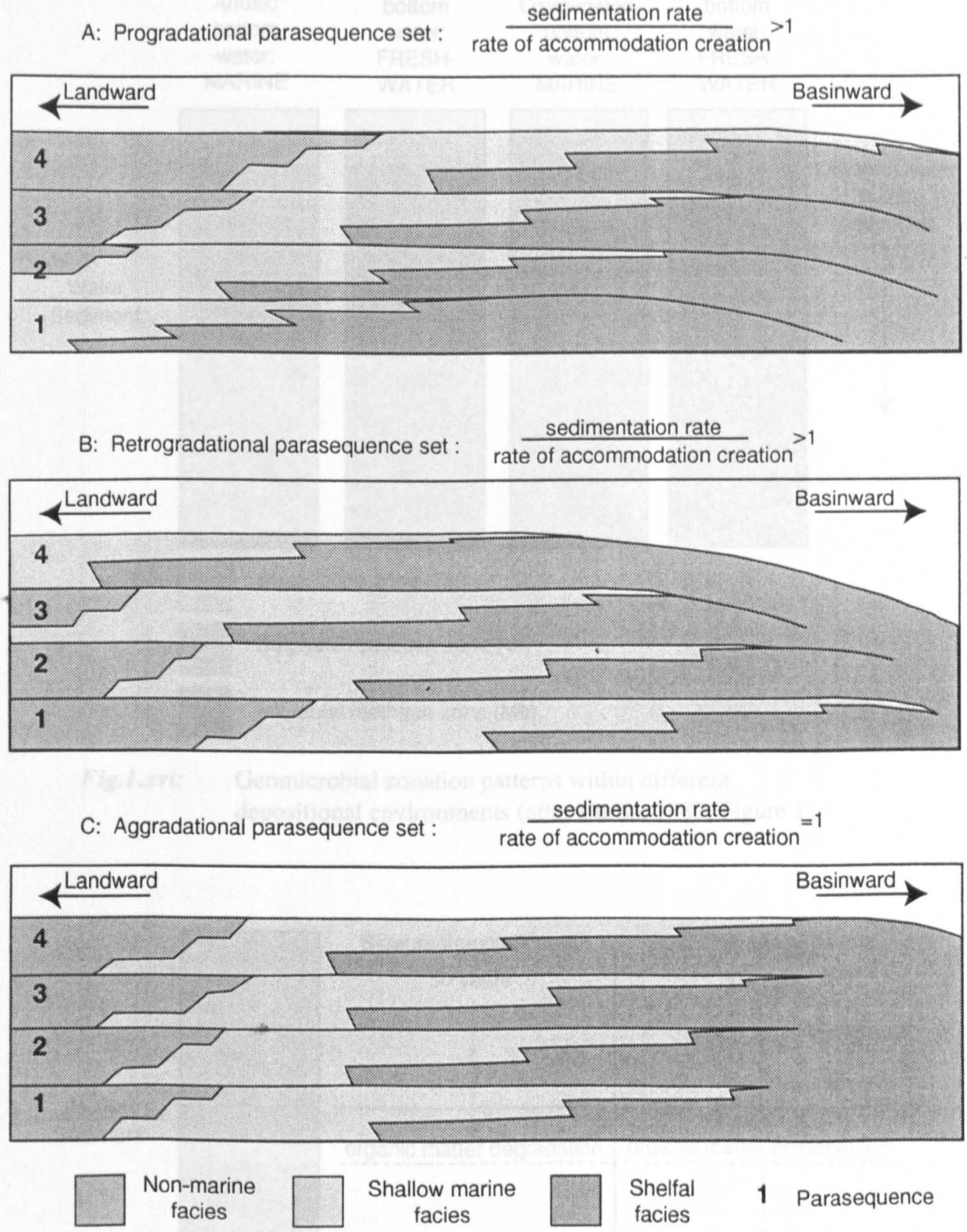

Fig.1.xv: Parasequence stacking patterns in parasequence sets, cross-section expression (from Van Wagoner *et al.*, 1990, Figure 10).

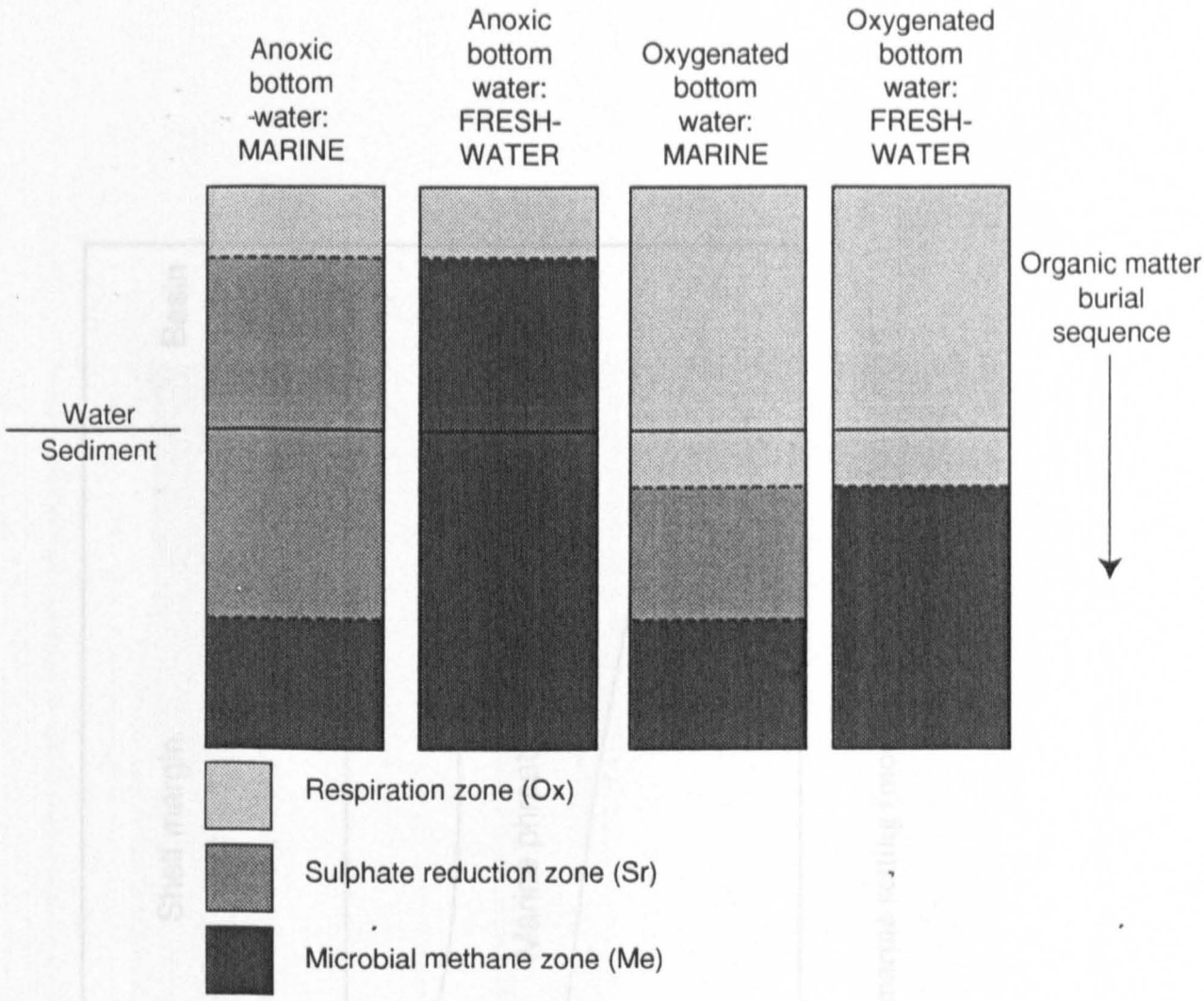

Fig.1.xvi: Geomicrobial zonation patterns within different depositional environments (after Curtis, 1987, Figure 1)

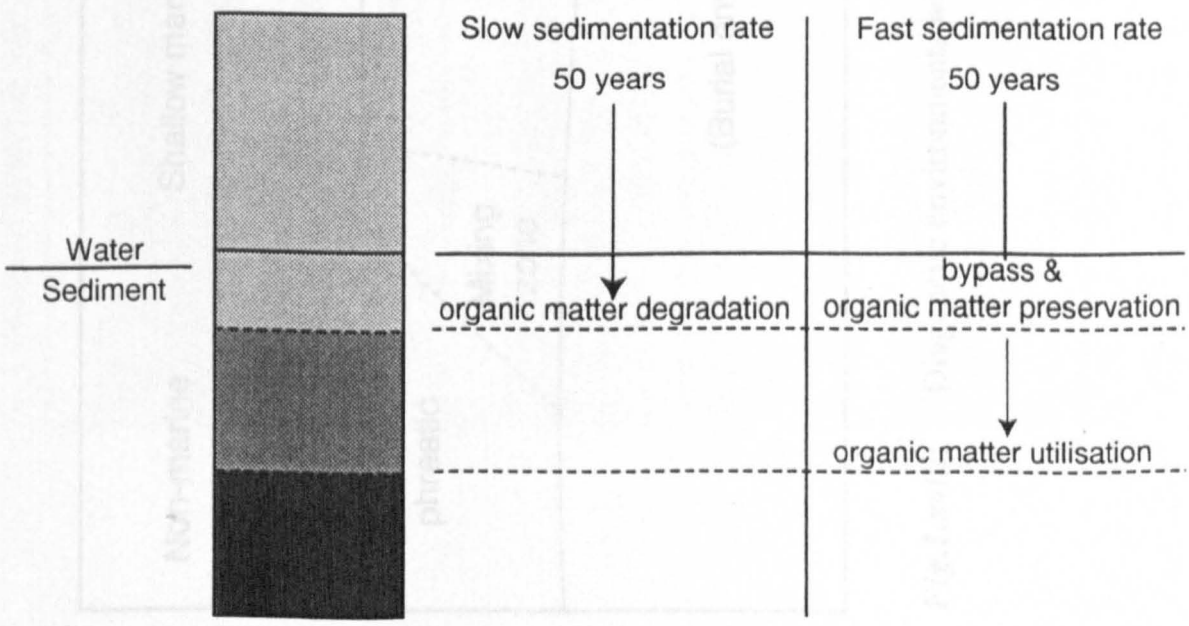

Fig.1.xvii: The influence of sedimentation rate on organic matter preservation. Rapid sedimentation carries material to zones of lower microbial activity, thus bypassing the Ox zone (after Curtis, 1987, Figure 3).

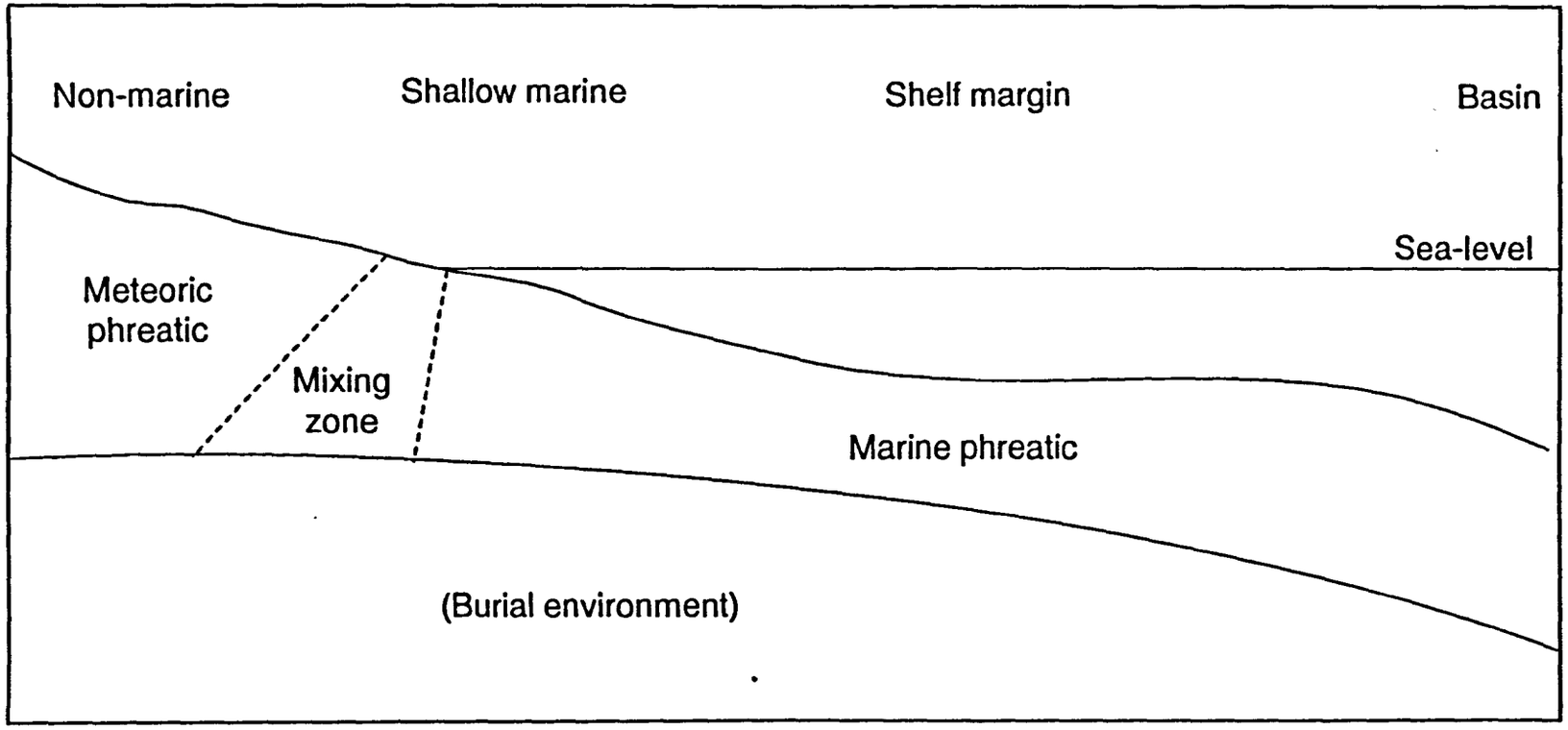

Fig.1.xviii: Diagenetic environments within a marginal marine setting (modified from Tucker, 1991, 1993)

A) Lowstand systems tract (LST)

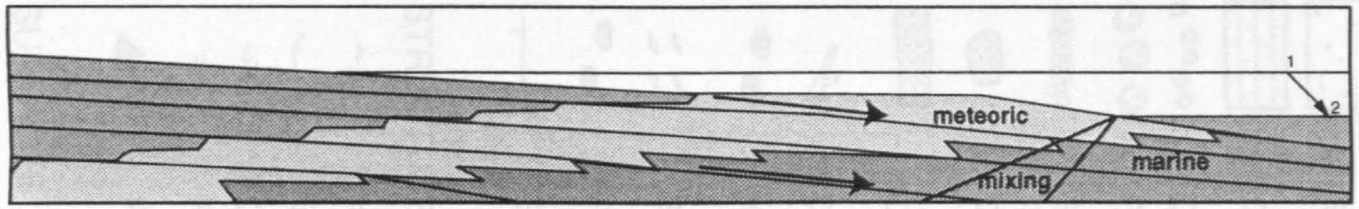

Marine diagenesis of LST sediments. Basinward movement of porewater zones during LST. Meteoric diagenesis of earlier TST and HST sediments

B) Transgressive systems tract (TST)

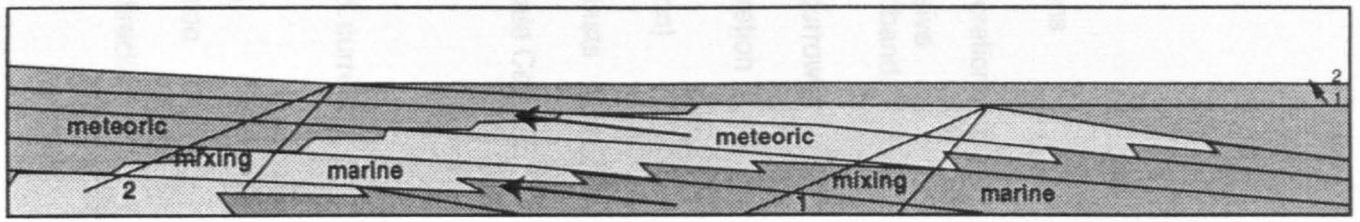

Landward movement of porewater zones (1 to 2) in response to relative sea-level rise (1 to 2). Marine diagenesis of TST sediments

C) Highstand systems tract (HST)

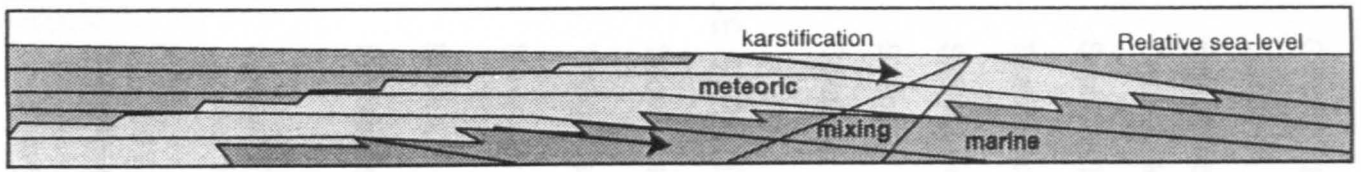

Basinward movement of porewater zones. Early marine then meteoric diagenesis of HST sediments, possible meteoric leaching and karstification.

Fig.1.xix: Models to show the movement of pore-water zones during the formation of LST, TST and HST (from Tucker, 1993 Figure 4.8)

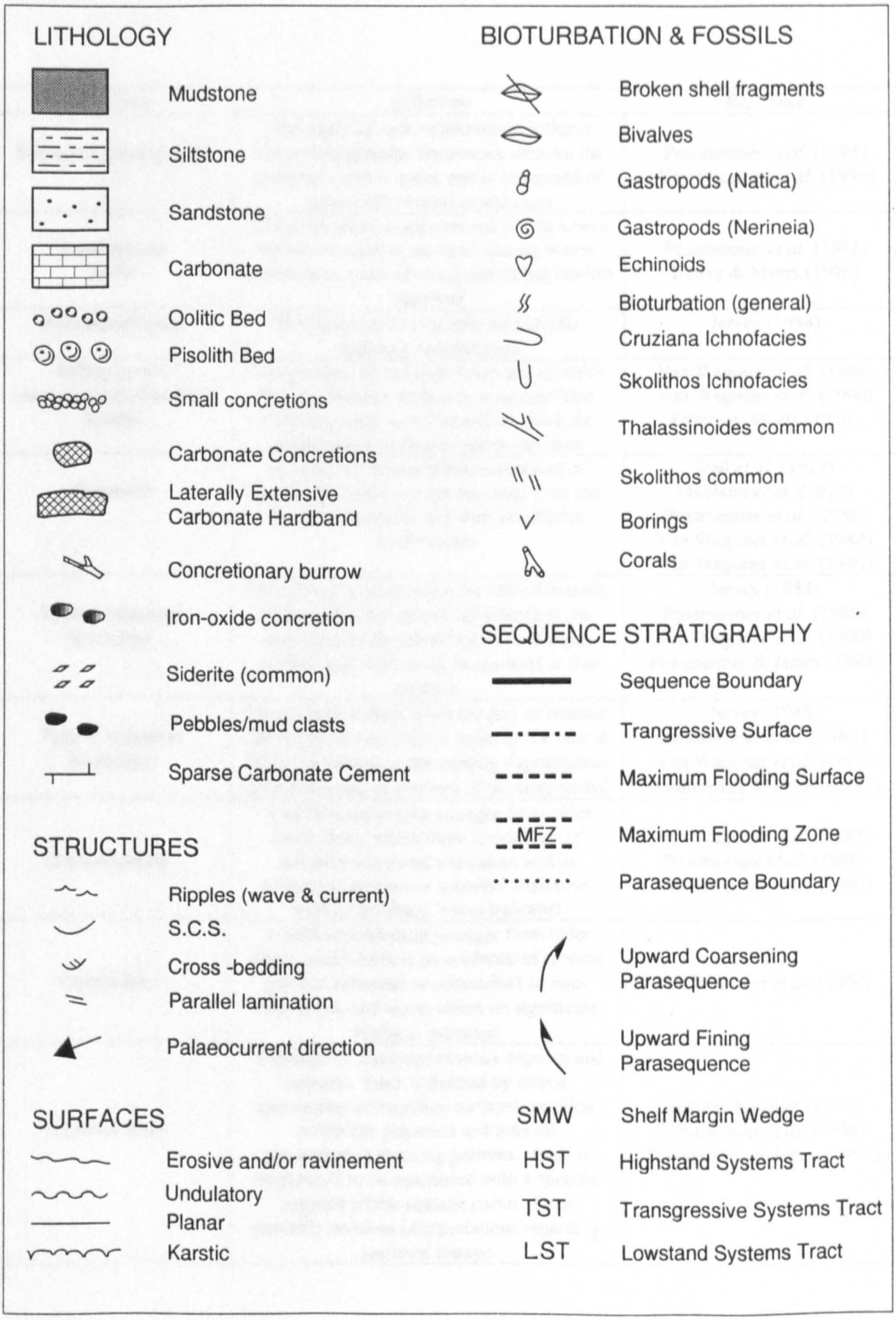

Fig.1.xx: Key to all Figures (unless otherwise stated)

Table 1.i: Glossary of key Sequence Stratigraphic terms & definitions

Key Term	*Definition*	*Reference*
Sequence Stratigraphy	The study of rock relationships within a chronostratigraphic framework wherein the study of rocks is cyclic and is composed of genetically related stratal units	Posamentier *et al.* (1988) Van Wagoner *et al.* (1990)
Equilibrium point	The point along a depositional profile where the rate of relative sea-level change is zero. It separates zones of rising and falling relative sea-level	Posamentier *et al.* (1988) Emery & Myers (1996)
Accommodation	The space made available for potential sediment accumulation	Jervey (1988)
Offlap break (depositional-shoreline break)	The position on the shelf landward of which the depositional surface is at or near base level/sea-level, and seaward of which the depositional surface is below sea-level	Van Wagoner *et al.* (1988) Van Wagoner *et al.* (1990) Emery & Myers (1996)
Sequence	A relatively conformable succession of genetically related strata bounded at its top by unconformities and their correlative conformities.	Vail *et al.* (1977) Mitchum *et al.* (1977) Posamentier *et al.* (1988) Van Wagoner *et al.* (1988) Van Wagoner *et al.* (1990)
Type-1 sequence boundary	Interpreted to form when the rate of eustatic fall exceeds the rate of subsidence at the depositional-shoreline break (shelf edge) producing a relative fall in sea-level at that position	Jervey (1988) Posamentier *et al.* (1988) Van Wagoner *et al.* (1990) Posamentier & James (1993)
Type-2 sequence boundary	Interpreted to form when the rate of eustatic fall is slightly less than or equal to the rate of basin subsidence at the existing depositional-shoreline break at the time of the eustatic fall	Jervey (1988) Posamentier *et al.* (1988) Van Wagoner *et al.* (1990) Posamentier & James (1993)
Unconformity	A surface separating younger from older strata along which there is evidence of subaerial-erosional truncation and/or submarine erosion or subaerial exposure, with a significant hiatus indicated	Van Wagoner *et al.* (1988) Posamentier *et al.* (1988) Van Wagoner *et al.* (1990)
Conformity	A surface separating younger from older strata which there is no evidence of erosion (neither subaerial or submarine) or non-deposition, and along which no significant hiatus is indicated	Van Wagoner *et al.* (1990)
Systems tract	A linkage of contemporaneous depositional systems. Each is defined by stratal geometries at bounding surfaces, position within the sequence and internal parasequence stacking patterns. Each is interpreted to be associated with a specific segment of the eustatic curve. Each explicitly involves interpretations regarding sea-level change	Brown & Fisher (1977) Posamentier *et al.* (1988) Posamentier & James (1993)

Table 1.i (cont.):

Key term	*Definition*	*Reference*
Condensed section	A stratigraphic interval consisting of thin hemipelagic or pelagic sediments, starved of terrigenous material, deposited on the middle to outer shelf, slope, and basin floor during a period of maximum relative sea-level rise and maximum transgression of the shoreline	Loutit *et al.*(1988)
Parasequence	A relatively conformable succession of genetically related beds or bedsets bounded by marine-flooding surfaces and their correlative surfaces	Van Wagoner (1985) Van Wagoner *et al.* (1988) Van Wagoner *et al.* (1990)
Parasequence set	A succession of genetically related parasequences that form a distinctive stacking pattern, bounded, in many cases, by major marine flooding surfaces and their correlative surfaces	Van Wagoner (1985) Van Wagoner *et al.* (1988)
Progradational Parasequence set	Successively younger parasequences are deposited farther basinward. Rate of deposition > rate of accommodation creation	Van Wagoner *et al.* (1990)
Retrogradational Parasequence set	Successively younger parasequences are deposited farther landward, in a backstepping pattern. Rate of deposition < rate of accommodation creation	Van Wagoner *et al.* (1990)
Aggradational Parasequence set	Successively younger parasequences are deposited above one another with no significant lateral shifts. Rate of deposition = rate of accommodation creation	Van Wagoner *et al.* (1990)
Transgressive lag	A sedimentary deposit, commonly less than 0.6m thick, of relatively coarse-grained material composed of shells, shell fragments, clay rip-up clasts, nodules and gravels	Van Wagoner *et al.* (1990)
Ravinement Surface	A surface of transgressive erosion formed by shoreface retreat during sea-level rise	Stamp (1921) Swift (1968) Emery & Myers (1996)

STRATAL UNIT	DEFINITION	RANGE OF THICKNESS (M)	RANGE OF LATERAL EXTENT (SQ. KM)	RANGE OF TIMES OF FORMATION (YEARS)	ORDER
		1000 100 10 1 0.1	10^3 1000 100 10 1	10^6 10^5 10^4 10^3 10^2	
Sequence	A relatively conformable succession of genetically related strata, bounded by unconformities and their correlative conformities				Third
Parasequence set	A succession of genetically related parasequences forming a distinctive stacking pattern and commonly bounded by major marine flooding surfaces and their correlative surfaces				Fourth
Parasequence	A relatively conformable succession of genetically related beds or bedsets bounded by marine flooding surfaces and their correlative surfaces				Fifth

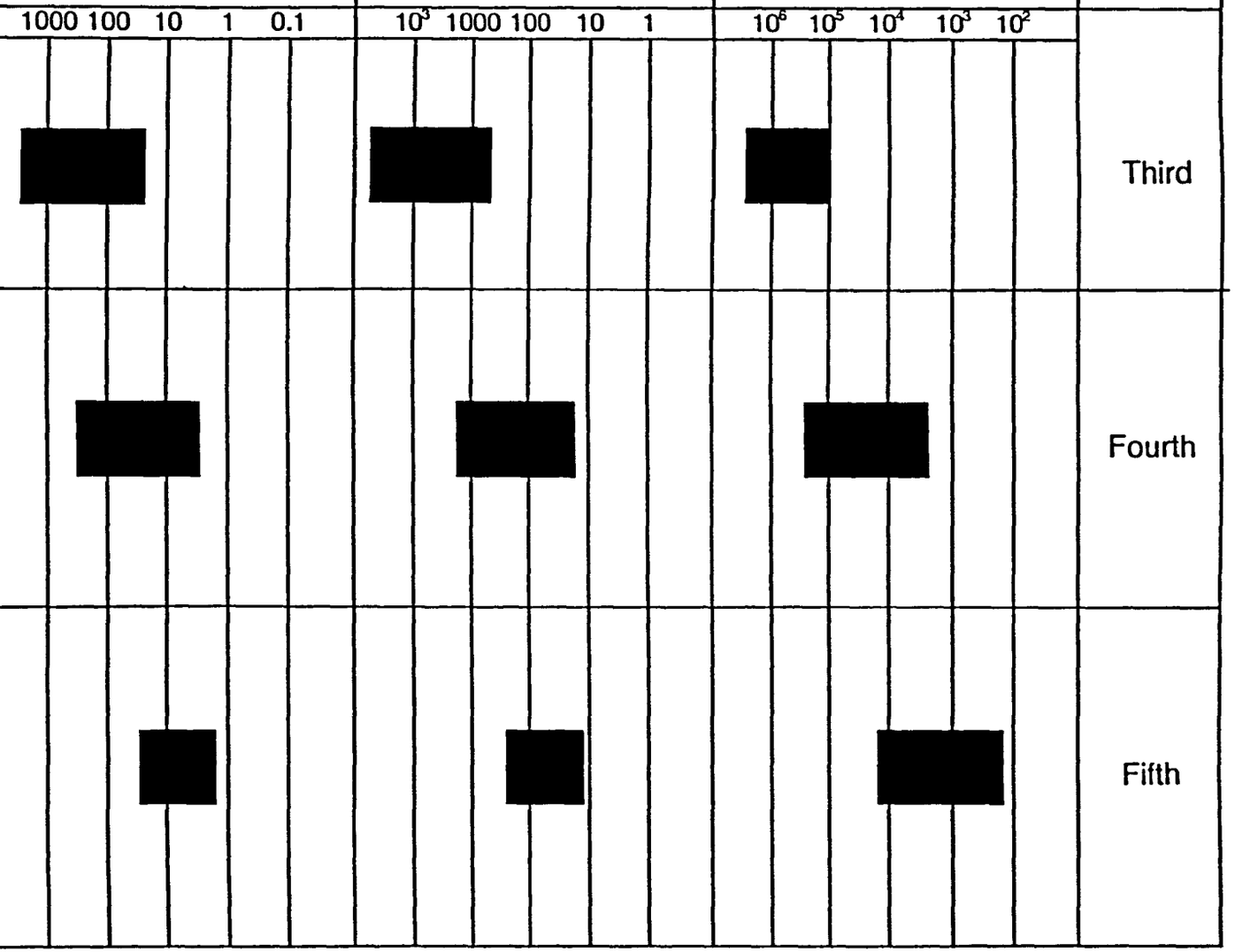

Table I.ii: Stratal units in hierarchy - definitions and characteristics (from Van Wagoner *et al.*, 1990)

2: A High Resolution Sequence Stratigraphic Model For The Corallian Group Of South Dorset

2.1: *Introduction*

2.1.1: Aims & organisation

2.1.1a: *Aims*

The overall aim of this research is to evaluate how specific diagenetic products can be related to sea-level change. A fundamental objective of this study therefore involves identification of successions and stratal surfaces, which indicate sea-level changes to as high a resolution as possible. Recent studies (e.g. Van Wagoner *et al.* 1990) have identified that the highest resolution units associated with sea level change are parasequences, high order sequences and associated stratal surfaces. The Corallian Group succession was chosen because it has been extensively studied and dated, including several recent sequence stratigraphic interpretations (e.g. Rioult *et al.*, 1991; Wilson, 1991; Coe, 1995). However none of these studies has attempted to identify parasequences or other high resolution sequence stratigraphic features. To satisfy the aims of the research, it was necessary to therefore re-interpret the succession at a high resolution. This approach has confirmed many of the observations made by previous workers, modified some and enabled a higher degree of resolution to which diagenetic features can be evaluated.

2.1.1b: *Organisation*

The chapter is divided into three main sections. In Section 2.2 the sedimentology and depositional environment of each lithostratigraphic unit are described and interpreted. This is necessary because Van Wagoner *et al.* (1990) state that any sequence stratigraphic interpretation must be based on a correct identification of facies. In Section 2.3, I the Corallian Group is divided into six sequences. Within each sequence, parasequences are identified where possible. Parasequence identification, together with the palaeoenvironmental interpretations from Section 2.2, are then used to identify systems tracts and 3rd and 4th order stratal surfaces. At some stratal surfaces a lack of unequivocal sedimentological data means that a number of interpretations are possible and these are discussed in turn. Regional data are also utilised, where available. Following each sequence description a comparison with previous interpretations is presented. In the final section (Section 2.4) the overall significance of the succession is discussed along with an indication where early diagenetic work may help to resolve the identification of certain key stratal surfaces and sequence stratigraphic units.

2.1.2: Regional geology of the Wessex Basin (Permian to Jurassic)

The Wessex Basin forms part of an extensive intracratonic basin that extends from southern central England to northern France. It evolved as the result of a phase of Permo-Triassic rifting which affected much of NW Europe (Stoneley, 1982; Chadwick, 1986; Stoneley & Selley, 1991).

During the Jurassic, the Wessex Basin lay at a latitude of approximately 35°N, one of the climatic implication being the deposition of a mixture of siliciclastics and carbonates and faunas intermediate between the Boreal and Tethyan realms (Callomon & Cope, 1995; Cope, 1995).

2.1.2a: *Tectonics*

The Wessex Basin was initiated in the Permian during a period of north-south extension which re-activated pre-existing east-west aligned Hercynian thrust faults (Chadwick, 1986). Fault bounded sub-basins developed within the Triassic in response to the early stages of Atlantic opening (Callomon & Cope, 1995). North-south extension continued throughout the Jurassic (Selley & Stoneley, 1987). During this period, syn-sedimentary growth faulting was also an important feature (Callomon & Cope, 1995). Rapid subsidence within the basin was controlled by wrench fault systems that were associated with crustal extension in the North Sea and Celtic Sea areas (Stoneley, 1982; Ziegler, 1990). By the time of the Oxfordian, regional flexural subsidence had become established, while syn-depositional faulting was rare (Sun, 1989).

2.1.2b: *Depositional history*

The Wessex Basin evolved in four distinct phases; the Permo-Triassic, the Jurassic to early Cretaceous, the late Cretaceous and the Tertiary to Recent (Stoneley & Selley, 1991). The first two of these phases are now described.

A period of continental desert sedimentation dominated Permo-Triassic times (Stoneley & Selley, 1991). Locally (particularly in the west of the basin) fan breccias, braided stream deposits and sheet flood conglomerates have been identified (Stoneley & Selley, 1991). Throughout the Late Permian and Triassic, deposition became more widespread across the basin and was dominated by playa lake mudstones interbedded with fluvial and aeolian sands (Stoneley & Selley, 1991).

Towards the end of the Triassic, a shallow intracratonic sea was gradually established across southern England. During the Early Jurassic this sea was periodically stagnant allowing dysaerobic bottom water conditions to develop. This led to the deposition of the Lower Lias (interbedded lime mudstones and shales) which are the major petroleum source rock for the basin. Succeeding this, sedimentation patterns within the Jurassic became cyclic, with individual cycles broadly consisting of a tripartite lithological sequence of clays, sands and limestones (Arkell, 1933, 1936; Stoneley & Selley, 1991; Callomon & Cope, 1995). It is one such cyclic succession which is the focus of this thesis.

The close of the Jurassic saw the gradual emergence of the entire region, with the development of the sabkhas and the brackish and fresh-water deposits of the Purbeck Group (Stoneley & Selley, 1991). Finally, the Cretaceous was dominated by marine chalk sedimentation and further tectonic activity which controlled subsequent deposition (Stoneley & Selley, 1991).

2.1.3: Summary of previous Corallian Group work

For the last sixty years, the coastal exposures of the Corallian Group around Osmington Mills in south Dorset (Fig.2.i) have been the focus of considerable sedimentological, stratigraphical, palaeontological and sequence stratigraphic study (Arkell, 1933, 1936, 1947a; Whatley, 1965; Wilson, 1968a, 1968b, 1975, 1991; Talbot, 1973, 1974; Fürsich, 1973, 1975; Brookfield, 1978; Wright, 1986a; Sun, 1989; Rioult *et al.*, 1991; Coe, 1992, 1995).

Arkell (1933, 1936) first recognised the cyclicity that is present within the Corallian Group. He identifies three shallowing-up cycles each beginning with a relatively deep water clay, overlain by a sandstone and capped by a shallow water carbonate deposit (Fig.2.ii). Thus, each of Arkell's cycles began with an abrupt deepening, but is subsequently related to a shallowing of sea-level.

Wilson (1968a, 1968b) re-interprets Arkell's three shallowing-up cycles, suggesting that each is controlled by the rate of siliciclastic sedimentation (Fig.2.ii). In his model, Wilson states that although each cycle begins with a "positive eustatic change", the subsequent deposition of sands and carbonates are linked to "events in the source area and not to sea-level changes".

In contrast, Talbot (1973) suggests that the Corallian Group consists of four eustatically controlled asymmetric shallowing-up cycles (Fig.2.ii). In this model, each cycle is characterised by the succession of limestone to clay to sand and is capped by an erosion

surface. The erosion surfaces mark a change from a restricted environment below (relating to the deposition of sand) to an open marine environment above and represent a marine transgression that is the result of a sudden rise in sea-level. According to Talbot, each erosion surface marks an abrupt change in lithology and truncates structures in the underlying sediments.

Wright (1986a) subdivides the Corallian Group into the six lithostratigraphical formations which are referred to throughout this thesis (the Nothe Grit Formation, the Redcliff Formation, the Osmington Oolite Formation, the Trigonia Clavellata Formation, the Sandsfoot Formation and the Ringstead Formation, see Fig.2.ii). Apart from the Nothe Grit Formation, all other formations are sub-divided into members. Within the middle four formations, Wright identifies cyclic sedimentation consisting of shelly siliciclastic sand to silty clay/lime mud to shallow-marine sandstones or limestones (Fig.2.ii). This cyclicity, he suggests, is a result of tectonically controlled changes, rather than eustatic sea-level changes. Wright (1986a) also expands on Sykes & Calloman's (1979) biostratigraphic proposals for the Corallian Group (refer to Fig.2.iv). In Wright's paper, a number of hiatus' have been positioned between ammonite subzones or within ammonite subzones (diagonal shading on Fig.2.iv). It is unclear however, whether Wright's hiatus' have been positioned on the basis of an absence of diagnostic ammonites, on the evidence of stratal erosion or a combination of both features.

In contrast to Talbot (1973), Sun (1989) identifies four symmetrical regressive-transgressive cycles (Fig.2.ii). According to Sun, each regressive shallowing-upward sequence is separated from a transgressive deepening-upward sequence by a sharp erosive

upper boundary. Sun also draws similarities between his interpretation and the global eustatic sea-level curves produced by Hallam (1978) and Haq (1987), and suggests that the sedimentary cycles are mainly produced by eustatic sea-level changes.

The advent of the application of sequence stratigraphy to the analysis of field exposures resulted in sequence stratigraphic interpretations by Wilson (1991), Rioult *et al.* (1991) and Coe (1992, 1995). Wilson (1991) divides the Corallian Group (up to the Sandsfoot Clay Member) into three sequences, each bounded by a type-1 sequence boundary and composed of a lowstand systems tract (divided into lower and upper lowstand wedge), transgressive systems tract and highstand systems tract (Fig.2.iii).

The sequence stratigraphic studies of Rioult *et al.* (1991) and Coe (1992, 1995) are part of regional studies of the Anglo-Paris Basin, and Oxfordian successions of Dorset, Oxfordshire and Yorkshire, respectively. Rioult *et al.* (1991) divide the Corallian Group strata into four sequences. Each is separated from the next by a sequence boundary which is assumed to have formed as a result of a relative sea-level fall. Sequences consist of either a shelf-margin or lowstand systems tract, a transgressive systems tract and a highstand systems tract (Fig.2.iii).

Coe (1992, 1995) recognises six major unconformities within the Corallian Group succession (Fig.2.iii). These unconformities divide the succession into five sedimentary packages, each of which is interpreted to be a cycle of relative sea-level change. The unconformities are thought to have formed during the maximum rate of sea-level fall and are, therefore, equivalent to sequence boundaries. Coe (1992, 1995) utilises lateral

changes in facies, an assessment of the amount of missing strata and the use of established biostratigraphy to construct her model.

Although Coe (1992) does not state whether her sequence boundaries are either type-1 or type-2, she does define her systems tracts based on the scheme proposed by Posamentier *et al.* (1988). This original scheme states that a type-1 sequence is bounded below by a type-1 sequence boundary and is composed of a basal lowstand, transgressive and highstand systems tracts (refer back to Section 1.2.3 for a fuller explanation). It is, therefore, assumed that Coe's lowstand systems tracts are bounded below by type-1 sequence boundaries.

As stated earlier, none of these workers have attempted to identify parasequences or parasequence boundaries within this succession..

2.2: *Facies Analysis*

Using the lithostratigraphic nomenclature proposed by Wright *et al.* (1986a) as a template, this section provides a detailed description and palaeoenvironmental interpretation of each lithostratigraphic formation within the Corallian Group. The lithostratigraphic units are used, because they have proven (in this study) to closely approximate to facies associations. Biostratigraphic data will be utilised where available (Fig.2.ii & Fig.2 iv) and reference to previous/alternative interpretations will also be given (Fig.2.ii).

2.2.1: The Nothe Grit Formation

The Nothe Grit Formation is located in the cliff sections of Bowleaze Cove and Ham Cliff (Fig.2.i). Biostratigraphically, it falls within the *cordatum* subzone (Fig.2.iv, Fig.2.v).

Lithostratigraphic boundary:

The lithostratigraphic boundary separating the Nothe Grit Formation from the underlying Oxford Clay Formation is best examined at the Bowleaze Cove exposure. Careful field analysis indicates that this boundary (at 0m on Fig.2.v) is gradational over a thickness of 0.5m from clay to silt to very fine sand. This observation is in agreement with Sun (1989) and Rioult *et al.* (1991) but disagrees with Wright (1986a), who describes it as planar and sharp.

Lithological description:

Grainsize measurements obtained from detailed fieldwork reveal that the Nothe Grit Formation represents an 11.8m thick gradually coarsening-up succession of silts to fine-grained sub-rounded and fairly well sorted sandstones, interrupted by two coarser, very fine to fine grained sandstone beds. This field observation is further supported by the analytical data of Wright (1986a, fig.2).

The trace fossil fauna from within the Nothe Grit Formation is dominated by *Rhizocorallium*, *Thalassinoides* and *Teichichnus* burrows which are especially abundant at

the top of each coarsening-up sequence. Whole (within concretions) and fragmented bivalves, notably *Pinna*, are abundant throughout the formation. Although a "spiculite bed" is identified by both Wright (1986a, fig.2 Bed 5) and Coe (1995, fig.6 Bed 5), no evidence of this was observed in the field during this research. Spicules are abundant throughout the formation, as indeed they are throughout the Corallian Group (*pers comm.* M.B. Hart); especially within the septarian concretions. It is unclear from the descriptions of both Wright (1986a) and Coe (1995) on what basis this spiculite bed has been defined.

The two prominent coarser grained beds are calcite cemented bioclastic sandstones. Each is clearly visible in the cliff sections at Bowleaze Cove, Ham Cliff and Red Cliff (at 6.5m and 10.4m on Fig 2.v and Fig.2.vii). These are equivalent to Beds 4 and 8 of Wright (1986a) and contain septarian concretions which are similar in character to concretions found within the underlying Oxford Clay Formation (Section 3.2.5a). The presence of these septarian concretions has not been noted by some previous workers (e.g. Coe, 1995).

Each cemented bed represents the top of a smaller scale coarsening-up sequence which is contained within the overall larger scale coarsening-up succession of the Nothe Grit Formation (refer to Fig.3v for a field view). The lower of the two coarsening-up sequences is 6.5m in thickness (between 0m and 6.5m on Fig.2.v) and grain-size measurements taken in the field (substantiated by analytical data from Wright, 1986a) indicate that it coarsens-up from silt (<44μm) to very fine sand (88-125μm). The upper coarsening-up sequence is 3.9m in thickness (between 6.5m and 10.4m on Fig 2.v) and coarsens-up (Wright, 1986a) from very fine sand (88-125μm) to fine sand (125-177μm). The boundary separating the two coarsening-up units is marked by an abrupt but slight

upward decrease in grain-size, a change in the amount of cementation (decrease in bioclastic content) and a weathered surface colour change from yellow to light grey (clearly identifiable in Fig.2.vii). A change from a laterally cemented shelly sand containing septarian concretions, to a predominantly uncemented sand also occurs across the boundary.

Palaeoenvironmental interpretation:

The lack of physical sedimentary structures and abundance of bioturbation within this formation indicates a relatively low energy environment, although the absence of clay suggests that deposition occurred above storm wave-base without any significantly long periods of quiet water in which fines could settle from suspension. The lack of structures may be the result of too high a degree of bioturbation. The shell beds at the top of each of the small-scale sequences are likely to be an indication of shallowing and winnowing above the level of fair-weather wave-base – hence each is bioclastic rich, of a coarser grain size and heavily bioturbated.

According to Whatley (1965), the ostracod fauna contained within the Nothe Grit Formation is indicative of deposition within an unrestricted marine environment. This evidence, coupled with the gradual coarsening-up grain-size trend and other dominantly shallow water marine fauna, indicates that the Nothe Grit Formation was most probably deposited in a prograding low energy lower shoreface environment (*sensu* Elliot, 1986; McCubbin, 1982; Walker & Plint, 1992). Similar low energy shorefaces occur on the present day coast of Texas (see McCubbin, 1982).

There is no sedimentological evidence for erosion or down-cutting at the lithostratigraphic boundary between the Nothe Grit Formation and underlying Oxford Clay Formation (e.g. load casts and/or elongate gutter casts: *sensu* Rosenthal & Walker, 1987; Davis & Byers, 1989; Plint, 1991) and it is therefore interpreted to be conformable. Because of the dominantly low energy environment (as interpreted above) there may not have been an efficient mechanism for removing sediment. Any sand deposited offshore would, therefore have been trapped within the lower shoreface environment with no (or a poorly developed) mechanism for offshore redistribution. This explains the "apparent" sharpness to the base of the formation, with shoreface sands sitting directly on top of mid- to outer-shelf mudstones. The gradational base of the Nothe Grit Formation would then represent the lower shoreface to inner-shelf transition zone (see Walker & Plint, 1992, fig.14).

2.2.2: The Red Cliff Formation

The Red Cliff Formation is located in the cliff sections of Ham Cliff, Red Cliff and Osmington Mills (Fig.2.i). It is composed of the Preston Grit Member, the Nothe Clay Member and the Bencliff Grit Member and lies within the *vertebrale* ammonite subzone (Fig.2.iv & Fig.2.v).

2.2.2a: *The Preston Grit Member*

Lithostratigraphic boundary:

The lithostratigraphic boundary between the Preston Grit Member and the underlying Nothe Grit Formation (at 11.8m on Fig.2.v) is erosional with some evidence of broken bioclastic debris immediately above it. Wright (1986a) has demonstrated that it represents a stratal/biostratigraphic gap, although it is unclear as to whether this "gap" is based on evidence of stratal erosion or the absence of diagnostic ammonites.

Lithological description:

The Preston Grit Member is a 1.1m thick coarsening-up succession of fine to medium grained (up to 250μm; Wright, 1986a) dominantly massive sandstone. Bioturbation is common (e.g. at 12m on Fig.2.v) and the member is characterised by a high faunal diversity (Arkell, 1936; Talbot, 1973; Rioult *et al.*, 1991; Coe, 1995). Particularly common are the shallow marine bivalves *Chlamys, Pleuromya* and *Myophorella hudlestoni* (dominant towards the top of the member), ammonites belonging to the *vertebrale* subzone (Fig.2.iv) and bioturbation dominated by *Thalassinoides* and *Rhizocorallium irregulare.* Whatley (1965) notes the presence of ostracods that are similar to those found within the underlying Nothe Grit Formation.

Palaeoenvironmental interpretation:

The lithostratigraphic boundary at the base of the Preston Grit could be interpreted two ways. It could either represent:-

1. an unconformity corresponding to a submarine regressive surface of erosion, more commonly referred to as a surface of forced regression (Fig 2.viiia *sensu* Walker & Plint, 1992). Surfaces of forced regression are commonly sharp based and interpreted to be the result of progradation due to a relative sea-level fall, resulting in abrupt shallowing above the surface; or,
2. a transgressive surface of erosion, more commonly referred to as a ravinement surface (Fig 2.viiib, e.g. Reinson, 1992). A ravinement surface generally occurs due to landward and upward movement of the shoreface during continued transgression resulting in abrupt deepening above the surface. Barrier and near-shore sands are commonly removed and a planar erosive surface will develop (the ravinement surface) upon which the redistributed lower shoreface-inner shelf sands are deposited.

Thus to interpret the lithostratigraphic boundary, the palaeoenvironmental interpretation of the Preston Grit Member needs to be established. The fossil evidence and bioturbation indicate that the Preston Grit Member was deposited in a shallow marine environment. Ostracods collected from the Preston Grit Member correspond to a similar shallow marine environment to that inferred for the underlying Nothe Grit Formation (Whatley, 1965). The absence of a clay-sized fraction further indicates that it was probably deposited above fair-weather wave-base. The lack of physical sedimentary structures can be explained by the high degree of biogenic activity - destroying all primary, physical sedimentary

structures. The dominant fine to medium grain-size indicates that it is likely to have been deposited in a transitional to upper shoreface zone (Elliot, 1986; Walker & Plint, 1992; Emery & Myers, 1996). This interpretation lends support for the lithostratigraphic boundary representing a surface of forced regression, with a sense of shallowing occurring above the boundary. A ravinement surface could only have formed at this lithostratigraphic boundary if shallower facies were deposited in the progradational phase of the upper Nothe Grit Formation, but were then totally removed by erosion during transgression. The Preston Grit Member is less likely to represent a transgressive deposit, for the reasons mentioned above and, the fact that there is less evidence for abrupt deepening above the lithostratigraphic boundary. Previous palaeoenvironmental interpretations (Fig.2.ii) indicate that the Preston Grit Member represents a shallow marine deposit.

2.2.2b: *The Nothe Clay Member*

Lithostratigraphic boundary:

The lithostratigraphic boundary that separates the Nothe Clay Member from the underlying Preston Grit Member (at 12.9m on Fig.2.v) is gradational and contains ooids and sandstone intraclasts.

Lithological description:

The Nothe Clay Member consists dominantly of claystone interbedded with at least six thin, cemented and occasionally laterally extensive siltstone beds (e.g. the bed at 17.3m on Fig.2.v). Each siltstone bed is rich in bioclastic material, sparsely oolitic and contains whole and fragmented bivalves such as *Lopha*, *Liostrea*, *Modiolus* (Wright, 1986a) and *Gryphea dilatata* (Arkell, 1936). The top surface of one siltstone bed (at 17.3m on Fig.2.v) is bored and this siltstone bed in particular displays an upward increase in faunal diversity. Ostracods similar to those found within the Preston Grit Member have been recorded by Whatley (1965). He also indicates that ostracod species associated with a restricted, less saline environment are only common within the top few metres of the Nothe Clay Member.

Palaeoenvironmental interpretation:

The fossil evidence indicates that the Nothe Clay Member was deposited in a marine environment, that became more restricted/less marine towards the very top of the member. A dominance of clays indicates that it was likely to have been deposited below storm wave-base within a deeper water environment than the underlying Preston Grit Member; probably a shallow shelfal environment (*sensu* Rine & Ginsberg, 1985; Johnson & Baldwin, 1986; Walker & Plint, 1992). This is supported by the ostracod data of Whatley (1965) and all other previous palaeoenvironmental interpretations (Fig.2.ii).

The depositional interpretation of the coarser, bioclastic rich sands has not been significantly discussed by previous workers. It is possible that each bed represents deposition from periodic storm activity and can be interpreted as "event" deposits. Davis *et al.* (1989) and Walker & Plint (1992) indicate that sharp-based coarser beds within shelf mudstone sequences are probably deposited from waning, storm generated flows. The muddier portion separating the coarser beds may be partly storm emplaced and partly reflecting the pelagic deposition between storms.

However, as mentioned previously, one coarser grained bed within the Nothe Clay Formation contains evidence of borings on its upper surface which may be an indication of shallowing above the level of wave winnowing. This particular surface could be interpreted as representing a marine hard-ground.

The distinct change in the depositional environment between the Nothe Clay Member and the underlying Preston Grit Member, is associated with an increase in water depth. The intervening lithostratigraphic boundary is thus interpreted as a transgressive surface. The presence of reworked pebbles, intraclasts and ooids on and immediately above this surface can be interpreted as representing a transgressive lag deposit (*sensu* Van Wagoner *et al.*, 1990).

2.2.2c: *The Bencliff Grit Member*

Lithostratigraphic boundary:

The lithostratigraphic boundary between the Bencliff Grit Member and underlying Nothe Clay Member is upwards gradational from claystone to fine grained sandstone. It shows no evidence of down-cutting or erosion, an observation also noted by Wright (1986a) and Sun (1989).

Lithological description:

The Bencliff Grit Member consists of four uniformly thick, sharp-based fining-up (sandstone to siltstone) facies associations (e.g. between 25.7m-27.4m on Fig.2.v & Fig.2.ix). Within each facies association is a mixed fresh-water/marine fauna indicated by fresh-water tolerant species of Ostracoda and Forminifera (Whatley, 1965 and Talbot, 1973) and a diverse dinoflagellate assemblage (Allen & Underhill, 1989). It is a predominantly uncemented, well sorted and contains large (average 1m diameter) calcareous concretions. The sandstones are interbedded with at least three, occasionally laterally persistent, well cemented silty heterolithic layers and rare impersistent thin claystone layers.

The sandstone beds of each facies association contain bedforms analogous to swaley cross-stratification (SCS) or amalgamated hummocky cross-stratification (HCS) that have formed under unidirectional currents (Allen & Underhill, 1989). Palaeocurrent directions,

taken from troughs within these bedforms, suggest variable flow directions towards the north and north-west. Trace fossils associated with the large scale SCS and ripple laminated sands are dominated by *Diplocraterion parallelum* (up to 0.2m in length). *D. parallelum* is often associated with unstable substrates that are subjected to high rates of sedimentation and erosion (Fürsich, 1975).

Palynological and micropalaeontological evidence (Goldring & Gabbott, 1993; Goldring *et al.* in press) indicate that "muddy" layers preserved within the cross-bedded sands are dominated by terrestrial palynomorphs and agglutinated foraminifera. This may indicate an input of fresh-water that contained land derived organic matter. Bioclastic shell debris is rare within the sandstone beds, but is locally concentrated within the large calcareous concretions.

The sandstones grade up into heterolithic facies, which occur at the top of individual fining-up facies associations. Each heterolithic bed contains flaser and wavy bedding. Ripple laminations indicate flow directions of northeast-southwest (wave ripples) and northwest (current ripples). Allen & Underhill (1989) suggest that the depositional characteristics of the heterolithic layers are controlled by flows reversing on either a tidal or gravity wave frequency. Talbot (1973) notes the presence of desiccation cracks within a heterolithic bed of the Bencliff Grit Member at Redcliff Point (although this is no longer exposed at this location). Facies association boundaries (e.g. at 25.7m on Fig.2.v) occur immediately above each heterolithic bed.

Trace fossils within the heterolithic layer of the uppermost facies association of the Bencliff Grit Member (29.2m on Fig. 2.v) are dominated by *Rhizocorallium irregulare.* Some of these burrows contain carbonate-coated grains that are not present in the Bencliff Grit Member and may have penetrated down from the overlying unit (Fig.2.x). The burrows are oriented approximately parallel to asymmetric ripple troughs, which contain a high amount of organic matter (Fürsich, 1975).

Palaeoenvironmental interpretation:

The biostratigraphic evidence indicates that the Bencliff Grit Member may represent a tidal-flat shoreline environment (*sensu* Elliot, 1986; Dalrymple, 1992), agreeing with the interpretation offered by Wilson (1968b, my Fig.2.ii). Individual facies associations represent tidal flat units that fine towards the high-tide level. Each facies association passes gradationally from a storm induced, sand dominated lower intertidal deposit through to an upper intertidal deposit represented by individual heterolithic beds (*sensu* Dalrymple, 1992). Facies association boundaries are characteristically sharp due to erosion by currents during transgression prior to the deposition of the succeeding sandstone. The presence of desiccation cracks within an heterolithic bed (observed by Talbot, 1973) would indicate shallowing and subaerial exposure associated with progradation. This would suggest that the heterolithic facies represent a shallower water environment than the SCS dominated coarser sandstone beds. Recent previous workers (e.g. Allen & Underhill, 1989) agree that the SCS bedforms within the sand dominated facies indicate periodic storm activity.

The presence of *R. irregulare* within the heterolithic layer at the top of the Bencliff Grit Member is significant. It is often associated with stable substrates in a lower energy environment (Fürsich, 1975). This suggests that the depositional environment gradually became more tranquil towards the top of the Bencliff Grit Member, which could be related to a gradually rising sea-level.

Two questions which remain unanswered in all previous work are:-

- why do SCS bedforms dominate the sand grade beds of each facies association? and,
- why are storm dominated sedimentary structures only prevalent in the Bencliff Grit Member of the Corallian Group and not seen elsewhere?

The latter question may be linked to changes in basin hydro-dynamics controlled by relative sea-level changes and will be discussed with reference to the high resolution sequence stratigraphic interpretation later (Section 2.3.3).

With reference to the first question, one would expect the dominant sedimentary structures within a tidal flat/tidal channel environment to include, for example, double mud-drapes, reactivation surfaces, tidal bundles and herringbone cross-stratification (Dalrymple, 1992). Generally, after minor storm events, a return to the dominant depositional regime (i.e. tidal flow) would be expected. Thus, the tidal flat/tidal channel depositional environment of the Bencliff Grit is not typical. Pickering (1995) has identified a concentration of similar storm induced bedforms within the shallow marine Middle Jurassic Bridport Sands of south Dorset and interprets them as "erosional wavy sandy bedforms formed.....during a very severe tropical cyclone, consistent with the low latitudes for that time". Pickering

also states that it is curious that these bedforms have been preserved within the Bridport Sands, but indicates that rising sea-level and decreased rates of sediment accumulation, allowing greater time periods for storm activity reworking, could lead to the preservation of the bedforms. It is quite possible, during the deposition of the Bencliff Grit Member, that the tidal flat depositional environment was subjected to numerous intense tropical cyclones lasting several days. This would have resulted in the re-working of sub-tidal sands and the deposition and preservation (coupled with a gradual rising sea-level) of storm induced beds. Thus storm deposition could well have been dominant over the more typical tidal flow depositional regime, during the deposition of the Bencliff Grit Member. After all, it is only the biostratigraphic evidence and recognition of intertidal heterolithic sands that allows a tidal flat interpretation of the Bencliff Grit Member.

Several workers (e.g. Allen & Underhill, 1989; Goldring *et al.* in press) have suggested that the Bencliff Grit Member represents deposition within an estuarine environment. However, Reinson (1992) states that the most important evidence for the interpretation of ancient estuarine environments, is the recognition of an incised valley within which the estuary develops during transgression. However, the lithostratigraphic boundary between the Bencliff Grit Member and the underlying Nothe Clay Member shows no evidence of the erosion or down-cutting that would usually be associated with valley incision.

2.2.3: The Osmington Oolite Formation

The Osmington Oolite Formation is exposed in the cliff sections 1km to the east of Osmington Mills and at Bran Point and Black Head (Fig.2.i). It is composed of the Upton Member, the Shortlake Member and the Nodular Rubble Member and lies within the *antecedens* and *parandieri* ammonite subzones (Fig.2.iv & Fig.2.v).

2.2.3a: *The Upton Member*

Lithostratigraphic boundary:

The lithostratigraphic boundary separating the Upton Member from the underlying Bencliff Grit Member (at 29.2m on Fig.2.v & Fig.2.ix) is wave-ripple cross-laminated. These wave ripples are draped by mm-scale mud drapes. Minor evidence of sub-marine erosion and sub-marine reworking is present in the form of small sandstone lithoclasts, which probably originate from the underlying Bencliff Grit Member. There is no evidence of sub-aerial exposure associated with this boundary although Wright (1986a) indicates that this lithostratigraphic boundary, also represents a small stratal/biostratigraphic gap. Immediately above this surface (at 29.5m on Fig.2.v) is a thin (approximately 0.5m) oolitic and bioclastic bed containing abundant reworked lithoclasts, ooids and whole or fragmented bioclastic material.

Lithological description:

The lowest 5m of the Upton Member (between 29.2m-35.5m on Fig.2.v) is composed of a series of interbedded silty claystones and coarser grained oolitic and bioclastic rich grainstones and packstones which are arranged into a series of two coarsening-up facies associations.

The lower facies association (between 30m and 31.8m on Fig 2.v) coarsens-up from silty claystone to a medium grained bioclastic, oolitic grainstone which is known as the *Chlamys qualicosta* bed (Wilson, 1968a, 1968b, 1975; Talbot, 1973; Wright, 1986a). The coarser grained bed at the top of this facies association contains well developed marine cements discussed in Section 3.2.

The upper facies association (between 31.8m-33.5m on Fig.2.v) coarsens-up from silty claystone to a coarse grained bioclastic and pisolitic packstone. The coarse grained bed contains poorly developed marine cements and a higher percentage of micrite than the lower facies association.

Both facies associations record an upward increase in faunal diversity, including an increase in the abundance of bivalves such as *Chlamys qualicosta* and *Nanogyra* (Talbot, 1973; Wright, 1986a; Sun, 1989). Both facies associations are highly bioturbated with *Diplocraterion, Arenicolites, Thalassinoides* and *Rhizocorallium* concentrated on, and towards, the upper surfaces. The upper surfaces are also bored, suggesting that early cementation occurred followed by winnowing and sub-aqueous exposure of the hardened

surface. This led to the formation of marine hardgrounds.

The upper 5.5m of the Upton Member (between 33.5m-38.9m on Fig.2.v) is composed of nodular micritic limestone interbedded with soft, occasionally silty, claystones. Physical sedimentary structures are absent from these beds. Fürsich (1973) has interpreted the nodular limestones as representing the cemented infillings of *Thalassinoides* burrows that had formed just beneath the sediment-water interface. As well as *Thalassinoides*, other trace fossils such as *Teichichnus*, *Rhizocorallium* (rare) and *Corophoides* (Fürsich, 1973) have been found. Apart from the presence of neomorphosed sponge spicules, macrofossils are rare.

Palaeoenvironmental interpretation:

The lithostratigraphic boundary separating the Upton Member from the underlying Bencliff Grit Member represents a change to a more open marine depositional environment and, as a result represents a transgressive surface. This interpretation agrees with all previous interpretations. The oolitic and bioclastic bed immediately above this surface (at 29.5m on Fig.2.v) can be interpreted as representing a transgressive lag deposit (*sensu* Van Wagoner *et al.*, 1990). Carbonate precipitation may have begun at this point due to a probable cut-off in clastic supply.

The presence of shallow marine fauna and a dominance of moderate to high energy carbonate grain types indicates that the lower 5m of the Upton Member was deposited within a shallow marine shoreface environment. Similar interpretations have been offered

by previous workers (Fig.2.ii). The presence of poorly developed marine cements and a high percentage of carbonate micrite mud in the upper facies association, indicates deposition within a deeper-water, less agitated (below fair-weather wave-base) depositional environment than the underlying facies association. Although oncoids are commonly associated with shallow lagoons, a similar interpretation has been offered for the Pea Grit Series (Middle Jurassic Inferior Oolite of the Cotswold area) by Kenyon-Roberts (1995) who identifies oncoids and pisolites and interprets them as having been deposited in a "mid-ramp" setting, equivalent to a shoal margin, but below fair-weather wave-base.

Fürsich (1973) has interpreted the upper 5.5m of the Upton Member as representing a tranquil, shallow subtidal environment, thus relating to a deeper water environment than that of the underlying relatively high energy, bioclastic and oolitc rich, shoreface sands.

2.2.3b: *The Shortlake Member*

Lithostratigraphic boundary:

The lithostratigraphic boundary separating the Shortlake Member from the underlying Upton Member has been defined by Wright (1986a). It can be described as planar and conformable at the Bran Point outcrop (white arrows on Fig.2.xi) but distinctly erosive 1km to the west of Osmington Mills at the Black Head outcrop (black arrows on Fig.2.xii). However, some confusion still exists as to the exact lithostratigraphic position of this boundary. Coe (1995) also notes the presence of a laterally conformable/erosive surface at

Bran Point, but identifies it as "the junction between a clear oolitic grainstone containing long 'U'-shaped burrows and a thin clay with sandy argillaceous oolites beneath. Here the unconformity is about 0.5m above the base of the Shortlake Member (taken as the first occurrence of oolite filled *Diplocraterion* burrows, Wright, 1986a)". Coe's (1995) lithostratigraphic boundary has been marked on Figure 2.xi with green arrows. It should be noted that it is very difficult to trace these surfaces laterally along the length of the Osmington Mills exposures due to the presence of a small normal fault, that is identified on Figure 2.xii.

Lithological description (lower to middle Shortlake Member):

The lower 2m of the Shortlake Member at Bran Point (between 39.8m-41.8m on Fig.2.v) is composed of three coarsening-up successions from sandy/silty calcareous claystones to medium grained oolitic and sparsely bioclastic packstones and grainstones. The upper packstone/grainstone bed of these three is more commonly known as the "middle white oolite bed" (Arkell,1947a). All are identified in the photograph and annotated sketch log on Figure 2.xi. Close field inspection indicates that the tops of the successions contain low angled planar cross-bedding with laminae dipping in a west-north-west direction.

Trace fossils are dominated by elements of the *Skolithos* and *Cruziana* ichnofacies assemblages, including *Arenicolites variablis*. This burrow type is common towards the top of all of the coarsening-up sequences indicating rapid deposition in a high energy environment (Fürsich, 1975).

At Black Head, the facies associations of the lower Shortlake Member thicken laterally (between 34.6m-41.6m on column 3 of Fig.2.v) and are associated with down-cutting into the underlying silty claystones. The oolitic grainstones are thicker and contain trough cross-bedding, indicating a dominant flow towards the southwest and a subordinate flow towards the west-northwest (also noted by Wilson, 1968b, 1975; Wright, 1986a & Sun, 1989, my Fig.2.xiii & Fig.2.xiv). Intraclasts, mud-draped wave-ripple laminations (indicating a southwest-northeast flow direction) and mud draped foreset laminae are also a common feature. Marine fossils are rare within the oolitic beds, except at Black Head where *Nucleolites* is common.

Palaeoenvironmental interpretation (lower to middle Shortlake Member):

The lithostratigraphic boundary separating the Shortlake Member from the underlying Upton Member is conformable to laterally erosive. Sedimentological evidence at this boundary indicates that it could represent either a surface of erosion at the base of a tidal inlet similar to modern day examples from Jade Bay, Germany (Dalrymple, 1992; fig. 13) or the Solway Firth, Scotland (Bridges & Leeder, 1976) or, a tidal/wave ravinement surface (*sensu.* Stamp, 1921) associated with a period of submarine transgression. However, because it marks a change in facies from the underlying subtidal muds of the Upton Member to the shallow water sands of the overlying Shortlake Member (representing overall shallowing, see below) it is likely that the first interpretation is more plausible.

The sedimentological and rare fossil evidence indicate that the silty claystones of the upper Upton Member represent deposition in a low energy subtidal environment, possibly a ramp setting. The oolitic grainstones of the overlying lower Shortlake Member have scoured bases, bimodal palaeo-currents and mud draped foreset laminae. All of these features are characteristic of laterally migrating tidal inlets/channels (*sensu.* Bridges & Leeder, 1976; Elliot, 1986; Dalrymple, 1992) within a high energy shoreface environment. Dominant flood tidal currents would have originated from the north-east (Fig.2.xiv). The west-north-west dipping bedsets identified at Bran Point can be traced laterally to the Black Head outcrop, where they thicken into north-east south-west trending tidal inlets/channels (as stated above). Tidal features (as stated above) are readily identifiable here, because tidal currents are likely to be exaggerated within tidal inlets. This may explain why similar tidal features were not as easy to identify within other similar depositional environments of the Corallian Group (e.g. the Bencliff Grit Member). The Bran Point bedsets are, likely to represent lateral accretion bedding (also called inclined heterolithic stratification, Bridges & Leeder, 1976; Thomas *et al.*, 1987) identifying a dominant west-north-west avulsion direction. Elliot (1986) cites the Georgia embayment of the eastern USA, which can be used as a modern day analogue of the lower to middle Shortlake Member.

Lithological description (upper Shortlake Member):

The upper Shortlake Member (above the "middle white oolite bed" of Arkell, 1947a and between 41.6m-48.5m on Fig.2.v) is composed of silty claystones that are interbedded with three coarser grained oolitic and bioclastic grainstone beds displaying sheet-like geometries (Wilson, 1968b, 1975). These coarser grained beds contain low angle planar

cross-bedding that indicates a dominant accretion direction towards the north-northwest (although Wilson, 1975 identifies a bidirectional pattern). Wave ripple lamination, indicate a north-northwest/south-southeast flow direction. (Fig.2.xv).

Biogenic sedimentary structures are concentrated at the top of the coarser grained beds and are dominated by *Planolites* and rare *Cylindrichus* burrows (Fürsich, 1975) along with evidence of borings. Marine fauna is scarce, although Arkell (1936) notes the presence of the bivalves *Exogyra, Ostrea* and *Placunopsis* within the coarser grained beds.

Palaeoenvironmental interpretation:

The physical and biogenic sedimentary structures along with the observed sheet-like bed geometries indicate that the upper Shortlake Member represents a marine shoal environment, probably equivalent to a middle shoreface environment (*sensu* Walker & Plint, 1992). Thus the deepening of the depositional environment between the lower/middle Shortlake Member (tidal channels/flats) and upper Shortlake Member (middle shoreface), indicates that they are likely to be separated by a transgressive surface positioned immediately above the "middle white oolite" bed (e.g. at 41.6m on column 3 of Fig.2.v). This interpretation is also supported by Wright (1986a).

2.2.3c: *The Nodular Rubble Member*

Lithostratigraphic boundary:

The lithostratigraphic boundary separating the Nodular Rubble Member from the underlying Shortlake Member (at 49.1m on Fig.2.v) is planar with no evidence of erosion or reworking. Wright (1986a) indicates that this surface also represents a small stratal/biostratigraphic gap.

Lithological description:

The Nodular Rubble Member consists of micritic limestone nodules containing common *Rhaxella*, which represent cemented infillings of *Thalassinoides* and *Teichichnus* burrows suspended within a laminated silty clay (between 49.1m and 52.1m on Fig.2.v and Fig.2.xv). A thin claystone occurs at 51.2m on Figure 2.v. The marine fauna is dominated by infaunal species such as *Pseudomelania*, *Ampullina*, *Pleuromya*, *Nucleolites* and the encrusting *Nanogyra nana* (Fürsich, 1973). Brookfield (1973) and Coe (1995) both suggest that the Nodular Rubble Member represents the whole of the *parandieri* subzone and so interpret it as being a condensed unit.

Palaeoenvironmental interpretation:

Evidence from biogenic sedimentary structures and marine fossils indicate that the Nodular Rubble Member represents a return to a low energy, oxygenated shelf

environment, deeper than the upper part of the Shortlake Member and similar to that of the upper part of the Upton Member.

2.2.4: The Trigonia Clavellata Formation

The Trigonia Clavellata Formation is located within the cliff sections of Black Head (Fig.2.i). It is composed of the Sandy Block Member, the Chief Shell Beds Member and the Red Beds Member and lies within the *cautisnigrae* ammonite subzone (Fig.2.iv & Fig.2.v).

2.2.4a: *The Sandy Block Member*

Lithostratigraphic boundary:

The lithostratigraphic boundary between the Sandy Block Member and the underlying Nodular Rubble Member is characterised by an irregular and undulatory surface, which was then draped by, laminated marls. In south Dorset, this boundary also corresponds to a major biostratigraphic gap. Wright (1986a) indicates that the latter part of the *parandieri* subzone, together with the whole of the *nunningtonense* subzone is missing (Fig.2.iv).

Coe (1995) measured oxygen and carbon stable isotopes extracted from bulk rock samples at the top of the Nodular Rubble Member. The values range between -2.3 to +2.2‰ PDB $\delta^{13}C$ and -2.3 to -6.1‰ PDB $\delta^{18}O$.

Lithological description:

The overlying Sandy Block Member (Fig.2.xvi and between 52.1m and 54m on Fig.2.v) consists of dominantly sandy, sparsely oolitic and bioclastic packstones that are interbeded with rare micritic partings. This agrees with the observations of Wilson (1968a), Talbot (1974), Brookfield (1978), Wright (1986a) and Coe (1995). Biogenic sedimentary structures are dominated by *Thalassinoides suevica*, *Planolites*, *Chondrites* and rare *Skolithos* burrows, as observed by Fürsich (1975), Sun (1989) and Coe (1995).

Palaeoenvironmental interpretation:

The irregular and undulatory characteristics of the lithostratigraphic boundary, along with the analytical evidence of Coe (1995) indicate that it is likely to represent a period of sub-aerial exposure. Coe (1995) interprets her oxygen and carbon stable isotope data to be the result of a phase of fresh water cementation. An increase in sand content within the Sandy Block Member (when compared to the underlying Nodular Rubble Member) together with a lack of clay and a dominantly *Cruziana* ichnofacies assemblage, indicates that it was deposited in a relatively high energy lower shoreface environment (*sensu* Elliot, 1986; Walker & Plint, 1992; Emery & Myers, 1996).

2.2.4b: *The Chief Shell Beds Member*

Lithostratigraphic boundary:

The lithostratigraphic boundary between the Chief Shell Beds Member and the underlying Sandy Block Member marks the first profusion of the bivalve *Myophorella clavellata.*

Lithological description:

The Chief Shell Beds Member consists of a series of three fine grained, sandy, oolitic and bioclastic beds that contain *M. clavellata* and rarer *Pleuromya.*

The lowest bed of the Chief Shell Beds Member (between 54m and 54.8m on Fig.2.v) contains an abundance of *M. clavellata* that are disarticulated, occasionally intact, heavily bored and concentrated into layers (Arkell, 1936; Talbot, 1974; Wright, 1986a and Coe, 1995).

Palaeoenvironmental interpretation:

The lithostratigraphic boundary separating the Chief Shell Beds Member from the underlying Sandy Block Member represents a return to a more open marine environment and can thus be interpreted as a transgressive surface.

The lowest bed of the Chief Shell Beds Member can be identified as a transgressive shell bed and is interpreted to represent a transgressive lag deposit, agreeing with the interpretation of Rioult *et al.* (1991). Goldring (1995, based on Fürsich & Oschmann, 1993) suggests that shell beds forming as a result of transgressive lag deposition show evidence of reworking, combined with randomly oriented, disarticulated, fragmented, encrusted and bored shells - observations that are characteristic of the Chief Shell Beds Member. Goldring (1995) continues by stating that this differs from the fabric of a shell bed that forms as a result of storm activity, which is generally cemented into a packstone or grainstone, has an erosive base, bimodal sorting and whole and broken randomly oriented shell debris.

2.2.4c: *The Red Beds Member*

Lithological description:

The Red Beds Member consists of a 0.6m thick clay band which lies conformably on top of the underlying Chief Shell Beds Member and a sparsely oolitic and bioclastic sideritic packstone with micritic mudstone partitions. Broken *M. clavellata* shell debris is common along with biogenic sedimentary structures, especially *Thalassinoides* burrows.

Palaeoenvironmental interpretation:

This upwards change in facies from the underlying Chief Shell Beds Member represents a continual deepening associated with a marine transgression, as suggested by previous

workers (Fig.2.ii).

2.2.5: The Sandsfoot Formation

The Sandsfoot Formation is located within the cliff sections of Black Head and beneath Sandsfoot Castle (Fig.2.i). It consists of the Sandsfoot Clay Member and the Sandsfoot Grit Member. The Formation lies between the upper *cautisnigrae* subzone and the *pseudocordata* subzone (Fig.2.iv & Fig.2.v). According to Wright (1986a) the *variocostatus* to *pseudoyo* subzones are missing from south Dorset (Fig.2.iv).

2.2.5a: *The Sandsfoot Clay Member*

Lithostratigraphic boundary:

The lithostratigraphic boundary between the Sandsfoot Clay Member and the underlying Red Beds Member (at 58.2m on Fig.2.v) is gradational from fine sand to claystone over a thickness of 0.1-0.2m. There is no evidence of erosion or reworking.

Lithological description & palaeoenvironmental interpretation:

The Sandsfoot Clay Member (between 58.2m-66.6m on Fig.2.v) is composed of a calcareous silty claystone, with occasional sandy laminations (Brookfield, 1978; Wright, 1986a and Coe, 1995). It is sparsely fossiliferous, containing rare examples of *Deltoideum*

delta, *Nanogyra* and belemnites (Brookfield, 1978; Coe, 1995). Wright (1986a) indicates that the Sandsfoot Clay Member represents the whole of the *variocostatus* subzone and has interpreted it as a condensed unit. Talbot (1974) has interpreted the Sandsfoot Clay Member as representing a subtidal depositional environment.

2.2.5b: *The Sandsfoot Grit Member*

Lithostratigraphic boundary:

The lithostratigraphic boundary separating the Sandsfoot Grit Member from the underlying Sandsfoot Clay Member (at 66.6m on Fig.2.v) is an erosional surface indicated by the extensive downcutting of the underlying strata (Brookfield, 1978) and, the removal of the upper part of the *variocostatus* subzone, the whole of the *caledonica* subzone and the lower *pseudoyo* subzone (Wright, 1986a, my Fig.2.iv).

Lithological description:

Lithologically, the Sandsfoot Grit Member (between 66.6m-71.2m on Fig.2.v) is a bioturbated ferruginous sandstone that is interbedded with a thin clay bed (at 70m on Fig.2.v). The macrofauna is dominated by the bivalves *Ctenostreon* and *Pinna*, often preserved in life position, suggesting periods of increased sedimentation (Talbot, 1974; Brookfield, 1978). Bioturbation is dominated by *Thalassinoides*, *Rhizocorallium* and *Chondrites*. A thin lag of shell debris occurs at 66.9m on Figure 2.v, as also noted by Coe (1995).

Within the lower beds of the Sandsfoot Grit Member (between 66.6m-69.7m on Fig.2.v) detailed grain-size measurements taken in the field and substantiated by analytical data from Wright (1986a), indicate an upwards-coarsening grain-size profile from siltstone (<44μm) to medium-grained sandstone (>177μm). Small sideritic, phosphatic and hollow or tube-like iron-oxide concretions are concentrated towards the top of this coarsening-up grain-size profile (at 69m on Fig.2.v).

Palaeoenvironmental interpretation:

The erosive base, coarsening-up grain-size profile, lack of clay within the sand units (indicating deposition above fair-weather wave-base) and the dominant shallow marine fauna, indicate that the Sandsfoot Grit Member was deposited in a middle to upper shoreface environment (*sensu* Elliot, 1986; Walker & Plint, 1992; Emery & Myers, 1996).

2.2.6: The Ringstead Formation

The youngest formation of the Corallian Group - the Ringstead Formation - is located within the cliff sections beneath Sandsfoot Castle and on the foreshore of Ringstead Bay (Fig.2.i). It consists of the Ringstead Waxy Clay Member and the Osmington Mills Ironstone Member and lies within the *evoluta* subzone (Fig.2.iv & Fig.2.v).

2.2.5a: *The Ringstead Waxy Clay Member*

Lithostratigraphic boundary:

The lithostratigraphic boundary separating the Ringstead Waxy Clay Member from the underlying Sandsfoot Grit Member (at 71.2m on Fig.2.v) is gradational from a medium grained sand to a claystone. This observation disagrees with Brookfield (1978), Wright (1986a) and Coe (1995), who all state that it is a sharp boundary. Wright (1986a) also indicates that this boundary corresponds to a thin, poorly developed stratal/biostratigraphic gap (Fig.2.iv).

Lithological description:

The Ringstead Waxy Clay Member is characterised by calcareous clays containing sparse ferruginous ooids, sand grains and an impoverished macrofauna (Brookfield, 1978; Coe, 1995).

Palaeoenvironmental interpretation:

The abrupt change in facies across the lithostratigraphic boundary is associated with a deepening of the depositional environment and can, therefore, be interpreted as a transgressive surface. The dominant clay sized grain-size fraction and impoverished macrofauna of the Ringstead Waxy Clay Member indicate that it probably represents deposition within a restricted bay or offshore shallow shelfal marine environment.

2.2.5b: *The Osmington Mills Ironstone Member*

Lithological description:

The Osmington Mills Ironstone Member (between 74m-74.8m on Fig.2.v) consists of a sandy, iron-rich, calcareous clay bed with a diverse, shallow marine fauna (Talbot, 1973, 1974; Brookfield, 1978; Wright, 1986a and Coe, 1995). The upper surface of this bed contains abundant bivalves, gastropods, serpulids and *in-situ* corals such as *Thamnasteria arachnoides* (Parkinson) and bored *Gastrochaenolites* (after Wright, 1986a and Coe, 1995).

Palaeoenvironmental interpretation:

The diverse shallow marine fauna indicate that the Osmington Mills Ironstone Member represents a return to a more open marine depositional environment when compared to the underlying Ringstead Waxy Clay Member.

2.3: *Sequence Stratigraphy*

The sequence stratigraphic approach and definitions used here follow those outlined in Chapter 1. The studied succession has been divided into six sequences, two of which (Sequence 1 and Sequence 6) are only partially represented within the studied sections (Fig.2.vi and Table 2.i). Within each sequence, the sequence boundary (if present) is

identified and interpreted (as either a Type-1 or Type-2 boundary). This is followed by an identification of parasequences (if present), systems tracts, transgressive surfaces and zones of maximum flooding. Where outcrop was clean enough, ichnofabric analysis has been used to help identify key stratal surfaces. However, more detailed ichnofabric work would be useful and should be a consideration when planning future studies (refer to Chapter 7). Reference to relevant regional data, and comparisons with previous interpretations, will be presented throughout. The sedimentological descriptions and interpretations presented in Section 2.2 are used throughout this Section.

2.3.1 Sequence 1

In this interpretation the upper part of Sequence 1 is equivalent to the Nothe Grit Formation. Only one systems tract is evident. The sequence boundary of Sequence 1 is not thought to occur within the sediments of the Corallian Group and therefore will not be discussed further.

2.3.1a: *Sequence 1: Parasequence identification*

Observations in the field indicate that the Nothe Grit Formation is composed of two parasequences (between 0m-6.5m and 6.5m-10.4m on Fig.2.vi, marked by white arrows on Fig.2.vii). These parasequences are the two small-scale coarsening-up facies sequences described in Section 2.2.1. Each parasequence contains a slight but definite and gradual increase in grain size and is capped by a prominent coarse grained bioclastic sandstone bed

containing septarian concretions. The shelly material can be interpreted as an indication of winnowing as each parasequence shallows into a higher energy environment at the shoreface equilibrium depth. Each parasequence boundary is marked by an abrupt but slight upward decrease in grain-size and a weathered surface colour change from yellow to light grey (picked out clearly in Fig.2.vii). A change from a laterally cemented shelly sand containing septarian concretions, to a predominantly uncemented sand also occurs across these boundaries. Diagenetic analysis presented in Section 3.2.5a has been used to help confirm the parasequence interpretation.

2.3.1b: *Sequence 1: Systems tract identification*

The highstand systems tract:

Although there are only two of them, the parasequences become thinner within an overall gradual coarsening-up succession (Fig.2.vi). With a fair degree of certainty, the reasoning presented in this thesis suggests that the two parasequences represent the top part of a progradational parasequence set. Van Wagoner *et al.* (1990) state that such a pattern could indicate progradation within a highstand systems tract. However, recent work by Church & Gawthorpe (1997) has indicated that the identification of systems tracts based on parasequence stacking patterns alone should be treated with a degree of caution. Their work indicates that basinal thickness trends should be considered when applying parasequence stacking patterns to systems tract identification. The logistical constraints on this research have meant that no such data was collected and this should be a priority in the planning of for future work (refer to Chapter 7).

The boundary separating the Nothe Grit Formation from the underlying Oxford Clay Formation, has already been described as conformable with no evidence of erosion or down-cutting (Section 2.2.1). This implies that an overall coarsening-up and shallowing-up succession occurs from the top of the deeper-water Oxford Clay Formation to the top of the shallower-water Nothe Grit Formation. It is not thought to represent a sequence boundary, but merely a transition from the inner shelf to lower shoreface environments (see Walker & Plint, 1992, fig.14) during normal progradation.

Previous & alternative sequence stratigraphic models:

The previous sequence stratigraphic interpretations of the Nothe Grit Formation (Fig.2.iii) are that: -

- the surface separating the Nothe Grit Formation from the underlying Oxford Clay Formation represents a sequence boundary (either type-1 or type 2, Rioult *et al.*, 1991 and Coe, 1995). Sun (1989) and Rioult *et al.* (1991) suggest that this boundary resulted from a relative sea-level fall that is comparable to a global eustatic sea-level fall at the end of the early Oxfordian (Hallam, 1978; Haq *et al.*, 1987); and,
- the Nothe Grit Formation represents either a lowstand (Coe, 1995) or shelf-margin systems tract (Rioult *et al.*, 1991).

The re-interpretation of the Nothe Grit Formation based on field observations and reasoning presented in this thesis, is that it represents the top part of a highstand systems tract. The evidence for this is:

1. At the lithostratigraphic boundary between the Nothe Grit Formation and the marine mudstones of the underlying Oxford Clay Formation (as interpreted by Wright, 1986b) there is no sedimentological evidence (erosion, down-cutting and abrupt shallowing) to support the identification of a type-1 sequence boundary[1]. Although sequence boundaries in marine successions can be traced laterally into correlative unconformities, there is no evidence for such an unconformity elsewhere in Dorset. A review of borehole data from North Dorset (Henderson, 1997), implies that a conformable sequence, with no evidence of erosion or down-cutting, occurs between the Oxford Clay Formation and the Hazelbury Bryan Formation (North Dorset Nothe Grit Formation equivalent). Bristow (1989) states that: "the lower boundary of the Hazelbury Bryan Formation is not well defined, as it is transitional with the Oxford Clay". This statement also implies that a conformable boundary exists between the two formations in North Dorset.

2. The dominantly low energy environment indicated by a lack of storm generated sedimentary structures within the Nothe Grit Formation, may indicate that there was no effective mechanism for removing sand from the shoreface environment into the deeper water setting represented by the Oxford Clay Formation. If this is so, the relatively abrupt facies change would not need to represent a major offshore shift in facies or, a sequence boundary (a similar explanation has been used for the base of the Safarujo Member, Ericeira Group discussed in Section 4.2.2).

[1] In a ramp setting (such as the depositional environment of the Corallian Group, a type-1 sequence boundary forms as a result of a period of forced regression (refer to Section 1.2.3a, page 17).

However, previous interpretations (e.g. Coe, 1995) have used this abrupt facies change as evidence for a sequence boundary.

3. Analysis of regional data (Coe, 1992, fig.25) does not indicate any stratal or biostratigraphic gap associated with this surface. It is suggested that the basin-wide incursion of sand at this time (as indicated by Coe, 1992, fig.25) could have occurred during the latter period of the highstand systems tract, when rates of sedimentation would have begun to outpace rates of accommodation creation resulting in net progradation of the shoreline (Posamentier & Vail, 1988). This would ultimately result in the deposition of a coarsening-up facies trend as reported in the field descriptions and lithostratigraphic interpretations presented in Section 2.2.1.

From the evidence and reasoning presented here the Nothe Grit Formation is more characteristic of deposition within a highstand systems tract. However, it should be noted that all interpretations (this, and previous research) are based on a limited number of exposures. Further field and analytical work is needed to unequivocally support any sequence stratigraphic interpretation of this unit. In Section 3.2.5, key diagenetic analyses of septarian concretions will be used to lend further support to the proposed sequence stratigraphic revision.

2.3.2 Sequence 2

Sequence 2 consists of the Preston Grit Member, the Nothe Clay Member and the lower 1.8m of the Bencliff Grit Member.

2.3.2a: *Sequence 2: Sequence boundary*

The lithostratigraphic boundary separating the Preston Grit Member from the Nothe Grit Formation is interpreted as the sequence boundary of Sequence 2. It has already been described and discussed in detail in Section 2.2.2a. In this account, a sequence boundary corresponding to a surface of forced regression is the preferred interpretation (Fig.2.viiia). This is based on three important pieces of evidence:

- Facies analysis (Section 2.2.2a) suggests that the Preston Grit Member was deposited in a shallower, higher energy depositional environment than the underlying Nothe Grit Formation, indicating that abrupt shallowing occurred across this boundary. The overlying Preston Grit Member (Section 2.3.2c) would then be classified as a lowstand deposit represented by a single shoreface or aggradational shoreface stack (*sensu* Ainsworth & Pattison, 1994).
- The boundary is erosional, implying a period of shoreface erosion associated with sequence boundary formation or base level fall.
- Wright (1986a) indicates that the boundary represents a stratal/biostratigraphic gap, although it is unclear from Wright whether this "gap" is based on evidence for stratal erosion or the absence of diagnostic ammonites. Again, this may indicate a period of shoreface erosion.

Alternative interpretations for the lithostratigraphic boundary are a transgressive surface of erosion or ravinement surface (Fig.2.viiib) as indicated by Coe (1995). This interpretation would agree with the erosional evidence presented for this boundary because shoreface erosion is also a common feature of ravinement surface formation (Reinson, 1992).

However, a transgressive surface implies shoreface retreat and the overlying facies (i.e. the Preston Grit Member) was deposited in deeper water than the underlying facies (i.e. the Nothe Grit Formation). This is not consistent with the facies evidence presented here and could only have occurred if shallower facies were deposited in the progradational phase of the Nothe Grit Formation, but were totally removed by erosion during transgression (e.g. Reinson, 1992; fig. 17).

Regional data (Coe, 1995) does not provide any additional evidence because in Oxfordshire strata immediately above the Lower Calcareous Grit (equivalent to the Nothe Grit Formation) is absent or unexposed. Therefore further evidence needs to be collected before this surface can be unequivocally interpreted.

2.3.2b: *Sequence 2: Parasequence identification*

The Preston Grit Member:

The Preston Grit Member (as described in Section 2.2.2a) can be interpreted as a single shoreface stack (*sensu* Ainsworth & Pattison, 1994) representing one coarsening-up parasequence (between 11.8m and 12.9m on Fig.2.vi) which is clearly overlain by a marine flooding surface. The abundant and varied fauna which is more abundant towards the top of the Preston Grit Member (Section 2.2.2a) would relate to a period of non-deposition (allowing more time for colonization) and prolonged marine flooding associated with parasequence boundary formation.

The Nothe Clay Member and lower 1.8m of the Bencliff Grit Member:

Within the Nothe Clay Member two parasequences can be identified (between 12.9m-17.3m and 22.4m-24.2m on Fig.2.vi). The lower parasequence coarsens-up from claystone to a bioturbated, bioclastic siltstone bed, the top of which is bored and is interpreted here as a marine hard-ground surface (Section 2.2.2b). This indicates shallowing above the level of wave winnowing and is consistent with an interpretation of a parasequence boundary. Hard-ground surfaces have been similarly used by Pope & Read (1997) to indicate parasequence boundaries in the Late Middle to Late Ordovician Foreland Basin Rocks of Kentucky and Virginia. The increase in faunal diversity towards the top of this parasequence is interpreted to be the result of either shallowing or a period of non-deposition that occurred during marine flooding at the parasequence boundary. The other laterally cemented siltstone beds that occur within this member cannot be interpreted as parasequence tops because they do not show any supporting evidence of shallowing. The interpretation of these beds has already been discussed in Section 2.2.2b.

The upper parasequence (from 22.4m-24.2m on Fig.2.vi) corresponds to the top of the Nothe Clay Member and the lower 1.8m of the overlying Bencliff Grit Member. It is a coarsening-up (from claystone to fine sandstone) and shallowing-up parasequence which contains a fauna typical of a reduced salinity environment (Whatley, 1965). The lithostratigraphic boundary between the Bencliff Grit Member and the underlying Nothe Clay Member (Section 2.2.2c) occurs within this parasequence.

2.3.2c: *Sequence 2: Systems tract identification*

The lowstand systems tract:

The Preston Grit Member (between 11.8m and 12.9m on Fig.2.vi) is interpreted as the lowstand systems tract of Sequence 2. As it directly overlies shoreface deposits of the Nothe Grit Formation, it can be interpreted as representing an "attached" shoreface (*sensu* Ainsworth & Pattison, 1994). It consists of one coarsening-up parasequence, as described in Section 2.3.2b.

Rioult *et al.* (1991) & Coe (1992, 1995) indicate that the Preston Grit Member represents a transgressive systems tract. This interpretation is plausible if the underlying lithostratigraphic boundary is interpreted as a transgressive surface, but it does not take into account the apparent shallowing of the depositional environment above the Nothe Grit Formation. Wilson (1991) indicates that the Preston Grit Member represents an upper lowstand wedge deposit.

The transgressive surface:

The upper bounding surface of the lowstand systems tract is defined by a surface of transgression (Ainsworth & Pattison, 1994). Thus, the lithostratigraphic surface separating the Nothe Clay Member from the underlying Preston Grit Member not only represents a parasequence boundary, but also a transgressive surface (at 12.9m on Fig.2.vi). It displays evidence of submarine erosion and reworking (associated with

periods of shoreface retreat) and marks the first deepening event after the deposition of the lowstand shoreface deposits. It probably also represents a prolonged period of non-deposition/marine flooding hi-lighted by the presence of an abundant and varied fauna.

Rioult *et al.* (1991) and Coe (1992, 1995) interpret this surface as a maximum flooding surface (MFS). By definition, an MFS should separate facies deposited during a maximum rate of relative sea-level rise below, from a decelerating rate of relative sea-level rise above (Posamentier & James, 1993). This would correspond to a gradual shallowing of the depositional environment above the boundary. However, facies analysis suggests that the lower part of the Nothe Clay Member was deposited in deeper water than the underlying Preston Grit Member.

The transgressive systems tract:

The lowest 4.5m of the Nothe Clay Member represents the transgressive systems tract of Sequence 2 (between 12.9m and ?17.3m on Fig.2.vi). It consists of one identifiable parasequence (Section 2.3.2b) and clearly represents a deeper marine depositional environment than the underlying Preston Grit Member; an interpretation that is supported by the ostracod data of Whatley (1965).

The zone of maximum flooding:

Due to a lack of parasequence identification in the remainder of the Nothe Clay Member, an MFS can not be clearly identified. However, a zone of maximum flooding (defined in

Section 1.2.3b) can be positioned within the Nothe Clay Member between ?17.3m and ?22.4m on Figure 2.vi because this most probably represents the deepest water facies of this sequence. It separates the transgressive systems tract below, from the highstand systems tract above.

The highstand systems tract:

The upper 0.5m of the Nothe Clay Member and lower 1.8m of the Bencliff Grit Member represent the highstand systems tract of Sequence 2 (between 22.4m-24.2m on Fig.2.vi). It consists of one coarsening-up and shallowing-up parasequence. Whatley (1965) suggests that any decrease of water depth (associated with a restricted, less saline environment) did not occur until the deposition of the upper Nothe Clay Member. This is likely to relate to highstand deposition when rates of relative sea-level rise begin to decelerate, resulting in shoreface progradation, a decrease in overall accommodation space and shallowing.

2.3.3: Sequence 3

Sequence 3 is composed of the upper 5m of the Bencliff Grit Member, the Upton Member and the lower two oolitic beds of the Shortlake Member (between 24.2m and 40.7m on Fig.2.vi, Bran Point outcrop).

2.3.3a: *Sequence 3: Sequence boundary*

A conformable surface, equivalent to a type-2 sequence boundary, is positioned in relation to the marine flooding surface of the parasequence that occurs at the top of the highstand systems tract of Sequence 2 (Section 2.2.2b and at 24.2m on Fig.2.vi). It is clearly marked on Figure 2.ix as relating to the lowermost mudstone bed of the Bencliff Grit Member. This sequence boundary does not relate to the lithostratigraphic boundary between the Bencliff Grit Member and the underlying Nothe Clay Member which occurs 1.8m below it (see enlargement photograph in Fig.2.ix). At the sequence boundary, there is no sedimentological evidence to indicate a fall in relative sea-level, such as an abrupt change in lithofacies, evidence of sub-aerial exposure or a biostratigraphic gap, supporting the interpretation that it represents a type-2 sequence boundary.

Regional data (Coe, 1992) indicate the presence of a stratal/biostratigraphic gap approximately correlatable to the base of the Bencliff Grit Member. This suggests that the conformable type-2 sequence boundary identified on the coast at this position, could be traced laterally into a correlative unconformity elsewhere in the basin (although evidence from North Dorset indicates that the Bencliff Grit Member is absent; Wright, 1981).

The positioning of this sequence boundary (based purely on field observations at the coastal sections) has been identified as the point at which there is a change in the style of parasequence stacking. The highstand systems tract of Sequence 2 consists of one coarsening-up parasequence (Section 2.3.2b), while the succeeding Bencliff Grit Member is composed of an aggradational stack of three fining-up parasequences (Sections 2.3.3b

and 2.2.3c). The positioning of the sequence boundary does not therefore correspond exactly to the lithostratigraphic boundary between the Nothe Clay Member and the Bencliff Grit Member (which would be positioned at 22.8m on Fig.2.vi and is no longer exposed at Osmington Mills).

Both Rioult *et al.* (1991) and Coe (1995) state that the sequence boundary is the lithostratigraphic surface separating the Bencliff Grit Member from the underlying Nothe Clay Member. These interpretations do not however, explain the change in parasequence stacking patterns that clearly occurs at the sequence boundary positioned at 24.2m on Figure 2.vi.

2.3.3b: *Sequence 3: Parasequence identification*

The Bencliff Grit Member:

The Bencliff Grit Member consists of three parasequences, each equivalent to one of the uniformly thick, sharp-based, fining-up facies association described in Section 2.2.2c (e.g. one occurs between 25.7m-27.4m on Fig.2.vi).

Parasequence boundaries (e.g. at 25.7m on Fig.2.vi) occur immediately above the finer heterolithic beds of each parasequence. These are sharp, probably due to current erosion during marine transgression prior to the deposition of the succeeding parasequence. Desiccation cracks identified by Talbot (1973) at the top of an heterolithic bed could represent shallowing and subaerial exposure associated with parasequence progradation.

The Upton Member (lower 5m):

The Upton Member is composed of two main coarsening-up parasequences (between 30m and 33.5m on Fig.2.vi) and a transgressive lag deposit (between 29.2m and 30m, Section 2.3.3c). The two parasequences are equivalent to the two coarsening-up facies associations described and identified in Section 2.2.3a. Both record an upward increase in faunal diversity, including an increasing abundance of bivalves such as *Chlamys qualicosta* and *Nanogyra* (Talbot, 1973; Wright, 1986a and Sun, 1989). Both are highly bioturbated, with *Diplocraterion, Arenicolites, Thalassinoides* and *Rhizocorallium* concentrated on and towards the upper surfaces. The upper surfaces of the parasequences are also bored, suggesting that early cementation occurred followed by winnowing and exposure of the hardened surface. This led to the formation of marine hard-grounds. Both the increase in faunal diversity and formation of hard-grounds provide clear evidence for the shallowing and drowning occurring during parasequence formation.

The Upton Member (upper 5.5m):

No parasequences were identified within the upper 5.5m of the Upton Member (equivalent to the *Thalassinoides* beds) due to a lack of clear evidence for shallowing-up.

The Shortlake Member:

The Shortlake Member consists of at least six coarsening-up parasequences, the lower two of which occur within Sequence 3. The remaining four parasequences will be described in their relevant sequence.

Both parasequences are equivalent to the lower two coarsening-up facies successions described in Section 2.2.3b. At the Bran Point outcrop, parasequences are generally thin (up to 1m thick) and coarsen-up/shallow-up from sandy/silty calcareous claystones (representing a low energy shelf depositional environment) to medium grained oolitic and sparsely bioclastic packstones and grainstones (representing higher energy shoreface sands, Section 2.2.3b).

At the Black Head outcrop, parasequences thicken laterally (e.g. between 35.6m-38.6m on column 3 of Fig.2.vi) and are associated with down-cutting into the underlying silty claystones. The oolitic grainstones are thicker and contain trough cross-bedding indicating a dominant flow towards the southwest and a subordinate flow towards the west-northwest (also noted by Wilson, 1968b, 1975; Wright, 1986a; Sun, 1989; Fig.2.xiii & Fig.2.xiv). Intraclasts, mud-draped wave ripple laminations indicating a southwest-northeast wave oscillation direction and mud-draped foreset laminae are also common within these parasequences. As noted earlier, these parasequences are interpreted to be deposited in tidal inlets (Section 2.2.3b).

2.3.3c: *Sequence 3: Systems tract identification*

The shelf-margin systems tract[2]*:*

The shelf-margin systems tract of Sequence 3 is represented by the upper 5m of the Bencliff Grit Member (between 24.2m-29.2m on Fig.2.vi) and is composed of the three, uniformly thick, fining-up parasequences. These stack to form a dominantly aggradational parasequence set.

The dominance of *Rhizocorallium irregulare* at the top of the Bencliff Grit Member (29.2m on Fig. 2.vi) indicates the onset of a more tranquil depositional environment (Section 2.3.2c). This would be expected to occur towards the end of a shelf-margin systems tract (or lowstand systems tract) when rates of relative sea-level are beginning to rise at an increasingly rapid rate.

Returning to the second question which I posed in Section 2.2.2c, that is - why are storm dominated sedimentary structures only prevalent in the Bencliff Grit Member of the Corallian Group? - the answer may be connected with changes in basin hydro-dynamics controlled by relative sea-level changes.

[2] The term shelf-margin systems tract is applicable because rather than relating to platform geometry, it relates to a particular rate of relative sea-level rise distinguishing it from a lowstand systems tract. Posamentier & James (1993) state that; "at a type-2 unconformity, no relative sea-level fall occurs to punctuate the succession. Rather the manifestation of a deceleration and then acceleration of relative sea-level rise will be a change from an increasingly to decreasingly progradational and subsequently aggradational stacking pattern"

Changes in relative sea-level can alter shelf bathymetry, shelf physiography and also basin hydro-dynamics, such that the effects of large storm events become prevalent at certain periods within the history of the basin (Pickering, 1995). Relative sea-level rises may then preserve the storm generated bed forms, as discussed previously in Section 2.2.2c. Changes in relative sea-level have been interpreted as being responsible for large scale storm events within the Jurassic period (e.g. the Middle Jurassic Bridport Sands, Pickering, 1995). Changes in relative sea-level may be the key as to why storm beds are not prevalent in other shoreface successions of the Corallian Group (e.g. the Nothe Grit Formation, the Shortlake Member).

The transgressive surface:

The surface that separates the Bencliff Grit Member from the overlying Upton Member has already been interpreted as a transgressive surface (Section 2.2.3a and at 29.2m on Fig. 2.vi & Fig.2.ix). The overlying Upton Member represents a more open marine depositional environment than that of the underlying Bencliff Grit Member and, as a result, this surface marks the first major deepening event of Sequence 3. Due to this important observation, this surface can not represent a surface of forced regression, which would imply a basinward shift in facies associated with a fall in relative sea-level and abrupt shallowing.

The transgressive systems tract:

The overlying 5m of the lower part of the Upton Member (between 29.2m-?35.9m on Fig.2.vi) represents the transgressive systems tract of Sequence 3 and was deposited within a shoreface environment during a period of rapid relative sea-level rise. The transgressive systems tract is composed of a transgressive lag deposit and at least two shallowing-up parasequences (described in Section 2.3.3b).

The transgressive lag deposit is represented by the lowest oolitic and bioclastic bed of the Upton Member (at 29.5m on Fig.2.vi). It contains reworked lithoclasts, ooids and whole or fragmented bioclastic material. Similar transgressive lags are common on marine flooding surfaces that occur due to a relative sea-level rise (Van Wagoner *et al.*, 1990).

The upper part of the transgressive systems tract is composed of the nodular micritic limestone of the lower *Thalassinoides* beds (between 33.4m-35.9m on Fig.2.vi). This represents a deeper water environment than that of the underlying parasequences indicating continued gradual relative sea-level rise.

The zone of maximum flooding:

The zone of maximum flooding has been positioned between 35.9m-38.9m on Figure 2.vi and is composed of the same nodular micritic limestones that are present at the top of the underlying transgressive systems tract. It separates the dominantly retrogradational transgressive systems tract below from the progradational highstand systems tract above

and probably represents the deepest depositional environment of Sequence 3 (see Section 2.2.3a). Identifying parasequences within this zone is difficult due to a lack of clear water depth criteria and the positioning of a maximum flooding surface based on parasequence stacking patterns within this zone is not possible.

Rioult *et al.* (1991) has suggested that a maximum flooding surface should correspond to the top of the *C. qualicosta* bed, while Coe (1992, 1995) has suggested the top of the pisolite bed. However, neither suggestion takes into account changes in the depositional environment. By definition, a maximum flooding surface should separate a deepening succession below, from an increasingly shallower one above. There is no sedimentological evidence to suggest that the *Thalassinoides* beds were deposited in increasingly shallower water than the underlying pisolite bed. The clear evidence for deepening, is the presence of *Thalassinoides* burrows indicating a subtidal environment (Fürsich, 1973).

The highstand systems tract:

The overlying highstand systems tract of Sequence 3 is composed of the lower two parasequences of the Shortlake Member and thickens laterally towards the west, a feature also observed by Wright (1986a), Sun (1989) and Coe (1995).

2.3.4: Sequence 4

Sequence 4 consists of the middle to upper 4.5m of the Shortlake Member and the Nodular Rubble Member.

2.3.4a: *Sequence 4: Sequence boundary*

A type-2 sequence boundary is thought to separate Sequence 3 from Sequence 4. Its location corresponds to the flooding surface of the upper parasequence of Sequence 3 marked by large blue arrows on Figure 2.xi. Lithostratigraphically it occurs within a thin mudstone layer, beneath the "middle white oolite bed" of Arkell (1947a).

The lithostratigraphic base of the Shortlake Member (as defined by Wright, 1986a; white arrows on Fig.2.xi) is not thought to represent a sequence boundary even though it represents an abrupt shift of facies. This surface represents a surface of tidal inlet accretion and downcutting associated with progradation during the development of a parasequence within the underlying highstand systems tract (refer to Section 2.2.3b).

Regional data (Coe, 1992) identify an important stratal/biostratigraphic gap approximately equivalent to the Upton Member/Shortlake Member lithostratigraphic boundary on the Dorset Coast (refer to Coe, 1992, fig.25). Within the Oxfordshire area, Coe (1995) provides evidence for erosion associated with this surface. This would suggest that it represents a type-1 sequence boundary (although Coe, 1995 does not use sequence stratigraphic terminology). However, at the coastal exposures there is no evidence for a

biostratigraphic gap or a period of sub-aerial exposure. Coe (1995) interprets her conformable/erosive surface (green arrows, Fig.2.xi) in south Dorset as an equivalent of a surface identified in Oxfordshire. Coe's (1995) overlying lowstand deposits are carbonate dominated, although several workers (e.g. Cant, 1995 and Emery & Myers, 1996), suggest that deposition after a relative sea-level fall in a carbonate depositional environment is generally dominated by siliciclastic deposition. A good example of this type of "facies partitioning" can be found within the Ericeira Group of west central Portugal (refer to Section 4.2.3).

Based on field evidence alone, my interpretation that a type-2 sequence boundary is the coastal equivalent of the type-1 sequence boundary observed by Coe (1995) in Oxfordshire, is plausible. Many workers (e.g. Emery & Myers, 1996) now believe that type-1 and type-2 sequence boundaries can pass laterally into one another (depending on basinal processes). Clearly more analytical work is needed at the coastal exposures in order to resolve this problem and this is taken further in Section 3.3.3, where results from early diagenetic studies are used to provide support for this model.

2.3.4b: *Sequence 4: Parasequence identification*

The middle to upper Shortlake Member:

The middle to upper Shortlake Member consists of at least four coarsening-up parasequences. The lower of these parasequences is similar in characteristics to the upper two parasequences of the underlying highstand systems tract. This parasequence relates to

the "middle white oolite bed" (Arkell, 1936). However, the upper three parasequences display very different geometries, primarily related to a change in the depositional setting from tidal inlet channels below to a deeper marine shoal environment above (refer back to Section 2.2.3b). Each of the three parasequences has a sheet-like geometry (as inferred by Wilson, 1968b, 1975) with no evidence of lateral thickening and, relate to the three coarsening-up facies associations described in Section 2.2.3b (e.g. one such parasequence is positioned between 41.6m-44.1m on Fig.2.vi and can be viewed in Fig.2.xv). The higher density and diversity in marine fauna (*Exogyra, Ostrea* and *Placunopsis*) within the coarser grained beds of each parasequence (refer back to Section 2.2.3b) is interpreted to be related to periods of non-deposition associated with marine flooding and parasequence boundary formation. The associated cut-off of sediment supply would provide favourable conditions for such epifaunal growth.

The Nodular Rubble Member:

Parasequences could not be identified within this member due to a lack of clear shallowing-up indicators.

2.3.4c: *Sequence 4: Systems tracts identification*

The shelf-margin systems tract[3]*:*

A thin shelf-margin systems tract of Sequence 4 is interpreted to correspond to the shallowing-up tidal inlet parasequence of the "middle white oolite bed" (*sensu* Arkell, 1947a, between 38.6m-41.6m on column 3 of Fig.2.vi). This parasequence represents a similar depositional environment to those of the highstand systems tract of Sequence 3. Coe (1992) has also identified a thin lowstand deposit which is approximately equivalent to this bed.

The transgressive surface:

A transgressive surface is positioned immediately above the "middle white oolite bed" (Arkell, 1947a) and is identified by red arrows on Fig.2.xi. The location of this surface is in agreement with Rioult *et al.* (1991) and Coe (1992). It marks a distinct deepening of the depositional environment from shallow water tidal inlets below (e.g. as in Fig.2.xiii) to a deeper marine shoal environment above (e.g. as in Fig.2.xv). This observation is in agreement with Wright (1986a) and is clearly observed at the Black Head outcrop.

[3] refer to footnote in Section 2.3.3c

The transgressive systems tract:

The transgressive systems tract of Sequence 4 corresponds to at least the three coarsening-up and sheet-like parasequences of the upper part of the Shortlake Member (above the "middle white oolite bed" of Arkell, 1947a) and, probably extends into the lower part of the Nodular Rubble Member (between 41.6m and ?50m on Fig.2.vi).

The change in sedimentation patterns and bed geometries, from tidal inlets of the shelf-margin systems tract to a nearshore, deepening shoal environment of the transgressive systems tract, is a consequence of deepening associated with the commencement of transgression. This interpretation is also supported by Wright (1986a). Further deepening occurred towards the top of the transgressive systems tract corresponding to the deposition of the lower Nodular Rubble Member. This represented a return to a low energy, oxygenated shelf environment, deeper than the upper Shortlake Member and similar to that of the deepest water environment of Sequence 3 (i.e. the *Thalassinoides* Beds).

The zone of maximum flooding:

The zone of maximum flooding must be contained within the Nodular Rubble Member which represents the deepest water facies of Sequence 4. Within the Nodular Rubble Member, a thin claystone occurs at 51.2m on Figure 2.vi which could indicate a period of condensation associated with a maximum flooding surface. However, without the aid of parasequence identification a maximum flooding surface can not be positively identified.

Rioult *et al.* (1991) and Coe (1995) have interpreted the lithostratigraphic boundary between the Shortlake Member and the overlying Nodular Rubble Member as representing a maximum flooding surface. If this was so then, by definition, it should separate deepening facies from overlying shallowing facies. There is no sedimentological evidence to suggest that the Nodular Rubble Member was deposited in shallower water than the underlying Shortlake Member.

The highstand systems tract:

There is very little sedimentological evidence for the highstand systems tract of Sequence 4. By definition, the facies above the maximum flooding surface marks the commencement of progradation and thus the highstand systems tract. Therefore, the upper Nodular Rubble Member above the ?MFS (between ?51.3m and 52.1m on Fig.2.vi) would be equivalent to at least the basal expression of a highstand systems tract. However, this cannot be substantiated by facies analysis alone. The top of the Nodular Rubble Member is characterised by an irregular and undulatory surface that also represents a major hiatus. Wright (1986a) states that the whole of the overlying *nunningtonense* subzone is missing, implying that a major period of erosion, non-deposition or winnowing occurred. This surface is likely to represent the overlying sequence boundary (Section 2.3.5a). Clearly, further analytical work is necessary before a highstand systems tract can be unequivocally identified within this sequence at this location. However, regional data (Coe, 1995) indicates that the equivalent strata in Oxfordshire is the Coral Rag Member which was likely to have been deposited during a period of regression associated with a highstand systems tract.

2.3.5 Sequence 5

Sequence 5 consists of the Trigonia Clavellata Formation and the overlying Sandsfoot Clay Member of the Sandsfoot Formation (between 52.1m & 66.6m on Fig.2.vi).

2.3.5a: *Sequence 5: Sequence boundary*

A type-1 sequence boundary is positioned beneath the Trigonia Clavellata Formation, equivalent to the lithostratigraphic boundary that separates this formation from the underlying Nodular Rubble Member (Fig.2.xvi and at 52.1m on Fig.2.vi). The field characteristics of this surface, along with oxygen and carbon isotope analysis (Coe, 1995), has already been discussed in Section 2.2.4a. All evidence is consistent with a period of subaerial exposure during the formation of this sequence boundary. Further assessment of regional data (Coe, 1992, fig.25) indicate a large stratal/biostratigraphic gap associated with this surface, extending across the Wessex Basin.

A shallowing of facies above this sequence boundary (Section 2.2.4a), together with evidence of fresh water cementation, winnowing and a large biostratigraphic gap indicate that the sequence boundary formed in response to an abrupt fall in relative sea-level resulting in an abrupt basinward shift in facies. Subsequent deposition of shoreface deposits (the Sandy Block Member, refer to Section 2.2.4a) indicates that the sequence boundary formed as a result of forced regression. In a ramp setting (which the Corallian Group may represent) it is now believed that forced regressions are generally the result of abrupt falls in relative sea-level (Emery & Myers, 1996).

This sequence boundary cannot represent a type-2 sequence boundary as indicated by Rioult *et al.* (1991). The abrupt shallowing of the depositional environment, coupled with the identification of a large biostratigraphic gap and bulk rock stable isotope data of Coe (1995), indicate that an abrupt fall in relative sea-level and subsequent subaerial exposure/erosion must have occurred.

2.3.5b: *Sequence 5: Parasequence identification*

The Trigonia Clavellata Formation:

As a result of a lack of shallowing-up indicators, it is difficult to identify parasequences within this formation. In North Sea cores, the presence of *Thalassinoides seuvica* in has been used to locate the position of firm grounds, associated with periods of marine flooding (R. Goldring, *pers. comm.*). The presence of similar burrows within the Sandy Block Member (refer back to Section 2.2.4a) could therefore indicate similar flooding surfaces associated with parasequence boundary formation.

The Sandsfoot Clay Member:

No parasequences have been identified within this member due to a lack of facies and sedimentary structures which would help determine water depths.

2.3.5c: *Sequence 5: Systems tracts identification*

The lowstand systems tract:

The Sandy Block Member is interpreted to represent the lowstand systems tract of Sequence 5 (between 52.1m and 54m on Fig.2.vi and Fig.2.xvi). The characteristics of this member have already been discussed in Section 2.2.4a. It was deposited during a period of relative sea-level fall and slow subsequent relative sea-level rise, in a distinctly shallower depositional environment than the underlying Nodular Rubble Member.

The transgressive surface:

A transgressive surface is positioned at the lithostratigraphic boundary between the Sandy Block Member and the overlying Chief Shell Beds Member (at 54m on Fig.2.vi and Fig.2.xv). As previously discussed in Section 2.2.4b, it marks the first abundance of the bivalve *Myophorella clavellata* which can be associated with a return to a more open marine environment. Overlying this (the lowest bed of the Chief Shell Beds Member) is a classic transgressive lag deposit, the features of which have been described in Section 2.2.4b.

Abundant *Myophorella* were also noted towards the top of the Preston Grit Member (refer back to Section 2.2.2b) which was not interpreted as a transgressive lag deposit. This is because the abundance occurs immediately beneath a transgressive surface, rather than above it. However, the abundance of the bivalve still indicates prolonged marine flooding

associated with a period of marine transgression.

Coe (1992) suggests that the transgressive surface should be amalgamated with the sequence boundary, indicating that the lowstand systems tract is completely missing. Her reasoning for this appears to be the presence of a demonstrable biostratigraphic gap at this surface (Trigonia Clavellata Formation lithostratigraphic boundary) and that the overlying Trigonia Clavellata Formation represents a transgressive succession. This is a plausible explanation, although it does not explain the sudden profusion of the bivalve *M. clavellata* at the Sandy Block Member and Chief Shell Beds Member lithostratigraphic boundary.

The transgressive systems tract:

The Chief Shell Beds Member, Red Beds Member and at least the lower 1.8m of the Sandsfoot Clay Member, are interpreted to represent the transgressive systems tract of Sequence 5 (between 54m and ?60m on Fig.2.vi and Fig.2.xv). The upwards change in facies from the relatively shallow water Chief Shell Beds to the deeper water Sandsfoot Clay Member, represents a continual deepening associated with a rapid rise in relative sea-level and marine transgression.

The zone of maximum flooding:

The zone of maximum flooding occurs within the Sandsfoot Clay Member and has been positioned between ?60m and ?65m on Figure 2.vi as this probably represents the deepest water facies of this sequence. As parasequences could not be identified within this

member, it would be unjustifiable to attempt to locate a maximum flooding surface.

Coe (1995) indicates that the maximum flooding surface should be positioned at the lithostratigraphic boundary between the Red Beds Member and the overlying Sandsfoot Clay Member. The positioning of a maximum flooding surface at this stratigraphic horizon implies that the overlying succession represents the onset of progradation. There is no sedimentological evidence to indicate that the Sandsfoot Clay Member was deposited within shallower water than the underlying Red Beds Member.

The highstand systems tract:

Due to an absence of parasequences, the sedimentological identification of the highstand systems tract of Sequence 5 is again unjustifiable (based on facies analysis alone). Regional data (Coe, 1992) does not give any indication of a highstand systems tract that could relate to the top part of the Sandsfoot Clay Member.

2.3.6: Sequence 6

Sequence 6 consists of the Sandsfoot Grit Member, the Ringstead Waxy Clay Member and the Osmington Mills Ironstone Member (between 66.6m & 74.8m on Fig.2.vi).

2.3.6a *Sequence 6: Sequence boundary*

A type-1 sequence boundary, that formed as a result of a period of forced regression, is positioned at the lithostratigraphic boundary between the Sandsfoot Grit Member and the underlying Sandsfoot Clay Member (at 66.6m on Fig.2.vi). Its erosional characteristics have been described in Section 2.2.5b. The field and biostratigraphic evidence clearly indicate an abrupt fall in relative sea-level and a subsequent basinward shift in facies belts. Deposition during a fall in relative sea-level and subsequent lowstand has resulted in the deposition of a "detached" lowstand systems tract (Section 2.3.6c). This lowstand systems tract (Sandsfoot Grit Member) could represent the "detached" lowstand equivalent of the Preston Grit Member (which was identified as an attached lowstand systems tract; refer back to Section 2.3.2c and Ainsworth & Pattison, 1994).

2.3.6b: *Sequence 6: Parasequence identification*

The Sandsfoot Grit Member:

At least one parasequence has been identified within the Sandsfoot Grit Member, relating to the coarsening-up facies succession identified in Section 2.2.5b. It is capped by a thin clay layer, which represents a period of non-sedimentation and marine flooding associated with parasequence boundary formation. Small sideritic, phosphatic and hollow, tube-like iron-oxide concretions are concentrated towards the top of this parasequence (at 69m on Fig.2.vi). An analysis of the early diagenetic phases associated with these concretions is used to provide further evidence to support the identification of this parasequence (Section

3.3.6). A second parasequence may be present above the thin clay layer, but could not be clearly identified (e.g. between 69.7m-71.2m on Fig.2.vi).

The Ringstead Formation:

The Ringstead Waxy Clay Member and the Osmington Mills Ironstone Member together correspond to one shallowing-up parasequence (between 71.2m-74.8m on Fig.2.vi). The base of the parasequence is characterised by calcareous clays containing sparse ferruginous ooids, sand grains and an impoverished macrofauna (Brookfield, 1978; Coe, 1995). In contrast, the top consists of sandy, iron-rich, calcareous clays and a diverse, shallow marine fauna (Talbot, 1973, 1974; Brookfield, 1978; Wright, 1986a and Coe, 1995). The upper surface of the parasequence contains abundant marine fauna (refer to Section 2.2.6b for details) and is interpreted to represent a period of non-deposition and marine flooding associated with parasequence boundary formation.

2.3.6b: *Sequence 6: Systems tract identification*

The lowstand systems tract:

The Sandsfoot Grit Member is interpreted to represent the lowstand systems tract of Sequence 6. This interpretation is based on two key points:

1. The shoreface succession was deposited after a period of forced regressions as a result of an abrupt basinward shift in facies and a fall in relative sea-level. Examples of

shoreface sequences prograding over surfaces of forced regression are well documented (e.g. sharp-based shoreface sandbodies of the Cardium Formation, Walker & Plint, 1992). This interpretation is different to that offered for the boundary between the Nothe Grit/Oxford Clay Formations (refer back to Section 2.3.2a) because at the lower boundary of the Sandsfoot Grit Member, there is clear sedimentological and biostratigraphic evidence for an unconformity.

2. The upper bounding surface of the Sandsfoot Grit Member marks a distinct deepening of the depositional environment from shoreface sandstones to deeper water mudstones, representing transgression.

Coe (1995) has interpreted the Sandsfoot Grit Member as representing a transgressive systems tract and its lower bounding surface to be an amalgamated sequence boundary and transgressive surface. Her evidence for this is based on the large biostratigraphic gap (Fig.2.iv) and erosional evidence that occurs at the Sandsfoot Grit Member, Sandsfoot Clay Member lithostratigraphic boundary. Based on the limited outcrop, her interpretation is equally plausible.

The transgressive surface:

The transgressive surface of Sequence 6 is positioned at the lithostratigraphic boundary between the Sandsfoot Grit Member and the overlying Ringstead Waxy Clay Member (at 71.2m on Fig.2.vi). The positioning of this surface is based on an abrupt change in facies from shallow marine shoreface sediments of the lowstand systems tract to deeper marine facies of the overlying transgressive systems tract. Wright (1986a) also indicates that this

boundary corresponds to a short lived, poorly developed, stratal/biostratigraphic gap (Fig.2.iv) which could indicate a period of sub-marine erosion and non-deposition associated with a marine transgression.

The transgressive systems tract:

At least the lower beds of the transgressive systems tract occur within the Corallian Group sediments. The transgressive systems tract corresponds to the coarsening-up parasequence that is equivalent to the Ringstead Waxy Clay Member and the overlying Osmington Mills Ironstone Member (between 71.2m-74.8m on Fig.2.vi).

2.4: *Discussion*

Within Section 2.3, the Corallian Group of south Dorset has been divided into six sequences with each sequence being further divided into systems tracts and, where possible, parasequences. Within this section, the overall significance of the succession is discussed in terms of sequence frequency, sea-level falls during a "green-house" period and siliciclastic/carbonate partitioning within sequences.

2.4.1: Sequence frequency, "green-house" period & facies partitioning

2.4.1a: *Sequence frequency*

The concept of sequence frequency reflecting a eustatic signal has been well documented by Van Wagoner *et al.* (1990) and Mitchum & Van Wagoner (1991). The eustatic signal can consist of the addition of sea-level curves of different frequencies and amplitudes superimposed onto a curve of average sedimentation rate for a particular basin or different parts of a basin. Within the context of this work, sequences are the product of third-order relative sea-level changes, on the time scale of 1-10 million years. These sequences are divisible into systems tracts and shallowing-up parasequences. Parasequences are thought to be the product of smaller scale fourth and fifth order relative sea-level changes on the time scale of 10,000-100,000 years, but maybe due to autocyclic processes too, particularly in deltaic settings where local cut-off of sediment supply can be dramatic.

Figure 2.xvii has been modified from Van Wagoner *et al.* (1990) to illustrate the sequence frequency within the Corallian Group succession of south Dorset. Simple sedimentary logs illustrating typical systems tracts, have been positioned to show their relationship to a relative sea-level curve. An enlargement of this curve is also displayed showing it to be made up of periods of parasequence progradation and parasequence drowning. Parasequence drowning is associated with a period of non-deposition and the formation of a parasequence boundary. The length of time of parasequence progradation and drowning, is dependent on its location within a parasequence set and the type of systems tract.

Generally, the Corallian Group in this field area was deposited during a long term sinusoidal relative sea-level rise, that has been punctuated by three periods of shallowing (Sequence Boundaries 1, 4 and 5). None of these periods of shallowing resulted in prolonged (if any) sub-aerial exposure or were associated by deep fluvial incision.

Sequence Boundaries 2 and 3 do not represent a relative sea-level fall, but rather the change from a decelerating to accelerating rate of relative sea-level rise. Overall however, it is clear that sedimentation rates were in balance with rates of relative sea-level change.

2.4.1b: *"Green-house" periods*

The amplitude of the different orders of relative sea-level change has varied through geological time, with the presence or absence of polar ice caps controlling the higher orders of sea-level change (Tucker, 1993). The Phanerozoic has been divided into various "ice-house" and "green-house" periods, based on the Earth's glacial record (Veevers, 1990). During "green-house" periods, such as the Oxfordian, a lack of polar ice caps resulted in small scale relative sea-level changes most likely of the order of, 1 to 10 metres amplitude (Tucker, 1993). This contrasts sharply with relative sea-level changes of 10 to 100 metres during an "ice-house" period (Tucker, 1993). The small scale changes in relative sea-level during a "green-house" period could still result in forced regressions (Sequence Boundaries 1, 4 and 5 on my model) but the degree of offlap would be limited. Similarly the duration of sub-aerial exposure associated with a fall in relative sea-level would be short and this had obvious consequences for the degree of surface related diagenesis (discussed further in Chapter 3 and Chapter 6).

The lack of periods of prolonged sub-aerial exposure at sequence boundaries within the Corallian Group is interpreted as a reflection of a lack of polar glaciation during the Upper Jurassic.

2.4.1c: *Facies partitioning*

Facies partitioning within mixed siliciclastic/carbonate sequences has been well documented (e.g. Mack & James, 1986; García-Mondéjar & Fernández-Mendiola, 1993;

and Osleger & Montañez, 1996).

During periods of falling sea-level, the landward portion of a carbonate ramp may become exposed. Any subsequent siliciclastic sediment supply may overwhelm carbonate production and a siliciclastic lowstand systems tract may be established across the old carbonate ramp surface (Emery & Myers, 1996).

Within the Corallian Group succession, facies partitioning is especially apparent within Sequence 3 and 5. In Sequence 3, the siliciclastic shelf-margin systems tract is associated with a major period of siliciclastic deposition which began within the early Oxfordian. The subsequent transgressive and highstand systems tracts were then dominated by carbonate deposition. In Sequence 5, the siliciclastic lowstand systems tract is associated with a type-1 sequence boundary which resulted in a small fall in relative sea-level.

However, facies partitioning is not apparent in some of the sequences of the Corallian Group. In Sequence 4, all systems tracts are pre-dominantly carbonate rocks. This is because there was no fall in relative sea-level at Sequence Boundary 3 and thus the underlying carbonate beds were not subaerially exposed. Alternatively for this sequence, if the transgressive surface had amalgamated with the sequence boundary due to wave/tidal ravinement, the lowstand systems tract would have been removed.

2.5: *Concluding Remarks*

The sequence stratigraphic framework that has been constructed in this chapter, identifies high frequency sea-level changes within a succession, by relating depositional environments to parasequences, systems tracts and key stratal surfaces. Listed below are

the key points of this chapter:

1. Field work and facies analysis of the coastal sections around Osmington Mills has divided the Corallian Group into six sequences.
2. Facies and grain-size analyses have identified coarsening-up and fining-up parasequences (e.g. within the Upton Member and Bencliff Grit Member, respectively).
3. Parasequence boundaries have been identified on the basis of, abrupt changes in lithology, truncation, hard-ground or ravinement surface development, an increase in the abundance of burrowing organisms and fauna and, an abrupt deepening of the depositional environment (e.g. hard-ground development at the top of parasequences within the Upton Member).
4. Major transgressive surfaces have been interpreted as representing the first major deepening event in each sequence (e.g. the Bencliff Grit Member/Upton Member lithostratigraphic boundary).
5. Using only facies analysis, maximum flooding surfaces were unidentifiable, due to a lack of clear water depth indicators which made parasequence identification unjustifiable. Instead, Maximum flooding zones were defined for each sequence. These zones always corresponded to the deepest water depositional environment of the sequence (e.g. the *Thalassinoides* beds of Sequence 3).
6. Type-1 sequence boundaries were identified where there was clear evidence for a period of forced regression. All such boundaries were associated with a stratal/biostratigraphic gap and were capped by a shoreface facies (e.g. the Sandsfoot Clay Member/Sandsfoot Grit Member lithostratigraphic boundary). However, at some horizons containing similar features, not enough data was available to unequivocally support a facies based, sequence stratigraphic interpretation (see below).

7. Type-2 sequence boundaries were identified on the basis of a change in the style of parasequences/parasequence stacking patterns and/or where there was no evidence of an abrupt offshore shift in facies. This has led to a slight re-positioning of some sequence boundaries when compared to previous interpretations (e.g. at the first mudstone bed within the Bencliff Grit Member). However, further diagenetic evidence is needed to unequivocally support these facies based interpretations.

Finally, although this is a new, higher resolution interpretation of the Corallian Group succession, it is recognised that within the limitations of the work and the current coastal exposures, only a relatively small amount of section was analysed. Therefore throughout this Chapter frequent reference to previous interpretations (and regional data) has occurred and, where necessary, more than one explanation has been offered (e.g. the Nothe Grit/Preston Grit boundary). This research has attempted to provide a high resolution sequence stratigraphic model for the Corallian Group of south Dorset, using a similar approach to that established by Van Wagoner *et al.* (1990). There is no doubt however, that this approach can not be applied as easily as in the examples from Van Wagoner *et al.* (1990). The main reasons for this are:

- difficulty in clearly defining parasequences due to a lack of clear relative water depth indicators. This is probably due to the relatively protected nature of the shoreface sediments;
- a difficulty in clearly defining some stratal surfaces (for the same reasons as stated above); and,
- relatively poor quality, non-continuous exposure.

Clearly, the identification of some stratal surfaces and units requires further work and in Chapter 3, an analysis of early diagenetic phases is used to help resolve sequence stratigraphic arguments. Listed below are some of the key areas where early diagenesis will be used to help resolve these arguments and following each point, is a brief description as to why and how early diagenetic analysis will be utilised;

- parasequence identification within the Nothe Grit Formation. It is clear that the small scale cycles (?parasequences) that are present within this Formation are controlling the distribution of septarian concretions. A diagenetic analysis of these concretions may help to support a parasequence based model;
- systems tract identification of the Nothe Grit Formation. Similarly a comparison of the volumes of key authigenic phases within the septarian concretions, may help to resolve whether relative sea-level was rising or falling and thus what systems tract the formation is likely to represent;
- parasequence identification within the Nothe Clay Member. A similar investigation to the Nothe Grit Formation will be implemented;
- identification and positioning of the sequence boundary at the base of the Bencliff Grit Member. Changes in the volume of key early diagenetic cements may be linked to changes in sedimentation rates and the amount of available accommodation space, both of which should vary around sequence boundaries ;
- identification of parasequences within the Bencliff Grit Member. Early diagenetic concretions appear to be controlled by small scale cycles (?parasequences). A diagenetic analysis of these concretions may help to support a parasequence based model;
- identification of parasequences within the Upton and Shortlake Member. Early

diagenetic cements appear to be controlled by small scale cycles (?parasequences);

- identification and location of the sequence boundary within the basal beds of the Shortlake Member. An analysis of the volumes of key early diagenetic cements may help to resolve this; and,
- identification of parasequences within the Trigonia Clavellata Formation and Sandsfoot Grit Member. Early diagenetic cements/concretions appear to be controlled by small scale cycles (?parasequences).

These points are discussed further in the following chapter.

Fig. 2.i: The location of Osmington Mills (also enlarged), Sandsfoot Castle & Ringstead Bay

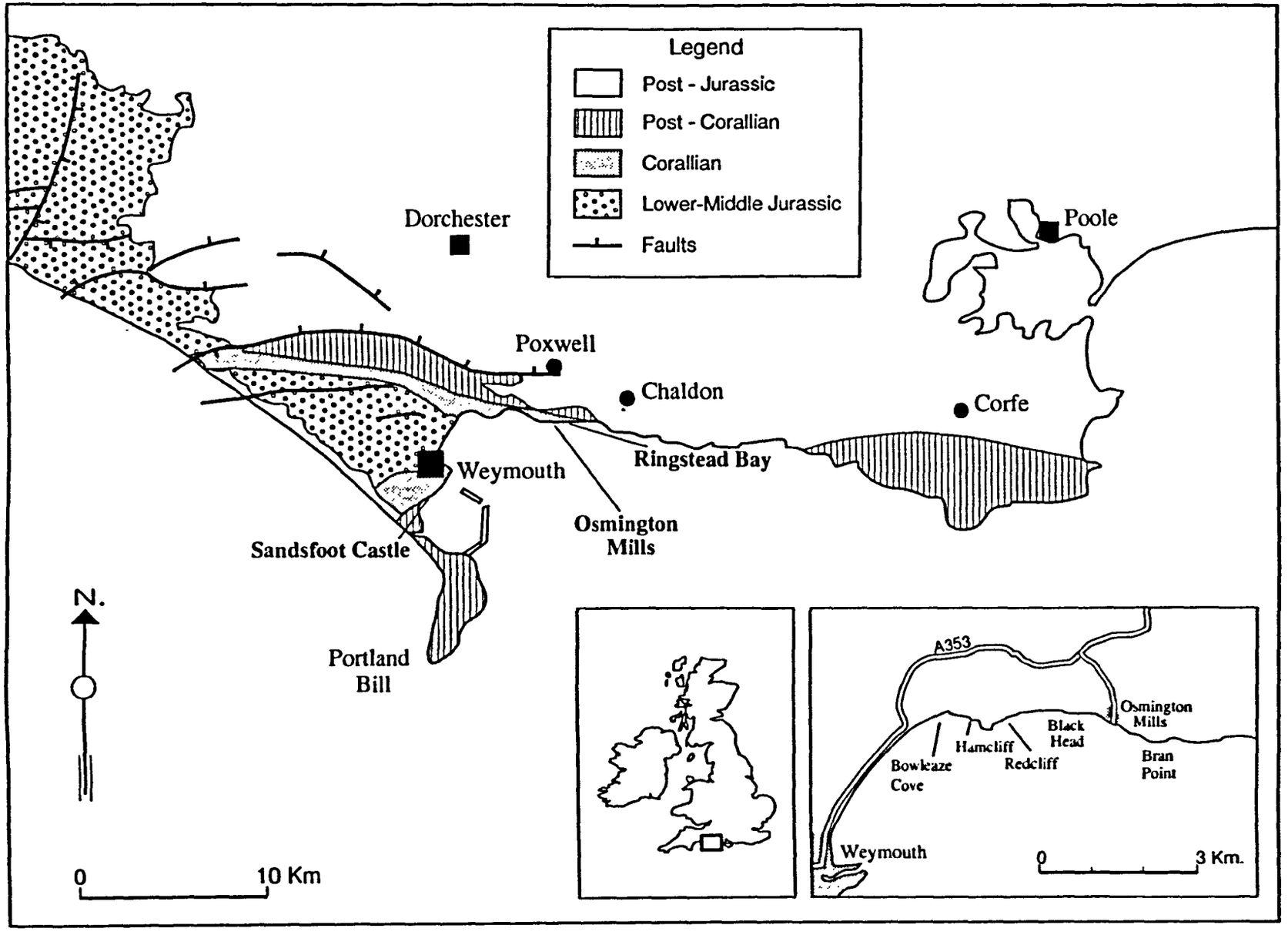

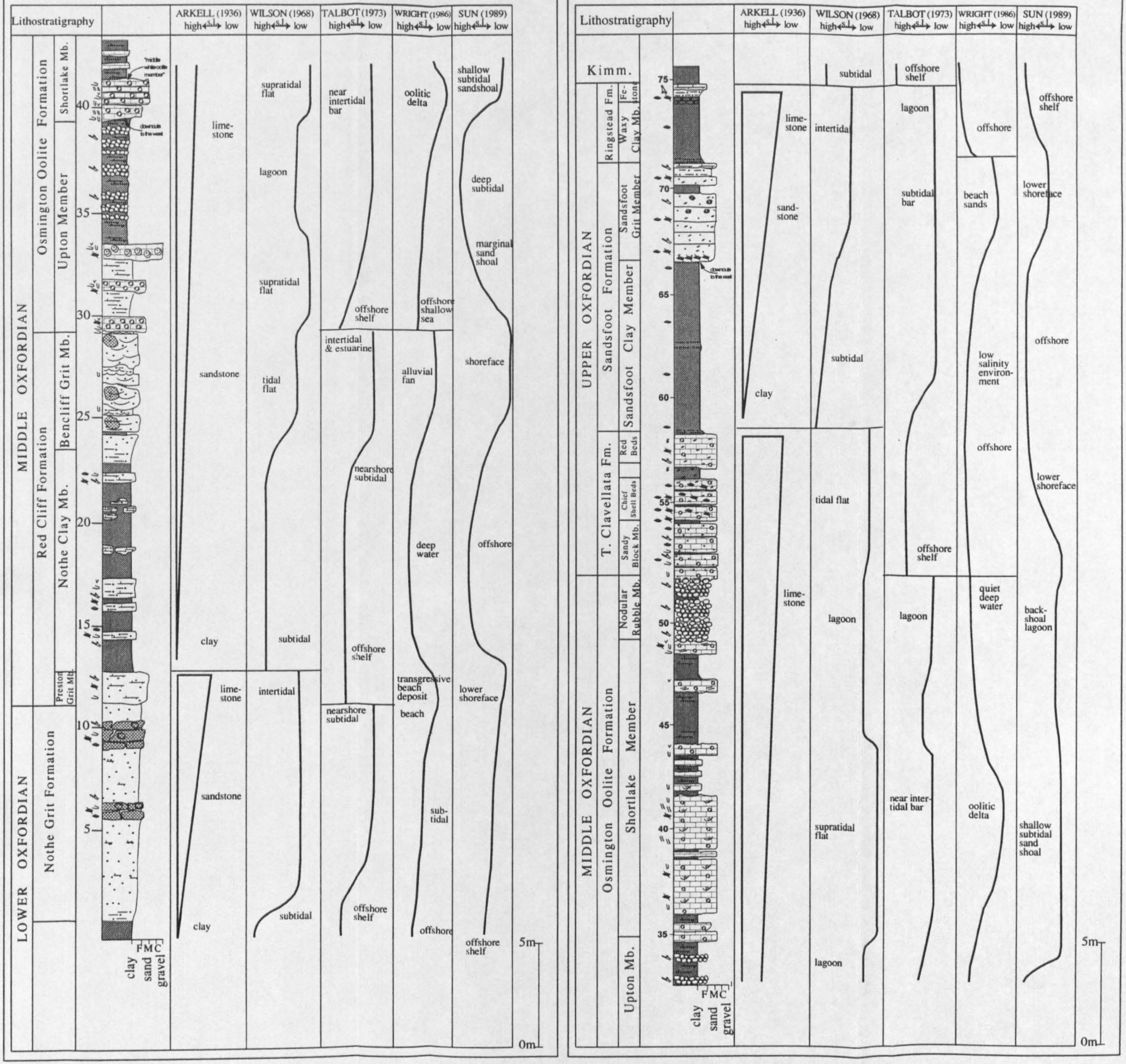

Fig. 2.ii: Previous interpretations of the Corallian Group of south Dorset (modified from Sun, 1989)

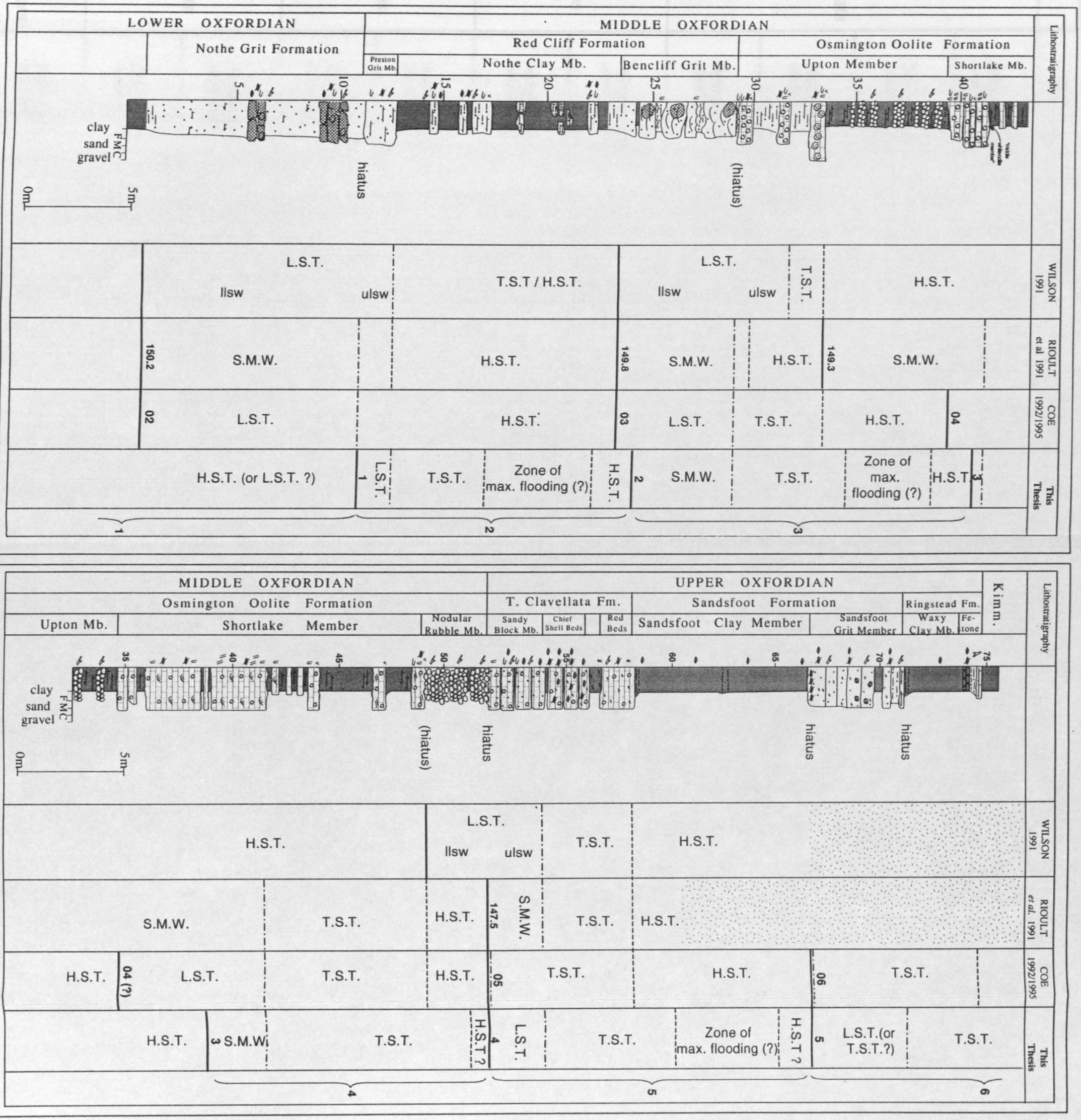

Fig. 2.iii: Previous sequence stratigraphic interpretations of the Corallian Group of south Dorset (including location of stratal/biostratigraphic hiatus' & a comparison with this thesis)

ZONE	SUBZONE	FORMATION/MEMBER
Ringsteadia pseudocordata	*Ringsteadia evoluta*	Ringstead Formation — Ironstone/ Coralbed Member, Waxy Clay Member
	Ringsteadia pseudocordata	Sandsfoot Formation — Sandsfoot Grit Member
	Ringsteadia pseudoyo	
	Ringsteadia caledonica	
Perisphinctes cautisnigrae	*Perisphinctes variocostatus*	Sandsfoot Formation — Sandsfoot Clay Member (?)
	Perisphinctes cautisnigrae	Trigonia Clavellata Formation — Red Beds Member, Chief Shell Beds Member, Sandy Block Member
Perisphinctes pumilus	*Amoeboceras nunningtonense*	
	Perisphinctes parandieri	Osmington Oolite Fm. — Nodular Rubble Member
Perisphinctes plicatilis	*Perisphinctes antecedens*	Osmington Oolite Fm. — Shortlake Member, Upton Member
	Cardioceras vertebrale	Red Cliff Fm. — Bencliff Grit Member, Nothe Clay Member, Preston Grit Member
Cardioceras cordatum (pars)	*Cardioceras cordatum*	Nothe Grit Formation

Fig. 2.iv: Ammonite biostratigraphy of the Corallian Group of south Dorset (after Sykes & Calloman, 1979; Wright, 1986a; Sun, 1989 & Coe 1995)

Fig. 2.v: Sedimentary logs and suggested depositional environments of the Corallian Group of south Dorset (also included are field locations for each log)

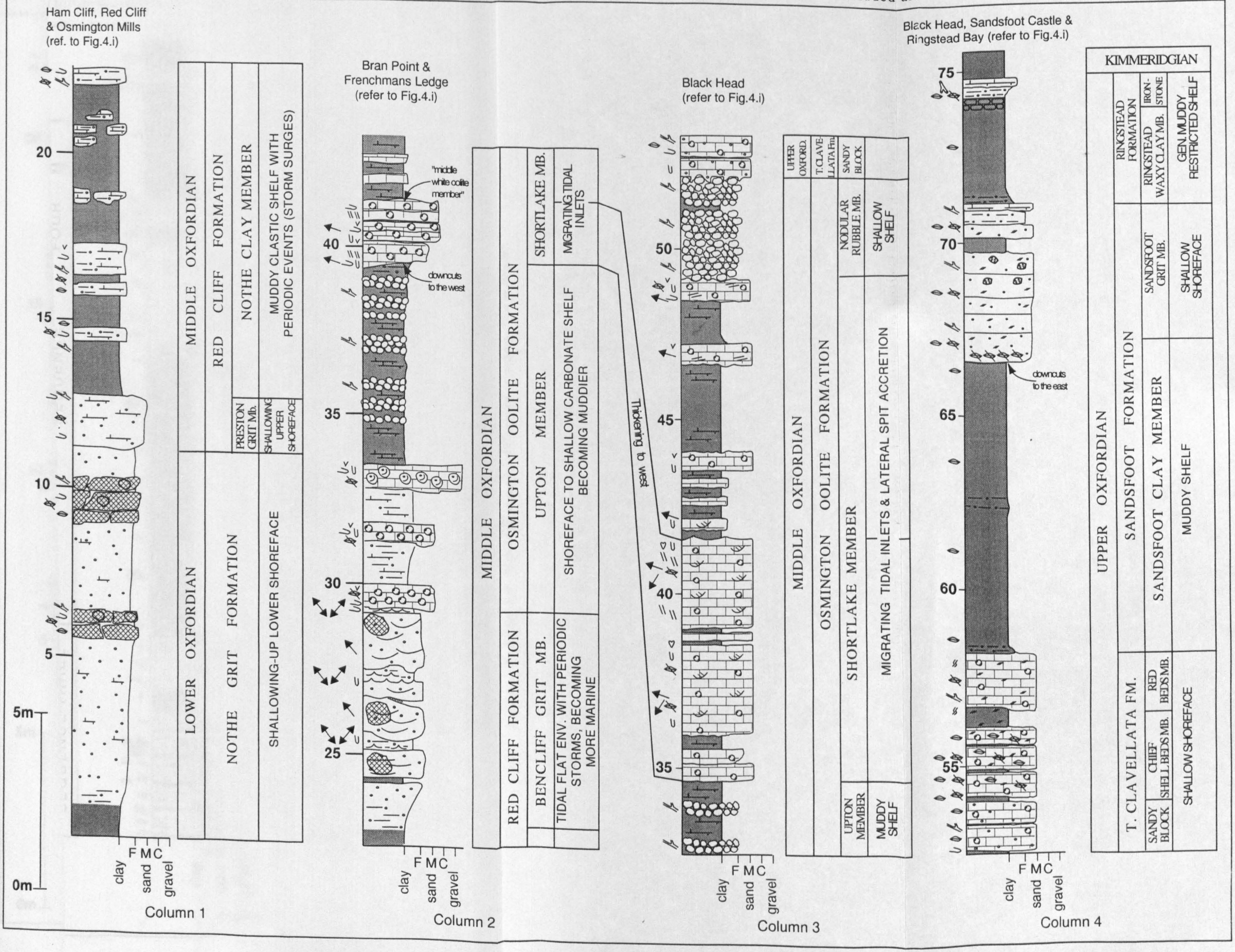

Fig. 2.vi: Sedimentary logs and suggested sequence stratigraphy interpretation of the Corallian Group of south Dorset (lithostratigraphy & field locations of logs as for Fig.2.v)

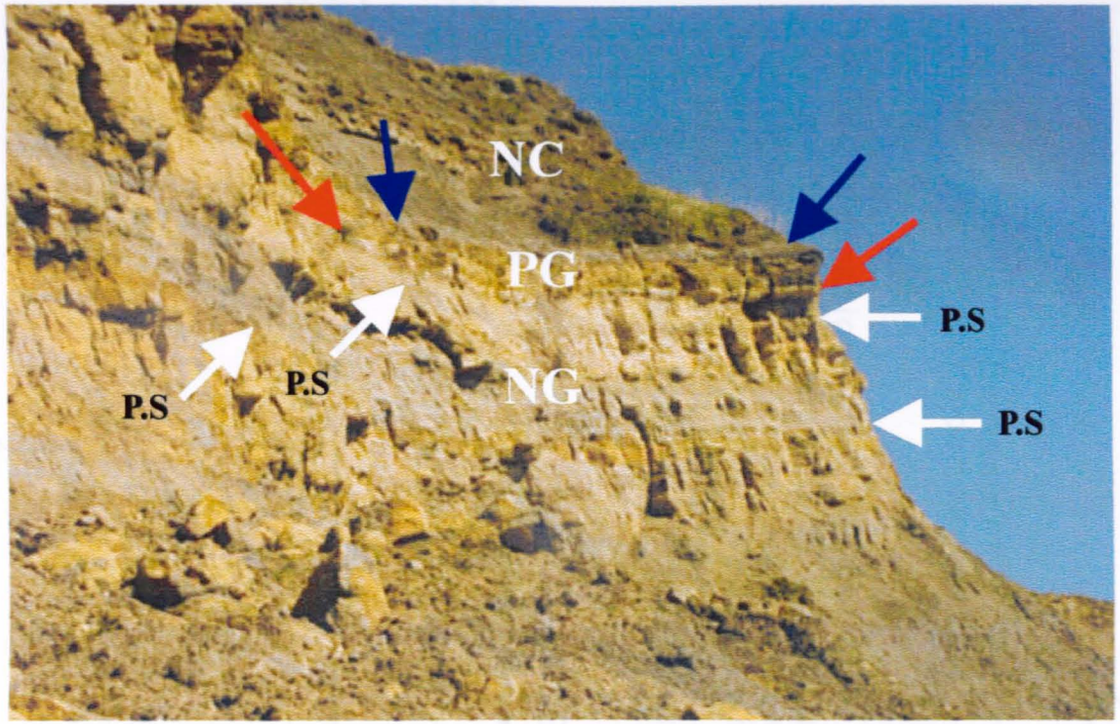

Fig. 2.vii: The Nothe Grit Formation (NG), Preston Grit Member (PG) & the Nothe Clay Member (NC)
White arrows indicate the tops of coarsening-up parasequences (P.S) within the Nothe Grit Fm.
In this interpretation, the Nothe Grit Formation represents a HST. Red arrows indicate position of a sequence boundary interpreted to have form ed as a result of a period of forced regression.
Alternative explanations indicate that it represents a transgressive surface.

The overlying Preston Grit Mb. represents a LST (or TST ?) & a shallow upper shoreface environment. Blue arrows indicate position of a well developed transgressive surface.
The lower Nothe Clay Mb. represents a deeper water depositional environment and the basal beds of a transgressive systems tract.
(see Sections 2.2.1, 2.2.2, 2.3.1 & 2.3.2 for further and alternative explanations).

Location: Red Cliff S.Y. 715814 (For scale, cliff section is approx. 15m in height)

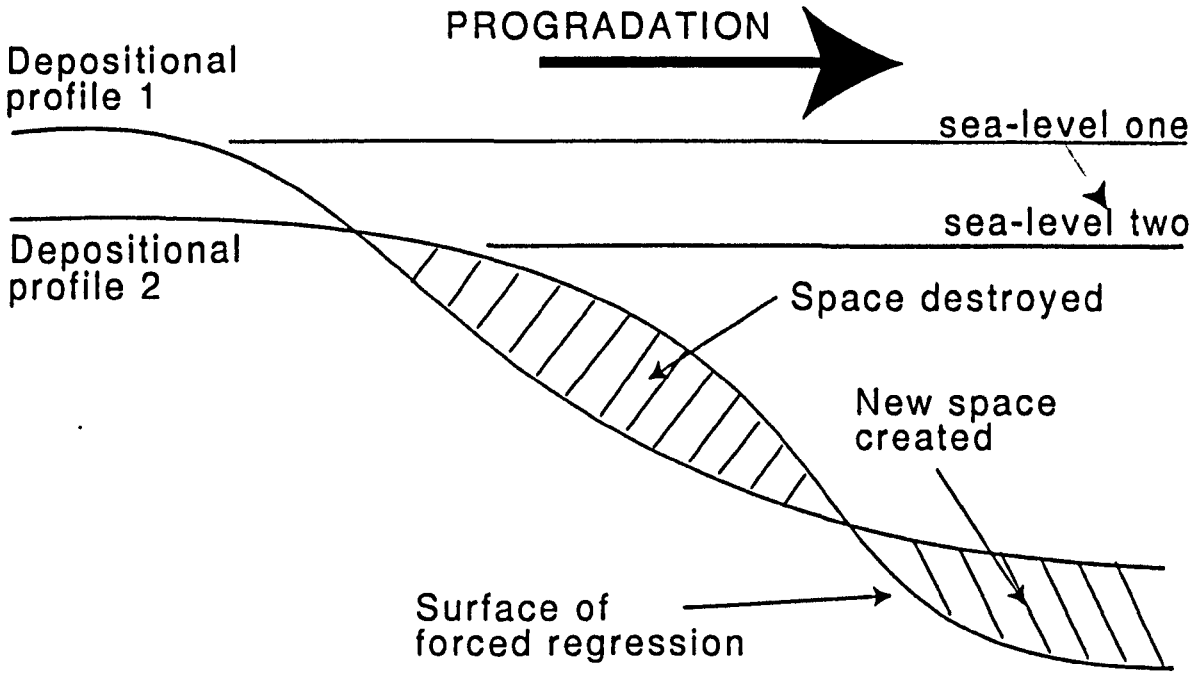

A: Forced regression (after Walker & Plint, 1992)
Sharp base interpreted to be the result of progradation due to a relative sea-level fall. This would cause wave scouring of the inner shelf, resulting in shoreface progradation over an erosive surface (e.g. the Cardium Formation of Alberta)

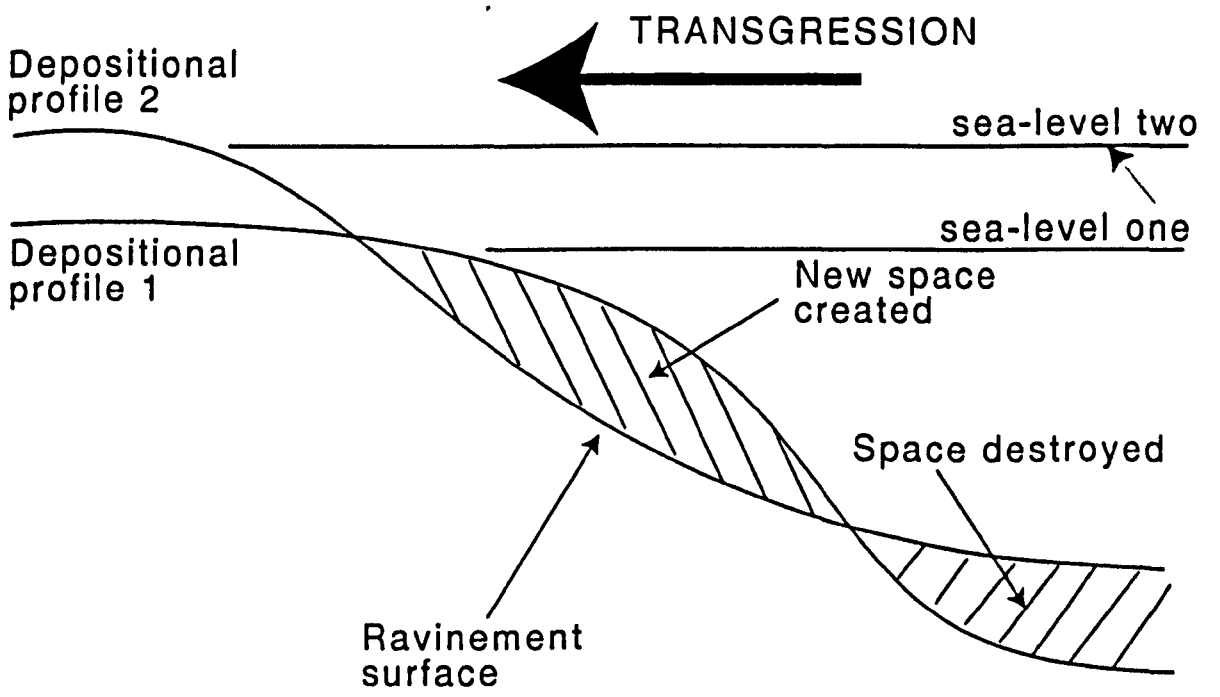

B: Ravinement surface (after Reinson, 1992)
As an upper shoreface zone moves landwardand upward during continued transgression, it will erode barrier wash-over and lagoon facies to form a planar erosive surface (ravinement surface) upon which the redistributed lower shoreface-inner shelf sands are deposited.

Fig.2.viii: Two alternative interpretations for the Nothe Grit/Preston Grit lithostratigraphic boundary

Fig. 2.ix: Bencliff Grit Member (BG), Upton Member (UM) & Shortlake Member (SM). Black arrows indicate parasequence tops, blue arrows indicate position of transgressive surfaces & red arrows indicate position of type-2 sequence boundaries. White arrows indicate the position of a conformable and laterally erosive surface that has been attributed to lateral accretion of tidal inlets or tidal/wave ravinement.
Bencliff Grit Member represents a shelf-margin systems tract, the lower Upton Member represents a transgressive systems tract and the upper Upton Member & lower Shortlake Member (up to the type-2 sequence boundary) represents a highstand systems tract. The overlying beds of the Shortlake Member represent a shelf-margin systems tract of Sequence 4.
(see Sections 2.2.3, 2.2.4, 2.3.3 & 2.3.4 for further explanation)

Location: Frenchman's Ledge
S.Y. 739814 (For scale, the cliff section is approx. 15m in height)

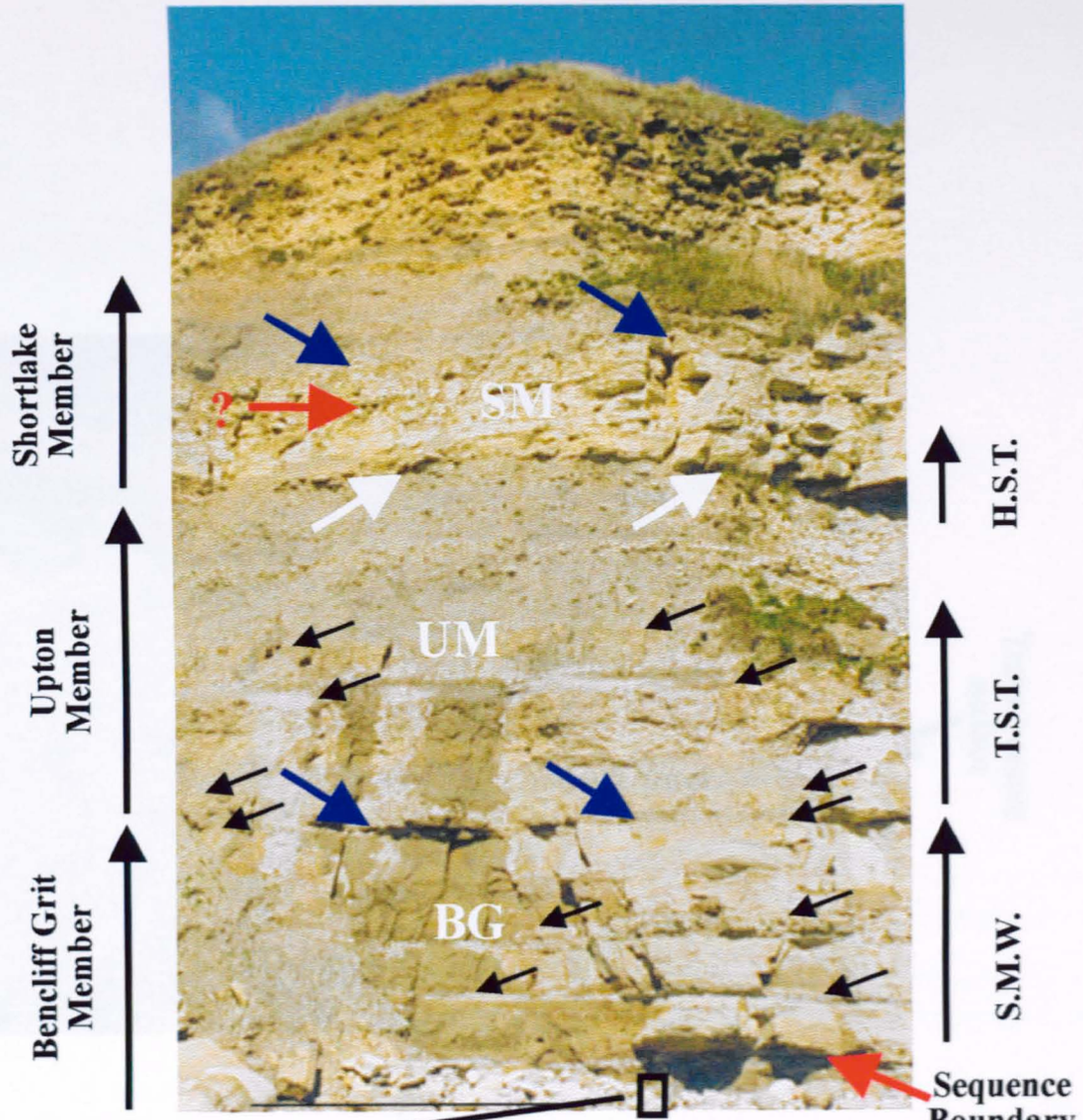

Blow-up of basal unit of the Bencliff Grit Member, clearly showing the gradational contact with the underlying Nothe Clay Member (below the 100% clay line). For scale the trowel 250mm in length

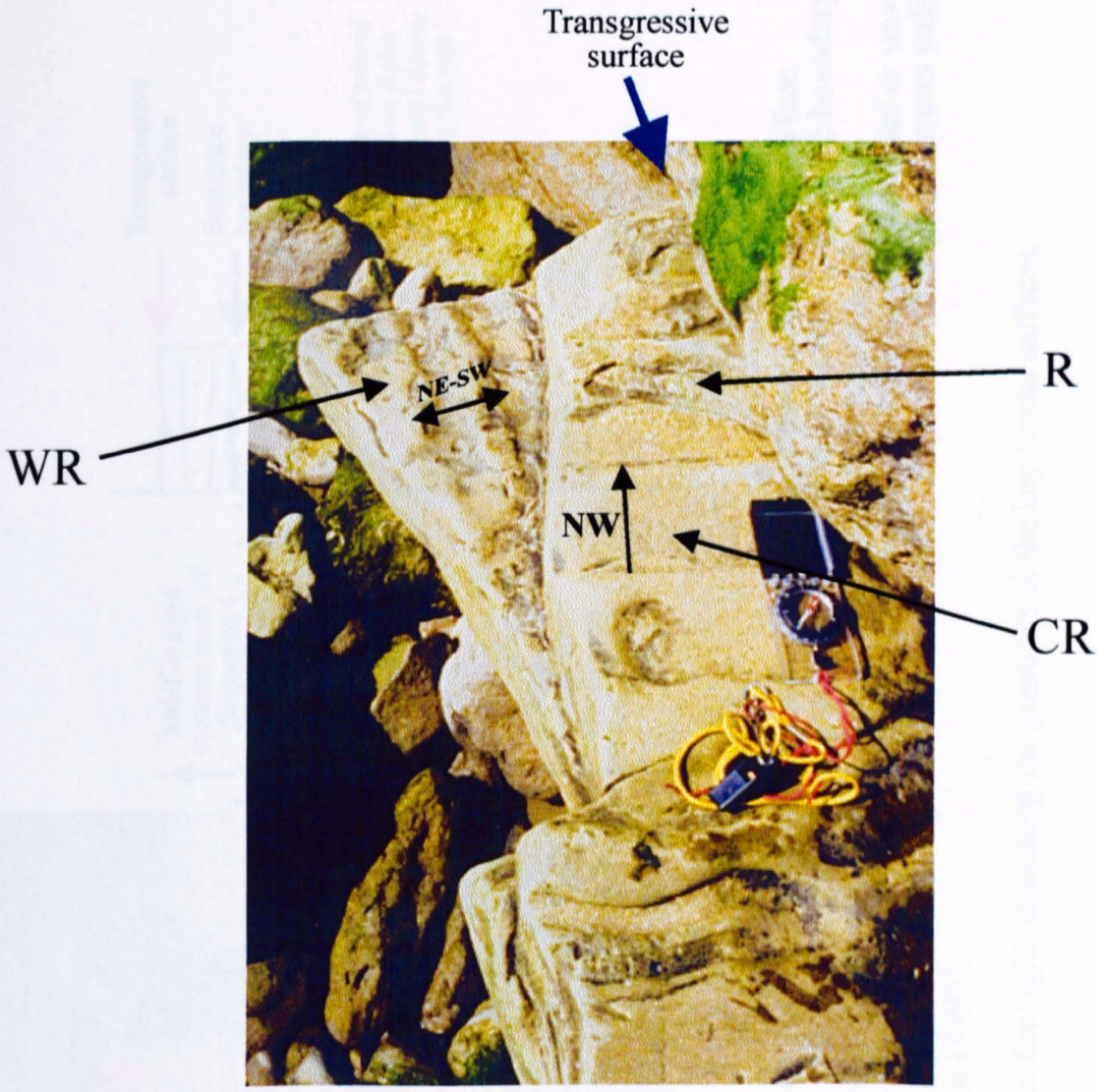

Fig. 2.x: Top heterolithic bed of Bencliff Grit Member. Note current ripples (CR), wave ripples (WR) & *Rhizocorallium irregulare* (R). Note that in this example Rhizocorallium burrows are foreign to the Bencliff Grit Member, & penetrate down from the overlying Upton Member. A transgressive surface is positioned immediately above this bed, as located by the blue arrow.

The Bencliff Grit Member represents the shelf-margin systems tract of Sequence 3

(see Section 2.2.3 & 2.3.3 for further explanation)

Location: Bran Ledge S.Y. 743813 (For scale, the compass/clinometer is 180mm in length)

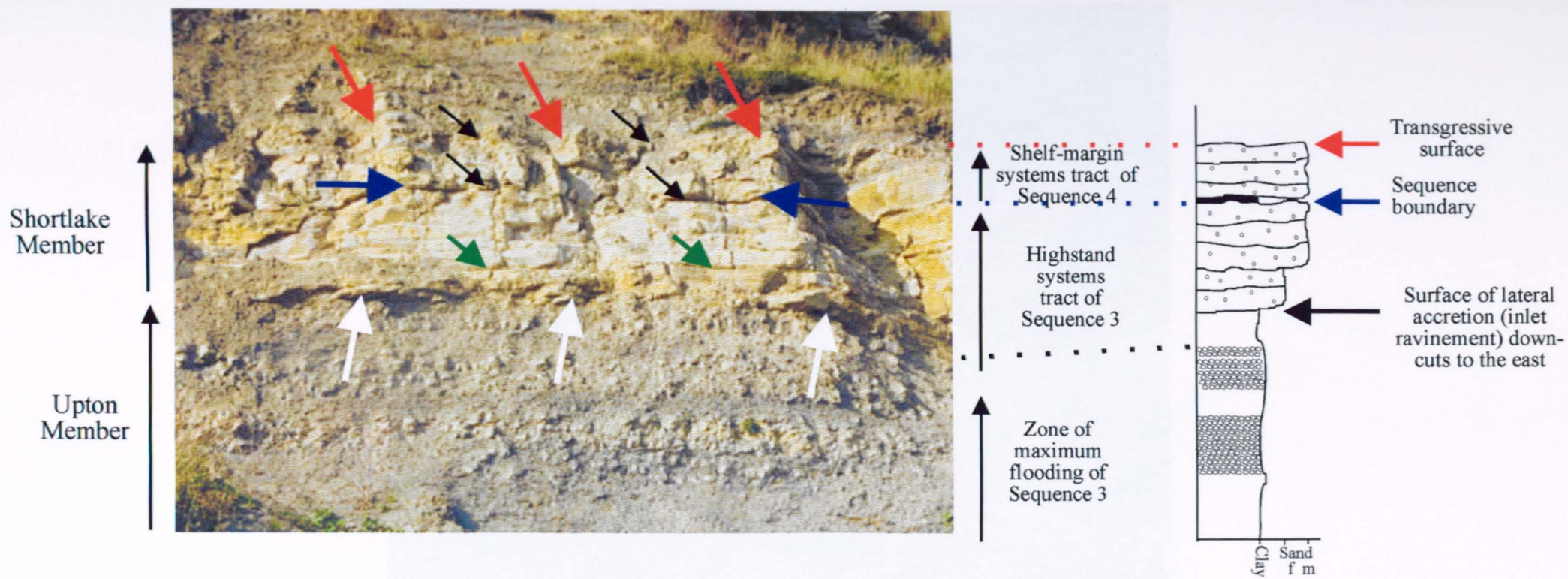

Fig. 2.xi: The lower beds of the Shortlake Member at Bran Point. White arrows indicate lithostratigraphic boundary/lower conformable surface which relates to lateral accretion of tidal inlets/tidal or wave ravinement. Blue arrows indicate the position of the type-2 sequence boundary that separates Sequences 3 and 4. Red arrows indicate position of the transgressive surface of Sequence 4. Black arrows indicate the tops of two coarsening-up parasequences. Note that the conformable surface relating to lateral tidal inlet accretion/tidal or wave ravinement (white arrows) is contained within the lower parasequence of the highstand systems tract of Sequence 3. The green arrows indicate the position of this conformable surface as interpreted by Coe (1995).

An annotated sketch log of the field-slide is also displayed on the right, indicating the positions of the key stratal surfaces.

(see Sections 2.2.3, 2.2.4, 2.3.3 & 2.3.4 for further and alternative explanations)

Location: Bran Point S.Y. 744814 (For scale, the cliff section is approx. 5m in height)

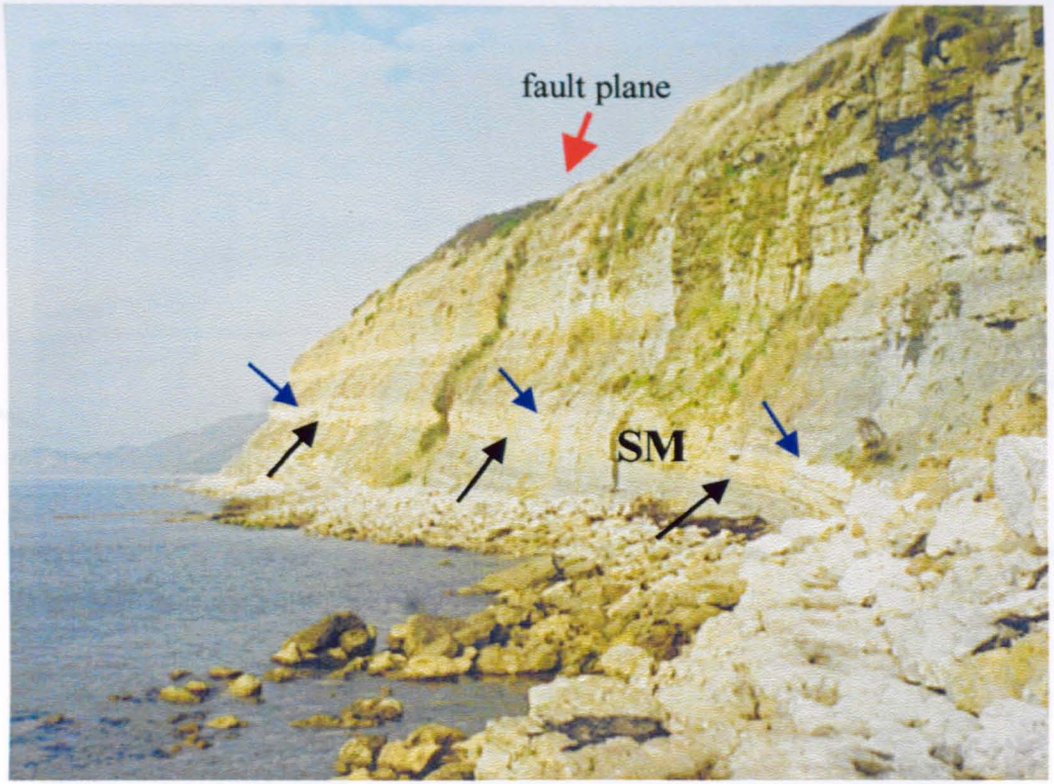

Fig. 2.xii: Lateral variations within the lower Shortlake Mb. (SM). Black arrows indicate position of a conformable (middle-ground) & erosive (back-ground) surface, which represents a surface of tidal inlet lateral accretion or wave/tidal ravinment. Blue arrows indicate the position of the transgressive surface of Sequence 4, which is also visable in the fore-ground. Note the location of a normal fault in the middle-ground of the phorograph. Photograph taken looking west.

(see Section 2.2.4 & 2.3.4 for further explanation)

Location: Bran Point S.Y. 744814 (Cliff section in background is approx. 25-30m in height).

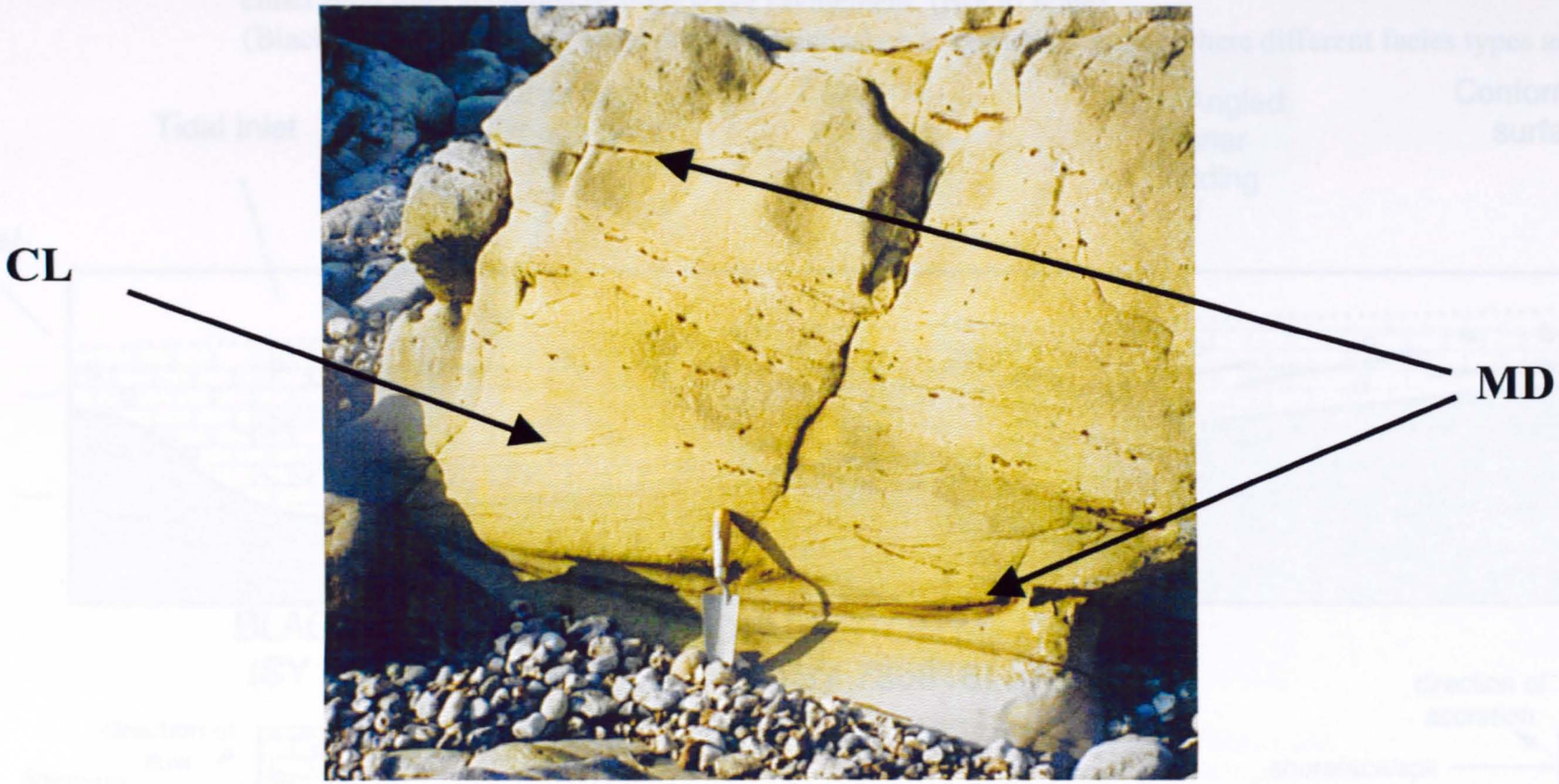

Fig. 2.xiii: Lower Shortlake Member at Black Head. Note mud drapes (MD) & large scale trough cross-laminae (CL) that indicate a north-westerly current flow direction
This bed represents the top of one parasequence and is the lateral equivalent of parasequences within the lower Shortlake Member at Bran Point (Fig. 2.x).
For scale, trowel is 0.25m in length. See Section 2.2.4 & 2.3.4 for further explanation.

Location: Black Head S.Y. 728819

Fig. 2.xiv: Cartoon to show lateral variations within the lower part of the Shortlake Member. Erosional surface could relate to either tidal inlet accretion or tidal/wave ravinement. (Not to scale)
(Black Head, Osmington Mills & Bran Point relate to coastal locations where different facies types are found)

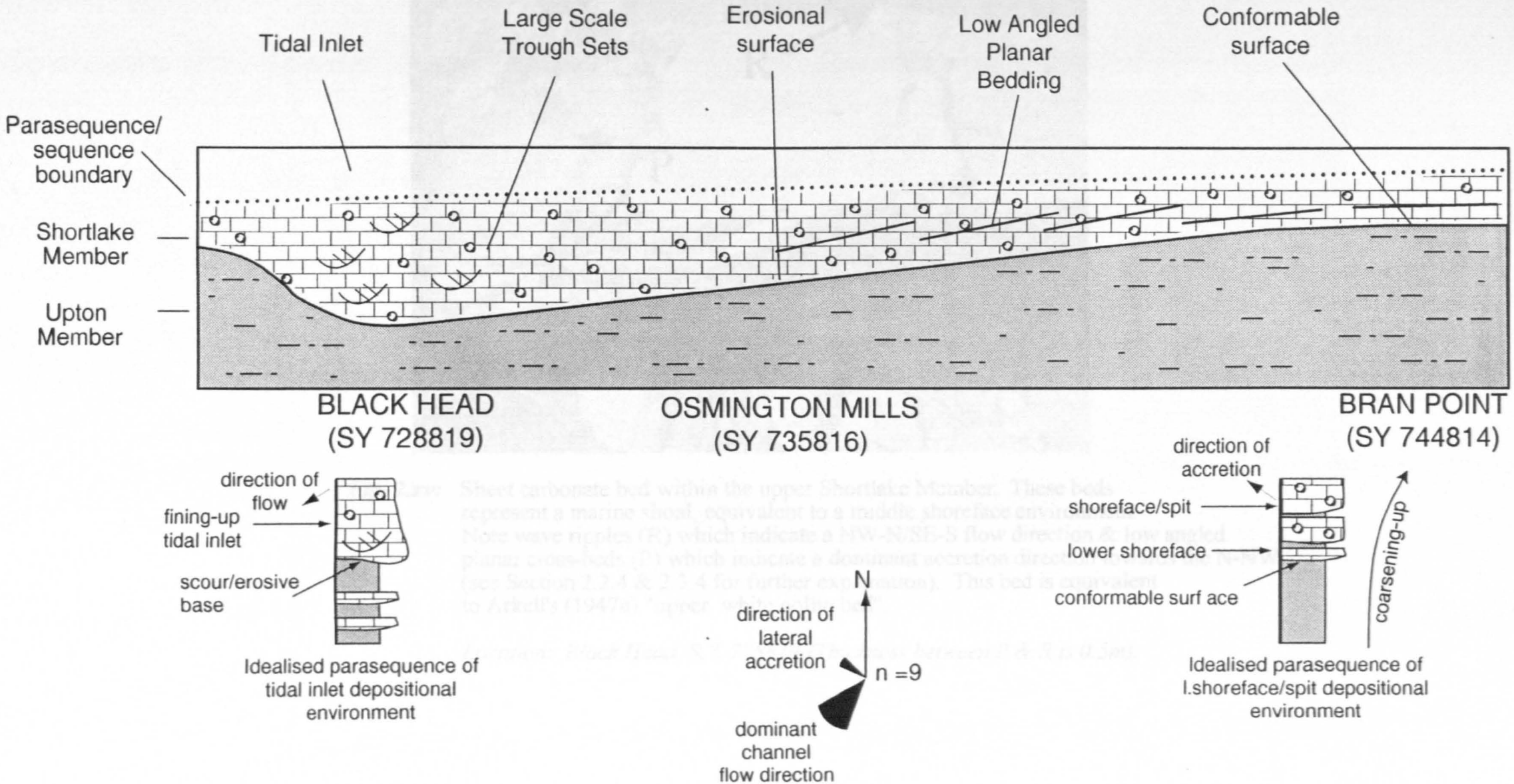

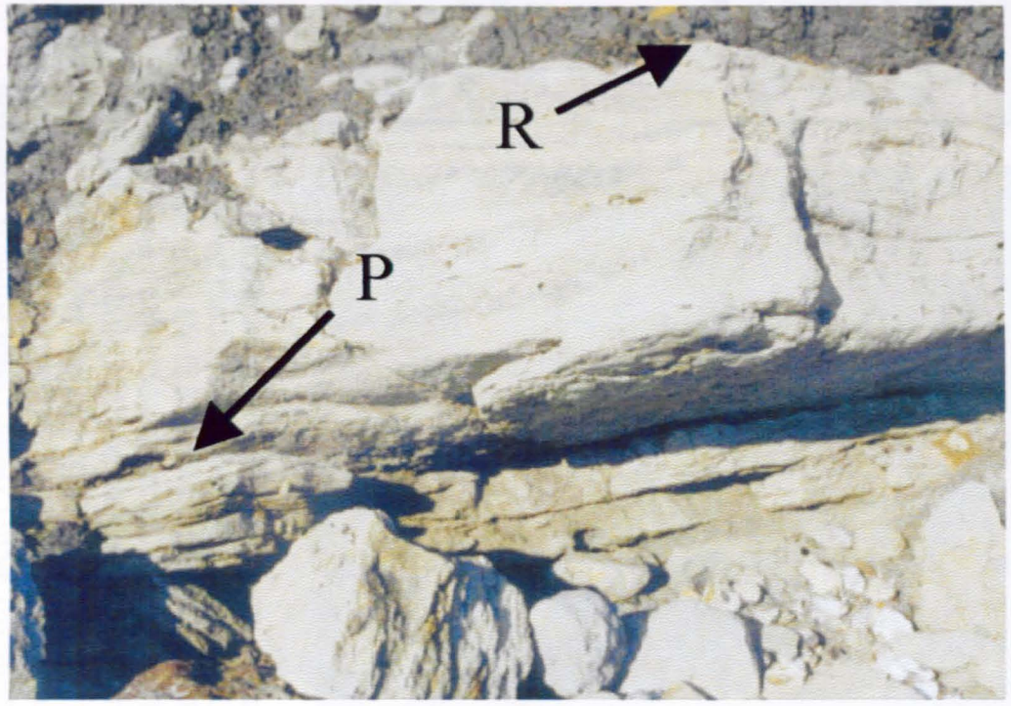

Fig. 2.xv: Sheet carbonate bed within the upper Shortlake Member. These beds represent a marine shoal, equivalent to a middle shoreface environment. Note wave ripples (R) which indicate a NW-N/SE-S flow direction & low angled planar cross-beds (P) which indicate a dominant accretion direction towards the N-NW. (see Section 2.2.4 & 2.3.4 for further explanation). This bed is equivalent to Arkell's (1947a) "upper white oolite bed".

Location: Black Head S.Y. 728819 (Thickness between P & R is 0.5m).

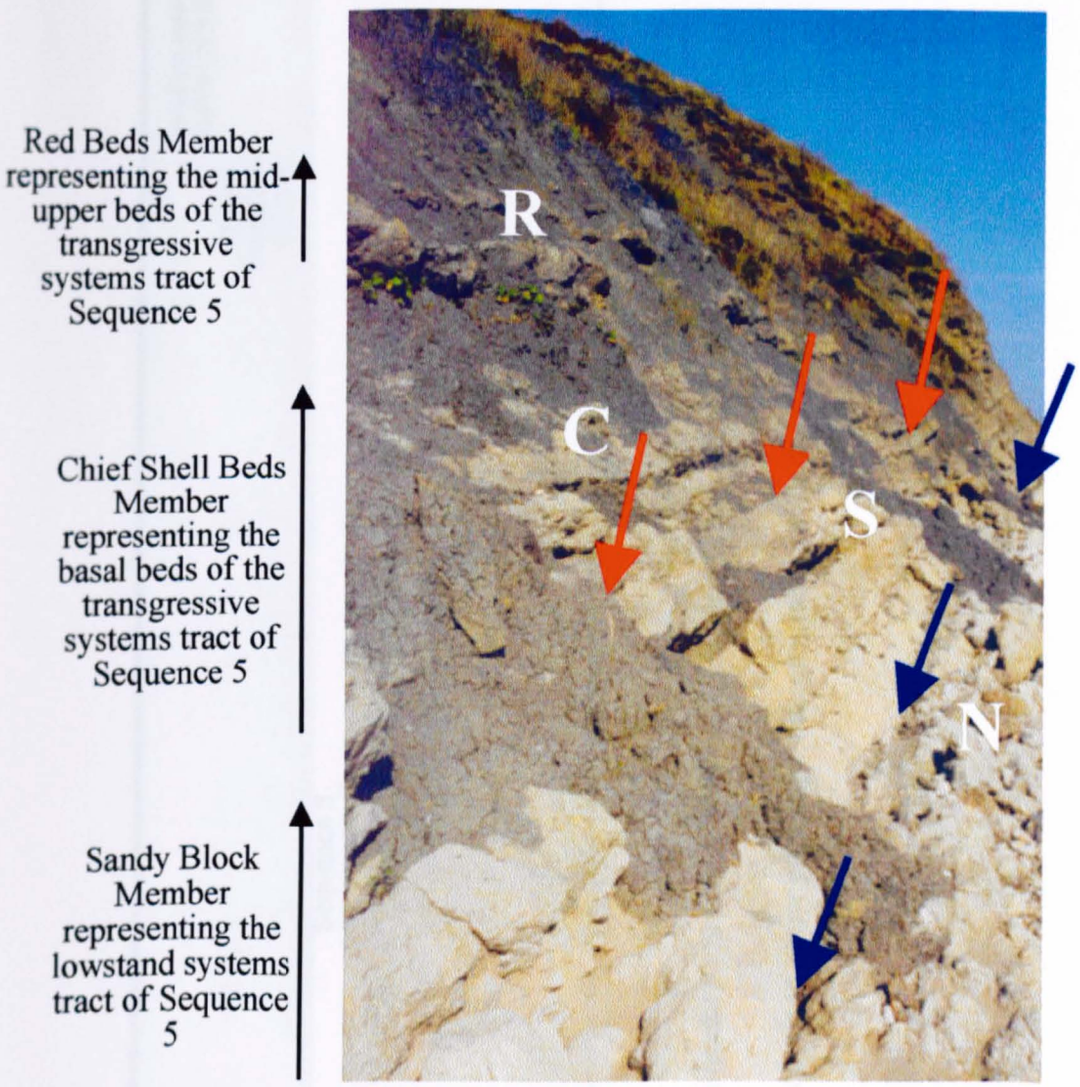

Fig. 2.xvi: Nodular Rubble Member (N) & Trigonia Clavellata Formation (consisting of the Sandy Block Member (S), Chief Shell Beds Member (C) and the Red Beds Member (R)). A type-1 sequence boundary that formed during a period of forced regression (blue arrows) separates the Nodular Rubble Member of Sequence 4, form the overlying Sandy Block Member of Sequence 5. Note the irregular nature of this surface. Within Sequence 5, a transgressive surface separates the lowstand systems tract (Sandy Block Member) from the basal beds of the transgressive systems tract (Chief Shell Beds Member).

(See Section 2.2.5 & 2.3.5 for further explanation)

Location: Black Head S.Y. 728819 (Cliff section in back-ground is approx. 10m in height).

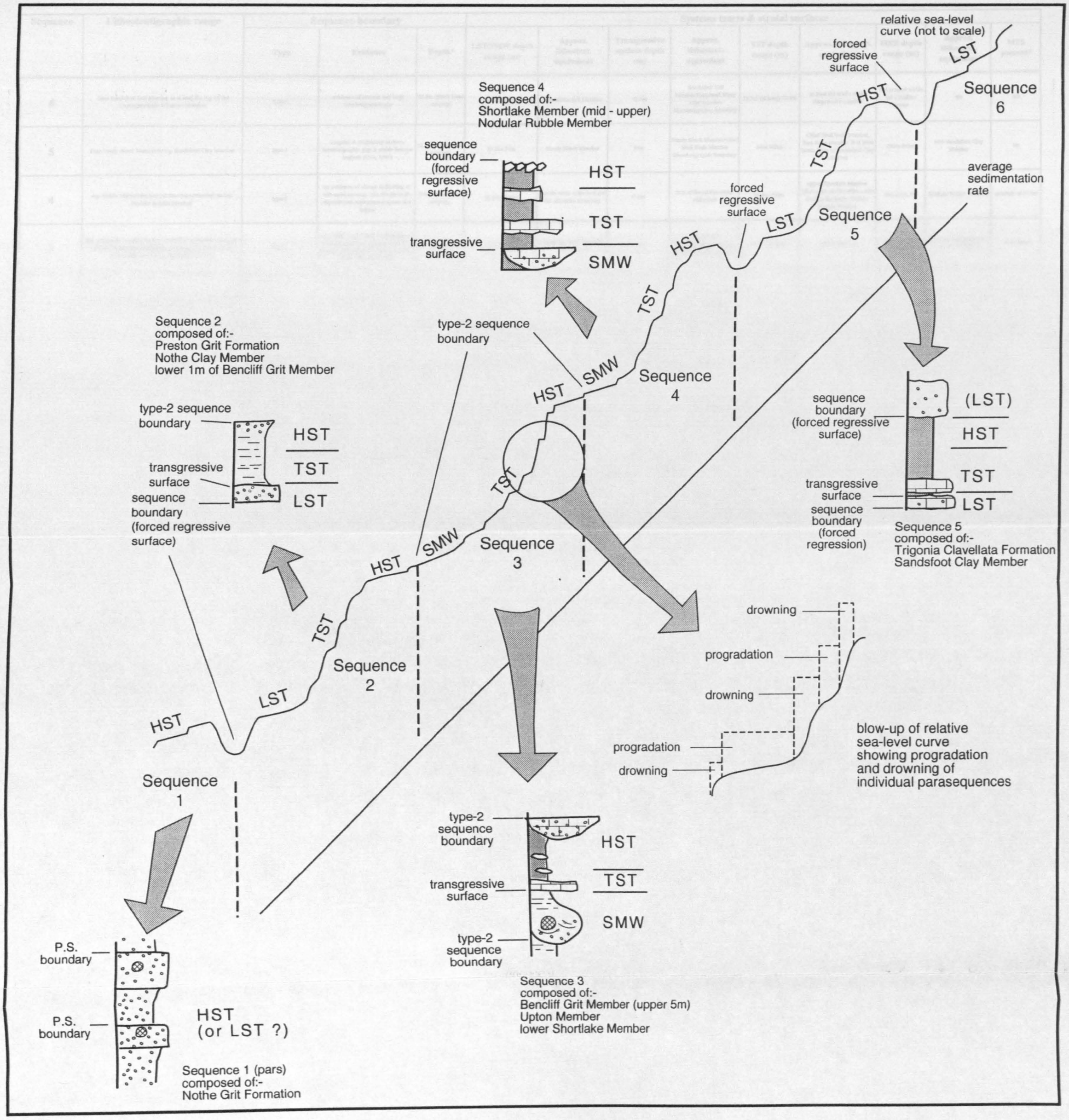

Fig. 2. xvii: The interaction of relative sea-level & average sedimentation rate within the Corallian Group of south Dorset
Each sequence is represented by a mini-log
Also shown is a blow-up of the relative sea-level curve to show parasequence progradation & drowning
(see Section 2.3.1a for further explanation)

Sequence	Lithostratigraphic range	Sequence boundary			Systems tracts & stratal surfaces								
		Type	Evidence	Depth*	LST/SMW depth range (m)	Approx. lithostrat. equivalent	Transgressive surface depth (m)	Approx. lithostrat. equivalent	TST depth range (m)	Approx. lithostrat. equivalent	MFZ depth range (m)	Approx. lithostrat. equivalent	MFS present?
6	base Sandsfoot Grit Member to at least the top of the Ossington Mills Ironstone Member	type-1	evidence of erosion and large biostratigraphic gap	66.6m (Black Head outcrop)	66.6m-71.2m	Sandsfoot Grit Member	71.2m	Sandsfoot Grit Member/Ringstead Waxy Clay Member lithostratigraphic boundary	71.2m-(at least) 74.8m	at least the whole of the Ringstead Formation	not present within the Corallian Group	n/a	n/a
5	base Sandy Block Member to top Sandsfoot Clay Member	type-1	irregular & undulatory surface, biostratigraphic gap & stable isotope analysis (Cox, 1995)	52.1m (Black Head outcrop)	52.1m-54m	Sandy Block Member	54m	Sandy Block Member/Chief Shell Beds Member lithostratigraphic boundary	54m-760m	Chief Shell Beds Member, Red Beds Member & at least lower 1.8m of Sandsfoot Clay Member	760m-765m	mid-Sandsfoot Clay Member	no
4	top middle white oolite bed (of Shortlake Member) to top Nodular Rubble Member	type-2	no evidence of abrupt shallowing or sub-aerial erosion. No change in the depositional environment above and below	38.6m (Black Head outcrop)	38.6m-41.6m	middle white oolite bed (of the Shortlake Member)	41.6m	top of the middle white oolite bed	41.6m-750m	upper Shortlake Member (above the middle white oolite bed) to the lower Nodular Rubble Member	750m-751.5m	Nodular Rubble Member	possibly at 51.2m
3	top of lowest mudstone bed of Bencliff Grit Member (approx. 1.8m above the lithostratigraphic boundary) to base middle white oolite bed (of the Shortlake Member)	type-2	no evidence of abrupt shallowing, or sub-aerial erosion. SB positioned at the change in the style of parasequence stacking above and below	24.2m	24.2m-29.2m	upper 5m of the Bencliff Grit Member	29.2m	Bencliff Grit Member/Upton Member lithostratigraphic boundary	29.2m-735.9m	Upton Member	735.9m-738.9m	mid-*Thalassinoides* beds (Upton Member)	no evidence
2	base of Preston Grit Member to top of lowest mudstone bed of the Bencliff Grit Member	type-1	some evidence of erosion, sharp surface and shallowing above	11.8m	11.8m-12.9m	Preston Grit Member	12.9m	Preston Grit Member/Nothe Clay Member lithostratigraphic boundary	12.9m-717.3m	lower 4.4m of Nothe Clay Member	717.3m-722.4m	mid-Nothe Clay Member	no evidence
1	at least the whole of the Nothe Grit Formation	not present within the Corallian Group	n/a	n/a	not present within the Corallian Group	n/a	not present within the Corallian Group	n/a	not present within the Corallian Group	n/a	not present within the Corallian Group	n/a	n/a

* Unless otherwise stated, the depth of the sequence boundary relates to the Bran Point outcrop. All depths connected with a particular sequence (unless otherwise stated) refer to the same outcrop.

N.B. For simplicity, the starting depth (0m) for the whole succession is based on the lowest occurrence of the Nothe Grit Formation, at the Bowleaze Cove outcrop. The starting depth at the Black Head outcrop is estimated at 34.6m of the Bran Point outcrop (which accounts for the down-cutting seen at the base of the Shortlake Member.

? Denotes where the actual depth of a stratal surface or the boundaries of a stratal unit are undefined.

TABLE 2.*i* Summary of sequence stratigraphic model for the Corallian Group of south Dorset (based on facies analysis) *Page 1 of 2*

Sequence	Lithostratigraphic range			Parasequences			Comments
		HST depth range (m)	Approx. lithostrat. equivalent	Number identified	Types identified	Depth ranges	
6	base Sandsfoot Grit Member to at least the top of the Ossington Mills Ironstone Member	not present within the Corallian Group	n/a	2, possibly 3	all coarsening-up	66.6m-69.7m & 71.2m-74.8m	
5	base Sandy Block Member to top Sandsfoot Clay Member	no evidence	probably upper Sandsfoot Clay Member	none (see comment)	n/a	n/a	the presence of *T. suevica* within the Sandy Block Member may be used to identify marine flooding surfaces associated with parasequence boundaries
4	top middle white oolite bed (of Shortlake Member) to top Nodular Rubble Member	no evidence	probably upper Nodular Rubble Member	4	all coarsening-up	38.6m-41.6m, 41.6m-44.1m, 44.1m-47.2m, 47.2m-49.1m.	distinct lateral thickening of parasequences from Brue Point to Black Head.
3	top of lowest sandstone bed of Bencliff Grit Member (approx. 1.8m above the lithostratigraphic boundary) to base middle white oolite bed (of the Shortlake Member)	738.9m (Brue Point outcrop)-38.6m (Black Head outcrop)	upper Upton Member to lower Shortlake Member	7	3 fining-up (SMW), 4 coarsening-up (TST & HST)	24.2m-25.7m, 25.m-27.4m, 27.4m-29.2m, 30-31.8m, 31.8m-33.5m, 38.9m-40.1m (the equivalent p.s. at Black Head is 34m-35.6m) & 40.1m-40.7m (the equivalent p.s. at Black Head is 35.6m-38.6m).	distinct lateral thickening of parasequences from Brue Point to Black Head.
2	base of Preston Grit Member to top of lowest sandstone bed of the Bencliff Grit Member	722.4m-24.2m	upper 0.5m of Nothe Clay Member to lower 1.8m of Bencliff Grit Member	3	all coarsening-up	11.8m-12.9m, 12.9m-17.2m & 22.4m-24.2m	Coe (1995) states that the lithostratigraphic boundary between the Nothe Grit Formation & Preston Grit Member represents a TS and, the boundary between the latter and the Nothe Clay Member, an MFS.
1	at least the whole of the Nothe Grit Formation	70m-11.8m	Nothe Grit Formation	2	both coarsening-up	0m-6.5m & 6.6m-10.4m	Coe (1995) and Rioult *et al.* (1991) state that the Nothe Grit Formation represents an LST and its lithostratigraphic boundary a sequence boundary.

TABLE 2.*i* **Summary of sequence stratigraphic model for the Corallian Group of south Dorset (based on facies analysis)** *Page 2 of 2*

3: Early Diagenesis & Its Relationship To Sequence Stratigraphy In The Corallian Group

3.1: *Introduction*

Aims & principles:

This chapter aims to evaluate the application of early diagenetic analyses in the construction of a high resolution sequence stratigraphic model for the Corallian Group. Field samples collected around key stratal surfaces and within key lithological horizons (as defined in the Methodology, Section 1.3) along with a range of analytical techniques have been used to create a petrographic dataset. It should be noted that sampling was not carried out within the clay-rich facies (which constitute approximately 32% of the Corallian Group) due to the high probability of later diagenetic over-printing by clay authigenesis and organic reactions.

Within the chapter, the early diagenesis of the Corallian Group will be broadly discussed, followed by an interpretation of the relationship of early diagenetic fabrics in an attempt to resolve, or provide further evidence in support of the facies related sequence stratigraphic framework outlined in Chapter 2. Hence, diagenetic sampling was concentrated within key stratal units and at key stratal surfaces.

Berner (1981) has defined the factors which control early diagenesis. Of particular importance, is the depositional environment, the organic content of the sediment and the sedimentation rate (Curtis, 1987) as well as the composition of the depositional pore-water, especially its sulphur, oxygen (Berner, 1981) and iron content (Curtis, 1987). The effect of changes in relative sea-level is of particular importance because this ultimately controls the basinward or landward movement of early diagenetic zones (Tucker, 1993; Taylor *et al.*, 1994; McKay *et al.*, 1995). Changes in relative sea-level are also responsible for the sequence stratigraphic architecture of nearshore sedimentary successions.

Previous interpretations:

Various aspects of the diagenesis of the Corallian Group across southern England have been studied by Wilson (1966, 1967); Talbot (1971); Fürsich (1973); Chowdhury (1982); Milodowski & Wilmot (1984); De Wet (1987) and Sun (1990).

Wilson (1966) was the first to report the presence of early diagenetic cements (especially calcite) within the Corallian Group. In his regional study of silica diagenesis in Upper Jurassic limestones (Corallian Group and Portland Group), he notes a distinct lack of silicification within the Corallian Group (despite their high sponge spicule content). This, he suggests is due to early calcite cements effectively reducing porosity prior to the phase of silica authigenesis.

In a later paper, Wilson (1967) classifies fossil shell fabrics within Jurassic limestones of

southern England. Wilson provides a model in which he identifies three types of fossil shell fabric (Type I - Type III). Type I fabrics show inclusion rich aragonite replacement calcite; Type II, inclusion free aragonite replacement calcite; and Type III, aragonite dissolution. Within the Corallian Group coastal successions, Wilson identifies a relationship between these and their host sediment. Type I fabrics are associated with large quantities of siderite (Wilson cites the Red Beds Member as an example - refer to Chapter 2, Fig.2.v for lithostratigraphic location); Type II fabrics are found in severely recrystallised limestone with very little or no siderite (Wilson cites the Chief Shell Beds Member as an example - refer to Chapter 2, Fig.2.v); and Type III fabrics are associated with pure limestone (Wilson cites the lower beds of the Upton Member as an example - refer to Chapter 2, Fig.2.v). Wilson suggests that within the Corallian Group especially, variations in the fabrics are due partly to "an unusual mineralogy" and are also related to "earth movements" or folding of beds at Bran Point where similar diagenetic fabrics have been identified within deformed veins.

Talbot (1971) presents a general study of calcite cements within the Corallian Group outcrops from the coastal successions of Dorset to inland exposures of Oxfordshire. This is one of the earliest papers to relate diagenetic products to changing diagenetic environments. In his paper, he identifies three generations of "sparry calcite" which are distinguishable by variations in cement fabrics, and differences in artificial staining colours.

According to Talbot (1971), non-ferroan calcite is the first generation cement and is

interpreted as having precipitated as a result of subaerial exposure of unconsolidated carbonate sediments. The next generation of cement is fibrous ferroan calcite. Talbot suggests four possible origins for this cement fabric: (i) a result of subaerial exposure; (ii) sea-floor precipitation; (iii) as a pseudomorph after fibrous aragonite, and (iv) precipitation within the shallow burial environment after the sediment had become sufficiently buried to isolate it from the subaerial and submarine depositional environments. The final generation of cement is granular ferroan calcite, which Talbot has reported to be the result of later burial diagenesis. Talbot shows that the ferroan cements have a widespread areal distribution, while the non-ferroan cements are more restricted.

Fürsich (1973) provides an interpretation of the origin of the nodular limestones that occur within the upper Upton Member (refer to Chapter 2, Fig. 2.v for lithostratigraphical location). Fürsich suggests that during early diagenesis, organic material (or mucus) lining *Thalassinoides* burrows acted as a nucleus for calcium carbonate precipitation - a theory that is now well accepted for the formation of similar concretionary beds (see Fleming, 1993).

The next three studies by Chowdhury (1982), Milodowski & Wilmot (1984) and De Wet (1987) have all used outcrop and subsurface data from the Corallian Group around the Oxfordshire and Berkshire area.

Chowdhury (1982) documents the variation in diagenetic environments of the Osmington Oolite Formation of the Oxfordshire-Berkshire area (refer to Chowdhury, 1982 - figs.1 &

2 for geographical and stratigraphical locations). Using petrographic and geochemical analysis, Chowdhury shows that the diagenetic environment changed from a dominantly marine phreatic, through a fresh-water phreatic to a dominantly vadose environment. Chowdury suggests that the changes in diagenetic environments are a consequence of tectonic uplift following the deposition of the Coral Rag Member (refer to Chowdhury, 1982 - figs.1 & 2 for stratigraphical location).

Milodowski & Wilmot (1984) investigate bore-hole material from the Horwell Research Site of south Oxfordshire and use this to determine how diagenesis influenced porosity and permeability evolution within the Corallian Group in the subsurface. They identify several phases of cementation, including calcite, pyrite, dolomite and silica, as well as phases of dissolution and compaction. In their model, they divide the Corallian Group into the upper calcareous sandstones and limestones and basal siliceous muddy sandstones (refer to Milodowski & Wilmot, 1984 - fig.1 for their lithological division).

Each of Milodowski & Wilmot's (1984) units underwent a different diagenetic history. The lower unit under-went early precipitation of iron sulphides. This was followed by precipitation of ferroan dolomite once sulphate diffusion had declined. Prior to compaction, opal, zeolite and smectite were precipitated and after compaction, minor late stage feldspar overgrowths formed. In contrast, the upper unit under-went early skeletal aragonite dissolution resulting in the creation of mouldic porosity. This porosity was subsequently infilled by non-ferroan or mildly ferroan calcite and micritic precipitates. This was followed by early precipitation of bladed ferroan calcite and pyrite precipitation.

Later, deeper burial diagenesis then followed in the form of compaction, stylotisation and the precipitation of authigenic clays.

Unfortunately, Milodowski and Wilmot (1984) do not interpret these products in terms of changing diagenetic environments (although they do make reference to the marine diagenetic environment when describing the diagenesis of the non-ferroan to mildly ferroan calcite). However, they do make the point that the paragenetic histories of both units had marked effects on the porosity and permeability of the different lithologies.

De Wet (1987) uses Chadwick's (1986) tectonic interpretation for the Wessex Basin as a framework for a petrographic and analytical study of the Corallian Group around the Oxford area (summarised in Table 3.i). In her model, De Wet identifies three phases of cementation - an early pre-burial, a shallow burial and a deep burial, which are influenced by depositional trends.

The first phase includes marine precipitates and non-ferroan, neomorphic and drusy spars. The second phase includes equant granular ferroan calcite spar and syntaxial overgrowths, with marine oxygen isotopic signatures similar to those of phase one. During burial of these two phases, pore-waters moved along conduits created by coarser grained sandstones and grainstones in a fresh-water phreatic system. Geochemical evidence led De Wet to suggest that the meteoric input may not have been isotopically very different from sea-water. Finally, early Cretaceous regional uplift exposed the Corallian strata to undersaturated meteoric water, initiating the final phase of vuggy dissolution followed by

later blocky poikilotopic calcite.

In the most recent paper on Corallian Group diagenesis, Sun (1990) describes the relationship between facies and diagenesis in the Osmington Oolite Formation of south Dorset (refer to Chapter 2, Fig.2.v for lithostratigraphical location). He accounts for his results within the context of one transgressive-regressive cycle of his sea-level model (Table 3.ii) (refer to Section 2.1.3 for a review of Sun's sea-level model).

The dominant cements within Sun's transgressive sequence (equivalent to the Upton Member) are early columnar isopachous ferroan calcite and pervasive strongly ferroan equant calcite, both of which have a dominantly non-zoned dull luminescence. Sun suggests that this represents a change from a marine phreatic diagenetic environment into a low-oxygen, deeper burial connate zone.

Within his regressive sequence (equivalent to the Shortlake Member and Nodular Rubble Member) Sun identifies early columnar isopachous calcite cement fringes as well as extensive leaching of formerly aragonitic grains, collapsed micrite envelopes and a pervasive, zoned, brightly luminescent mildly ferroan to non-ferroan calcite cement. Sun interprets this paragenesis as representing replacement of marine phreatic pore-water (precipitation of early columnar isopachous calcite) by meteoric pore-water, which dissolved unstable grains and precipitated non-ferroan carbonate cements in a sub-oxic environment.

The descriptions and interpretation presented in this chapter differ from previous studies because:-

- they provide an integrated study of the whole succession (siliciclastic and carbonate units);
- the emphasis (particularly in Section 3.2) is on establishing a link between the processes and products of early diagenesis specifically within a high resolution sequence stratigraphic framework, rather than simply investigating the causes of diagenesis within the Corallian Group.

Organisation:

In Section 3.2, I provide a detailed petrographical and analytical description of all early diagenetic products within the lithostratigraphic nomenclature of the Corallian Group, which broadly fall into the categories: glauconite, phosphate (apatite), pyrite, calcite, dolomite and siderite. Within this section, additional published data is also highlighted. Following this (in Section 3.3) early diagenetic products are interpreted and used to support (or refute) the facies based sequence stratigraphic model proposed in Chapter 2. Therefore each early diagenetic product will be interpreted as a factor of:-

- the depositional environment;
- the composition of the depositional pore-water;
- the sedimentation rate;
- the iron and organic content of the sediment;
- changes in relative sea-level; and,

- providing support or rebuttal of facies based sequence stratigraphic interpretations offered in Chapter 2.

Where possible, comparisons with previous work (especially the analytical data of De Wet, 1986 and Sun,1990) will also be assessed.

3.1.1: Detrital mineralogy

Within the context of this chapter, only a brief qualitative outline of the detrital mineralogy will be discussed here (with reference to the inferred depositional environments as defined in Fig.2.v & Fig.2.vi of Chapter 2).

3.1.1a: *Shoreface sandstones*

Detrital grains within the siliciclastic shoreface sandstones of the Nothe Grit Formation, Preston Grit Member and Sandsfoot Grit Member (between 0m-12.7m & 67.7m-71.1m on Fig.2.v) are dominated by very fine to medium grained subrounded quartz, rare feldspar and matrix, classifying them as dominantly sub-arkosic arenites. The matrix within the shoreface sandstones of the Sandsfoot Grit Member was revealed by preliminary XRD studies as being iron-rich (results not included within thesis). Bioclastic debris (the majority of which has been neomorphosed or replaced) is also present.

3.1.1b: *Siliciclastic shelfal deposits:*

The siliciclastic shelf deposits of the Nothe Clay Member and Sandsfoot Clay Member (between 12.8m-23m & 58.2m-66.5m on Fig.2.v) are dominated by silt sized quartz grains and fine grained replaced or neomorphosed bioclastic debris.

3.1.1c: *Tidal flat shoreline sandstones:*

These sandstones of the Bencliff Grit Member (between 24.2m-29.2m on Fig.2.v and Fig.2.vi) are texturally and compositionally sub-mature and dominated by fine grained subrounded quartz, classifying this rock as a quartz arenite. Feldspar and detrital clay are rare within these sandstones which still retain excellent primary porosity and permeability and are oil stained. Bioclastic debris (the majority of which has been neomorphosed or replaced) is rare, and concentrated within large (up to 1m in diameter) spherical and oblate carbonate concretions. The finer grained heterolithic layers which separate each sandstone, are dominated by silt sized quartz grains and detrital clay.

3.1.1d: *Shallow marine and shelf carbonates:*

The detrital mineralogy within the shallow marine and shelf mudstone to grainstone carbonate units of the Upton Member, Shortlake Member and Trigonia Clavellata Formation (between 29.2m-33.4m, 39.4m-49.1m & 52.2m-58.3m on Fig.2.v) is dominated by bivalve, gastropod and echinoderm debris, along with rare occurrences of foraminifera

and corals. The bivalve and gastropod debris may be either unaltered and/or replaced; this being dependant on the original mineralogy - calcitic material generally remaining unaltered. Other allochems identified are peloids, intraclasts and ooids. The *Thalassinoides* Beds and Nodular Rubble Member (between 33.4m-39.4m & 49.1m-52.2m on Fig.2.v) also contain a patchy micritic matrix.

Well developed micrite envelopes that have been precipitated around bioclastic allochems, are a common feature within all of the shallow marine carbonate sands. However, where these occur around aragonite bioclasts which have subsequently dissolved, the micrite envelopes have often collapsed and broken. Features associated with aragonite dissolution are common within all of the carbonate facies analysed in this research and will be discussed further in Section 3.2 and Section 3.3. However, it is important to stress that collapsed micrite envelopes are found within all carbonate beds and not just the Upton Member as previously stated by Sun (1990).

3.2: *Description of early diagenetic products*

3.2.1: Procedure

The criteria, sampling procedure and methodology for each of the analytical methods used in this thesis are described in detail in the appendices (Appendix 1 describes the methods used in the petrographic analysis; Appendix 2 describes the methods used in the X-ray

diffraction analysis; Appendix 3 describes the methods used in the stable isotope analysis; and Appendix 4 describes the cathodoluminescence study). Initially, samples were also viewed with the aid of a scanning electron microscope, but it was decided that this type of analysis was not relevant to the proposed study and so was discontinued.

Petrographic analyses:

Detailed petrographic analyses (transmitted light and scanning electron microscopy) was performed on seventy samples extracted from cemented beds, non-cemented beds and concretionary bodies throughout the vertical (and lateral) extent of the studied Corallian Group with specific emphasis on key stratal surfaces and units (Fig.3.i). Fifty-eight thin-sections were stained for carbonate using Dickson's staining technique (1966), point counted using a "Swift Model F" electronic counter, assessed for early diagenetic phases and photographed. The results are plotted in Figure 3.ii.

Cathodoluminescence:

Cathodoluminescence (using equipment at Camborne School of Mines) was performed on seventeen polished thin-sections cut from hand-specimens that contained examples of all early diagenetic products (Fig.3.i & Table 3.iii). This was used to confirm (i) the singularity of the cement phases that was to be analysed isotopically and (ii) to assess each phase in terms of its luminescence. Cement types are described as either non-luminescent, dull luminescent, moderately luminescent, brightly luminescent or a combination of these.

The presence or absence of zoning is also noted.

Stable isotopes:

Examples of all concretionary calcite, ferroan fringing calcite, ferroan equant calcite, non-ferroan equant calcite, concretionary siderite and siderite cement were isolated and extracted from 15 samples (Fig.3.i) using a scalpel and micro-drill, and were further analysed by X-ray diffraction to detect singular or multiple precipitates (x-ray diffraction plots are included within Appendix 2). The extracted cement phases (between 90 - 100% pure) were analysed at the Postgraduate Research Institute for Sedimentology Isotope Laboratory at Reading University, where oxygen and carbon isotopes were extracted and measured (Table 3.iii & Fig.3.iii). All carbon and oxygen isotopic data are reported in the standard δ-notation relative to the belemnite *Belemnitella americana* from the PeeDee Formation (PDB, Craig, 1957). The reproducibility of $\delta^{13}C$ and $\delta^{18}O$ values for a random calcite sample within each batch of samples was ± 0.05‰ and ± 0.07‰ respectively.

X-ray diffraction:

Finally, it should be noted that the XRD results support the identification of all carbonate cements discussed in this section. XRD results will not be discussed in detail here because they are only qualitative. However as mentioned above, the results can be found within Appendix 2.

3.2.2: Glauconite

Minor, (up to 6.6% total pore filling volume[1]) small, (average size is between 0.25mm and 0.5mm) peloidal and pore filling glauconite is present throughout the Corallian Group successions (although in many of samples, the resolution of the point counting technique was unable to distinguish its presence). Glauconite is more common within the higher energy siliciclastic facies, such as the tidal flat shoreface sands of the Bencliff Grit Member (sample numbers 30, 32, 34 and 36 on Fig.3.ii) and the prograding shoreface sands of the Sandsfoot Grit Member (sample numbers 111-120 on Fig.3.ii).

3.2.3: Phosphate (apatite)

Minor apatite (up to 5% total pore filling volume) is only present within the siliciclastic prograding shoreface sands of the Sandsfoot Grit Member (sample numbers 111-120 on Fig.3.ii). It occurs as small spheroidal and oblate pellets, as laminae within ooids and as a pore filling cement. Individual pellets range in size from 0.1 to 0.5mm.

[1] Through-out this chapter, each diagenetic phase is expressed as a percentage of the total pore filling volume of the sediment. The percentage pore-filling volume of each diagenetic phase is a calculation of the arithmetic mean of all occurrences of that phase - as shown in Appendix 1, Table 1. The pore filling volume takes into account other pore filling diagenetic phases, pore filling matrix and any porosity/permeability. It is independent of the detrital mineralogy.

3.2.4: Pyrite

Pyrite, (average 12.6% of the total pore filling volume) is present throughout the Corallian Group successions. However within the prograding shoreface sandstones of the Nothe Grit Formation, the abundance of pyrite increases to between 30-40% of the total pore filling volume (sample numbers B4 & B1 on Fig.3.ii and sample numbers A4 & A5 on Fig.3.vi). Within this formation, pyrite occurs preferentially within septarian concretions (see Section 3.2.5).

Pyrite commonly occurs as disseminated, small (average crystal size is 0.05mm) framboidal to euhedral crystals (Fig.3.iv) although framboidal pyrite is generally more common than euhedral pyrite. It is always associated with ferroan and non-ferroan calcite, ferroan dolomite and siderite, both of which it pre-dates (see Fig.3.xviii). Pyrite is also strongly associated with concentrations of organic matter either within pore spaces, or as membranes within bioclastic shell debris and ooid cortices Concretions of the Nothe Grit Formation contain some evidence of preserved organic matter (in the form of plant debris).

3.2.5: Authigenic calcite

Evidence of early authigenic calcite is present throughout the Corallian Group succession. However, the abundance, habit, texture and composition of the calcite varies considerably. Four general groups can be recognised:-

- non-ferroan calcite within zoned septarian concretions of the Nothe Grit Formation (at 6.3m and 10.1m on Fig.3.i and 3.ii);
- ferroan poikilotopic calcite within non-zoned concretions of the Bencliff Grit Member (at 26.7m and 28.8m on Fig.3.i and 3.ii);
- non-ferroan calcite within concretionary burrows of the *Thalassinoides* beds and Nodular Rubble Member (between 33.6m-39.4m & 48.5m-52.1m respectively, on Fig.3.i and 3.ii); and
- pore-filling ferroan to non-ferroan calcite within the lower Upton Member, Shortlake Member, Trigonia Clavellata Formation, Sandsfoot Grit Member and Ringstead Formation (between 29.1m-33.5m, 39.4m-49.1m, 52.1m-58.2m & 66.6m-74.8m on Fig.3.i and 3.ii).

Each group is discussed separately incorporating petrographic, stable isotope, CL data and published elemental data from the work of De Wet (1987) and Sun (1990).

3.2.5a: *Non-ferroan septarian concretionary calcite*

Occurrence:

Septarian concretions (Fig.3.v) only occur within the two coarser, shelly cemented units of the Nothe Grit Formation (at 6.2m and 9.6m on Fig.3.i & Fig.3.ii). Detailed analyses were performed on one septarian concretion (at 6.2m on Fig.3.i, Fig.3.ii & Fig.3.vi). Individual concretions are oblate to ellipsoidal, approximately 0.3m in diameter and concentrically

zoned (Fig.3.v & Fig.3.vi). The presence of septarian cracks suggests a very early diagenetic origin for these concretions (Raiswell, 1971; Astin, 1986; Scotchman, 1991 and McKay *et al.*, 1995).

Petrographical description:

The interior of the septarian concretion (zone 1, Fig.3.vi) contains 60-70% non-ferroan fine grained sparry calcite and 30-40% framboidal and euhedral pyrite (Fig.3.iv). The exterior zone (zone 2, Fig.3.vi) contains a similar volume of non-ferroan calcite, but less pyrite (approximately <15%) and a small volume of siderite cement (8.3%).

Stable isotope analysis:

Zone 1 calcite has highly depleted $\delta^{13}C$ values of -31.10‰ PDB and $\delta^{18}O$ values of -0.83‰ PDB, while zone 2 calcite has less depleted $\delta^{13}C$ values of -26.60‰ PDB and slightly heavier $\delta^{18}O$ values of -1.75‰ PDB (Table 3.iv, Fig.3.iii & Fig.3.vi). This is insufficient for accurate palaeotemperature determination, but may be used for a working estimate. Shackleton & Kennett (1975) have produced a modified version of the palaeotemperature equation of Epstein *et al.* (1953):

$$T°C = 16.9 - 4.38\,(\delta_c - \delta_w) + 0.10\,(\delta_c - \delta_w)^2 \quad [Eq.1]$$

where δ_c is the average measured isotope value of CO_2 (-0.46‰ PDB) and δ_w is the

isotopic composition of Jurassic sea-water, assumed to be approximately -1.2 ‰ P.D.B. (Shackleton & Kennett, 1975). Using the above data, Equation 1 suggests an average palaeotemperature estimation of 13.7°C at the time of concretion formation, which is consistent with Hudson's (1978) palaeotemperature estimations of 13°C obtained from similar concretions of the Oxford Clay Formation which immediately underlies the Nothe Grit Formation.

The principal cement of the septarian cracks within these concretions is ferroan equant sparry calcite. $D^{13}C$ isotope values are +2.23‰ PDB (slightly heavier than Hudson's average results of 1.66‰ PDB) and $\delta^{18}O$ values are -3.52‰ PDB (also less depleted than Hudson's average results of -7.37‰ PDB). Thus the $\delta^{18}O$ and $\delta^{13}C$ trends from concretionary fill to septarian fracture fill follow a trend to heavier carbon and lighter oxygen, agreeing with Hudson's data.

Cathodoluminescence analysis:

Zone 1 calcite is moderately to brightly luminescent and non-zoned (Fig.3.vii), while zone 2 calcite is also moderately to brightly luminescent but reveals very slight zoning (Table 3.iii). Septarian cracks are well zoned and reveal dull centres and bright outer zones.

3.2.5b: *Ferroan poikilotopic concretionary calcite*

Occurrence:

Ferroan poikilotopic calcite concretions (Fig.3.viii) only occur within the sandstone facies of the Bencliff Grit Member (at 26m and 28.8m on Fig.3.i, Fig. 3.ii & Fig.3.ix). Detailed analyses were performed on three concretions collected from within the Bencliff Grit Member, 1km to the east of Osmington Mills (refer to Fig.2.i of Chapter 2 for location). The concretions are generally oblate to spherical and approximately 1m in diameter (Fig.3.viii & Fig.3.ix), although at the top of the member, concretions have amalgamated to form a laterally extensive carbonate cemented horizon (Fig.3.viii).

Petrographic description:

Sample numbers 32a and 36a on Figure 3.ii, and E1-E4 on Fig.3.ix reveal that the concretions are composed of large (0.5-1.5mm in size) ferroan poikilotopic calcite crystals, (up to 98% pore-filling volume) each enclosing a number of smaller detrital quartz grains and bioclastic debris as well as preserving a depositional open grain fabric (Fig.3.x). Rare small (0.01-0.05mm in size) ferroan dolomite rhombs also occur within the concretions, concentrated within detrital clay laminae, along with rare pyrite and glauconite.

Stable isotope analysis:

Due to the scope and logistics of the work, only a limited number of samples were obtained for stable isotope analysis. Clearly further work is needed before any interpretation can be substantiated, however the available data reveals two increasingly heavy $\delta^{18}O$ trends (Table 3.iii, Fig.3.iii and Fig.3.ix). The first trend is within individual concretions which have an $\delta^{18}O$ trend from -6.30‰ PDB to -5.77‰ PDB (± 0.07‰) from the centre to the perimeter. The second trend is an upwards one within the Bencliff Grit Member, where $\delta^{18}O$ values increase from -9.23‰ PDB to -5.60‰ PDB. The $\delta^{13}C$ values also display a "heavying" trend from centre to perimeter within individual concretions (+1.64‰ PDB to +1.86‰ PDB) and vertically upwards through the member (-0.34‰ PDB to -0.24‰ PDB, Fig.3.ix).

Cathodoluminescence analysis:

Cathodoluminescence analysis performed on sample numbers 32a, E2 and E4 (Table 3.iii) indicates that the ferroan poikilotopic calcite is dull to non-luminescent with very subtle patches of zoning (Fig.3.xi).

Other occurrences of ferroan poikilotopic calcite:

Ferroan poikilotopic calcite has also been identified within the three coarser grained sandstone and siltstone beds of the Nothe Grit Formation and the Nothe Clay Member

(e.g. sample numbers B9, B3 and B12 on Fig.3.ii). Within the Nothe Grit Formation, the poikilotopic calcite surrounds the septarian concretions described in Section 3.2.5a, suggesting that here, it clearly post-dates septarian concretionary growth.

3.2.5c: *Non-ferroan concretionary (burrow) calcite*

Occurrence:

Early diagenetic concretions that developed around *Thalassinoides* burrows are only common within the *Thalassinoides* beds (upper Upton Member) and lower Nodular Rubble Member (between 33.5m-39.2m & 49.1m-52.1m on Fig.3.i & Fig.3.ii).

Petrographic description:

Concretionary burrows are composed of abundant (approximately 80-90%) very fine grained non-ferroan sparry calcite (<0.01mm in size) and rare to vertically increasing volumes of ferroan dolomite and framboidal and euhedral pyrite (10-20% increasing in abundance upwards).

Cathodoluminescence analysis:

Cathodoluminescence analysis performed on sample numbers 50 and 78 of Figure 3.i and 3.ii reveals two different responses. The pore filling cement of sample number 50 has a

dull luminescence, while in sample number 78, it is brightly luminescent and zoned.

3.2.5d: *Pore filling non-concretionary ferroan to non-ferroan calcite*

These phases incorporate ferroan isopachous fringing calcite, ferroan equant sparry calcite, ferroan calcite overgrowths and non-ferroan equant sparry calcite, which all occur within coarser grained carbonate beds of the lower Upton Member, Shortlake Member, Trigonia Clavellata Formation, Sandsfoot Formation and Ringstead Formation (between 29.1m-33.5m, 39.4m-49.1m, 52.1m-58.2m & 66.6m-74.8m on Fig.3.i and 3.ii). Some, of these coarser grained beds show evidence for marine hard-ground development (e.g. at 29.5m, 31.5m, 33m, 44m, 47m and 48.7m on Fig.3.i & Fig.3.ii - as noted in Section 2.2).

Ferroan fringing calcite:

Well developed ferroan isopachous fringing calcite is the dominant cement type (up to 60% total pore filling volume) within the coarser grained beds of the lower Upton Member and rare to common (20 - 40% total pore filling volume) within the Shortlake Member (e.g. sample numbers 40, 61, C8, C9 and C15 on Fig 3.ii).

Petrographic description:

The most abundant form of ferroan fringing calcite is the columnar variety, in which crystals have length to width ratios of more than 6:1 (Tucker & Wright, 1990). These

cements are seen to grow from grain boundaries and micrite envelopes (broken and intact) into both primary pore space and secondary pore space (mouldic porosity created from aragonite dissolution) (Fig.3.xiia). The most common fabric is fascicular-optic fibrous calcite where crystals display an undulose extinction pattern that is caused by convergent fast vibration directions (Kendall, 1985). Within crystals, sub-crystal boundaries and inclusions are common. Crystals also show well developed polygonal compromise boundaries and point terminations between fringe sets (Fig.3.xiia). Where the cement is particularly well developed (Fig.3.xiia), individual crystal lengths can reach up to 0.35mm and widths up to 0.05mm; however, where it is poorly developed, (Fig.3.xiib) crystal dimensions can be an order of magnitude smaller and their shape can be described as acicular (see Fig.3.xvii).

Well developed early fringing calcite has considerably reduced the effects of grain compaction within the lower Upton Member (Fig.3.xiia), while in the Shortlake Member where it is absent or poorly developed, early grain compaction is evident (Fig.3.xiii).

Stable isotope analysis:

Stable isotope analysis of ferroan fringing calcite extracted from sample number 40 on Figure 3.ii, reveals slightly depleted $\delta^{18}O$ values of -2.19‰ PDB and slightly positive $\delta^{13}C$ values of +0.73‰ PDB (Table 3.iv & Fig.3.iii). As noted before, such limited data is not sufficient for true palaeotemperature determination, but may be used for a working estimate. Using Shackleton & Kennett's (1975) modified palaeotemperature equation

[Eq.1], an average temperature of 20.9°C at the time of this cement formation is estimated. This is consistent with De Wet's (1987) estimation of 20.5°C for the equivalent cement type of the Corallian Group of Oxfordshire.

Cathodoluminescence analysis:

Cathodoluminescence analysis performed on samples 40, 61, C11, C12 and 88 (Table 3.iii) reveal some variability in the response of ferroan fringing calcite. In samples 40, C11, C12 and 88, which occur within the Upton Member and Shortlake Member, ferroan fringing calcite is dominantly non-luminescent to dull or weakly luminescent with some zoning (Fig.3.xiv). In these samples the ferroan fringing calcite is generally associated with a later pore-filling ferroan equant calcite. However, within sample 61, of the Shortlake Member, poorly developed, acicular ferroan fringing calcite is brightly luminescent and zoned (Fig.3.xv). In this sample, it is also associated with non-ferroan fringing calcite (see below). These results indicate that the CL response is controlled by the type of fringing calcite and its association with ferroan or non-ferroan equant calcite.

Previously published analytical data:

Sun (1990) measured the manganese and iron content of ferroan fringing calcite cements from within the Osmington Oolite Formation. He found these to be between 0.08 - 0.17 wt % and up to 1.8 wt % respectively (Table 3.ii). In contrast to my results, Sun notes that these cements do not luminesce under CL and he does not report any variation throughout

the Formation (Table 3.ii). This is clearly not the case.

Isopachous fibrous calcite cements are also found within the Corallian Group successions of the Oxford area (De Wet, 1987). These cements have similar isotope values to my results from the coastal successions, but their CL response and iron content are different (Table 3.i). De Wet has reported that these cements are distinctly non-ferroan with a non-luminescent to brightly luminescent CL response (Table 3.i).

Ferroan equant calcite:

Ferroan equant calcite (and ferroan calcite overgrowths) are common (up to 60% of the total pore filling volume) within (i) tops of coarser grained beds of the lower Upton Member (between 29.1m-33.5m on Fig.3.i & Fig.3.ii) (ii) coarser grained beds of the Trigonia Clavellata Formation (between 52.1m-58.2m on Fig.3.i & Fig.3.ii) and (iii), the bioclastic rich Ringstead Coral Bed (at 74.5m on Fig.3.i & Fig.3.ii). However, the cement type is very abundant (up to 80% of the total pore filling volume) within the coarser grained beds of the Shortlake Member (between 39.4m-49.1m on Fig.3.i & Fig.3.ii). In the field, most of the coarser grained beds in these lithostratigraphic units show clear evidence of hard-ground formation (see Section 2.2).

Petrographic description:

Ferroan equant calcite occurs as a pore filling mosaic of small crystals (average crystal

size is between 0.05 and 0.1mm) which are strongly to mildly ferroan in composition (Figs.3.xii, 3.xiii & 3.xvi). Where the cement is the dominant type (as in sample numbers C9-C15), crystals are seen to grow directly from detrital grain boundaries (Fig.3.xiii & 3.xvi). However, if fibrous ferroan calcite is the dominant cement (as in sample number 40), then ferroan equant calcite preferentially grows from fibrous calcite crystal terminations (Fig.3.xiia). Within some samples of the Shortlake Member, ferroan equant calcite post-dates early grain compaction, which has resulted due to an absence/poor development of ferroan fringing calcite (Fig.3.xiii).

Stable isotope analysis:

Stable isotope analysis of ferroan equant calcite extracted from the intergranular pore-spaces of sample number C12 (Shortlake Member) reveal slightly depleted $\delta^{18}O$ values of -3.07‰ PDB and slightly negative $\delta^{13}C$ values of -0.35‰ PDB (Table 3.iv & Fig.3.iii). The $\delta^{18}O$ values are, however, very similar to the values reported by Marshall & Ashton (1980) which were obtained from oyster samples within Jurassic hard-grounds of the Lincolnshire Limestone Formation, eastern England. Thus, using the palaeotemperature equation defined earlier [Eq.1], a working palaeotemperature estimate of 25.4°C at the time of cementation is obtained, which is consistent with other estimates of palaeotemperatures for the British Jurassic (e.g. Irwin *et al.*, 1977 and Marshall & Ashton, 1980). It is however, approximately 4°C higher than the estimates obtained from the ferroan fibrous calcite of the Upton Member (described earlier). This could be a factor of sample contamination by later ^{16}O enriched pore-waters (Marshall & Ashton, 1980) but,

$\delta^{18}O$ isotope values measured from ooids within the same sample, were found to be similar (-3.29‰ PDB) suggesting that sample contamination was not a factor. The implications of this will be discussed further in Section 3.3.

Cathodoluminescence analysis:

Cathodoluminescence analysis of ferroan equant calcite from samples 40, 42, C10, C12 and C13 (refer to Fig.3.i & Fig.3.ii) reveals a general non-luminescence to dull/moderate luminescence with well developed zoning (Table 3.iii & Fig.3.xiv).

Published analytical data:

Sun (1990) measured the manganese and iron content for ferroan equant calcite from the lower Osmington Oolite Formation as being between 0 - 0.2 wt % and 2.1 - 3.5 wt % respectively and stated that it did not luminesce (Table 3.ii). Sun's results generally agree with those presented in this thesis.

Ferroan equant calcite cements are also found within the Corallian Group successions of the Oxford area (De Wet, 1987). These cements have similar CL responses and $\delta^{18}O$ values to the results from the coastal successions presented here, but are slightly more depleted in $\delta^{13}C$ (Table 3.i).

Non-ferroan equant calcite:

Non-ferroan equant sparry calcite is restricted in lateral and vertical extent and is confined to three coarser grained oolitic beds within the lower Shortlake Member at the Bran Point outcrop (sample numbers 57-61 between 39.4m-41.2m on Fig.3.i & Fig.3.ii). The equivalent beds at the Black Head outcrop (sample numbers C8-C10 on Fig.3.i & Fig.3.ii) are cemented by ferroan to mildly ferroan equant calcite (see Fig.3.xiii).

Petrographic characteristics:

Non-ferroan equant sparry calcite, has similar petrographic characteristics to the ferroan equant sparry calcite described above, apart from its iron content (Fig.3.xvii). Within sample numbers 57-61 on Figure 3.ii, non-ferroan equant calcite accounts for between 30-40% of the total pore-filling volume and always post-dates ferroan fringing calcite (Fig.3.xvii).

Stable isotope analysis:

Stable isotope analysis of non-ferroan equant sparry calcite extracted from sample number 61 on Figure 3.ii, revealed more depleted $\delta^{18}O$ values of -4.42‰ PDB and heavier $\delta^{13}C$ values of +2.60‰ PDB when compared to its ferroan equivalent (Table 3.ii & Fig.3.iii).

Cathodoluminescence analysis:

Cathodoluminescence analysis of non-ferroan equant calcite from samples 57 and 61 (refer to Fig.3.ii) revealed a generally non-to moderately luminescent and partially zoned response (Table 3.iii & Fig.3.xv).

Published analytical data:

Sun (1990) states that the manganese content of samples of non-ferroan equant calcite collected from the upper Osmington Oolite Formation, range from 0.08-0.15 wt %, while the iron content is less than 1.0 wt %. Sun also states that this cement reveals bright luminescence and zoning (Table 3.ii). These results contradict those presented in this thesis, both in terms of the CL response and the distribution of non-ferroan calcite within the Osmington Oolite Formation.

Non-ferroan equant calcite also occurs within the Corallian Group successions around Oxford (De Wet, 1987). De Wet's results reveal a zoned, dull to bright luminescence, along with similar $\delta^{13}C$ values, but heavier $\delta^{18}O$ values, when compared to the results presented here (Table 3.i).

3.2.6: Authigenic ferroan dolomite

Occurrence

Authigenic ferroan dolomite occurs throughout the Corallian Group, except in the Nothe Grit Formation (between 0m and 12.8m on Fig.3.i & 3.ii). It is most abundant (20-30% of the total pore filling volume) within the heterolithic beds of the Bencliff Grit Member (at 25.3m, 27.3m & 29.1m on Fig.3.i & Fig.3.ii); the upper beds of the Upton Member to lower beds of the Shortlake Member (at 39.1m on Fig.3.i & Fig.3.ii); and the Sandsfoot Grit Member (between 66.5m-71.2m on Fig.3.i & Fig.3.ii). Through-out the remainder of the Corallian Group, if ferroan dolomite is present, it occurs as traces (less than 10% of the total pore filling volume, refer to Fig.3.ii).

Petrographic description:

Euhedral to subhedral ferroan dolomite rhombs (average individual crystal size is between 0.01 and 0.05mm, although occasionally 0.1 to 0.3mm) are closely associated with pyrite, siderite and micro-porosity within detrital clays (Fig.3.xviii). Ferroan dolomite clearly post-dates pyrite and siderite formation (Fig.3.xviii). When abundant (on a micron scale) ferroan dolomite forms mildly pervasive, idiotopic mosaics (after Freidman, 1964).

Stable isotope analysis:

The isotopic composition of ferroan dolomite could not be determined due to its fine grained nature.

Cathodoluminescence analysis:

Ferroan dolomite from samples 116 and 120 (refer to Fig.3.1 & Fig.3.ii) was non-luminescent.

3.2.7: Authigenic siderite

Authigenic siderite is present as traces within the Corallian Group succession, but is abundant within the Trigonia Clavellata Formation to the Ringstead Formation. Two types of siderite are recognised:-

- concretionary siderite; and,
- pore filling siderite cement

3.2.7a: *Concretionary siderite*

Occurrence:

Siderite concretions only occur within the lower beds of the Sandsfoot Grit Member (at 19.2m on Fig.3.i & 3.ii). These concretions range from 0.05-0.1m in size, are oblate to elongate in shape and composed entirely of siderite (Fig.3.xixa). Also seen within these sands are hollow/voidal iron-oxide concretions. Pettijohn (1975) suggests such features are due to oxidation of precursor siderite bodies [concretions]. The oxidation can be attributed to present day surface processes.

Petrographic characteristics:

In thin-sections of samples 115 and 116, siderite is brown to red in colour, has a high birefringence and is rhombic in cross-section.

Stable isotope analysis:

Stable isotope analysis was performed on one concretion from the lower beds of the Sandsfoot Grit Member (at 69m on Fig.3.i & Fig.3.ii). This concretion was collected from the Sandsfoot Grit Formation at Sandsfoot Castle. The results revealed strongly depleted $\delta^{13}C$ values of -15.28‰ PDB and slightly negative $\delta^{18}O$ values of -0.66‰ PDB (Table 3.iv & Fig.3.iii).

Cathodoluminescence analysis:

The CL response of concretionary siderite from within sample number 116 was non-luminescent.

3.2.7b: *Pore filling siderite cement*

Occurrence:

Pore-filling siderite cement is only abundant within the Trigonia Clavellata Formation (between 52.1m-58.4m on Fig.3.i & Fig.3.ii) and the Sandsfoot Grit Member (between 66.5m-71.2m on Fig.3.i & Fig.3.ii), where it constitutes between 10% and 50% of the total pore-filling volume. Within the Trigonia Clavellata Formation, the abundance of siderite cement increases upwards (between sample numbers 87 to C27 on Fig.3.ii) until it accounts for up to 50% of the total pore-filling volume (the remaining pore-space is occluded by ferroan equant calcite - refer to Section 3.2.5).

Petrographic characteristics:

Siderite cement is brown to red in colour, has a high birefringence and is rhombic in cross-section. It is closely associated with ferroan equant calcite which it post-dates and ferroan dolomite which it pre-dates (Fig.3.xixb).

Stable isotope analysis:

Stable isotope analysis of siderite cement extracted from sample C27 of the Red Beds Member (Trigonia Clavellata Formation, refer to Fig.3.iii) revealed slightly depleted $\delta^{13}C$ values of -0.54‰ PDB and strongly depleted $\delta^{18}O$ values of -5.91‰ PDB. However, analysis of similar cements extracted from sample 113 of the Sandsfoot Grit Member yielded depleted $\delta^{13}C$ values of -14.84‰ PDB which are similar to the siderite concretions described in Section 3.2.7b, and $\delta^{18}O$ values of -5.87‰ PDB, which are similar to the siderite cements of the Trigonia Clavellata Formation of Sequence 5.

Cathodoluminescence analysis:

The CL response of siderite cement from within sample numbers 88 and 120 was non-luminescent.

3.2.8: Summary of the distribution of early diagenetic products within the Corallian Group

Figures 3.i, 3.ii and Table 3.v summarise the early diagenetic products and processes within each lithostratigraphic unit of the Corallian Group succession. Early diagenetic products are broadly contained within either concretions or cemented beds.

3.2.8a: *Concretions*

Concretions of the Nothe Grit Formation and Bencliff Grit Formation are contained within coarser grained sandstone facies. During the deposition of the Nothe Grit Formation, two episodes of concretion growth occurred. Within the Bencliff Grit Member, at least two phases of concretion growth occurred, implying that in both cases their origin is related to periods of cyclic deposition. The early diagenetic interpretation of these concretions will be discussed in Section 3.3.1 and 3.3.3. Within the Sandsfoot Grit Member, only one episode of concretion growth occurred corresponding to the layer of small siderite concretions beneath the thin clay layer that occurs at 70m on Figure 3.ii. These concretion will also be interpreted within Section 3.3.6.

Nodular concretionary beds or concretionary burrows occur in two main episodes throughout the Corallian Group relating to a shallow shelfal depositional environment. These correspond to the *Thalassinoides* Beds (upper Upton Member) and the Nodular Rubble Member and will be discussed in Sections 3.3.3 and 3.3.4.

3.2.8b: *Cemented beds*

Carbonate cemented beds are seen to occur throughout the Corallian Group and are especially common within the Nothe Clay Member, Osmington Oolite Formation and Trigonia Clavellata Formation. These beds are composed dominantly of fringing and equant ferroan calcite and rarely poikilotopic ferroan calcite and non-ferroan calcite.

Traces of pyrite, ferroan dolomite and siderite are also present. Ferroan dolomite is seen to increase upwards within the Nothe Clay Member and Upton/Shortlake Member. Within the Osmington Oolite Member, carbonate cemented beds generally cap small metre thick coarsening-up carbonate cycles emphasising the cyclic repetition of these early diagenetic phases.

3.3: *Discussion - interpretation of early diagenetic products*

Introduction:

This section interprets the diagenetic phases described in Section 3.2 and discusses the validity of each phase in terms of supporting (or refuting) the facies based sequence stratigraphic model proposed in Chapter 2. Figure 3.xx and Table 3.vi provide graphical and tabulated summaries of the early diagenetic products and processes with relation to the sequence stratigraphic model outlined in Chapter 2.

Background:

Within the context of this study, early diagenesis is considered to include those processes occurring at or just after sediment deposition, at relatively low temperatures and within a shallow burial environment (Friedman, 1964; McKay *et al.*, 1995).

Early diagenetic processes are strongly influenced by depositional pore-water chemistry and microbial activity which are ultimately controlled by the depositional environment. Early diagenesis occurs in four main depth related zones, from the sediment-water interface downwards (Curtis, 1978, 1980, 1987; Irwin *et al.*, 1977; Berner, 1981 and Curtis & Coleman, 1986). These zones can be broadly described as the oxic zone, the sub-oxic /post-oxic zone, the zone of sulphate reduction and the zone of methanogenesis. In these zones, degradation of organic matter (primarily by bacteria) is controlled by the oxygen and sulphate content, the amount of available organic matter, iron and temperature (refer to Section 1.3 for an introduction to organic early diagenesis).

Stable isotope values of early diagenetic cements, reflect the composition of the pore-water at the time of cementation and are controlled by the method of organic degradation - each revealing specific $\delta^{13}C$ and $\delta^{18}O$ signatures (McKay *et al.*, 1995). For example, CO_3^{2-} produced within the zone of sulphate reduction, will commonly yield depleted $\delta^{13}C$ values of approximately -25‰ PDB (Irwin *et al.*, 1977), whereas low positive $\delta^{13}C$ values may suggest a methanogenic source (Coleman *et al.*, 1993 and McKay *et al.*, 1995). Generally, only during early diagenesis will the $\delta^{13}C$ value of the depositional water be a significant factor (McKay *et al.*, 1995).

Similarly, the $\delta^{18}O$ value of a cement is controlled by the composition of the depositional pore-water, which is ultimately controlled by the depositional and diagenetic environments (refer to Section 1.3 for an introduction to diagenetic environments). Thus within the Corallian Group, $\delta^{18}O$ values of cements that are similar to those of Jurassic sea-water

(inferred to be approximately -1.2‰ PDB *sensu* Marshall & Ashton, 1980) suggest a marine diagenetic environment, while depleted $\delta^{18}O$ values could relate to a mixed marine/meteoric diagenetic environment and strongly depleted $\delta^{18}O$ values could relate to a fresh-water (or burial) diagenetic environment. However, as will be discussed in the relevant sub-sections, a number of other possibilities exist to explain depleted oxygen values.

The degree of luminescence in carbonate cements [rocks] is controlled by the Fe/Mn ratio (not by the absolute concentration of either cation, Frank *et al.*, 1982) which itself can be controlled by the chemical composition of the pore-water. Meyers (1974) states that cathodoluminescence is derived from the incorporation of manganese into the calcite lattice (acting as an activator), while the reduction of iron, commonly acts as a luminescent quencher. Frank *et al.* (1982) state that there is no critical amount of Fe^{2+} in a calcite lattice, above which there is no luminescence, and regardless of the amount of Fe^{2+} present, calcite will luminesce if sufficient Mn^{2+} is present.

The CL intensity is a useful expression of the possible iron and manganese content of a calcite crystal and may be a guide to deciding whether the sedimentary carbonate was formed under oxidising or reducing conditions (Marshall, 1988). Various authors have suggested that the CL intensity reflects the pH, redox potential and total sulphur content of the pore-water (Carpenter & Oglesby, 1976; Frank *et al.*, 1982; Coleman, 1985 and Miller, 1988). Generally speaking, in an oxidising environment (where Mn^{3+} and Fe^{3+} are not reduced) both cations are excluded from the calcite crystal lattice and CL is not produced.

During sub-oxic conditions, Mn^{3+} is reduced to Mn^{2+} and is incorporated into the calcite lattice. However Fe^{3+} is not reduced and is not incorporated as a quencher. Thus the corresponding CL response is bright. In a strongly reducing environment, both Mn and Fe are reduced, which would lead to a dull CL response. But in all situations, it must be re-emphasised that the overall controlling factor on luminescence is the Fe/Mn ratio (Frank *et al.*, 1982).

3.3.1: The Nothe Grit Formation

Analysis of septarian concretions:

Further evidence to support the facies based identification of parasequences within the Nothe Grit Formation (refer back to Section 2.3.1) may be found by analysing the early diagenetic products of the septarian concretions that are located directly below the proposed marine flooding surfaces of each parasequence. This analysis is summarised as Stages 1-3 of Figure 3.xxi.

Sedimentological evidence (e.g. bioturbation) indicates that the shoreface sandstone facies of the Nothe Grit Formation was deposited under normal marine conditions (i.e. aerobic bottom waters, Section 2.2.1). Within this progradational shoreface, sedimentation rates would have been fairly high, and accordingly, any reactive iron and organic matter would have been rapidly buried into the deeper diagenetic zones, beyond the influence of the

zone of respiration (the oxic zone). Here, it would have been made available for intense sulphate reduction and/or microbial methanogenesis.

Pyrite formation:

The abundance of pyrite within the septarian concretions is consistent with reactions within the zone of sulphate reduction (Stage 1, Fig.3.xxi). Authigenic pyrite is a product of simultaneous reduction of organic matter, $Fe(III)$ compounds and SO_4^{2-}, which yield Fe^{2+} and HS^- (Curtis, 1987). The balanced reaction responsible for pyrite formation is:-

$$15CH_2O + 2Fe_2O_3 + 8SO_4^{2-} \rightarrow 4FeS_2 + 7H_2O + 15HCO_3^- + OH^- \quad \text{[Eq.2]}$$

As stated in Section 1.3, this reaction is limited by the concentration and reactivity of organic matter, and the rates of sediment accumulation - an increase in either, resulting in an increase in pyrite abundance (Berner, 1984; Curtis, 1987). From Equation 2, it is also clear that intense sulphate reduction and pyrite formation will result in the production of large quantities of bicarbonate which, when combined with calcium, from the dissolution of unstable bioclastic material, will result in the precipitation of calcite:-

$$Ca^{2+} + HCO_3^- \leftrightarrow CaCO_3^{2-} + H^+ \quad \text{[Eq.3]}$$

Concretionary growth:

Fleming (1993) has produced a model to explain the geometry and growth of carbonate concretions. In this model, calcite nucleation occurs preferentially upon aragonitic shell material due to a low activation energy (this process will occur during Stage 1 on Fig.3.xxi). This causes a reduction of the dissolved carbonate content in the surrounding pore fluids. As a result, a diffusion gradient of cement forming components develops around the nucleus which initially increases rapidly in response to rapid calcite precipitation, but over time increases at a slower rate in response to concretion growth.

The very low $\delta^{13}C$ values (-31.10‰ PDB) of zone 1 non-ferroan calcite (Stage 1, Fig.3.xxi) indicate that oxidation of organic matter during sulphate reduction was the major source of carbonate (e.g. Irwin *et al.*, 1977; Curtis & Coleman, 1986; Curtis, 1987; Raiswell, 1987; Mozley & Burns, 1993; Hendry, 1993b and McKay *et al.*, 1995). Similarly, the moderate to bright luminescence of zone 1 calcite is consistent with the generation of calcite during organic matter diagenesis within a dominantly sub-oxic environment (Carpenter & Oglesby, 1976; Frank *et al.*, 1982; Coleman, 1985; and Miller, 1988) assuming a low Fe/Mn ratio. The absence of zoning within zone 1 calcite suggests that small fluctuations in pore-water chemistry were minimal at the time of precipitation.

Oxygen isotope results obtained from zone 1 calcite (-0.83‰ PDB) should closely approximate to the isotope composition of the depositional pore-water. The $\delta^{18}O$ results suggest that (i) the original calcite source was from normal marine ^{18}O pore-water and (ii)

that the palaeotemperature of the depositional pore-water was between 13°C and 14°C.

Zone 2 calcite of these concretions (Stage 2, Fig.3.xxi) also has very low $\delta^{13}C$ values (-26.60‰ PDB), although slightly less depleted than in zone 1. This, coupled with the decreasing volume of pyrite and the introduction of traces of siderite and slight zoning as revealed by CL, may suggest that zone 2 calcite was forming close to the lower boundary of the sulphate reduction zone. Zoning suggests that small fluctuations in pore fluid chemistry occurred, which would be expected close to the boundary of the Sr and Me zones. Also, the crystallization of siderite would have begun once iron was no longer being fixed by pyrite formation (McKay *et al.*, 1995).

Siderite precipitation within the zone of sulphate reduction requires pore-waters with very low dissolved sulphide (Pearson, 1979) as well as bicarbonate and Fe^{2+}, the principal products of sulphate reduction. The extensive removal of iron during the early formation of pyrite within zone 1 of the concretions, may explain the very low siderite content of zone 2. Similarly, as both calcite cements of zone 1 and zone 2 are non-ferroan, this suggests that rates of $Fe(III)$ reduction were less than the rate of sulphate reduction - an observation that is supported by the moderate to bright luminescence response. This could have occurred due to a low iron content in the host sediment (Coleman, 1985; Curtis, 1987). Thus, limited Fe^{2+} would have been available for siderite crystallisation.

The formation of septarian fractures within similar concretions elsewhere, has been attributed to:- (i) chemical dehydration and shrinkage (Raiswell, 1971; Pettijohn, 1975); or

(ii) tensile stress relating to overpressure development during shallow burial (Astin, 1986; Astin & Scotchman, 1988). All authors agree however that their formation is synonymous with early growth prior to any significant compaction and dewatering (McKay *et al.*, 1995). $D^{13}C$ values for calcite within the septarian fractures are slightly positive (+2.23‰ PDB). Mozley & Burns (1993) suggest that calcite with low positive $\delta^{13}C$ values can be explained by low rates of organic-carbon oxidation which will either extend the zone of sulphate reduction deeper into the sediment, or result in very slow rates of methanogenesis (Stage 3, Fig.3.xxi).

Sequence stratigraphic interpretation:

The analytical results presented in this sub-section suggest that early diagenesis was controlled by parasequence formation. During parasequence progradation, sedimentation rates were high enough to allow for the rapid burial of organic material into the zone of sulphate reduction (Stage 1, Fig.3.xxi). During the development of the parasequence boundary (an example of one such boundary is at 6.4m on Fig.3.xx) the parasequence would have effectively "drowned" as the amount of accommodation space exceeded the sedimentation rate and a cut-off in sediment supply would have occurred. This phase of "drowning" must have been long enough for sediment to remain in the Sr zone for a sufficient length of time to allow the septarian concretions to grow (Stages 1-3 of Fig.3.xxi). The carbon isotope, CL and cement types all suggest that zone 1 and 2 diagenesis occurred within the zone of sulphate reduction, although zone 2 calcite must have precipitated closer to the Sr/Me boundary.

Parasequence progradation and drowning provides a plausible interpretation to account for the rapid burial, followed by prolonged residence times within early diagenetic zones - conditions which were necessary for concretion growth.

The proposed interpretation of the septarian concretions is in agreement with those of Hudson (1978) for similar concretions within the Oxford Clay Formation underlying the Nothe Grit Formation. Hudson also suggests that organic/sulphate reduction was the source for the carbon and the concretions formation at sea-water temperatures of 13-16°C. Hudson's $\delta^{13}C$ and $\delta^{18}O$ values reveal the same trends as described here (refer to Sections 3.2.5). The similarity between my results and those of Hudson suggests a strong similarity in the composition of early diagenetic pore-fluids within the Nothe Grit Formation and underlying Oxford Clay Formation even though they are composed of distinctly different lithologies. This is further evidence that these two formations are part of the same sequence and not separated by an abrupt basinward shift in facies (refer to Section 2.3.1 for sequence stratigraphic model). Such a shift in facies would undoubtedly evoke a change in pore-water fluids. Thus it is still conceivable to suggest that the Nothe Grit Formation could represent the upper highstand systems tract of Sequence 1 at a time when sedimentation rates were increasingly outpacing rates of accommodation creation.

There is no evidence of meteoric diagenesis associated with the period of forced regression that caps Sequence 1 and is responsible for the formation of Sequence Boundary 1 (at 11.2m on Fig.3.xx). This suggests that the period of forced regression did not result in any sub-aerial exposure at this location, an interpretation in keeping with the facies analysis

(see Section 2.2). Alternatively, this could also support the interpretation of a ravinement surface at this boundary where the presence of meteoric cements would also be highly unlikely.

Other cements within the Nothe Grit Formation:

The laterally extensive ferroan poikilotopic calcite cements of the coarsest sandstone facies at the top of each parasequence, formed after the septarian concretions and so were unrelated to relative sea-level changes at a parasequence or intracyclic scale. However, this cement is preferentially found within the coarser grained sandstone facies, suggesting that pore fluids responsible for its formation required a porous and permeable medium for movement. This can be termed facies related diagenesis, which would have been ultimately controlled by the type and development of the individual parasequences and their depositional environment. It is therefore quite possible that cements of this type (that are clearly not formed during the deposition of the parasequence) can still be predicted within a sequence stratigraphic framework.

3.3.2: Preston Grit Member & Nothe Clay Member

Pore filling pyrite, ferroan dolomite and rare siderite cement, along with rare non-ferroan concretionary calcite and common ferroan poikilotopic calcite, are present within the coarser grained beds of the Preston Grit and Nothe Clay Member (at 12m, 14.5m, 17m and

22.4m on Fig.3.xx). From Figure 3.xx, it is clear that the volume of pore-filling ferroan dolomite increases upwards through the Nothe Clay Member into the lower one metre of the Bencliff Grit Member, while the relative abundances of the other authigenic phases remains level.

Ferroan dolomite:

The data presented in Figure 3.xx (sample numbers B12 to B18) indicates that the upwards increase in ferroan dolomite occurs within the proposed highstand systems tract of Sequence 2. As such, this would support the interpretation of a highstand systems tract and the positioning of a sequence boundary corresponding to the first mudstone bed of the Bencliff Grit Member, both of which were originally based on facies analysis, as described in Sections 2.3.2 and 2.3.3. Van Wagoner *et al.* (1990) state that sedimentation rates are greater than the rates of accommodation creation within a highstand systems tract. One response to this net increase in sedimentation rates is a rapid burial of sediment to the zone of sulphate reduction. The precipitation of ferroan dolomite [and siderite] in association with pyrite, requires rapidly depleted sulphate levels, which can be effectively reduced to zero by the action of microbial sulphate reduction (Curtis & Coleman, 1986). Unstable primary carbonates (e.g. aragonitic shell debris) and pore-water solutes can then react with the products of organic degradation (Equation 2 of Section 3.3.1) to produce the authigenic phases. The overall low volumes of ferroan dolomite (up to a maximum of 30% pore-filling volume within sample number B18 on Fig.3.xx) is a factor of low iron and organic content, both of which would have been extensively removed during the

formation of pyrite.

Non-ferroan concretionary calcite:

Within the lower beds of the Nothe Clay Member, one coarser grained siltstone bed (at 17m on Fig.3.xx) contains fine grained non-ferroan calcite (sample number B13 on Fig.3.ii). The presence of borings (refer back to Section 2.2) indicates that the top surface of this bed is a hard-ground suggesting that these cements are a marine precipitate. In Section 2.3.2, this bed was identified as the top of a proposed parasequence, based on facies analysis. The early diagenetic evidence indicates a sea-floor marine environment, thus supporting this interpretation. This is the only bed within the Nothe Clay Member that contains such cements.

Ferroan poikilotopic calcite:

As in the Nothe Grit Formation, ferroan poikilotopic calcite is confined to coarser sandstone and siltstone beds and is of a similar form and habit to that described in sub-section 3.3.1. This cement is interpreted to be unrelated to parasequence formation. This cement is therefore a facies related diagenetic product which required a porous and permeable medium for pore fluid movement - hence its preferential growth within coarser sandstone and siltstone beds.

3.3.3: Bencliff Grit Member to Shortlake Member

Early diagenetic analyses can be used as further evidence to support the proposed sequence stratigraphic framework (primarily based on facies analysis) of Sequence 3 (Bencliff Grit Member to second oolitic bed of the Shortlake Member). They can be divided into two groups:- (i) glauconite, large ferroan poikilotopic calcite concretions and ferroan dolomite cement within fining-up facies sequences of the Bencliff Grit Member and (ii) pyrite, calcite, ferroan dolomite and concretionary burrows within coarser grained carbonate beds and nodular horizons of the Upton Member and lower two oolitic beds of the Shortlake Member.

3.3.3a: *The Bencliff Grit Member*

Early diagenesis within the Bencliff Grit Member was controlled within cyclic facies sequences. It is characterised by (i) large calcite concretions within what is otherwise a relatively uncemented fine grained sand facies (refer to Section 2.2.3 for lithological description) and (ii) the precipitation of authigenic dolomite within laterally extensive heterolithic units (refer to Section 2.2.3 for lithological description). Due to this cyclicity, early diagenesis can be convincingly related to parasequence formation. Figure 3.xxii (Stages 1-4) summarises the early diagenetic reactions within one such parasequence.

Stage 1, Figure 3.xxii:

Interpretation of sedimentological data indicates that these sediments were deposited in an aerobic environment (see Section 2.2.3). The presence of diffuse glauconite within the fine grained sandstone facies of each parasequence (sample numbers 30, 32, 34 and 36 on Figure 3.xx) is interpreted to be related to condensation during periods of prolonged flooding at the time of parasequence boundary formation (Fig.3.xxii). Glauconite is indicative of reworking, slow sedimentation rates or sediment starvation within mildly reducing conditions (Pettijohn, 1975; Desrochers & Al-Aassm, 1993 and McKay *et al.*, 1995). Interestingly, samples 30 to 36 (see Fig. 3.xx) show an upward decreasing volume of glauconite. The fact that the largest volumes of glauconite are found towards the base of the Bencliff Grit Member can be related to greater amounts of winnowing, sediment transportation and turbulence which would be associated with sequence boundary formation and a change in depositional environments from dominantly muddy shelfal to dominantly tidal flat shoreline (refer back to Section 2.2.3 and 2.3.3).

Stage 2, Figure 3.xxii:

Due to the low sedimentation rates associated with prolonged flooding at parasequence boundaries, organic degradation may occur in the oxic and post-oxic zones if present. The inevitable result is that less organic matter is likely to reach the sulphate reduction zone and there will be lower amounts of sulphide supersaturation (Berner, 1978; Raiswell, 1982 and Curtis 1987). This is reflected in the low volumes of pyrite (Section 3.3.1).

Stage 3, Figure 3.xxii:

A combination of excellent poroperm properties and low sedimentation rates resulted in the formation of large poikilotopic calcite crystals and the growth of large oblate and spherical concretions (refer back to Section 3.2.5). The shape of each concretion is defined by the concentration and location of shell debris (refer back to Section 3.1.1c) within the sandstone facies (*sensu* Fleming, 1993).

The $\delta^{13}C$ values of the ferroan poikilotopic calcite within the concretions range from -0.24‰ PDB to +1.86‰ PDB. This suggests a combination of marine carbonate and carbonate sourced from low rates of organic-carbon oxidation deep within the zone of sulphate reduction (Mozley & Burns, 1993). The fact that the carbon values are not strongly depleted supports my interpretation that levels of sulphate reduction were low. This interpretation is also supported by the CL data which shows a dominantly dull to non-luminescence for the ferroan poikilotopic calcite. The dull luminescence coupled with the ferroan nature of the calcite indicates the presence of a strongly reducing environment, in which iron reduction was common.

$D^{18}O$ values for calcite within the concretions are increasingly depleted (ranging from -9.23 to -5.60) from the core to perimeter (Fig.3.ix). These values are consistent with a pore-water chemistry of mixed marine/meteoric composition. According to Mozley & Burns (1993) this is the most common explanation in the literature for anomalously depleted oxygen values during early diagenesis. Bearing-in-mind the depositional

environment of these sediments (tidal flat shoreline), it seems logical that pore-waters of mixed marine/meteoric chemistry would have percolated through the sediment. This explanation is supported by palynological work of Goldring *et al.* (in press) who report the presence of terrestrial organic matter within the muddy horizons of the Bencliff Grit Member. All this evidence strongly points to an input of meteoric water.

A second explanation for low $\delta^{18}O$ values can also be offered, but due to the limited amount of data, this can not be substantiated and further samples need to be analysed. This explanation states that the effect of carbonate precipitation on the $\delta^{18}O$ composition of the pore-water is dependant upon the rate at which the concretion forms (Mozley & Burns, 1993). Carbonate precipitation rates will lead to a greater depletion in the $\delta^{18}O$ composition of the pore-waters. The difference in oxygen isotope values between normal Jurassic sea-water (approximately -1.2‰ PDB) and the core of the concretions described here (-6.30‰ PDB) is 5.1‰, whereas the difference between the core and outer zone of the concretion is only 0.53‰. This suggests that the initial growth of the concretion occurred at a very rapid rate. As discussed previously (Section 3.3.1), Fleming's (1993) model for concretion growth includes an initial period of very high growth rate, where volumes of calcite precipitation are substantially greater than aragonite dissolution. The growth rate subsequently declines until calcite precipitation and aragonite dissolution rates equilibrate.

Discussion:

The ferroan poikilotopic calcite found within the concretions cannot be a late generation cement because it preserves an open grain framework and has an unlikely carbonate source for a burial phase. De Wet (1987) interprets similar calcite within the Oxfordshire outcrops of the Corallian Group (although their form and habit in terms of concretionary bodies or cemented beds, was not discussed) as having formed during burial. However, De Wet's measured $\delta^{18}O$ values averaged at -3‰ PDB, which is not too dissimilar to Marshall & Ashton's (1980) results that were extracted from bivalve shells. In Saigal & Bjørlykke's (1987) study of North Sea Jurassic sandstone reservoirs, $\delta^{18}O$ values of less than -10‰ PDB are interpreted to indicate later burial cements.

The $\delta^{18}O$ depletion is also unlikely to have been caused by recrystalisation of the calcite during later burial. Assuming that the calcite was originally low-magnesium, the norm. for Jurassic marine precipitates (Sandberg, 1983; Wilkinson *et al.*, 1985), it should have been relatively stable and unsusceptible to recrystalisation (Mozley & Burns, 1993).

The $\delta^{18}O$ values increase with younging within the Bencliff Grit Member (Fig.3.ix). This is interpreted to indicate an overall decrease in the meteoric influence during the deposition of this member. This pattern might be expected at the top of a shelf-margin systems tract, where rates of relative sea-level are rising increasingly quickly (although it should be noted that this explanation is based on a limited amount of data). Further analytical data is needed to unequivocally support this statement.

In conclusion, the two distinct $\delta^{18}O$ trends observed within the concretions, are interpreted to be the result of an overall change from a mixed marine/meteoric to dominantly marine pore-water chemistry, associated with a slow and gradual change to a more open marine depositional environment.

Stage 4, Figure 3.xxii:

Precipitation of ferroan dolomite would have followed once sulphate levels had effectively been reduced to zero. Ferroan dolomite (refer back to Section 3.2.6) occurs in organic rich zones, such as clay laminae within the sands, burrows and the laterally extensive heterolithic layers, again suggesting that sulphate supersaturation was very low.

Sequence stratigraphic interpretation:

Analysis of analytical data obtained from concretions and heterolithic beds, supports the proposed facies based identification of parasequences and provides further, limited evidence that the Bencliff Grit Member represents a shelf-margin systems tract. The upward decreasing volume of glauconite also provides further support for the positioning of the sequence boundary at the first mudstone bed of the Bencliff Grit Member, rather than at the lithostratigraphic boundary (as suggested by previous workers, e.g. Coe, 1995).

3.3.3b: *Upton Member to second oolitic bed of the Shortlake Member*

Early diagenesis within these two lithostratigraphic units (between 29.2m and 40.7m on Fig.3.xxiii) was dominated by sea-floor cementation within shallow water depositional environments (i.e. the proposed early transgressive and late highstand systems tracts between 29.2m-33.5m & 39m-40.7m respectively on Fig.3.xxiii). Concretionary burrow formation dominates the deeper water depositional environment corresponding to the proposed zone of maximum flooding (between 33.5m-39m on Fig.3.xxiii).

The Upton Member:

The principal cements are ferroan grain fringing calcite and ferroan equant sparry calcite, both of which totally occlude pore space and mouldic porosity (Fig.3.xii) and both of which reveal dull to moderate luminescence and well developed zoning (Fig.3.xiv). Characteristically, these cements occur at the top of small scale coarsening-up carbonate cycles which have been identified as parasequences (at 29.8m, 31.6m and 33.3m on Fig.3.xxiii). The top of each parasequence has been interpreted as a marine hard-ground (refer back to Section 2.3.3) and the early diagenetic and analytical evidence supports this (see below).

Early growth of well developed fringing calcite significantly reduced the degree of grain repacking during burial. Contrary to Sun (1990), both intact and collapsed micrite envelopes are present within these sediments. Collapsed micrite envelopes are the result

of dissolution of unstable aragonite bioclasts forming large solution pores, poorly developed fringing calcite cements and subsequent compaction/collapse. The stable isotope values of the fringing calcite cements are consistent with a normal marine carbonate source ($\delta^{13}C$ values of +0.73‰ PDB) precipitating within normal marine pore-waters ($\delta^{18}O$ values of -2.19δ‰ PDB suggesting pore-water temperatures of 20.9°C at the time of cementation). Stable isotope values of similar ferroan equant sparry calcite are also consistent with a normal marine carbonate source ($\delta^{13}C$ values of -0.35‰ PDB) precipitating within normal marine pore-waters ($\delta^{18}O$ values of -3.07‰ PDB). As well as the calcite cements, pyrite is present, within the organic rich zones of bioclastic shell debris and ooid laminae and rarely as a pore filling precipitate. Siderite is also present in trace quantities.

Similar observations have been made by Wilkinson *et al.* (1985) who note the presence of dull to bright luminescent, equant sparry calcite and acicular isopachous calcite within Upper Jurassic hard-grounds of southeastern Wyoming. Purser (1969) describes abundant early equant, to slightly elongate, calcite cement in oolitic Jurassic hard-grounds from the Paris Basin. Both interpret these cements as being the products of sea-floor precipitation.

Sun (1990) suggests that the fringing cements precipitated either as low magnesium calcite, or from neomorphism of high magnesium calcite in anoxic marine or meteoric phreatic water; while the ferroan equant sparry calcite owes its origin to an oxygen depleted, deep burial environment. De Wet (1987) suggests a marine to oxidising meteoric phreatic origin for the equivalent non-ferroan fringing cements of the Corallian

of dissolution of unstable aragonite bioclasts forming large solution pores, poorly developed fringing calcite cements and subsequent compaction/collapse. The stable isotope values of the fringing calcite cements are consistent with a normal marine carbonate source ($\delta^{13}C$ values of +0.73‰ PDB) precipitating within normal marine pore-waters ($\delta^{18}O$ values of -2.19δ‰ PDB suggesting pore-water temperatures of 20.9°C at the time of cementation). Stable isotope values of similar ferroan equant sparry calcite are also consistent with a normal marine carbonate source ($\delta^{13}C$ values of -0.35‰ PDB) precipitating within normal marine pore-waters ($\delta^{18}O$ values of -3.07‰ PDB). As well as the calcite cements, pyrite is present, within the organic rich zones of bioclastic shell debris and ooid laminae and rarely as a pore filling precipitate. Siderite is also present in trace quantities.

Similar observations have been made by Wilkinson *et al.* (1985) who note the presence of dull to bright luminescent, equant sparry calcite and acicular isopachous calcite within Upper Jurassic hard-grounds of southeastern Wyoming. Purser (1969) describes abundant early equant, to slightly elongate, calcite cement in oolitic Jurassic hard-grounds from the Paris Basin. Both interpret these cements as being the products of sea-floor precipitation.

Sun (1990) suggests that the fringing cements precipitated either as low magnesium calcite, or from neomorphism of high magnesium calcite in anoxic marine or meteoric phreatic water; while the ferroan equant sparry calcite owes its origin to an oxygen depleted, deep burial environment. De Wet (1987) suggests a marine to oxidising meteoric phreatic origin for the equivalent non-ferroan fringing cements of the Corallian

Group in the Oxford area, and a reduced meteoric and shallow burial environment for the ferroan equant calcite phase. However, in her analysis, both phases of cement have similar $\delta^{18}O$ values, averaging -2.0 to -2.5 ‰ PDB, instead of an expected stronger depleted value for the meteoric phase. She explains this by suggesting that the isotopic composition of the meteoric water was not greatly different from the sea-water. Talbot (1971) suggests that the early fibrous cements, which are widespread across southern England, appear to have formed as low magnesium calcite in a shallow burial reducing environment.

The isotopic and sedimentological results presented in this thesis suggest that the formation of the fringing and equant calcite could not have occurred within a reducing environment. Stable isotope, CL and petrographic results indicate that both cements are sea-floor precipitates, and the presence of bioturbation indicates that the sea-floor was oxygenated. Therefore the dull to moderate luminescence must be controlled by the Fe/Mn ratio of the calcite (Frank *et al.*, 1982) suggesting that the luminescence is a primary attribute - a suggestion also made by Wilkinson *et al.* (1985). Wilkinson *et al.* (1985) also infer that if luminescence was acquired during initial marine cement precipitation, then initial cement compositions must have been low-magnesium calcites. It is unlikely that the luminescence was a late diagenetic attribute (e.g. if the original cement was of high-magnesium composition and was then stabilised to low-magnesium calcite) because this would have resulted in depleted $\delta^{18}O$ values, which clearly are not the case.

The variation in crystal morphologies within the documented hard-grounds, may result from differing *Mg/Ca* ratios or surface/active cation ratios (Wilkinson *et al.*, 1985).

According to Wilkinson *et al.* (1985) such a variation in Jurassic marine cement morphologies must be related to a factor [kinetic?] which influences crystal growth during hardground lithification.

The occurrence of low volumes of pyrite and siderite emphasises that very low rates of sulphide supersaturation occurred, and only then within organic rich micro-environments (e.g. ooid cortices, bioclastic shell debris, burrows or clay rich laminae). Similar observations have been made by Milodowski & Wilmot (1984) and Sun (1990).

Sequence stratigraphic interpretation:

Interpretation of isotopic, diagenetic, CL and sedimentological evidence indicates that the dominant calcite cements were precipitated within agitated marine pore-waters during the phase of parasequence progradation, and were then exposed to the sub-marine environment by winnowing during the phase of parasequence boundary formation. This exposure resulted in the development of marine hard-grounds. These analyses provide unequivocal evidence for parasequence identification. Similarly, the dominance of marine cements and lack of sub-aerial exposure indicates precipitation within a transgressive systems tract (*sensu* Tucker, 1993).

Thalassinoides Beds:

The deeper water facies (between 33.5m-39.3m on Fig.3.xxiii) are characterised by

concretionary diagenesis within *Thalassinoides* burrows. The dominant cement type is fine grained non-ferroan calcite, although quantities of ferroan dolomite increase upwards towards the top of this unit (Fig.3.xxiii). Cementation of these, and similar burrow networks, has been well documented by Fürsich (1973) and Fleming (1993); my Section 3.1. Cementation of these burrows must have been early, as there is no evidence of burrow collapse or compaction. The increase in the volume of ferroan dolomite towards the top of this unit must be related to a net increase in sedimentation rates associated with the commencement of progradation. This would ensure rapid burial of organic matter into organic reducing zones, which would then be available for sulphate reduction (as depicted in Equation 2 of Section 3.3.1). Thus a similar scenario to that described within the highstand systems tract of Sequence 2 is envisaged (refer back to Section 3.3.2).

The Shortlake Member:

Within the coarser grained beds of the Shortlake Member, ferroan fringing calcite is poorly developed (Fig.3.xii), cross-cutting fractures filled with a late generation ferroan drusy calcite spar are present and locally (at the Bran Point outcrop) pore-filling and non-luminescent non-ferroan calcite is present (Fig.3.xvii & Fig.3.xxiii). The lack of fringing calcite has already been interpreted to be the main contributing factor of grain compaction within these highstand sediments (Fig.3.xiii & refer back to Section 3.2.5).

Stable isotope results obtained from ferroan equant sparry calcite are consistent with a normal marine carbonate source ($\delta^{13}C$ values of -0.35‰ PDB) precipitating within normal

marine pore-waters ($\delta^{18}O$ values of -3.07‰ PDB suggesting pore-water temperatures of 25.4°C at the time of cementation[2]).

However, stable isotope results obtained from non-ferroan equant calcite extracted from the Bran Point outcrop are consistent with a normal marine carbonate source ($\delta^{13}C$ values of -0.35‰ PDB) precipitating within mixed marine/meteoric porewaters ($\delta^{18}O$ values of -4.42‰ PDB). The $\delta^{18}O$ values of the non-ferroan cements are more depleted than their ferroan equivalent. This observation supports Sun (1990) who interpreted them as representing cementation during an incursion of mixed marine/meteoric water that originated from a subaerially exposed area of the basin. However, these cement types are not as extensive as Sun has reported. In his work, he infers that non-ferroan equant calcite is common through-out the whole of the overlying Shortlake Member. This is clearly not the case (see sub-section 3.3.4). The only evidence of non-ferroan equant calcite is within the lower three oolitic beds of the Shortlake Member at the Bran Point outcrop. The most abundant cement in the laterally equivalent beds at the Black Head outcrop is ferroan equant calcite.

The CL response of the non-ferroan calcite would suggest an oxidising environment. Its characteristic dull to non-luminescence must be related to limited Mn^{3+} and Fe^{3+} reduction. However, Sun (1990) states that non-ferroan equant calcite from the Shortlake

[2] Interestingly, the palaeotemperature estimation of these cements is marginally higher than that estimated for the fringing calcites of the transgressive systems tract and indeed significantly higher than that obtained from concretionary calcite within sequence 1. Of course this could be a factor of experimental error and small sample size, but it is worth pointing out that Hallam (1994) using a range of data (floral, faunal, sediment, isotope and computer generated models) infers that the palaeoclimate of the late Jurassic was warmer than the that of the early Jurassic. Clearly, further evaluation and work is required to link pore-water palaeotemperatures to Jurassic palaeoclimates.

Member has a bright luminescence which suggests a sub-oxic diagenetic environment. The isotopic data presented in this thesis does not agree with Sun's (1990) diagenetic environment for these particular cements.

Sequence stratigraphic interpretation:

The presence of localised non-ferroan calcite is interpreted to indicate an incursion of meteoric derived pore-water. Within the context of the sequence stratigraphic framework defined in Chapter 2, this could be associated with the development of the sequence boundary positioned above the second oolitic bed of the Shortlake Member (at 40.7m on Fig.3.xxiii). However in the coastal successions, there is no field evidence for subaerial erosion associated with this sequence boundary. Thus any influx of meteoric water must have been in the form of an hydraulically driven fresh-water lens that originated from a subaerial exposed area of the basin during this time of sequence boundary formation.

Coe (1995) suggests that within the Oxfordshire area, a sequence boundary associated with a period of erosion can be positioned between the Highworth Grit Member and the Third Trigonia Bed (refer to Coe, 1995, fig.11 for stratigraphic location). Coe (1995) has correlated this surface in Oxfordshire to a conformable/erosive surface positioned 0.5m above the base of the Shortlake Member in the coastal exposures (Fig.3.xxiii & refer to Section 2.2.3f for detailed description). However the presence of meteoric cements within the lower beds of the Shortlake Member supports my interpretation of the positioning of a sequence boundary at the top of the second oolitic bed of the Shortlake Member

(Fig.3.xxiii). The fact this cement is of a limited extent and formed as a result of a fresh-water lens, further supports the interpretation that the sequence boundary was a type-2 boundary and thus did not result in any sub-aerial exposure.

Immediately above the sequence boundary, (sample number 61 on Fig.3.xx) there is also evidence of meteoric cementation within the overlying shelf-margin systems tract (equivalent to the "middle white oolite bed" Arkell, 1947a). This would not necessarily have to result in further re-positioning of this sequence boundary, because sample number 61 was collected directly above the surface separating the second oolitic bed of the Shortlake Member from the overlying "middle white oolite bed" (Arkell, 1947a) when the effects of meteoric infiltration would still have been evident.

3.3.4: Shortlake Member to the Nodular Rubble Member

Early diagenetic processes can be used as further evidence to support the proposed sequence stratigraphic framework of Sequence 4 ("middle white oolite bed" to top of Nodular Rubble Member). They are similar to those of the underlying Upton and Shortlake Members, except that there is little evidence of a meteoric influence. Only sample 61 on Figure 3.xx, shows any evidence of non-ferroan pore filling calcite that could be related to a period of meteoric diagenesis and this has been discussed in Section 3.3.3. As indicated in Section 3.3.3, this observation is inconsistent with Sun's (1990) findings that the upper Osmington Oolite Formation (approximately equivalent to

Sequence 4) is dominated by pervasive mildly ferroan to non-ferroan meteoric calcite cements.

Poorly developed dull luminescent to moderately luminescent marine ferroan fringing calcite and marine ferroan equant calcite within the "middle white oolite bed" (samples 61, C9 & C10 on Fig.3.xx) are replaced upwards by marine ferroan equant sparry calcite within the remainder of the Shortlake Member (sample numbers C11-C15 on Fig.3.xx). The Nodular Rubble Member (samples 78-84 on Fig.3.xx) is dominated by concretionary burrows, brightly luminescent calcite and upwardly increasing volumes of pyrite. The pyrite is contained within ooid cortices and bioclastic shell debris, although the upwards increase in volume may represent a net increase in sedimentation rates associated with progradation, as has been documented in the highstand systems tracts of Sequence 2 (Section 3.3.2) and Sequence 3 (Section 3.3.3). The dominantly bright luminescence of the concretionary calcite must be related to either (i) early diagenesis within a sub-oxic environment (i.e. the Sr zone) and/or (ii) a low Fe/Mn ratio.

Interestingly, early diagenetic analysis provided no evidence of dissolution or meteoric cementation associated with the top of the Nodular Rubble Member which has been interpreted as a sequence boundary. This would indicate that any period of sub-aerial exposure was of very limited duration. However, Coe (1995) measured bulk rock $\delta^{18}O$ and $\delta^{13}C$ isotopes of samples collected from the top of the Nodular Rubble Member. Although her data is variable (-2.3 to -6.1‰ PDB $\delta^{18}O$ and -2.3 - +2.2‰ PDB $\delta^{13}C$) and not an exact measurement of early diagenetic cements, it does appear to indicate a phase of

meteoric porewater at the top of the Nodular Rubble Member. This is further evidence to indicate a fall in relative sea-level associated with this surface, thus supporting the facies based sequence stratigraphic interpretation.

3.3.5: Trigonia Clavellata Formation to Sandsfoot Clay Member

Sedimentological analysis (refer back to Section 2.2.5) suggests that the bioturbated shoreface sediments (Trigonia Clavellata Formation) were deposited in an aerobic environment and therefore organic degradation in the oxic and post-oxic zones probably occurred (depending on relative rates of sedimentation). This would explain the low pore filling volume of pyrite (apart from in sample number 86, on Fig.3.xx which must have been rich in organic matter) which is a by-product of reactions within the zone of sulphate reduction (refer back to Equation 2 of Section 3.3.1). Thus less organic matter reached the sulphate reduction zone, resulting in lower levels of sulphide supersaturation (Berner, 1978; Raiswell, 1982; Curtis, 1987).

The early diagenetic reactions are dominated by upward decreasing amounts of fine grained ferroan equant calcite (Fig.3.xxiv) and upward increasing amounts of siderite and ferroan dolomite (Fig.3.xxiv). Within the Red Beds Member at 56.7m-58.3m on Fig.3.xxiv) the pore filling cements comprise approximately 50% ferroan calcite and 50% siderite.

The fine grained ferroan sparry calcite that is dominant within the Sandy Block Member, and less so within the Red Beds Member, is very similar in form and habit (although finer grained) and has a similar dull luminescent response to that seen within the Shortlake Member. It is therefore assumed to be of an early marine origin. Due to the fine grained nature of the sediments, it was not possible to extract the cement by scalpel or micro-drill for isotope analysis.

In contrast to earlier lithostratigraphic units, the Trigonia Clavellata Formation is characterised by abundant volumes of siderite cement (Fig.3.xviii & Fig.3.xxiv). This high abundance could be related to (i) low volumes of pyrite, which would have resulted in more iron being made available for siderite formation during ferric iron reduction (McKay *et al.*, 1995); or (ii) precipitation of siderite as a by-product of chemical reactions that involve sulphate reducing bacteria (Coleman *et al.*, 1993). Coleman *et al.* (1993) state that this type of reaction utilises an enzymatic mechanism which reduces H_2S compounds rather than reducing $Fe(III)$ (siderite being unstable in the presence of H_2S).

An alternative explanation by Canfield (1989) is that siderite may have a bacterial origin from the microbial reduction of iron oxides. Distinct micro-environments may exist in marine sediments where in one, sulphides react with iron oxides locally producing pyrite whilst in another, iron reduced by micro-organisms migrates freely into solution to be combined with bicarbonate to produce siderite.

Within the Red Beds Member, the calculated $\delta^{13}C$ value for the pore filling siderite

(-0.54‰ PDB) is consistent with crystallisation as a result of ferric iron reduction in a sub-oxic environment during or immediately after sulphate reduction (Mozley & Wersin, 1992), although a contribution from marine carbonate cannot be ruled out. Sub-oxic conditions are favoured in marine environments that display relatively low concentrations of organic matter and low sedimentation rates (Berner, 1981; Coleman, 1985). Siderite crystallising under sub-oxic conditions has been well documented by numerous workers (e.g. Li *et al.*, 1969; Lynn & Bonatti, 1965; Maynard, 1982; Walker, 1984; Coleman, 1985; Mozley & Carothers, 1992 and Taylor & Curtis, 1995).

From Equation 2 (Section 3.3.1) it is clear that due to the action of sulphate reducing bacteria, carbonate production is inevitable. If the rate of *Fe(III)* reduction is greater than the rate of sulphate reduction, then iron rich carbonates (e.g. siderite) will precipitate (Curtis, 1987). As noted in Section 3.3.1, siderite precipitation requires pore-waters with very low dissolved sulphide levels (Pearson, 1979), high bicarbonate levels and high Fe^{2+} levels (associated with *Fe(III)* reduction). Therefore from Equation 2, any free Fe^{2+} may combine with HCO_3^- to produce siderite:-

$$Fe^{2+} + HCO_3^- + OH^- \rightarrow FeCO_3 + H_2O \quad \text{[Eq. 4]}$$

Measured $\delta^{18}O$ isotope values for the siderite cements are light (-5.91‰ PDB). Mozley & Burns (1993) suggest that anomalously low oxygen values could be due to water-mineral interactions. At low temperatures during early diagenesis, authigenic minerals are considerably enriched in ^{18}O relative to the pore-waters from which they precipitate

(Lohman & Walker, 1989). If significant volumes are precipitated, then authigenic minerals, such as carbonates, may lower the pore-water oxygen values by selectively removing ^{18}O.

These pore-filling siderite cements post-date the earliest marine calcite cements, which could have selectively removed ^{18}O from the pore-waters. It is unlikely that the depleted oxygen values are the result of an input of meteoric pore-water, because there is no other evidence (depositional, sedimentological or other) to support this. Similarly, the depleted values are unlikely to have been the result of recrystalisation, because siderite is a relatively stable mineral, that is unsusceptible to recrystalisation (Mozley & Burns, 1993). Similar explanations have been used to explain anomalously low $\delta^{18}O$ values for early carbonate cements within the Upper Jurassic Kimmeridge Clay Formation of Dorset (Irwin *et al.*, 1977) and $\delta^{18}O$ depleted siderite concretions within the Kuparuk Formation of Alaska (Mozley & Carothers, 1992). Ferroan dolomite which would have been a product of sulphate reduction, can be seen to post-date the siderite (Fig.3.xviii).

Sequence stratigraphic Implications:

The early diagenetic phases of the Sandy Block Member and Chief Shell Beds Member are consistent with an initial phase of marine cementation and would thus support the positioning of the proposed lowstand and transgressive systems tracts of Sequence 5 (Fig.3.xxiv). The increase in siderite precipitation within the Red Beds Member would also support continued transgression, at a time when sedimentation rates would have been

low and sediment ponding in the zone of sulphate reduction was dominant. However no further evidence was found for the identification of parasequences.

3.3.6: Sandsfoot Grit Member to Ringstead Coral Bed

Early diagenetic products are dominated by upward decreasing volumes of glauconite, apatite and pyrite within the Sandsfoot Grit Member (Fig.3.xxv) as well as large volumes of siderite cement, concretionary siderite and ferroan dolomite within both lithostratigraphic units (Fig.3.xxv). Within the Ringstead Coral Bed, equant ferroan calcite is also present (Fig.3.xxv).

Glauconite & apatite:

The presence of glauconite and apatite within the Sandsfoot Grit Member is associated with slow rates of sedimentation or even sediment starvation, during slightly reducing conditions within the post-oxic zone (Pettijohn, 1975; Desrochers & Al-Aassm, 1993 and McKay *et al.*, 1995) or at the oxic/suboxic boundary (Taylor & Curtis, 1995).

Sequence stratigraphic interpretation:

The presence of glauconite and apatite may help to identify the lower parasequence boundary of the Sandsfoot Grit Member (at 69.8m on Fig.3.xxv). Apatite in particular, is

associated with marine flooding surfaces and periods of sediment starvation or slow net sediment accumulation, in settings where there is a rapid increase in accommodation space and very little input from detrital sediment (Macquaker *et al.*, 1996). This would therefore suggest that parasequence flooding surfaces within the Sandsfoot Grit Member represent a prolonged period of sediment starved time.

Siderite:

Two phases of siderite precipitation occur within the Sandsfoot Grit Member:- (i) small early forming siderite concretions, and (ii) a dominant later pore-filling siderite cement (Fig.3.xix & 3.xxv).

The calculated $\delta^{13}C$ isotope values of both siderite phases (-15.28‰ PDB & -14.84‰ PDB respectively) are consistent with crystallisation as a result of ferric iron reduction in sub-oxic conditions during or immediately after sulphate reduction (Mozley & Wersin, 1992) although carbonate sources from other diagenetic environments (e.g. sulphate reduction, high temperature abiotic reactions or even soil derived meteoric water) cannot be ruled out. Thus the growth of siderite concretions must be related to prolonged residence time within the sub-oxic zone. As for interpretations of other concretions within the Corallian Group, this indicates a period of non-deposition associated with the formation of a parasequence boundary and provides further evidence for the identification of a parasequence at the base of the Sandsfoot Grit Member.

The $\delta^{18}O$ values of each type of siderite are distinctly different. The early formed concretions have values of -0.66‰ PDB which is consistent with a normal marine carbonate source, while the pore-filling cements have a value of -5.87‰ PDB. Again, a number of explanations can be offered to explain this depletion, such as, water-mineral interactions, meteoric water input, and recrystalisation. However, within the Sandsfoot Grit Member, pore filling siderite is the dominant cement type. The situation is therefore different from the transgressive systems tract of Sequence 5 where siderite and ferroan carbonate were seen to occur in approximately equal proportions. It is unlikely therefore that earlier water-mineral interactions were significant enough to reduce the ^{18}O value of the pore-water.

Mixing of marine and meteoric water could significantly lower the oxygen value of a cement precipitating from its pore-waters (Mozley & Burns, 1993). Further evidence which could support this is the dissolution and etching of rare calcite crystal faces, which could have occurred during a period of meteoric input. The positioning of a sequence boundary that is related to a period of forced regression beneath these sediments, would imply a period of sub-aerial exposure, and thus a meteorically driven water input could have been likely. This would refute Coe's (1995) sequence stratigraphic interpretation (transgressive systems tract) of this member.

Sequence stratigraphic interpretation of the overlying Ringstead Formation:

Within the overlying Ringstead Formation (transgressive systems tract) one parasequence

has been identified (Fig.3.xxv). This parasequence is composed of dominantly dysaerobic muddy shelfal sediments which shallow-up to a thin faunally rich bioclastic bed. The early diagenetic cements of the bioclastic bed are dominated by fine grained ferroan equant sparite and rare ferroan dolomite and siderite, with pyrite abundant in locally organic rich micro-environments. These cements are similar in habit and form to those occurring within the transgressive systems tracts of Sequences 3 and 4 (Sections 3.3.3 and 3.3.4) and thus relate to similar diagenetic environments. The top of the mudstone unit is very iron rich containing abundant siderite and apatite, which have precipitated into localised small nodules. As in the Sandsfoot Grit Member, the growth of these concretions must relate to slow sediment accumulation within a sub-oxic/reducing environment beneath the parasequence flooding surface (Macquaker *et al.*, 1996) which has been positioned on top of the bioclastic rich bed (Fig.3.xxv).

3.4: *Concluding Remarks*

- A range of analytical and petrographical techniques have identified twelve early diagenetic phases within the Corallian Group succession. These include glauconite, phosphate (apatite), pyrite, six forms of calcite concretion and cement, ferroan dolomite cement and two forms of siderite concretion and cement.
- The study has indicated that an analysis of early diagenetic products has helped to identify, or provide further evidence for the identification of, parasequences, systems tracts and sequence boundaries thus providing support for the facies based sequence

stratigraphic framework outlined in Chapter 2.

- Within the Nothe Grit Formation, the interpretation of concretion growth strongly supports the proposed facies identification of parasequences and may provide further evidence to support a highstand systems tract interpretation. Interpretation of the growth phases of concretions has indicated an initial period of rapid burial followed by a prolonged period of stillstand, which relate to parasequence progradation and drowning/non-deposition respectively.
- There is no evidence for surface related diagenetic processes at Sequence Boundary 1. This may indicate that periods of forced regression during the deposition of the Corallian Group did not result in any significant duration of sub-aerial exposure, which would be expected during a global "green-house" period such as the late Jurassic (Veevers, 1990). This is because a fall in relative sea-level would not be a prolonged event and thus the amount of time of sub-aerial exposure and surface related diagenetic processes would be of a limited duration. Alternatively, this observation could also be in keeping with a ravinement surface interpretation at this boundary, as suggested by some workers.
- In the Bencliff Grit Member and Sandsfoot Grit Member, a similar interpretation of concretion growth has also provided strong support for parasequence identification.
- Parasequences are easily identifiable within the Upton Member and Shortlake Member and analyses of early diagenetic marine cements strongly supports this. One parasequence was identified within the Nothe Clay Member, agreeing with the interpretation offered in Chapter 2.
- However no further evidence could be found to identify parasequences within the

remainder of the Nothe Clay Member, the *Thalassinoides* Beds, the Nodular Rubble Member and the Trigonia Clavellata Formation.

- Upward increasing volumes of ferroan dolomite support the proposed identification of highstand systems tracts at the top of the Nothe Clay Member/lower sandstone bed of the Bencliff Grit Member (up to the first mudstone bed) and the *Thalassinoides* beds/lower two oolitic beds of the Shortlake Member. However no ferroan dolomite was identified within the proposed highstand systems tract of the Nothe Grit Formation or the upper beds of the Nodular Rubble Member.
- Analysis of upward increasing volumes of ferroan dolomite in conjunction with highstand systems tract identification also supports the positioning of a sequence boundary at the first mudstone bed of the Bencliff Grit Member (rather than the alternative position at the lithostratigraphic contact between this and the underlying Nothe Clay Member).
- Identification of meteoric cements within the first two oolitc beds of the Shortlake Member supports the positioning of a type-2 sequence boundary above the second of these beds. No evidence of exposure occurs at this sequence boundary and the meteoric cement is deemed to be the result of a small scale meteoric lens, originating from an up-dip/exposed area of the basin. An analysis of regional data indicates a correlatable sub-aerial erosion surface in the Oxfordshire area.
- Finally, the emphasis of this chapter was to utilise the analyses of early diagenetic cements to support a facies based sequence stratigraphic model. This theme is continued in Chapter 6, where generalised models are produced that combine facies analysis with analyses of early diagenetic fabrics and are related to differing scales of

relative sea-level change.

Fig. 3.i: Sample nos., locations & types of analysis. B4 (etc.) = sample no., CB = cemented bed, NCB = non-cemented bed & C = concretion. i = thin section petrography, ii = XRD, iii = stable isotope & iv = CL. Sedimentology & sequence stratigraphy as for Figs.2.v & 2.vi.

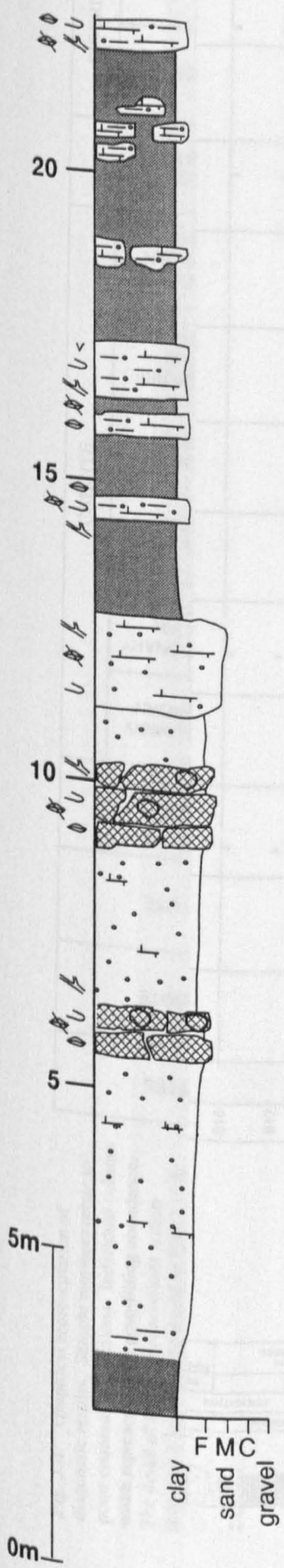

B18	CB	i
B17	CB	i
B14	CB	i
B13	CB	i
B12	CB	i
B3	CB	i
B9	CB	i
A4-8	C	i,ii,iii,iv
B1	CB	i
B2	NCB	i
B4	CB	i

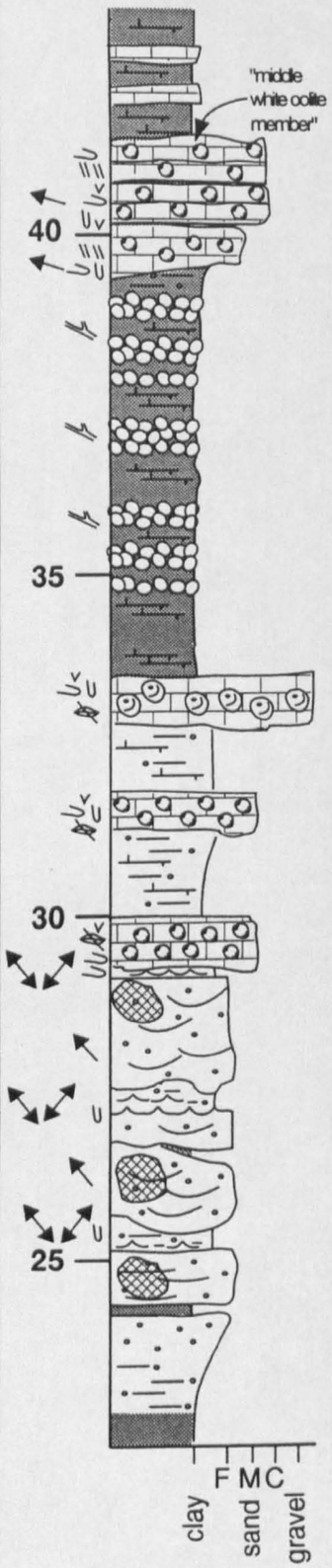

61	CB	i,ii,iii,iv
59	CB	i
57	CB	i,iv
54	CB	i
52	C	i
50	C	i,iv
48	C	i
42	CB	i,iv
40	CB	i,ii,iii,iv
GO1	CB	i
E1-4	C	i,ii,iii,iv
39a		
36	NCB	i
34	NCB	i
32a	C	i,ii,iii
32	NCB	i
31	CB	i
30	NCB	i

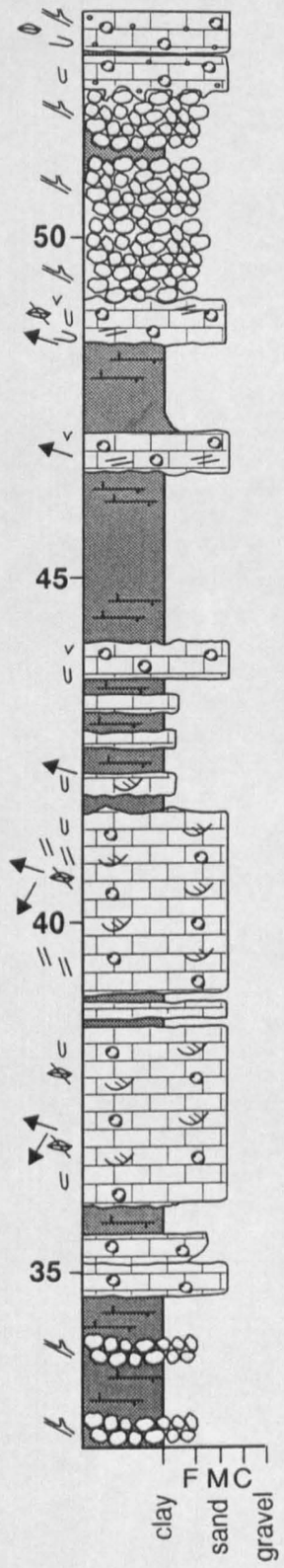

86	CB	i
85	CB	i
84	C	i
82	C	i
80	C	i
78	C	i,iv
C15	CB	i
C13	CB	i,iv
C12	CB	i,ii,iii,iv
C11	CB	i
C10	CB	i,iv
C9	CB	i
C8	CB	i
C4	CB	i
C2	C	i
C1	C	i

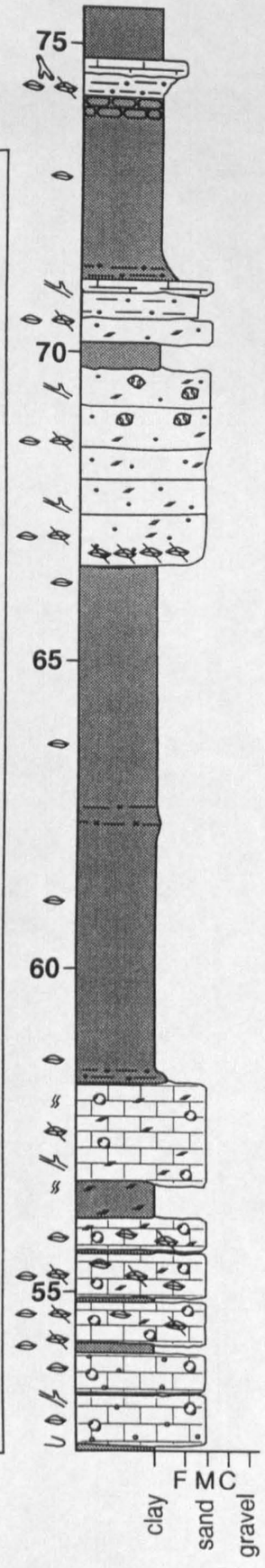

D17	CB	i
D15	CB	i
120	CB	i,iv
116	C	i,iv
115	C	i,ii,iii
113	CB	i,ii,iii
112	CB	i
111	CB	i
C27	CB	i,ii,iii
C26	CB	i
C24	CB	i
C23	CB	i
C22	CB	i
88	CB	i,iv
87	CB	i

Fig. 3.ii: Graphical representation of diagenetic results. Sample numbers relate to point counted thin-sections. Individual column width represents % of pore-filling abundance. The detail of sampled concretions within sequence 1 and 3 can be found in Figs.3.vi & vii respectively. Please note log overlap & the different symbols used for each. Point count number for each sample = 500. (see Appendix 1 for tabulated results).

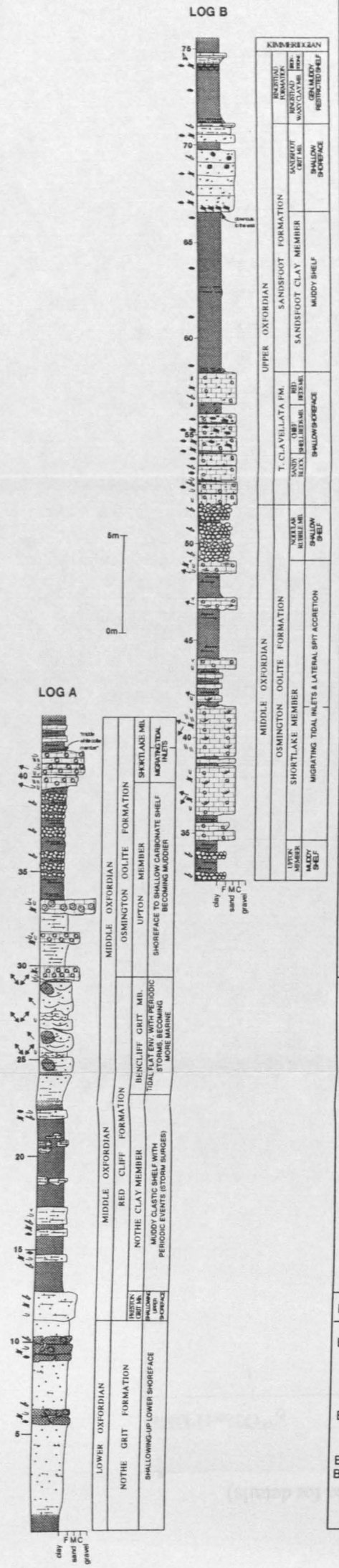

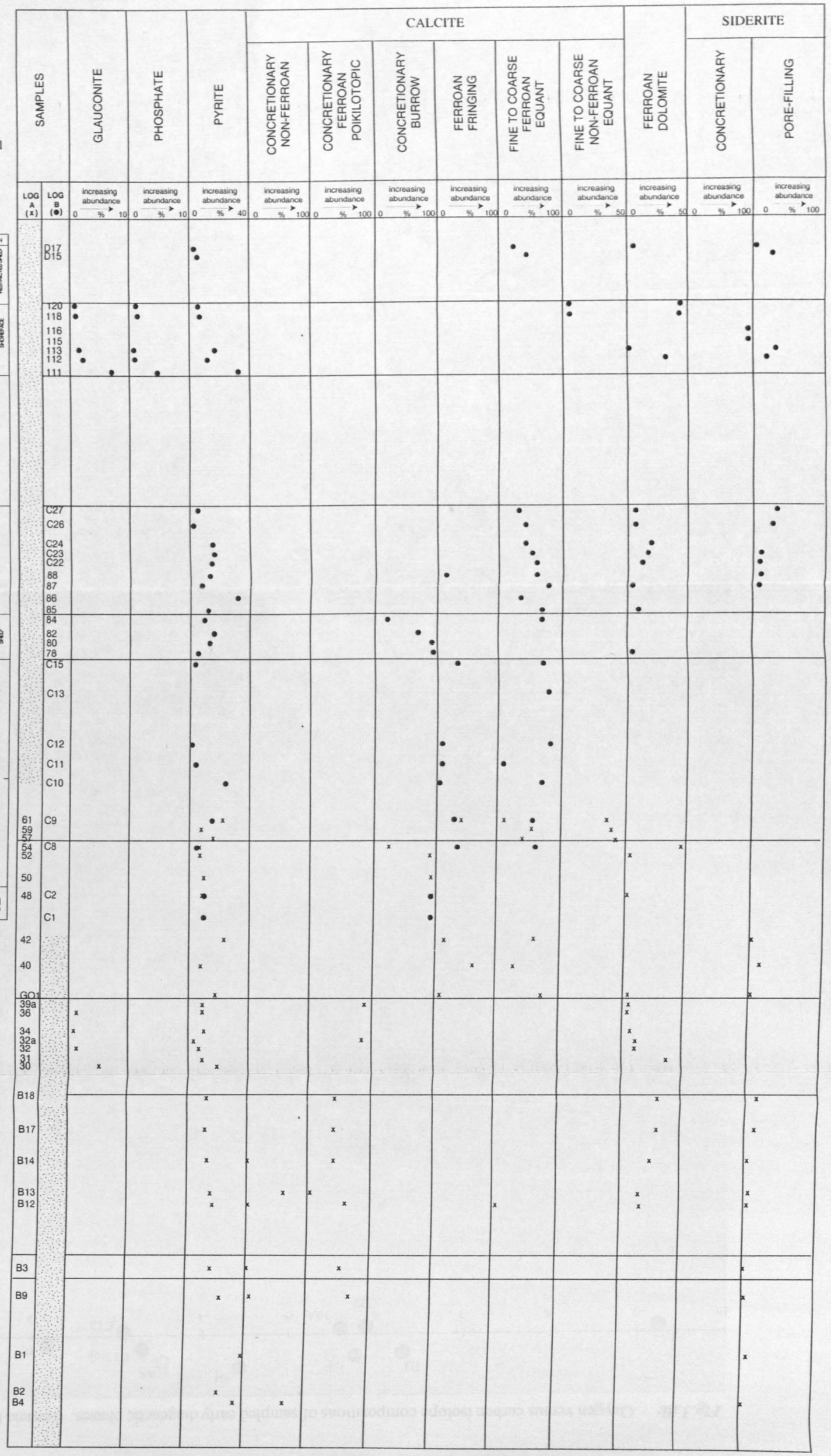

Fig.3.iii: Oxygen versus carbon isotope compositions of sampled early diagenetic phases. (see text for details)

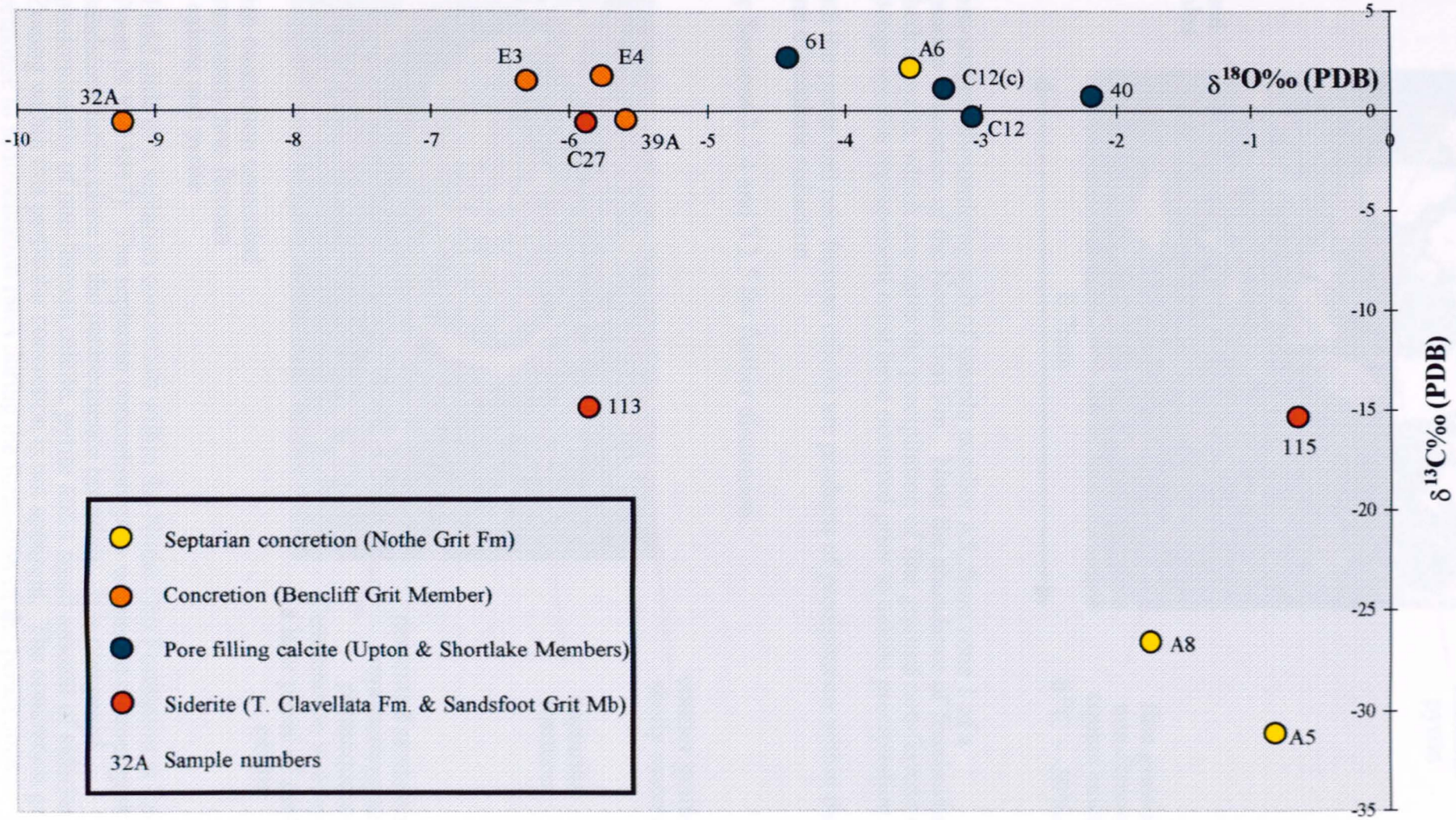

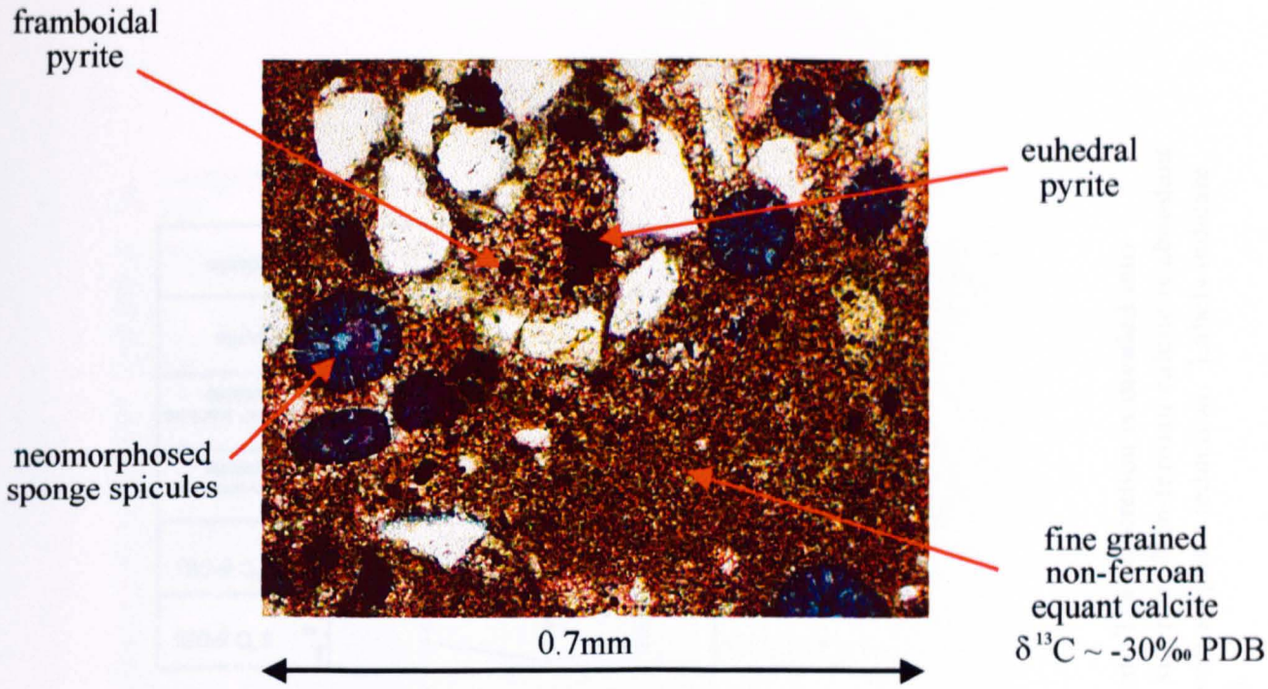

Fig.3.iv. Thin-section photomicrograph of sample number A5, from zone 1 of a septarian concretion of the Nothe Grit Fm.. Note the abundance of framboidal and euhedral pyrite, which pre-dates the precipitation of fine grained non-ferroan calcite. Sponge spicule replacement must have occurred prior to calcite precipitation.

Both the pyrite and non-ferroan calcite are products of precipitation within the zone of sulphate reduction.

See Sections 3.2.4 and 3.2.5 for further discussion.

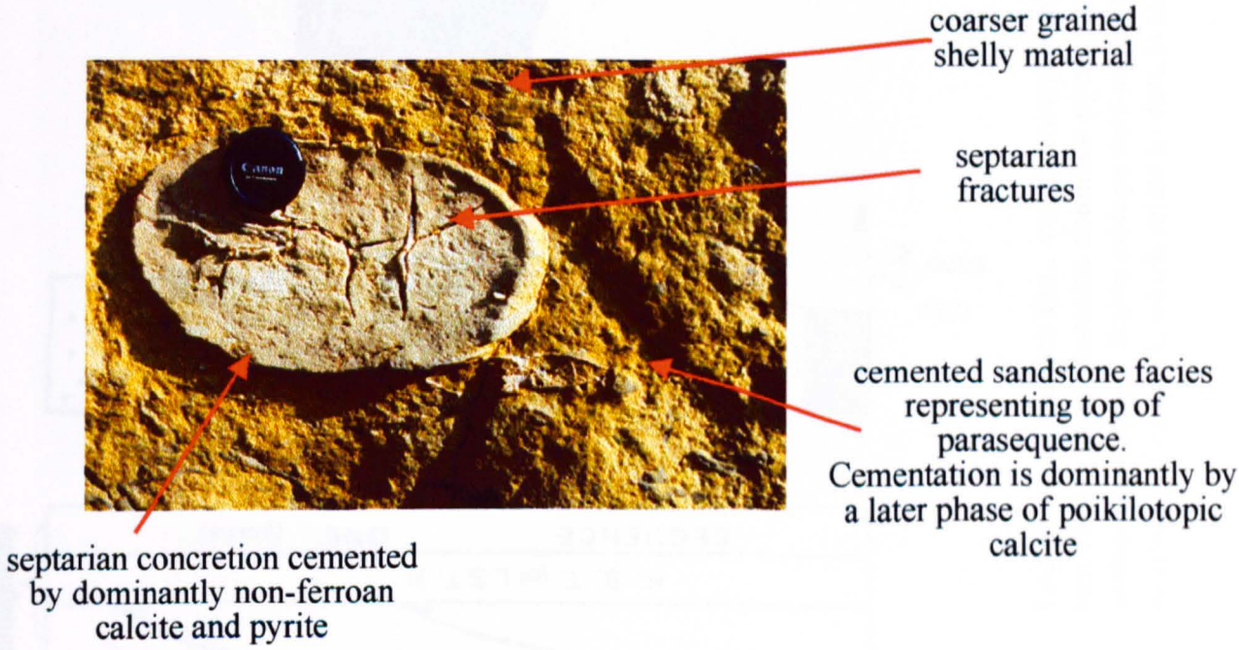

Fig.3.v. Field slide of a septarian concretion within the Nothe Grit Formation at Red Cliff Point (S.Y.713817). The septarian concretion grew within the coarser grained sandstone facies close to the parasequence boundary. It is composed predominantly of non-ferroan calcite, pyrite and a small amount of siderite. Zoning within this particular concretion is not apparent. The concretion grew in response to sedimentation rates during the formation of the parasequence. The host sandstone is cemented by a later phase of poikilotopic calcite which is unrelated to the deposition of the parasequence. See Section 3.2.5 for further explanation.

For scale, camera lens cap is approximately 0.05m in diameter.

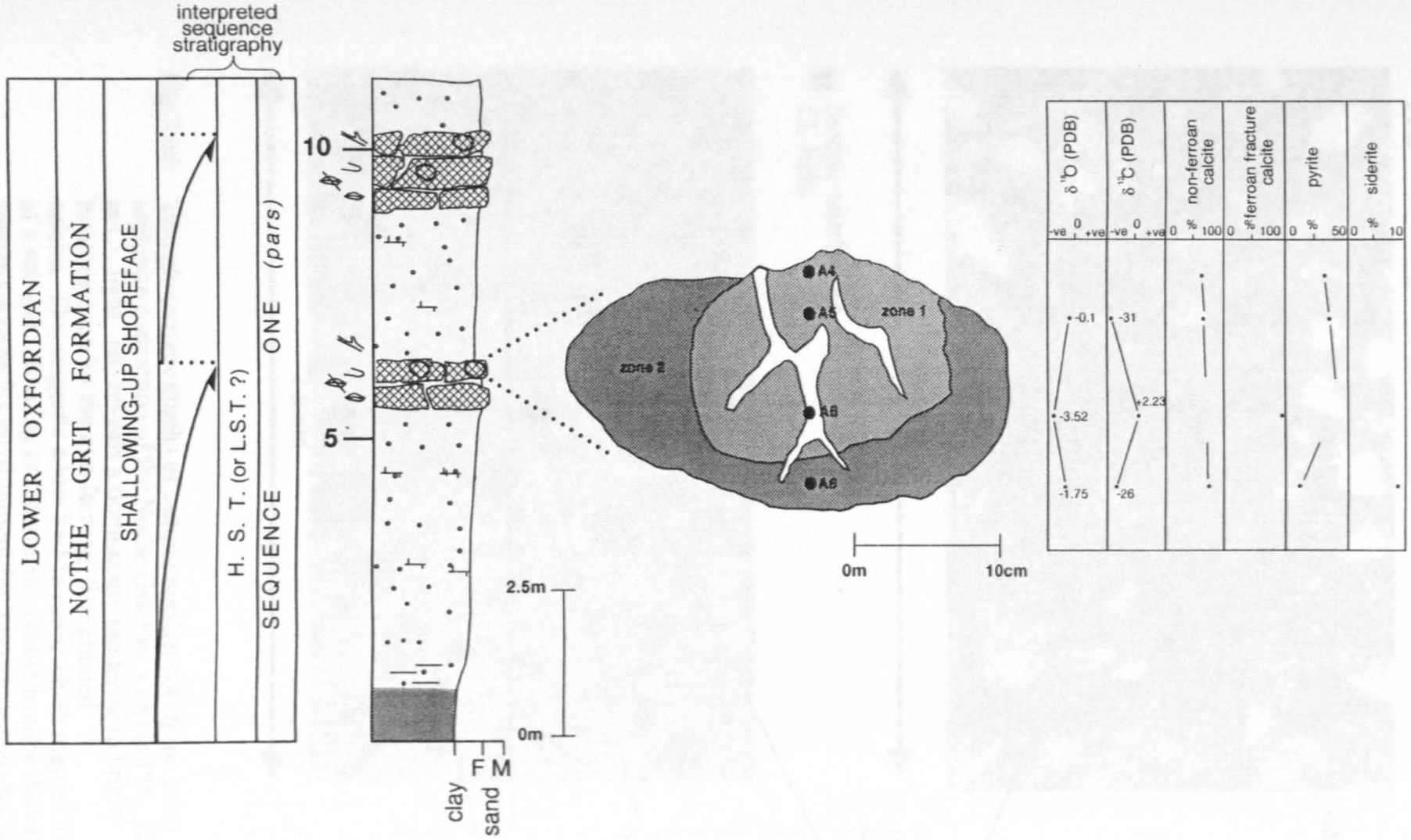

Fig.3.vi: Log of the Nothe Grit Fm., and an enlargement of a typical septarian concretion. The concretion is divided into two zones: zone 1 contains abundant pyrite; zone 2 shows less pyrite and rare siderite. Non-ferroan calcite is abundant within both zones. Stable isotope data suggests the source of carbonate was from sulphate reduction. Labels indicate positions of samples, which relate to data in table (right-hand side of diagram).

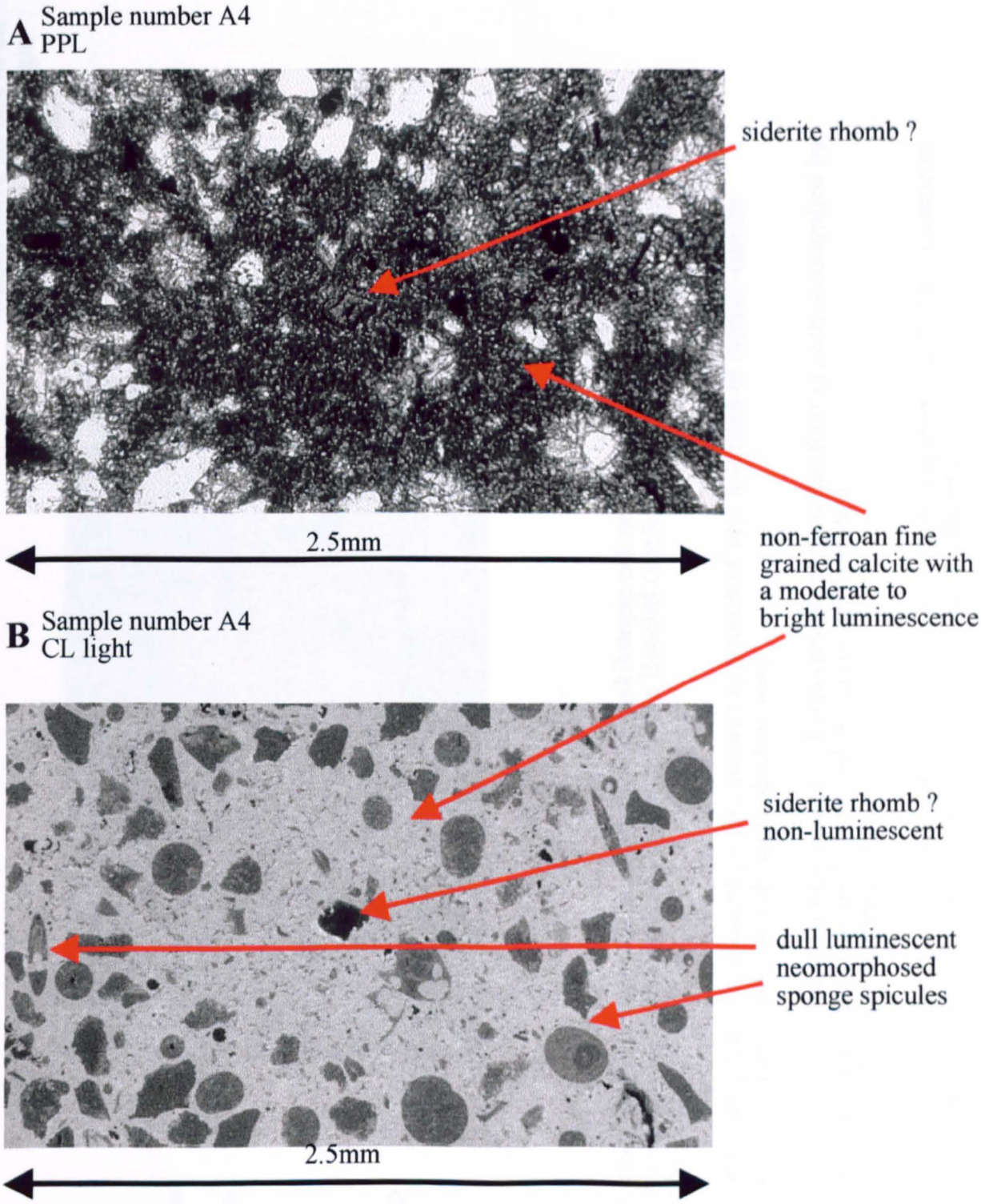

Fig.3.vii: Two photomicrographs of sample number A4, from zone 1 of a septarian concretion of the Nothe Grit Fm. - (A) in PPL, (B) in CL light. (B) reveals a dominantly moderate to bright luminescence for the non-ferroan fine grained calcite. This suggests a low Fe/Mn ratio, which may be indicative of a sub-oxic reducing environment. Stable isotope data also suggests a reducing environment for this calcite (see Section 3.2.5 for further explanation).

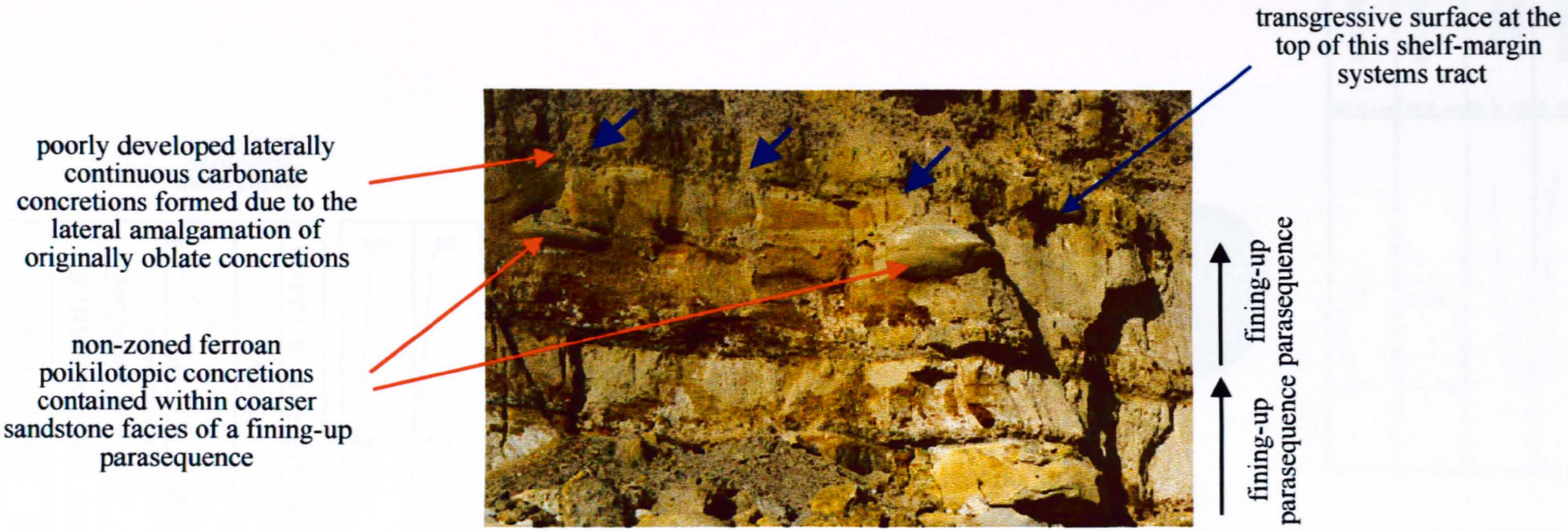

Fig.3.viii. Field slide to show two non-zoned, ferroan poikilotopic calcite concretions within the coarser grained facies of a parasequence of the Bencliff Grit Member at Osmington Mills (SY 738815).

These concretions are thought to have formed as a result of very low rates of organic-carbon oxidation, deep within the sulphate reduction zone

Trends within the stable isotope analysis of concretions, suggest that their growth is controlled by parasequence formation as well as overall systems tract formation.
See Section 3.2.5 for further explanation.

For scale, the concretion on the right-handside of the photograph is approximately 1m in diameter (All sequence stratigraphic interpretations are as defined in Chapter 2).

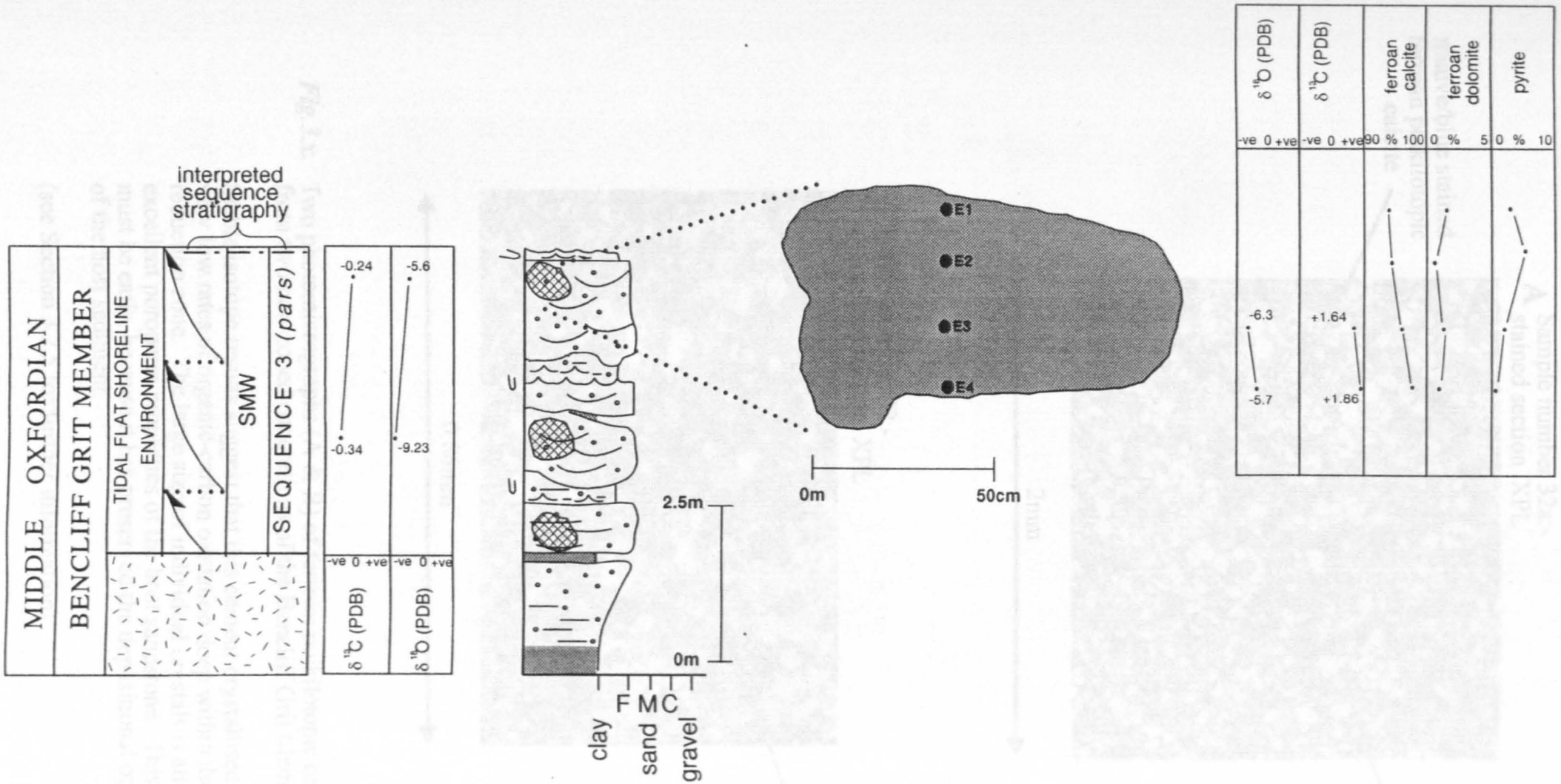

Fig.3.ix: Log of the Bencliff Grit Member, and a typical concretion. The concretion is dominated by ferroan poikilotopic calcite. Stable isotopes suggest dominant source of carbonate was marine, although within a mixed marine/meteoric environment that became more marine. Labels indicate positions of samples, which relate to data in table (right-hand side of diagram). Also note isotope values for the systems tract, which indicate a vertically waning meteoric influence.

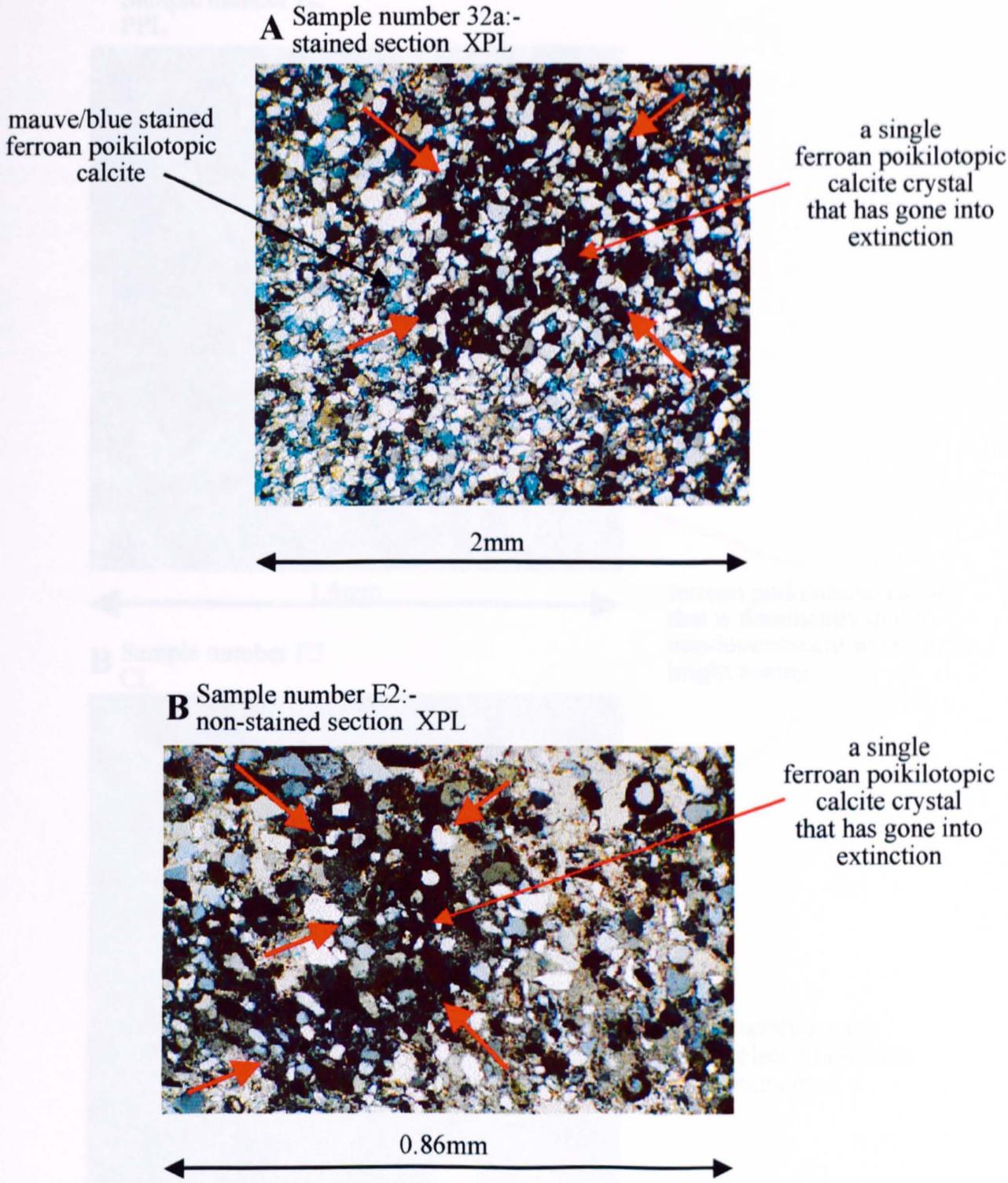

Fig.3.x. Two photomicrographs (A & B) of ferroan poikilotopic calcite extracted from two non-zoned concretions of the Bencliff Grit Member..

Stable isotope results suggest that this cement crystallised as a result of very low rates of organic-carbon oxidation deep within the sulphate reduction zone. The large size of individual crystals is attributed to excellent poroperm properties of the host sandstone. This cement type must be early, because it has preserved the depositional open grain fabric of the host sediment.

(see Section 3.2.5 for further information)

Sample number E2
PPL

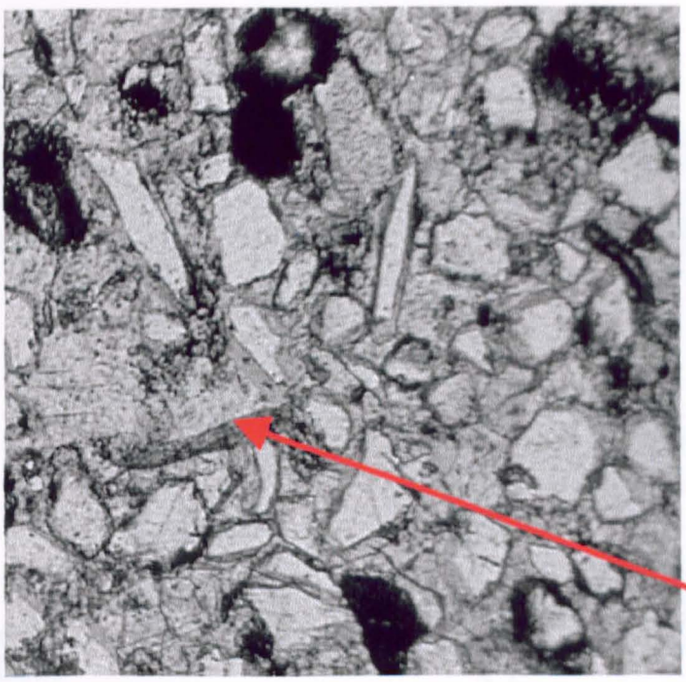

1.6mm

ferroan poikilotopic calcite that is dominantly dull to non-luminescent with subtle bright zoning.

B Sample number E2
CL

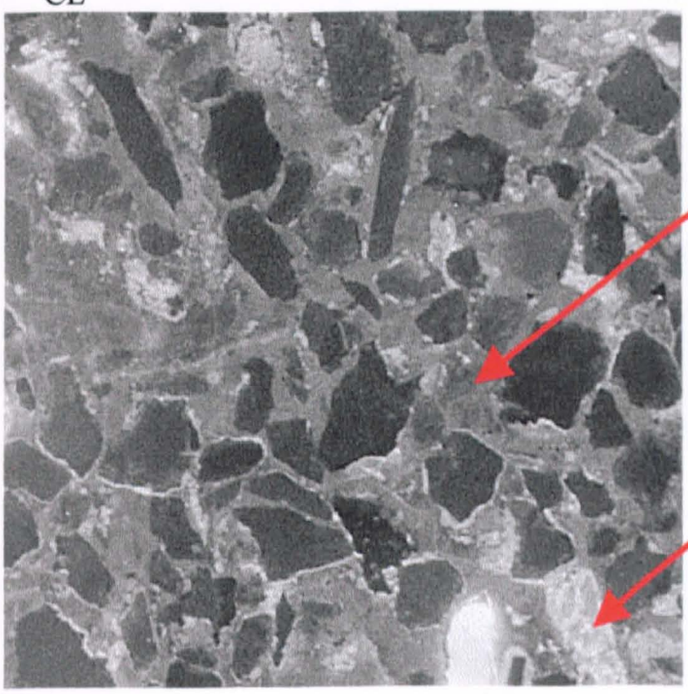

brightly zoned replaced bioclastic fragments ?

1.6mm

Fig.3.xi. Two photomicrographs of sample number E2, from a concretion of the Bencliff Grit Member - (A) in PPL and (B) in CL light. The CL photomicrograph clearly shows that the ferroan poikilotopic calcite which forms these concretions is dull to non-luminescent (with some zoning). This suggests a very high Fe/Mn ratio which may be indicative of a strongly reducing environment (see Section 3.2.5 for further explanation). (A) & (B) are not exactly coincident views.

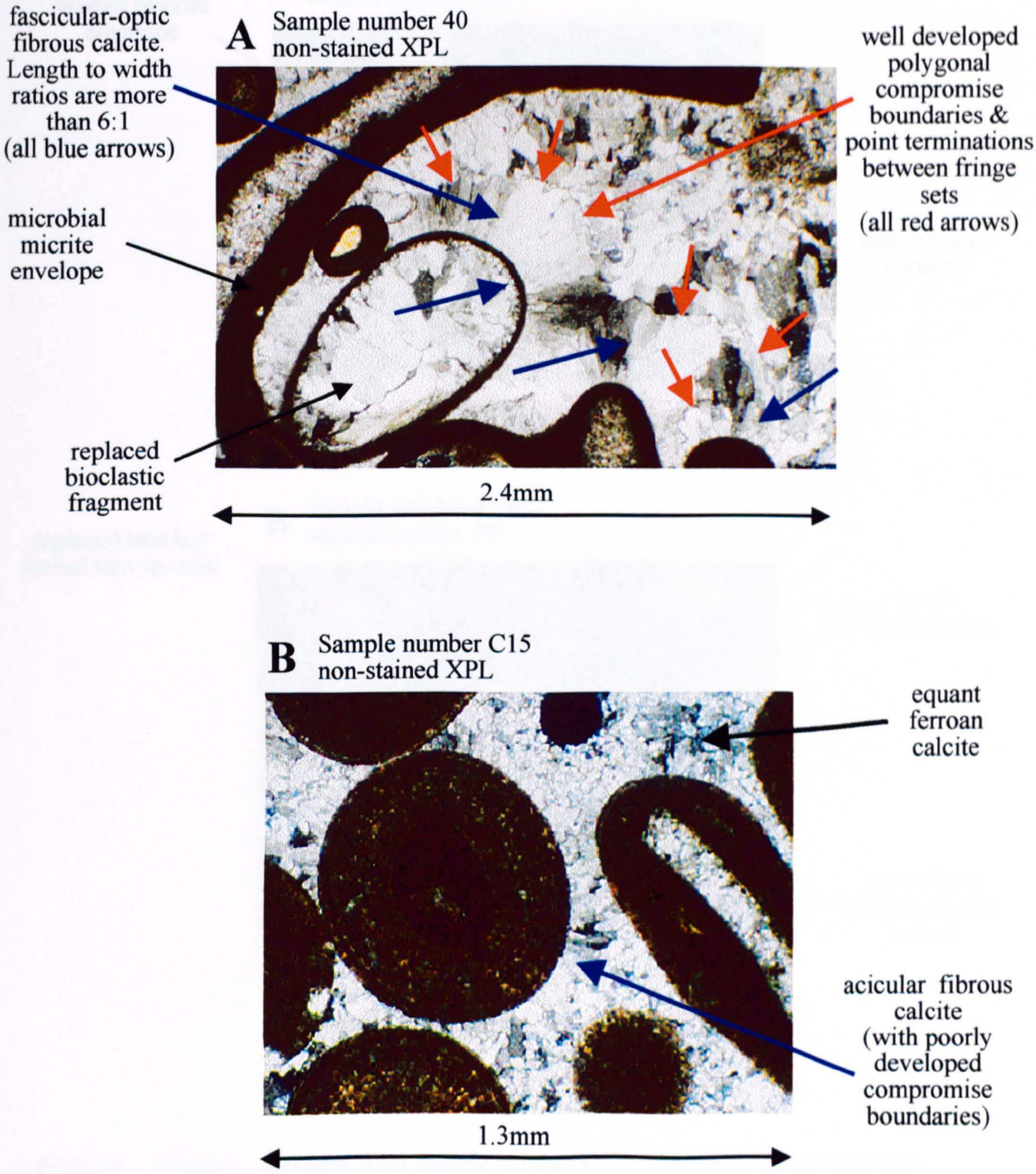

Fig.3.xii. Photomicrographs of two different types of ferroan fringing calcite, (A) is of sample number 40 extracted from the top of a parasequence of the lower Upton Member, (B) is of sample number C15 extracted from the top of a parasequence of the upper part of the Shortlake Member).

(A) shows well developed columnar, fascicular optic fibrous calcite that have well developed compromise boundaries; (B) shows poorly developed acicular fringing calcite. However, in both examples the fringing calcite is clearly an early cement phase. Stable isotope results have confirmed a marine origin for these cements.

(see Section 3.2.5 for further information)

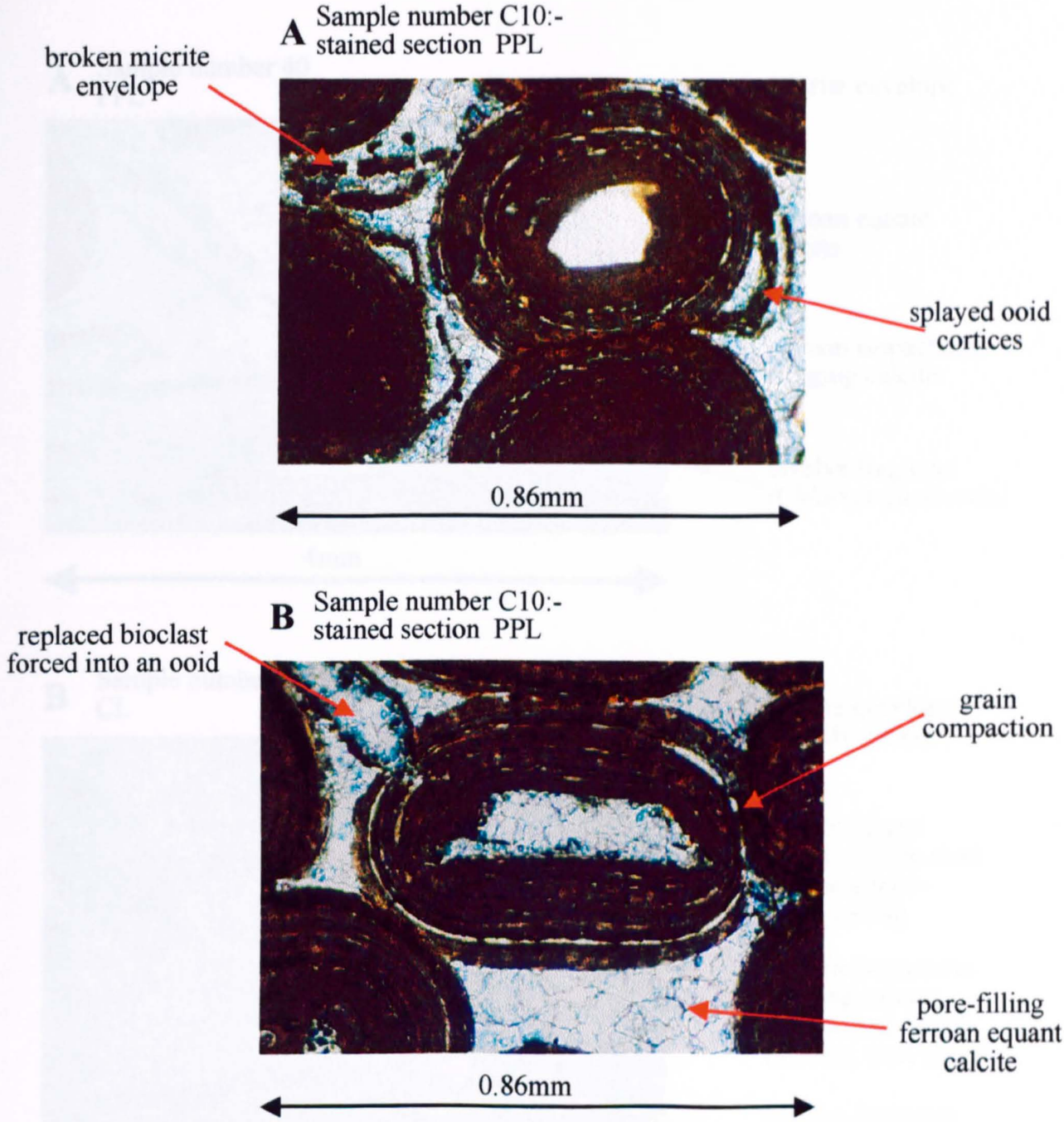

Fig3.xiii. Photomicrographs from sample number C10 (lower beds of the Shortlake Member at the Black Head outcrop) to show the effect of early grain compaction. Note the presence of grain contacts, collapsed micrite envelopes and splayed ooid cortices (A & B). Also note that bioclastic material that has been replaced by ferroan equant calcite, has been forced into an ooid (B).

The equant ferroan calcite cement is an early pore-filling cement that was crystallising during and after the minor compaction phase. The compaction phase occurred due to an absence of fringing calcite. Stable isotope data from samples containing similar equant ferroan calcite, suggests that it is clearly a marine precipitate (see Section 3.2.5 for further details).

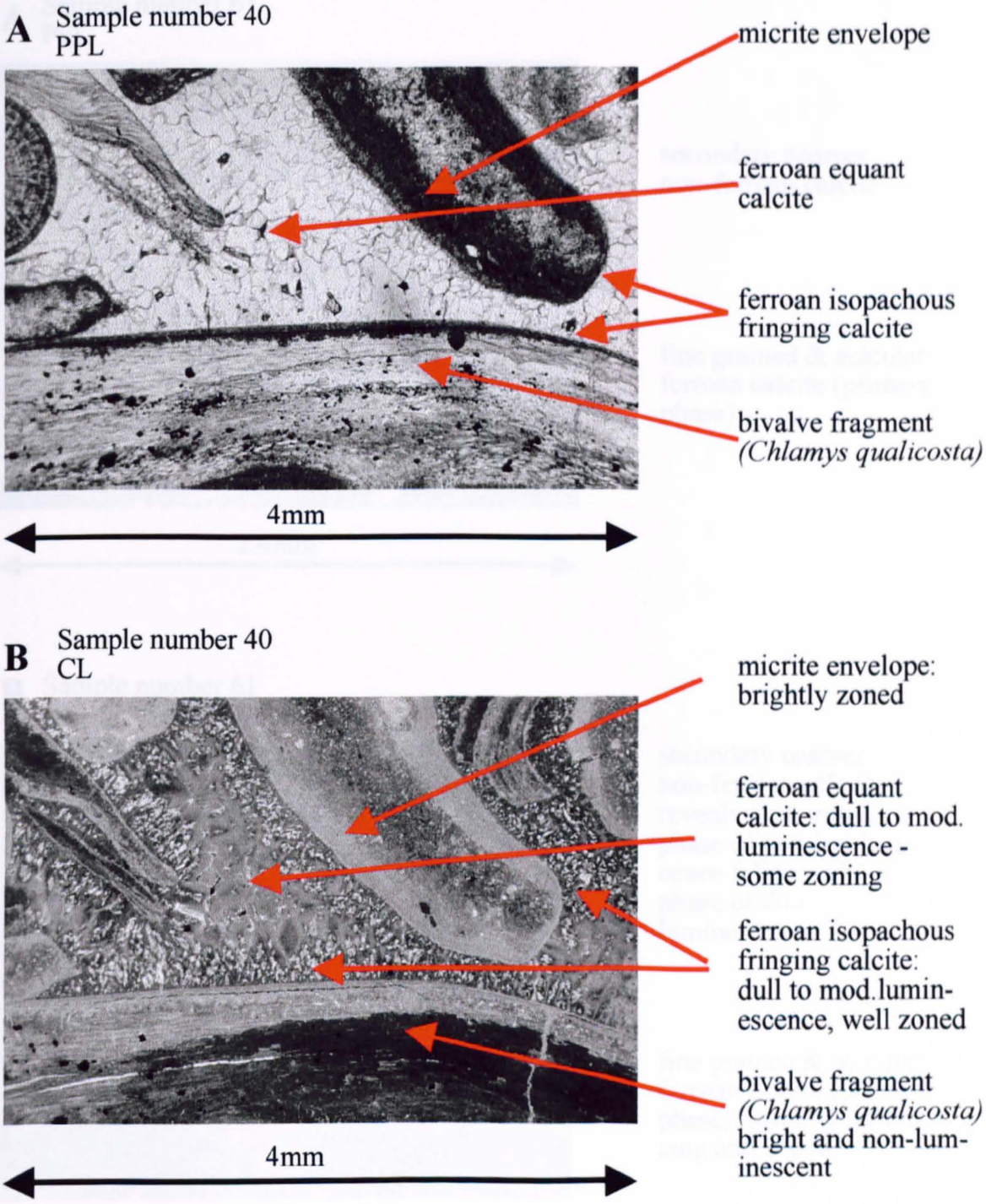

Fig.3.xiv. Two photomicrographs (A & B) of sample number 40 from a parasequence top of the TST of Sequence 3 (lower Upton Member). The CL photomicrograph (B) clearly shows that both the ferroan fringing calcite and the ferroan equant calcite have a dull to moderate luminescence. The ferroan fringing calcite is also well zoned. These results suggest that both cements have a low Fe/Mn ratio, but due to cement fabrics and stable isotope data, these cements are unlikely to have precipitated in a reducing environment. It is suggested that the low Fe/Mn ratio is due to a primary low-magnesium composition of both cement phases (see Section 3.2.5 for further explanation).

A Sample number 61
PPL

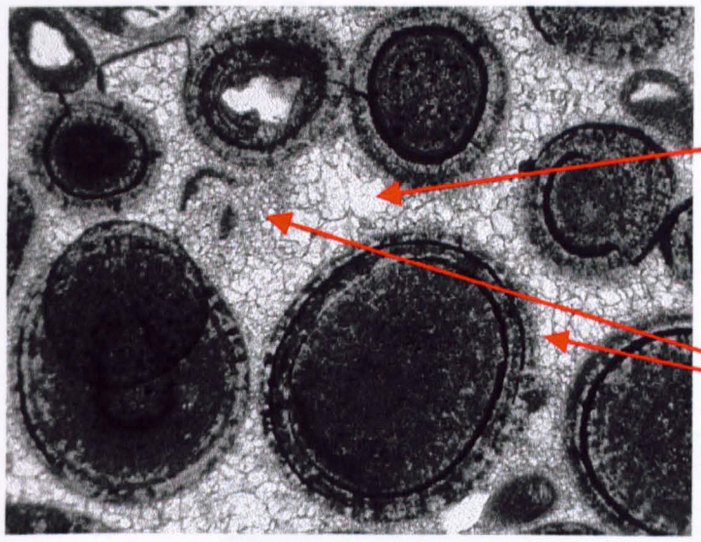

secondary coarser non-ferroan calcite

fine grained & acicular ferroan calcite (primary phase)

2.4mm

B Sample number 61
CL

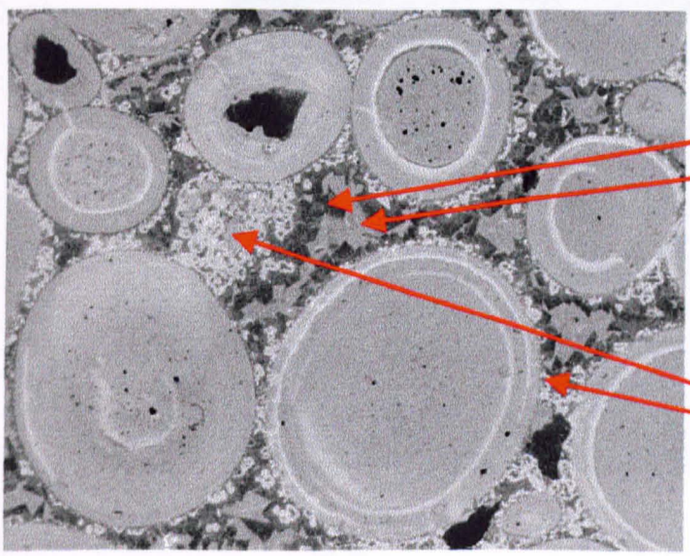

secondary coarser non-ferroan calcite: revealing an initial phase of non-luminescence followed by a phase of dull luminescence

fine grained & acicular ferroan calcite (primary phase): brightly luminescing and zoned.

2.4mm

Fig.3.xv. Two photomicrographs (A & B) of sample number 61 from the middle white oolite bed of the Shortlake Member. This sample contains fine grained acicular and pore filling ferroan calcite which is a marine precipitate and is brightly luminescent and zoned. Similar to sample number 40, (B) suggests a low Fe/Mn ratio for these cements. The remaining pore space is infilled with coarser, non-ferroan equant calcite which is non-luminescent to mod. luminescent. This would suggest an initial period of oxidation where neither Fe or Mn were reduced, followed by a period of reduction, where Fe would have begun to reduce.

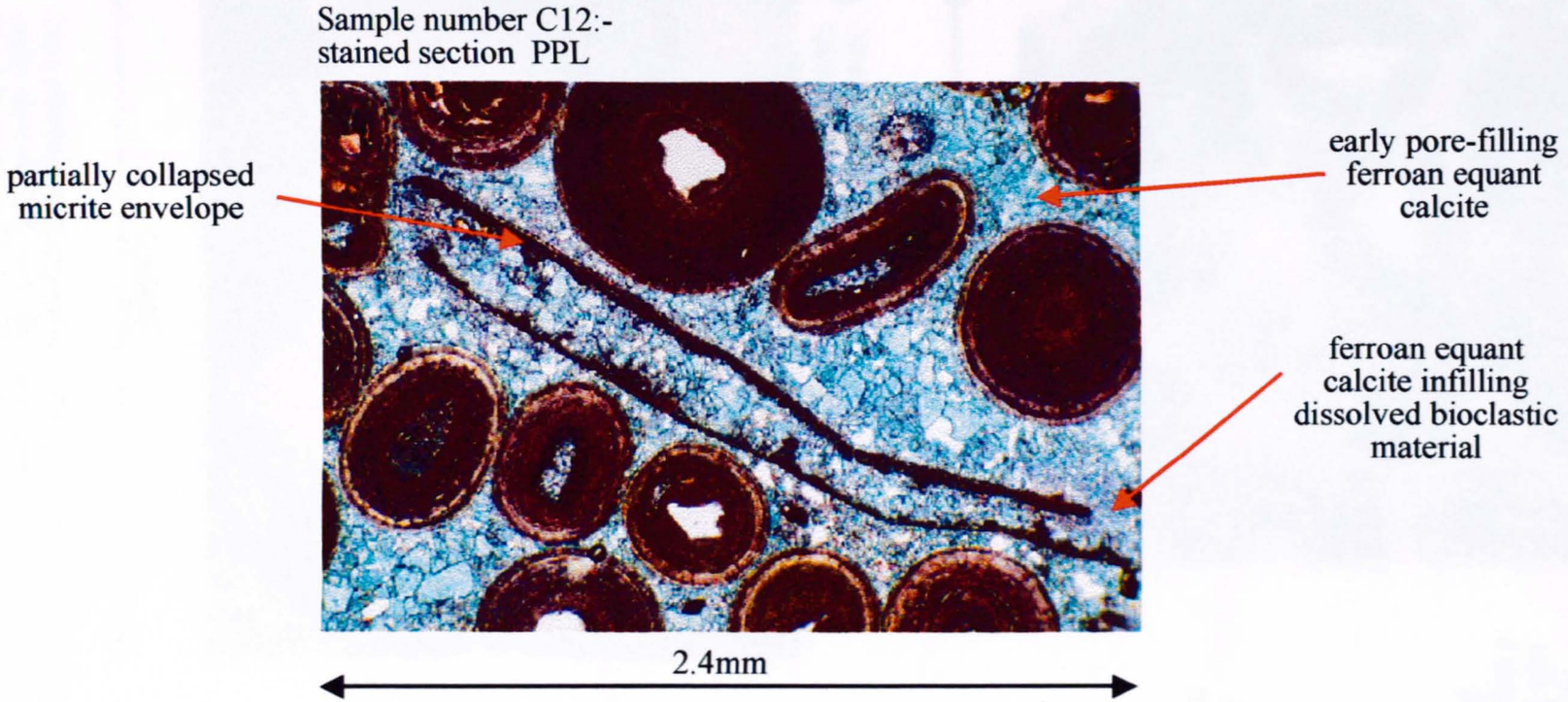

Fig.3.xvi. Thin section photomicrograph to show early pore-filling ferroan equant calcite within the Shortlake Member. Note that due to a lack of fringing calcite, this cement grows directly from grain boundaries. Stable isotope data taken from this sample, clearly suggests that this cement is a marine precipitate. The cement is also seen to clearly infill mouldic porosity that was formed as a result of aragonite bioclast dissolution due to the action of calcite rich marine pore-waters (see Section 3.2.5 for further explanation).

A Sample number 61:-
stained section PPL

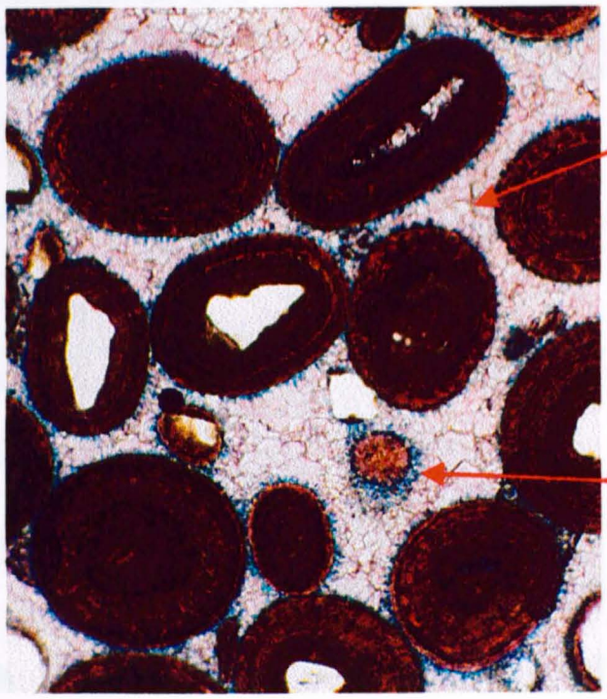

B Sample number 59:-
stained section PPL

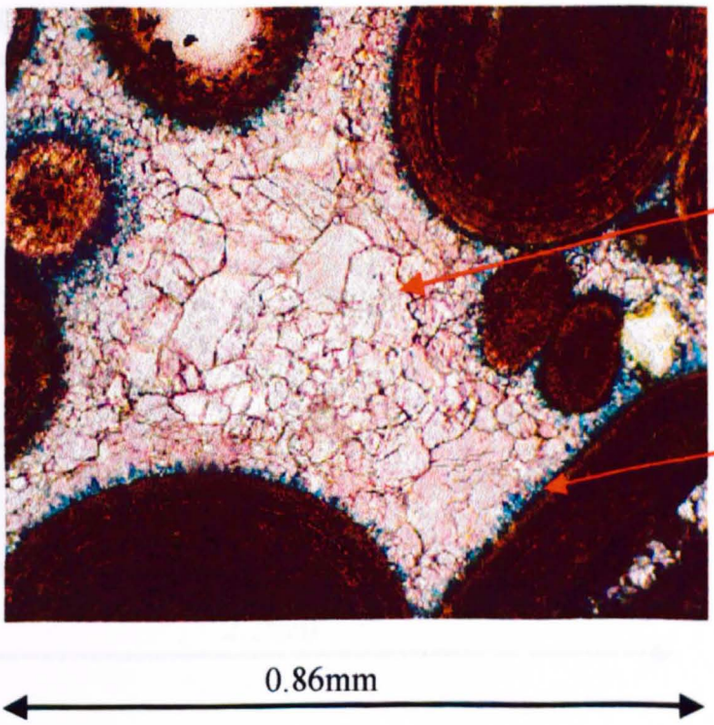

Fig.3.xvii. Two photomicrographs to show early acicular ferroan fringing calcite and early pore-filling non-ferroan equant calcite. Both samples were collected from the Shortlake Member at the Bran Point outcrop (please refer to Fig.3.ii for exact location).

Stable isotope data suggests that the non-ferroan equant calcite was precipitated from meteoric pore-waters. This cement is not laterally or vertically extensive and is assumed to have formed as a result of a small meteoric lens (see Section 3.2.5 for further explanation).

A Sample number 112:-
stained section PPL

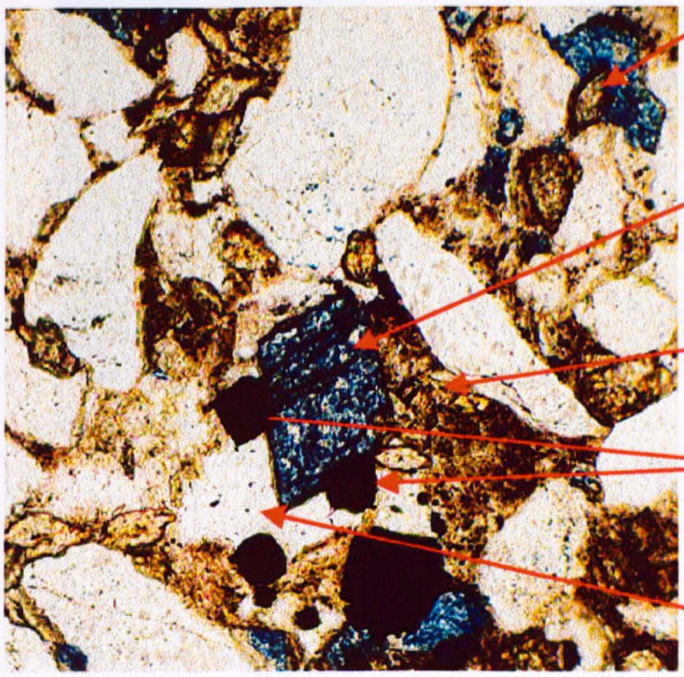

B Sample number 31:-
stained section PPL

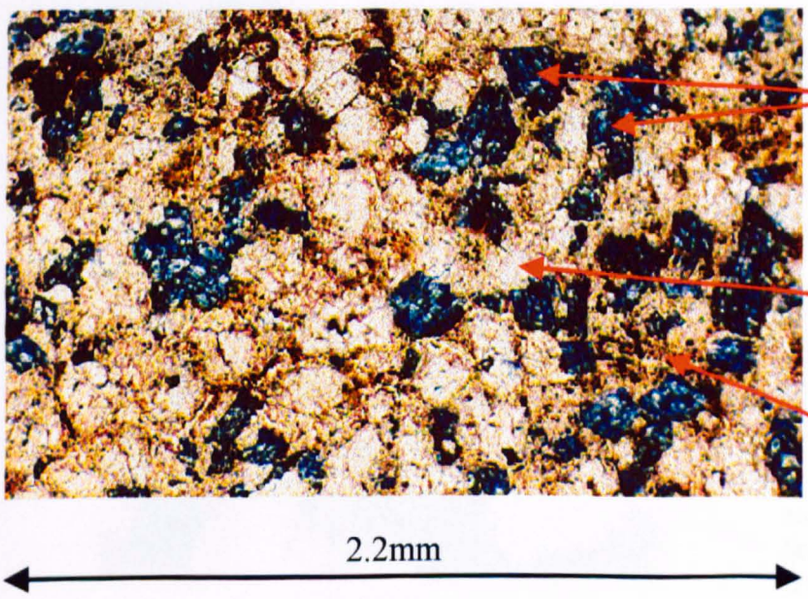

Fig.3.xviii. Photomicrographs to show the relationship between pyrite, ferroan dolomite and siderite within two samples. Sample number 31 (B) was collected from a heterolithic bed of the Bencliff Grit Member). Sample number 112 (A) was collected from the lower beds of the Sandsfoot Grit Member. Pyrite, siderite and ferroan dolomite are all primary phases and have precipitated as a result of reactions that took place within the zone of sulphate reduction. Within sample number 112, pyrite was the first diagenetic phase, followed by siderite and ferroan dolomite once sulphate levels had effectively been reduced to zero (see Sections 3.2.6 & 3.2.7 for further explanation).

Fig.3xixa. Small oblate siderite concretions from the Sandsfoot Grit Formation. Stable isotope data from siderite crystals within these concretions, suggest that they grew within the zone of sulphate reduction (see Section 3.2.7 for further explanation).

Photograph taken at Sandsfoot Castle (S.Y. 675774). For scale, the camera lens cover is approximately 50mm in diameter.

Sample number 112:-
stained section PPL

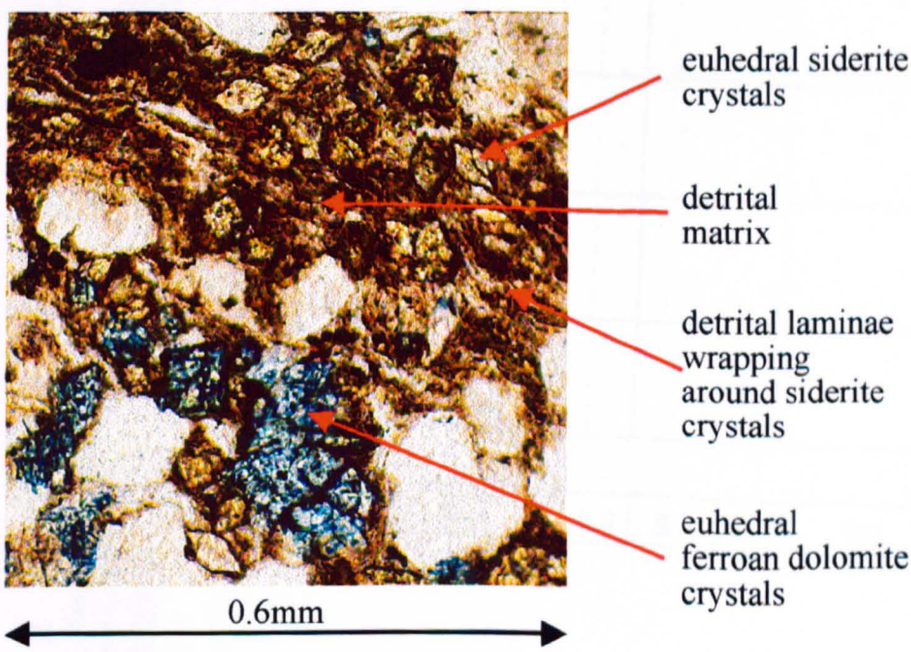

Fig.3.xixb. Photomicrograph of sample number 112 extracted from the lower beds of the Sandsfoot Grit Formation. Note the abundance of pyrite, preferentially growing within micro-porosity of the detrital matrix and note that laminae wrap around siderite crystals implying that crystal growth occurred before any significant compaction. Stable isotope data suggests that this siderite grew as a result of reactions within the zone of sulphate reduction (see Section 3.2.7 for further explanation).

Fig. 3.xx: Graphical representation of diagenetic results. Sample numbers relate to point counted thin-sections. Individual column width represents % of pore-filling abundance. The detail of sampled concretions within sequence 1 and 3 can be found in Figs.3.vi & vii respectively. Please note log overlap & the different symbols used for each. Point count number for each sample = 500. (see Appendix 1 for tabulated results). Sequence stratigraphic framework as for Chapter 2

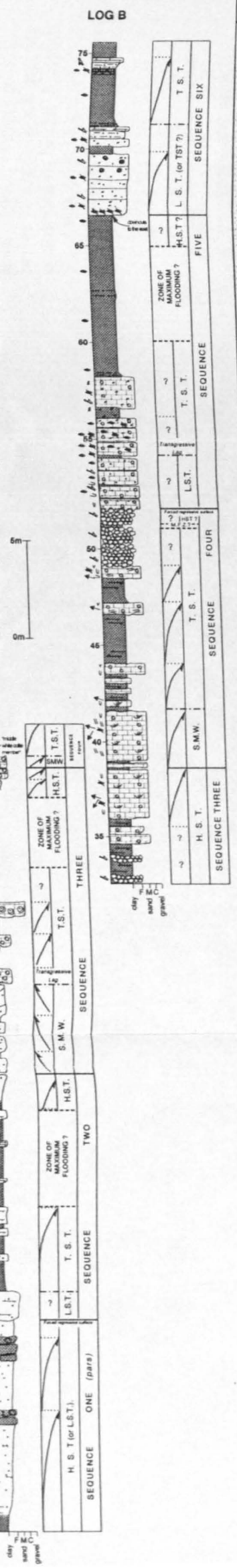

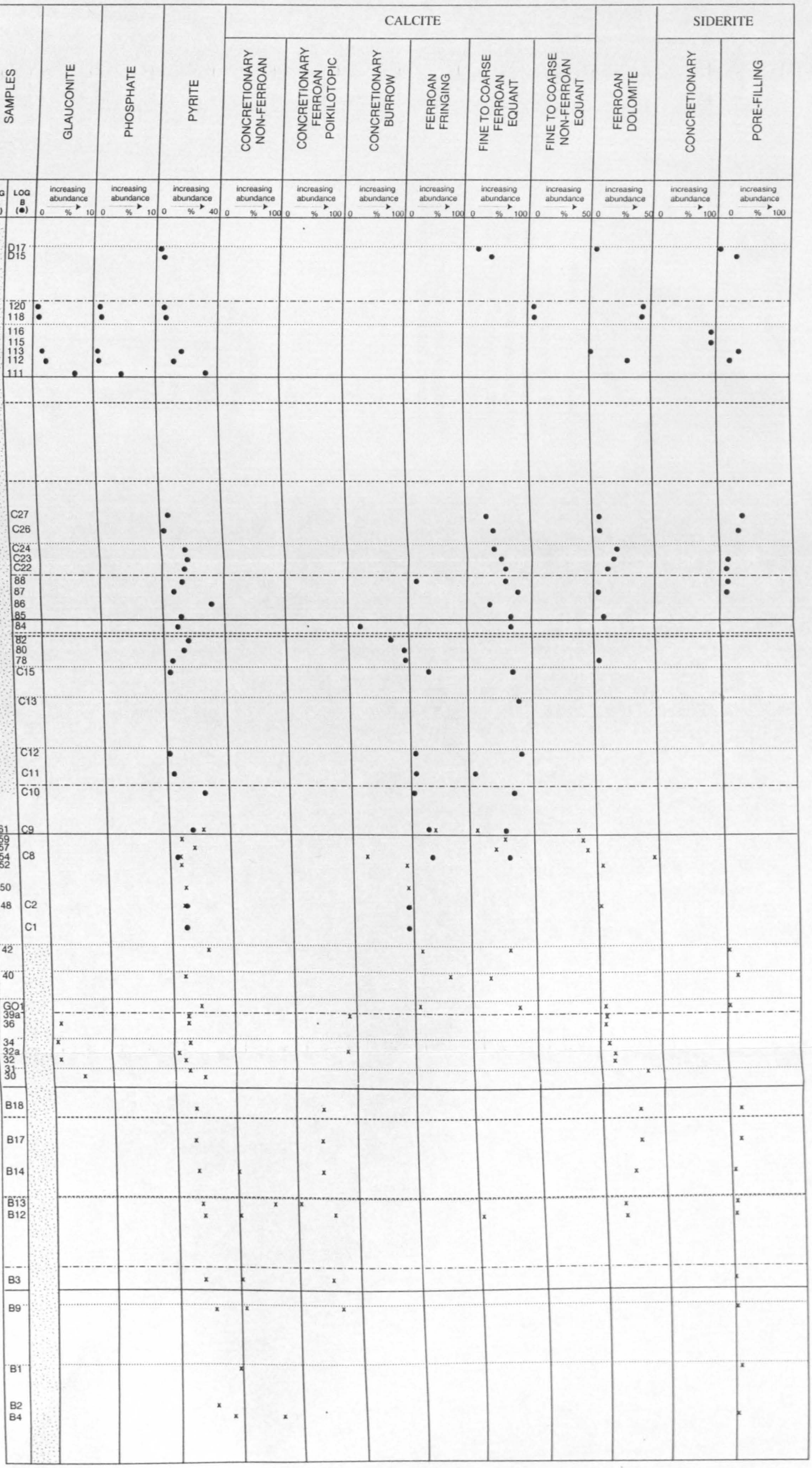

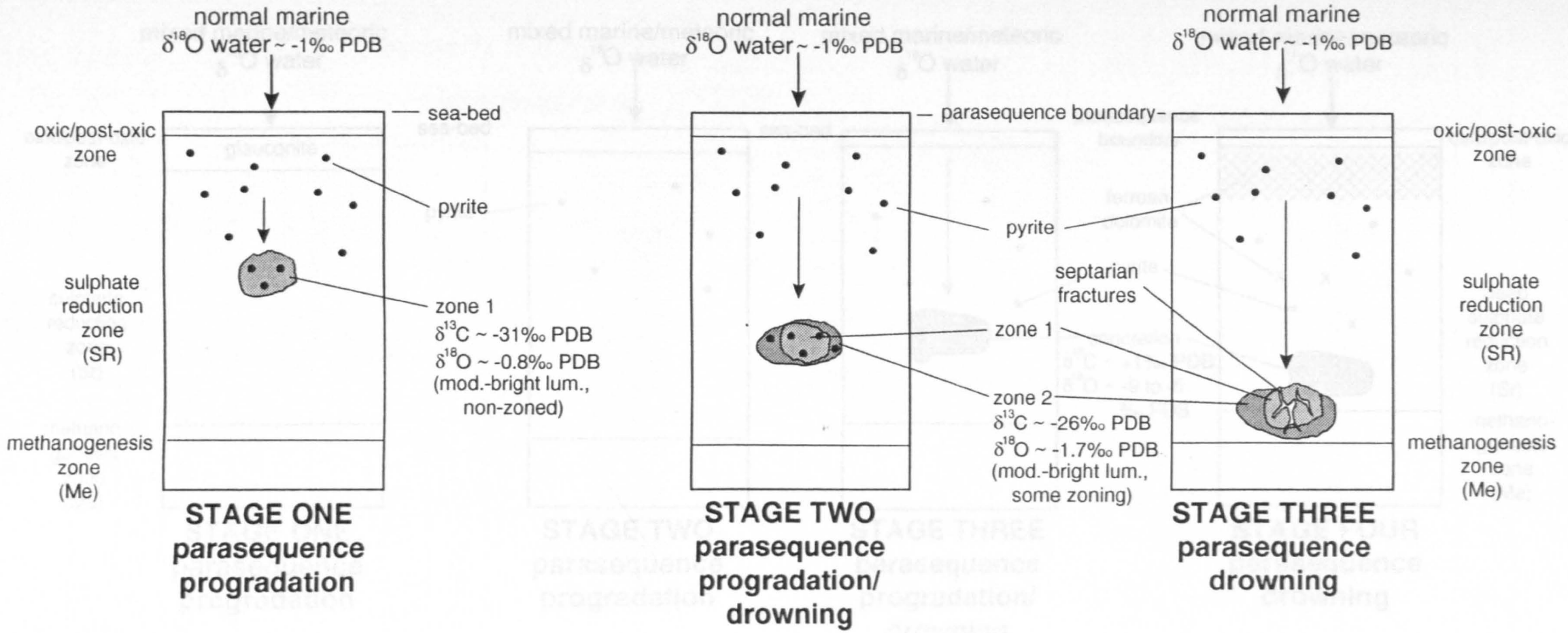

Fig.3.xxi: Early diagenesis within a parasequence of the Nothe Grit Fm. (Sequence 1). During stage 1, pyrite and zone 1 calcite are precipitated in the sulphate reduction zone (Sr). Due to high sedimentation rates, sediment quickly by-passes the oxic/post-oxic zone, thus preserving organic material. With development of parasequence boundary, burial continued at a slower rate, and zone 2 calcite, siderite and less pyrite began to precipitate closer to the lower boundary of the Sr zone. Finally, during stage 3, continued growth of zone 2 calcite occurred, along with development of septarian fractures, which were infilled with calcite that crystallised, very deep into the Sr zone, or just within the zone of methanogenesis (Me). The dominance of calcite with Sr isotope values, suggests that after initially high sedimentation rates, sedimentation became "stagnant" during the formation of the parasequence boundary.

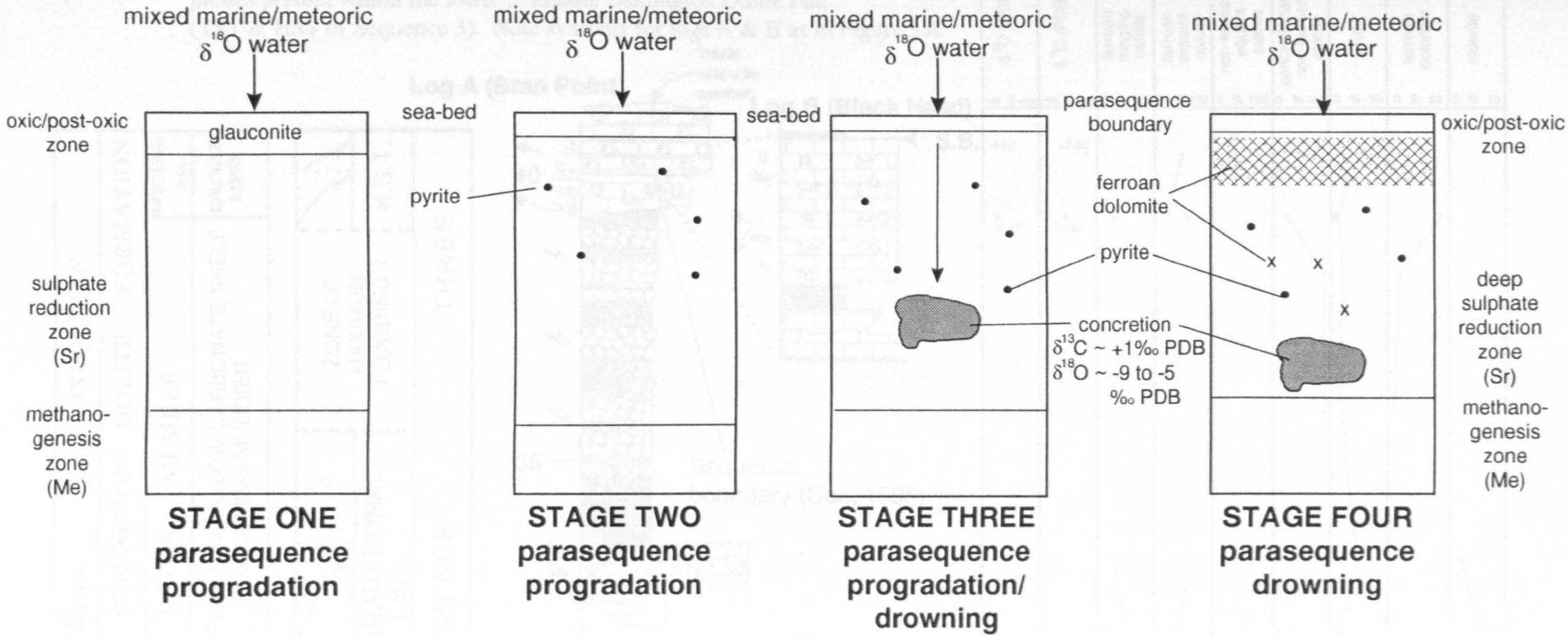

Fig.3.xxii: Early diagenesis within a parasequence of the aerobic tidal flat sands, Bencliff Grit Member (Sequence 3). During Stage 1, rare glauconite crystallises within the post-oxic zone. During Stage 2, low sedimentation rates have resulted in a reduction in the amount of organic matter entering into the sulphate reduction zone. Thus, only a limited amount of pyrite crystallises. During Stage 3, very low rates of organic-carbon oxidation deep within the sulphate reduction zone, result in the growth of large calcite concretions. Finally, during stage 4, ferroan dolomite is precipitated within organic rich facies of the heterolithic beds, and clay laminae (see text for further details).

Fig 3.xxiii: Vertical (& lateral) variations in the abundance of the main early diagenetic phases present within the lower to middle Osmington Oolite Fm. (TST & HST of Sequence 3). Note symbols for logs A & B as in Figure 3.ii.

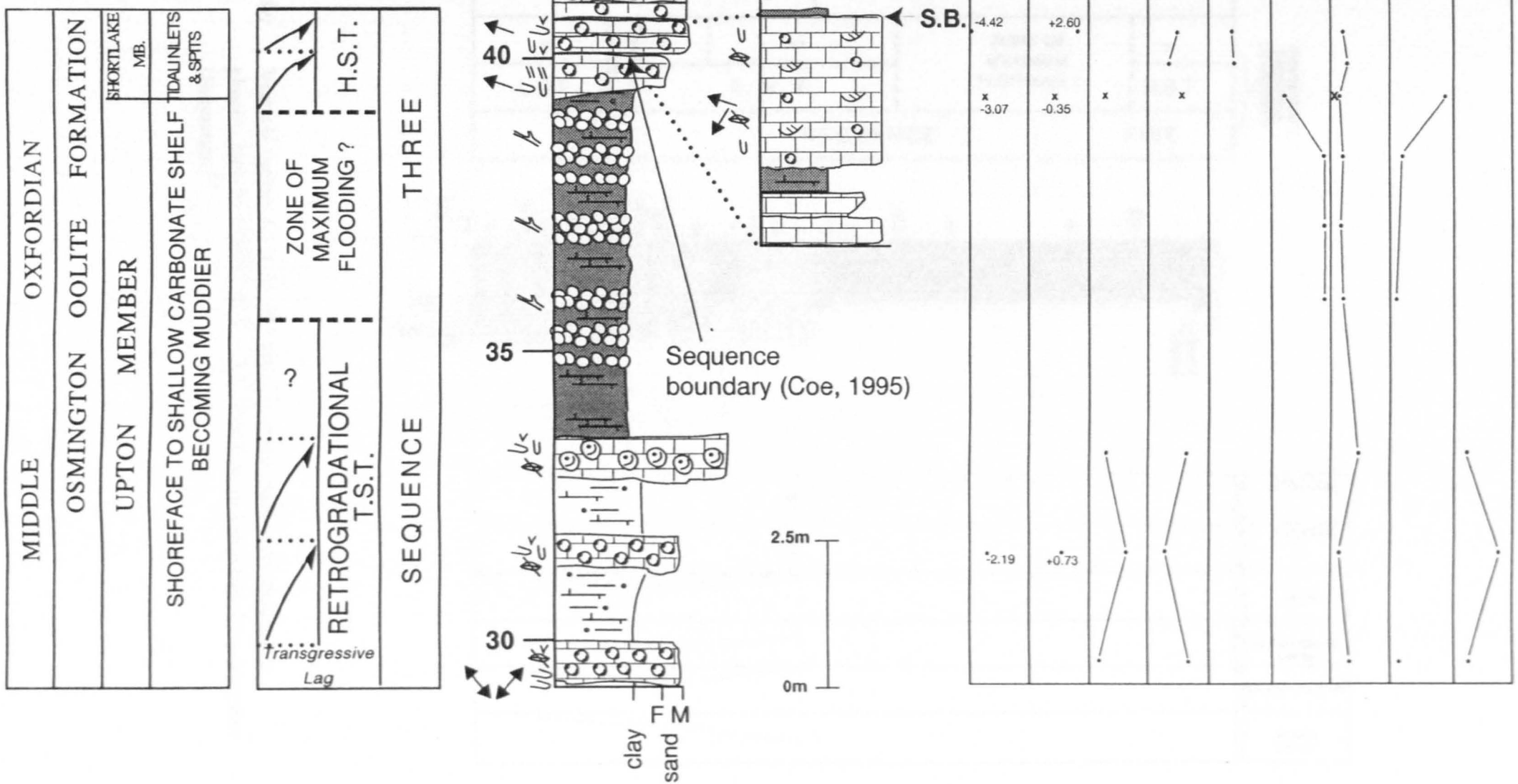

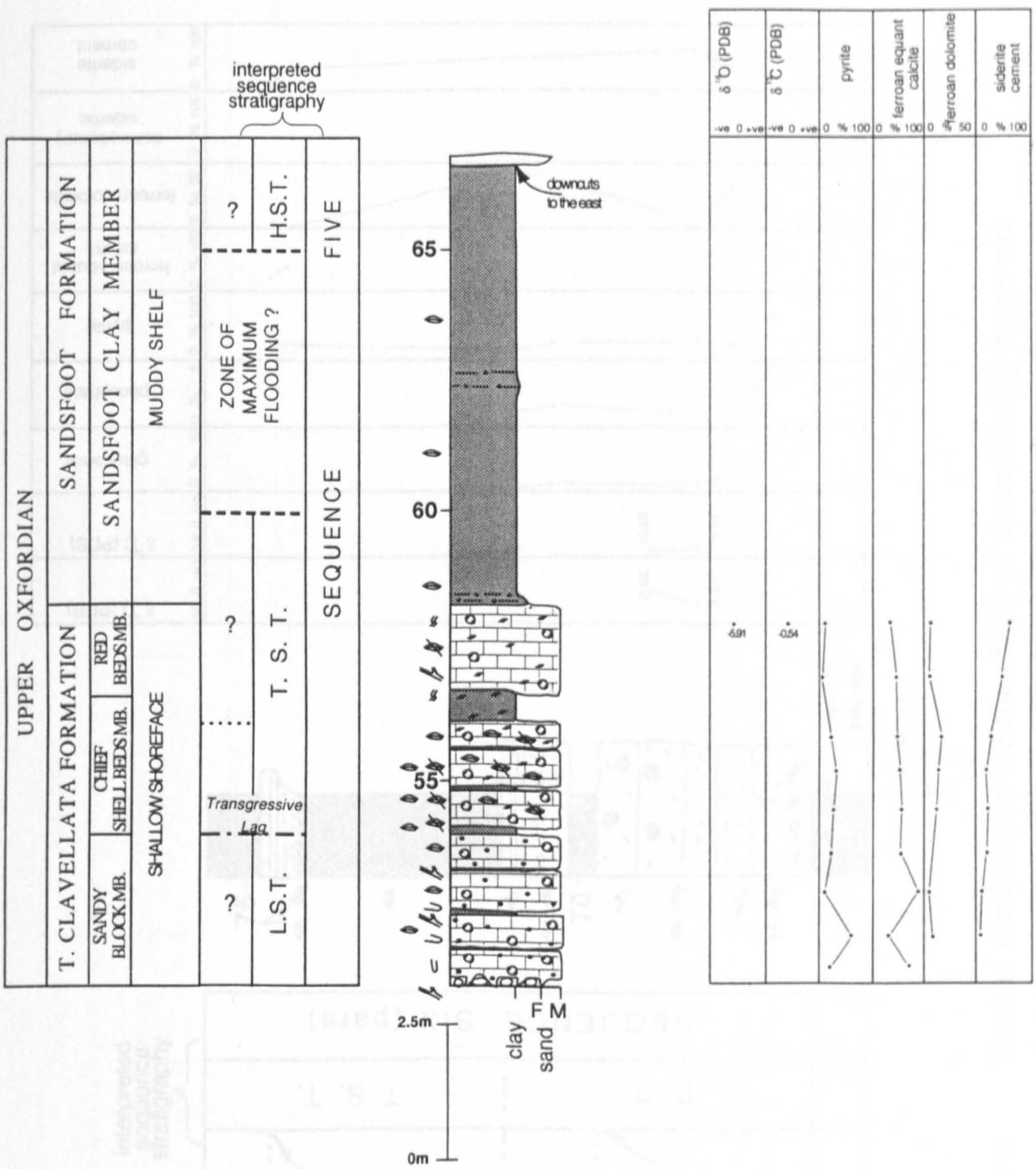

Fig.3.xxiv: Vertical variations in the abundance of the main early diagenetic phases, present within the T. Clavellata Fm. to Sandsfoot Clay Member (Sequence 5)

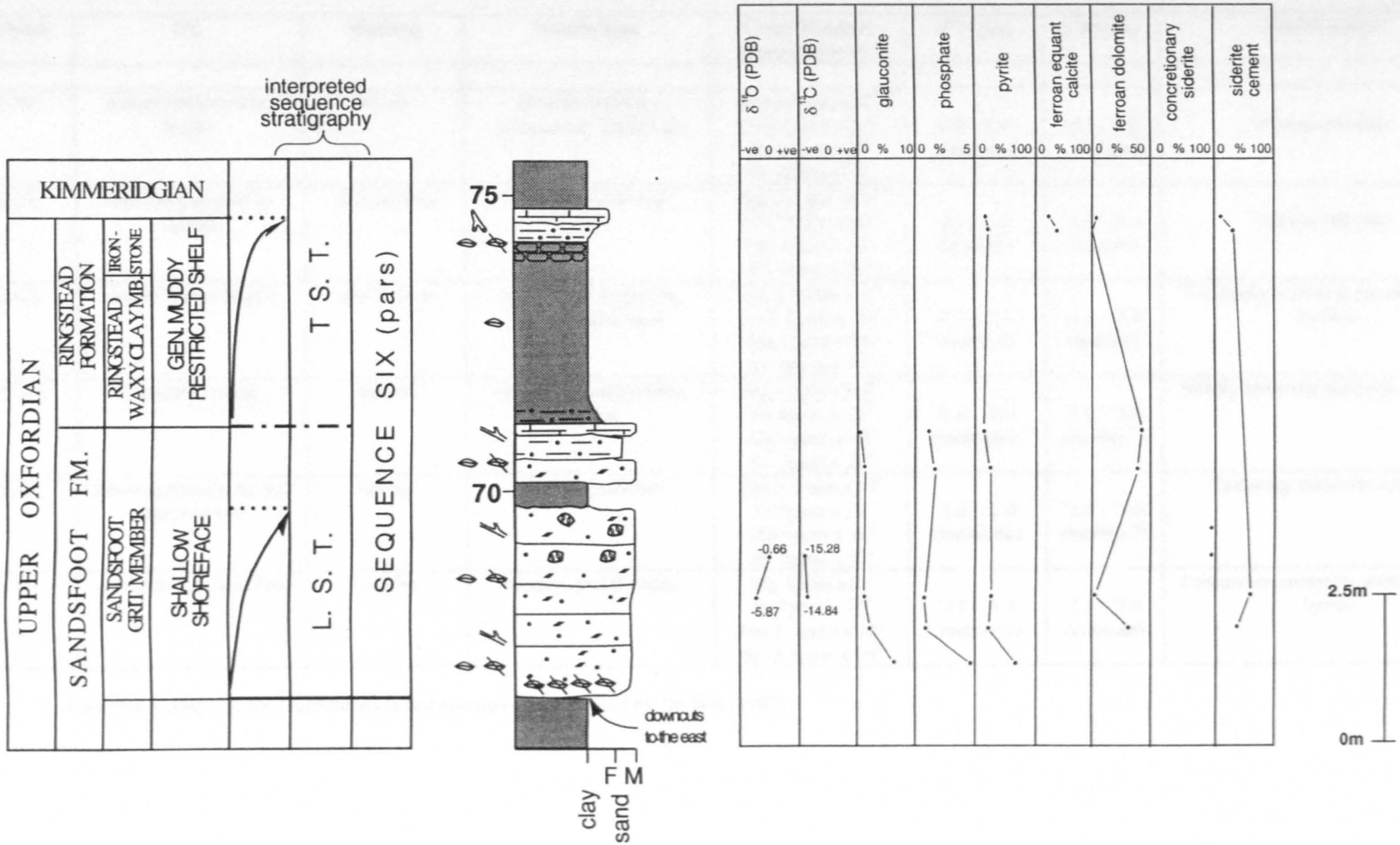

Fig.3.xxv: Vertical variations in the abundance of the main early diagenetic phases, present within the Sandsfoot Grit Member to Ringstead Fm. (Sequence 6)

Cement Phase	CL	Staining	Description	Trace Element (approximates)	$\delta^{13}C$ (‰)	$\delta^{18}O$ (‰)	Environment
Phase 1 (a)	non-luminescent to bright	brown	micritic peloids, grapestone, intraclast	Mg 2.5ppm $x10^3$ Fe 2.5ppm $x\ 10^3$ Mn 3ppm $x\ 10^2$ Sr 4ppm $x\ 10^2$	0.5 - 2.5 (marine)	¯1.0 - ¯3.0 (marine)	Marine phreatic
Phase 1 (b)	non-luminescent to bright	non-ferroan	isopachous fibrous	Mg 2.5ppm $x10^3$ Fe 2.5ppm $x\ 10^3$ Mn 3ppm $x\ 10^2$ Sr 4ppm $x\ 10^2$	0.5 - 2.5 (marine)	¯1.0 - ¯3.0 (marine)	Marine phreatic
Phase 1 (c)	zoned dull to bright	non-ferroan	isopachous dogtooth, equant, microspar	Mg 2.5ppm $x10^3$ Fe 2.5ppm $x\ 10^3$ Mn 3ppm $x\ 10^2$ Sr 4ppm $x\ 10^2$	0.5 - 2.5 (marine)	¯1.0 - ¯3.0 (marine)	Oxidising meteoric phreatic near surface
Phase 2 (a)	complex zoning	ferroan	syntaxial overgrowths, equant	Mg 1.5ppm $x10^3$ Fe 9ppm $x\ 10^3$ Mn 6ppm $x\ 10^2$ Sr 3ppm $x\ 10^2$	¯1.0 - ¯2.0 (meteoric)	¯1.0 - ¯3.0 (marine ?)	Mildly reducing meteoric phreatic
Phase 2 (b)	non-luminescent to dull luminescent	ferroan	equant, granular	Mg 1.5ppm $x10^3$ Fe 9ppm $x\ 10^3$ Mn 6ppm $x\ 10^2$ Sr 3ppm $x\ 10^2$	¯1.0 - ¯2.0 (meteoric)	¯1.0 - ¯3.0 (marine ?)	Reducing meteoric connate
Phase 3	dull with dark patches	variable	blocky, poikilotopic	Mg 1ppm $x10^3$ Fe 5ppm $x\ 10^3$ Mn 2-7ppm $x\ 10^2$ Sr 3.5ppm $x\ 10^2$	¯0.5 - ¯4.0 (meteoric)	¯3.5 - ¯5.0 (connate)	Cretaceous meteoric connate deep burial

Table 3.i: Corallian Group calcium carbonate cement summary as classified by De Wet (1987)

Sequence	Diagenetic Phase	CL	Description	Trace element (wt %)	Environment
Transgressive	1	luminescent	Neomorphism of skeletal aragonite and ooids	Fe <1.2 Mn 0.08 - 0.17	Marine phreatic
Transgressive	2	non-zoned dull	Early columnar isopachous cement fringes	Fe 1.8 Mn 0.08 - 0.17	Anoxic marine phreatic
Transgressive	3	non-zoned dull	ferroan calcite	Fe 2.1 - 3.5 Mn 0.01 - 0.17	Anoxic deep burial
Regressive	1	luminescent	ooids	Fe < 1.2 Mn 0.08 - 0.17	Marine phreatic
Regressive	2	non-zoned dull	Early columnar isopachous cement fringes	Fe 1.8 Mn 0.05 - 0.18	Anoxic marine phreatic
Regressive	3	zoned bright	Blocky calcite non-ferroan to mildly ferroan	Fe <1.0 Mn 0.08 - 0.15	shallow burial/sub-oxic meteoric
Regressive	4	dull	ferroan fracture calcite	(no data)	Anoxic deep burial

Table 3.ii: Osmington Oolite Formation calcium carbonate cement summary as classified by Sun (1990)

Sample No.	Sample Type	Authigenic Phase	Depositional Environment	Lithostrat. unit	CL response
A4, A6	interior zone of septarian concretion	non-ferroan calcite pseudospar	prograding shoreface	Nothe Grit Formation	moderate to bright luminescence, non-zoned
A8	exterior zone of septarian concretion	non-ferroan calcite pseudospar	prograding shoreface	Nothe Grit Formation	moderate to bright luminescence, subtle zoning
E2, E4, 32A	interior & exterior of concretion	ferroan poikilotopic calcite	tidal flat shoreline	Bencliff Grit Member	dull to non-luminescence, subtle zoning
40	pore filling	ferroan fibrous & equant calcite	lower shoreface	Upton Member	dull to moderate luminescence, subtle zoning
42	pore filling	ferroan fibrous & equant calcite	lower shoreface	Upton Member	moderate luminescence, zoned
50	concretion-ary burrow	non-ferroan calcite microspar	shallow shelfal	Upton Member	dominantly dull luminescence
57	pore filling	non-ferroan equant	tidal inlet and accretionary spit	Shortlake Member	very dull to non-luminescent
61	pore filling	ferroan fringing & non-ferroan equant	tidal inlet and accretionary spit	Shortlake Member	fringing calcite is brightly luminescent and zoned, non-ferroan calcite is non to mod. luminescent
C10	pore filling	ferroan equant calcite	tidal inlet and accretionary spit	Shortlake Member	non-luminescent to dull luminescent
C12	pore filling	ferroan equant calcite	tidal inlet and accretionary spit	Shortlake Member	dull to brightly luminescent with rare zoning
C13	pore filling	ferroan equant	tidal inlet and accretionary spit	Shortlake Member	moderate luminescent with some zoning
78	concretion-ary burrow	mildly ferroan microspar	shallow shelfal	Nodular Rubble Member	brightly luminescent and zoned
88	pore filling	ferroan equant calcite	lower shoreface/shallow shelfal	T. Clavellata Formation	dull luminescent and non-zoned
116, 120	pore filling	siderite & ferroan dolomite	prograding shoreface	Sandsfoot Grit Formation	non-luminescent

Table 3.iii: Cathodoluminescence (CL) results for selected cement samples of the Corallian Group succession of south Dorset. CL response described as either non-luminescent, dull luminescent, moderately luminescent or brightly luminescent & either zoned or non-zoned

Sample No.	Sample Type	Authigenic Phase	Depositional Environment	Lithostratigraphic unit	$\delta^{18}O$‰ PDB	$\delta^{13}C$‰ PDB
A5	interior zone of septarian concretion	non-ferroan calcite pseudospar	prograding shoreface	Nothe Grit Fm.	-0.83	-31.10
A6	fracture of septarian concretion	ferroan drusy calcite	?	Nothe Grit Fm.	-3.52	+2.23
A8	exterior zone of septarian concretion	non-ferroan calcite pseudospar	prograding shoreface	Nothe Grit Fm.	-1.75	-26.60
32A	exterior zone of concretion	ferroan poikilotopic calcite	tidal flat shoreline	Bencliff Grit Member	-9.23	-0.34
E3	interior of concretion	ferroan poikilotopic calcite	tidal flat shoreline	Bencliff Grit Member	-6.30	+1.64
E4	exterior of concretion	ferroan poikilotopic calcite	tidal flat shoreline	Bencliff Grit Member	-5.77	+1.86
39A	exterior of concretion	ferroan poikilotopic calcite	tidal flat shoreline	Bencliff Grit Member	-5.60	-0.24
40	pore filling	ferroan fibrous calcite	lower shoreface	Upton Member	-2.19	+0.73
61	pore filling	non-ferroan sparry calcite	tidal inlet and accretionary spit	Shortlake Member	-4.42	+2.60
C12	pore filling	ferroan sparry calcite	tidal inlet and accretionary spit	Shortlake Member	-3.07	-0.35
C12 (c)	control	ooid	tidal inlet and accretionary spit	Shortlake Member	-3.29	+1.14
C27	pore filling	siderite	lower shoreface/shallow shelfal	Red Beds Member	-5.91	-0.54
115	concretion	siderite	prograding shoreface	Sandsfoot Grit Member	-0.66	-15.28
113	pore filling	siderite	prograding shoreface	Sandsfoot Grit Member	-5.87	-14.84

Table 3.iv: $\delta^{18}O$ & $\delta^{13}C$ (‰ PDB) results for selected cement samples of the Corallian Group succession of south Dorset

Lithostratigraphy	Depositional environment	Cement form	Sulphides	Early Carbonates			Paragenetic sequence (early diagenesis only)
Formation/Member				Dolomite	Calcite	Siderite	
Nothe Grit Fm.	prograding shoreface	septarian concretions	abundant pyrite	absent	non-ferroan concretionary calcite	rare siderite	pyrite - calcite - siderite
Preston Grit Mb.	prograding shoreface	cemented bed	pyrite	ferroan dolomite	absent	absent	
Nothe Clay Mb.	muddy offshore shelf	cemented beds	as above	as above	rare non-ferroan calcite	rare siderite	pyrite - calcite - siderite - dolomite
Bencliff Grit Mb.	shallowing shelf tidal flat shoreline	as above concretions and cemented beds	as above pyrite	as above common ferroan dolomite	absent ferroan concretionary calcite	rare siderite absent	pyrite - calcite - dolomite
Upton Mb.	transgressing shoreface	cemented beds & concretionary burrows	as above	rare ferroan dolomite	fringing - equant ferroan calcite	rare pore-filling siderite	calcite - pyrite - siderite/dolomite
Shortlake Mb.	tidal inlets and accretionary spits	cemented beds	as above	as above	fringing - equant ferroan calcite & non-ferroan calcite	rare pore-filling siderite	calcite (ferroan) - pyrite - siderite - dolomite - calcite (non-ferroan)
	tidal inlets and accretionary spits	cemented beds	pyrite	rare ferroan dolomite	fringing - equant ferroan calcite	rare pore-filling siderite	calcite - pyrite - siderite - dolomite
Nodular Rubble Mb.	shallow shelf	concretionary burrows	as above	as above	non-ferroan conc. burrow calcite	rare pore-filling siderite	as above
Sandy Block Mb. Chief Shell Beds Mb	shoreface	cemented beds	pyrite	rare ferroan dolomite	equant ferroan calcite	rare pore-filling siderite	as above
Red Beds Mb.	transgressing shoreface to restricted shelf	cemented beds	as above	common ferroan dolomite	rare equant ferroan calcite	abundant pore-filling siderite	as above
Sandsfoot Grit Mb.	prograding shoreface	cemented beds & siderite concretions	as above	rare ferroan dolomite	rare equant ferroan calcite	abundant concretionary & pore filling siderite	calcite (?) - dissolution - pyrite - siderite - dolomite
Ringstead Coral Bed	restricted shelf to shallow coral bed	cemented beds	rare pyrite	rare ferroan dolomite	ferroan calcite	pore-filling siderite	pyrite - calcite - siderite

Table 3.v: A summary of early diagenetic products within the Corallian Group succession (excluding glauconite & phosphate)

Lithostratigraphy	Depositional environment	Cement form	Sulphides	Early Carbonates			Paragenetic sequence (early diagenesis only)
Formation/Member				Dolomite	Calcite	Siderite	
Nothe Grit Fm.	prograding shoreface	septarian concretions	abundant pyrite	absent	non-ferroan concretionary calcite	rare siderite	pyrite - calcite - siderite
Preston Grit Mb.	prograding shoreface	cemented bed	pyrite	ferroan dolomite	absent	absent	
Nothe Clay Mb.	muddy offshore shelf	cemented beds	as above	as above	rare non-ferroan calcite	rare siderite	pyrite - calcite - siderite - dolomite
Bencliff Grit Mb.	shallowing shelf tidal flat shoreline	as above concretions and cemented beds	as above pyrite	as above common ferroan dolomite	absent ferroan concretionary calcite	rare siderite absent	pyrite - calcite - dolomite
Upton Mb.	transgressing shoreface	cemented beds & concretionary burrows	as above	rare ferroan dolomite	fringing - equant ferroan calcite	rare pore-filling siderite	calcite - pyrite - siderite/dolomite
Shortlake Mb.	tidal inlets and accretionary spits	cemented beds	as above	as above	fringing - equant ferroan calcite & non-ferroan calcite	rare pore-filling siderite	calcite (ferroan) - pyrite - siderite - dolomite - calcite (non-ferroan)
	tidal inlets and accretionary spits	cemented beds	pyrite	rare ferroan dolomite	fringing - equant ferroan calcite	rare pore-filling siderite	calcite - pyrite - siderite - dolomite
Nodular Rubble Mb.	shallow shelf	concretionary burrows	as above	as above	non-ferroan conc. burrow calcite	rare pore-filling siderite	as above
Sandy Block Mb.	shoreface	cemented beds	pyrite	rare ferroan dolomite	equant ferroan calcite	rare pore-filling siderite	as above
Chief Shell Beds Mb	transgressing	cemented beds		common ferroan	rare equant ferroan	abundant pore-	as above
Red Beds Mb.	shoreface to restricted shelf		as above	dolomite	calcite	filling siderite	
Sandsfoot Grit Mb.	prograding shoreface	cemented beds & siderite concretions	as above	rare ferroan dolomite	rare equant ferroan calcite	abundant concretionary & pore filling siderite	calcite (?) - dissolution - pyrite - siderite - dolomite
Ringstead Coral Bed	restricted shelf to shallow coral bed	cemented beds	rare pyrite	rare ferroan dolomite	ferroan calcite	pore-filling siderite	pyrite - calcite - siderite

Table 3.v: A summary of early diagenetic products within the Corallian Group succession (excluding glauconite & phosphate)

Sequence	Systems tract	Depositional environment	Sulphides	Early Carbonates			Paragenetic sequence (early diagenesis only)
				Dolomite	Calcite	Siderite	
Sequence 1	HST	prograding shoreface	abundant pyrite	absent	non-ferroan concretionary calcite	rare siderite	pyrite - calcite - siderite
Sequence 2	LST	prograding shoreface	pyrite	ferroan dolomite	absent	absent	pyrite - calcite - siderite - dolomite
	TST	muddy offshore shelf	as above	as above	rare non-ferroan calcite	rare siderite	
	HST	shallowing shelf	as above	as above	absent	rare siderite	
Sequence 3	SMW	tidal flat shoreline	pyrite	common ferroan dolomite	ferroan concretionary calcite	absent	pyrite - calcite - dolomite
	TST	transgressing shoreface	as above	rare ferroan dolomite	fringing - equant ferroan calcite	rare pore-filling siderite	calcite - pyrite - siderite/dolomite
	HST	tidal inlets and accretionary spits	as above	as above	fringing - equant ferroan calcite & non-ferroan calcite	rare pore-filling siderite	calcite (ferroan) - pyrite - siderite - dolomite - calcite (non-ferroan)
Sequence 4	SMW	tidal inlets and accretionary spits	pyrite	rare ferroan dolomite	fringing - equant ferroan calcite	rare pore-filling siderite	calcite - pyrite - siderite - dolomite
	TST	marine shoal to shallow shelf	as above	as above	as above & non-ferroan conc. burrow calcite	rare pore-filling siderite	as above
Sequence 5	LST	shoreface	pyrite	rare ferroan dolomite	equant ferroan calcite	rare pore-filling siderite	as above
	TST	transgressing shoreface to restricted shelf	as above	common ferroan dolomite	rare equant ferroan calcite	abundant pore-filling siderite	as above
Sequence 6	LST	prograding shoreface	as above	rare ferroan dolomite	rare equant ferroan calcite	abundant concretionary & pore filling siderite	calcite (?) - dissolution - pyrite - siderite - dolomite
	TST	restricted shelf to shallow coral bed	rare pyrite	rare ferroan dolomite	ferroan calcite	pore-filling siderite	pyrite - calcite - siderite

Table 3.vi: Corallian Group sequences, depositional environments and associated early diagenesis (excluding glauconite & phosphate)

4: A High Resolution Sequence Stratigraphic Model For The Lower Cretaceous Ericeira Group Of West Central Portugal

4.1: *Introduction*

4.1.1: Aims

The aim of this chapter is to present a high resolution sequence stratigraphic framework for the lower to middle part of the Ericeira Group through the analysis of depositional environment, facies changes and the identification of key stratal surfaces and sequence stratigraphic units. A consideration of published data on basin-wide facies changes and biostratigraphy is not yet possible for this succession, although unpublished regional data provided by Dr M. Watkinson (*pers comm.* 1996) is presented where available.

The interpretation presented here is that of the author but draws on unpublished material provided by Dr M. Watkinson (*pers comm.* 1996). It differs from previous interpretations because it employs high resolution sequence stratigraphic principles (parasequence stacking patterns - where parasequences can be identified - and systems tracts) to depositional environments, much in the same way that the Corallian Group was interpreted in Chapter 2. In this way, the interpretation relates individual stratal packages and key surfaces to high frequency sea-level changes.

Organisation:

In Section 4.2 of this chapter, I provide a detailed description and interpretation of the Ericeira Group succession and develop a high resolution sequence stratigraphic model. Where applicable, a number of sequence stratigraphic interpretations are offered. In Section 4.3 this interpretation is compared to previous work and highlights similarities and differences with the Corallian Group succession discussed in Chapter 2.

4.1.2: A general introduction to the regional geology of the Lusitanian Basin (Upper Jurassic to Lower Cretaceous)

The Lusitanian Basin of west central Portugal extends more than 250km to the north of the city of Lisbon, and its onshore area totals 23000km^2 (Wilson *et al.*, 1990). To the east, it is bounded by Hercynian basement rocks of the Iberian massif. Offshore, to the west, the boundary is less clearly defined (Wilson *et al.*, 1990). The majority of the structures which formed within the basin since the initial phase of late Triassic extension, can be attributed to the reactivation of Hercynian basement faults (Wilson *et al.*, 1990).

The middle Oxfordian to Berriasian interval was characterised by rapid basement subsidence rates (Wilson *et al.*, 1990). The resulting sub-basins that developed during this syn-rift interval, were primarily due to salt withdrawal and/or NE-SW extension (Wilson *et al.*, 1990). Freshwater and brackish limestones and/or shales were deposited in the north of the basin during the late Oxfordian. These were the first sediments to be

deposited in the basin since the development of the preceding early Oxfordian hiatus (Hiscott *et al.*, 1990b). Following this, a rapid marine transgression occurred during the late Oxfordian and Kimmeridgian, which resulted in the deposition of slope marls, deep sea sands and conglomerates (Hiscott *et al.*, 1990b).

The Tithonian period was characterised by a series of marine transgressions and regressions, which deposited alternations of carbonates and siliciclastic strata within the south of the basin, and marine limestones around the Ericeira region (Hiscott *et al.*, 1990b).

Uppermost Tithonian to lower Berriasian deltaic environments resulted in the deposition of coarsening-up successions which were subsequently exposed and eroded, leading to the development of a major upper Berriasian unconformity (Hiscott *et al.*, 1990a).

During the latest Berriasian to Valanginian, coarse fluvial sandstones were deposited unconformably on top of older strata (Hiscott *et al.*, 1990b). A later transgressive episode produced a change from continental to marine depositional environments during the Valanginian to Hauterivian time interval, during which the deposition of marine shales and carbonates occurred within the basin (Whiteman, 1990).

Table 4.i (after Hiscott *et al.*, 1990b) provides a summary of the main stratigraphic elements of the Lusitanian Basin from Lower Oxfordian to Hauterivian. The inset map of Figure 4.i depicts the palaeogeography and distribution of the major facies types during the Hauterivian.

4.1.3: Previous work

Over the last twenty five years, the lower Cretaceous coastal sections to the north of the town of Ericeira, west central Portugal (Fig.4.i) have been the focus of sedimentological, stratigraphical and palaeontological study (Rey, 1972, 1979; Hiscott *et al.*, 1990a; Whiteman, 1990).

Rey (1972) recognises four distinct stratigraphic units and assigned informal names to them (Fig.4.ii). The lowermost unit is named "dolomies, argilles et grés à foraminiféres", followed by "marnes et grés de Santa Susana", "calcaires à rudist de praia dos coxos" and finally "grés à trigonies".

Hiscott *et al.* (1990a) subdivide the outcrop into six lithostratigraphical members assigned to geological formations (Fig.4.ii). The lowermost member is named the Calada Member, which is equivalent to Rey's (1972) basal unit. This is succeeded by the Sao Lourenço Mudstone Member and Safarujo Member, both equivalent to Rey's (1972) second unit. Succeeding these are the Cabo Raso Limestone Member and Dois Irmãos Member which are broadly equivalent to the upper two units of Rey (1972). In their work, Hiscott *et al.* (1990a) conclude that the lower Cretaceous sediments of the Lusitanian Basin were deposited in an open marine setting characterised by low wave energy. Within the Ericeira Group they recognise at least one marine transgression which is separated from the underlying regression by a submarine hard-ground surface.

Finally, Whiteman (1990) performs a micropalaeontological study of the Kimmeridgian to Barremian deposits of Portugal, which encompassed the Ericeira sections (Fig.4.ii). In his work, he adopts Hiscott *et al.*'s lithostratigraphy, and uses this to locate sample sites (generally mudstone horizons) for micropalaeontological investigation. His palaeoecological interpretations suggest that the succession represents one major regression (Calada Member and Sao Lourenço Member) succeeded by a marine transgression (Safarujo Member to Dois Irmãos Member).

4.2: *Descriptions & Interpretations*

As in Chapter 2, the sequence stratigraphic approach and definitions follow those outlined in Chapter 1. The part of the Ericeira Group studied has been subdivided into four proposed sequences. For each sequence I will outline the lithostratigraphic formations it incorporates (using Hiscott *et al.*, 1990a lithostratigraphy), followed by a detailed description and palaeoenvironmental interpretation. This is then followed by a detailed sequence stratigraphic interpretation incorporating stratal packages and key sequence stratigraphic surfaces. The interpretation incorporates the sequence stratigraphic hierarchy that was outlined in Chapter 1 (parasequence, parasequence set/systems tract and sequence). However, as will be demonstrated, the identification of parasequences is not always possible, particularly in some transgressive and highstand systems tracts where evidence of shallowing-up does not exist.

Throughout Section 4.2, I will refer to Figure 4.iii (sedimentary logs and suggested depositional environments of the Ericeira Group) and Figure 4.iv (sedimentary logs and suggested sequence stratigraphy interpretation of the Ericeira Group) frequently. Table 4.ii provides a tabulated summary of sequence, systems tract and stratal surface depth.

4.2.1: Sequence 1

Sequence 1 is located in the cliff sections to the north of Praia de São Lourenço & the Ribeira do Safarujo (Fig.4.i). Within this study, only the upper third of Sequence 1 is described and this is composed of 13m of the Calada Member (Fig.4.iii & Fig.4.v). The base of Sequence 1 is no longer accessible in the position identified by Hiscott *et al.* (1990a).

4.2.1a: *Lithological description*

The succession begins with 6.5m of fine to coarse trough cross-bedded carbonate cemented sandstones and pebbly sandstones which are interbedded with thin carbonaceous siltstones (up to 6.5m on Fig.4.iii). Palaeocurrent directions taken from trough cross-bedding (average 0.15 - 0.20m thick) indicate current flow was to the south (at 190°). The trough cross-bedded sandstones often grade upwards into low angle planar cross-bedding and wave ripple laminations. The coarser grained beds commonly display concave-up erosional bases, rip-up clasts in lag deposits and have lensoid geometries. Towards the top of these sandstone beds, large pieces of fossil wood are seen which are oriented in an east-

west direction (at 5.9m on Fig.4.iii). *Skolithos* and *Cruziana* ichnofacies assemblages characterise these beds.

Succeeding the sandstones are 6.2m of interbedded fine to very fine sandy, vuggy ferroan dolomitic limestones and silty claystones (between 6.5m-12.7m on Fig.4.iii and Fig.4.v). The coarser grained beds contain a number of small septarian concretions of approximately 0.1m in diameter (Fig.4.v). The septarian concretions increase in abundance towards the top of each bed and are composed of non-ferroan dolomite. The upper bed of this succession contains abundant vugs but no septarian concretions. Whiteman (1990) has reported the presence of the ostracod *Fabanella* and the foraminifera *Trochammina* and *Ammobaculites* in the sandy dolomitic limestones of this succession.

4.2.1b: *Palaeoenvironmental interpretation*

The coarse grained trough cross-bedded sands represent a series of channels within a low to moderate energy nearshore shallow marine environment. The trace fossils and fossil wood further indicate a distributary channel/delta mouth environment (*sensu* Bhattacharya & Walker, 1992). These are replaced upwards by a restricted lagoonal or estuarine bay environment as indicated by the palaeontology and a lack of marine reworking.

Previous palaeoenvironmental interpretations:

The lower sandstone beds have previously been interpreted as representing river mouth estuaries or low energy sand flat deposits flanking river mouths, but showing a lack of

marine reworking (Hiscott *et al.*, 1990b), while the upper fine grained sandstones and silty claystones have been interpreted as lower marsh, lagoonal deposits (Whiteman, 1990).

4.2.1c: *Sequence stratigraphic interpretation*

The lower 6.5m of the succession described above represents at least three fining-up parasequences which are each capped by a marine flooding surface/parasequence boundary (e.g. at 5m on Fig.4.iv). Each parasequence boundary is marked by an abrupt change in lithology from silty mudstone below, to sandstone above the boundary and an abrupt increase in bed thickness relating to a deepening of the depositional environment.

The clearest flooding surface of the three is the uppermost one (at 6.5m on Fig.4.iv) which contains carbonaceous material and separates the channelised sandstone facies, below from the restricted lagoonal deposits above. This surface also marks a change in depositional environment, resulting from a rise in relative sea-level and therefore corresponds to a transgressive surface. The upper 7m of Sequence 1 (between 6.5m and 12.7m on Fig.4.iv) is interpreted to represent the transgressive and highstand systems tracts (Fig.4.v). Positioning of a maximum flooding surface based on parasequence identification within this sequence is problematic. However the presence of septarian concretions towards the top of some coarse beds, may suggest a prolonged residence within a particular diagenetic zone (see Chapter 5 Section 5.3.1). Their growth could be directly related to succeeding marine flooding surfaces/parasequence boundaries. The presence of septarian concretions within the lower 3.5m of the lagoonal facies, indicates that this may represent the

transgressive systems tract, where prolonged periods of flooding at parasequence boundaries would be expected.

Succeeding the restricted lagoonal deposits, are another series of channel fill facies. (see Sub-section 4.2.2). The surface that separates the two distinctly different depositional environments must therefore represent a period of abrupt shallowing which indicates the presence of a type-1 sequence boundary.

4.2.2: Sequence 2

Sequence 2 is located in the cliff sections to the north and south of Praia de São Lourenço and beneath the Forte de São Lourenço (Fig.4.i). It is composed of the upper 4m of the Calada Member, the succeeding São Lourenço Mudstone Member and the lower 14m of the Safarujo Member. The total thickness of this sequence at the Ericeira outcrops is 27.7m (between 12.7m-40.4m on Fig.4.iii).

4.2.2a: *Lithological description (Calada Member & São Lourenço Mudstone Member)*

The Calada Member sediments within this sequence are similar to the distributary channel deposits described in Sequence 1. Thus they are coarse grained sandstones often with granular bases that fine upwards and display well developed lensoid geometries. They can clearly be seen down-cutting into muddy flood-plain deposits (Fig.4.vi). As in Sequence 1, the trough cross bedding indicates flow in a dominant southerly direction.

The overlying São Lourenço Mudstone Member is composed of approximately 10m of interbedded silty mudstones and coarser grained fossiliferous beds (between 16.5m-25.8m on Fig.4.iii and Fig.4.vii). The silty mudstones are absent of macrofossils, but the coarser grained fossiliferous beds contain gastropods, (e.g. *Natica*) bivalves, (e.g. *Exogyra tuberculifera* and *Neithea* sp.) and fish teeth (Rey, 1972). An epifaunal solitary coral was observed within one of these beds (at 24m on Fig.4.iii) (Watkinson *pers comm.*). Whiteman (1990) notes the presence of the foraminifera *Trochammina* and *Ammobaculites* within the silty mudstones, but an absence of ostracod species.

4.2.2b: *Palaeoenvironmental interpretation (São Lourenço Mudstone Member)*

The sedimentological and palaeontological evidence indicates that the São Lourenço Mudstone Member may represent a shallow outer to inner shelf marine environment, accumulating below fair-weather wave base, with probable periodic incursions of storms depositing beds of bioclastic debris. This interpretation is similar to Hiscott *et al.* (1990a). Alternatively, the lower part of this member could represent a similar restricted lagoonal environment to that seen within the Calada Member (because it shows similar facies characteristics) and only the top few metres could represent a true marine environment (based on the discovery of the solitary coral at 25m on Fig.4.iii).

Previous palaeoenvironmental interpretations:

This member has previously been interpreted as representing open marine shelfal deposits (Hiscott *et al.*, 1990a) and fluctuating high and low marsh environments which vertically

grade into a lower mudflat estuarine environment (Whiteman, 1990).

4.2.2c: *Lithological description (lower part of Safarujo Member)*

The basal 14m of the Safarujo Member is dominated by three thick bedded medium grained, moderately cemented sandstones, interbedded with two thin silty mudstone units (between 26.8m-40.4m on Fig.4.viii). Both of the silty mudstone units are well bioturbated with abundant well cemented *Thalassinoides* burrows, (some having amalgamated) that often extend into the surrounding sandstones. The two sandstone beds that occur within the lower 4.5m of the member contain sparse physical sedimentary structures apart from rare, relict parallel laminations and rarely preserved current ripple cross-laminations (Watkinson *pers comm.*). The third sandstone bed is 7.5m thick, has a coarse granular base and contains abundant, large (~0.5-1.0m diameter) elongate and oblate to spherical carbonate concretions (Fig.4.viii). Sedimentary structures within this sandstone bed are dominated by trough cross-bedding vertically grading into low angled, planar cross-bedding towards the top. Palaeocurrent directions from the trough-cross bedding indicate a southerly flow direction. The top of the unit is heavily bioturbated.

Whiteman (1990) notes a monospecific assemblage of the foraminifera *Ammobaculites* within the silty mudstone layers.

4.2.2d: *Palaeoenvironmental interpretation (Safarujo Member)*

The bioturbated sands of the lower Safarujo Member (between 25.8m-31.5m on Fig.4.iii) containing relic sedimentary structures which would indicate a lower shoreface environment (*sensu* McCubbin, 1982; Elliot, 1986 and Walker & Plint, 1992). The lack of sedimentary structures (most of which would have been destroyed by bioturbation) and a dominance of browsing burrowers indicates a low energy environment, although the lack of clay indicates deposition above fair-weather wave-base.

Sedimentary structures within the sand unit occurring above this (31.5m-40.4m on Fig.4.iii) indicate a change to upper shoreface (trough cross-bedding) and foreshore/beach (low angled planar cross-bedding) depositional environments (Fig.4.viii). Thus the lower part of the Safarujo Member provides an excellent example of a prograding shoreface environment (*sensu* McCubbin, 1982; Elliot, 1986 and Walker & Plint, 1992).

The surface separating the São Lourenço Mudstone Member and Safarujo Member appears sharp in the field, but on close examination shows no evidence of erosion or down-cutting (i.e. gutter casts, erosional surface or mudstone intraclasts). This sharp base is not thought to be related to an abrupt fall in relative sea-level, but is interpreted to be the result of an inefficient mechanism of sand removal from the shoreface environment. For example, there is no sedimentary evidence for storm driven offshore directed currents. A similar interpretation was offered for the Nothe Grit Formation of the Corallian Group (refer to Section 2.2.1).

An alternative explanation offered by Hiscott *et al.* (1990a) indicates that the planar surface separating the two members represents a basinward movement of the shoreline caused by a relative sea-level fall (*sensu* Posamentier *et al.*, 1992). The Safarujo Member would then represent an "attached shoreface" (*sensu* Ainsworth & Pattison, 1994). A lack of erosional or down-cutting evidence at this surface (e.g. gutter casts, down-cutting or mudstone intraclasts) indicates that the first explanation is more preferable. However, with a lack of biostratigraphic control or regional data, an unequivocal palaeoenvironmental interpretation is not possible.

Previous palaeoenvironmental interpretations:

The Safarujo Member has previously been interpreted as representing a low energy, micro-tidal beach deposit/foreshore environment with migrating tidal inlets (Hiscott *et al.*, 1990a). In their interpretation, low angled planar laminations are thought to represent beach deposits; the trough cross beds represent megaripples migrating onshore or alongshore under the influence of wave generated currents and the granule layers represent lag deposits formed due to reworking in the swash zone. The lower 4.5m of massive sandstones have been interpreted as representing middle/lower shoreface deposits, where burrowing organisms would have been relatively active. Finally, the contact between the sandstones and the underlying São Lourenço Mudstone Member is interpreted as representing an erosional surface formed at the level of the lower shoreface due to longshore migration of tidal inlets. However Whiteman (1990), using foraminiferal data, suggests that the silty mudstone layers of the Safarujo Member represent a mudflat/estuarine environment.

4.2.2e: *Sequence stratigraphic interpretation*

The boundary between Sequence 1 and Sequence 2 (at 12.7m on Fig.4.iv) has already been interpreted as the equivalent of a type-1 sequence boundary which formed as a result of an abrupt shallowing of water depth from a deeper water lagoonal environment, to a shallow water, dominantly nearshore distributary channel environment. Thus the lower 4m of Sequence 2 represents a lowstand systems tract forming within a distributary channel environment, that is composed of three fining-up parasequences, similar in character to the fining-up parasequences of Sequence 1 (between 12.7m-16.5m on Fig.4.iv).

The overlying São Lourenço Mudstone Member and lower 14m of the Safarujo Member are interpreted as representing the transgressive and highstand systems tracts of Sequence 2 (between 16.5m-40.4m on Fig.4.iv). This would therefore suggest that the surface separating the underlying Calada Member from the offshore mudstones represents a transgressive surface relating to an abrupt deepening of the depositional environment (Fig.4.vii). The immediately overlying coarser grained shelly bed (17m, Fig.4.iv) represents a transgressive lag deposit that formed as a result of shoreface erosion during the commencement of a marine transgression (Fig.4.vii). However, not all of the features commonly associated with basal transgressive lags (e.g. rip-up clasts, gravels or pebbles) are present.

The depositional environment of the upper São Lourenço Mudstone Member and lower Safarujo Member has been interpreted as representing a prograding shoreface

beach/strand-plain environment. Therefore, a zone of maximum flooding would have to occur within the São Lourenço Mudstone Member (suggested to occur between ?24m-?25.8m on Fig.4.iv). Its exact stratigraphical location is indeterminable as parasequences are not present, however the limited palaeontological evidence suggests that conditions were increasingly marine towards the top of this member. Their is no field evidence (shallowing and subsequent hard-ground formation) to suggest that the coarser grained bioclastic beds (e.g. at 18.3m and 20.3m on Fig.4.iv) represent shallowing associated with parasequence formation, however diagenetic analysis supports the interpretation of parasequences (see Section 5.3.2).

Unpublished regional data (Watkinson *pers comm.*) indicates that the São Lourenço Mudstone Member represents an extensive transgressive unit. At Cabo Espichel (approximately 70km to the south of the town of Ericeira) the São Lourenço Mudstone Member is also interpreted to contain a period of maximum flooding, followed by highstand progradation above (Watkinson *pers comm.*).

The lower part of the Safarujo Member (between 25.8m and 40.4m on Fig.4.iv and Fig.4.viii) is composed of three well defined shallowing-up parasequences. Each parasequence is composed of a basal silty mudstone unit and a coarser grained sand unit. Basal lag deposits at the base of each sand unit are likely to have been deposited as a result of shoreface erosion that occurred during the preceding marine flooding event. The zone of bioturbation at the top of each parasequence is related to the formation of the succeeding marine flooding surface, enabling colonisation by a burrowing fauna as current energy dropped. Facies analysis indicates that this set of three parasequences represents a

prograding parasequence set, equivalent to a highstand systems tract.

A conformable boundary, equivalent to a type-2 sequence boundary is positioned immediately above the third parasequence of the Safarujo Member (at 40.4m on Fig.4.iv and Fig.4.viii). The surface shows no evidence of either subaerial exposure or an abrupt fall in relative sea-level. Its positioning also corresponds more or less to the change from dominant progradation (below) to dominant aggradation (above, see Section 4.2.3) indicating that the Safarujo Member (as a whole) represents two parasequence sets (*pers comm.* Watkinson). If a sequence boundary was positioned at the top of the other sandstone units (e.g. at 27.9m or 31.9m on Fig.4.iv) it would not correspond to the maximum amount of progradation or, the change from dominant progradation to dominant aggradation.

Unpublished regional data (Watkinson *pers comm.*) indicates that at Cabo Espichel, a progradational muddy deltaic unit representing a highstand systems tract, can be correlated to the lower part of the Safarujo Member, thus supporting this sequence stratigraphic interpretation.

4.2.3: Sequence 3

Sequence 3 is located beneath, and to the south of the Forte de São Lourenço and cliff sections to the north and south of Praia dos Coxos (Fig.4.i). It is composed of the upper 10m of the Safarujo Member and the succeeding Cabo Raso Limestone Member. The

total thickness of this sequence at the Ericeira outcrops is 17m (Fig.4.iii).

4.2.3a: *Lithological description & palaeoenvironmental interpretation (upper Safarujo Member)*

The sedimentology and depositional environment of the upper 10m of the Safarujo Member is very similar to that described in Sequence 2. Thus it represents a series of three small mixed upper shoreface/foreshore prograding units, each being capped by a pronounced ravinement surface (e.g. 44.5m and 47m on Fig.4.iii). These units contain elongate, spherical and oblate carbonate cemented concretions, trough cross bedding (indicating a bi-directional current flow to the SW and N) and horizontal to low angled planar cross-lamination.

4.2.3b: *Lithological description (Cabo Raso Limestone Member)*

The succeeding Cabo Raso Limestone Member is a 7.5m succession of carbonate deposits. These are composed of basal sandy, bioclastic grainstones, grading up into sparsely bioclastic wackstones and mudstones (Fig.4.ix). Locally, especially within the coarser grained carbonate beds, marine fossils are present including oyster fragments, large nerineid and naticid gastropods, rare rudists and scleractinian corals (see also Rey, 1972). One *in situ* coralline red algae was also noted (Watkinson *pers comm.*). Whiteman (1990) mentions "large colonial corals", but these are more likely to be solitary coralline algae (Watkinson *pers comm.*). Thin section analysis of the finer grained upper beds reveals the presence of *Dasycladacea* green algae fragments and stromatoporids. Abundant bioclastic

material has been dissolved out of these sediments to create secondary vuggy and mouldic porosity.

The tops of some of the lower carbonate beds and the uppermost surface of the member have a distinct undulatory and rubbly appearance (e.g. at 55.1m and 58.7m on Fig.4.iii and Fig.4.ix). Finally, within the coarser grained beds, small (approximately 20mm diameter) spherical carbonate concretions are also present.

4.2.3c: *Palaeoenvironmental interpretation (Cabo Raso Limestone Member)*

The lower, coarser grained carbonate beds of the Cabo Raso Limestone Member represent a series of shallow water, open marine carbonate deposits, rather than "reef build-ups". A reef build-up implies an element of topography. Although Whiteman (1990) suggests that the beds thin laterally, there was no evidence for this along the studied outcrops. The upper finer grained carbonates containing green algae and macro-fossils, suggest that the depositional environment changed to a less agitated, probably slightly deeper, stenohaline lagoon.

The undulatory upper surfaces of the lower limestone beds can be clearly interpreted as representing ravinement surfaces relating to erosion associated with shoreface transgression. The top surface of the member has previously been interpreted by Hiscott *et al.* (1990a) to represent a marine hard-ground or omission surface (Fig.4.ix). Due to its undulatory appearance and associated surface related diagenetic products (Section 5.3.3), it is interpreted as representing a small (poorly developed) karst surface that developed as

a result of subaerial exposure to a humid climate (Fig.4.ix).

Previous palaeoenvironmental interpretations:

Rey (1979) indicates that the depositional environment of these carbonate beds relates to "reefal build-ups, which formed during a regressive phase that followed on from a marine transgression." However, at the Ericeira outcrop, this interpretation is undoubtedly incorrect because coral specimens are very rare.

4.2.3d: *Sequence stratigraphic interpretation*

The surface that separates Sequence 2 from Sequence 3 (at 40.4m on Fig.4.iv) is interpreted as representing a type-2 sequence boundary because it displays no evidence of exposure or an abrupt fall in relative sea-level and separates a dominantly progradational parasequence set below, from a dominantly aggradational parasequence set above. The succeeding upper 10m of the Safarujo Member represents a series of three coarsening-up parasequences (e.g. one occurs between 40.4m-44.5m on Fig.4.iv) which stack to form the aggradational shelf-margin systems tract[1] of Sequence 3. Each parasequence is separated from the next by a well developed ravinement surface and capped by a small lag deposit - both representing elements of short-lived marine transgressions associated with parasequence boundary formation. Within this parasequence set, the depositional environment fluctuated between an upper shoreface and foreshore environment.

[1] refer to Section 2.3.3 for definition of terminology

The change from clastic shoreface deposits to shallow water open marine carbonates, is indicative of a transgression. The transgressive surface (Fig.4.ix) is situated at 51.8m on Figure 4.iv. The depositional environment of the Cabo Raso Limestone Member represents transgression from a shallow water open marine environment to a less agitated marly lagoonal environment, followed by a very abrupt shallowing, and the creation of a distinct karstic surface. Very abrupt shallowing at the top of the member represents a small poorly developed highstand systems tract.

Three parasequences can be identified within the Cabo Raso Limestone Member - two within the lower open marine facies (between 51.4m-55m on Fig.4.iv) and one at the very top within the less agitated marly facies (between 58.1m-59.2m on Fig.4.iv). It is likely that the zone of maximum flooding could be positioned between these sets of parasequences, within the less agitated marly facies (between ?55m and ?58.1m on Fig.4.iv). However, accurate positioning of a maximum flooding surface within this zone is not possible using currently available data. The lower two parasequences are capped by well developed and pronounced ravinement surfaces which must have developed as a result of submarine transgression associated with marine flooding periods and parasequence boundary formation (Fig.4.ix). The third parasequence is positioned at the top of the member and is capped by a sub-aerial erosive surface that displays evidence of karstification and records a period of emergence (Fig.4.ix).

The top surface of the upper parasequence is also equivalent to the sequence boundary at the base of Sequence 4 (at 59.2m on Fig.4.iv and Fig.4.ix). As noted earlier, it displays evidence of karstification which indicates a period of sub-aerial exposure. Above this

surface, rests a well sorted approximately 2m thick, lensoid sand-body which, in agreement with Hiscott *et al.* (1990a) is interpreted as representing a spit (see Sub-section 4.2.4). As this surface is the only one within the member that clearly records a prolonged period of emergence/sub-aerial exposure it is therefore interpreted to represent a type-1 sequence boundary.

Unpublished regional data (Watkinson *pers comm.*) indicates that, in the south of the basin, a transgressive period occurred above the laterally equivalent type-2 sequence boundary leading to the development of a 20m thick reef-like biostrome. Present data indicate that this maybe correlatable with the upper part of the Safarujo Member. However there is no evidence for a fall in relative sea-level at this time (Watkinson *pers comm.*). This supports the positioning and identification of a type-2 sequence boundary within the Safarujo Member.

4.2.4: Sequence 4

Sequence 4 is exposed above the modern day foreshore and cliff sections around Dois Irmãos (Fig.4.i). It is composed of the Dois Irmãos Member and is 11.3m thick at this location (between 59.2m-70m on Fig.4.iii).

4.2.4a: *Lithological description*

The basal 2m of the Dois Irmãos Member is composed of a fine grained well sorted sandstone that contains trough cross-beds up to 2m thick dipping in a northerly direction (59.2m to 60.3m on Fig.4.iii & Fig.4.x). Its upper surface is dominated by *Thalassinoides* burrows, mud clasts, wood fragments and polygonal desiccation cracks (Hiscott *et al.*, 1990a). Smaller scale structures are also present including current ripples, parting lineation, small scale trough cross bedding (oriented SW) and reactivation surfaces. This sandstone unit grades laterally into a thin marly limestone bed and is draped by mudstones and wackstones (Fig.4.x).

The remainder of the Dois Irmãos Member fines upwards and is composed of 10m of interbedded silty calcareous mudstones and fine to coarse grained carbonate cemented sandstones (60.3m to 70m on Fig.4.iii) with evidence of marine fossils (brachiopods and echinoids). One such bed, (69m on Fig.4.iii) is approximately 1m in thickness, coarsens-up, contains low angled laminations and common vertical burrows from the *Skolithos* ichnofacies assemblage. Laterally, the bed can be seen to down-cut into the underlying mudstones (Fig.4.xi).

The mudstone/wackstone units contain abundant examples of the foraminifera *Choffatella decipiens* and sparse examples of trachyleberid ostracods (Whiteman, 1990).

4.2.4b: *Palaeoenvironmental interpretation*

The basal sandstone bed of the member represents a small prograding spit, which is in agreement with the interpretation offered by Hiscott *et al.* (1990a). Spit accretion relates to foreset dip direction (i.e. northerly). Sedimentological and palaeontological evidence indicates that the remaining 8m of the member, represents a quiet water marine or lagoonal environment (as indicated by the presence of *Choffatella decipiens*) that was barred by small regressive sand barriers containing marine fossils (of which the uppermost 1m thick, coarsening-up sandstone bed containing *Skolithos* burrows, is a good example).

Previous palaeoenvironmental interpretations:

Hiscott *et al.* (1990a) have interpreted the basal sandstone bed to represent a thin spit building out across the hard-ground surface that relates to the sequence boundary at the top of Sequence 3. The main direction of spit growth relates to the large foreset dip direction (i.e. northerly) with the small scale features relating to seaward flow across the spit (i.e. south-westerly). This is such a well exposed feature that there is little doubt that this interpretation is correct. Whiteman (1990) interprets the Dois Irmãos Member as a shallow marine intertidal environment.

4.2.4c: *Sequence stratigraphic interpretation*

The basal 2m thick sandstone bed that has been interpreted as a spit, represents a shoreface equivalent of a lowstand systems tract, that prograded over the highstand sediments of

Sequence 3. The top of the spit represents a transgressive surface, separating it from the quieter and deeper water facies of the interbedded silty mudstones and sandstones (Fig.4.x and Fig.4.xii). This is further evidence to indicate that the spit could represent a lowstand deposit. Alternatively, the spit could represent a transgressive systems tract which would imply that the sequence boundary and transgressive surface have amalgamated. Spits (and barriers) are commonly deposited during a rising relative sea-level, which would occur during both a lowstand and transgressive systems tract (Reinson, 1992). Without regional data or additional outcrop, either interpretation is valid.

The succeeding 8m of the Dois Irmãos Member represent both the transgressive and highstand systems tracts of Sequence 4. Parasequences are difficult to identify, although the presence of marine fossils on the upper surface of the coarser grained carbonate cemented sandstones, would suggest periods of non-deposition relating to marine flooding and parasequence boundary formation. A clear coarsening-up parasequence does occur around 69m on Figure 4.iv. Its upper surface contains evidence of trace fossils indicative of a high energy environment, which would indicate an element of shallowing also associated with parasequence progradation.

As is the case for Sequences 1-3, there is insufficient evidence to accurately identify a maximum flooding surface. On Figure 4.iv, a zone of maximum flooding has been positioned between probable stacked parasequences at ?63.9m and ?65.7m. This zone would thus contain the maximum flooding surface.

There are two candidate surfaces for the sequence boundary above Sequence 4. The first is at the top of the upper parasequence (62.9m on Fig.4.iv). It is capped by silty mudstones and sandstones similar in character to those of the underlying facies. This would suggest that the depositional environment and thus relative sea-level, did not alter significantly across the sequence boundary - corresponding to the definition of a type-2 sequence boundary. The parasequence would then represent the uppermost parasequence of Sequence 4. Its lower surface (which is clearly erosive - 68.1m on Fig.4.iv) could be interpreted as representing a ravinement surface.

An alternative explanation would position a sequence boundary to correspond with this erosive surface (68.1m on Fig.4.iv). The erosion and down-cutting would then relate to the development of a type-1 sequence boundary that would have formed in response to a relative sea-level fall/period of forced regression. The succeeding parasequence would then become the basal unit of the subsequent lowstand systems tract of the succeeding sequence (Sequence 5).

In the present study, not enough field evidence exists to accurately determine the location of this sequence boundary, however petrographic evidence (Section 5.3.4) indicates that early diagenetic cements within all of the carbonate cemented sandstone beds of the Dois Irmãos Member, are similar. This would indicate that pore-water chemistry was similar and that all of these parasequences are of the same sequence (refer to Section 5.3.4a).

4.3: *Summary, discussion and comparison with the Corallian Group succession*

4.3.1: Summary & discussion

Figure 4.xiii summarises the proposed sequence stratigraphic model in terms of sequence frequency, and is based on the concept defined in Figure 2.xvi of Chapter 2. Simplified logs illustrating typical sequences have been positioned to show their relationship to a relative sea-level curve. A blow-up of this curve is also displayed showing it to be made up of periods of parasequence progradation and parasequence drowning. The length of time of parasequence progradation and drowning is controlled by the position of the parasequence within a parasequence set, and the type of parasequence set (either aggradational, retrogradational or progradational).

Two periods of abrupt shallowing, relating to the formation of type-1 sequence boundaries, separate Sequences 1 and 2 and Sequences 3 and 4. The latter of these is in agreement with Hiscott *et al.* (1990a) who identify a major shallowing phase, succeeded by spit development across older highstand deposits. Sequence boundary numbers 2 and 4 are both interpreted as type-2 sequence boundaries, indicating no fall in relative sea-level.

Similar to the Corallian Group succession that was described and interpreted in Chapter 2, the Ericeira Group succession was also deposited during a global "green-house" period

(Veevers, 1990). The implications of this, are that relative sea-level falls at sequence boundaries are unlikely to be large and of a long duration. Consequently, any periods of sub-aerial exposure associated with type-1 sequence boundary formation would have been relatively short-lived (when compared to global "ice-house" periods).

Hiscott *et al.* (1990a) and Whiteman (1990) both suggest (or imply) that the lithostratigraphic boundary separating the São Lourenço Mudstone Member from the Safarujo Member relates to a period of erosion, succeeding a major progradational phase. As already stated, this differs from the interpretation offered in this thesis, which suggests that the succession from the São Lourenço Mudstone Member to Safarujo Member relates to continued shoreface progradation.

4.3.2: Comparison of the Corallian and Ericeira Groups

A comparison of the sequence stratigraphic frameworks of the two studied successions reveals a number of similarities and some differences.

Similarities:

- Both of the studied successions contain clear evidence for parasequence formation, although the identification of parasequences within late TST and early HST are problematic.
- Parasequence boundaries in both successions show clear evidence of shallowing

(associated with parasequence progradation) and subsequent drowning/non-deposition (associated with marine transgression and parasequence boundary formation). Within the Corallian Group, parasequence boundaries are collectively represented by abrupt changes in lithology, changes in bed thickness, increases in the intensity of bioturbation, small transgressive surfaces, formation of marine hard-grounds and a deepening of the depositional environment across the boundary. The Ericeira Group succession contains all of these features, as well as clear ravinement formation associated with periods of sub-marine transgressive erosion.

- Both successions contain evidence of fining-up parasequences (occurring in similar nearshore depositional environments) and coarsening-up parasequences often associated with shoreface/beach-strandplain progradation.
- Both successions contain examples of highstand, lowstand, transgressive and shelf-margin systems tract which relate to particular depositional environments.
- Both successions contain examples of major marine transgressive surfaces which clearly represent changes in the depositional environment (i.e. a change from shallow to deeper water environments across the transgressive surface).
- Both successions provide clear evidence of type-1 and type-2 sequence boundary development.
- Both successions show facies partitioning above type-1 sequence boundaries (e.g. Sequence 5 in the Corallian Group succession and Sequence 4 in the Ericeira Group succession).

Differences:

- The main difference between the two successions is that the Ericeira Group succession contains evidence of karstification and sub-aerial exposure indicating a potentially humid palaeoclimate. This feature is also reflected in the early diagenetic processes and products that are related to this surface (see Section 5.3.3). By comparison, little evidence of karstification occurs within the Corallian Group succession (even though it contains a number of sub-aerial erosion surfaces), which may indicate that the climate was less humid.

4.3.3: Concluding remarks

- The Ericeira Group succession of west central Portugal comprises a series of mixed clastic/carbonate nearshore depositional environments that are the result of high resolution changes in relative sea-level.
- The sequence stratigraphic model identifies high frequency sea-level changes by relating depositional environments to parasequence and systems tract development.
- Within this model, the Ericeira Group is interpreted to be composed of four sequences which are each composed of systems tracts and parasequences (where evidence of shallowing-up is available).
- Facies analysis identifies coarsening-up and fining-up parasequences within these sequences.
- Parasequence boundaries can be identified by abrupt changes in lithology, changes in

bed thickness, truncation or ravinement surface development, transgressive lag development and abrupt deepening of depositional environments.

- Sequences 1 and 3 (the Calada Member and middle to upper Safarujo Member to Cabo Raso Limestone Member, respectively) are both capped by type-1 sequence boundaries, suggesting an abrupt lowering of relative sea-level. The top of Sequence 3 also displays evidence of karstification, suggesting an element of sub-aerial exposure.
- Sequence 2 (the Calada Member to lower part of the Safarujo Member) is capped by a type-2 sequence boundary which has been positioned more-or-less at the change from a progradational parasequence set below to an aggradational parasequence set above.
- Major transgressive surfaces are well developed in all sequences and relate to an abrupt deepening of the depositional environment manifested as a change in the facies associations.
- Unpublished regional data are used to support this sequence stratigraphic model, although it is recognised that further regional and biostratigraphic data are required.

Facies analysis of the Ericeira Group of west central Portugal has resulted in the construction of a high resolution sequence stratigraphic model (using the approach established by Van Wagoner *et al.*, 1990). There is no doubt that this approach has been more successful on this succession, than the south Dorset Corallian Group succession. One of the main reasons for this, is parasequence and stratal surface identification are a lot clearer in the Ericeira Group succession, due to the probable unprotected nature of the shoreface sediments and, clearer water-depth indicators. Accepting the lack of regional and biostratigraphic control, this has led to the development of a plausible facies based high resolution sequence stratigraphic model on which an early diagenetic framework can

be based (Chapter 5).

The early diagenetic evidence presented in Chapter 5 will be used to lend further support for this model and, to aid in the identification of certain stratal surfaces and stratal packages, where facies evidence alone was not conclusive (i.e. parasequence identification within the Calada Member; positioning of a sequence boundary within or at the base of the Safarujo Member; identification of a sequence boundary at the base of the Dois Irmãos Member and positioning of a sequence boundary within the Dois Irmãos Member).

Fig. 4.i: (A): The location of Ericeira & the Ericeira sections of west central Portugal
(B): Palaeogeography for the Hauterivian

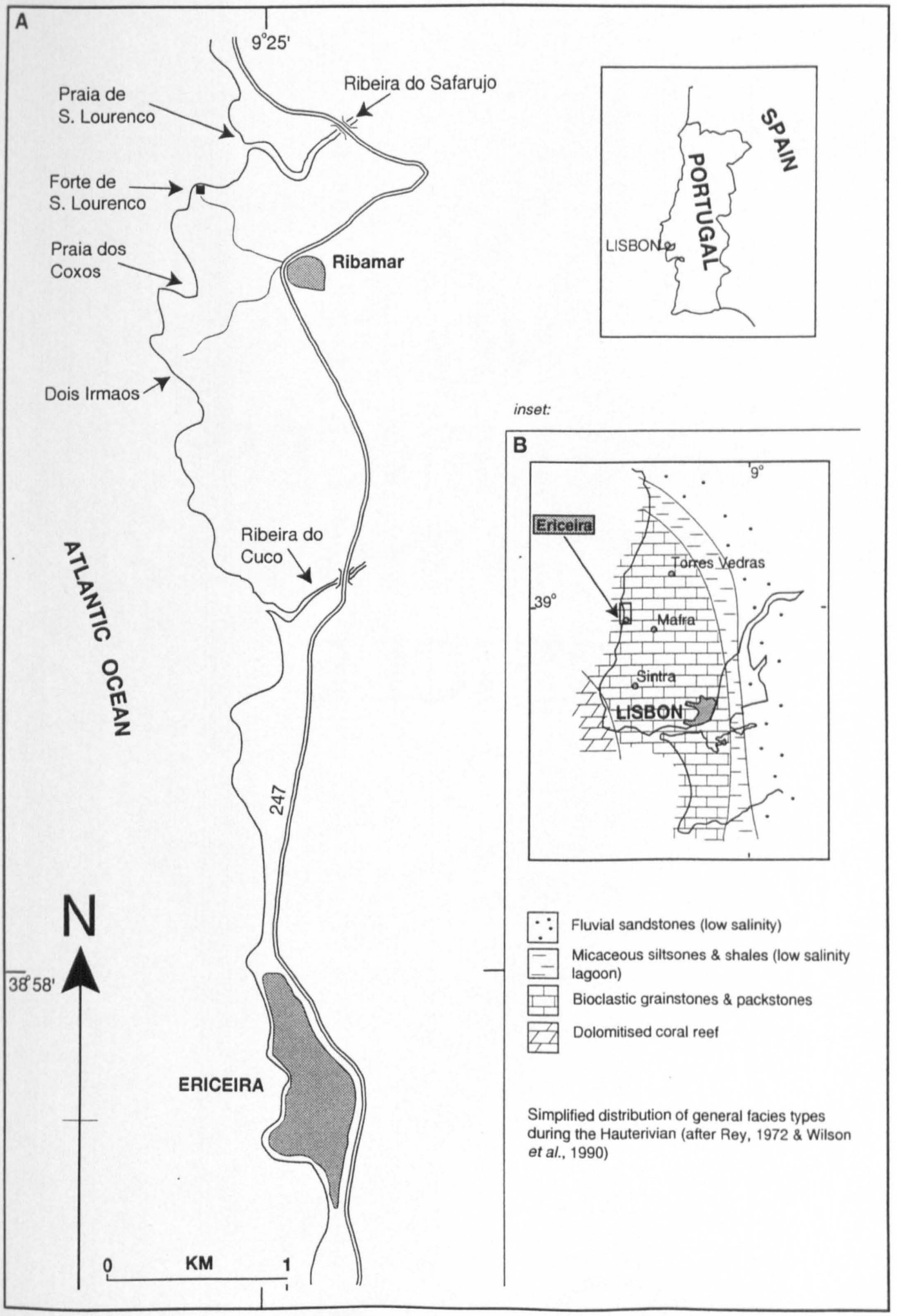

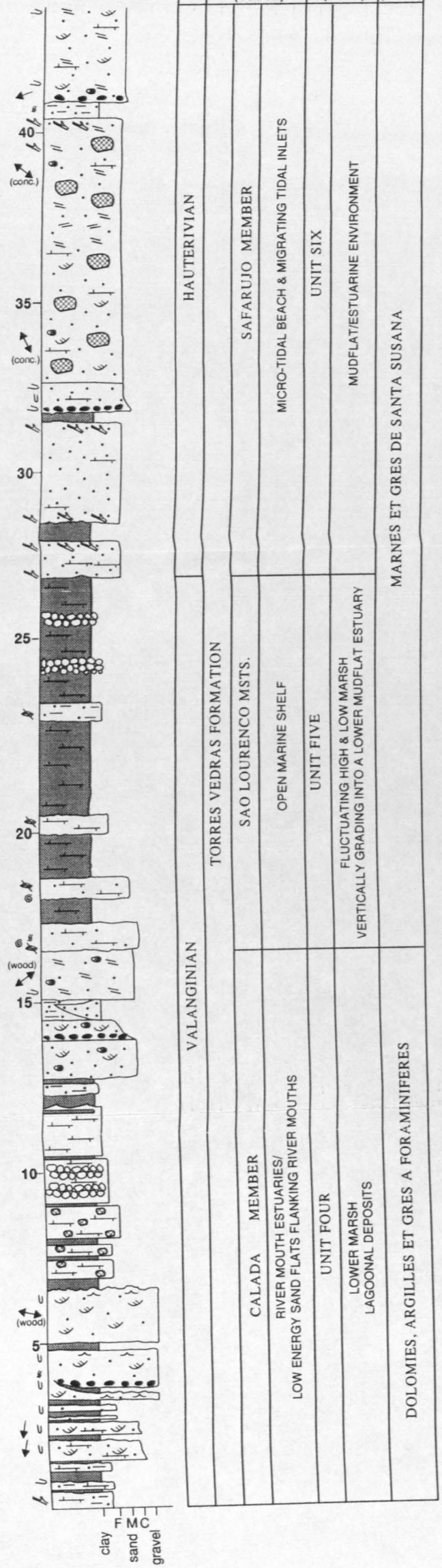

	Hiscott *et al.* (1990b)	Whiteman (1990)	Rey (1972)
HAUTERIVIAN			
TORRES VEDRAS FORMATION	SAFARUJO MEMBER	UNIT SIX	MARNES ET GRES DE SANTA SUSANA
	MICRO-TIDAL BEACH & MIGRATING TIDAL INLETS	MUDFLAT/ESTUARINE ENVIRONMENT	
VALANGINIAN			
TORRES VEDRAS FORMATION	SAO LOURENCO MSTS.	UNIT FIVE	
	OPEN MARINE SHELF	FLUCTUATING HIGH & LOW MARSH VERTICALLY GRADING INTO A LOWER MUDFLAT ESTUARY	
	CALADA MEMBER	UNIT FOUR	
	RIVER MOUTH ESTUARIES/ LOW ENERGY SAND FLATS FLANKING RIVER MOUTHS	LOWER MARSH LAGOONAL DEPOSITS	
			DOLOMIES, ARGILLES ET GRES A FORAMINIFERES

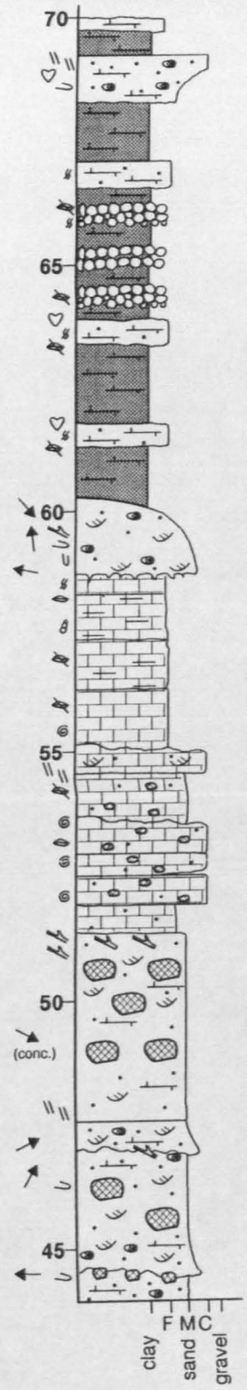

	Hiscott *et al.* (1990b)		Whiteman (1990)	Rey (1972)
HAUTERIVIAN				
TORRES VEDRAS FORMATION	DOS IRMAOS MEMBER	RIVER DOMINATED DELTAS MOUTH BARS & DISTRIBUTARY FILLS	UNIT EIGHT	GRES A TRIGONIES
	CABO RASO LIMESTONES	SPIT	UNIT SEVEN	CALCAIRES A RUDIST DE PRAIA DOS COXOS
	SAFARUJO MEMBER		UNIT SIX	MARNES ET GRES DE SANTA SUSANA
	MICRO-TIDAL BEACH & MIGRATING TIDAL INLETS			
	MUDFLAT/ESTUARINE ENVIRONMENT		SHALLOW MARINE UNTERTIDAL	?

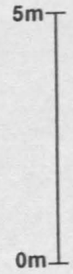

Fig. 4.ii: Previous lithostratigraphical & depositional interpretations of the lower to middle Ericeira Group of west central Portugal

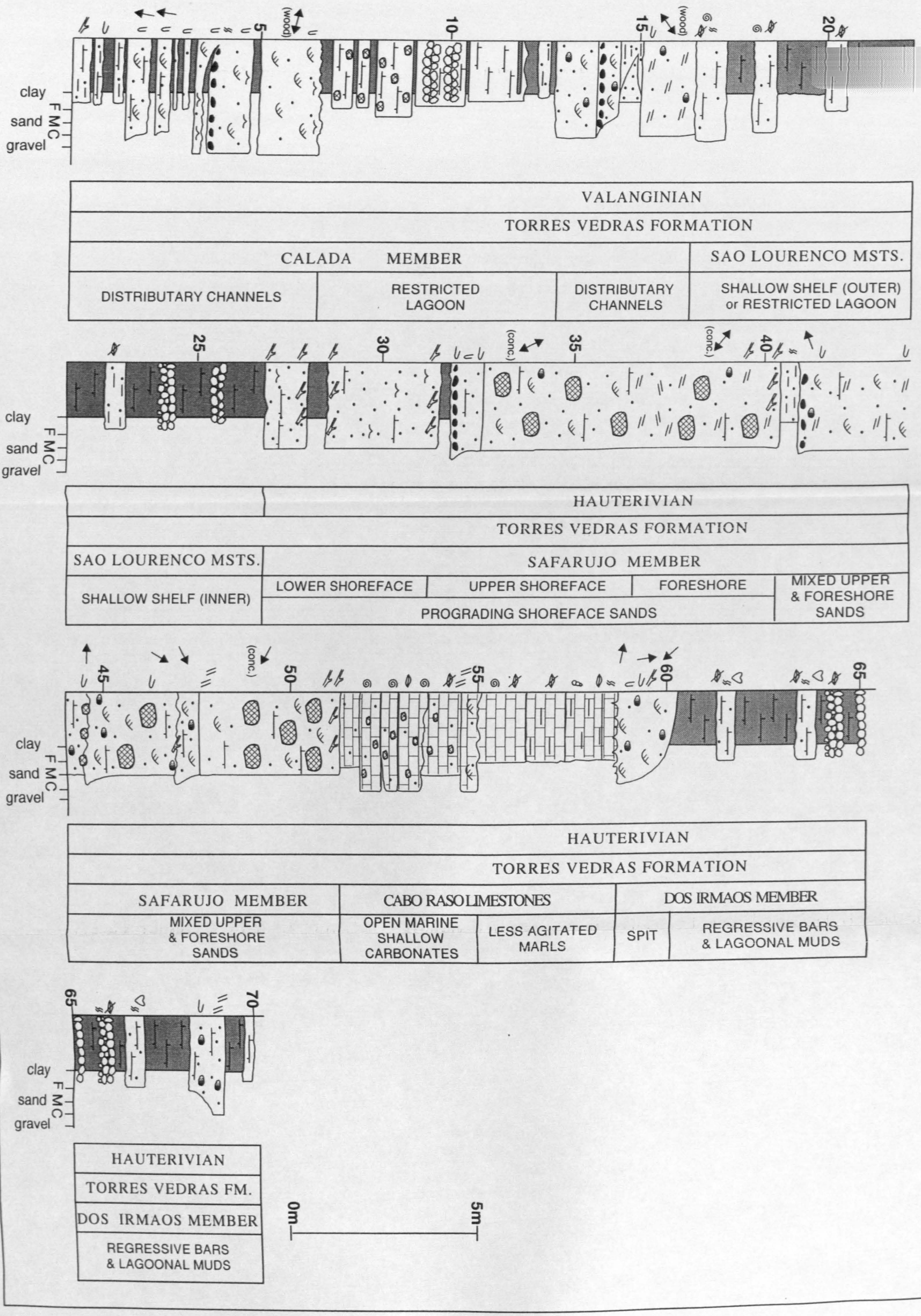

Fig. 4.iii: Sedimentary logs and suggested depositional environments of the lower to middle Ericeira Group of west central Portugal

Fig. 4.iv: Sedimentary logs and suggested sequence stratigraphy interpretation of the lower to middle Ericeira Group of west central Portugal

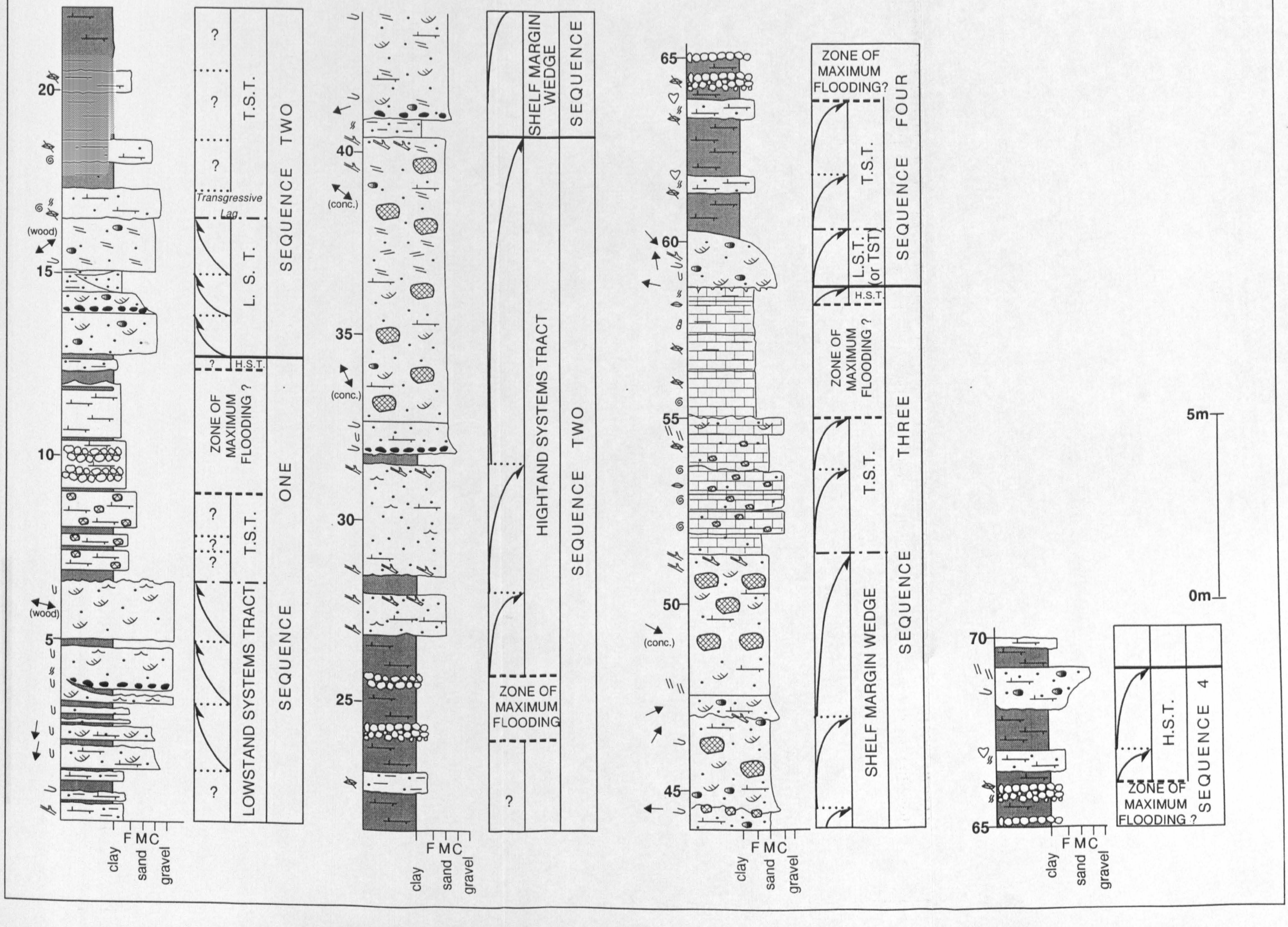

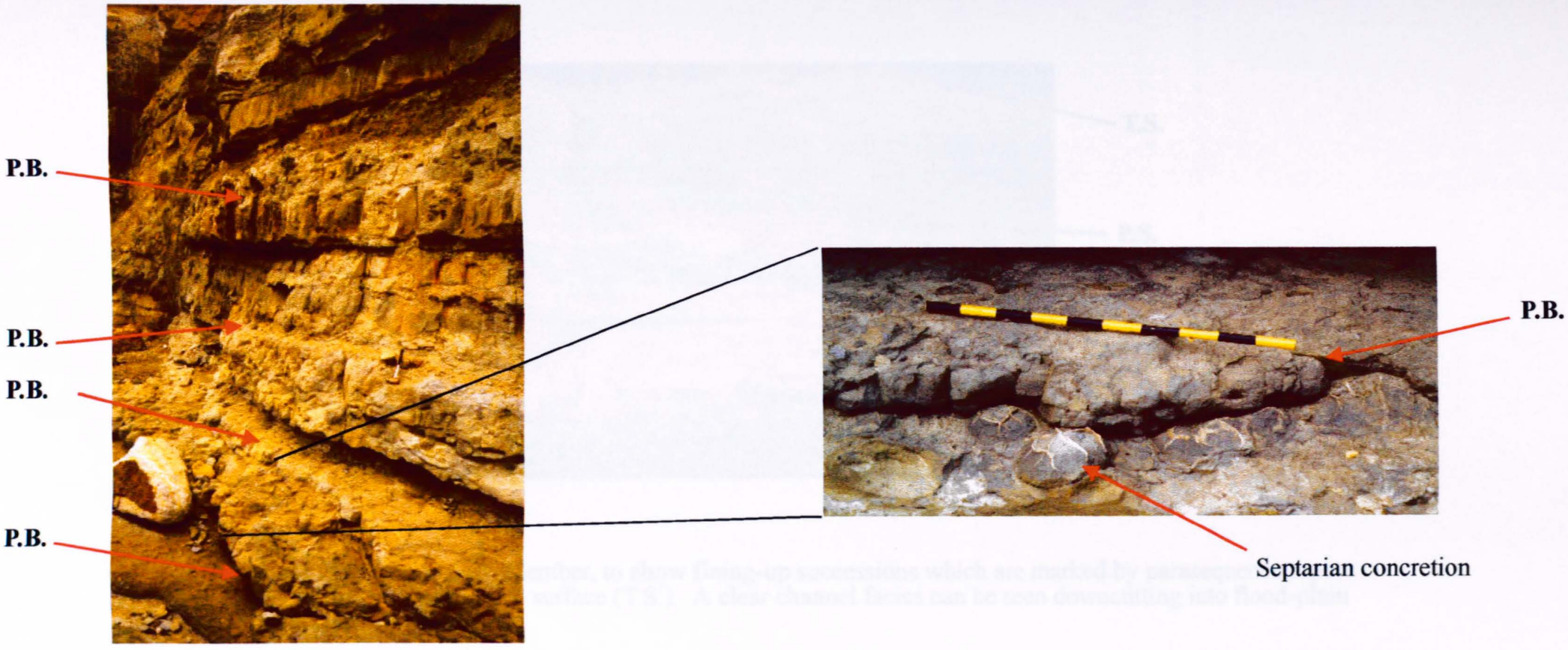

Fig.4.v. The restricted lagoonal deposits of the Calada Member. Red arrows point to the tops of coarsening-up successions which may represent parasequence boundaries (P.B.). Sequence stratigraphically, this unit represents the transgressive systems tract of Sequence 1. Hammer is 0.4m in length.

The photograph on the right is a blow-up of the top of a coarsening-up succession to show septarian concretionary growth. Scale bar on blow-up photograph is 1m.

Photograph taken at the cliff section to the north of Praia de S. Lourenco (see Fig.4.i for location).

Fig.4.vi. Upper beds of the Calada Member, to show fining-up successions which are marked by parasequence tops (P.S.) and/or a transgressive surface (T.S.). A clear channel facies can be seen downcutting into flood-plain or over-bank deposits.

Sequence stratigraphically, this succession represents the lowstand systems tract of Sequence 2.

For scale, hammer is 0.4m in length.

Photograph taken to the north of Praia de S. Lourenco (see Fig.4.i for location).

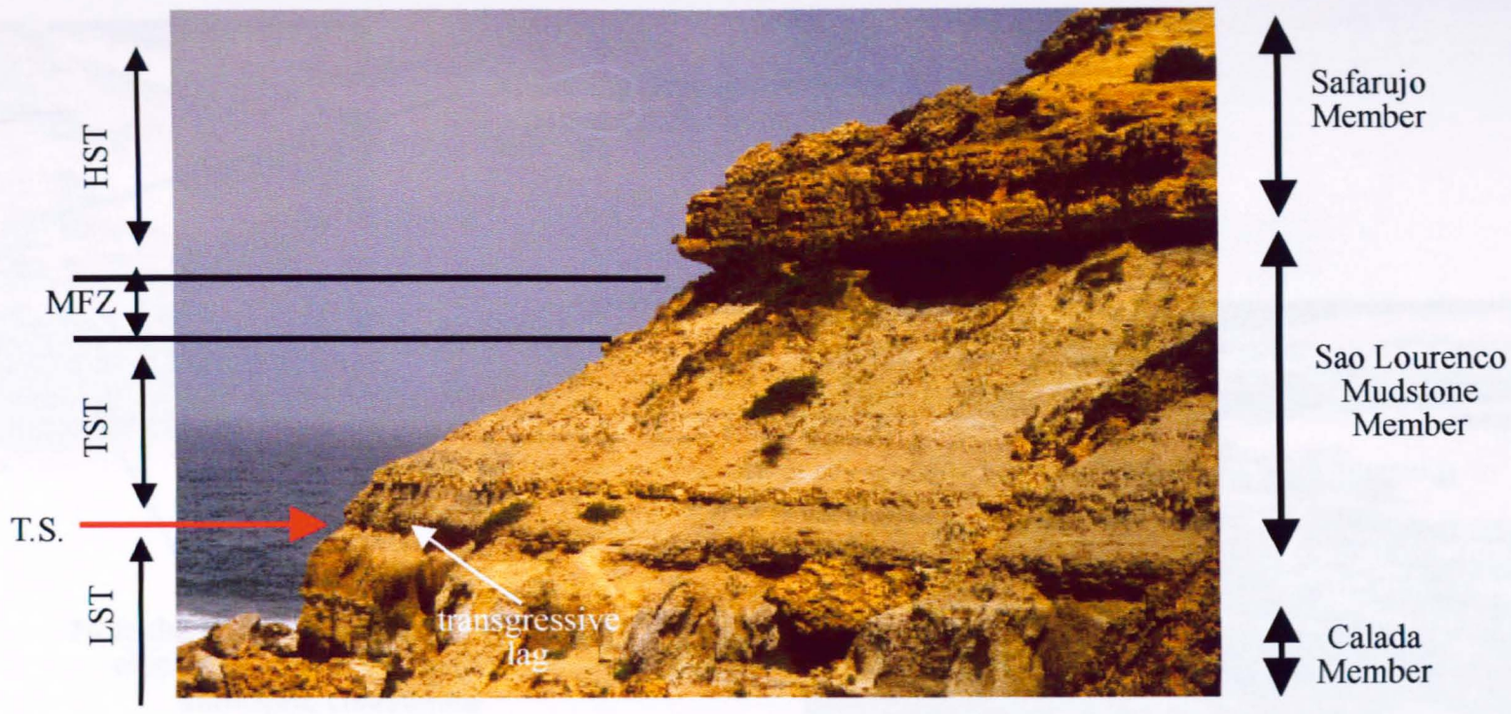

Fig.4.vii. Upper beds of the Calada Member, together with the overlying Sao Lourenco Mudstone Member and the lower Safarujo Member.

Sequence stratigraphically, the upper Calada Member represents the lowstand systems tract (LST) of Sequence 2 and is separated from the overlying transgressive systems tract (TST) by a transgressive surface (T.S. & red arrow). The unit that is interpreted to represent a thin transgressive lag has also been identified. Overlying this, the Sao Lourenco Mudstone Member represents a transgressive systems tract (TST) while the lower Safarujo Member represents the highstand systems tract (HST) of Sequence 2. Separating these is a zone of maximum flooding (MFZ) which represents the more open marine/inner shelfal depositional environment of the upper Sao Lourenco Mudstone Member.

Photograph was taken looking approximately north from Praia de S. Lourenco. Cliff section is approx. 20m in height. (See Fig.4.i for location).

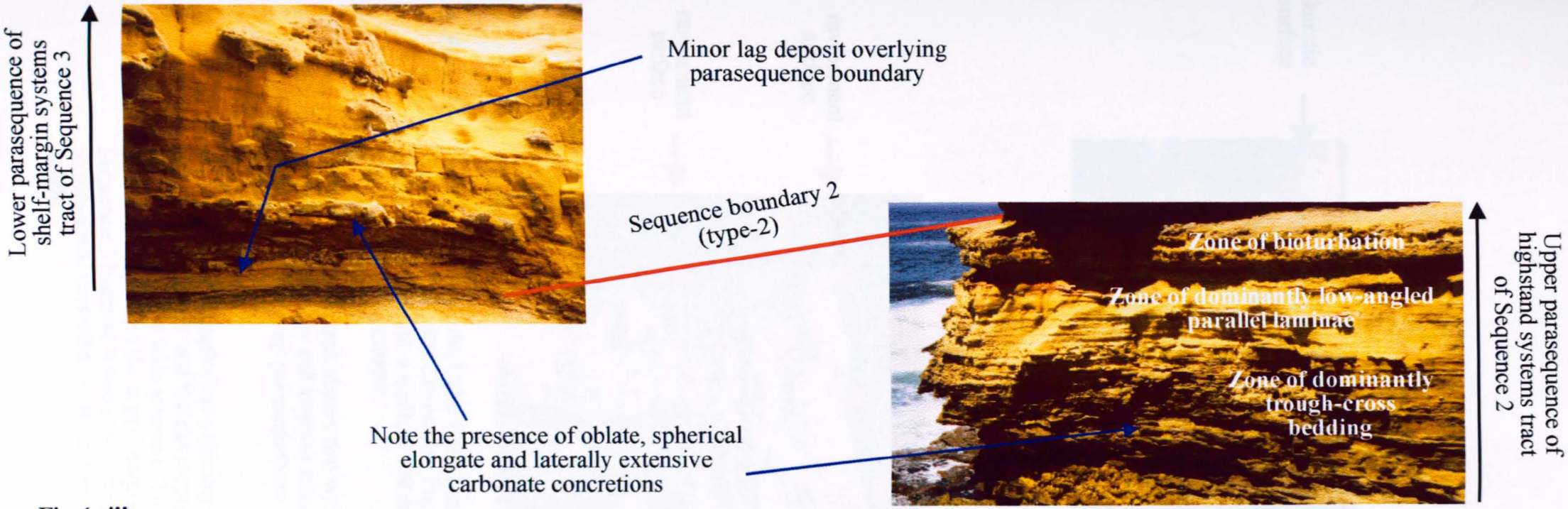

Fig.4.viii.

The Safarujo Member beneath the Forte de S. Lourenco (see Fig.4.i for location).

Right-hand photograph shows a 7.5m thick sandstone bed (equivalent to the third sandstone bed of the Safarujo Member. Note the abundance of carbonate concretions as pointed out by the blue arrow. This is separated from the overlying sandstone bed (enlarged photo on left hand-side) by a thin silty mudstone layer which has been labelled a thin transgressive lag. This sandstone bed also contains carbonate concretions. Both sandstone beds are inferred to represent prograding shoreface deposits, due to the vertical change in sedimentary structures, as shown by the white lettering on the right-hand photo.

Sequence stratigraphically, both sandstone beds represent coarsening-up (and shallowing-up) parasequences. The lower parasequence (right-hand photo) represents the top of the HST of Sequence 2, while the upper parasequence (left-hand photo) represents the lower unit of the overlying SMW of sequence 3. A sequence boundary has been positioned between these two parasequences (red line) coinciding with the formation of the parasequence boundary. As there is no evidence of sub-aerial erosion or a hiatus at this horizon, the sequence boundary is inferred to represent a type-2 sequence boundary. It has been positioned on the basis of a change in the style of parasequence stacking patterns.

For scale, the hammer in the left-hand photo (enlarged) is 0.4m in length, and the cliff section in the right-hand photo is approx. 8m in height.

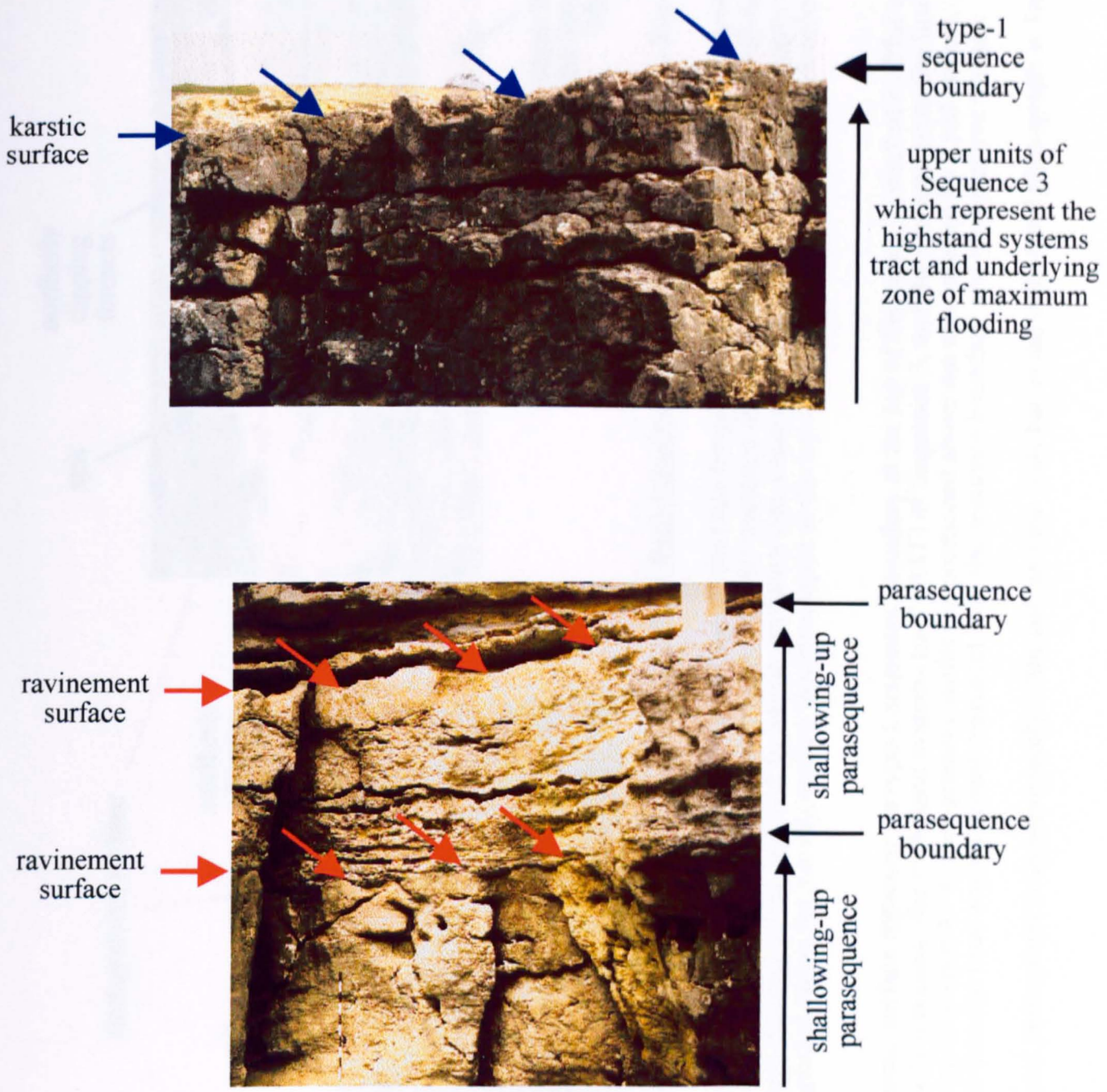

Fig.4.ix. The upper beds of the Cabo Raso Limestone Member to the south of Praia dos Coxos (see Fig.4.i for location). These beds represent a shallow marine carbonate depositional environment.

The lower photograph shows two well defined ravinement surfaces (marked by red arrows) which also mark the tops of two shallowing-up parasequences. Note metre stick for scale (lower left).

The upper photograph shows the top of the Cabo Raso Limestone Member and the development of a small karstic surface (marked by blue arrows). This surface is also inferred to represent the type-1 sequence boundary of Sequence 3 because it must represent a prolonged period of sub-aerial exposure. Cliff section is approx. 3m in height.

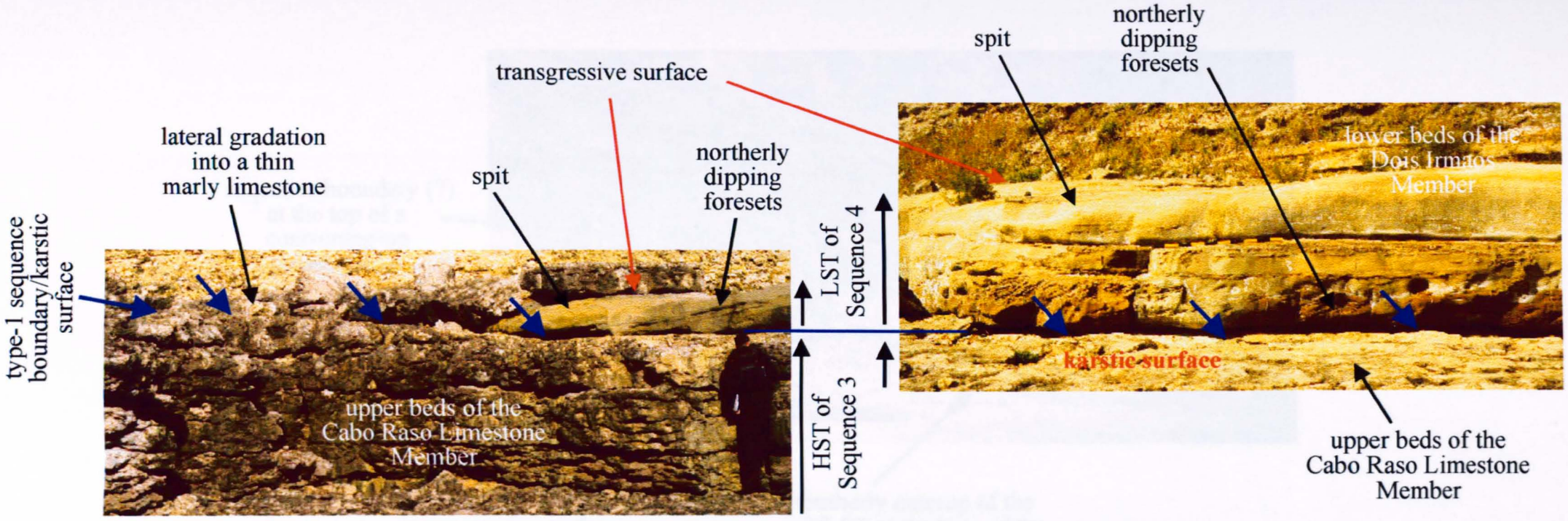

Fig.4.x. Two photographs to show the lower Dois Irmaos Member overlying the Cabo Raso Limestone Member at Dois Irmaos (see Fig.4.i for location)

Both photographs show the fine grained, well sorted sandstone at the base of the Dois Irmaos Member which is inferred to represent a laterally prograding spit. Large scale northerly dipping foresets suggest that the accretion direction was to the north. The left-hand photograph also shows the northerly thinning of the spit and its lateral gradation into a thin marly limestone. Both photographs also show clearly that the spit has prograded across the karstic surface that developed at the top of the Cabo Raso Limestone Member (marked by blue arrows).

Sequence stratigraphically, the karstic surface represents a type-1 sequence boundary at the top of Sequence 3 (marked by blue arrows and blue line). Thus the underlying beds represent the highstand systems tract (HST) of Sequence 3, and the spit represents the lowstand systems tract (LST) of the overlying Sequence 4. A transgressive surface is positioned above the spit (marked by a red arrow). Alternatively the spit could represent a TST and then the blue arrows would represent both the sequence boundary and transgressive surface.

For scale, the person in the left-hand photograph is approximately 1.8m tall, and the scale bar in the right-hand photograph is 1m in length.

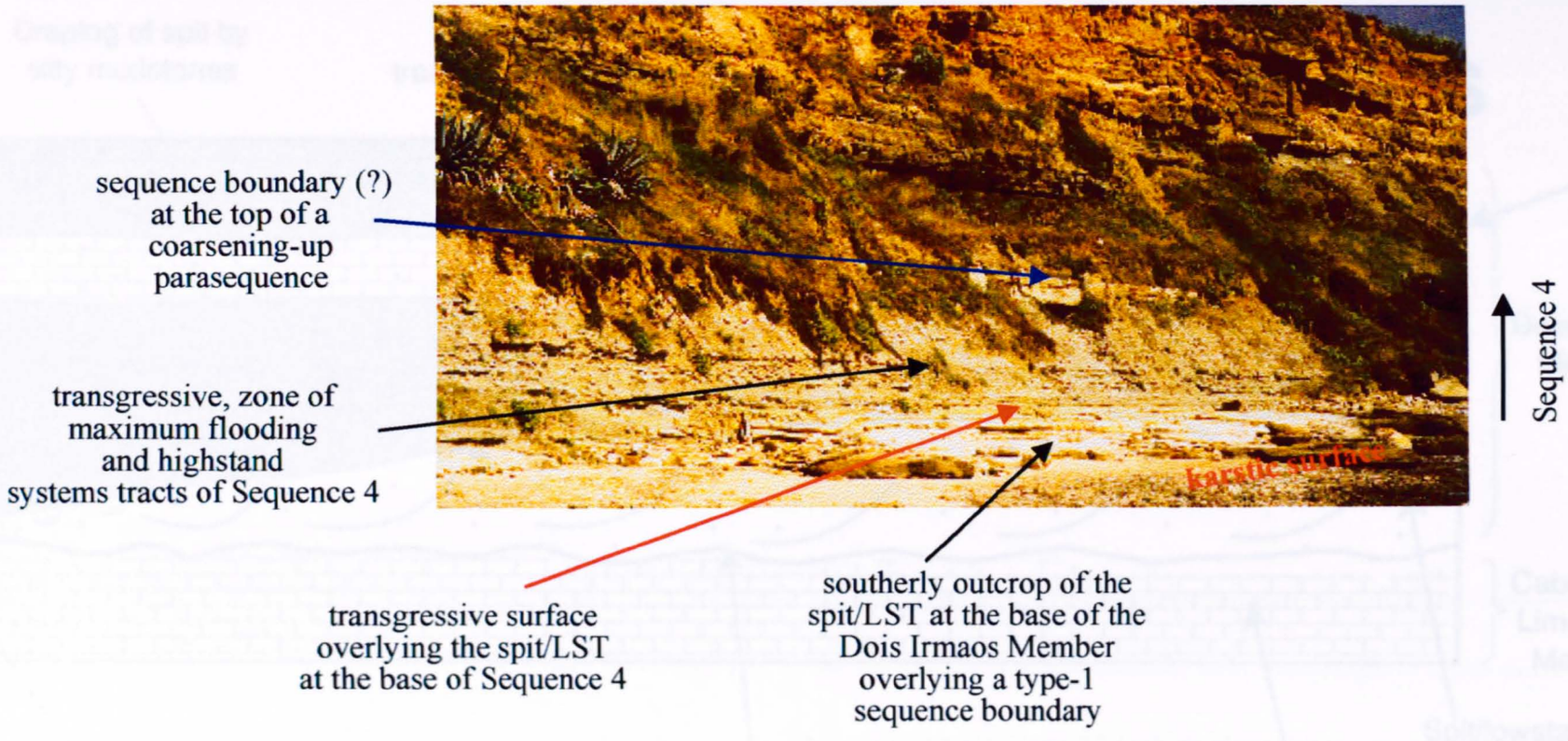

Fig.4.xi. Photograph of the Dois Irmaos Member at Dois Irmaos (see Fig.4.i for location) to show the characteristics of Sequence 4.

The photograph shows the southerly outcrop of the spit/LST of Sequence 4, which has prograded over the karstic surface which represents a type-1 sequence boundary. Above the spit/LST is a transgressive surface, which is overlain by the TST, zone of maximum flooding and HST deposits. The coarser grained beds that can be picked out in the photograph probably do represent parasequence tops (see text for an explanation of the evidence). A probable sequence boundary has been positioned at the top of an obvious coarsening-up parasequence (marked by a blue arrow). The strata above this bed were not studied within this thesis..

For scale, the cliff section is approximately 20m in height.

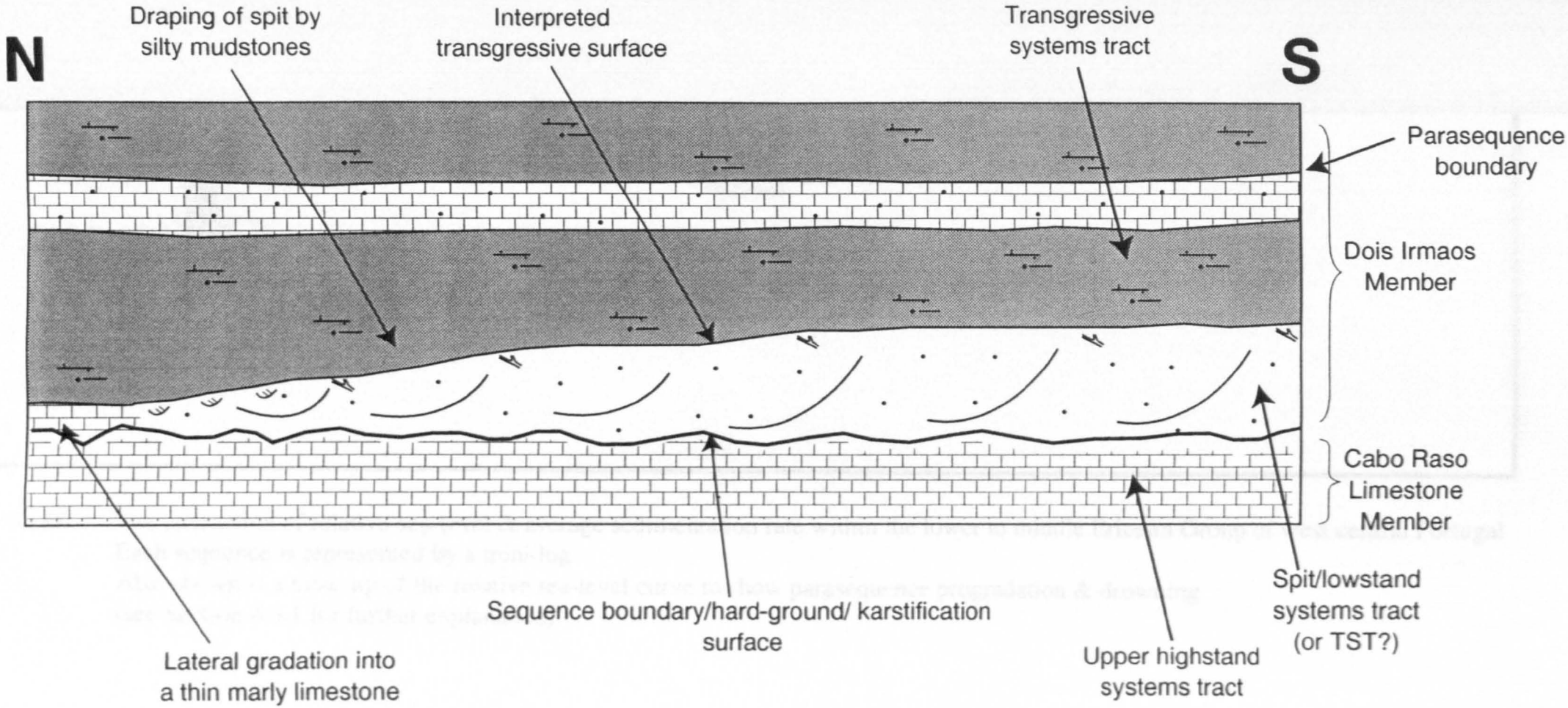

Fig.4.xii: Summary diagram to show the depositional and sequence stratigraphic characteristics of the upper Cabo Raso LimestonesMember and the lower Dois Irmaos Member. Note the northerly thinning and lateral gradation of the spit/LST (or TST?) into a thin marly limestone. (not to scale)

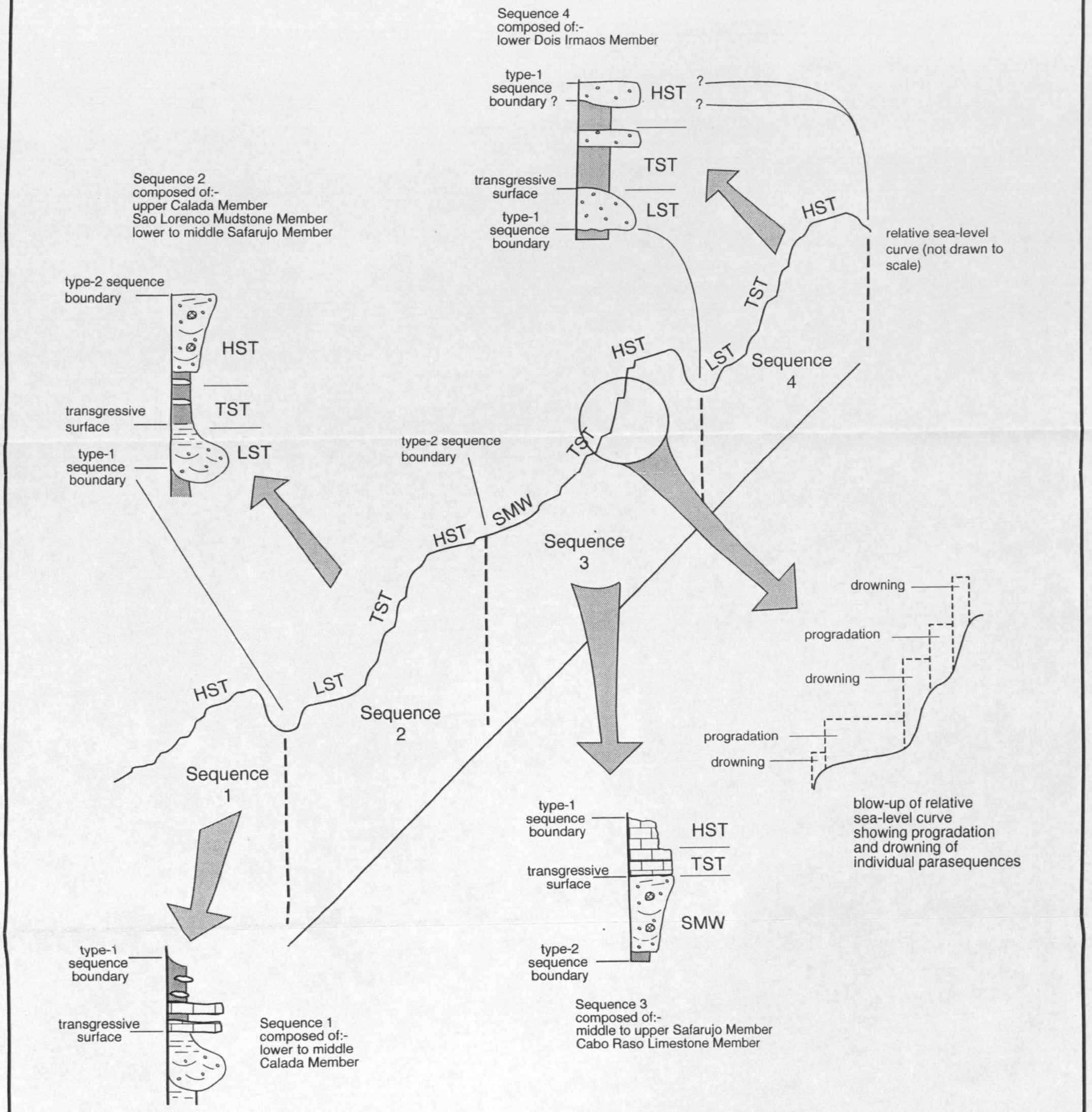

Fig. 4.xiii: The interaction of relative sea-level & average sedimentation rate within the lower to middle Ericeira Group of west central Portugal
Each sequence is represented by a mini-log
Also shown is a blow-up of the relative sea-level curve to show parasequence progradation & drowning
(see Section 4.3.1 for further explanation)

AGE	DESCRIPTION
Valanginian-Hauterivian	Fining upward transgression
latest Berriasian-Valanginian	Unconformity beneath sandstones
early Berriasian	Regressive sandstones and deltas
Tithonian	Transgressive-regressive cycles
Kimmeridgian	Backfills of palaeovalleys (?)
early Kimmeridgian	Deep basins with siliciclastic influx
early Oxfordian	Hiatus and restricted brackish or hypersaline basins

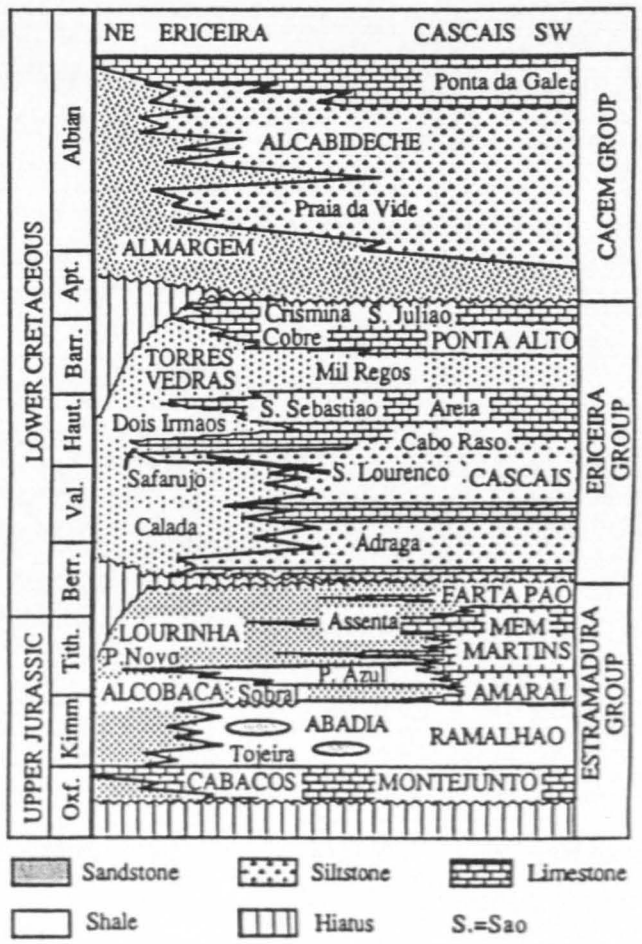

Table 4.i.: Tabular & stratigraphic summary of the main elements of the Lusitanian Basin of west central Portugal from upper Jurassic to lower Cretaceous (after Hiscott *et al.*, 1990a)

Sequence	Lithostratigraphic range	Sequence boundary			Systems tracts & stratal surfaces								
		Type	Evidence	Depth*	LST/SMW depth range (m)	Approx. lithostrat. equivalent	Transgressive surface depth (m)	Approx. lithostrat. equivalent	TST depth range (m)	Approx. lithostrat. equivalent	MFZ depth range (m)	Approx. lithostrat. equivalent	MFS present?
4	Dois Irmãos Member	type-1	abrupt shallowing above sequence boundary and development of karstic surface coincident with sequence boundary	59.2m	59.2m-60.3m	basal 2m of Dois Irmãos Member	60.3m	n/a	60.3m-763.9m	Dois Irmãos Member (?mid.)	763.9m-765.7m	Dois Irmãos Member (?mid.-?upper)	no
3	Upper Safaruja Member to Cabo Raso Limestone Member	type-2	distinct change in parasequence stacking patterns above and below sequence boundary - becoming aggradational above	40.45m	40.45m-51.4m	Upper Safaruja Member	51.4m	n/a	51.4m-755m	Upper Safaruja Member	755m-758.1m	Lower to Middle Cabo Raso Limestone Member	no
2	Calada Member (?upper) to Middle Safaruja Member	type-1	abrupt shallowing above sequence boundary	12.7m	12.7m-16.5m	Upper Calada Member	16.5m	Calada Member, São Lourenço Mudstone Member lithostratigraphic boundary	16.5m-724m	Lower São Lourenço Mudstone Member	724m-725.8m	Middle to Upper São Lourenço Mudstone Member	no
1	Calada Member (?lwr.-mid.)	no outcrop available	n/a	n/a	0m-6.5m	Calada Member (?lwr.)	6.5m	n/a	6.5m-78.9m	Calada Member (?mid)	78.9m-712.3m	Calada Member (?mid.)	no

* For simplicity, the starting depth (0m) for the whole succession is based on the lowest occurrence of the Calada Member, to the north of Praia de São Lourenço.

? Denotes where the actual depth of a stratal surface or the boundaries of a stratal unit are undefined.

TABLE *4.ii* Summary of sequence stratigraphic model for the Ericeira Group of west central Portugal (based on facies analysis) ***Page 1 of 2***

Sequence	Lithostratigraphic range			Parasequences			Comments
		HST depth range (m)	Approx. lithostrat. equivalent	Number identified	Types identified	Depth ranges	
4	Dois Irmãos Member	765.7m-770m	Dois Irmãos Member (?upper)	at least 5	all coarsening-up	59.2m-60.3m, 60.3m-61.8m, 61.8m-63.9m, 65.7m-67m, 67m-69.3m	the basal 2m of the Dois Irmãos Member could alternatively represent a TST, implying that the sequence boundary and t.s. have amalgamated
3	Upper Safarajo Member to Cabo Raso Limestone Member	758.1m-59.2m	Upper Cabo Raso Limestone Member	at least 6	all coarsening-up	40.45m-44.5m, 44.5m-47m, 47m-51.4m, 51.4m-53.7m, 53.7m-55m, 58.1m, 59.2m	HST is represented by very abrupt shallowing at the top of the Cabo Raso Limestone Member
2	Cabo Member (?upper) to Middle Safarajo Member	725.8m-40.45m	Lower to Middle Safarajo Member	at least 6	3 fining-up (LST), and 3 coarsening-up (HST)	12.7m-13.8m, 13.8m-15m, 15-16.5m, 25.8m-27.9m, 27.9m-31.9m, 31.9m-40.45m	5th. boundary between Safarajo & São Lourenço Mudstone Members may represent a relative fall in sea-level (Hiscott *et al.*, 1990b)
1	Cabo Member (?low.-mid.)	712.3m-12.7m	Cabo Member (?mid.)	at least 3	all fining-up (LST)	1.5m-3.3m, 3.3m-5m, 5m-6.5m	base of sequence no longer accessible in the position identified by Hiscott *et al.* (1990b)

TABLE *4.ii* Summary of sequence stratigraphic model for the Ericeira Group of west central Portugal (based on facies analysis) *Page 2 of 2*

5: Early Diagenesis & Its Relationship To Sequence Stratigraphy In The Lower To Middle Ericeira Group

5.1: *Introduction*

Aims & principles:

This chapter aims to evaluate the application of early diagenetic analyses in the construction of a high resolution sequence stratigraphic model for the Ericeira Group. Sample collection concentrated only around key stratal surfaces and within key lithological horizons (as stated in the Methodology, Section 1.3) along with a range of analytical techniques have been used to create a petrographic data-set. As with the Corallian Group succession, clay-rich facies (which constitute approximately 24% of the Ericeira Group section) have not been sampled.

Within this chapter, the early diagenesis of the Ericeira Group will be broadly discussed. This is followed by an interpretation of the relationship of early diagenetic fabrics in an attempt to resolve, or provide further evidence for the facies based sequence stratigraphic framework outlined in Chapter 4.

Early diagenetic processes are strongly influenced by the depositional environment (Berner, 1981; Curtis, 1987) the composition of depositional water relating to rises and

falls of relative sea-level and influxes of meteoric water (Tucker, 1993; Taylor *et al.*, 1994; McKay *et al.*, 1995), iron and organic content of the sediment (Curtis, 1987) and sedimentation rate (Curtis, 1987).

Previous work:

There are no published diagenetic studies of the lower Cretaceous Ericeira Group. Studies by both Rey (1972, 1979) and Hiscott *et al.* (1990a) make reference to some diagenetic features, but do not interpret them or relate them to high frequency fluctuating sea-levels.

Rey (1972, 1979) notes the presence of sparite, microsparite and dolomitic beds within the "marnes et grès de Santa Susana" which is equivalent to Hiscott *et al's* (1990b) São Lourenço Mudstone Member and Safarujo Member. Within the "Calcaires à Rudistes de Praia dos Coxos" (equivalent to the Cabo Raco Limestone Member) Rey (1972, 1979) mentions crystalline cements and nodules. Finally, within the "Grès à Trigonies" (equivalent to the Dois Irmãos Member) Rey (1972, 1979) notes the presence of cryptocrystalline cements and dolomitic beds.

Hiscott *et al.* (1990a) make reference to a "firm or diagenetically hardened carbonate surface or marine hard-ground" at the top of the Cabo Raco Limestone Member. Their interpretation suggests that it represents the top of a shallowing-up cycle, which was succeeded by the progradation of a spit.

Organisation:

The chapter begins with a detailed description of all early diagenetic products, which broadly fall into the categories, pyrite, dolomite, calcite, siderite and iron-oxide (haematite). Following this (in Section 5.3) early diagenetic products are interpreted and used to support (or refute) the facies based sequence stratigraphic model proposed in Chapter 4. In Section 5.3.5, I highlight the similarities and differences between the diagenesis of the Ericeira and Corallian Group successions.

5.1.1: Detrital mineralogy

5.1.1a: *Restricted lagoonal deposits & distributary channel sands*

Detrital mineralogy within the restricted lagoonal deposits and channel sands of the Calada Member is dominated by rare silt sized sub-rounded quartz and rare feldspar within a matrix of detrital clay, interbedded by angular to sub-angular fine to coarse quartz, feldspar and rock fragments within a detrital clay matrix. Bioclastic debris is rare to absent.

5.1.1b: *Prograding shoreface sands*

Detrital mineralogy within the coarser silty layers of the outer to inner shelfal deposits of the São Lourenço Mudstone Member includes rare sub-rounded quartz grains, bioclastic

fragments and detrital clays within a sparse matrix. The prograding shoreface sands of the Safarujo Member are dominated by sub-rounded quartz grains, rare feldspar (plagioclase, potassium feldspar and microcline), rock fragments and muscovite mica contained within a detrital matrix. Texturally, these sediments possess a narrow range of grain-sizes from fine to fine-medium. There is very little evidence of bioclastic debris left within these sediments. The majority of quartz grains show evidence of etching while the majority of feldspars have been partially dissolved, often along cleavage planes which are now infilled by an intraparticle pore filling cement.

5.1.1c: *Shallow shelfal carbonates*

The detrital mineralogy within the carbonate dominated Cabo Raso Limestone Member is dominated by bivalve, gastropod, echinoderm and other bioclastic shell debris which is either unaltered, neomorphosed or replaced. Peloids and intraclasts are also present. The carbonate beds deposited in deeper marine environments contain a micritic matrix. Well developed micrite envelopes around bioclastic allochems are a common feature within the carbonate beds.

5.1.1d: *Laterally accreting spit*

Detrital mineralogy within the spit of the Dois Irmãos Member is dominated by sub-angular to sub-rounded detrital quartz grains (including finely crystallised vein quartz) feldspars, rock fragments and broken muscovite mica flakes, contained within a detrital matrix.

5.2: *Early diagenetic results*

5.2.1: Procedure

A detailed outline of the procedure used in this study can be found in Section 3.2.1. and within Appendices 1 to 4. Detailed petrographic analysis was performed on 76 stained thin-sections sampled from cemented beds, non-cemented beds and concretionary bodies (Fig.5.i). The results are plotted in Figure 5.ii, and exact volumes can be found within tables of Appendix 1. Detailed cathodoluminescence (using equipment at Camborne School of Mines) was performed on seventeen polished thin-sections, the procedure of which has been outlined in Section 3.2.1 (Fig.5.i and Table 5.ii). Finally, nine samples of septarian concretion, elongated concretion and pore-filling cement from different sequences were selected for stable isotope analysis (Fig.5.i) the procedure of which has been discussed in Section 3.2.1. Table 5.i and Figure 5.iii plot the results of this analysis.

5.2.2: Authigenic Pyrite

Pyrite is most abundant (up to 30% of the total pore filling volume[1]) within the restricted lagoonal facies of the Calada Member (sample numbers P14-P17A, P26 and P28 on Fig.5.ii) and the inner shelfal facies of the São Lourenço Mudstone Member (sample

[1] see footnote 1 of Section 3.2.2 for definition

numbers P19-P21 and P31-P38 on Fig.5.ii) where it is commonly associated with both ferroan and non-ferroan dolomite (Fig.5.iv). In these samples, clusters of pore filling framboidal pyrite (average crystal size is between 0.01 and 0.05mm) are more common than pore filling euhedral pyrite (average crystal size approximately 0.03mm). Both forms of pyrite pre-date the dolomite which they are associated with.

Pore filling and euhedral pyrite is also present as traces (generally between 0% and 2% of total pore filling volume) within the remainder of the studied succession, although commonly within concretionary bodies (e.g. sample numbers P43B-P44A on Fig.5ii). It is also associated with small haematite concretions and hollow iron-oxide tubes (e.g. sample numbers P43B, P43A, P57 and P57A on Fig.5.ii).

5.2.3: Authigenic dolomite

Evidence of early authigenic dolomite is present throughout the whole succession. However, within the middle to upper units of the Safarujo Member upwards into the Dois Irmãos Member, all original early dolomite has been either replaced leaving behind only rhombic iron-oxide "ghost" structures within one or more calcite crystals, or dedolomitised leaving behind isolated or large volumes of rhombic calcite crystals. Both types of replaced dolomite will be described in Section 5.2.4.

Within the remainder of the succession, the abundance, habit, texture and composition of individual dolomite varies considerably. Four distinct groups can be recognised:-

- non-ferroan dolomite in septarian concretions present within the restricted brackish lagoonal facies of the Calada Member (between 7m-10.4m on Fig.5.i & Fig.5.ii);
- ferroan dolomite present within the restricted brackish lagoonal, channel sands and inner shallow shelfal facies of the Calada Member and São Lourenço Mudstone Member (between 0m-6.9m & 16.5m-27.4m on Fig.5.i & Fig.5.ii);
- zoned non-ferroan dolomite within prograding shoreface sands of the lower units of the Safarujo Member (between 26.5m-32.6m on Fig.5.i & Fig.5.ii), and;
- zoned non-ferroan dolomite in elongate/oblate concretions present within prograding shoreface sands of the Safarujo Member (between 27.9m-40.4m on Fig.5.i & Fig.5.ii).

All phases are common except for the non-concretionary zoned dolomite. Each group is described separately below, with isotopic and CL analyses where recorded.

5.2.3a: Non-ferroan dolomite in septarian concretions

Occurrence:

Small (up to 0.2m diameter) oblate to ellipsoidal septarian concretions (Fig.5.v) are only present within the coarser grained siltstone beds of the Calada Member (between 7m-9m on Fig.5.i & Fig.5.ii). Detailed analysis was performed on two such concretions (at 7.1m & 8.9m on Fig.5.vi) which were found to be composed of pervasive, isolated, non-ferroan dolomite rhombs (up to 70% total pore filling volume) with crystal sizes generally between 0.1 and 0.3mm (Fig.5.vii). The presence of septarian cracks suggests a very early diagenetic origin for these concretions (Raiswell, 1971; Astin, 1986; Scotchman, 1991 and

McKay *et al.*, 1995).

Petrographical description:

Individual dolomite crystals are generally inclusion free. Rarely they show petrographic evidence of etched outer surfaces. When pervasive, these cements form idiotopic and xenotopic mosaics (*sensu* Friedman, 1964) and are strongly associated with microporosity within detrital clays. By comparison, isolated non-ferroan dolomite (e.g. sample P19 at 9.5m on Fig.5.ii) is associated with micrite, shows good textural preservation and is often smaller, with average crystal sizes of 0.05mm.

Stable isotope analysis:

Stable oxygen and carbon isotope values extracted from the non-ferroan dolomite of two septarian concretions revealed depleted $\delta^{18}O$ values of approximately -4.18 ‰ PDB and slightly negative $\delta^{13}C$ values of -1.3 ‰ PDB (Table 5.i & Figs.5.iii & vi).

The septarian cracks that fracture these concretions contain a ferroan drusy calcite cement that has a more depleted $\delta^{18}O$ value of -6.74 ‰ PDB and a more negative $\delta^{13}C$ value of -3.09 ‰ PDB than the concretionary non-ferroan dolomite (Table 5.i, Figs.5.iii & vi).

Cathodoluminescence analysis:

Cathodoluminescence analysis of sample numbers P14 and P17 reveals an abundant dull to occasionally non-luminescent response for all non-ferroan dolomite within these concretions. In comparison, the ferroan drusy calcite of the septarian fractures has a dull to bright luminescence and is well zoned.

5.2.3b: Ferroan dolomite

Occurrence:

Pore filling and pervasive ferroan dolomite rhombs (up to 70% total pore filling volume) are present within the Calada Member (between 0m-6.9m on Fig.5.ii), the São Lourenço Mudstone Member and the lower part of the Safarujo Member (between 16.5m-27.4m on Fig.5.ii). They commonly have crystal sizes of between 0.1-0.3mm, and are associated with framboidal and euhedral pyrite (Fig.5.iv).

Petrographical description:

Individual ferroan dolomite rhombs are generally inclusion free, although occasionally contain a thin iron-oxide outer rim (possibly a result of recent surface oxidation) and some signs of etched outer surfaces. Pervasive ferroan dolomite cements form idiotopic and xenotopic mosaics (*sensu* Friedman, 1964) and are strongly associated with micro-porosity within detrital clays (Fig.5.iv).

Stable isotope analysis:

Stable oxygen and carbon isotope values for the ferroan dolomite cements from sample number P21 of the Calada Member, reveal slightly depleted $\delta^{18}O$ values of -3.78‰ PDB compared to normal Cretaceous sea-water (between -2.0 - 0 ‰ PDB Veizer *et al.*, 1980) and slightly negative $\delta^{13}C$ values of -0.63 ‰ PDB (Table 5.i & Figs.5.iii & vi).

Cathodoluminescence analysis:

Cathodoluminescence analysis of ferroan dolomite cement from sample numbers P1 and P3 are non-luminescent.

5.2.3c: Zoned ferroan to mildly ferroan dolomite

Occurrence:

Pore filling and zoned ferroan to mildly ferroan (based on qualitative artificial staining response) dolomite rhombs (up to 65% of the total pore filling volume) are present within the lower units of the Safarujo Member (between 26m-32.5m on Fig.5.ii).

Petrographic description:

Individual crystal sizes do not exceed more than 0.1mm and commonly have highly etched crystal faces. Zoning typically consists of either an iron-oxide rich centre with three outer

zones, one of which is iron-oxide rich; or a clear centre and three outer zones, two of which are iron-oxide rich (Fig.5.viii). Both forms of zoned dolomite commonly occur in association with one another as well as with non-ferroan sparry or poikilotopic calcite which they pre-date.

Stable isotope analysis:

Stable isotope values reveal slightly less depleted $\delta^{18}O$ values of -3.59 ‰ PDB than the results obtained from the non-zoned dolomites, and similar negative $\delta^{13}C$ values of -0.95 ‰ PDB (Table 5.i & Fig.5.iii).

Cathodoluminescence analysis:

Cathodoluminescence analysis of sample numbers P35 and P38H reveals zoned, non-luminescent to brightly luminescent dolomite (Fig.5.ix). Luminescence is controlled by the presence of iron-oxide rich centres and/or zones within individual dolomite crystals

5.2.3d: Zoned ferroan to mildly ferroan concretionary dolomite

Occurrence:

Pore filling and zoned ferroan to mildly ferroan dolomite rhombs (up to 30% of the total pore filling volume) are present within oblate, spherical, elongated and burrow concretions of the prograding shoreface sands of the lower units of the Safarujo Member (at 33.3m,

36.4m and 39.8m on Fig.5.ii).

Petrographic description & stable isotope analysis:

This dolomite is petrographically identical to that described in Section 5.2.3c. However, stable isotope values extracted from zoned ferroan dolomites within elongated concretions (sample number P38G) reveal slightly more depleted $\delta^{18}O$ values (-3.90‰ PDB), when compared to similar zoned dolomites of the cemented beds, and similar $\delta^{13}C$ values (-0.71‰ PDB) (Table 5.i & Fig.5.iii).

Cathodoluminescence analysis:

Cathodoluminescence analysis of ferroan to mildly ferroan zoned dolomite cement from sample number P38G reveals a non-luminescent to dull luminescent response. Very rarely, isolated zoned dolomite crystals reveal brightly luminescent centres.

5.2.4: Authigenic calcite

Evidence of early authigenic calcite is present within the majority of the succession. However the abundance, habit, texture and composition of individual calcite types varies considerably. Five general groups can be recognised:-

- non-ferroan pore filling sparry calcite within prograding shoreface sands (rare) and

concretionary burrows (common) of the lower units of the Safarujo Member (between 27.7m-34m on Fig.5.i & Fig.5.ii);

- non-ferroan poikilotopic (concretionary and pore-filling) calcite within prograding shoreface sands of the lower units of the Safarujo Member (between 25.7m-40.3m on Fig.5.i & Fig.5.ii);
- non-ferroan calcite (sparry and poikilotopic) replacing originally zoned dolomite within the Safarujo Member (between 41m-51.3m on Fig.5.i & Fig.5.ii);
- non-ferroan to ferroan pore filling calcite within shallow marine carbonates of the Cabo Raso Limestone Member (between 51.3m-58.6m on Fig.5.i & Fig.5.ii); and
- dedolomite (rhombic calcite), within the Cabo Raso Limestone Member and Dois Irmãos Member (between 55m-58.6m and 63.6m-69.9m respectively, on Fig.5.i & Fig.5.ii).

Each group is discussed separately in terms of petrographic, isotopic and CL characteristics.

5.2.4a: Non ferroan sparry calcite

Occurrence & petrographic description:

Pore filling non-ferroan sparry calcite (up to 30% total pore filling volume) is present within the lower beds of the Safarujo Member (between 25.5m-34m on Fig.5.ii). Individual calcite crystal sizes are commonly between 0.1 and 0.2mm and are always associated with, but do not replace, zoned non-ferroan dolomite (Fig.5.viii). Where they occur together, this group of calcite is observed to pre-date the growth of zoned non-

ferroan dolomite.

Cathodoluminescence analysis:

Cathodoluminescence analysis of sample number P35 and P38G, reveals a dominantly non-luminescent response for the non-ferroan sparry calcite (Fig.5.ix).

5.2.4b: Non-ferroan poikilotopic concretionary calcite

Occurrence & petrographic distribution:

Common, large (average crystal size is 0.3-0.5mm) non-ferroan poikilotopic concretionary calcite crystals (up to 70% of total pore filling volume) are present within large (average 0.5-1m diameter) spherical, oblate and elongated (greater than 4m long axis) concretions and host sands of the lower units of the Safarujo Member (between 32.6m-40.2m on Fig.5.ii & refer back to Chapter 4, Fig.4.viii for field view).

5.2.4c: Replacive non-ferroan calcite

Occurrence & petrographic description:

Poikilotopic and sparry calcite (up to 100% total pore filling volume), is similar in character to those described in Sections 5.2.4a and 5.2.4b. Both replace earlier zoned dolomite, commonly within elongated and oblate concretions (Fig.5.x) and less commonly

within host sediments of the middle to upper units of the Safarujo Member (between 40.4m-52.5m on Fig.5.ii). Characteristic iron-oxide ghost structures can be clearly seen within large non-ferroan poikilotopic calcite crystals and across sparry and poikilotopic crystal boundaries. This is clear evidence that the calcite replaced early zoned dolomite crystals (Fig.5.xi).

Stable isotope analysis:

Stable oxygen and carbon isotope results extracted from replacive non-ferroan poikilotopic calcite of an elongated concretion of the Safarujo Member (sample number P43E on Fig.5.ii) reveal depleted $\delta^{18}O$ values of -3.32 ‰ PDB and negative $\delta^{13}C$ values of -8.37‰ PDB (sample number P43E on Table 5.i & Fig.5.iii). This is insufficient for accurate palaeotemperature determination, but may be used to provide a working estimate. Using Shackleton & Kennett's (1975) palaeotemperature equation (equation 1 as defined in Section 3.2.5) a palaeotemperature at the time of calcite crystallisation of between 27°C and 32°C is estimated.

Stable oxygen and carbon isotope analyses were also performed on replacive non-ferroan poikilotopic calcite cements within the host sands of the Safarujo Member (e.g. sample number P44 on Fig.5.ii). Results of these analyses reveal almost normal marine $\delta^{18}O$ values of -2.84 ‰ PDB (when compared to normal Cretaceous sea-water of between -2.0 - 0 ‰ PDB, Veizer *et al.*, 1980) and strongly negative $\delta^{13}C$ values of -8.74 ‰ PDB (sample number P44 on Table 5.i & Fig.5.iii). Again, using the palaeotemperature equation of Shackleton & Kennett (1975) a working palaeotemperature estimate of ~26°C (range

between 20.64 and 35°C) is obtained, which is similar to that obtained from the concretionary calcite.

Cathodoluminescence analysis:

Cathodoluminescence analysis of sample numbers P45C and P45D (both from elongate concretions) reveal a strongly zoned dull to brightly luminescent response (Fig.5.xii). Zoning can be seen to pass through relic dolomite structures where it changes to a dull response. There is characteristically no luminescence associated with relic dolomite structures.

5.2.4d: Non-ferroan to ferroan pore filling calcite (within carbonate sand bodies)

Occurrence:

Non-ferroan fringing prismatic calcite, non-ferroan calcite overgrowths and equant non-ferroan to ferroan sparry calcite (up to 90% of total pore filling volume) are present within the Cabo Raso Limestone Member.

Petrographic description:

Non-ferroan fringing prismatic calcite is particularly well developed in samples P50 to P53 on Figure 5.ii. Crystals are approximately 0.01mm in length and up to 0.04mm in width and can be described as acicular (Fig.5.xiiia). Non-ferroan pore filling equant

sparry calcite, calcite overgrowths and microspar (Fig.5.xiiib-c) are common within sample numbers P48 to P56 on Figure 5.ii. Ferroan sparry calcite becomes more common upwards, especially within samples P52 to P53 (Fig.5.xiiid). Sparry calcite always post-dates the fringing prismatic calcite when they occur together (Fig.5.xiii). When the fringing calcite is absent then equant sparry calcite is seen to grow directly from grain boundaries (Fig.5.xiii).

Non-ferroan sparry calcite is also found within very small (5-10mm in size.) concretions that occur within the lower beds of the Cabo Raso Limestone Member (between 52m-54.5m on Fig.5.ii). The majority of these small concretions are composed entirely of non-ferroan sparry calcite, however some have a prismatic outer rim. Locally, concretions have amalgamated to form small scale laterally continuous cemented horizons.

Stable isotope analysis:

Carbon and oxygen stable isotope values were obtained from non-ferroan pore filling sparry calcite cements of sample number P52C (Table 5.i & Fig.5.iii). Strongly depleted $\delta^{18}O$ values of -5.35‰ PDB are recorded, along with slightly negative $\delta^{13}C$ values (-2.95‰ PDB).

Cathodoluminescence analysis:

Cathodoluminescence analysis performed on sample numbers P52A, C, B and P53 on Figure 5.ii reveal a variable non-luminescence to dull luminescence with rare zoning, for

the fringing and equant pore-filling calcite (Fig.5.xiv). Also evident on Figure 5.xiv is a patchy bright to moderate luminescence, which is infilling pore-spaces. This is clearly a different phase of cementation, which is not identifiable using standard petrographic techniques. Within sample number P53 pore filling ferroan equant calcite is generally dull to non-luminescent.

5.2.4e: Dedolomite (rhombic calcite)

Occurrence:

Non-ferroan, often zoned rhombic calcite crystals (up to 0.2mm in size) occur within the Cabo Raso Limestone Member (between 55m-58.7m on Fig.5.ii) and within the fine to coarse grained sandstone beds of the Dois Irmãos Member (at 63.8m, 69m and 69.9m on Fig.5.ii).

Petrographic description:

This form of calcite is described as dedolomite because within the samples where it is abundant (sample numbers P61, P65 and P67 on Fig.5.ii) it has either replaced earlier dolomite, or has crystallised within rhombic pore spaces (Fig.5.xv). Its abundance ranges from less than 1% within the Cabo Raso Limestone Member to greater than 95% within the fine to coarse sandstone beds of the Dois Irmãos Member (Fig.5.ii).

Cathodoluminescence analysis:

Cathodoluminescence analysis performed on pore filling dedolomite and rhombic calcite of sample numbers P63 and P65 reveals a generally dull to bright luminescence with good zoning (Fig.5.xvi). In sample number P63, rhombic calcite crystals generally have moderate to dull luminescent and bright luminescent outer zones.

5.2.5: Authigenic siderite

Occurrence:

Authigenic siderite is present (up to 20% but generally <5% of the total pore filling volume) within the Safarujo Member and the Dois Irmãos Member (between 25.5m-70m on Fig.5.ii). It is completely absent from the Calada Member and the São Lourenço Mudstone Member.

Petrographic description:

Within all samples, siderite occurs as isolated rhombs (average crystal size, 0.01mm) and is commonly associated with non-ferroan poikilotopic calcite, non-ferroan to ferroan sparry calcite and iron-oxide. Siderite stains a brown to red colour, has a high birefringence and is rhombic in cross-section.

5.2.6: Authigenic iron oxide

Occurrence & petrographic description:

Minor iron-oxide (haematite) occurs as small (up to 50mm) oblate concretions, burrow in fills, iron rich laminae and hollow tubes. These features are only commonly seen within the Calada Member, the Safarujo Member and within the coarser grained beds of the Dois Irmãos Member. Within some concretions, haematite is associated with pyrite, but is the dominant cement type (over 50% total pore filling volume). Within certain laminae of host sediments, haematite is rare (accounting for up to 10% total pore filling volume). In thin-section, haematite is pervasive, and generally opaque, but occasionally a blood red colour.

5.2.7: Summary of the distribution of early diagenetic products within the Ericeira Group

Figure 5.ii and Table 5.iii summarise the distribution of the early diagenetic products and processes within each lithostratigraphic unit of the Ericeira Group succession. Early diagenetic products are broadly contained within concretions and cemented beds.

5.2.7a: *Concretions*

Septarian concretions of the Calada Member are contained within very fine grained sandy/silty beds. They are composed of non-ferroan dolomite. The interpretation of these concretions is discussed in Section 5.3.1. In contrast, large oblate, spherical and elongate concretions dominate the stacked, coarsening-up shoreface sands that comprise the Safarujo Member. Within the lower part of the Safarujo Member (between 26.5m and 40m on Fig.5.ii) these concretions are composed of zoned ferroan to non-ferroan dolomite and non-ferroan calcite, while above this, in the middle to upper part of the Safarujo Member (between 40m and 51.5m on Fig.5.ii) they are composed dominantly of non-ferroan calcite. Relic dolomite rhombs can be seen within these calcite crystals. Thus there is a significant difference in the early diagenetic history of the lower and middle to upper Safarujo Member, which is discussed in Section 5.3.2 and 5.3.3.

Other small iron-oxide concretions and minor concretionary burrows are found to occur above and below well developed ravinement surfaces particularly within the Safarujo Member.

5.2.7b: *Cemented beds*

Cemented beds are common within the Calada Member, the São Lourenço Mudstone Member, the Cabo Raso Limestone Member and the Dois Irmãos Member (Figures 5.i and 5.ii). Within the Calada Member and São Lourenço Mudstone Member, these beds are composed of ferroan dolomite. Within the Cabo Raso Limestone Member they are

dominantly composed of non-ferroan calcite with rare occurrences of marine fringing calcite and replaced dolomite. Finally within the Dois Irmãos Member, the cemented beds are dominantly composed of dedolomite. The significance of all of these cemented beds and their different early diagenetic histories will be discussed in Section 5.3.

5.3: *Discussion - interpretation of early diagenetic products*

This section interprets the diagenetic phases described in Section 5.2 and discusses the validity of each phase in terms of supporting (or refuting) the facies based sequence stratigraphic model proposed in Chapter 4. Figure 5.ii and Table 5.iv provide graphical and tabulated summaries of the early diagenetic products and early diagenetic processes with relation to the sequence stratigraphic model outlined in Chapter 4.

As noted in Section 3.3, early diagenetic processes are strongly influenced by depositional pore-water chemistry and microbial activity. (Refer to Sections 3.3 and 1.3 for a full introduction to early diagenesis and sequence stratigraphy, including the relevance of stable isotope and CL data).

5.3.1: The Calada Member

5.3.1a: *Distribution*

The early diagenesis of the Calada Member can be divided into those reactions that took place during/after the deposition of the distributary channels and those that took place during the deposition of the restricted lagoonal facies. To recap, the distributary channel facies is dominated by abundant ferroan dolomite and upwards decreasing volumes of pyrite, while the restricted lagoonal facies is dominated by vertically increasing volumes of pyrite, large volumes of non-ferroan dolomite within small septarian concretions and low to vertically increasing volumes of ferroan dolomite.

Sedimentological evidence (Section 4.2.1) indicates that the fine to coarse distributary channel sandstones were deposited under high energy aerobic conditions, and the restricted lagoonal silty claystones, under more dysaerobic conditions (as indicated by a lack of bioturbation). A combination of generally stable to high sedimentation rates during the deposition of the distributary channels and a reduction (or absence) in the effectiveness of reactions in the oxic zone of the restricted lagoonal deposits, indicates that large amounts of organic matter and reactive iron survived into the sub-oxic and/or sulphate reducing zones.

The early diagenetic reactions (especially those that occur within individual coarsening-up beds of the restricted lagoonal deposits) can be explained in three stages (Fig.5.xviii).

5.3.1b: *Stage 1*

Pyrite:

The large volumes of pyrite are consistent with reactions that occur within the zone of sulphate reduction (Stage 1, Fig.5.xviii). Authigenic pyrite is a product of simultaneous reduction of organic matter, $Fe(III)$ compounds and SO_4^{2-}, which yield Fe^{2+} and HS^- (Curtis, 1987). Equation 3 of Section 3.3.1 indicates the balanced reaction responsible for pyrite formation.

The volume of pyrite decreases towards the top of the distributary channel facies suggesting that there was a reduction in the amount of organic matter reaching the sub-oxic or sulphate reducing zones. This can be explained by a reduction of sedimentation rates prior to the development of a transgressive surface resulting in prolonged residence of sediment within the oxic zone and subsequent degradation of organic matter. A decrease in sedimentation rates could also be related to non-deposition/drowning at parasequence flooding surfaces, thus supporting the positioning of parasequences within the proposed sequence stratigraphic scheme.

5.3.1c: *Stage 2*

Dolomite:

Dolomite precipitation followed that of pyrite. Curtis & Coleman (1986) state that for dolomite to precipitate as an early authigenic mineral, sulphate must be rapidly depleted prior to any significant compaction. Unstable primary carbonates and pore-water solutes will then react with organic degradation products to produce authigenic dolomite. Microbial sulphate reduction can reduce sulphate levels effectively to zero (Curtis & Coleman, 1986) within tens of centimetres of the sediment/water interface (e.g. Nissenbaum *et al.*, 1972).

Coleman (1985) and Curtis (1987) suggest that if rates of *Fe(III)* reduction exceed rates of sulphate reduction, iron-rich authigenic carbonate minerals can be expected to co-precipitate with iron sulphide. Within the restricted lagoonal facies, the converse must have been the case resulting in the growth of non-ferroan dolomite concretions (Stage 2, Fig.5.xviii). As commented upon in Section 3.3, Fleming (1993) shows how concretion shape is defined by the concentration and location of shell debris within the sandstone. These models would ultimately suggest that the source of individual concretions was iron-poor bioclastic debris.

Septarian concretions:

The $\delta^{13}C$ values of the non-ferroan dolomite within the concretions range from -1.03‰

PDB to -1.63‰ PDB, indicating derivation from a combination of marine carbonate and carbonate sourced from low rates of organic-carbon oxidation, deep within the zone of sulphate reduction (Mozley & Burns, 1993). Hird *et al.* (1987) show that slightly negative $\delta^{13}C$ values obtained from peritidal dolomicrites within the Carboniferous of south Wales are also the result of an organic matter source.

Cathodoluminescence within dolomite is considered to be controlled by the concentrations of Mn^{2+} as an activator and Fe^{2+} as a quencher (Medlin, 1961b, 1968 - i.e. in a similar way to calcite, see Section 3.3). As a result, the common dull luminescent response of the dolomites within these septarian concretions suggests a high Fe/Mn ratio which is characteristic of a diagenetic environment where Fe^{3+} is reduced to Fe^{2+} (Carpenter & Oglesby, 1976; Frank *et al.*, 1982; Coleman, 1985 and Miller, 1988). Such an environment can be associated with reduction deep within the zone of sulphate reduction.

The depleted $\delta^{18}O$ values of these concretions indicate a near-surface mixing zone origin, reflecting precipitation from mixed marine/meteoric or brackish pore-waters. This interpretation agrees with the inferred depositional environment of the host sediments. It is unlikely that these dolomites are the result of burial for two reasons:- (i) their obvious early concretionary nature, and (ii) dolomite of burial origin should have highly depleted $\delta^{18}O$ isotope values when compared to the composition of the depositional pore-water (Gawthorpe, 1987). An evaporation origin is also considered unlikely, because dolomites of this origin should result in heavier $\delta^{18}O$ isotope values when compared to the composition of the depositional pore-water (Bechrens & Land, 1972) and no evaporites or evaporite pseudomorphs are present anywhere in these successions.

Septarian concretion growth was closely followed by the precipitation of pore filling ferroan dolomite which surrounds and has similar isotope values to individual concretions. This indicates that dolomite was sourced from similar carbonate (although more Fe-rich) within a similar pore-water environment. Thus the ferroan dolomite is interpreted to have formed in the sub-oxic/sulphate reducing zone within a dominantly mixed marine/meteoric pore-water environment.

It is also clear that both types of dolomite are not of a replacive origin, but are dolomite cements that have displaced ?detrital clay minerals to form diagenetic beds. Tucker & Wright (1990) state that replacive dolomite typically have "cloudy" crystal centres, as a result of the presence of inclusions and mineral relics of a previous calcium carbonate precursor. The dolomite crystals identified here are dominantly inclusion free and have clear crystal centres. Similarly, if dolomite replaced a calcite precursor, then CL analysis would have revealed some evidence of an original crystal structure - which it did not.

5.3.1d: *Stage 3*

Septarian fractures:

All concretions in the coarser grained beds of the restricted lagoonal facies contain septarian fractures. Formation of septarian fractures has been attributed to chemical dehydration and shrinkage (Raiswell, 1971; Pettijohn, 1975) or tensile stress related to overpressure development during shallow burial (Astin, 1986; Astin & Scotchman, 1988). All authors agree that their formation is synonymous with early growth prior to significant

compaction (and dewatering, McKay *et al.*, 1995). However as these sediments show no evidence of rapid compaction it is unlikely that overpressure would have been a significant factor. Therefore, my interpretation supports the model presented by Raiswell (1971) and Pettijohn (1975). $D^{18}O$ values for drusy calcite within the septarian fracture are strongly negative (-6.74 ‰ PDB) indicating crystallisation occurred during shallow burial before significant compaction (Stage 3, Fig.5.xviii). Finally, the characteristic zoned moderate to dull luminescence that the septarian fractures reveal can be interpreted as representing crystallisation within a shallow to deep reducing environment.

Sequence stratigraphic interpretation:

The interpretation outlined above indicates that the early diagenetic precipitates (septarian concretions) grew as a result of prolonged residence time within the zone of sulphate reduction. This can be associated with periods of marine flooding and non-deposition at parasequence boundaries (Stages 1-3 on Fig.5.xviii). Therefore, although the field evidence for parasequences is inconclusive (particularly within the restricted lagoonal facies) the early diagenetic evidence for parasequence identification is more conclusive.

5.3.2: Upper Calada Member to lower Safarujo Member

5.3.2a: *Distribution*

Early diagenetic patterns within these lithostratigraphic units (up to 40m on Fig.5.ii) are characterised by upward increasing volumes of ferroan dolomite and non-ferroan dolomite within the São Lourenço Mudstone Member (sample numbers P26-P34 on Fig.5.ii). Within the lower part of the Safarujo Member (sample numbers P36-P41D on Fig.5.ii) these authigenic phases are replaced upwards by zoned non-ferroan dolomite, non-ferroan sparry calcite, poikilotopic calcite and small volumes of siderite. Fluctuating trends in pyrite and small volumes of iron-oxide (haematite) are present throughout, especially within small concretions and concretionary burrows (between sample numbers P25-P41D on Fig.5.ii).

5.3.2b: *Upper Calada Member*

Only small volumes of pyrite and haematite are present within the distributary channel facies. The absence of a carbonate phase suggests a lack of calcium carbonate ions available for carbonate cement crystallisation. The small volumes of pyrite suggest that reactions within the zone of sulphate reduction were limited, possibly due to low volumes of organic matter. The latter explanation would support the formation of small iron-oxide concretions which require low net sediment accumulation rates and long periods of residence within the zone of aerobic respiration (oxic and post-oxic zones, Taylor & Curtis, 1995).

Sequence stratigraphic interpretation:

Iron-oxide concretion growth can be related to marine flooding/non-deposition at parasequence boundaries (Taylor & Curtis, 1995), thus supporting the identification of parasequences in this facies. However no further evidence was obtained for the identification of a particular systems tract for this unit.

5.3.2c: *São Lourenço Mudstone Member*

As in the Calada Member, the presence of pyrite indicates diagenesis within the zone of sulphate reduction. The presence of ferroan and small volumes of non-ferroan dolomite also indicate that prior to their crystallisation, levels of sulphate reduction had effectively been reduced to zero. As interpreted in Section 5.3.1c, this dolomite is not of a replacive origin, but is a cement. Therefore the beds that contain it are diagenetic, relating to precipitation during a period of increased residence time within an early diagenetic zone.

Sequence stratigraphic interpretation:

The laterally extensive dolomite beds are interpreted to have precipitated during periods of non-deposition. This therefore provides strong diagenetic evidence that these beds have formed below parasequence boundaries (parasequence boundary formation being related to periods of non-deposition and marine flooding). This is a good example of where an analysis of early diagenetic products can help to identify sequence stratigraphic units, when field evidence is poor.

5.3.2d: *Lower beds of the Safarujo Member*

The presence of bioturbation indicates that the prograding shoreface sands that characterise the lower part of the Safarujo Member, were deposited in an aerobic environment and therefore organic degradation in the oxic and post-oxic zones probably occurred. Small iron oxide concretions and cemented laminae are likely to have grown during a period of prolonged residence within the zones of aerobic respiration (Taylor & Curtis, 1995).

Due to the effects of organic degradation in the oxic and post-oxic zones less organic matter reached the sulphate reduction zone resulting in lower sulphide supersaturation (Berner, 1978; Raiswell, 1982; Curtis 1987). This is reflected in the low volumes of pyrite which are only found within highly organic zones such as cemented *Thalassinoides* burrows.

5.3.2e: *Concretions*

The sandstone facies of the lower part of the Safarujo Member (between 32m-44m on Fig.5.ii) is characterised by the presence of large spherical, oblate, elongate and burrow concretions cemented by zoned non-ferroan dolomite, non-ferroan equant sparry calcite and poikilotopic spar. Similar patchy cements are also found within the more poorly cemented host sandstone. The zoning within individual dolomite rhombs that is revealed by artificial staining and CL is interpreted as resulting from slow, incomplete and periodic precipitation from an alternating iron-rich or iron-poor source. The CL response indicates

that non-luminescent dark zones have a high Fe/Mn ratio, whereas the brightly luminescent zones have a low Fe/Mn ratio. Similar observations and interpretations from zoned dolomites have been made by Smith & Stenstrom (1965).

The calculated $\delta^{13}C$ value of zoned non-ferroan dolomite (-0.71‰ PDB) within these concretions is consistent with crystallisation in a sub-oxic or slightly reducing environment, where incorporated CO_3^{2-} is as a result of organic matter reduction, although a contribution of marine bicarbonate cannot be ruled out. The calculated $\delta^{18}O$ values of -3.90‰ PDB suggests crystallisation from within mixed marine/meteoric depositional pore-waters.

McBride *et al.* (1994) and McBride *et al.* (1995) look at oriented and elongated Pleistocene concretions along the Basilicata coast of the Ionian Sea, southern Italy and within the Tertiary sandstones of the northern Apennines, Italy. $D^{18}O$ isotope values for the carbonates that cement the Pleistocene concretions suggest a meteoric origin, resulting in the conclusion that the concretions were growing parallel to groundwater flow directions.

A similar interpretation is indicated for the elongate concretions here. The concretions are aligned NW-SE, while palaeocurrent readings taken from the low-angled planar laminations (variable between 180° and 230°) suggest an east-west to northwest-southeast oriented palaeo-shoreline (Section 4.2.1). Thus it is conceivable to suggest that porewater lenses originating from subaerially exposed portions of the basin, flowed in an offshore direction along permeability pathways that were parallel to ground-water flow directions

(Fig.5.xix). Stable isotope data indicates that subsequent cementation of non-ferroan dolomite within these concretions, occurred within the mixed marine/meteoric diagenetic porewater zone.

Cementation within the concretionary burrows, is interpreted to be due to the abundance of faecal/organic material, associated bacteria and the presence of an organic membrane lining, all of which must have survived (in sufficient quantities) the reactions within the oxic and post-oxic zones. Similar interpretations have been made for concretionary burrows found within the Corallian Group succession (Sections 3.3.3 and 3.3.4).

Sequence stratigraphic interpretation:

The work of Taylor & Curtis (1995) indicates that the presence of iron-oxide concretions suggests that periods of non-deposition associated with parasequence boundary formation are likely to have occurred. This diagenetic evidence supports the facies related sequence stratigraphic framework and identification of parasequences outlined in Chapter 4.

Identification of mixed marine/meteoric cements within the elongate concretions would indicate a period of sub-aerial exposure, possible related to a sequence boundary. Based on facies analysis and changes in parasequence stacking patterns, a sequence boundary has been positioned at 40.4m on Fig.5.ii. However this has been related to a type-2 sequence boundary, where exposure would not normally have occurred. It is therefore suggested that the pore-water source of the elongate concretions originated from an up-dip area of the basin, relating to a period of sub-aerial exposure and type-1 boundary formation

(Fig.5.xix). However without regional data, this statement cannot be supported.

Further support for the interpretation of a type-2 sequence boundary at 40.4m on Fig.5.ii is that early diagenetic cements beneath this surface have been preserved. Formation of a type-2 sequence boundary is not related to a basinward movement of the shoreline and thus diagenetic pore-water zones would be static, preserving early diagenetic precipitates.

5.3.3: Middle to upper Safarujo Member to Cabo Raso Limestone Member

5.3.3a: *Distribution*

Early diagenesis within these lithostratigraphic units is characterised by upward increasing volumes of replacive non-ferroan sparry and poikilotopic calcite within elongate concretions of the Safarujo Member (sample numbers P43-P45D on Fig.5.ii). Within the Cabo Raso Limestone Member (sample numbers P46-P54 on Fig.5.ii) these phases are replaced upwards by non-ferroan fringing and equant calcite, non-replacive poikilotopic calcite and traces of ferroan calcite and dedolomite. Low volumes of pyrite, siderite and iron-oxide (haematite) are seen through-out.

5.3.3b: *Safarujo Member*

The most striking characteristic of the cements within the elongated concretions of the middle to upper Safarujo Member (sample numbers P43-P45D on Fig.5.ii) is that they

have replaced an earlier phase of zoned dolomite precipitation. This would have originally been similar to that preserved within the lower Safarujo Member described previously (Section 5.3.2). The only evidence of early dolomite in these concretions is in the form of iron oxide relics that would have formed the iron-rich zoning within individual crystals. These are characteristically found within single poikilotopic calcite crystals, or across a number of equant crystal boundaries (Fig.5.xi). There is also no response under CL of these early dolomites, which would indicate replacement. By comparison, a CL response was apparent within the dolomite crystals of the lower part of the Safarujo Member (Section 5.2.3d).

Evamy (1967) and Pettijohn (1975) state that the process of calcitisation [dedolomitisation] requires solutions with a high Ca-Mg ratio, rapid flow and temperatures under 50°C - restrictions which imply near-surface conditions. Tucker (1991) states that this process predominantly takes place through contact with meteoric waters. The overall reaction can be represented by the equation originally proposed by Morlot (1848) :-

$$CaCO_3.MgCO_3 + Ca^{2+} \xrightarrow{dedolomite} 2CaCO_3 + Mg^{2+} \quad \text{[Eq.5]}$$

The depleted $\delta^{18}O$ values (-3.32‰ PDB) of the poikilotopic calcite from an elongated concretion suggests that crystallisation could have taken place within a meteoric pore-water environment. The $\delta^{13}C$ results (-8.37‰ PDB) suggest the incorporation of CO_3^{2-} from the precursor dolomite which itself would have most probably had negative $\delta^{13}C$ values (Section 5.3.2) although additional input of HCO_3^{2-} from within the zone of

sulphate reduction or sub-oxic zone cannot be ruled out.

5.3.3c: *Cabo Raso Limestone Member*

A similar change from dominantly marine to dominantly meteoric cementation can be clearly identified within the cemented beds of these shallow water carbonates. Early fringing calcite and micrite precipitation (which has later been neomorphosed to microspar) with a dominant non-luminescent response, is typical of cementation within a marine environment (Tucker & Wright, 1990). However, pore-filling non-ferroan sparry calcite with strongly negative $\delta^{18}O$ values (-5.35 ‰ PDB), patchy bright to dull luminescence and dedolomitisation (although rare) are indicative of cementation within a meteoric environment. Also present in these deposits are rhombohedral pores, that have subsequently been infilled by non-ferroan calcite (probably of meteoric origin) suggesting selective leaching or replacement of original dolomite rhombs.

5.3.3d: *Sequence stratigraphic interpretation*

Stage 1:

Figure 5.xx is a model for the diagenetic processes that are interpreted to have affected the proposed Sequence 3. During Stage 1, which relates to the deposition of the shelf-margin systems tract, a similar situation to that already described for the development of the concretions in the highstand systems tract of Sequence 2 is envisaged. Early diagenesis would however, have been controlled by the progradation and subsequent drowning of

each parasequence. Relatively high net sedimentation rates during the progradation of each parasequence[2] would have resulted in rapid burial of sediment into the sulphate reduction zone. However due to a lack of organic matter within the host sandstones, only small volumes of pyrite crystallised. This was followed by siderite and zoned dolomite as levels of sulphate reduction had effectively been reduced to zero. During the progradation of each parasequence, pore-water zones would have been moving in an offshore direction and, as in the highstand systems tract of Sequence 2, any dolomite preferentially crystallised along permeability pathways within a mixed marine/meteoric zone. Finally small iron-oxide concretions, which are concentrated beneath and within parasequence boundaries, grew as a result of prolonged residence within the zone of aerobic respiration. This suggests that parasequence boundaries represented prolonged periods of drowning and non-deposition.

Stage 2:

During Stage 2, which equates to the deposition of the transgressive and highstand systems tracts (Fig.5.xx) carbonate sediments were deposited above the siliciclastic shoreface sandstones. Initial cementation was dominated by non-luminescent marine fringing calcite cements and rare dolomite growth within vuggy/mouldic porosity.

[2] sedimentation rates within parasequences of the shelf-margin wedge systems tract are deemed not to be too dissimilar from those that occurred within the preceding highstand systems tract, bearing in mind that both systems tracts represent the same depositional environment.

Stage 3:

During Stage 3, which equates to the development of the type-1 sequence boundary, a sharp fall in sea-level occurred, resulting in the basinward movement of all pore-water zones (Fig.5.xx). Thus the cements that formed within Stages 1 and 2 were now within the meteoric zone. Strongly meteoric pore-waters ($\delta^{18}O$ values from sparry and poikilotopic calcite range from -3.32 to -5.35 ‰ PDB) flushed through the sediments, partially dissolving and fully replacing original dolomite within concretions and host sediments and crystallising within open pore spaces. This process of dissolution and replacement of dolomite would have required solutions with a high Ca-Mg ratio, rapid flow and temperatures under 50°C (Pettijohn, 1975; Tucker, 1991). These conditions are likely to have occurred through contact with meteoric waters (Pettijohn, 1975; Tucker, 1991). A characteristic patchy bright to moderate luminescence within pore-spaces of the carbonate sediments could be attributed to growth within a dominantly reducing, meteoric pore-water environment. Patchy bright luminescence has been associated with calcrete formation during sub-aerial exposure (Miller, 1988, fig.6.4). If this is the case in these samples, then it must provide further evidence for the development of a karst surface which is associated with Sequence Boundary 3 (at 58.6m on Fig.5.ii) and was originally identified by facies analysis and described within Section 4.2.3.

This interpretation provides unequivocal support for the facies based sequence stratigraphic interpretation of the Safarujo Member and Cabo Raso Limestone Member (Sequence 3).

5.3.4: Dois Irmãos Member

5.3.4a: *Distribution*

Early diagenetic products within the spit facies of the Dois Irmãos Member are characterised by upward increasing volumes of iron-oxide (haematite) and upward decreasing volumes of siderite and pyrite (sample numbers P57 and P57A on Fig.5.ii). The remainder of the studied Dois Irmãos Member is characterised by upward increasing volumes of dedolomite (sample numbers P61-P67 on Fig.5.ii). Pyrite and siderite are present in low volumes. Non-ferroan sparry calcite and microspar is also common.

5.3.4b: *Spit facies of the Dois Irmãos Member*

The presence of bioturbation, cross-bedding and cross-lamination suggests deposition in an aerobic environment (Section 4.2.5) and therefore organic degradation within the oxic and post-oxic zones probably occurred. Small iron oxide concretions and cemented laminae increase in volume towards the top of this facies succession. As discussed previously (Section 5.3.3), this indicates prolonged residence time within the zones of aerobic respiration (Taylor & Curtis, 1995).

Due to the effects of organic degradation in the oxic and post-oxic zones a limited amount of organic matter would have reached the sulphate reduction zone resulting in lower sulphide supersaturation (Berner, 1978; Raiswell, 1982; Curtis, 1987). This is reflected in the upward decreasing volumes of pyrite.

Relatively abundant siderite is also found within this facies. The crystallisation of siderite would have begun once iron was no longer being fixed by pyrite formation (McKay *et al.*, 1995). Siderite precipitation within the zone of sulphate reduction requires pore-water with very low dissolved sulphide (Pearson, 1979) as well as bicarbonate and Fe^{2+}, which are the principal products of sulphate reduction. Alternatively, the siderite may have had a bacterial origin as a result of bacterial reduction of iron oxide (Canfield, 1989). Canfield (1989) suggests that two distinct microenvironments may exist in marine sediments. In the first, sulphides react with iron-oxides, locally producing iron sulphide. In the other environment, iron reduced by micro-organisms migrates freely into solution where it is combined with bicarbonate (produced by sulphate reduction reactions) to produce siderite.

Sequence stratigraphic interpretation:

The growth of iron-oxide concretions can be related to prolonged periods of marine flooding at parasequence boundaries (Taylor & Curtis, 1995). This implies that the spit facies can be interpreted as a single parasequence, which is in keeping with the proposed facies based sequence stratigraphic model of Chapter 4. However the diagenetic evidence does not provide any further support for the interpretation of either a lowstand or transgressive systems tract for this facies succession.

5.3.4c: *Dois Irmãos Member*

Upwards increasing volumes of dedolomite characterise the coarser grained beds of the remainder of the Dois Irmãos Member. No isotope analysis was performed on these

cements, but the process of dedolomitisation has already been defined as requiring solutions with a high Ca-Mg ratio, rapid flow and temperatures under 50°C which predominantly take place through contact with meteoric waters (Pettijohn, 1975; Tucker, 1991). As a result of these conditions, a similar interpretation to that for replaced dolomite of the Safarujo Member and Cabo Raso Limestone Member is envisaged (Section 5.3.3). Large volumes of pore-filling dolomite would have crystallised within the sulphate reduction zone once the levels of sulphate reduction had effectively been reduced to zero.

Sequence stratigraphic interpretation:

It is feasible to suggest that the original process of dolomite precipitation occurred during the formation of individual parasequences (much in the same way as those described in the São Lourenço Mudstone Member) implying that each coarser grained bed represents the top of an individual parasequence. Subsequently, during the formation of Sequence Boundary 4 (at 69.2m on Fig.5.ii) the original dolomite cements would then have been flushed by meteoric pore-waters, calcitising the dolomite. Positioning a sequence boundary above the coarse grained bed at 69m on Figure 5.ii (as has been suggested in the facies based sequence stratigraphic proposal) implies that all of the coarser grained beds were affected by similar meteoric pore-waters. Therefore the early diagenetic evidence supports the sequence stratigraphic proposal outlined in Chapter 4. However it is still not clear whether the sequence boundary relates to a type-1 or a type-2 boundary and further analysis needs to be performed.

5.3.5: Comparison of the early diagenesis of the Corallian and Ericeira Groups

General remarks:

Early diagenesis within the two successions studied for this thesis was dominated by the growth of concretions within the siliciclastic dominated facies; and marine/meteoric cementation, dissolution and replacement within the carbonate dominated facies.

Septarian concretions:

Septarian concretions are present within both successions, but occur within different depositional environments. Within the Corallian Group, septarian concretions are found within prograding shoreface highstand/lowstand systems tracts (refer to Section 2.2.1b). Within the Ericeira Group, similar concretions are found within restricted lagoonal siltstones that are likely to represent a transgressive systems tract.

Stable isotope values taken from both sets of concretions indicate that their growth is related to prolonged residence within the suboxic/sulphate reducing zone. An interpretation that could substantiate this evidence is that their growth is related to progradation and subsequent drowning of parasequences.

Therefore, although septarian concretions occur in a range of environments, lithologies and sequence stratigraphic units, the available data indicates that they are likely to occur within porous and permeable mediums, at or below parasequence boundaries.

Other carbonate concretions:

Oblate and spherical non-septarian concretions that are present within siliciclastic facies are also common within both successions. Within the Corallian Group, carbonate concretions are found within tidal flat shoreline sandstones. Within the Ericeira Group, oblate and elongate concretions are found within prograding shoreface sandstones. In both successions, stable isotope evidence indicates that their growth is also related to prolonged residence time within sub-oxic/sulphate reducing zones of a mixed marine/meteoric diagenetic environment.

As is the case with septarian concretions, the available data indicates that these carbonate concretions must have grown in response to parasequence progradation and drowning. They are similarly located below parasequence boundaries, along permeability pathways within parasequences or within more porous and permeable lithologies.

Pore-filling calcite cements:

Within the carbonate dominated facies of both successions, common early marine cements are seen to be replaced in time by phases of meteoric diagenesis during major progradational periods (interpreted as highstand systems tracts).

Within the Corallian Group Shortlake Member, evidence of meteoric cementation is sparse. By comparison, in the Cabo Raso Limestone Member of the Ericeira Group, evidence of meteoric diagenesis is widespread. This is because this succession has been

proven to be capped by a type-1 sequence boundary (based on early diagenetic and facies data), which resulted in subaerial exposure and a large scale basinward shift in pore-water zones. Consequently the affects of meteoric dissolution, replacement and cementation resulted in poor preservation of subsequent early precipitated phases.

Sequence 3 of the Corallian Group succession was interpreted to be capped by a type-2 sequence boundary which did not result in a significant fall in relative sea-level, sub-aerial exposure or a basinward shift of pore-water zones. Any meteoric cementation probably occurred as a result of hydrostatically driven, small scale fresh-water lenses that would have originated from an updip, subaerially exposed area of the basin. Early diagenetic phases of the earlier precipitates within the lower Shortlake Member and Upton Member were thus preserved.

Therefore the amount of meteoric dissolution (on the one-hand) and early cement preservation (on the other) is controlled by the degree of relative sea-level fall at the time of sequence boundary formation.

5.4: *Concluding Remarks*

- A range of analytical and petrographical techniques have identified fourteen early diagenetic phases within the Ericeira Group succession. These include pyrite, four forms of dolomite cement and concretionary growth, six forms of calcite (occurring as concretions, cements and replacement cements), dissolution associated with sub-aerial

exposure, siderite and iron-oxide (haematite). Petrographic and isotope evidence indicates that both the ferroan and non-ferroan dolomite is a primary precipitate/cement rather than a product of replacement of an original calcium carbonate precursor.

- As for Chapter 3, this study has indicated that an analysis of early diagenetic products had helped to identify, or provide further evidence for the identification of parasequences, systems tracts and sequence boundaries thus providing additional support for the facies based sequence stratigraphic framework outlined in Chapter 4.
- Within the Calada Member, the interpretation of concretion growth has provided further support for the identification of parasequences. Analysis of the cements within individual concretions (carbonate and iron-oxide) has indicated that their growth is related to prolonged periods of residence within early diagenetic zones. This observation can be related to marine flooding and non-deposition at parasequence boundaries.
- However, analysis of early diagenetic phases has not helped to further identify systems tracts within the distributary channel facies of the Calada Member.
- Within the São Lourenço Mudstone Member, analysis of laterally cemented dolomitic beds provides evidence for the identification of parasequences. As for concretionary interpretation, cements within these beds are related to prolonged residence within an early diagenetic zone which can be related to non-deposition/marine flooding at parasequence boundaries.
- Within the Safarujo Member, the habit and stable isotope values of dolomite within elongate concretions indicate that it crystallised as a result of a general offshore movement of marine/meteoric pore-water along permeability pathways during progradational periods. Generally;

  - within the lower beds of the Safarujo Member, these cements have been preserved, lending further early diagenetic support for the positioning of a type-2 sequence boundary at 40.4m on Figure 5.ii. Generation of a type-2 sequence boundary would not have resulted in any further movement of pore-water zones; and,
  - within the middle to upper beds of the Safarujo Member, early diagenetic dolomite within concretions has been replaced by a phase of meteoric calcite. This is related to a period of sub-aerial exposure at the top of the overlying Cabo Raso Limestone Member. This strongly supports the positioning of a type-1 sequence boundary at the top of the Cabo Raso Limestone Member.
- Within the Cabo Raso Limestone Member, analytical and petrographic data indicates a phase of meteoric cementation. This strongly supports the facies based sequence stratigraphic model for the positioning of a karst/sequence boundary at the top of this member.
- Within the spit facies of the Dois Irmãos Member, iron oxide concretions provide support for the identification of a parasequence, but not for the type of systems tract. Further analysis/regional data needs to be acquired before unequivocal systems tract identification can be made. The presence of abundant dedolomite within the remainder of this member, indicates a phase of meteoric diagenesis which may provide further support for the positioning of a sequence boundary at 68.9m on Figure 5.ii.
- Finally, as in Chapter 3, the emphasis of this chapter was to utilise the analyses of early diagenetic cements to support a facies based sequence stratigraphic model. This theme is continued in Chapter 6, where generalised models are produced that combine facies analysis with analyses of early diagenetic fabrics and are related to differing scales of

relative sea-level change.

Fig. 5.i: Sample nos., locations & types of analysis. B4 (etc.) = sample no., CB = cemented bed, NCB = non-cemented bed & C = concretion. i = thin section petrography, ii = XRD, iii = stable isotope & iv = CL. Sedimentology & sequence stratigraphy as for Figs.4.iii & 4.iv.

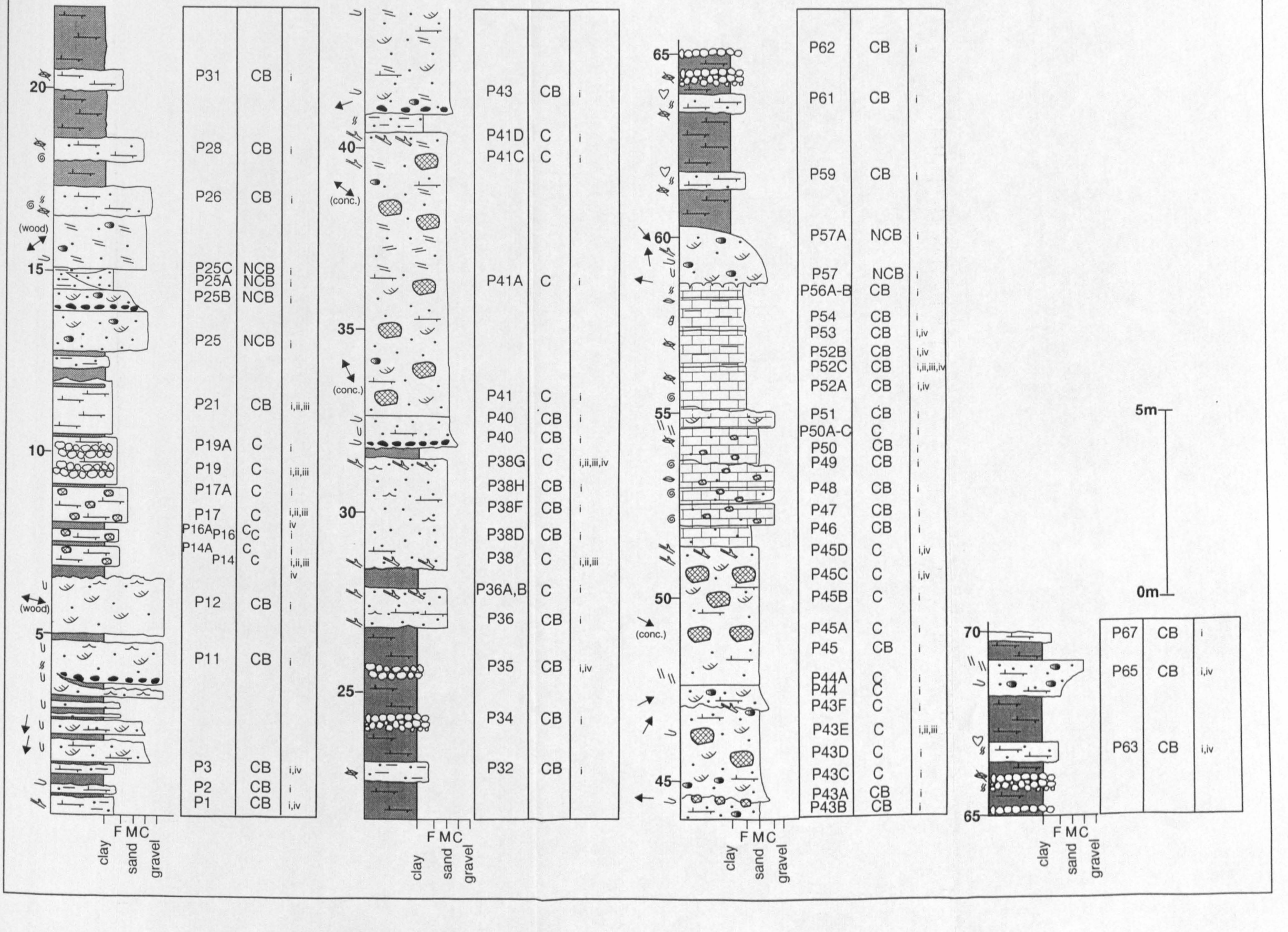

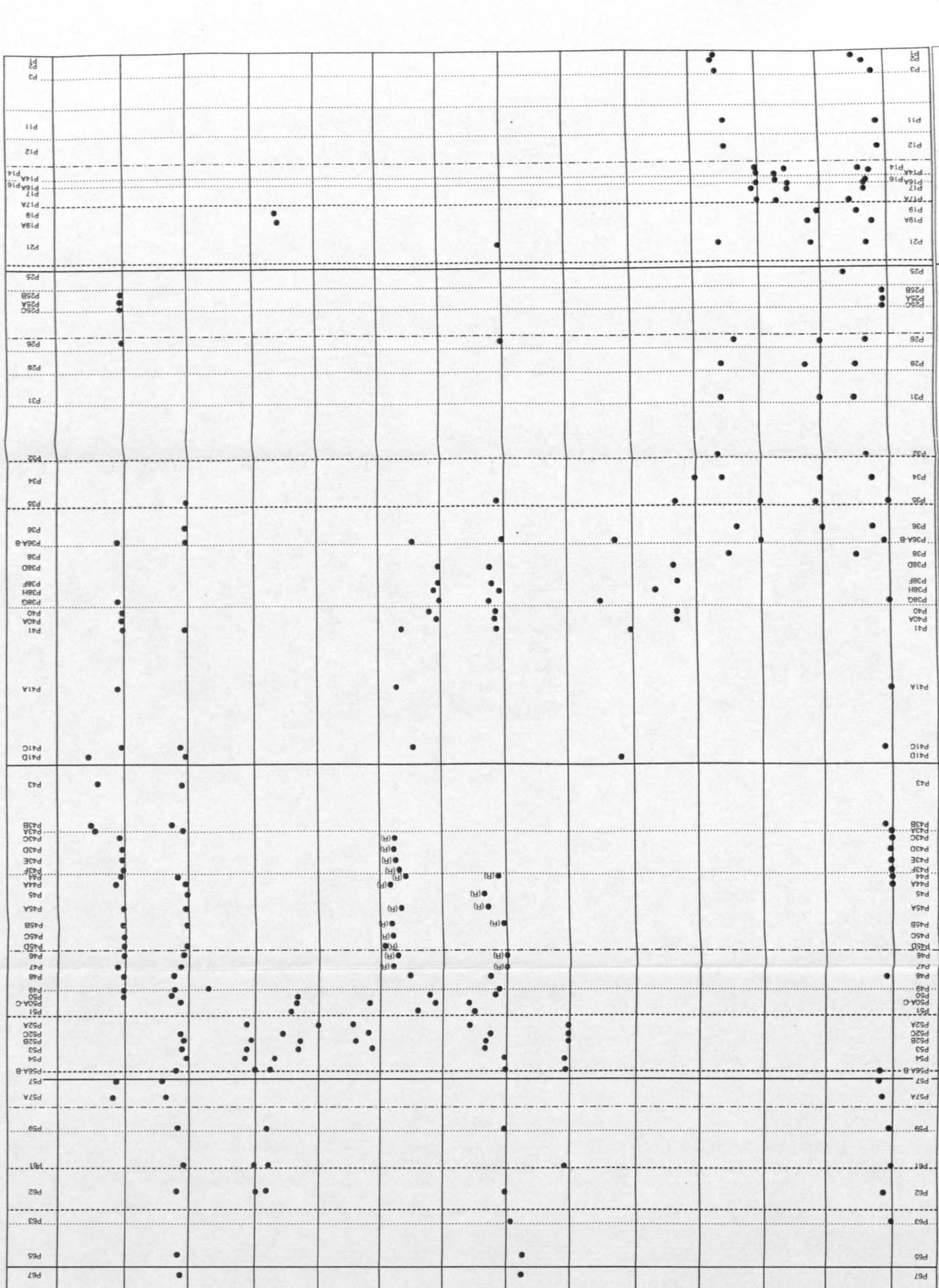

Fig. 5.ii: Graphical representation of diagenetic results. Sample numbers relate to point counted thin-sections. Individual column width represents % of pore-filling abundance. Point count number for each sample = 500. (see Appendix 1, Table 2 for detailed results). Note sequence stratigraphy (as in Chapter 4) & lithostratigraphy

SAMPLES

DOLOMITE PHASES

- PYRITE — increasing abundance 0 → 500
- NON-FERROAN DOLOMITE — increasing abundance 0 → 1000
- FERROAN DOLOMITE — increasing abundance 0 → 1000
- ZONED FERROAN TO MILDLY FERROAN DOLOMITE — increasing abundance 0 → 1000
- ZONED NON-FERROAN CONC. DOLOMITE — increasing abundance 0 → 500

CALCITE PHASES

- DEDOLOMITE — increasing abundance 0 → 1000
- NON-FERROAN SPARRY CALCITE (R = replacing original zoned dolomite) — increasing abundance 0 → 1000
- NON-FERROAN POIKILOTOPIC CALCITE (R = replacing original zoned dolomite) — increasing abundance 0 → 1000
- NON-FERROAN FRINGING CALCITE — increasing abundance 0 → 500
- NON-FERROAN MICROSPAR — increasing abundance 0 → 1000
- FERROAN SPARRY CALCITE — increasing abundance 0 → 1000
- PORE FILLING SIDERITE — increasing abundance 0 → 500
- PORE FILLING & CONCRETIONARY IRON-OXIDE (HEAMATITE) — increasing abundance 0 → 100

SAMPLES

Fig.5.iii: Oxygen versus carbon isotope compositions of sampled early diagenetic phases. (see text for details)

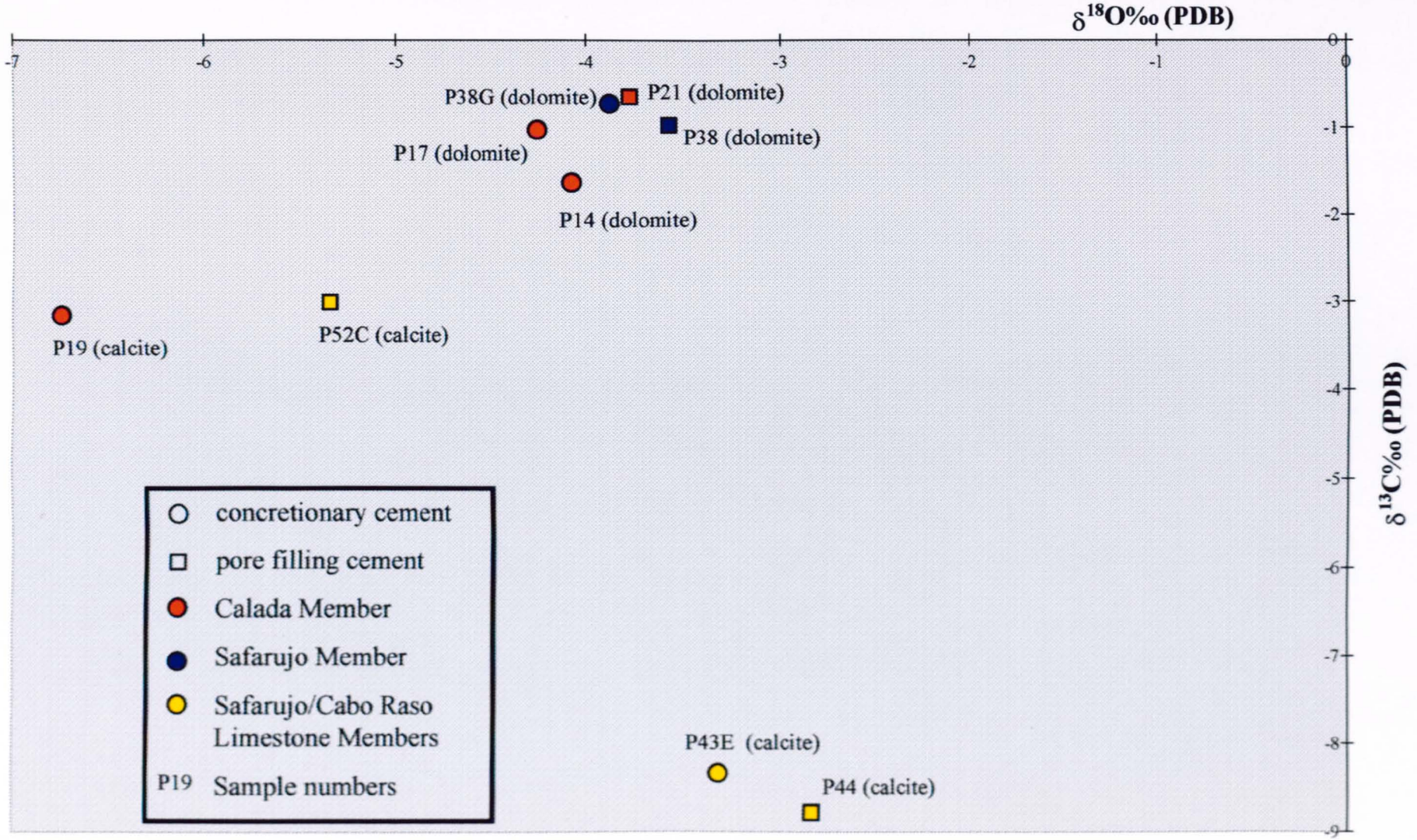

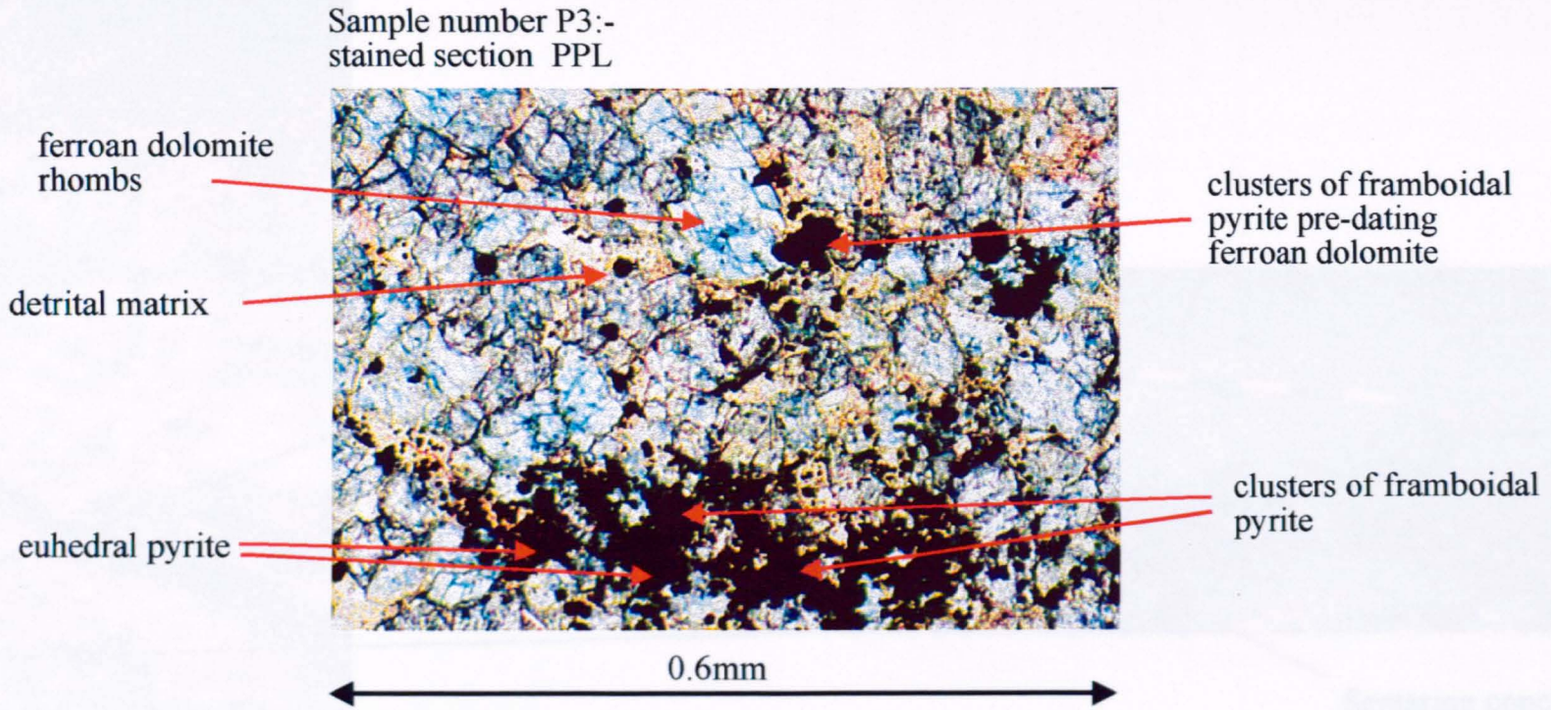

Fig.5.iv. Thin-section photomicrograph of sample number P3 from a parasequence within the lowstand systems tract of Sequence 1 (the Calada Member).

Photograph shows the abundance of framboidal and euhedral pyrite, and its association with ferroan dolomite. The abundance of pyrite and the depleted carbon isotope values for the ferroan dolomite indicate that they are both products of reactions within the zone of sulphate reduction. These reactions have been interpreted to be controlled by sea-level changes at a parasequence scale - parasequence progradation resulting in rapid burial of sediment deep into the Sr zone, followed by prolonged residence associated with parasequence flooding.

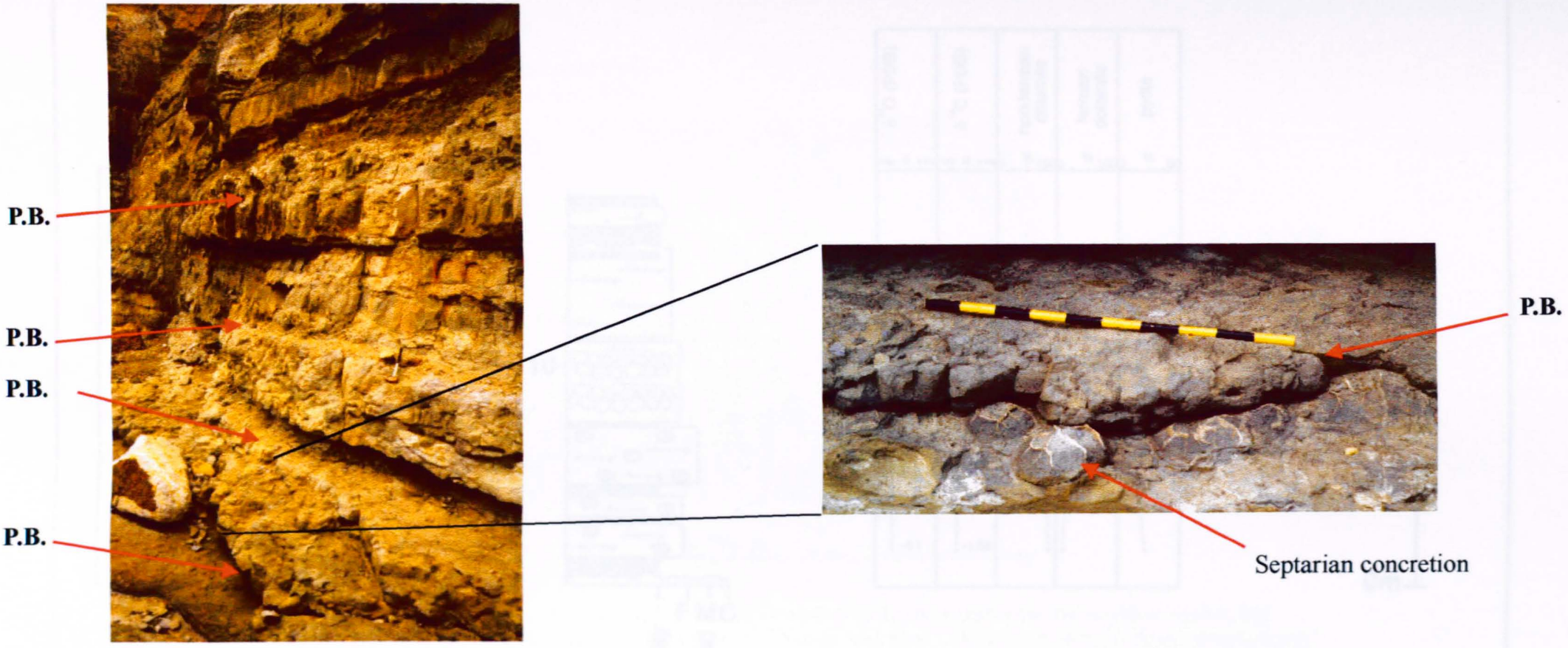

Fig.5.v. The restricted lagoonal deposits of the Calada Member. Red arrows point to the tops of coarsening-up successions which may represent parasequence boundaries (P.B.). Sequence stratigraphically, this unit represents the transgressive systems tract of Sequence 1. (For scale, the hammer is 0.4m in length)

The photograph on the right is a blow-up of the top of a coarsening-up succession to show septarian concretionary growth. Septarian concretions are composed of dominantly non-ferroan dolomite, pyrite and ferroan calcite septarian cracks. Stable isotope and CL data all suggest that concretion growth was deep within the zone of sulphate reduction.

Scale bar on blow-up photograph is 1m.

Photograph taken at the cliff section to the north of Praia de S. Lourenco (see Fig.4.i for location).

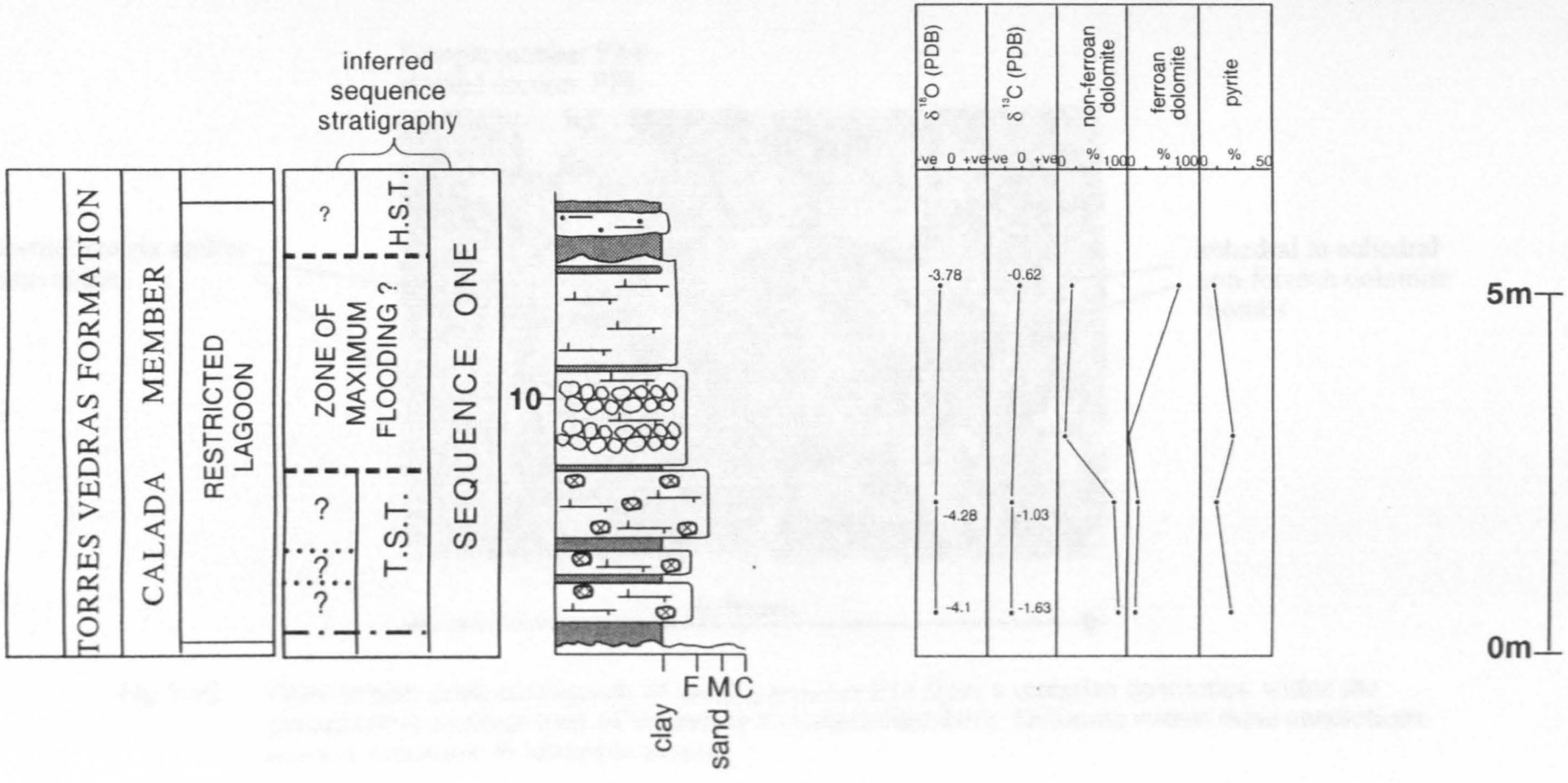

Fig.5.vi: Illustration of the restricted lagoonal deposits of the Calada Member (Sequence 1). The systems tracts are dominated by pore-filling ferroan dolomite, pyrite and small non-ferroan dolomite septarian concretions. Stable isotope data implies dolomite precipitation occurred within a sub-oxic/sulphate reduction zone, of a mixed marine/meteoric pore-water environment. Data points relate to sample numbers as in Figs.5.i & 5.ii.

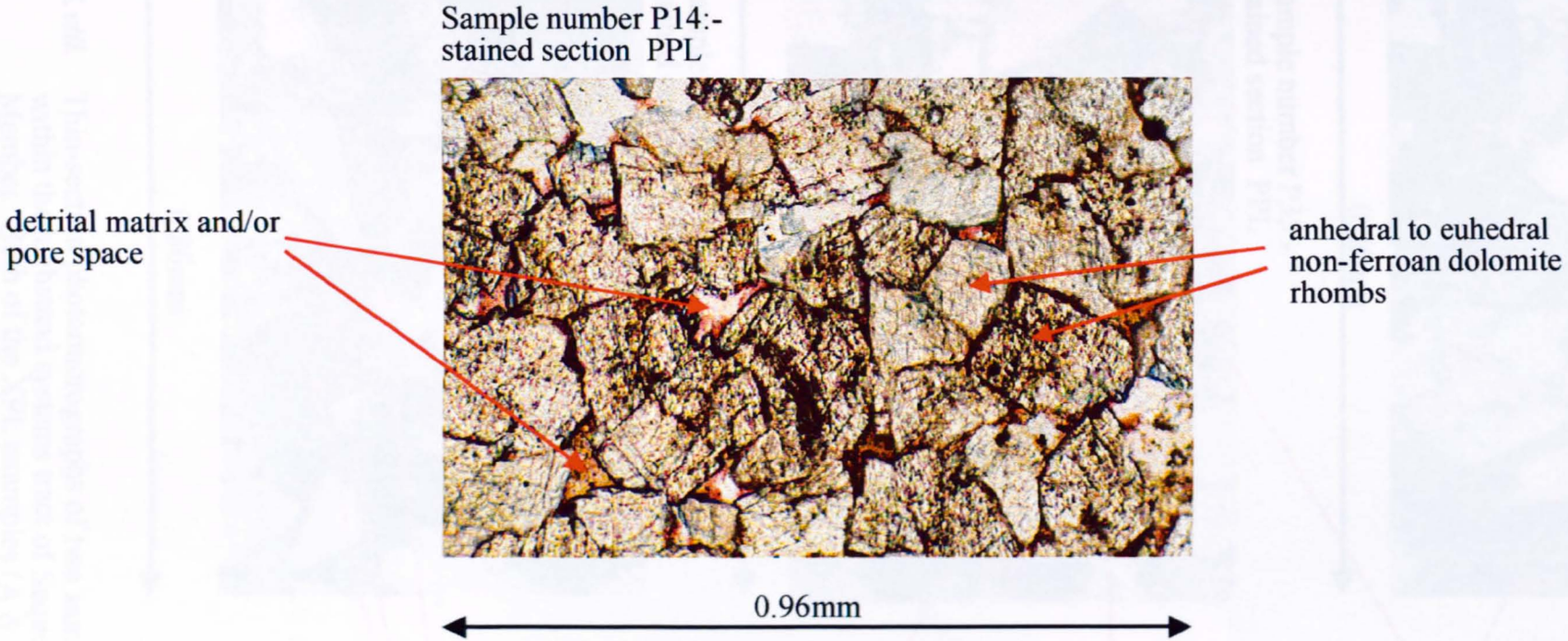

Fig.5.vii. Thin-section photomicrograph of sample number P14 from a septarian concretion within the transgressive systems tract of Sequence 1 (Calada Member). Dolomite within these concretions forms a xenotopic to idiotopic mosaic.

Stable isotope and CL data from these dolomites suggests that they were precipitated during a period of prolonged residence within the zone of sulphate reduction as a result of marine flooding at parasequence boundaries.

A Sample number P35:-
stained section XPL

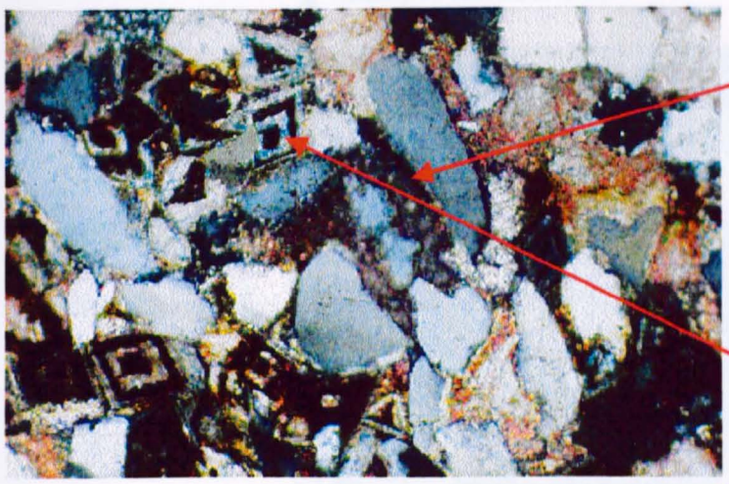

non-ferroan poikilotopic calcite crystal in extinction. This calcite does not replace the zoned dolomite that is present within this sample

zoned mildly ferroan dolomite, consisting of an iron-oxide rich core and one iron-oxide rich zone. Note that this dolomite rhomb has not been replaced by poikilotopic calcite

0.86mm

B Sample number P35:-
stained section PPL

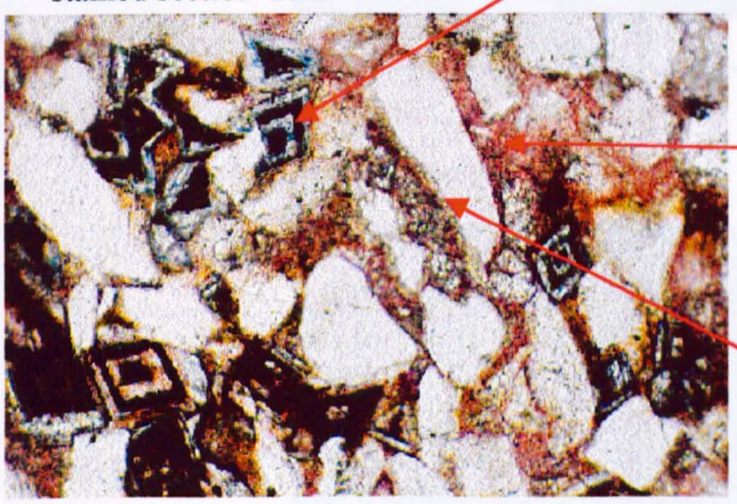

non-ferroan poikilotopic calcite

diffuse quartz boundaries suggest some etching by alkaline rich pore-fluids

0.86mm

C Sample number P38H:-
stained section XPL

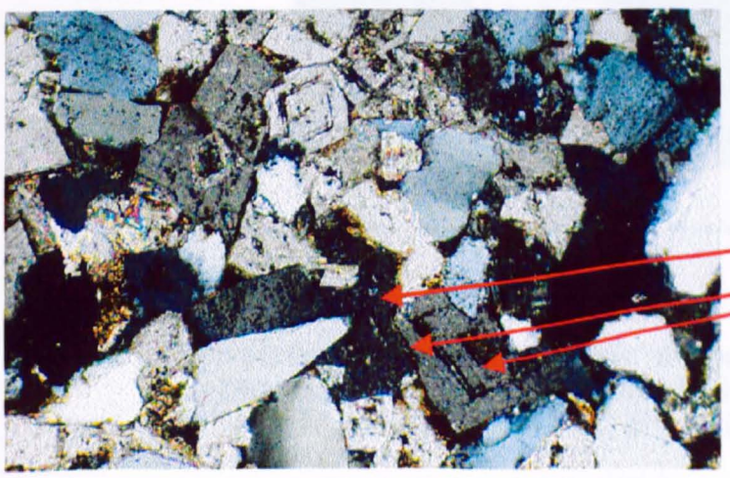

zoned dolomite crystal juxtaposed against a poikilotopic calcite crystal. A clear boundary can be seen between these two crystals implying that there has been no replacement.

0.86mm

Fig.5.viii. Thin-section photomicrographs of two samples (P35 & P38H) from within the highstand systems tract of Sequence 2 (lower beds of the Safarujo Member. Both of the XPL examples (A & B) clearly show the non-replacive relationship between the non-ferroan poikilotopic/equant calcite and the mildly ferroan zoned dolomite. Zoning within the dolomite rhombs is related to slow, incomplete and periodic precipitation either from an iron-rich or iron-poor source.

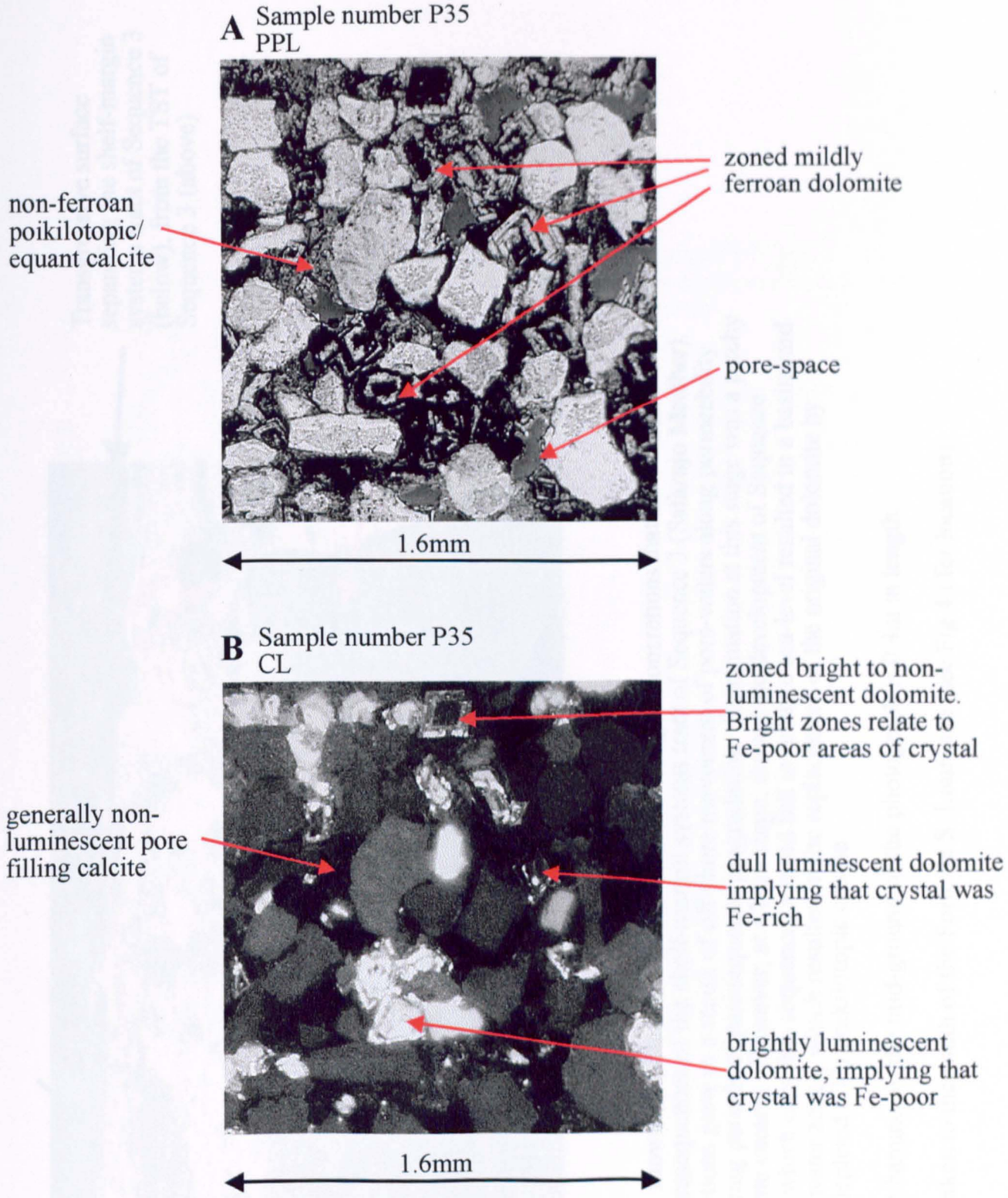

Fig.5.ix. Two photomicrographs of sample number P35 from the highstand systems tract of Sequence 2 (lower beds of the Safarujo Member) - (A) in PPL, (B) under CL.

Zoning within individual dolomite crystals is well revealed by CL responses. Brightly luminescent zones correspond to Fe-poor zones, whereas non/dull luminescent zones correspond to Fe-rich zones. Bright luminescence also implies a sub-oxic reducing environment of precipitation. The remaining pore-space is occluded by non-luminescent calcite which implies an earlier oxidising environment of precipitation.

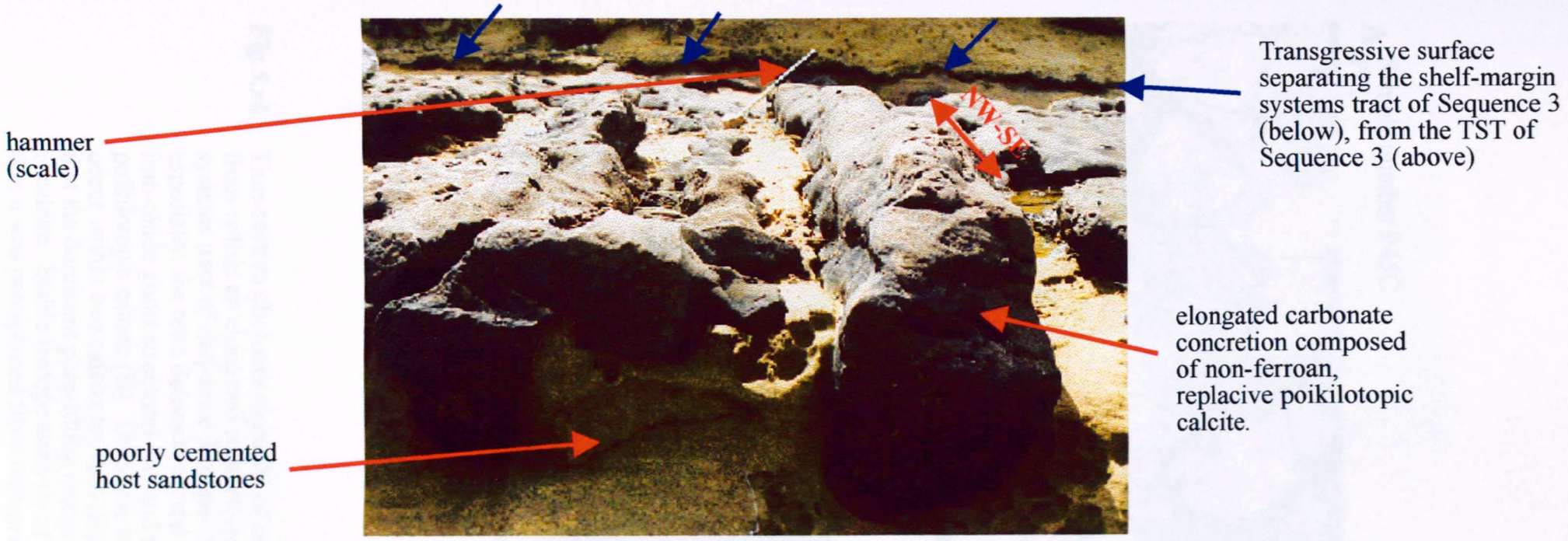

Fig.5.x. Field slide to show the habit and orientation of the elongate concretions that are common within the parasequences of the shelf-margin systems tract of Sequence 3 (Safarujo Member). These concretions grew as a result of off-shore movement of pore-waters along permeability pathways during periods of parasequence progradation. Cementation at this stage was a patchy zoned dolomite cement. However, at a later stage, during the development of Sequence Boundary 3 (which caps this sequence) a rapid fall in relative sea-level resulted in a basinward shift in pore-water zones, which resulted in the replacement of the original dolomite by isotopically depleted (O^{18}) poikilotopic calcite.

For scale, the hammer in the mid-ground of the photograph is 0.4m in length.

Photograph taken to the south of the Forte de S. Lourenco (see Fig.4.i for location).

A Sample number P45C
PPL

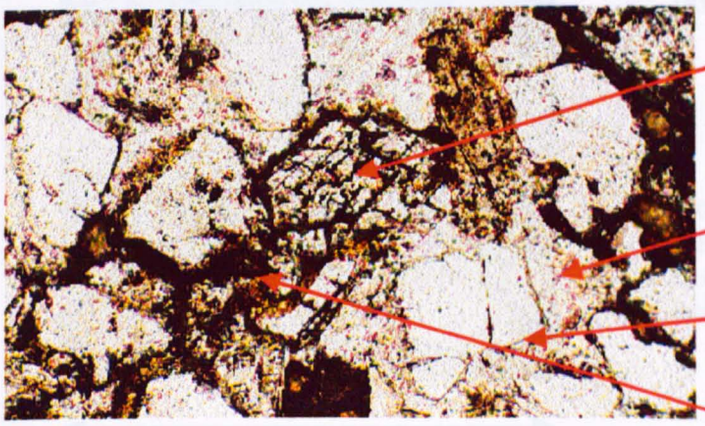

iron-oxide "ghost" structure marking a relic dolomite crystal

pore-filling poikilotopic calcite

etched quartz crystals

detrital matrix within pore spaces

0.8mm

B Sample number P45C
XPL

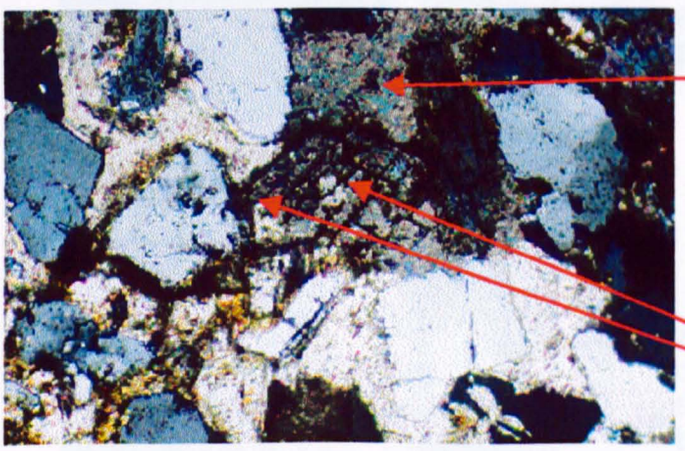

poikilotopic calcite in extinction, clearly replacing original dolomite

dolomite relic can be seen to occur within two poikilotopic calcite crystals

0.8mm

Fig.5.xi. Thin-section photomicrographs of sample number P45C from within an elongated concretion of the shelf-margin systems tract of Sequence 3 (upper Safarujo Member). Note especially, the relic dolomite crystal that can be picked out by iron-oxide ghost structures (A) and the replacive nature of the poikilotopic calcite (B). Dolomite relic can also been seen to occur within two calcite crystals (B). XRD analysis proves that the dominant pore-filling component in these samples is calcite. Stable isotope analysis of this calcite implies that it was precipitated from meteoric pore-waters.

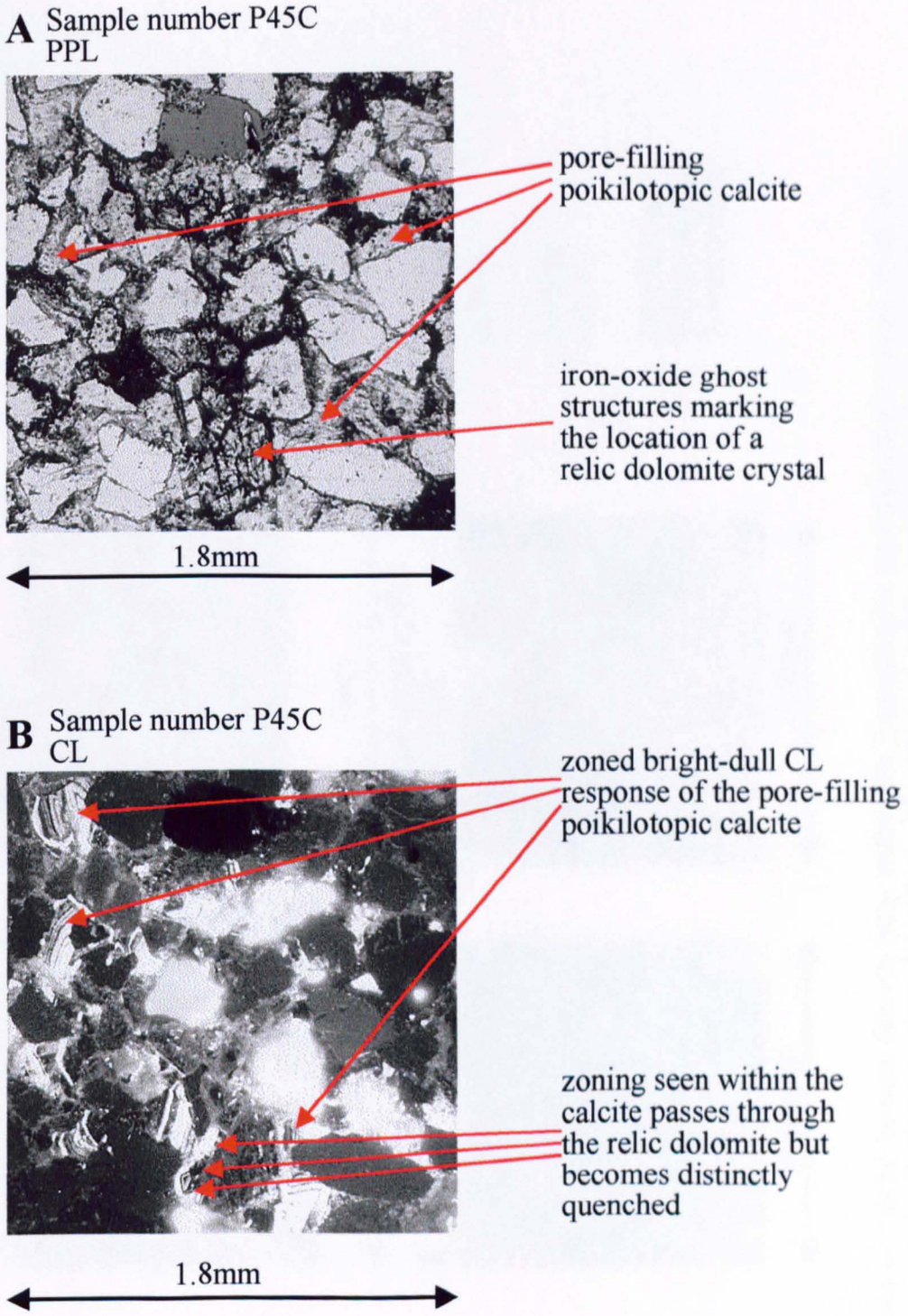

Fig.5.xii. Two photomicrographs of sample number P45C, from an elongate concretion within the shelf-margin systems tract of Sequence 3 (upper Safarujo Member) - (A) in PPL, (B) in CL light.

(B) clearly shows the common bright luminescence of the poikilotopic calcite, with zoning originating from detrital grain boundaries. This response implies crystal growth within a dominantly meteoric, reducing environment. The relic dolomite reveals no luminescence (unlike dolomite crystals within concretions of Sequence 2) apart from dull zoning that originates from within the calcite crystals - dull zoning is due to the high Fe content.

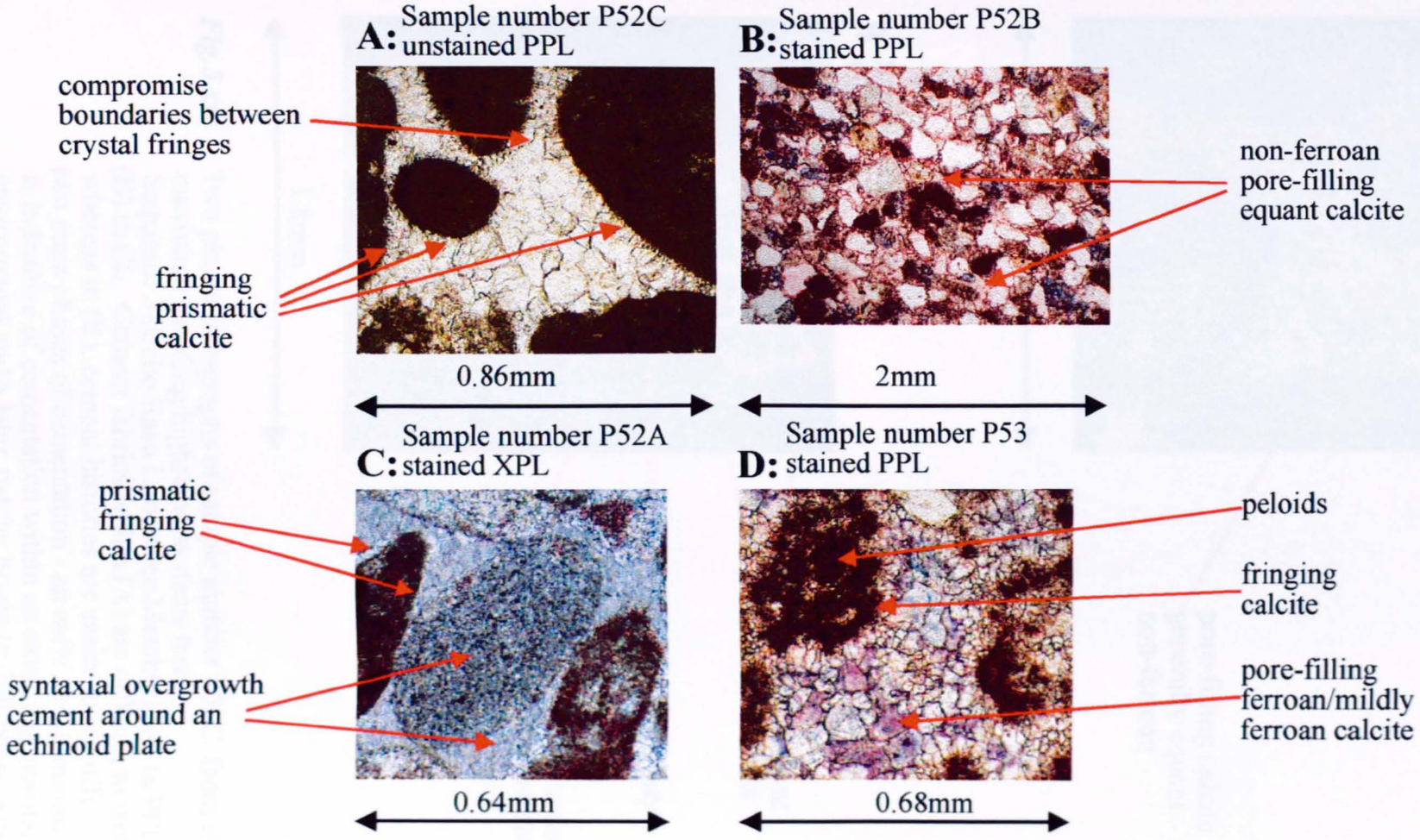

Fig.5.xiii. Four examples of calcite cement fabrics from within the transgressive and highstand systems tracts of Sequence 3 (the Cabo Raso Limestone Member). The fringing calcite and syntaxial overgrowth cements of A and C are marine precipitates, while stable isotope and CL results suggest that the non-ferroan equant calcite is a meteoric precipitate. The pore filling ferroan/mildly ferroan calcite is not vertically extensive and could be related to a later phase of shallow burial cementation. (see Section 5.2.4d for further explanation).

A Sample number P52C
PPL

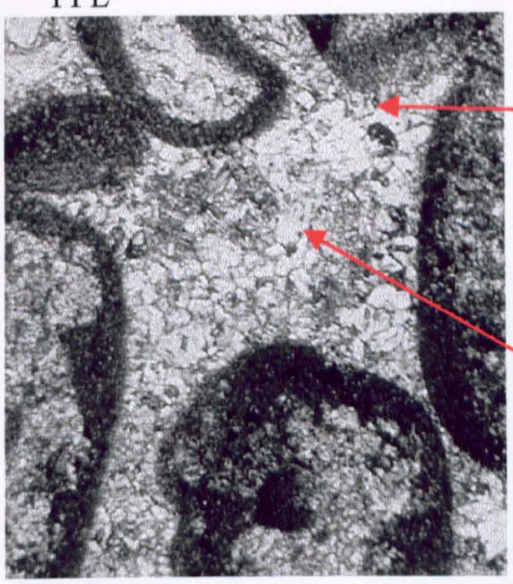

B Sample number P52C
CL

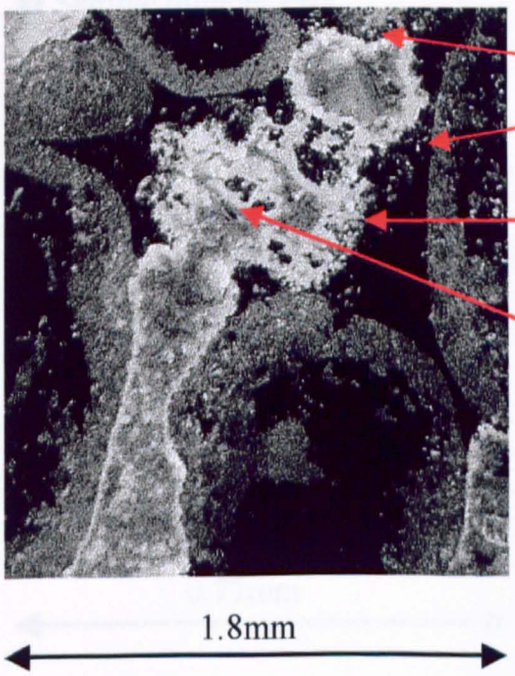

Fig.5.xiv. Two photomicrographs of sample number P52C, from the zone of maximum flooding/highstand systems tract of Sequence 3 (Cabo Raso Limestone Member) (A) in PPL, (B) in CL. Cement fabrics within (A) are difficult to isolate, whereas in (B), cement histories are easier to identify. (B) clearly shows two main phases of cementation - an early non-luminescent phase which is indicative of cementation within an oxidising, marine environment and a later, patchy bright to dull phase which is indicative of precipitation within a sub-oxic meteoric environment. The diffuse boundary between the two phases suggests that dissolution occurred prior to the precipitation of the second phase. This second phase is also related to karstification that occurred during the development of Sequence Boundary 3. (see Section 5.2.4d for further explanation).

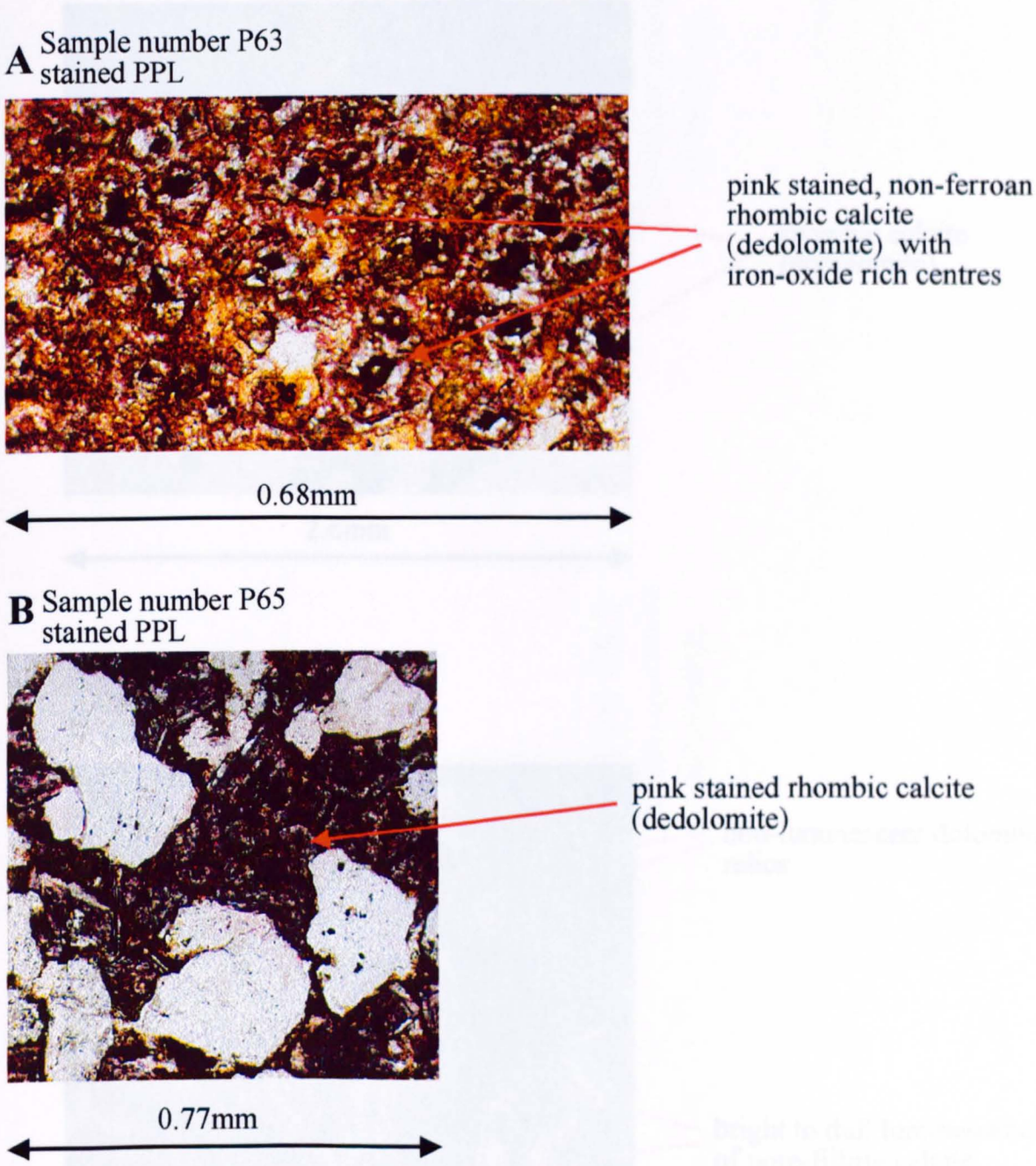

Fig.5.xv. Photomicrographs of two samples from Sequence 4 (the Dois Irmaos Member) to show common pink stained rhombic calcite (dedolomite) This form of calcite is a product of replacement of primary dolomite by calcite precipitated from meteoric waters. Dark centres within individual calcite crystals are due to iron-oxide rich cores of primary dolomite. (see Section 5.2.4e for further explanation).

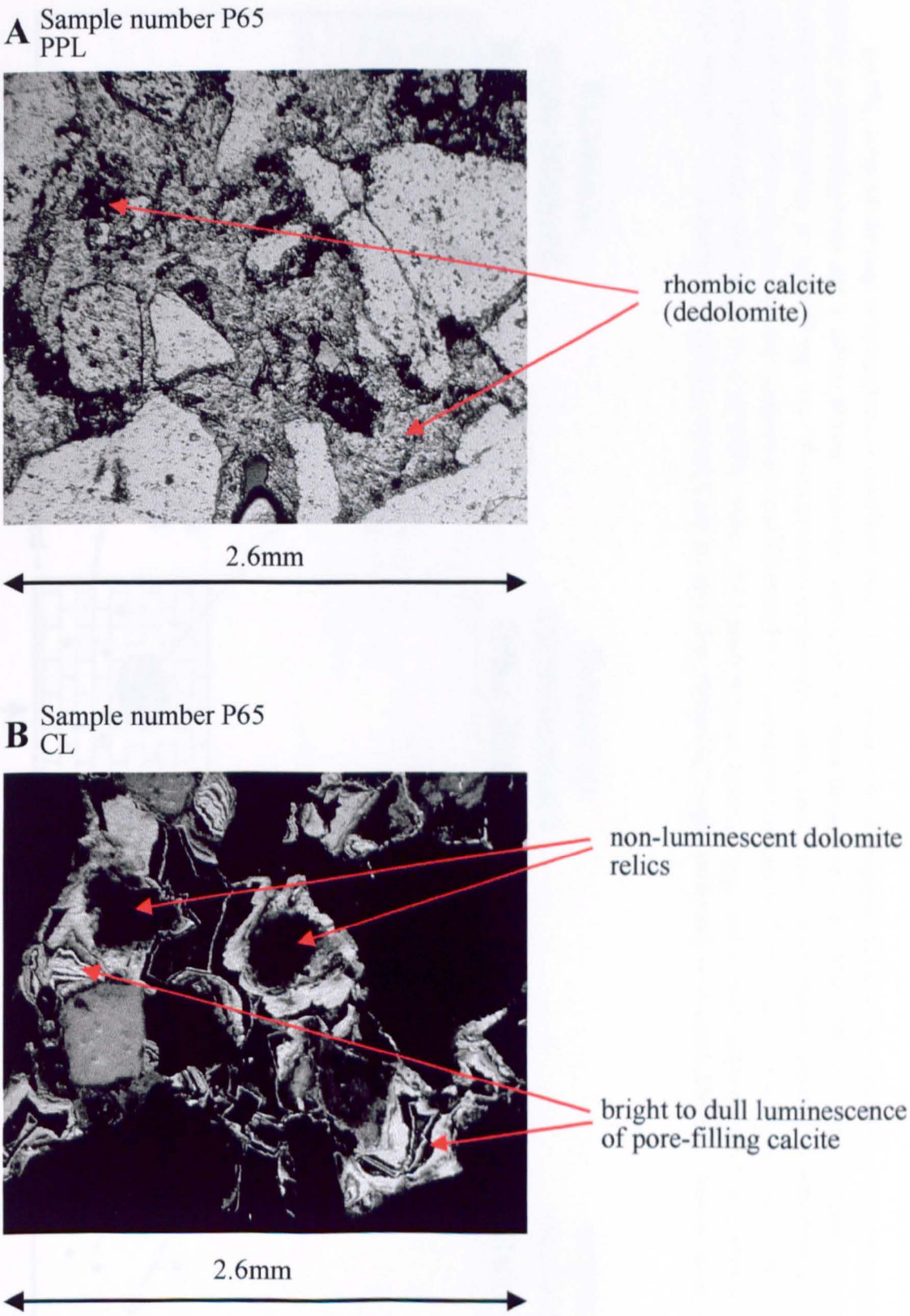

Fig.5.xvi. Two photomicrographs of sample number P65 from the highstand systems tract of Sequence 4 (the Dois Irmaos Member) (A) in PPL, (B) in CL.

The CL response (B) of the pore-filling calcite clearly shows bright to dull luminescence which is indicative of precipitation within a sub-oxic meteoric environment. (see Section 5.2.4e for further information)

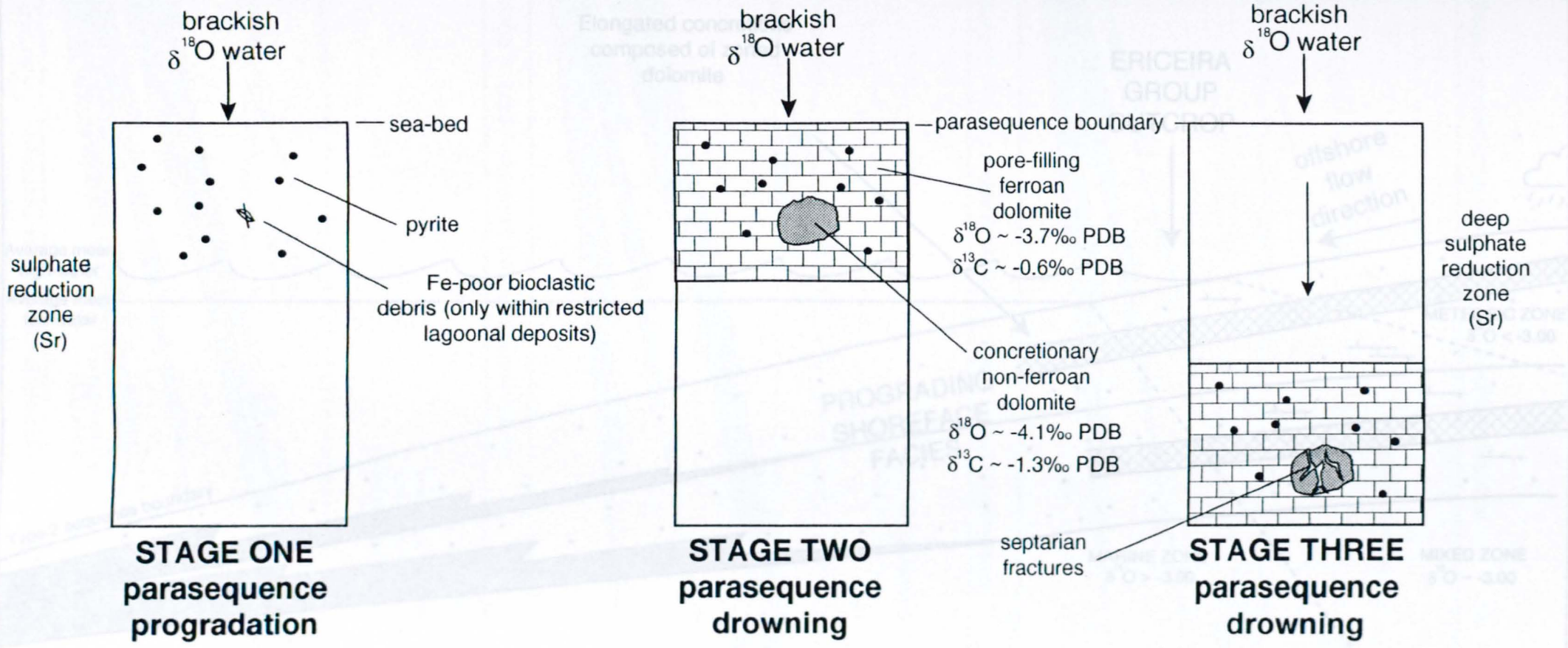

Fig.5.xviii: Early diagenesis within a parasequence of the dysaerobic, lagoonal deposits of the Calada Member (Sequence 1). During stage 1, pyrite crystallises within the sulphate reduction zone (Sr). A lack of oxic/post-oxic zones suggests a lot of organic material is preserved and available for sulphate reduction. With marine flooding & the development of a parasequence boundary, burial may have continued at a slower rate, while levels of sulphate reduction would have effectively been reduced to zero allowing:- (i), the growth of small concretions around Fe-poor bioclastic debris and (ii), the crystallisation of pore-filling ferroan dolomite. Finally, during stage 3, the development of septarian fractures within the concretions occurred, which were infilled with a drusy calcite that suggests crystallisation during shallow burial.

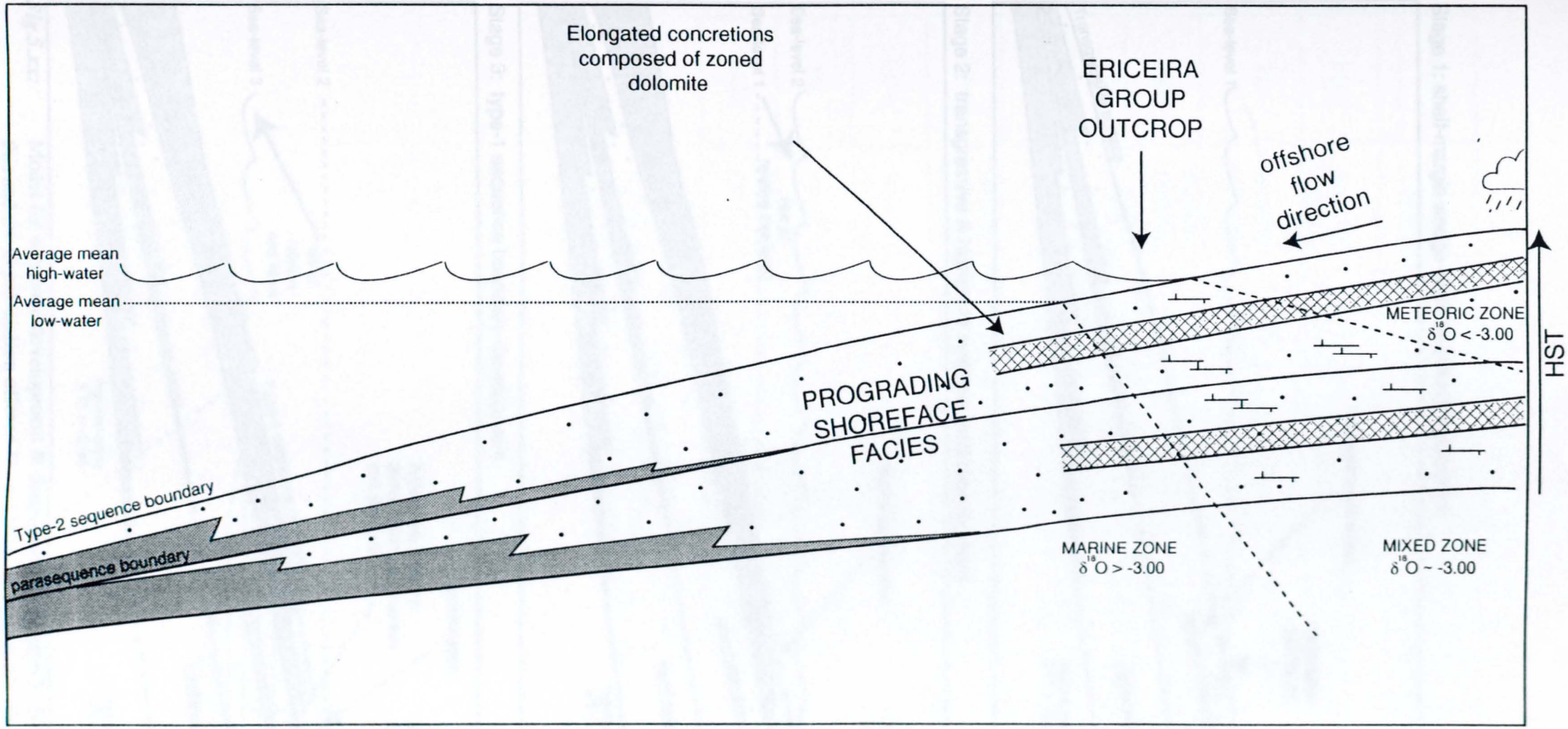

Fig.5.xix: Model to show the formation of elongate concretions within the Safarujo Member of Sequence 2. Prograding shoreface parasequences stack to form a progradational parasequence set. Within the shoreface depositional environment, a mixed marine/meteoric pore-water zone develops resulting in patchy carbonate cementation. During HST/sequence boundary formation, pore-water lenses that originated within subaerially exposed parts of the basin, flow along permeability pathways in an offshore direction, parallel to ground-water flow. Based on stable isotope data, cementation of non-ferroan dolomite occurred within the mixed marine/meteoric pore-water zone. The type-2 sequence boundary that developed resulted in no net relative fall in sea-level & no subsequent basinward shift in diagenetic pore-water zones. Thus all cements were initially preserved, & no subsequent meteoric dissolution/replacement occurred.

Stage 1: shelf-margin wedge systems tract development

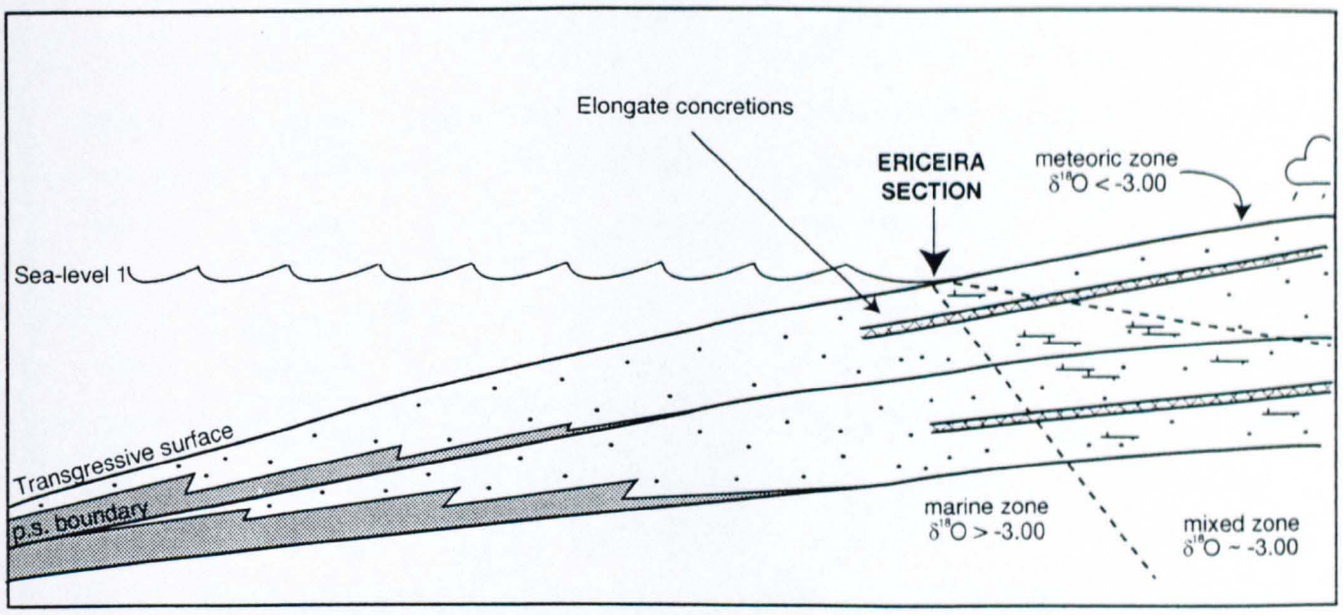

Stage 2: transgressive & highstand systems tract development

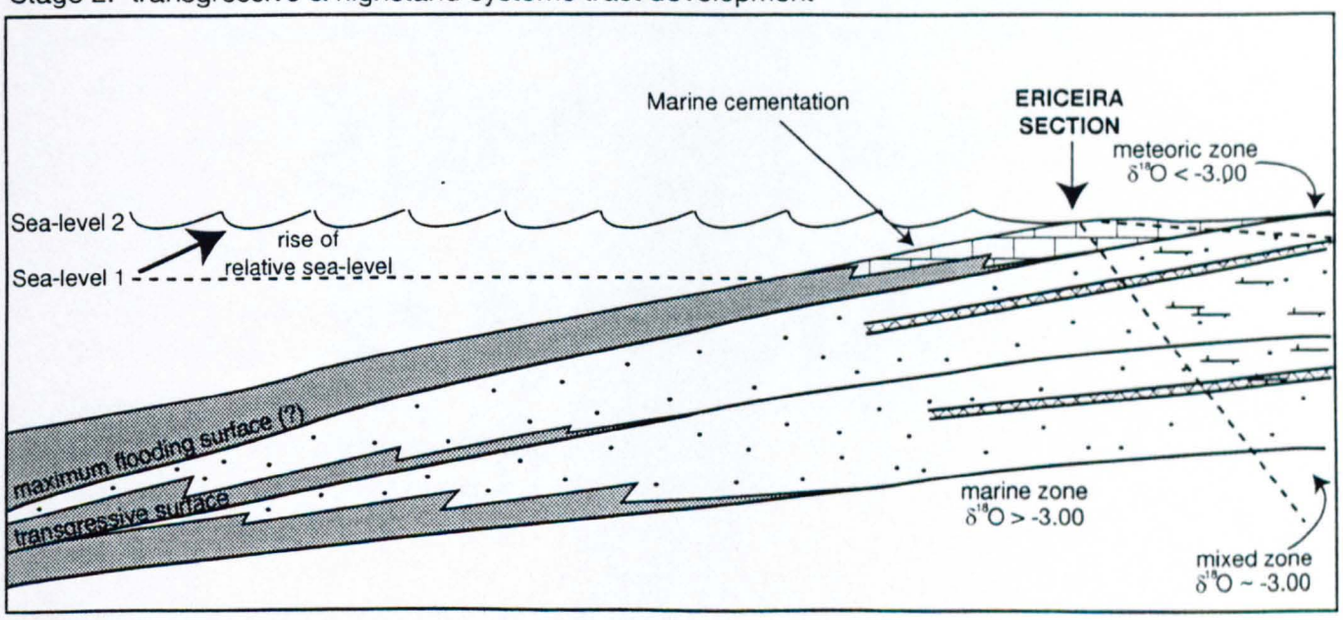

Stage 3: type-1 sequence boundary development

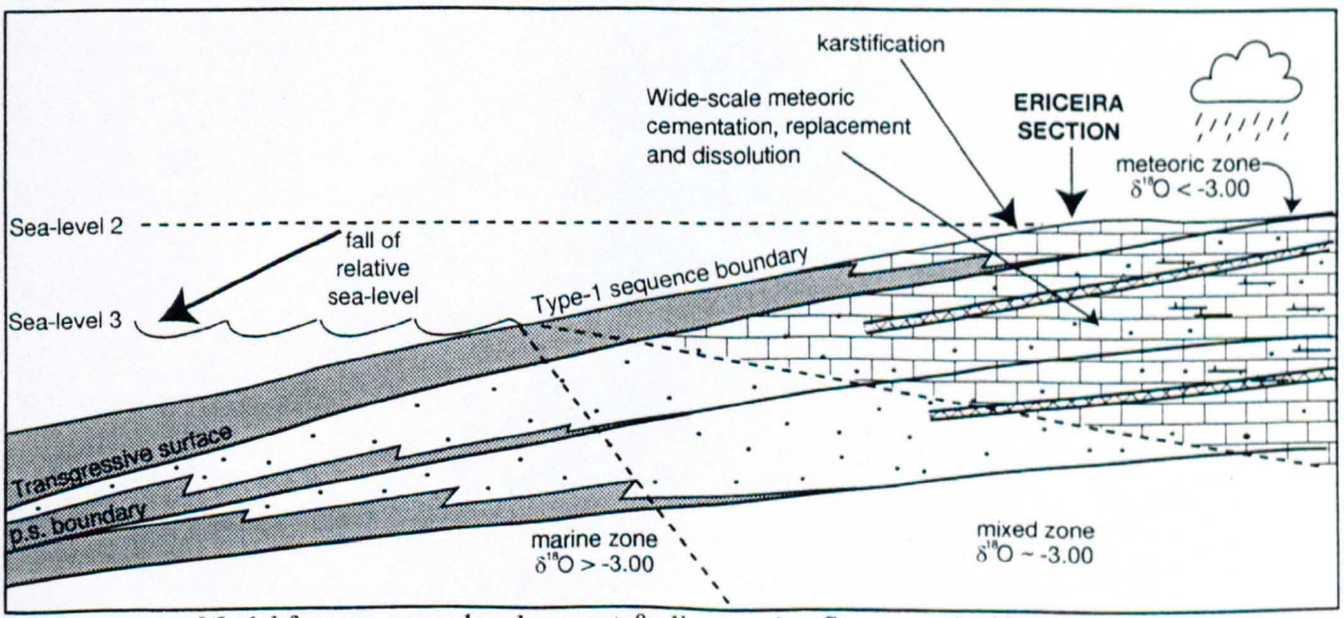

Fig.5.xx: Model for sequence development & diagenesis - Sequence 3. Note difference between this and the interpretation offered for the HST of Sequence 2 (Fig.5.xix). See section 5.3.3d for further explanation.

Sample No.	Sample Type	Authigenic Phase	Depositional Environment	Lithostrat-igraphy	$\delta^{18}O$‰ PDB	$\delta^{13}C$‰ PDB
P14	septarian concretion	non-ferroan dolomite	restricted lagoonal	Calada Member	-4.10	-1.63
P17	septarian concretion	non-ferroan dolomite	restricted lagoonal	Calada Member	-4.28	-1.03
P19	fracture of septarian concretion	ferroan drusy calcite	restricted lagoonal	Calada Member	-6.74	-3.09
P21	pore filling	ferroan dolomite	restricted lagoonal	Calada Member	-3.78	-0.62
P38	pore filling	non-ferroan zoned dolomite	prograding shoreface	Safarujo Member	-3.59	-0.95
P38G	elongated concretion	non-ferroan zoned dolomite	prograding shoreface	Safarujo Member	-3.90	-0.71
P43E	elongated concretion	non-ferroan poikilotopic calcite	prograding shoreface	Safarujo Member	-3.32	-8.37
P44	pore filling	non-ferroan poikilotopic calcite	prograding shoreface	Safarujo Member	-2.84	-8.74
P52C	pore filling	non-ferroan sparry calcite	shallow marine carbonates	Cabo Raso Limestone Member	-5.35	-2.95

Table 5.i: $\delta^{18}O$ & $\delta^{13}C$ (‰ PDB) results for selected cement samples of the lower to middle Ericeira Group successions of west central Portugal

Sample No.	Sample Type	Authigenic Phase	Depositional Environment	Lithostrat-igraphy	CL response
P1, P3	pore-filling	ferroan dolomite	channel sands (delta mouth?)	Calada Member	Non-luminescent
P14, P17	septarian concretion	non-ferroan dolomite	restricted lagoonal	Calada Member	dull to non-luminescent
P35	pore filling	zoned dolomite & pore filling calcite	inner shelf	Safarujo Member	dolomite is non to brightly luminescent; calcite is non-luminescent
P38G	concretion	zoned dolomite & pore filling calcite	prograding shoreface	Safarujo Member	dolomite is non to dull luminescent; calcite is non-luminescent
P45C, P45D	concretion	poikilotopic calcite	prograding shoreface	Safarujo Member	zoned, dull to bright luminescence
P52A-P52C, P53	pore filling	fringing & equant non-ferroan to mildly ferroan calcite	shallow marine carbonates	Cabo Raso Limestone Member	variable non-luminescent to patchy bright to moderate luminescent
P63, P65	pore filling	dedolomite (rhombic calcite)	regressive sand bars	Dois Irmãos Member	zoned, dull to bright luminescence

Table 5.ii: Cathodoluminescence (CL) results for selected cement samples of the lower to middle Ericeira Group succession to the north of the town of Ericeira. CL response described as either non-luminescent, dull luminescent, moderately luminescent or brightly luminescent & either zoned or non-zoned

Lithostrat-igraphy	Cement type	Depositional environment	Sulphides	Carbonates			Iron-oxide (heamatite)	Paragenetic sequence (early diagenesis only)
				Dolomite	Calcite	Siderite		
Calada Member	concretions	delta mouth/ distributary channels	Absent	Common ferroan dolomite	Absent	Absent	Rare	Dolomite heamatite
Calada Member	cemented beds	restricted lagoonal	Abundant pore-filling framboidal pyrite & pyrite within dolomite lattice	Common ferroan dolomite. Common septarian concretionary non-ferroan dolomite	Rare non-ferroan microspar	Absent		Pyrite ferroan dolomite non-ferroan dolomite non-ferroan microspar
São Lourenço Mudstone Member	cemented beds	restricted lagoonal/ inner shelf	Abundant pore-filling framboidal pyrite & pyrite within dolomite lattice	Common ferroan dolomite	Absent	Absent		Pyrite dolomite
Safarujo Member	concretions	"normally" prograding shoreface sands	Rare pore-filling euhedral pyrite	Common concretionary zoned non-ferroan dolomite. Rare zoned non-ferroan dolomite	Non-ferroan pore-filing sparry calcite. Non-ferroan poikilotopic concretionary calcite. Non-ferroan poikilotopic calcite	Rare	Rare	Pyrite dolomite/sparry calcite poikilotopic calcite siderite heamatite
Cabo Raso Limestone Member	cemented beds	Shallow marine carbonates	Rare pore-filling euhedral pyrite	All dolomite calcitised/dissolved	Non-ferroan to ferroan pore filling calcite	Rare		Pyrite dolomite calcite/calcitisation siderite
Dois Irmãos Member	cemented beds	Spits, regressive sand bars and marine muds	Rare pore-filling euhedral pyrite	All dolomite calcitised/dissolved	Non-ferroan poikilotopic calcite	Rare	Rare	Pyrite dolomite poikilotopic calcite siderite heamatite

Table 5.iii: Lower to middle Ericeira Group, depositional environments and associated early diagenetic phases

Sequence	Systems tract	Depositional environment	Sulphides	Carbonates			Iron-oxide (heamatite)	Paragenetic sequence (early diagenesis only)
				Dolomite	Calcite	Siderite		
Sequence 1 & 2	LST	delta mouth/distributary channels	Absent	Common ferroan dolomite	Absent	Absent	Rare	Dolomite heamatite
Sequence 1	TST HST	restricted lagoonal	Abundant pore-filling framboidal pyrite & pyrite within dolomite lattice	Common ferroan dolomite. Common septarian concretionary non-ferroan dolomite	Rare non-ferroan microspar	Absent		Pyrite ferroan dolomite non-ferroan dolomite non-ferroan microspar
Sequence 2	TST lower HST	restricted lagoonal/ inner shelf	Abundant pore-filling framboidal pyrite & pyrite within dolomite lattice	Common ferroan dolomite	Absent	Absent		Pyrite dolomite
Sequence 2 Sequence 3	upper HST SMW	"normally" prograding shoreface sands	Rare pore-filling euhedral pyrite	Common concretionary zoned non-ferroan dolomite. Rare zoned non-ferroan dolomite	Non-ferroan pore-filing sparry calcite. Non-ferroan poikilotopic concretionary calcite. Non-ferroan poikilotopic calcite	Rare	Rare	Pyrite dolomite/sparry calcite poikilotopic calcite siderite heamatite
Sequence 3	TST HST	Shallow marine carbonates	Rare pore-filling euhedral pyrite	All dolomite calcitised/dissolved	Non-ferroan to ferroan pore filling calcite	Rare		Pyrite dolomite calcite/calcitisation siderite
Sequence 4	LST TST HST	Spits, regressive sand bars and marine muds	Rare pore-filling euhedral pyrite	All dolomite calcitised/dissolved	Non-ferroan poikilotopic calcite	Rare	Rare	Pyrite dolomite poikilotopic calcite siderite heamatite

Table 5.iv: Lower to middle Ericeira Group, depositional environments and associated early diagenetic phases

Chapter 6: Early Diagenesis & High Resolution Sequence Stratigraphy For Mixed Carbonate/Siliciclastic Nearshore Successions

6.1: *Aims*

The previous chapters have demonstrated that the application of diagenetic analyses can be used to support a facies-based identification of key sequence stratigraphic units and surfaces. The principal aim of this chapter is to synthesise these results and combine with other examples from the literature. Recognising the limitations and scope of the data, generalised models are formulated which account for the relationship between early diagenesis and high resolution sequence stratigraphy in nearshore successions. The objectives of these models are to facilitate the: (i) distribution of diagenetic products; (ii) correct identification of sequence stratigraphic units; and, (iii) identification of key correlative stratal surfaces at a variety of scales.

Although the available data-set is limited, the models formulated will provide building-blocks on which more detailed modelling can be produced. The approach taken in this research is demonstrated to be of great value in refining high resolution sequence stratigraphic interpretations and in the prediction of the distribution of diagenetic heterogeneities within reservoir units. At all scales, examples from the two studied sections and, relevant examples from the literature will be used to illustrate key features.

6.2: *Early diagenesis & sequence stratigraphy*

In the two case studies described in this thesis, products of early diagenesis are related to facies-based high resolution sequence stratigraphic models to identify parasequences, systems tracts and sequences. Therefore, early diagenesis was controlled by changes in relative sea-level on three time scales:- (i) the parasequence scale (10^2-10^4 year duration, refer back to Table 1.ii): (ii) the systems tract scale (10^4-10^5 year duration, refer back to Table 1.ii): and, (iii) the sequence scale (10^5-10^6 year duration, refer back to Table 1.ii).

Both successions studied in this research were deposited during "greenhouse" periods (Veevers, 1990) indicating that prolonged duration, high amplitude falls in relative sea-level were rare. Relative sea-level falls were generally of relatively low amplitude and therefore of a short time duration. The majority of sequence boundaries in both successions described in this study have been interpreted as representing no, or relatively minor, falls in relative sea-level. As a direct consequence of this, meteoric diagenesis associated with sub-aerial exposure at sequence boundaries is confined to the relatively shallow sub-surface.

6.2.1: The parasequence scale

Within both the Corallian Group and Ericeira Group successions, there is strong evidence to indicate that early diagenetic processes are controlled by high frequency sea-level changes (10^2-10^4 year duration) on a parasequence scale. This section describes the types

of diagenetic processes and products which can be demonstrated to have formed as a result of sea-level changes at this frequency.

6.2.1a: *Siliciclastic parasequences containing oblate/spherical concretions*

Analysis of concretions within coarser grained sand facies (e.g. the Nothe Grit Formation, Bencliff Grit Member, Sandsfoot Grit Member- all of the Corallian Group succession; and the Calada Member of the Ericeira Group succession) indicates that growth was related to parasequence formation. The preservation of original depositional fabric along with bioclastic material within carbonate concretions, indicates that cementation was predominantly early.

Carbonate concretions:

The presence of pyrite and carbonate with depleted $\delta^{13}C$ isotope values within the concretions, indicates that growth occurred principally within the sub-oxic/sulphate reducing zone. Early diagenetic reactions occurring within this zone were the result of either: (i) dsyaerobic bottom water conditions with no oxidation zone in the upper sediment layers; or, (ii) high sedimentation rates leading to rapid burial of sediment into the zone of sulphate reduction and reduced residence time within the oxidation zone.

Sedimentological and palaeontological evidence from most of the siliciclastic parasequences in both successions indicates that bottom waters were normally oxygenated. This implies that high sedimentation rates associated with parasequence progradation

rapidly buried sediment through the early diagenetic zones (Fig.6.i). Concretions subsequently grew during a period of marine flooding associated with the formation of a parasequence boundary (Fig.6.i). During marine flooding an increase in the rate of accommodation creation and a decrease in the rate of sedimentation results in a period of depositional hiatus (Taylor *et al.*, 1994). As a result, sediments have a longer residence time within early diagenetic zones (i.e. the sub-oxic/sulphate reduction zone) and, as a consequence, a greater amount of early diagenetic precipitation occurs. The presence of well-developed concretions (some up to 1m in size) indicates that periods of low sediment accumulation, associated with marine flooding surfaces, were of sufficient duration to allow the significant build-up of early diagenetic products.

Iron-oxide concretions:

Small iron-oxide concretions are present in some identified siliciclastic parasequences. These formed as the result of slow net sediment accumulation rates during slightly reducing periods within the zone of aerobic respiration (for iron-oxide concretions, after Taylor & Curtis, 1995), the post-oxic zone (Pettijohn, 1975; Desrochers & Al-Aassm, 1993 and McKay *et al.*, 1995), or at the oxic/suboxic boundary (Taylor & Curtis, 1995). A reduction in sedimentation rate occurs in association with marine flooding at parasequence boundaries, due to an increase in the rate of accommodation creation and a cut-off in sediment supply (Fig.6.i). Thus, the common occurrence of these diagenetic products, particularly towards the top of parasequences, suggests that periods of low sediment accumulation associated with marine flooding surfaces were of sufficient duration to allow a significant build-up of diagenetic solutes.

Implications to reservoir geology:

Early diagenesis, controlled by high frequency sea-level changes on a parasequence scale, may lead to the formation of laterally cemented layers beneath parasequence boundaries. This would inevitably result in highly compartmentalised and layered reservoir units, with each lateral heterogeneity (laterally cemented layer) acting as a barrier to vertical fluid flow (Fig.6.i).

Similarly, when free iron is abundant in sediments, this could lead to extensive laterally cemented layers occurring beneath marine flooding surfaces. Consequently, this would result in highly compartmentalised reservoir units and a decrease in vertical permeability flow. The occurrence of these concretions can be used to identify parasequence boundaries and, therefore, aid in interwell and across-field reservoir prediction, reducing the necessity of stochastic modelling techniques.

Field examples:

- **Parasequences in the Nothe Grit Formation (Corallian Group):** Facies and diagenetic analyses indicate that parasequences were deposited within a prograding shoreface environment. Within each parasequence septarian concretions, that grew within the zone of sulphate reduction, occur below marine flooding surfaces in the coarser grained shelly beds. The formation of septarian fractures within such concretions have been attributed to either chemical dehydration and shrinkage (Raiswell, 1971; Pettijohn, 1975), or tensile stress relating to overpressure development

during shallow burial (Astin, 1986; Astin & Scotchman, 1988). As overpressure is unlikely to have occurred in shallow buried sandstones, the hypothesis offered by Raiswell (1971) and Pettijohn (1975) seems to be the more likely mechanism for the concretions described here (see Sections 2.3.1, 3.2.5a and 3.3.1).

- **Parasequences of the Bencliff Grit Member (Corallian Group):** Facies and diagenetic analyses have identified parasequences within this tidal flat environment. The coarser grained beds at the bottom of each parasequence contain large carbonate concretions that grew within a reducing environment. Carbonate concretion growth has been attributed to preferential calcite nucleation upon aragonitic shell material due to a low activation energy (Fleming, 1993) (see Sections 2.3.3, 3.2.5b and 3.3.3a).
- **Parasequences of the Sandsfoot Grit Member (Corallian Group):** Facies and diagenetic analyses have identified one parasequence within this shallowing shoreface environment. The coarser grained beds at the top of the parasequence contain siderite concretions with depleted $\delta^{13}C$ values indicating growth within a sulphate reducing environment. Siderite concretions will grow within the zone of sulphate reduction when pore-waters have very low levels of dissolved sulphide (Pearson, 1979) as well as bicarbonate and Fe^{2+} (see Sections 2.3.6, 3.2.7 and 3.3.6).
- **Parasequences of the middle Calada Member (Ericeira Group):** Facies and diagenetic evidence indicate that parasequences were deposited within a restricted lagoonal environment. The coarser grained beds at the top of each parasequence contain septarian concretions that grew within a sub-oxic/sulphate reducing environment (see Sections 4.2.1, 5.2.3a and 5.3.1).
- **Parasequences within the siliciclastic beds of the Ericeira Group:** Facies and diagenetic evidence have identified parasequences within a range of nearshore

depositional environments. These contain common iron-oxide (haematite) concretions which are associated with parasequence boundary formation. Iron-oxide concretions require low net sediment accumulation rates and prolonged residence time within the zone of aerobic respiration (Taylor & Curtis, 1995) (see Sections 5.2.6 and 5.3.2).

All of the above examples indicate that concretion growth occurs within the coarser grained sandstone facies (which possess greater porosity and permeability values) of each coarsening-up or fining-up parasequence. As parasequence growth is controlled by the depositional setting (i.e. fining-up parasequences are typically found in tidal flat environments), then the position of the sand-body and thus the location of the concretions will vary.

The analysis of early diagenetic processes and products in all of the above examples have aided in the interpretation and identification of parasequences and parasequence boundaries and have highlighted the importance of the marine flooding surface. The importance of the "parasequence model" is that, without the prolonged period of non-deposition associated with parasequence boundary formation, concretion growth would not have been contained within single diagenetic zones.

Other examples from the literature:

- Taylor *et al.* (1994) indicate the presence of early carbonate concretions and laterally extensive carbonate sheets below marine flooding surfaces within lowstand deposits of the Blackhawk Formation, Book Cliffs, Utah. During periods of non-sedimentation

associated with parasequence boundary formation, sediment has a longer residence time within early diagenetic zones. However, evidence obtained from this work indicates that such concretions are not restricted to parasequences in lowstand systems tracts, but are also present in all other systems tracts. This indicates that it is the duration of marine flooding associated with parasequence boundary formation that influences concretion growth and this may be similar in a range of systems tracts depending on the balance between longer term accommodation creation and sedimentation rates. This is an important conclusion in that these concretions are not diagnostic of any specific systems tract, as inferred by Taylor *et al.*(1994).

- Taylor & Curtis (1995) indicate that ironstones of the Lower Lias (Frodingham and Pecten Ironstones) of eastern England have formed under low net sediment accumulation rates during the formation of parasequence-bounding disconformities. These findings are consistent with the interpretations of iron-oxide concretions offered in this thesis.

6.2.1b: *Siliciclastic parasequences containing elongate concretions*

Analysis of carbonate concretions within coarser grained sand facies of the Safarujo Member (Ericeira Group) indicate that during the progradational phase of parasequence formation, pore-waters originating from an up-dip landward location, would flow in an offshore direction along permeability conduits (Fig.6.ii). During the marine flooding phase of parasequence formation, prolonged residence of sediment within the sub-oxic/reducing zone resulted in the growth of elongated concretions, parallel to the original offshore pore-water flow direction.

Implications to reservoir geology:

The growth of elongate concretions on a parasequence scale is likely to lead to highly compartmentalised and layered reservoir units. Concretions will result in the formation of laterally extensive heterogeneities to vertical fluid flow and will also affect directional permeability.

Field examples:

- **Parasequences of the Safarujo Member (Ericeira Group):** Facies and diagenetic evidence indicate that these parasequences were deposited within a prograding shoreface environment and contain elongate non-ferroan dolomite concretions that grew within permeability conduits, parallel to ground-water flow directions (see Sections 4.2.2 and 5.3.2).

Other examples from the literature:

McBride *et al.* (1994) and McBride *et al.* (1995) indicate the presence of oriented and elongated concretions within Tertiary and Pleistocene sandstones of northern and southern Italy. Although their work is unrelated to high resolution sequence stratigraphy, it does indicate that concretions may grow parallel to groundwater flow directions, which is in agreement with my interpretations.

6.2.1c: *Parasequences within carbonate facies*

Parasequences within the carbonate facies of both successions (e.g. the Upton Member and Shortlake Member of the Corallian Group and the Cabo Raso Limestone Member of the Ericeira Group) contain evidence of both marine and meteoric cementation. The type of cementation is dependant on the stratigraphic position of the parasequence within the overall sequence. Parasequences of transgressive systems tracts (e.g. within the Upton Member) are dominated by marine carbonate cements (Fig.6.iiia) and parasequence boundaries are commonly represented by marine hard-grounds. This indicates that periods of marine flooding, winnowing and sub-marine exposure occurred.

Parasequences of highstand systems tracts (e.g. the Cabo Raso Limestone Member) reveal a range of cements that include an early marine phase that is replaced in time by a later meteoric phase (Fig.6.iiib). Meteoric diagenesis may include evidence of minor dissolution/leaching, replacement, cementation and calcrete formation, if the climate was humid or, evaporative dolomite and anhydrite precipitation if the climate was arid. Parasequence boundaries are represented by marine hard-grounds, ravinement or minor karstification surfaces. However the type of parasequence boundary is ultimately dependant on the rate of relative sea-level rise throughout the systems tract and the formation of either a type-1 or type-2 sequence boundary.

Highstand systems tracts that are bounded by type-1 sequence boundaries (e.g. the Cabo Raso Limestone Member) contain parasequences that show strong evidence of meteoric processes and products along with the possible formation of palaeosols at the

parasequence boundary. Highstand systems tracts that are bounded by type-2 sequence boundaries (e.g. the lower beds of the Shortlake Member) contain less evidence of meteoric diagenesis and more evidence of marine diagenesis. The lack of sub-aerial exposure in the latter case means that pedogenic processes will not affect the parasequence boundary.

Implications to reservoir geology:

Parasequences of transgressive systems tracts are likely to contain a high amount of early marine fringing cement. This may prevent grain compaction on burial and so result in the preservation of primary porosity. If hydrocarbons are being generated in a basin, the coarser grained facies of carbonate parasequences in transgressive systems tracts would make desirable reservoir units, particularly as they are likely to be capped by a relatively impermeable zone relating to the period of maximum flooding which would act as a reservoir seal.

On the other hand, carbonate parasequences of highstand and early lowstand systems tracts are likely to contain less marine fringing calcite and so grain compaction and a reduction in the amount of primary porosity are likely to occur (refer back to Fig.3.xiii). However, subsequent meteoric diagenetic processes would lead to extensive dissolution and leaching of the original unstable mineralogy, particularly if the climate was humid, resulting in the creation of secondary porosity. Subsequent meteoric calcite cementation would lead to localised occlusion of porosity and the development of permeability baffles. (NB it must be stressed that if hydrocarbon generation was late in a particular basin, then later burial

diagenetic processes could destroy all porosity making both types of parasequence unsuitable as reservoir units).

Field examples:

- **Parasequences of the lower Upton Member (Corallian Group):** These parasequences were deposited within a shallow shelf environment that represents a transgressive systems tract. The coarser grained facies at the top of parasequences contain clear evidence of laterally extensive marine cementation (fringing calcite and marine stable isotope signatures) and parasequence boundaries are represented by marine hard-grounds (see Sections 2.3.3, 3.2.5d and 3.3.3b);
- **Parasequences of the lower Shortlake Member (Corallian Group):** These parasequences were deposited within laterally accreting spit/tidal inlet environments that represent a highstand systems tract. This systems tract is situated below a type-2 sequence boundary (which ultimately overprinted the diagenesis on this scale, refer to Section 6.2.3). Locally, parasequence tops contain clear evidence of an early phase of marine cementation (fringing calcite cements which prevented early grain compaction) but little evidence of meteoric cementation. Where this does occur, it is represented by non-ferroan pore-filling equant calcite. The parasequence boundaries are generally represented by marine hard-grounds (see Sections 2.3.3, 3.2.5d and 3.3.3b);
- **Parasequences of the Cabo Raso Limestone Member (Ericeira Group):** These parasequences were deposited within shallow shelfal carbonate environments that represent both a transgressive and highstand systems tract. This systems tract is situated below a type-1 sequence boundary (which ultimately overprinted the

diagenesis on this scale, refer to Section 6.2.3). Parasequences contain clear evidence of an early phase of marine cementation (fringing calcite cement preventing early grain compaction) which is replaced in time by extensive replacement, dissolution and further meteoric calcite cementation. Parasequence boundaries are generally represented by ravinement and minor karstic surfaces, indicating that the climate was likely to have been humid (see Sections 4.2.3, 5.2.4d, 5.2.4e, 5.3.3c and 5.3.3d).

Other examples from the literature:

- Read & Horbury (1993) indicate that carbonate parasequences tend to have a "layer cake" stacking pattern. In an arid climate, parasequence cycles can be partly, to completely, dolomitised by pore fluids sourced from the tidal/supratidal surface. Reservoir facies are likely to occur in parasequence tops, where intercrystalline porosity is preserved and porosity occlusion by calcite is rarely significant (apart from marine and beachrock cementation). Dissolution is also negligible. These features result in strongly stratified, layered reservoirs with multiple pay zones. Read & Horbury (1993) cite major producing fields such as the Upper Permian of the Permian Basin, Texas and the Upper Jurassic Arab/Hith of Arabia, as examples.
- According to Read & Horbury (1993), parasequence tops developed in humid climates are planar to microkarsted. Within parasequences, aragonite fossils are commonly leached out, although any secondary porosity is likely to be occluded by either fibrous marine or meteoric equant calcite. Such occlusion of porosity is likely to lead to layered reservoir units containing permeability baffles. These points are in agreement with my findings (although examples of arid climate processes do not occur within

either of the successions studied in this research). However, I have stated that carbonate parasequences of transgressive systems tracts are likely to be more desirable reservoir units, due to the preservation of primary porosity and the stratigraphic location of parasequences beneath a relatively impermeable zone of maximum flooding.

6.2.2: The systems tract scale

The role of sea-level changes at this scale has already been touched on in Section 6.2.1. Ultimately the type of systems tract, and its position within a sequence, will control the early diagenetic products at this scale. Within both of the successions studied in this research, vertical changes in the abundance and type of early diagenetic products (over a time scale of 10^4-10^5 years; refer back to Table 1.ii) indicate that sea-level changes controlled diagenetic processes at this scale. Taking into account the limitations of the data (low-resolution analysis) four generalised models can be formulated. Additional data would ultimately build on these proposals.

6.2.2a: *Upwards increasing values of $\delta^{18}O$ associated with a shelf-margin systems tract*

The low resolution sampling scheme indicates a broad upward increase in the $\delta^{18}O$ value for carbonate cements (from depleted to normal marine signatures). This implies a change in pore-water composition from an earlier mixed marine/meteoric phase to a later marine phase, indicating a progressive increase in the rate of relative sea-level rise leading to a change from a brackish to a more marine pore-water environment. This can be associated

with the development of a shelf-margin systems tract (Fig.6.iv).

Implications to reservoir geology:

An upwards return to a deeper, more tranquil, marine depositional environment from a higher energy shallow marine or tidal flat environment, may lead to an upwards deterioration in the reservoir quality of the systems tract.

Field example:

- **The Bencliff Grit Member (Corallian Group):** This systems tract represents a dominantly tidal flat depositional environment and contains carbonate concretions that reveal a progressive upwards increase in $\delta^{18}O$ values from an initial mixed marine/meteoric composition to a dominantly marine pore-water composition (see Sections 2.3.3, 3.2.5b, 3.2.8a and 3.3.3a).

6.2.2b: *Typical marine diagenetic products associated with a transgressive systems tract*

The main diagenetic process occurring within carbonate transgressive systems tracts was marine cementation (as well as the formation of marine hard-grounds in association with parasequence boundaries). Early diagenetic processes occurring within siliciclastic transgressive systems tracts are less clear. Again, due to the low resolution sampling scheme, this model is generalised and needs to be supported by further work.

Implications for reservoir geology:

The implications for reservoir geology within transgressive systems tracts are similar to those previously discussed in Section 6.2.1d.

Field examples:

- **The lower Upton Member (Corallian Group):** Marine diagenetic products that change upwards from common, well developed, fringing calcite to poorly developed fringing calcite and micrite, dominate this systems tract (see Sections 3.2.5d and 3.3.3b);
- **The lower Cabo Raso Limestone Member (Ericeira Group):** Similarly, marine diagenetic products (fringing calcite cements and micrite) dominate this systems tract (see Sections 5.2.4 and 5.3.3).

Other examples from the literature:

- Loutit *et al.* (1988) report on condensed sections in continental margin sequences which are most extensive at the time of maximum transgression (i.e. during the deposition of the transgressive systems tract). In their model, they state that a decrease in terrigenous sedimentation rates produced by a sea-level rise, can be associated with a concentration of organic matter and authigenic minerals such as glauconite, phosphorite and siderite. Although their model does not include any detail on how these authigenic phases grow, it does state that concentration and preservation of organic matter in particular, is

dependant on bottom water conditions.

- Tucker (1993) states that, as relative sea-level is rising throughout the duration of a transgressive systems tract, sediments will be buried with marine pore-fluids filling pore spaces. The consequence of this is that further diagenetic changes are likely to be reduced until the composition of the pore-waters changes (i.e. during a fall in relative sea-level) or, burial continues into the zone of compaction. Early marine fringing cementation will prevent any subsequent burial compaction, enhancing the reservoir potential of the rock. This is in agreement with the interpretations offered in this thesis.

6.2.2c: *Upward increasing volumes of early diagenetic products associated with a highstand systems tract*

Both of the successions described in this thesis show one to ten metre thick upward increasing trends in the volume of pore-filling authigenic products that were precipitated within the zone of sulphate reduction (Fig.6.v). These are contained within coarser grained beds of individual parasequences and the process of precipitation is that described in Section 6.2.1a. An upward increase in authigenic products indicates that the rate of sedimentation/sediment burial of each parasequence increases with time, a pattern which is consistent with a progradational period during a highstand systems tract. With an increase in the rate of progradation of each parasequence, sediment will be rapidly buried thus spending less residence time within the zone of oxidation and more residence time within the zone of sulphate reduction. As a consequence, during periods of marine flooding associated with parasequence boundary formation, the intensification of large values of early diagenetic reactions within the zone of sulphate reduction would allow the build-up

of solutes within the sediment and the precipitation of large volumes of early diagenetic products.

Implications to reservoir geology:

Highstand systems tract reservoir units would be expected to show an upward increase in the degree of cementation. This would lead to an upward increase in the size and extent of laterally extensive cemented horizons or reservoir heterogeneities (Fig.6.va). If the highstand systems tract is bounded above by a type-2 sequence boundary (e.g. the HST of Sequence 3, the Shortlake Member, Corallian Group), then the lack of sub-aerial exposure would render the effects of dissolution and subsequent secondary porosity creation as negligible. Reservoir heterogeneities would remain laterally extensive resulting in a "layer cake" geometry (after Weber & Geuns, 1990, my Fig.6.va(A)). If the highstand systems tract is bounded above by a type-1 sequence boundary and the climate is humid (e.g. the HST of Sequence 3, the Cabo Raso Limestone Member, Ericeira Group), then reservoir heterogeneities would be partially to completely dissolved by meteoric processes. Reservoir heterogeneities would then be "broken" leading to vertical connectivity of reservoir pay-zones. This type of reservoir unit would result in a "jigsaw puzzle" geometry (after Weber & Geuns, 1990, my Fig.6.va(B)).

Field examples:

- **The upper Nothe Clay Member/lower Bencliff Grit Member (Corallian Group):** This contains patchy, upward increasing volumes of authigenic pyrite and ferroan

dolomite, both products of bio-chemical reactions occurring within the zone of sulphate reduction. This systems tract is bounded above by a type-2 sequence boundary (Fig.6.va(A) and see Sections 2.3.2, 3.2.8 and 3.3.2).

- **The upper Upton Member/lower Shortlake Member (Corallian Group):** This contains upwards increasing volumes of authigenic pyrite and ferroan dolomite that were precipitated within the zone of sulphate reduction. It is bounded above by a type-2 sequence boundary (Fig.6.va(A) and see Sections 2.3.3, 3.2.8 and 3.3.3).
- **The lower Safarujo Member (Ericeira Group):** Contains upward increasing volumes of pyrite and dolomite that were precipitated within a sub-oxic/sulphate reducing environment. Non-ferroan to ferroan dolomite cement forms laterally extensive cemented beds which would act as permeability baffles to vertical fluid flow. The lower Safarujo Member is bounded above by a type-2 sequence boundary (Fig.6.va(A) and see Section 5.3.2).

6.2.2d: *Upwards change from marine to meteoric early diagenetic products associated with a highstand systems tract*

The main diagenetic patterns of highstand systems tracts that developed during phases of carbonate deposition are an initial marine phase that is replaced upward by a meteoric phase. Carbonate cements also reveal a progressive upward decrease in $\delta^{18}O$ values. The meteoric processes that may occur, will be dependant on the amount of relative sea-level fall at the sequence boundary, and whether the climate is humid or arid. The prolonged duration of systems tract formation indicates that early diagenetic processes at this scale will be more pronounced than at the parasequence scale.

Field examples:

- **The upper Upton Member/lower Shortlake Member (Corallian Group):** This example is characterised by an initial phase of marine diagenesis represented by laterally extensive fringing calcite cements, that was replaced in time by meteoric cementation in the form of a locally extensive meteoric lens. This later phase was not associated with a relative sea-level fall or a period of sub-aerial exposure. Subsequent dissolution associated with surface related processes was therefore negligible. The lower Shortlake Member is bounded above by a type-2 sequence boundary (Fig.6.va(A) and see Sections 3.2.5d and 3.3.3b).
- **The Cabo Raso Limestone Member (Ericeira Group):** This example is characterised by an initial phase of marine diagenesis (fringing calcite cement) that was replaced in time by the processes of meteoric diagenesis (laterally extensive cementation, dissolution and replacement of dolomite). This later phase was extensive because: (i) the systems tract was capped by a period of sub-aerial exposure; and (ii) the presence of a karstic surface indicates that the climate was humid. The Cabo Raso Limestone Member is bounded above by a type-1 sequence boundary (Fig.6.va(B) and see Sections 4.2.3 and 5.3.3).

Other examples from the literature:

- Tucker (1993) states that marine cementation will be initially important along carbonate ramp shorelines during highstand progradation. However, due to continued progradation, marine sediments soon come under the influence of the subaerial

diagenetic environment where supratidal diagenesis and evaporite dolomitisation may be dominant.

- In a humid climate, Tucker (1993) states that initial marine diagenesis will be replaced by meteoric dissolution and cementation resulting in the formation of karstic surfaces and calcretes. The effect of these will be more pronounced towards the top of a highstand systems tract. This is in agreement with the interpretations offered in this thesis.

6.2.3: The sequence scale

Diagenetic processes that occur on a time scale of 10^5-10^6 years, can be associated with a fall in relative sea-level and subsequent sub-aerial exposure, or no fall in relative sea-level and no period of sub-aerial exposure. Both successions studied in this research were deposited during global "green-house" periods when third order sea-level changes were not necessarily of a large enough amplitude to result in extensive sub-aerial exposure. Thus, sequences are not always bounded above by type-1 boundaries. Even when a sequence boundary does represent a fall in relative sea-level, it may be of such a small duration that it results in only minor sub-aerial exposure.

Two examples of early diagenesis controlled by sea-level changes at the sequence scale will be cited: (i) a sequence bounded above by a type-2 sequence boundary; and, (ii) a sequence bounded above by a type-1 sequence boundary that formed in a humid climate. Other examples from the literature, in particular the differences between "ice-house" and

"green-house" periods will be discussed at the end of this section.

6.2.3a: *Preservation of early diagenetic products during the formation of a type-2 sequence boundary*

With the formation of a type-2 sequence boundary, the rate of eustatic sea-level fall is equivalent to the rate of subsidence, resulting in little or no basinward shift in coastal onlap and limited or no subaerial exposure (Posamentier & Vail, 1988). This implies that there will be no basinward shift in diagenetic environments and early diagenetic products of the underlying sequence would be preserved (Fig.6.vi). A small meteoric pore-water lens may develop, originating from an up-dip location in response to any sub-aerial exposure, which would flow in an offshore direction. Any dissolution or replacement of earlier diagenetic products will be rare.

Implications for reservoir geology:

The low rates of dissolution associated with a type-2 sequence boundary, would result in a reduction in the amount of secondary porosity, particularly in the highstand systems tract. This would inevitably reduce reservoir quality. However, low rates of further replacement and meteoric cementation, would result in less destruction of primary porosity, which would have been particularly well developed in the transgressive systems tract (refer back to Section 6.2.2b). Thus, reservoir units that are bounded above by a type-2 sequence boundary may have small pay-zones, predominantly contained within the lower systems tracts of the sequence.

Field example:

- **Sequence 3 of the Corallian Group (Bencliff Grit Member, Upton Member and lower Shortlake Member):** This sequence is bounded above by a type-2 sequence boundary, which shows no evidence of an abrupt fall in relative sea-level. Consequently, the extensive early diagenetic cementation of the underlying systems tracts have been preserved, with no evidence of dissolution or replacement by meteoric pore-fluids. A small meteoric lens developed within the upper parasequences of the highstand systems tract as indicated by petrographic and analytical characteristics. This was not associated with phases of dissolution or replacement (see Sections 2.3.3 and 3.3.3).

6.2.3b: *Dissolution & replacement of early diagenetic products during the formation of a type-1 sequence boundary*

With the formation of a type-1 sequence boundary, the rate of eustatic sea-level fall is greater than the rate of subsidence, resulting in a basinward shift in coastal onlap and a period of prolonged subaerial exposure (Posamentier & Vail, 1988; Hendry, 1993a). Associated with a fall in relative sea-level, a basinward shift in diagenetic environments would lead to extensive dissolution, replacement and further cementation of the old sequence (Fig.6.vii). Meteoric pore-waters would penetrate deep into the underlying sediments and karst surfaces would develop on the sequence boundary if the climate is humid.

Implications for reservoir geology:

Depending on the level of relative sea-level fall, all systems tracts within the sequence may be effected by meteoric processes including dissolution. This would ultimately improve reservoir quality by creating secondary porosity, although replacement and further cementation may actually counteract the improvement. Laterally cemented layers within the highstand systems tract are likely to be partially dissolved, leading to a "jigsaw puzzle" geometry and multiple vertically and laterally connected pay-zones (Fig.6.va(B)).

Field example:

Sequence 3 of the Ericeira Group (upper Safarujo Member and the Cabo Raso Limestone Member): This sequence is bounded above by a type-1 sequence boundary, which shows evidence of karstification and sub-aerial exposure. Consequently, the early diagenetic cements within the underlying systems tracts were subjected to extensive replacement and dissolution, along with further meteoric cementation. Early formed dolomitic concretions within the siliciclastic shelf-margin systems tract have been replaced by a phase of meteoric calcite cement. Early forming marine cements and authigenic products of the sulphate reducing zone, found within the carbonate systems tracts have been partially dissolved while pore-space has been occluded by a phase of meteoric calcite that contains a patchy bright luminescence (as revealed by CL, see Sections 4.2.3 and 5.3.3).

Other examples from the literature:

- Tucker (1993) states that during "green-house" periods third order relative sea-level changes produce thick sequences that are bounded above and below by unconformities or correlative conformities. Such third order sequences dominate the two successions studied in this research. However, during "ice-house" periods, much thinner sequences are produced by high amplitude fourth/fifth order sea-level changes on a much greater scale than any third order sea-level change. Tucker (1993) cites the Quaternary carbonate sequences of Barbados and the Bahamas as representing fourth/fifth order sequences.
- Tucker (1993) states that the type of sequence will also control the style and degree of diagenesis. Under a humid climate, sequences that formed during "ice-house" periods will have deep karsts developed on sequence bounding surfaces during lowstand periods. Tucker (1993) cites "the blue holes" of the Bahama platform as an example. However, during "green-house" periods, minor karst may develop at parasequence or sequence boundaries. Sequence 3 of the Ericeira Group cited above provides a good example of a similar "green-house" sequence.
- Tucker (1993) also states that relative sea-level changes during "ice-house" periods will lead to more rapid pore-fluid movements than during "green-house" periods. As a consequence, deep meteoric penetration will lead to extensive leaching and grain dissolution during "ice-house" periods, but will be confined to the near-surface during "green-house" periods.
- Read & Horbury (1993) cite a number of examples of reservoir units that are associated with "ice-house" periods (high amplitude fourth/fifth order sea-level changes) and

"green-house" periods (long-term third order sea-level changes). Amongst these are the Miocene carbonate reservoirs of Northeast Syria, Northwest Iraq and the Red Sea which were deposited during "ice-house" periods and, the Upper Jurassic Smackover Formation of the U.S. Gulf Coast which was deposited during a "green-house" period.

6.3: *Concluding remarks*

- The combination of facies and early diagenetic analyses within a high resolution sequence stratigraphic framework has led to the development of generalised models (taking into account the scope of the available data). These models are designed to help predict the distribution of heterogeneities (cemented beds/concretions) within petroleum geology reservoirs and simulation studies.
- Early diagenesis can be modelled on the three main high resolution sequence stratigraphic scales:-
    - the parasequence scale (10^2-10^4 year duration);
    - the systems tract scale (10^4-10^5 year duration);
    - and the sequence scale (10^5-10^6 year duration);

  Each scale is controlled by differing amplitudes and durations of relative sea-level change. As both successions described in this thesis occur within a "green-house" period, large scale falls in relative sea-level are rarely associated with sequence boundary formation and no periods of deep fluvial incision occur during lowstands. However, in some sequences, the processes of surface related meteoric diagenesis are

still evident.

- Analysis of concretions not only supports a facies based identification of parasequences, but also allows for a generalised prediction of such reservoir heterogeneities within siliciclastic successions. The available data have indicated that such concretionary bodies are not restricted to lowstand systems tract, as previously stated.
- Similarly, analysis of early diagenetic cements can be modelled at a systems tract and sequence scale. This has led to the development of generalised models which predict the distribution of reservoir heterogeneities at these scales. An important factor in improving reservoir heterogeneity is the amplitude and duration of relative sea-level fall associated with sequence boundary formation, coupled with the duration of any sub-aerial exposure and the climate.
- With no fall in relative sea-level (i.e. the formation of a type-2 sequence boundary) preservation of earlier formed diagenetic products will occur. The lack of sub-aerial exposure will only provide a small elevation head for meteoric diagenetic processes and as a result, there will be little evidence of the effects of meteoric diagenesis. Due to a lack of grain dissolution, the reservoir quality of this sequence would not be high (although any primary porosity may be preserved by early marine fringing calcite). Based on facies and diagenetic evidence, Sequence 3 of the Corallian Group (Bencliff Grit Member to lower two oolitic beds of the Shortlake Member) provides a good example of this.
- With an abrupt fall in relative sea-level (i.e. the formation of a type-1 sequence boundary) a period of sub-aerial exposure will occur. This will provide a large elevation head for deep penetration by meteoric pore-waters, resulting in extensive

replacement, dissolution and cementation of the underlying systems tract. Any dissolution and creation of secondary porosity, may improve the reservoir quality of this type of sequence. Sequence 3 of the Ericeira Group succession (mid-upper Safarujo Member to Cabo Raso Limestone Member) provides an excellent example of this.

- Finally, the proposed models have been formulated using a low resolution data-set. They will however form the foundations for further higher resolution analyses.

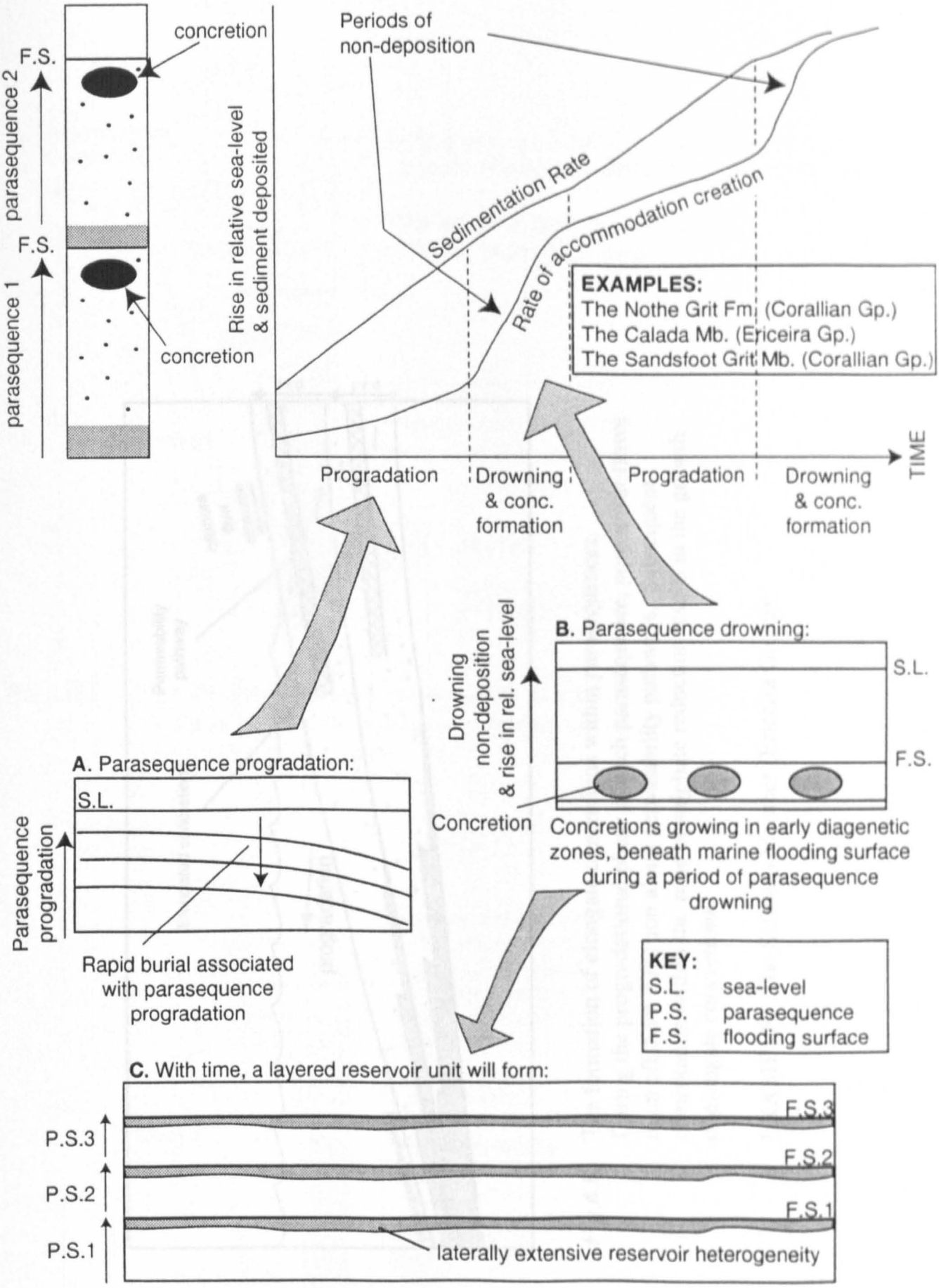

Fig.6.i: Sedimentation rate vs. accommodation creation rate during the progradation of two parasequences. Block diagrams (A & B) illustrate rapid burial during parasequence progradation (A), followed by concretionary growth during marine flooding, non-deposition and parasequence boundary formation (B). (C) illustrates how a layered reservoir unit will form over a period of time, due to the progradation & drowning of subsequent parasequences. Individual concretions beneath marine flooding surfaces will act as laterally extensive reservoir heterogeneities.

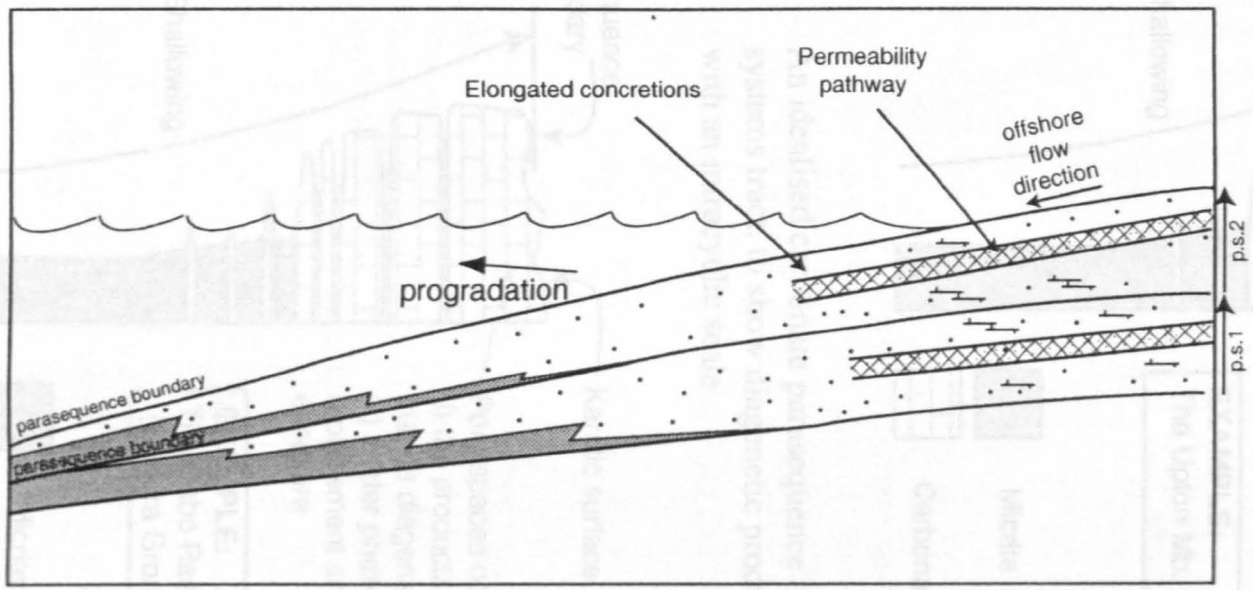

Fig.6.ii: The formation of elongate concretions within parasequences. During the progradational phase of each parasequence, pore-water flows in an offshore direction along permeability pathways. Subsequent cementation within the zone of sulphate reduction results in the growth of elongate concretions.

EXAMPLE: The Safarujo Member (Ericeira Group)

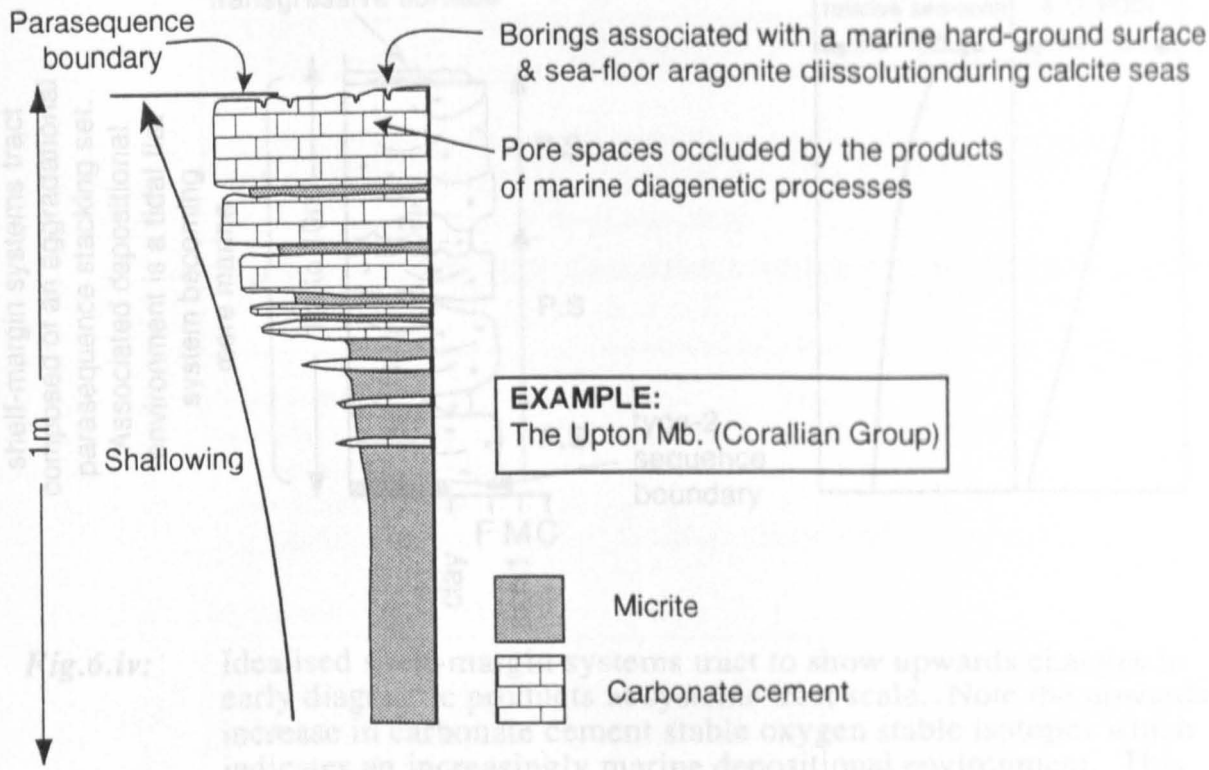

Fig.6.iiia: An idealised carbonate parasequence of a transgressive systems tract, to show diagenetic products associated with an intracyclic scale

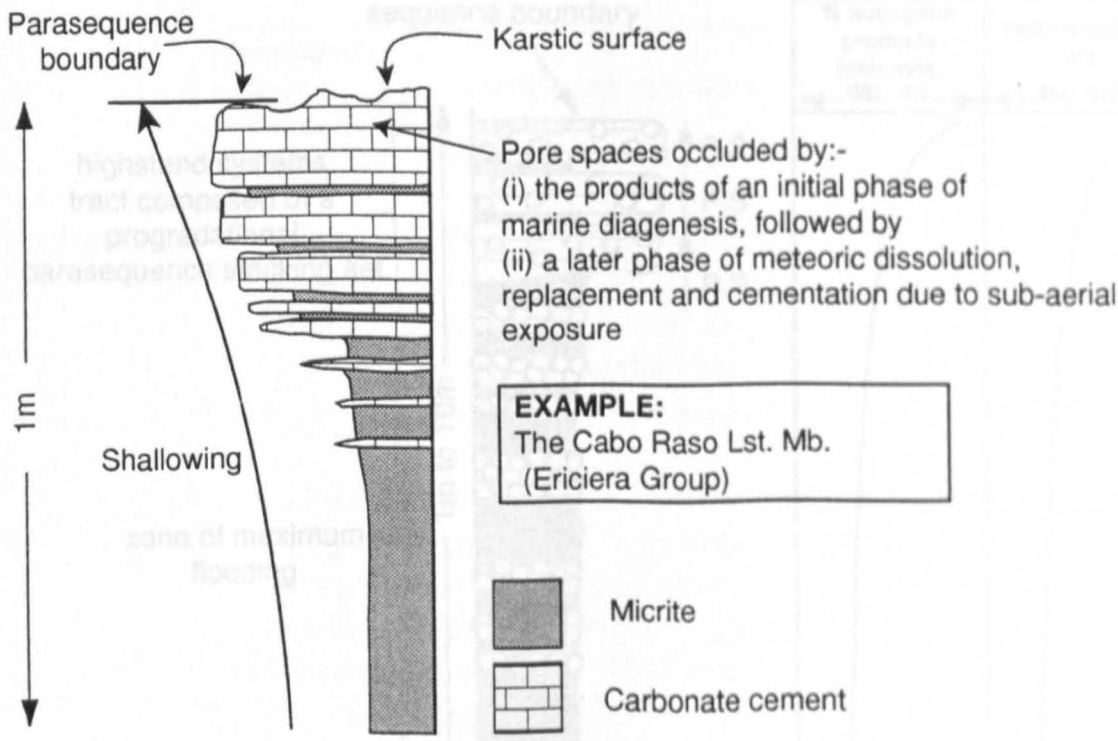

Fig.6.iiib: An idealised carbonate parasequence of a highstand systems tract (humid climate & bounded above by a type-1 sequence boundary) to show diagenetic products associated with an intracyclic scale

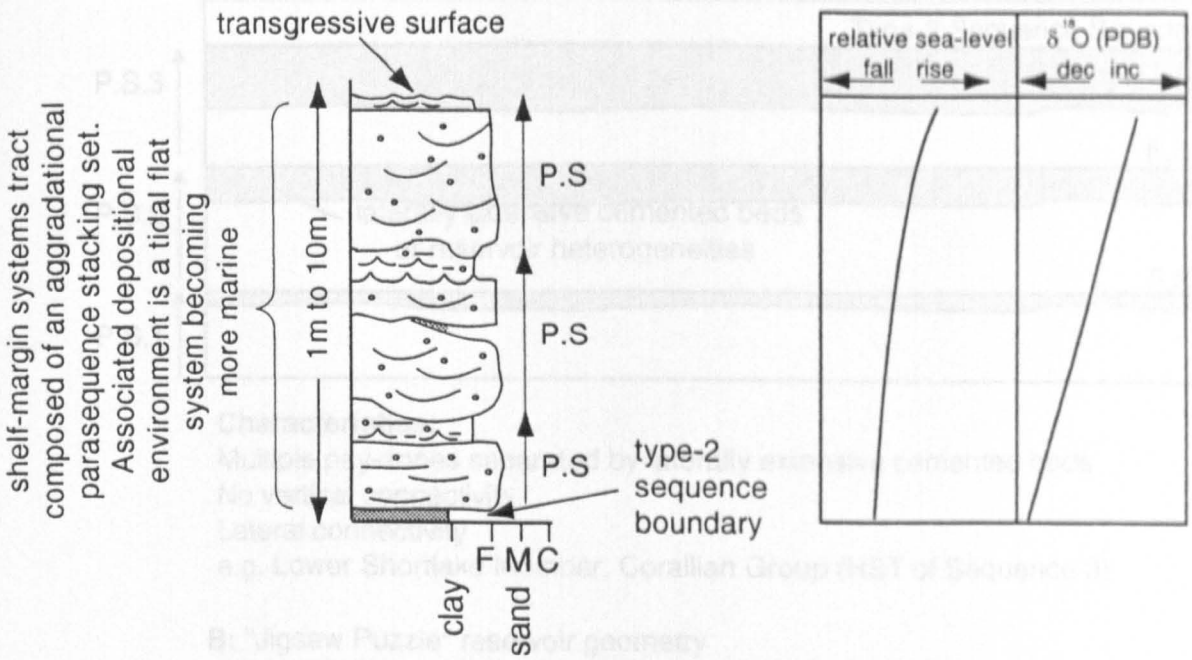

Fig.6.iv: Idealised shelf-margin systems tract to show upwards changes in early diagenetic products at systems tract scale. Note the upwards increase in carbonate cement stable oxygen stable isotopes which indicates an increasingly marine depositional environment. This can also be associated with a gradual rise in relative sea-level. (N.B. BASED ON A LIMITED NUMBER OF SAMPLES)

EXAMPLE: The Bencliff Grit Mb. (Corallian Group)

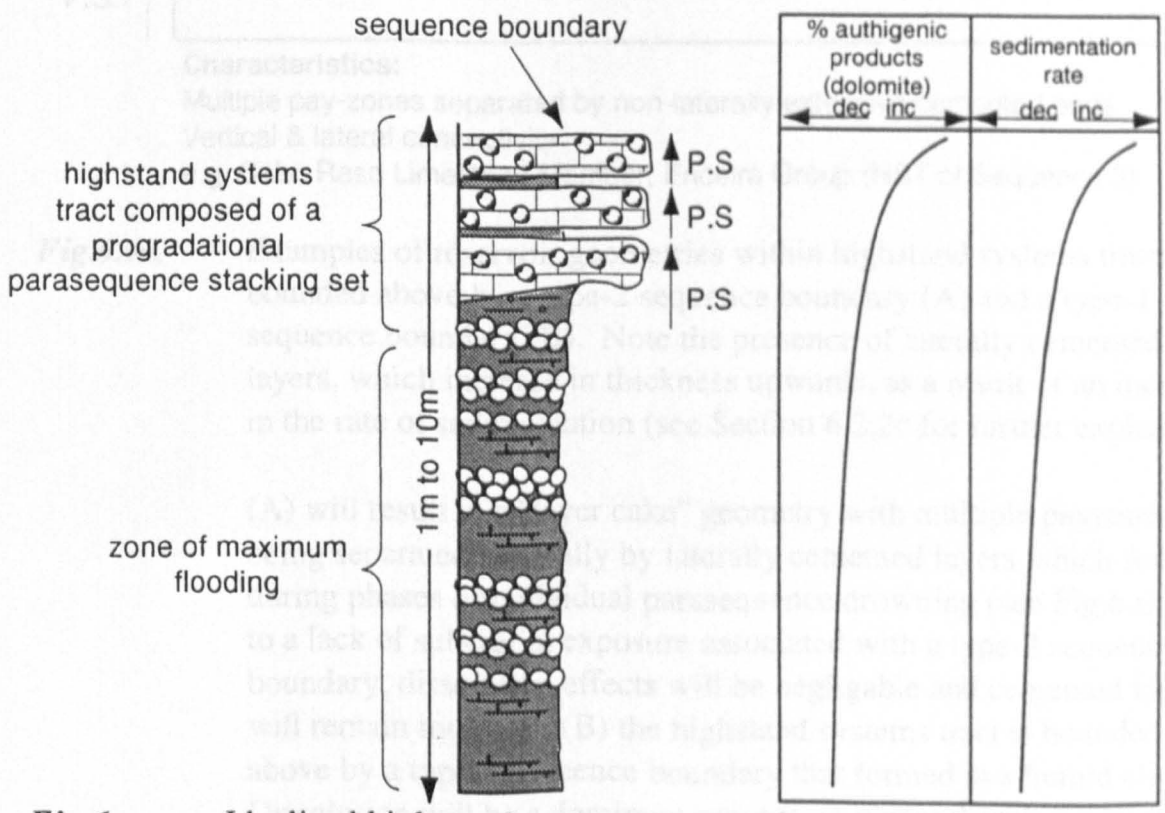

Fig.6.v: Idealised highstand systems tract to show upwards changes in early diagenetic products at a systems tract scale. Note the upwards increase in % authigenic products which can be associated with an upwards increase in sedimentation rates (at this scale).
EXAMPLE: The upper Upton Mb. to lower Shortlake Mb. (Corallian Group) (N.B. BASED ON A LIMITED NUMBER OF SAMPLES

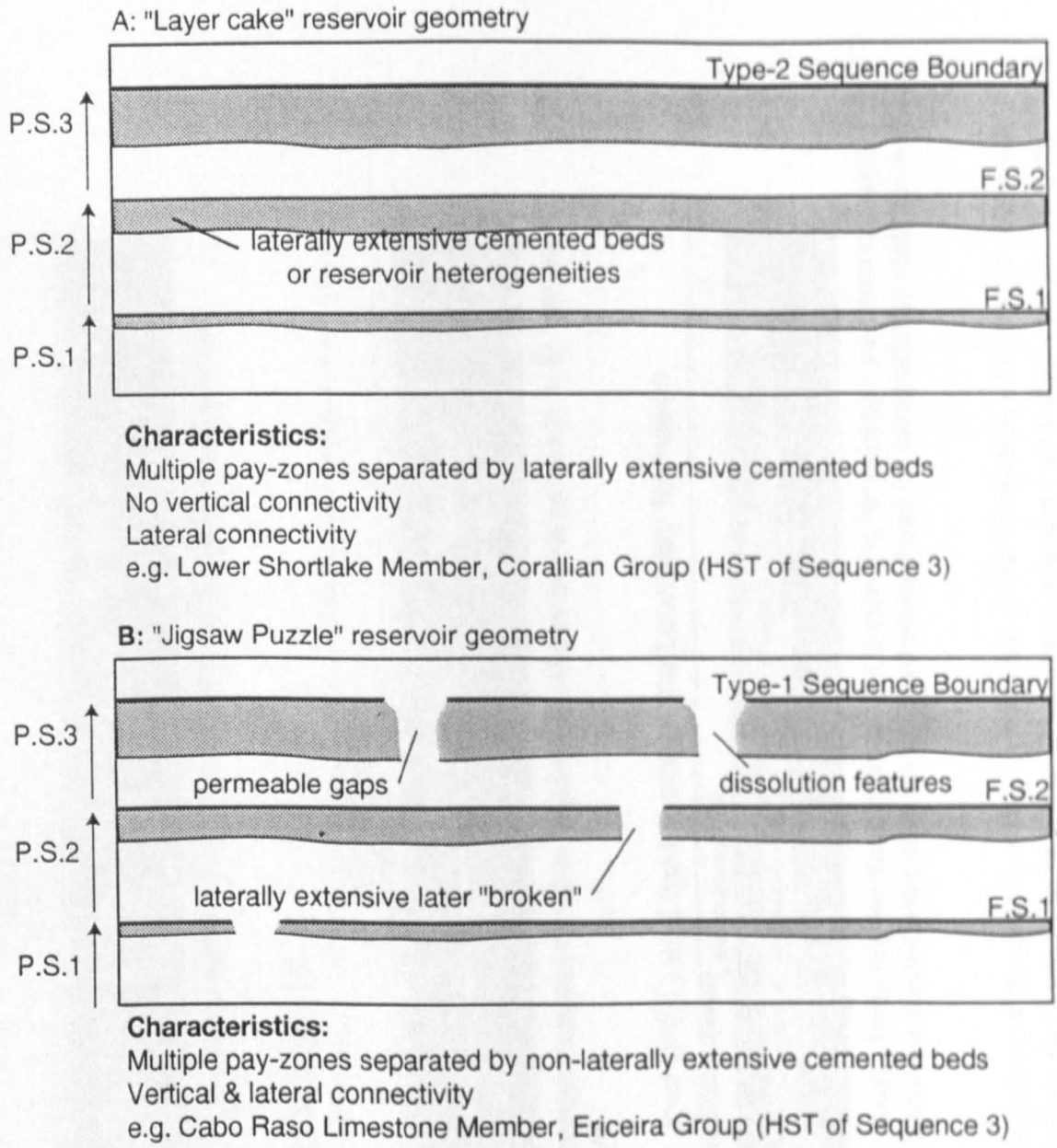

Fig.6.va. Examples of reservoir geometries within highstand systems tracts bounded above by a type-2 sequence boundary (A) and a type-1 sequence boundary (B). Note the presence of laterally cemented layers, which increase in thickness upwards, as a result of an increase in the rate of sedimentation (see Section 6.2.2c for further explanation).

(A) will result in a "layer cake" geometry with multiple payzones being separated vertically by laterally cemented layers which formed during phases of individual parasequence drowning (see Fig.6.i). Due to a lack of sub-aerial exposure associated with a type-2 sequence boundary, dissolution effects will be negligable and cemented layers will remain intact. In (B) the highstand systems tract is bounded above by a type-1 sequence boundary that formed in a humid climate. Dissolution will be a dominant process, in places dissolving laterally cemented layers. This will result in vertical connectivity between reservoir pay-zones.

P.S. - parasequence; F.S. - flooding surface

A) Shelf-margin systems tract (SMW)

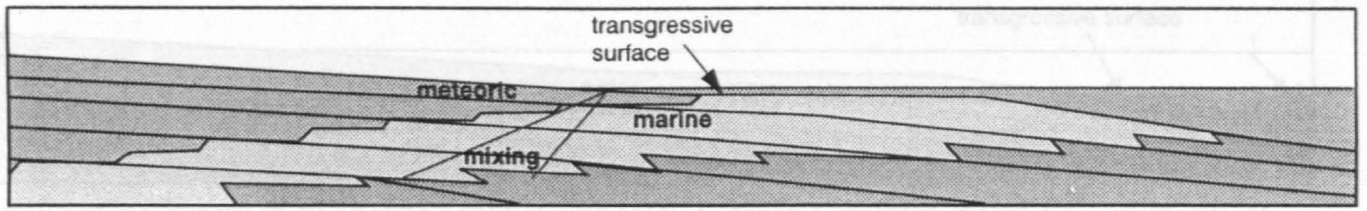

Generally static diagenetic zones during SMW. Thus earlier cements of the old sequence will be preserved

B) Transgressive systems tract (TST)

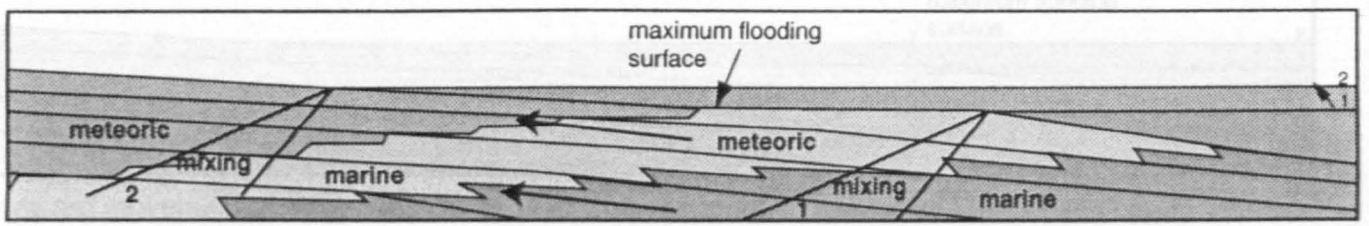

Landward movement of diagenetic zones (1 to 2) in response to relative sea-level rise (1 to 2). Marine diagenesis of TST sediments

C) Highstand systems tract (HST) and type-2 sequence boundary formation

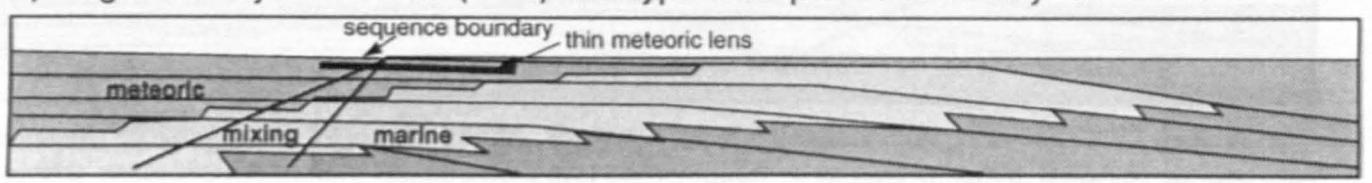

Generally static diagenetic zones. Early marine diagenesis of HST sediments folowed by rare & thin meteoric lens development providing there is a sufficiently large enough hydrostatic head for penetrationby meteoric waters.

Fig.6.vi: Model to show the movement of diagenetic zones in response to the formation of a type-2 sequence boundary. Note that during the formation of a type-2 sequence boundary and shelf-margin systems tract, there is little movement of diagenetic zones.

EXAMPLE: Sequence 3 of the Corallian Group (comprising the Bencliff Grit Mb. - lower Shortlake Mb.)

A) Lowstand systems tract (LST)

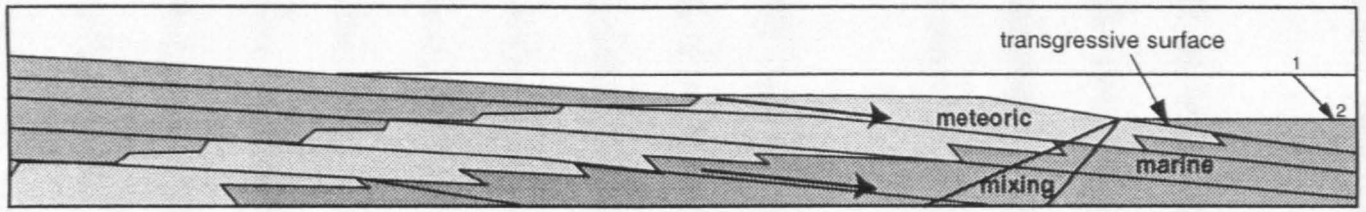

Basinward movement of diagenetic zones during LST. Extensive meteoric dissolution, replacement and cementation of older sequence

B) Transgressive systems tract (TST)

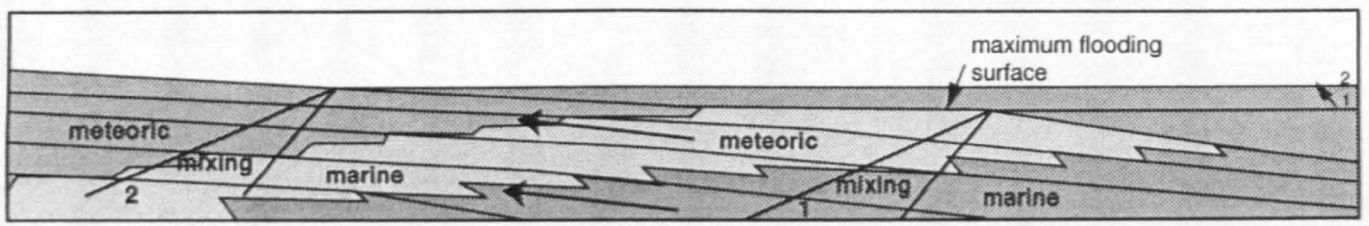

Landward movement of diagenetic zones (1 to 2) in response to relative sea-level rise (1 to 2). Marine diagenesis of TST sediments

C) Highstand systems tract (HST) and type-1 sequence boundary formation

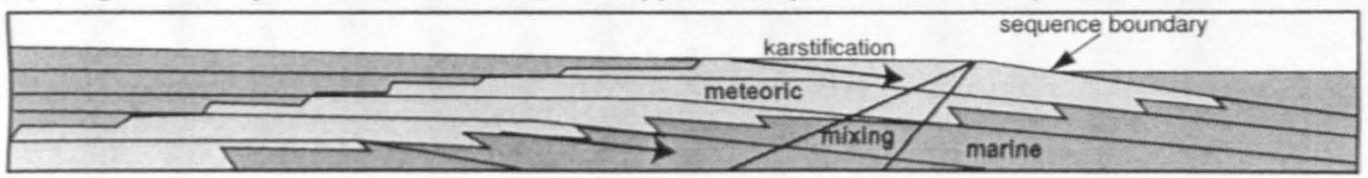

Basinward movement of diagenetic zones. Early marine then meteoric diagenesis of HST sediments, including meteoricdissolution, replacement and cementation. If climate is humid, a karstic surface may develop.

Fig.6.vii: Model to show the movement of diagenetic zones in response to the formation of a type-1 sequence boundary. Note that during the formation of a type-1 sequence boundary and lowstand systems tract, the movement of diagenetic zones is in a basinward direction, which exposes older sediments to the effects of surface related meteoric diagenetic processes. (N.B. The mixing zone has been simplified to represent a "wedge". However changing poroperm values would greatly affect the shape of this zone) **EXAMPLE:** Sequence 3 of the Ericeira Group (upper Safarujo Mb. - top of the Cabo Raso Lst. Mb.)

Chapter 7: Conclusions

7.1: *Introduction*

In this research, high resolution sequence stratigraphic frameworks have been established for two nearshore mixed carbonate/siliciclastic successions, using facies and early diagenetic analyses. These are the Upper Jurassic Corallian Group of south Dorset and the Lower Cretaceous, lower to middle Ericeira Group of west central Portugal.

For each succession, a facies-based sequence stratigraphic model was constructed from field-work based on available exposures within a relatively small area and previously published biostratigraphy. Published data were incorporated where available to further constrain each model within a regional context. In each succession it was discovered that at certain key stratal surfaces or within key stratal units, the field evidence and published data were not sufficient to produce an unequivocal sequence stratigraphic interpretation. This was especially true for the Corallian Group succession and led to a change in the diagenetic objectives of the research. The new objectives were to see whether an analysis of the type and distribution of early diagenetic products would provide further evidence to support the facies-based sequence stratigraphic proposals.

A relatively low resolution sampling scheme was implemented, with sample collection concentrated within concretions, cemented beds, at key stratal surfaces and within facies which would yield results. Clay-rich facies (which constitute approximately 32% of the

Corallian Group and 24% of the Ericeira Group) were not sampled due to the effects of clay authigenesis and organic reactions over-printing earlier diagenetic evidence. Petrographic, analyses were performed on a 142 samples, with further XRD, CL and stable isotope analyses on selected samples. The early diagenetic evidence from within the majority of these cemented bodies supported the proposed facies-based sequence stratigraphic interpretation of parasequences, systems tracts and sequences, although some uncertainties remain.

Both of the successions studied during this research were deposited in the Mesozoic "green-house" period, when large scale falls in relative sea-level associated with sequence boundary formation were rare. Instead, relative sea-level falls were generally of a shorter duration and smaller scale and this has had an important input on the nature of sedimentological and diagenetic processes.

Once it had been established that early diagenesis could be used to support a facies based sequence stratigraphic interpretation, generalised were constructed with the view to predicting the distribution of early diagenetic products within the hierarchical range of high resolution sequence stratigraphy (the parasequence, systems tract and sequence). It is accepted that these are based on a relatively low resolution sampling procedure. It is hoped that these models may be expanded and utilised to help predict the distribution of early diagenetic products between well control points within reservoirs. This is of key importance when predicting the performance of particular reservoir units in simulation studies.

7.1.1: Summary of key points

The overall aims of the research were to:-

- assess whether the distribution of diagenetic features in nearshore successions could be explained within a sequence stratigraphic context;
- to assess whether the identification and analysis of these features could be used to aid sequence stratigraphic interpretations; and,
- to use sequence stratigraphy to predict the distribution of early diagenetic heterogeneities at the field/interwell scale.

The results of this thesis indicate that early diagenesis is a valuable tool when interpreting the high resolution sequence stratigraphy of nearshore successions, particularly when a field based high resolution sequence stratigraphic approach is not always possible, or does not yield equivocal results. A facies based high resolution analysis was found to be much more problematic when applied to the Corallian Group succession than the Ericeira Group. Some of the reasons for this have been stated in the concluding paragraphs of Chapters 2 and 4, but can be summarised as:-

- the difficulty in clearly defining parasequences within much of the Corallian Group due to a lack of unequivocal relative water depth indicators. This is probably due to the relatively protected nature of the shoreface sediments, identified by an absence of storm generated bedforms. Conversely, in the Ericeira Group, the shoreface was probably less protected and relative water depth indicators were often more obvious;
- difficulty in the interpretation of some stratal surfaces within the Corallian Group (for the same reasons as stated above); and,

- relatively poor quality, non-continuous exposure of the Corallian Group.

Despite these restrictions, the following conclusions have been made in support of the aims of the thesis.

7.1.1a: *The Parasequence Scale*

1. Early diagenetic analyses of carbonate and iron-oxide concretions supported a facies-based identification of parasequences within both successions (e.g. parasequences of the Nothe Grit Formation, Corallian Group and parasequences of the restricted lagoonal facies of the Calada Member, Ericeira Group). These analyses have indicated that concretionary growth is controlled by an initial phase of rapid burial, equating to the period of parasequence progradation, followed by a period of prolonged residence within a single diagenetic zone. This equates to a period of non-deposition/marine flooding at a parasequence boundary.
2. Analysis of early diagenetic features in carbonate cemented beds supports facies-based identification of parasequences (e.g. the parasequences of the Upton Member, Corallian Group). In the São Lourenço Mudstone Member of the Ericeira Group, facies analysis gave no indication of parasequences. However, subsequent analysis of early diagenetic dolomite within coarser grained cemented beds successfully defines parasequences, because this diagenetic phase is related to a prolonged residence time within an early diagenetic zone, which is related to non-deposition/marine flooding at a parasequence boundary.

7.1.1b: *The Systems Tract Scale*

3. A general upward increase in the volume of early diagenetic products (particularly dolomite) occurs within highstand systems tracts (e.g. the upper Nothe Clay Member/lower bed of the Bencliff Grit Member of the Corallian Group). This was attributed to an increase in residence time within early diagenetic zones as the rate of progradation/burial increased and the rate of non-deposition/marine flooding at parasequence boundaries remained constant.
4. An upward increase in the $\delta^{18}O$ isotope values of carbonate cements (to a more marine value) occurs within shelf-margin or lowstand systems tracts (e.g. the Bencliff Grit Member of the Corallian Group). This pattern would be expected towards the top of such systems tracts, where rates of relative sea-level are rising increasingly quickly.
5. A dominance of marine cements occurs within coarser grained beds of transgressive systems tracts (e.g. the lower part of the Upton Member, Corallian Group).

7.1.1c: *The Sequence Scale*

6. Within carbonate successions, early diagenesis are particularly useful in discriminating between type-1 and type-2 sequence boundaries (bearing in mind that both successions were deposited within the Mesozoic "green-house" period (Veevers, 1990)). Associated with type-1 sequence boundaries was evidence of cementation, dissolution and replacement of early phases by meteoric pore-water. A good example is the mid-upper part of the Safarujo Member and Cabo Raso Limestone Member (Sequence 3) of the Ericeira Group. In this example, field analysis suggested a possible karstic surface

that capped this sequence.

7. Type-2 sequence boundaries are associated with minor meteoric cementation which is confined to localised areas immediately beneath the sequence boundary. An example here is the Bencliff Grit Member to lower part of the Shortlake Member (Sequence 3) of the Corallian Group. In this example the identification of meteoric cements has resulted in a slight repositioning of the sequence boundary from existing sequence stratigraphic models (Coe, 1995).

7.1.1d: *Limitations*

Limitations to this method of study can be summarised as follows.

1. The method failed to support a facies based sequence stratigraphic interpretation of parasequences where there was no early diagenetic cement control or where there was later diagenetic over-printing.
2. The use of early diagenesis in the identification of some systems tracts (particularly in siliciclastic successions) is problematic. This may be a factor of the low resolution sampling scheme and/or poor exposure making sampling more difficult. More detailed analysis is needed to provide unequivocal interpretations.
3. The method employed does not allow an unequivocal identification of maximum flooding surfaces. This again is probably a factor of the low resolution sampling scheme and the fact that all of the maximum flooding surfaces in the two successions would have occurred within unconsolidated, mud rich facies where sampling was extremely difficult. However, various workers (e.g. Pope & Read, 1997) have shown that maximum flooding surfaces cannot be identified in outcrop or core and the only

tool that can identify them is the Gamma Log.

4. The use of early diagenesis to identify sequence boundaries (and key stratal surfaces) in siliciclastic successions can be problematic. This is partly due to the low resolution sampling scheme, the limited exposure and dominantly "green house" geological time period in which these successions were deposited (i.e. not relating to any prolonged periods of sub-aerial exposure). Thus, within the scope of this work, certain lithological units and stratal surfaces were given more than one sequence stratigraphic interpretation. Examples are the Nothe Grit Formation (interpreted as either a highstand or lowstand systems tract); and the lithological boundary between the Nothe Grit Formation and Preston Grit Member (interpreted as either a surface of forced regression or a ravinement surface), both of the Corallian Group. In these examples more detailed sampling, better biostratigraphic control and new outcrop/bore-hole data may help resolve the interpretation (see Section 7.2).

To summarise, diagenetic analyses at this level of study, is a useful tool, when used in conjunction with other evidence.

7.1.1e: *Diagenetic Analyses as a Predictive Tool*

The second and third aims of the research were to assess if early diagenesis could be used to predict a sequence stratigraphic framework and to use sequence stratigraphy to predict the distribution of diagenetic heterogeneities at the field/interwell scale. In answer to these points, this thesis has demonstrated that early diagenesis can be used as a predictive tool and, like-wise, sequence stratigraphy can be used to predict the distribution of early

diagenetic products. However, like any other tool, this is only possible when used in conjunction with all other knowledge and data. Key points in support of these statements can be summarised as follows

1. The analysis of early diagenetic concretions can help to identify parasequences and parasequence boundaries/marine flooding surfaces (surfaces of non-deposition, e.g. septarian concretions within the Nothe Grit Formation have aided in the identification of parasequences). Similarly, the application of sequence stratigraphic theory in terms of parasequence progradation and subsequent drowning can be used to predict the presence and location of early diagenetic concretions (e.g. within shoreface successions, it is possible to predict that concretions will develop within the coarser grained beds of individual parasequences).
2. The analysis of laterally extensive carbonate cemented marine hard-grounds can also be associated with parasequence boundary formation, particularly in transgressive systems tracts. This is a common feature in both successions (e.g. parasequences of the Upton Member, Corallian Group and parasequences of the Cabo Raso Limestone Member, Ericeira Group). The available data indicate that it is possible to predict such features within systems tracts of similar successions.
3. The available data indicated that an upward increase in early diagenetic products (particularly dolomite) is expected within highstand systems tracts. An upward increase in $\delta^{18}O$ isotope values of carbonate cements is expected within shelf-margin or lowstand systems tracts. A dominance of marine cements is expected within transgressive systems tracts.
4. An analysis of the early diagenetic products associated with exposure surfaces (i.e. karst surfaces), could help to locate and identify type-1 sequence boundaries (e.g.

sequence boundary 3 of the Ericeira Group). Type-2 sequence boundaries are more difficult to predict using this method, but there is some evidence to suggest that fresh-water lenses could develop beneath such boundaries. However, in such cases, a combination of early diagenetic analysis and facies analysis is still necessary (e.g. sequence boundary 3 of the Corallian Group).

The approach taken in this research has demonstrated that early diagenesis is a useful tool in refining high resolution sequence stratigraphic interpretations and in the prediction of the distribution of early diagenetic heterogeneities within reservoir units. But it must be stressed that it should not be used in isolation from other analytical techniques.

7.1.2: Implications for future high resolution sequence stratigraphic studies and reservoir geology

The aims, objectives and methodology employed throughout this study can help towards creating more geologically realistic high resolution sequence stratigraphic frameworks of sedimentary successions and petroleum plays. In this respect, a number of important points have come to light while completing this research:-

1. Analysis of early diagenetic features and their relationship to changes in relative sea-level are a useful a tool when creating a high resolution sequence stratigraphic framework and it should not be disregarded. Carbonate sedimentologists have always used early diagenesis as an indicator of changes in the depositional environment and this has been carried into the sequence stratigraphic realm. Only recently has early

diagenesis been considered as a useful tool in siliciclastic sequence stratigraphic studies. Its use as a tool has implications in reservoir geology. For example, diagenetic samples extracted from a core could help in the identification of key stratal surfaces and stratal packages which would then be of use in well correlation and reservoir characterisation studies.

2. Early diagenetic concretions that form due to a period of non-sedimentation at parasequence boundaries are not diagnostic of a particular systems tract, as previously indicated by other workers (e.g. Taylor *et al.*, 1994).
3. The identification of early diagenetic products within a high resolution sequence stratigraphic framework can lead to the prediction of the distribution of early diagenetic heterogeneities within reservoir units. Cementation below marine flooding surfaces associated with parasequence boundary formation, may lead to highly compartmentalised and layered reservoir units. Further meteoric dissolution associated with a fall in relative sea-level and subsequent sub-aerial exposure, would result in partially dissolved heterogeneities leading to lateral and vertical connectivity between pay-zones.
4. The identification of early diagenetic bodies such as iron-oxide or carbonate concretions are of particular use in identifying parasequence boundaries in interwell or across-field studies. These features may be identifiable in bore-hole core or on well logs during petrophysical analysis.

7.2: *Recommendations for further work*

Within both successions, more detailed sampling is recommended, along with an improved biostratigraphic control (e.g. the use of microfossils that can be linked to published ammonite biostratigraphy) and further facies analysis of new exposures and/or bore-hole data. Further early diagenetic and facies analyses at the regional scale would also improve the identification of major correlative surfaces.

Within the Corallian Group, further sampling and biostratigraphic control at a local and regional scale would help to resolve the sequence stratigraphic interpretation of :-

1. the Nothe Grit Formation;
2. the lithostratigraphic boundary between the Nothe Grit Formation and the Preston Grit Member;
3. the Bencliff Grit Member;
4. the positioning of a sequence boundary within the lower part of the Shortlake Member; and,
5. the Sandsfoot Grit Member.

Similarly, within the Ericeira Group, further sampling and a biostratigraphic control at a local and regional scale would improve the sequence stratigraphic interpretation of the:-

1. the Calada Member; and,
2. the Dois Irmãos Member.

To complement this study it is recommended that additional successions representing different depositional environments are studied using a similar approach. Successions that are blessed with uninterrupted outcrop, or reservoir units that have a close well spacing would also be advantageous.

It would be useful to approach the methodology with the aim of providing input for petroleum reservoir simulation models. In petroleum reservoirs with poor well control, the approach outlined in this thesis could lead to a more realistic, rather than stochastic geological input.

Additional geochemical work would complement the analytical results already obtained. For example, micro-probe work would provide a quantitative analysis of the CL results particularly within the analysis of the concretions within the Bencliff Grit Member. Additional stable isotope data would also improve palaeoenvironmental interpretations, help to define upward changes in pore-water composition and strengthen the proposed predictive models of Chapter 6.

The use of ichnofabric analysis would be another useful tool, when attempting to identify stratal surfaces, especially if core was available. Sequence stratigraphic studies using ichnofabric analysis have been performed on a number of successions (e.g. Martin, 1993).

Finally, it would be useful to conduct further studies from successions deposited during global "ice-house" periods and compare the results with those of this study. During "ice-house" periods, large scale (up to 100m) falls in relative sea-level should have a greater

impact on sedimentary and early diagenetic processes.

References

Ainsworth, R.B. & Pattison, S.A.J. 1994. Where have all the lowstands gone? Evidence for attached lowstand systems tracts in the Western Interior of North America *Geology* **22**, 415-418.

Allen, P.A. & Underhill, J.R. 1989. Swaley cross-stratification produced by unidirectional flows, Bencliff Grit (Upper Jurassic), Dorset, UK. *Journal of the Geological Society, London.* **146**, 241-252.

Arkell, W.J. (ed.) 1933. The Jurassic System in Britain. Oxford University Press, Oxford.

Arkell, W.J. 1936. The Corallian Beds of Dorset. *Proceedings of the Dorset Natural History and Archaeological Society.* **57**, 59-93.

Arkell, W.J. 1947a. The geology of the country around Weymouth, Swanage, Corfe & Lulworth. *Memoirs of the Geological Survey of Great Britain* 386pp

Astin, T.R. 1986. Septarian crack formation in carbonate concretions from shales and mudstones. *Clay Minerals.* **21**, 617-631.

Astin, T.R. & Scotchman, I.C. 1988. The diagenetic history of some septarian concretions from the Kimmeridge Clay, England. *Sedimentology.* **35**, 349-368.

Bechrens, E.W. & Land, L.S. 1972. Subtidal Holocene dolomite, Baffin Bay, Texas *Journal of Sedimentary Petrology* **42**, 155-161.

Berner, R.A. 1978. Sulphate reduction and the rate of deposition of marine sediments. *Earth & Planetary Science Letters.* **37**, 492-498.

Berner, R.A. 1981. A new geochemical classification of sedimentary environments. *Journal of Sedimentary Petrology.* **51**, 359-369.

Berner, R.A. 1984. Sedimentary pyrite: an update *Geochimica et Cosmochimica Acta* **448**, 605-615.

Bhattacharya, J.P. & Walker, R.G. 1992. Deltas *In:* Walker, R.G. & James, N.P. (eds) *Facies Models Response To Sealevel Change* Geological Association of Canada 157-178.

Bjørkum, P.A., Knarud, R. & Bergan, M. 1993. How important is the late Cimmerian unconformity in controlling the formation of kaolinite in sandstones of the North Sea? (Examples from the Snorre Field). *In:* Horbury, A.D. & Robinson, A.G. (eds) *Diagenesis and Basin Development.* American Association of Petroleum Geologists Studies in Geology. **36**, 261-269.

Bridges, P.H. & Leeder, M.R. 1976. Sedimentary model for intertidal mudflat channels, with examples from the Solway Firth, Scotland. *Sedimentology* **23**, 533-552.

Bristow, C.R. 1989. Geology of sheets ST71NE & SE (Marnhull-Struminster Newton, Dorset). *Britisg Geological Survey* Technical Report WA/89/59.

Brookfield, M.E. 1973. Palaeogeography of the Upper Oxfordian and Lower Kimmeridgian (Jurassic) in Britain. *Palaeogeography, Palaeoclimatology, Palaeoecology.* **14**, 137-167.

Brookfield, M.E. 1978. The lithostratigraphy of the upper Oxfordian-Lower Kimmeridgian Beds of south Dorset, England. *Proceedings of the Geologists' Association, London.* **89 (1)**, 1-32.

Brown, L.F. & Fischer, W.L. 1977. Seismic-stratigraphic interpretation of depositional systems: examples from Brazil rift and pull-apart basins. *In:* Payton, C.E. (ed.) *Seismic stratigraphy - applications to hydrocarbon exploration.* American Association of Petroleum Geologists Memoir. **26**, 213-248.

Burchette, T.P., Wright, V.P. & Faulkner, T.J. 1990. Oolitic sandbody depositional models and geometries, Mississippian of southwest Britain: implications for petroleum exploration in carbonate ramp settings *Sedimentary Geology* **68**, 87-115.

Callomon, J.H. & Cope, J.C.W. 1995. The Jurassic Geology of Dorset. *In:* Taylor, P.D. (ed.) *Field Geology of the British Jurassic.* Geological Society of London. 51-103.

Canfield, D.E. 1989. Reactive iron in marine sediments. *Geochimica et Cosmochimica Acta.* **53**, 619-632.

Cant, D.J. 1995. Sequence Stratigraphic Analysis of Individual Depositional Successions: Effects of Marine/Nonmarine Sediment Partitioning and Longitudinal Sediment Transport, Mannville Group, Alberta Foreland Basin, Canada *American Association of Petroleum Geologists* **79 (5)**, 749-762.

Carpenter, A.B. & Oglesby, T.W. 1976. A model for the formation of luminescently zoned calcite cements and its implications. *Abstracts with Programs.* **8**, 469-470. Boulder, CO: Geological Society of America

Chadwick, R.A. 1986. Extension tectonics in the Wessex Basin, Southern England. *Journal of the Geological Society of London* **140**, 893-911.

Chowdhury, A.N. 1982. Variations in diagenetic environments of the Coral Rag and underlying oolite of the Osmington Oolite Formation (Upper Oxfordian) of the Oxford-Berkshire area, U.K., and their implications. *Sedimentary Geology.* **32**, 247-263.

Church, K.D. & Gawthorpe, R.L. 1997. Sediment supply as a control on the variablity of sequences: an example from the late Namurian of northern England. *Journal of the Geological Society of London* **154**, 55-60.

Coe, A.L. 1992. The Oxfordian and Portlandian *In:* Coe, A.L., Hesselbo, S.P., Parkinson, D.N., & Jenkyns, H.C. (eds) *Sequence stratigraphy of the Dorset Jurassic: a field guide.* Field guide for a field trip in conjunction with Sequence Stratigraphy of European Basins meeting, CNRS- IFP, Dijon, France.

Coe, A.L. 1995. A comparison of the Oxfordian successions of Dorset, Oxfordshire and Yorkshire. *In:* Taylor, P.D. (ed.) *Field Geology of the British Jurassic* Geological Society of London 151-172.

Coleman, M.L. 1985. Geochemistry of diagenetic non-silicate minerals: kinetic considerations *Philosophical Transactions of the Royal Society of London* **315**, 39-56.

Coleman, M.L., Hedrick, D.B., Lovley, D.R., White, D.C. & Pye, K. 1993. Reduction of Fe(III) in sediments by sulphate-reducing bacteria. *Nature.* **361**, 436-438.

Cope, J.C.W. 1995. Introduction to the British Jurassic. *In:* Taylor, P.D. (ed.) *Field Geology of the British Jurassic.* Geological Society of London. 1-7.

Craig, H. 1957. Isotopic standards for carbon and oxygen and correction factors for mass-spectrometric analysis of carbon dioxide. *Geochimica et Cosmochimica, Acta.* **12**, 133-149.

Curtis, C.D. 1978. Possible links between sandstone diagenesis and depth-related geochemical reactions occurring in enclosing mudstones. *Journal of the Geological Society of London.* **135**, 107-117.

Curtis, C.D. 1980. Diagenetic alteration in black shales. *Journal of the Geological Society of London.* **137**, 189-191.

Curtis, C.D. & Coleman, M.L. 1986. Controls on the precipitation of early diagenetic calcite, dolomite and siderite concretions in complex depositional sequences. *In:* Gautier, D.L. (ed.) *The Relationship of Organic Matter & Mineral Diagenesis.* Special Publication of the Society of Palaeontologists and Mineralogists. **38**, 23-33.

Curtis, C.D. 1987. Mineralogical Consequences of Organic Matter Degradation in Sediments: Inorganic/Organic Diagenesis. *In:* Leggett, J.K. & Zuffa, G.G. (eds) *Marine Clastic Sedimentology.* 108-123.

Dalrymple, R.W. 1992. Tidal depositional systems. *In:* Walker, R.G. & James, N.P (eds) *Facies Models - response to sea-level change* Geological Association of Canada 195-218.

Davis, H.R. & Byers, C.W. 1989. Shelf sandstones in the Mowry shale: evidence for deposition during Cretaceous sea-level falls. *Journal of Sedimentary Petrology.* **59,** 548-560.

Davis, H.R., Byers, C.W. & Pratt, L.M. 1989. Depositional mechanisms and organic matter in Mowry Shale (Cretaceous), Wyoming. *American Association of Petroleum Geologists.* **73,** 1103-1116.

De Wet, C.B. 1987. Deposition and diagenesis in an extensional basin: the Corallian Formation (Jurassic) near Oxford, England. *In:* Marshall, J.D. (ed.) *Diagenesis of Sedimentary Sequences* Geological Society Special Publication **36, 339-353.**

Desrochers, A. & Al-Aassm, I. 1993. The formation of septarian concretions in Queen Charlotte Islands, B.C.: evidence for microbially and hydrothermally mediated reactions at shallow burial depth. *Journal of Sedimentary Petrology.* **63 (2),** 282-294.

Dickson, J.A.D. 1966. Carbonate identification and genesis as revealed by staining. *Journal of Sedimentary Petrology.* **36,** 491-505.

Elliot, T. 1986. Siliciclastic shorelines *In:* Reading, H.G. (ed) *Sedimentary Environments and Facies* Blackwell Scientific Publications (2nd edition) 155-188.

Emery, D. & Myers, K.J. (eds). 1996. *Sequence Stratigraphy.* Blackwell Science Ltd., 297pp.

Epstein, S., Buchsbaum, H.A., Lowenstam, H.A. & Urey, H.C. 1953. Revised carbonate-water isotopic temperature scale. *Bulletin of the Geological Society of America.* **64,** 315-1326.

Erskine, R.D. & Vail, P.R. 1988. Seismic stratigraphy of the Exmouth Plateau. *In:* Baily. A.W. (ed.) *Atlas of Seismic Stratigraphy.* American Association of Petroleum Geologists - Studies in Geology. **27,** 163-173.

Evamy, B.D. 1967. Dedolomitization And The Development Of Rhombohedral Pores In Limestones *Journal of Sedimentary Petrology* **37 (4),** 1204-1215.

Fleming, N. 1993. Calcium carbonate cementation of sandstones. *Geology Today.* **9 (6),** 223-226.

Frank, J.R., Carpenter, A.B. & Oglesby, T.W. 1982. Cathodoluminescence and composition of calcite cement in the Taum Sauk Limestone (Upper Cambrian), southeast Missouri. *Journal of Sedimentary Petrology* **52,** 631-638.

Friedman, G.M. 1964. Early diagenesis and lithification in carbonate sediments. *Journal of Sedimentary Petrology.* **34 (4),** 777-813

Fürsich, F.T. 1973. *Thalassinoides* and the origin of nodular limestone in the Corallian Beds (Upper Jurassic) of southern England. *Neues Jahrebuch Geologische Paläontologische Abhundlungen.* **3**, 136-156.

Fürsich, F.T. 1975. Trace fossils as environmental indicators in the Corallian of England and Normandy. *Lethia.* **8**, 151-172.

Fürsich, F.T. 1976. The use of macroinverterbrate associations in interpreting Corallian environment. *Palaeogeography, Palaeoclimatology, Palaeoecology.* **20**, 235-256.

Fürsich, F.T. & Oschmann, W. 1993. Shell beds as tools in basin analysis: the Jurassic of Kachchh, western India. *Journal of the Geological Society of London.* **50**, 169-185.

García-Mondéjar, J. & Fernández-Mendiola, P.A. 1993. Sequence Stratigraphy and Systems Tracts of a Mixed Carbonate and Siliciclastic Platform-Basin Setting: The Albian of Lunada and Soba, Northern Spain. *Bulletin of the American Association of Petroleum Geologists.* **77 (2)**, 245-275.

Gawthorpe, R. 1987. Burial dolomitization and porosity development in a mixed carbonate-clastic sequence: an example from the Bowland Basin, northern England *Sedimentology* **34**, 533-558.

Given, R.K. & Wilkinson, B.H. 1987. Dolomite abundances and stratigraphic age: constraints on rates and mechanisms of Phanerozoic dolostone formation. *Journal of Sedimentary Petrology.* **57**, 1068-1078.

Goldring, R. & Gabbott, S. 1993. An Integrated View of the Bencliff Grit (Upper Jurassic, Dorset Coast). Abstract presented at *BSRG* annual conference, University of Manchester, 15th-17th December 1993.

Goldring, R. 1995. Organisms and the substrate: response and effect. *In:* Bosence, D.W.J. & Allison, P.A. (eds). *Marine Palaeoenvironmental Analysis from Fossils.* Geological Society Special Publication **83**, 151-180.

Goldring, R., Astin, T.R., Marshall, J.E.A., Gabbott, S. & Jenkins, C.D. *in press* Towards an integrated study of the depositional environment of the Bencliff Grit (U. Jurassic) of Dorset *In:* Underhill, J.R. (ed) *Development & Evolution of the Wessex Basin* Special Publication of the Geological Society of London.

Hallam, A. 1978. Eustatic cycles in the Jurassic. *Palaeogeography, Palaeoclimatology, Palaeoecology.* **23**, 1-32.

Hallam, A. 1994. Jurassic climates as inferred from the sedimentary and fossil record. *In:* Allen, J.R.L., Hoskins, B.W., Sellwood, B.W., Spicer, R.A & Valdes, P.J. (eds) *Palaeoclimates and their modelling* The Royal Society 79-88.

Haq, B.U., Hardenbol, J. & Vail, P.R. 1987. Chronology of fluctuating sea-levels since the Triassic. *Science.* **235**, 1156-1167.

Henderson, A.H. 1997. *The Palaeo-ecology and Biostratigraphy of the foraminifera from the Oxfordian of north Dorset* Unpublished Ph.D Thesis, University of Plymouth.

Hendry, J.P. 1993a. Geological controls on regional subsurface carbonate cementation - an isotopic-palaeohydrological investigation of middle Jurassic limestones in central England. *In:* Horbury, A.D. & Robinson, A.G. (eds) *Diagenesis and Basin Development.* American Association of Petroleum Geologists - Studies in Geology **36**, 231-260.

Hendry, J.P. 1993b. Calcite cementation during bacterial manganese, iron and sulphate reduction in Jurassic shallow marine carbonates. *Sedimentology.* **40**, 87-106.

Hird, K., Tucker, M.E. & Waters, R.A. 1987. Petrography, geochemistry and origin of Dinantian dolomites from south-east Wales. *In:* Miller, J., Adams, A.E. & Wright, V.P. (eds.) *European Dinantian Environments.* John Wiley, Chichester 359-377p.

Hiscott, R.N., Wilson, R.C.L., Harding, S.C., Pujalte, V. & Kitson, D. 1990a. Contrasts in Early Cretaceous depositional environments of marine sandbodies, Grand Banks- Iberian Corridor. *Bulletin of Canadian Petroleum Geology.* **38(2)**

Hiscott, R.N., Wilson, R.C.L., Gradstein, F.M., Pujalte, V., Garcia-Mondejar, J., Boudreau, R.R. & Wishart, H.A. 1990b. Comparative stratigraphy and subsidence history of Mesozoic syn-rift basins of the North Atlantic. *The American Association of Petroleum Geologists Bulletin.* **74 (1)**, 60-76.

Horbury, A.D. & Robinson, A.G. 1993. Diagenesis, basin development and porosity prediction in exploration - an introduction. *In:* Horbury, A.D. & Robinson, A.G. (eds) *Diagenesis and Basin Development.* American Association of Petroleum Geologists - Studies in Geology. **36**, 1-4.

Howell, J.A. & Aitken, J.F. 1996. High resolution sequence stratigraphy: innovations, applications and future prospects. *In:* Howell, J.A. & Aitken, J.F. (eds) *High Resolution Sequence Stratigraphy: Innovations and Applications.* Geological Society Special Publication. **104**, 1-9.

Hudson, J.D. 1978. Concretions, isotopes and diagenetic history of the Oxford Clay (Jurassic) of central England. *Sedimentology.* **25**, 339-370.

Hunt, D. & Tucker, M.E. 1993. Sequence stratigraphy of carbonate shelves with an example from the mid-Cretaceous (Urgonian) of southeast France. *In:* Posamentier, H.W., Summerhayes, C.P., Haq, B.U. & Allen, G.P. (eds) *Sequence Stratigraphy and Facies Associations* Special Publications of the International Association of Sedimentologists, **18**, 307-341.

Irwin, H., Curtis, C.D. & Coleman, M. 1977. Isotopic evidence for source of diagenetic carbonates formed during burial of organic-rich sediments. *Nature.* **269**, 209-213.

James, N. 1984. Shallowing-upward sequences in Carbonates *In:* Walker, R. (ed.) *Facies Models (2nd. edition)* The Geological Association of Canada, Geoscience Reprint Series **1**, 213-228.

Jennette, D.C. & Riley, C.O. 1996. Influence of relative sea-level on facies and reservoir geometry of the Middle Jurassic lower Brent Group, UK North Viking Graben *In:* Howell, J.A. & Aitken, J.F. (eds.) *High Resolution Sequence Stratigraphy: Innovations and Applications* Geological Society Special Publication **104**, 87-114.

Jervey, M. T. 1988. Quantitative Geological Modelling of Siliciclastic Rock Sequences and their Seismic Expression. *In:* Wilgus, C. K., Hastings, B. S., Kendall, G. St. C., Posamentier, H. W., Ross, C. A. & Van Wagoner, J. C. (eds) *Sea-level Changes: An Integrated Approach.* Special Publication of the Society of Economic Palaeontologists and Mineralogists. **42**, 47-70.

Johnson, H.D. & Baldwin, C.T. 1986. Shallow siliciclastic seas *In;* Reading, H.G. (ed) *Sedimentary Environments & Facies* Blackwell Scientific Publications (2nd edition) 229-282).

Kendall, A.C. 1985. Radiaxial fibrous calcite: a reappraisal *In:* Schneidermann, N. & Harris, P.M. (eds.) *Carbonate Cements* Special Publication of the Society of Economic Palaeontologists and Mineralogists **36**, 59-77.

Kendall., C.G. st. C., & Schlager, W. 1981. Carbonates and relative changes in sea-level. *Marine Geology.* **44**, 181-212.

Kenyon-Roberts, S. 1995. Hardgrounds and sequence stratigraphy of Jurassic carbonate sand-bodies in the Cotswolds. Field Trip Guidebook for *The 10th Bathurst Meeting of carbonate Sedimentologists.* Royal Holloway University of London 2nd-5th July.

Leeder, M.R. (ed.) 1982. *Sedimentology: Process and Product* Chapman & Hall (London) 344pp.

Li, Y.H., Bischoff, J. & Mathieu, G. 1969. The migration of manganese in Arctic Basin sediments *Earth & Planetary Science Letters* **7**, 265-270.

Lohmann, K.C. & Walker, J.C.G. 1989. The $\delta^{18}O$ record of Phanerozoic abiotic marine calcite cements *Geophysical Research Letters* **16**, 319-322.

Loutit, T.S., Hardenbol, J., Vail, P.R. & Baum, G.R. 1988. Condensed sections: the key to age determination and correlation of continental margin sequences. *In:* Wilgus, C. K., Hastings, B. S., Kendall, G. St. C., Posamentier, H. W., Ross, C. A. & Van Wagoner, J. C. (eds) *Sea-level Changes: An Integrated Approach.* Special Publication of the Society of Economic Palaeontologists and Mineralogists. **42**, 183-213.

Lynn, D.C. & Bonatti, E. 1965. Mobility of manganese in diagenesis of deep-sea sediments. *Marine Geology* **3**, 457-474.

Mack, G.H. & James, W.C. 1986. Cyclic sedimentation in the mixed siliciclastic-carbonate Abo-Hueco transitional zone (Lower Permian), southwestern New Mexico. *Journal of Sedimentary Petrology.* **56 (5)**, 635-647.

Macquaker, J.H.S., Taylor, K.G., Young, T.P. & Curtis, C.D. 1996. Sedimentological and geochemical controls on ooidal ironstone and "bone-bed" formation and some comments on their sequence stratigraphical significance. *In:* Hesselbo, S.P. & Parkinson, D.N. (eds) *Sequence Stratigraphy in British Geology.* Geological Society Special Publication **103**, 97-108.

Marshall, D.J. (ed.) 1988. Cathodoluminescence of Geological Materials Allen & Unwin, Boston 128pp.

Marshall, J.D. & Ashton, M. 1980. Isotopic and trace element evidence for submarine lithification of hardgrounds in the Jurassic of eastern England. *Sedimentology.* **27**, 271-289.

Martin, M.A. 1993. *Trace fossil analysis and sequence stratigraphy of the Upper Jurassic Fulmar Formation, Western Central Graben (U.K.C.S.).* Unpublished Ph.D Thesis, University of Manchester.

Maynard, J.B. 1982. Extension of Berner's "New geochemical classification of sedimentary environment's" to ancient sediments. *Journal of Sedimentary Petrology.* **50**, 1325-1331.

McBride, E.F., Picard, M.D. & Folk, R.L. 1994. Oriented Concretions, Ionian Coast, Italy: Evidence of Groundwater Flow Direction *Journal of Sedimentary Research* **64 (3)**, 535-540.

McBride, E.F., Milliken, K.L., Cavassa, W., Cibin, U., Fontana, D., Picard, M.D., Zuffa, G.G. 1995. Heterogeneous Distribution of Calcite Cement at the Outcrop Scale in Tertiary Sandstones, Northern Apennines, Italy *Bulletin of the American Association of Petroleum Geologists* **79 (7)**, 1044-1063.

McCubbin, D.G. 1982. Barrier Island and Strand Plain Facies. *In:* Scholle, P.A. & Spearing, D. (eds) *Sandstone Depositional Environments.* American Association of Petroleum Geologists Memoir. **31**, 247-279.

McKay, J.L, Longstaffe, F.J. & Plint A.G. 1995. Early diagenesis and its relationship to depositional environment and relative sea-level fluctuations (Upper Cretaceous Marshybank Formation, Alberta and British Columbia). *Sedimentology.* **42,** 161-190.

Medlin, W.L. 1961b. Thermoluminescence in dolomite. *Journal of Chemical Physics* **34,** 672-677.

Medlin, W.L. 1968. The nature of traps and emission centres in thermoluminescent rock materials. *In:* McDougall, D.J. (ed) *Thermoluminescence og geological materials* New York Academic Press 193-223.

Meyers, W.J. 1974. Carbonate cement stratigraphy of the Lake Valley formation (Mississippian) Sacramento Mountains, New Mexico. *Journal of Sedimentary Petrology.* **44,** 837-61.

Miller, J. 1988. Cathodoluminescence microscopy *In:* Tucker, M.E. (ed.) *Techniques in Sedimentology* Blackwells, Oxford. 174-190.

Milodowski, A.E. & Wilmot, R.D. 1984. Diagenesis, porosity and permeability in the Corallian Beds (Upper Oxfordian) from the Harwell Research Site, south Oxfordshire, U.K. *Clay Minerals* **19,** 323-341.

Mitchum, R.M. 1977. Seismic stratigraphy and global changes of sea level, Part 1: glossary of terms used in seismic stratigraphy. *In:* Payton, C. E. (ed) *Seismic stratigraphy - applications to hydrocarbon exploration.* American Association of Petroleum Geologists Memoir **26,** 131-160

Mitchum, R.M. & Van Wagoner, J.C. 1991. High frequency sequences and their stacking patterns: sequence stratigraphic evidence of high frequency eustatic cycles. *Sedimentary Geology.* **70,** 135-144.

Morlot, A. von 1848. Sur l'origine de la dolomie (extrait d'une lettre d'A. von Morlot à E. de Beaumont) *Academic Science Paris comptes rendus* **26,** p.313.

Mozley, P.S. & Carothers, W.W. 1992. Elemental and isotopic composition of siderite in the Kuparuk Formation, Alaska: effect of microbial activity and water/sediment interaction on early pore-water chemistry. *Journal of Sedimentary Petrology.* **62,** 681-692.

Mozley, P.S. & Wersin, P. 1992. Isotopic composition of siderite as an indicator of depositional environment. *Geology.* **20,** 817-820.

Mozley, P.S. & Burns, S.J. 1993. Oxygen and carbon isotopic composition of marine carbonate concretions: an overview. *Journal of Sedimentary Petrology.* **63,** 73-83.

Nissenbaum, A., Presley, B.J. & Kaplan, I.R. 1972. Early diagenesis in a reducing fjord, Saanich Inlet, British Columbia - I. Chemical and isotopic changes in major components of interstitial water *Geochemica et Cosmochimica Acta* **36**, 1007-1027.

Osleger, D.A. & Montañez, I.P. 1996. Cross-platform architecture of a sequence boundary in mixed siliciclastic-carbonate lithofacies, Middle Cambrian, southern Great Basin, USA. *Sedimentology.* **43**, 197-217.

Pearson, M.J. 1979. Geochemistry of the Hepworth Carboniferous Sediment Sequence and origin of the diagenetic iron minerals and concretions. *Geochimica et Cosmochimica Acta.* **43**, 927-941.

Pemberton, S.G. 1992. *Applications of Ichnology to Petroleum Exploration: A Core Workshop.* Society of Economic Paleontologists and Mineralogists Core Workshop No. **17**, 429pp.

Pettijohn, F.J. (ed.) 1975. Sedimentary Rocks (third edition) Harper & Row Publishers 628pp.

Pickering, K.T. 1995. Are enigmatic sandy wave-like bedforms in Jurassic Bridport - Sands, Dorset, due to standing waves? *Journal of the Geological Society, London.* **152**, 481-485.

Plint, A.G. 1991. High-frequency relative sea-level oscillations in Upper Cretaceous shelf clastics of the Alberta foreland basin: possible evidence for a glacio-eustatic control? *In:* MacDonald, D.I.M. (ed) *Sedimentation, tectonics and eustacy.* International Association of Sedimentologists, Special Publication **12**, 409-428.

Pope, M. & Read, J.F. 1997. High-resolution surface and subsurface sequence stratigraphy of Late Middle to Late Ordovician (Late Mohawkian-Cincinnatian) Forelan Basin Rocks, Kentucky and Virginia. *American Association of Petroleum Geologists* **81**, 1866-1893.

Posamentier, H. W., Jervey, M. T. & Vail, P. R. 1988. Eustatic controls on clastic deposition I: conceptual framework. *In:* Wilgus, C. K., Hastings, B. S., Kendall, G. St. C., Posamentier, H. W., Ross, C. A. & Van Wagoner, J. C. (eds) *Sea-level Changes: An Integrated Approach.* Special Publication of the Society of Economic Paleontologists and Mineralogists. **42**, 109-124.

Posamentier, H. W. & Vail, P. R. 1988. Eustatic controls on clastic deposition II: sequence and system tract models. *In:* Wilgus, C. K., Hastings, B. S., Kendall, G. St. C., Posamentier, H. W., Ross, C. A. & Van Wagoner, J. C. (eds) *Sea-level Changes: An Integrated Approach.* Special Publication of the Society of Economic Paleontologists and Mineralogists. **42**, 125-154.

Posamentier, H.W., Allen, G.P., James, D.P. & Tesson, M. 1992. Forced Regressions in a Sequence Stratigraphic Framework: Concepts, Examples and Exploration Significance. *American Association of Petroleum Geologists Bulletin.* **76 (11),** 1687-1709.

Posamentier, H.W., Summerhayes, C.P., Haq, B.U. & Allen G.P. (eds) 1993. Sequence Stratigraphy and Facies Associations. *Special Publication Number 18 of the International Association of Sedimentologists.* Blackwell Scientific Publications

Posamentier, H.W. & James, D. P. 1993. An overview of sequence-stratigraphic concepts: uses and abuses. *In:* Posamentier, H.W., Summerhayes, C.P., Haq, B.U. & Allen, G.P. (eds) *Sequence Stratigraphy and Facies Associations* Special Publication of the International Association of Sedimentologists. **18,** 3-18.

Posamentier, H.W. & Weimer, P. 1993. Siliciclastic Sequence Stratigraphy and Petroleum Geology-Where to From Here? *Bulletin of The American Association of Petroleum Geologists* **77 (5),** 731-740.

Purser, B.H. 1969. Synsedimentary marine lithification of Middle Jurassic limestones in the Paris Basin. *Sedimentology.* **12,** 205-230.

Raiswell, R. 1971. The growth of Cambrian and Liassic concretions. *Sedimentology.* **17,** 147-171.

Raiswell, R. 1982. Pyrite texture, isotopic composition and the availability of iron. *American Journal of Science.* **282,** 1244-1263.

Raiswell, R. 1987. Non-steady state microbiological diagenesis and the origin of concretions and nodular limestone. *In:* Marshall, J.D. (ed.) *Diagenesis of Sedimentary Sequences.* Special Publication of the Geological Society of London. **36,** 41-54.

Read, J.F. & Horbury, A.D. 1993. Eustatic and tectonic controls on porosity evolution beneath sequence-bounding unconformities and parasequence disconformities on carbonate platforms. *In:* Horbury, A.D. & Robinson, A.G. (eds). *Diagenesis and Basin Development.* American Association of Petroleum Geologists - Studies in Geology. **36,** 155-198.

Reinson, G.E. 1992. Transgressive barrier island and estuarine systems *In:* Walker, R.G. & James, N.P. (eds) *Facies Models - response to sea-level change* Geological Association of Canada. 179-194.

Rey, J. 1972. Récherches géologiques sur le Crétace inférieur de l'Estremadura (Portugal). *Mémoires Service Géologique Portugal* **21,** 477pp.

Rey, J. 1979. Le Crétace Inférieur de la marge Atlantique portugaise: biostratigraphie, organisation sequentielle, evoultion páléogeographique. *Ciençias da Terra (UNL) Lisboa.* **5**, 97-120.

Rine, J.M. & Ginsburg, R.N.. 1985. Depositional facies of a mud shoreface in Suriname, South America - a mud analogue to sandy shallow-marine deposits. *Journal of Sedimentary Petrology,* **55**, 633-652.

Rioult, M., Dugue, O., Jan Du Chene, R., Ponsot, C., Fily, G., Moron, J. & Vail, P. R. 1991. Outcrop Sequence Stratigraphy of the Anglo-Paris Basin, Middle to Upper Jurassic (Normandy, Maine, Dorset). *Bulletin de la centres Recherches Exploration-Production, Elf Aquitaine,* **15**, 101-194.

Rosenthal, L.R.P. & Walker, R.G. 1987. Lateral and vertical facies sequences in the Upper Cretaceous Chungo Member, Wapiabi Formation, southern Alberta. *Canadian Journal of Earth Sciences.* **24**, 771-783.

Saigal, G.C. & Bjørlkke, K. 1987. Carbonate cements in clastic reservoir rocks from offshore Norway - relationships between isotopic composition, textural development and burial depth. *In:* Marshall, J.D. (ed.) *Diagenesis of Sedimentary Sequences.* Geological Society Special Publication **36**, 313-324.

Sandberg, P.A. 1983. An oscillating trend in Phanerozoic non-skeletal carbonate mineralogy. *Nature* **305**, 19-22.

Sandberg, P.A. 1985. Aragonite cements and their occurrence in ancient limestones. *In:* Schneiderman, N. & Harris, P.M. (eds) *Carbonate Cements* Special Publication of the Society of Economic Palaeontologists and Mineralogists. **36**, 33-57.

Sarg, J.F. 1988. Carbonate sequence stratigraphy. *In:* Wilgus, C. K., Hastings, B. S., Kendall, G. St. C., Posamentier, H. W., Ross, C. A. & Van Wagoner, J. C. (eds) *Sea-level Changes: An Integrated Approach.* Special Publication of the Society of Economic Paleontologists and Mineralogists. **42**, 155-181.

Savrda, C.E. 1991. Ichnology in Sequence Stratigraphic Studies: An example from the Lower Paleocene of Alabama. *Palaios.* **6**, 39-53

Schlager, W. 1981. The paradox of drowned reefs and carbonate platforms. *Geological Society of America Bulletin.* **92**, 197-211.

Schlager, W. 1992. Sedimentology and Sequence Stratigraphy of Reefs and Carbonate Platforms. *American Association of Petroleum Geologists, Continuing Education Course Note Series* **34**, 71pp.

Scotchman, I.C. 1991. The geochemistry of concretions from the Kimmeridge Clay Formation of southern and eastern England. *Sedimentology.* **38**, 79-106.

Selley, R.C. (ed) 1985. *Ancient Sedimentary Environments (3rd. edition).* London Chapman & Hall 317pp.

Selley, R.C. & Stoneley, R. 1987. Petroleum habitat in south Dorset. *In:* Brooks J. and Glennie K. (eds) *Petroleum Geology of North West Europe.* Graham & Trotman, London 139-148.

Shackleton, N.J. & Kennett, J.P. 1975. Palaeotemperature history of the Cenozoic and the initiation of the Antarctic glaciation: oxygen and carbon isotope analysis in DSDP sites 277, 279 and 281. *In:* Kennett, J.P. & Houtz, R.E. (eds) *Initial Reports of the Deep Sea Drilling Project.* **XXIX**, 743-755.

Shinn, E. A. 1983. Tidal Flat Environments. *In:* Scholle, P. A., Bebout, D. G. & Moore, C. H. (eds) *Carbonate Depositional Environments.* The American Association of Petroleum Geologists Memoir **33** p171-210.

Smith, J.V. & Stenstrom, R.C. 1965. Electron excited luminescence as a petrologic tool. *Journal of Geology* **73**, 627-635.

Stamp, L.D. 1921. On cycles of sedimentation in the Eocene strata of the Anglo-France-Belgium Basin. *Geological Magazine.* **58**, 108-114.

Stemmerik, L. & Larssen, G.B. 1993. Diagenesis and porosity evolution of lower Permian palaeoaplysinid buildups on Bjornoya: an example of high frequency sea level fluctuations controlling diagenesis in a transgressive sequence. *In:* Horbury, A.D. & Robinson, A.G. (eds) *Diagenesis and Basin Development.* American Association of Petroleum Geologists - Studies in Geology **36**, 199-212.

Stoneley, R. 1982. The structural development of the Wessex Basin. *Journal of the Geological Society of London* **139**, 543-554.

Stoneley, R. & Selley, R.C. (eds) 1991. A Field Guide To the Petroleum Geology of the Wessex Basin (3rd edition) Imperial College, London. 49pp.

Sun, S.Q. 1989. A New Interpretation of the Corallian (Upper Jurassic) Cycles of the Dorset Coast, Southern England. *Geological Journal* **24**, 139-158.

Sun, S.Q. 1990. Facies related Diagenesis in a Cyclic Shallow Marine Sequence: The Corallian Group (Upper Jurassic) of the Dorset Coast, Southern England. *Journal of Sedimentary Petrology* **60 (1)**, 42-52.

Swift, D.J.P. & Thorne, S.A. 1991. Sedimentation on continental margins, I: a general model for shelf sedimentation *In:* Swift, D.J.P., Oertal, G.F., Tillman, P.W. & Thorne, J.A. (eds) *Shelf Sands & Sandstone Bodies Special* Publication of the International Association of Sedimentologists. **14**, 3-33

Sykes, R.M. & Callomon, J.H. 1979. The *Amoeboceras* zonation of the Boreal Upper Oxfordian. *Sedimentology* **22 (4)**, 839-903.

Talbot, M.R. 1971. Calcite cements in the Corallian Beds (Upper Oxfordian) of southern England. *Journal of Sedimentary Petrology* **41 (1)**, 261-273.

Talbot, M.R. 1973. Major sedimentary cycles in the Corallian Beds (Oxfordian) of Southern England. *Palaeogeography, Palaeoclimatology, Palaeoecology* **14**, 293-317.

Talbot, M.R. 1974. Ironstones in the Upper Oxfordian of southern England. *Sedimentology* **21**, 433-450.

Taylor, K., Gawthorpe, R. & Van Wagoner, J.C. 1994. Cementation below marine flooding surfaces: examples from the Blackhawk formation, Book Cliffs, Utah. *In:* Johnson, S.D. (ed.) *High Resolution Sequence Stratigraphy: Innovations & Applications.* Abstract Volume, 340-342.

Taylor, K.G. & Curtis, C.D. 1995. Stability and facies association of early diagenetic mineral assemblages: an example from a Jurassic ironstone-mudstone succession, U.K. *Journal of Sedimentary Research.* **A65 (2)**, 358-368.

Thomas, R.G., Smith, D.G, Wood, J.M, Visser, J., Calverley-Range, E.A. & Koster, E.H. 1987. Inclined heterolithic stratification - terminology, description, interpretation and significance. *Sedimentary Geology* **53**, 123-179.

Tucker, M.E. & Wright, V.P. (eds) 1990. *Carbonate Sedimentology.* Blackwell Scientific Publications 482pp.

Tucker, M.E. (ed) 1991. *Sedimentary Petrology - an introduction to the origin of sedimentary rocks (2nd. edition)* Blackwell Scientific Publications, Oxford. 260pp

Tucker, M. E. 1993. Carbonate diagenesis and sequence stratigraphy. *In:* Wright, V. P. (ed) *Sedimentology Review/1.* Blackwell Scientific Publications, Oxford. 51-72.

Vail, P.R., R.M. Mitchum, & S. Thompson, III 1977. Seismic stratigraphy and global changes in sea-level, part 3: relative changes of sea-level from coastal onlap. *In:* Payton, C.W. (ed.) *Seismic stratigraphy applications to hydrocarbon exploration.* American Association of Petroleum Geologists Memoir. **26**, 63-97.

Van Wagoner, J. C. 1985. Reservoir facies distribution as controlled by sea-level change. Abstract presented at *Society of Economic Palaeontologists and Mineralogists*, Golden Colerado., 11th - 14th August, p91-92.

Van Wagoner, J. C., Posamentier, H.W., Mitchum, R.M, Vail, P.R., Sarg, J.F., Loutit, T.S. & Harbendol, J. 1988. The key definitions of sequence stratigraphy. *In:* Wilgus, C. K., Hastings, B. S., Kendall, G. St. C., Posamentier, H. W., Ross, C. A. & Van Wagoner, J. C. (eds) *Sea-level Changes: An Integrated Approach.* Special Publication of the Society of Economic Paleontologists and Mineralogists. **42**, 39-45.

Van Wagoner, J. C., Mitchum, R.M., Campion, K.M. & Rahmanian, V.D. 1990. *Siliciclastic Sequence Stratigraphy in Well Logs, Cores and Outcrops: Concepts for High-Resolution Correlation of Time and Facies.* American Association of Petroleum Geologists Methods in Exploration Series, No. 7

Veevers, J.J. 1990. Tectonic-climatic supercycle in the billion-year plate-tectonic eon: Permian Pangean icehouse alternates with Cretaceous dispersed-continents greenhouse. *Sedimentary Geology* **68**, 1-16.

Veizer, J., Holser, W.T. & Wilgus, C.K. 1980. Correlation of $^{13}C/^{12}C$ and $^{34}S/^{32}S$ secular variations. *Geochemica et Cosmochimica Acta.* **44**, 579-587.

Walker, J.C.G. 1984. Suboxic diagenesis in banded iron formations *Nature* **309**, 340-342.

Walker, R.G. 1982. Hummocky and swaley cross-stratification. *In:* Walker, R.G. (ed) *Clastic units of the front Ringes, Foothills and Plains in the area between field B.C. and drumheller, Alberta.* Hambleton, International Association of sedimentologists. Guidebook for Excursion. 22-30

Walker, R.G. 1992. Facies, facies models and modern stratigraphic concepts *In:* Walker, R.G. & James, N.P. (eds.) *Facies Models, response to sea-level change* Geological Association of Canada 1-14.

Walker, R.G. & Plint, G.A. 1992. Wave and storm dominated shallow marine systems *In:* Walker, R.G. & James, N.P. (eds.) *Facies Models, response to sea-level change* Geological Association of Canada 219-238.

Weber, K.J. & Geuns, L.C. 1990. Framework for constructing clastic reservoir simulation models *Journal of Petroleum Technology* **42**, 1248-1297.

Wehr, F.L. & Brasher, L.D. 1996. Impact of sequence-based correlation style on reservoir model behaviour, lower Brent Group, North Cormorant Field, UK North Sea. *In:* Howell, J.A. & Aitken, J.F. (eds.) *High Resolution Sequence Stratigraphy: Innovations and Applications* Geological Society Special Publication **104**, 115-128.

Weimer, R. J., Howard, J. D. & Lindsay, D. R. 1982. Tidal Flats and Associated Tidal Channels. *In:* Scholle, P. A. & Spearing, D. (eds) *Sandstone Depositional Environments.* American Association of Petroleum Geologists Tulsa. Memoir **31** p191-246

Whatley, R.C. 1965. Callovian & Oxfordian Ostracoda from England & Scotland. *Unpublished PhD. thesis* - University of Hull.

Whiteman, W.G. 1990. Micropalaeontology of the Kimmeridgian to Barremian deposits of Portugal and the Grand banks of Newfoundland. *Unpublished PhD thesis* Dalhousie University, Halifax, Nova Scotia. 406pp.

Wilgus, C.H., Hastings, B.S., Kendall, C.G.St.C., Posamentier, H., Ross, C.A. & Van Wagoner, J. (eds) 1988. Sea-level Changes: An Integrated Approach. *Special Publication of the Society of Economic Palaeontologists and Mineralogists* **42** 407pp.

Wilkinson, B.H., Janecke, S.V. & Brett, C.E. 1982a. Low magnesium calcite marine cement in Middle Ordovician hardgrounds from Kirkfield, Ontario. *Journal of Sedimentary Petrology* **52**, 47-57.

Wilkinson, B.H., Owen, R.B. & Carroll, A.R. 1982b. Submarine hydrothermal weathering, global eustacy and carbonate polymorphism in Phanerozoic marine oolites. *Journal of Sedimentary Petrology* **55**, 171-183.

Wilkinson, B.H., Smith, A.L. & Lohmann, K.C. 1985. Sparry calcite marine cement in Upper Jurassic limestones of southeastern Wyoming. *In:* Schneiderman, N. & Harris, P.M. (eds) *Carbonate Cements.* Special Publication of the Society of Economic Palaeontologists and Mineralogists. **36**, 169-183.

Wilson, R.C.L. 1966. Silica diagenesis in upper Jurassic limestones of southern England. *Journal of Sedimentary Petrology* **36 (4)**, 1036-1049.

Wilson, R.C.L. 1967. Diagenetic carbonate fabric variations in Jurassic limestones of southern England. *Proceedings of the Geologists Association of England* **78**, 535-554.

Wilson, R. C. L. 1968a. Carbonate facies variations within the Osmington Oolite series in Southern England. *Palaeogeography, Palaeoclimatology, Palaeoecology* **4**, 89-123.

Wilson, R. C. L. 1968b. Upper Oxfordian Palaeogeography of Southern England. *Palaeogeography, Palaeoclimatology, Palaeoecology* **4**, 5-28.

Wilson, R. C. L. 1975. Upper Jurassic Oolite Shoals, Dorset Coast, England. *In:* Guisby, R. N. (ed) *Tidal deposits, a case book of recent examples and fossil counterparts.* Springer Verlag, New York, 355-362.

Wilson, R.C.L., Hiscott, R.N., Willis, M.G. & Gradstein, F.M. 1990. The Lusitanian Basin of west central Portugal: Mesozoic and Tertiary tectonics, stratigraphic and subsidence history. *In:* Tankard, A.J. & Balkwill, H. (eds) *Extensional tectonics and stratigraphy of the North Atlantic margins.* American Association of Petroleum Geologists Memoir. **46**, 341-361.

Wilson, R.C.L. 1991. Sequence Stratigraphy: an Introduction. *Geoscientist* **1(1)**, 13-23.

Wright, J.K. 1981. The Corallian rocks of north Dorset. *Proceedings of the Geological Association* **92 (1)**, 17-32.

Wright, J. K. 1986a. A new look at the stratigraphy, sedimentology and ammonite fauna of the Corallian Group (Oxfordian) of south Dorset. *Proceedings of the Geological Association* **97 (1)**, 1-21.

Wright, J.K. 1986b. The Upper Oxford Clay at Furzy Cliff, Dorset: stratigraphy, palaeoenvironment and ammonite fauna. *Proceedings of the Geological Association* **97 (3)**, 221-228.

Ziegler, P.A. (ed.) 1990. Geological Atlas of Western and Central Europe (2nd edition) Shell International Petroleum Maatschappij 239pp.

Appendix 1: Petrographic point counting technique & detailed results

In standard petrographical studies of samples, point counting is a method used to establish the modal composition of a sediment - both detrital and authigenic. However, in this thesis the authigenic components of each sample were of particular interest, so the standard point counting procedure was modified slightly to compensate this.

Point counting of individual thin sections was performed using a "Swift Model F" electronic counter. Thin sections obtained from representative samples were placed on a mechanical stage which was screwed to the rotating stage of the microscope, which was then clamped. Under a moderate to high magnification, several traverses were made of each thin section and a total of 500 points per section were counted. Only components that were seen in pore spaces were counted. These were, individual authigenic phases (data of which is displayed in the following tables) porosity and matrix. Any detrital components were by-passed using the "stage only" button. Data was then displayed as a percentage of the total pore filling components. Where a samples' components do not add up to 100% (see following tables) then the remainder is composed of either porosity, matrix or both.

Table 1 (data expressed as a % of total pore filling components)

Appendix 1

Sample No.	Glauconite (%)	Phosphate (%)	Pyrite (%)	Non-ferroan concretionary calcite (%)	Ferroan poikilotopic calcite (%)	Concretionary burrow calcite (%)	Ferroan fringing calcite (%)	Ferroan equant sparry calcite (%)	Non-ferroan equant sparry calcite (%)	Ferroan dolomite (%)	Concretionary siderite (%)	Pore filling siderite (%)
B4			33.6	65.6								0.6
B2			22.3									
B1			39.0									
A4			33	62.6								
A5			35.4	64.6								
A6								100 (drusy)				
A8			13.6	78.0								8.3
B9			22	7	69							1.3
B3			17.6	4	51.4							2
B12			16	3	56			4.3		16		4.6
B13			15	60	6					15		4
B14			13	2	43					24		5
B17			11.3		47					28.6		13.0
B18			13		45					28		13.6
30	5	0.6	18									
31			9.3							34.6		
32	1.3		7.3							8.3		
32a			2.6		87					10.3		
34	1		10							6.2		
36	1.2		8.6							4.8		
36a			8.6		88					3.3		
E1			3		94			1.6		1.3		
E2			5.3		94.3					0.3		
E3			2		96.3					1.6		
E4	1.0		0.6		97.6					0.6		
GO1			17				6.6	70.3		2.6		3.3
40			7.3				56.6	27.3				8.0
42			22.6				12.6	61				3.6
48			8.3			91.3				0.3		

Table 1 (data expressed as a % of total pore filling components)

Appendix 1

Sample No.	Glauconite (%)	Phosphate (%)	Pyrite (%)	Non-ferroan concretionary calcite (%)	Ferroan poikilotopic calcite (%)	Concretionary burrow calcite (%)	Ferroan fringing calcite (%)	Ferroan equant sparry calcite (%)	Non-ferroan equant sparry calcite (%)	Ferroan dolomite (%)	Concretionary siderite (%)	Pore filling siderite (%)
50			9.3			90.6						
52			7.3			89.4				4.3		
54			6.6			23.3				44		
57			15.6					40.3	43.3			
59			7.6					54.3	38			
61			21.6				36.3	9	33.3			
C1			8.8			91.2						
C2			9.1			90.9						
C8			4.6				35.3	60				
C9			14.9				28.7	57.4				
C10			23.3				4.0	72.6				
C11			4.3				5.3	10.3				
C12			1.3				6.3	84				
C13								80.3				
C15			3.6				27.3	69				
78			4.6			91.6			3.6			
80			12.6			87.3						
82			15.4			69.5						
84			9.3			20.6		70				
85			10.6					69.4				
86			30					3.6		8.0		
87	0.3		6.6			10.3		80.3		2.3		
88			12.9				11.6	56.3				18.3
C22			14.3					55		12.2		18.5
C23			15.6					52.6		14.3		17.3
C24			14.5					46.4		18.3		20.5
C26			2.0					45.3		3.9		48.6
C27			5.3					33.3		4.6		56.6
111	6.6	4.6	31.6									

Table 1 (data expressed as a % of total pore filling components)

Appendix 1

Sample No.	Glauconite (%)	Phosphate (%)	Pyrite (%)	Non-ferroan concretionary calcite (%)	Ferroan poikilotopic calcite (%)	Concretionary burrow calcite (%)	Ferroan fringing calcite (%)	Ferroan equant sparry calcite (%)	Non-ferroan equant sparry calcite (%)	Ferroan dolomite (%)	Concretionary siderite (%)	Pore filling siderite (%)
112	2	1	11							30		35.6
113	1.3	0.6	14.3							0.6		56.6
115											100	
116											100	
118	0.6	1	6						5	42		
120	1	2	4.7						5	40		
D15			5					47				48
D17			3					20		5		5

Table 2 (data expressed as a % of total pore filling components)

Appendix 1

Sample No.	Pyrite (%)	Non-ferroan conc. Dolomite (%)	Ferroan dolomite (%)	Zoned non-ferroan dolomite (%)	Zoned non-ferroan conc. dolomite (%)	Dedolomite (%)	Non-ferroan sparry calcite (%)	Non-ferroan poikilotopic calcite (%)	Non-ferroan fringing calcite (%)	Non-ferroan microspar (%)	Ferroan sparry calcite (%)	Siderite (%)	Iron-oxide (%)
P1	24		66.6										
P2	16.6		70										
P5	10		65.3										
P11	8.4		52.1										
P12	7.3		53										
P14	21.3	56.3	6.3										
P14A	12.3	70.6	4.0										
P16	16.3	69											
P16A	17.3	50.0	4.3										
P17	17.6	50.3	12.3										
P17A	28.6	68.2	2.9										
P19	23.3	5								64.6			
P19A	11.3	18.3								62			
P21	15.6	14.3	62.6				0.6						
P25	33.8												
P25A	5												5 (matrix)
P25B	5												5 (matrix)
P25C	5												5 (matrix)
P26	17.3	1	42.9				0.6						0.6
P28	24.3	0.3	66.6										
P31	25.1	1.3	64.2										
P32	19.3		69.3										
P34	13.3	2	64.3	1.3									
P35	0.6	11	0.3	33			13.2					0.6	
P36	13.6	0.6	41									1.6	
P36A	5		0.3		13.6			47				1.6	15.3
P36B	3.6				13.2		4.5	41				0.8	2.4
P38	26		55.6										
P38D				34.6			25	4					
P38H				63.6			10.3	7.6					
P38F				30.7			24.8	5.4					
P38G					26.3		27.3	2.6					8.6
P40				31.3			14.3	22.6					3.3
P40A				32.5			19.6	10.2					3.5

Table 2 (data expressed as a % of total pore filling components)

Appendix 1

Sample No.	Pyrite (%)	Non-ferroan conc. Dolomite (%)	Ferroan dolomite (%)	Zoned non-ferroan dolomite (%)	Zoned non-ferroan conc. dolomite (%)	Dedolomite (%)	Non-ferroan sparry calcite (%)	Non-ferroan poikilotopic calcite (%)	Non-ferroan fringing calcite (%)	Non-ferroan microspar (%)	Ferroan sparry calcite (%)	Siderite (%)	Iron-oxide (%)
P41					2.3		16	61.6				2	0.3
P41A								70.6					11
P41C	5.6							52.3				6	5.3
P41D			2		5.6							1.3	56
P43												5.3	42.3
P43A	0.9											4.9	45.7
P43B	6											13.6	53.3
P43C	0.3							76 (r)					7.6
P43D	1.6							78 (r)					3.6
P43E	1.2							74 (r)					4
P43F	0.6							70.6 (r)					2.3
P44	0.3						13.6 (r)	62.3 (r)				7	5.3
P44A	0.6							84.3 (r)				2.6	12
P45							37.3 (r)					0.3	
P45A							29 (r)	65.3 (r)				2.3	0.6
P45B							2 (r)	85.6 (r)				1	3.3
P45C								82.6 (r)					0.3
P45D								96 (r)				0.6	0.6
P46							0.6 (r)	76.6 (r)				3.3	0.6
P47							0.6 (r)	82 (r)				5.6	9.6
P48	4.6						28	53.3				12.3	0.3
P49							13				75	10.3	1.6
P50							23.3	27		36.3		13	0.3
P50A							16.6	14		37.3		0.6	
P50B							35	18.6				3.6	
P50C							18	9	10.3	48		10	
P51							54.3	45.6		45.6			
P52A						0.8	62.3		22.3	0.3	15		
P52C						1.5	26.6		9.6	57.3		6.3	
P52B						2.2	37		20	31.0	8	4	
P53							37.9		7.6	34.6	15.1	5	
P54						6	0.3			71.3	20.6	1.6	
P56										85.3	1.3	13.3	

Table 2 (data expressed as a % of total pore filling components)

Appendix 1

Sample No.	Pyrite (%)	Non-ferroan conc. Dolomite (%)	Ferroan dolomite (%)	Zoned non-ferroan dolomite (%)	Zoned non-ferroan conc. dolomite (%)	Dedolomite (%)	Non-ferroan sparry calcite (%)	Non-ferroan poikilotopic calcite (%)	Non-ferroan fringing calcite (%)	Non-ferroan microspar (%)	Ferroan sparry calcite (%)	Siderite (%)	Iron-oxide (%)
P56A	10.3					5.3	0.6			70	2.3	8	3.3
P57	10.9											21.9	12.6
P57A	9.6											16.9	18.6
P59	3.3						1.3			86.3		9	
P61	1					8.3				83.3	3.3	4	
P62	7						1.6			81.3	0.6	9.3	
P63	1.3					95.3							
P65						76.7						8.3	
P67						72.5						6.9	

(r) = calcite replacing original zoned dolomite.

Appendix 2: The preparation & qualitative x-ray diffraction analysis of carbonate cement phases

A2.1: *Preparation & analysis*

The purpose of x-ray diffraction (XRD) within the context of this thesis was to provide an estimation of the purity of samples that were selected for stable isotope analysis.

Using a scalpel, micro-drill and binocular microscope, carbonate cement phases (ferroan dolomite, non-ferroan dolomite, siderite, ferroan fringing calcite, ferroan equant calcite and non-ferroan equant calcite) were cut out of stained sample off-cuts. At least 10mg of sample was obtained, which was gently ground down to a mean particle size of between 5-10μm. The sample was pushed through a sieve to test this. Each sample was then smear mounted onto an aluminium mounting stage and inserted into a diffractometer. Analysis was performed on a Philips PW 1729 x-ray generator. The Kv was set to 40 and the amps was set to 50mA. The output device was a PW 1710 diffractometer control unit which records the results in both analogue and digital form.

After the samples had been analysed, pure samples of calcite, dolomite and quartz were also tested so that quick comparisons could be made with actual samples. X-ray diffraction charts were then analysed by identifying diffraction peaks (2θ angles and *d* spacings) to obtain a qualitative analysis of each sample. Analysis of diffraction peak

height (x-ray intensity counts per second) allows for an estimation of the relative abundance of mineral types in impure samples. All samples were found to be between 90 to 100% pure for the type of carbonate sampled. It should be noted that the presence of quartz does not affect stable isotope analysis of carbonates.

The results that follow are for each sample and are displayed in both tabular and graphical format. In each sample listed below, the carbonate compound required for analysis is listed as the sample name. For every compound detected in each sample, the $2\theta_{Cu}$ angle, *d*-value and number of counts is given.

A2.2: *Results*

A2.2.1: Selected Corallian Group samples

Sample A5:- Calcite

Analysis also reveals quartz

Calcite:-	$2\theta_{Cu}$	29.57
	d(Å)	3.02
	counts	496
Quartz:-	$2\theta_{Cu}$	26.72
	d(Å)	3.33
	counts	920

Sample A6:- Fracture Calcite

Analysis also reveals some pyrite (trace)

Calcite:	$2\theta_{Cu}$	29.50	39.60	43.36	47.76
	d(Å)	3.02	2.27	2.08	1.90
	counts	2638	588	386	1086

Pyrite:	$2\theta_{Cu}$	57.54			
	d(Å)	1.59 ($^{+}$/.0.04)			
	counts	208			

Sample A8:- Calcite (non-ferroan)

Analysis also reveals quartz and pyrite (trace)

Calcite:-	$2\theta_{Cu}$	29.54	39.58	43.33	47.37
	d(Å)	3.02	2.27	2.08	1.92
	counts	3422	676	786	242
Quartz:-	$2\theta_{Cu}$	26.71	60.89		
	d(Å)	3.33	1.52		
	counts	710	242		
Pyrite:-	$2\theta_{Cu}$	57.63	47.71		
	d(Å)	1.59	1.90		
	counts	412	558		

Sample 32A:- Calcite

Analysis also reveals quartz

Calcite:	$2\theta_{Cu}$	29.60	39.64	43.33	47.74
	d(Å)	3.01 ($^{+}$/.0.02)	2.27 ($^{+}$/.0.01)	2.09	1.90
	counts	2432	294	290	2846
Quartz:	$2\theta_{Cu}$	26.75	20.99	50.21	60.03
	d(Å)	3.33	4.23 ($^{+}$/.0.03)	1.81	1.54
	counts	1550	384	490	514

Sample E3:- Calcite (ferroan)

Analysis also reveals quartz and pyrite (trace).

Calcite:-	$2\theta_{Cu}$	29.73	39.75	43.52	47.48
	d(Å)	3.00	2.26	2.07	1.91
	counts	5722	772	774	324
Quartz:-	$2\theta_{Cu}$	26.88	21.08	50.38	60.14
	d(Å)	3.31	4.20	1.81	1.53
	counts	6514	748	632	672
Pyrite:-	$2\theta_{Cu}$	56.91	40.55		
	d(Å)	1.61	2.22		
	counts	222	232		

Sample E4:- Calcite (ferroan)

Analysis also reveals quartz, siderite, pyrite and dolomite (trace quantities).

Calcite:-	$2\theta_{Cu}$	29.74	39.72	43.45	47.45
	d(Å)	3.00	2.27	2.08	1.91
	counts	1206	492	278	242

Quartz:-	$2\theta_{Cu}$	26.92	21.12	50.40	60.23
	d(Å)	3.31	4.20	1.81	1.54
	counts	3002	420	320	506
Siderite:-	$2\theta_{Cu}$	32.05			
	d(Å)	2.79			
	counts	226			
Pyrite:-	$2\theta_{Cu}$	57.67			
	d(Å)	1.59			
	counts	222			
Dolomite:-	$2\theta_{Cu}$	67.89			
	d(Å)	1.38			
	counts	254			

Sample 39A:- Calcite

Analysis also reveals quartz, pyrite and dolomite (both trace quantities)

Calcite:-	$2\theta_{Cu}$	39.58	42.56		
	d(Å)	2.28	2.12		
	counts	464	376		
Quartz:-	$2\theta_{Cu}$	26.80	20.98	50.29	60.03
	d(Å)	3.32	4.23	1.81	1.54
	counts	3986	970	1052	774
Pyrite:-	$2\theta_{Cu}$	55.01	40.43		
	d(Å)	1.67	2.23		
	counts	226	338		
Dolomite:-	$2\theta_{Cu}$	67.80			
	d(Å)	1.38			
	counts	290			

Sample 40:- Calcite

Analysis also reveals quartz and pyrite (trace).

Calcite:-	$2\theta_{Cu}$	29.56	39.59	43.34	47.71
	d(Å)	3.01	2.27	2.09	1.90
	counts	1814	320	230	428
Quartz:-	$2\theta_{Cu}$	26.73			
	d(Å)	3.33			
	counts	216			
Pyrite:-	$2\theta_{Cu}$	57.63			
	d(Å)	1.59			
	counts	264			

Sample 61:- Calcite

Analysis also reveals pyrite (trace).

Calcite:	$2\theta_{Cu}$	29.57	39.58	43.32	47.72

	d(Å)	3.02	2.27	2.09	1.90
	counts	1224	264	270	276
Pyrite:	$2\theta_{Cu}$	57.60			
	d(Å)	1.59 (+/.0.04)			
	counts	156			

Sample C10:- Calcite

Analysis also reveals quartz

Calcite:-	$2\theta_{Cu}$	29.46	39.53	47.61	48.68
	d(Å)	3.03	2.28	1.91	1.87
	counts	452	164	420	254
Quartz:-	$2\theta_{Cu}$	61.01			
	d(Å)	1.52			
	counts	264			

Oolitic Control Sample

Small trace of detrital quartz interpreted to be nucleus for ooid growth

Calcite:-	$2\theta_{Cu}$	29.59	39.60	43.34	47.72
	d(Å)	3.02	2.27	2.08	1.90
	counts	1054	428	224	294
Quartz:-	$2\theta_{Cu}$	26.66			
	d(Å)	3.33			
	counts	476			

Sample C27:- Siderite

Hand picked siderite crystals (small volume). Also detected - quartz and calcite

Siderite:	$2\theta_{Cu}$	48.68		
	d(Å)	1.88 (+/.0.08)		
	counts	216		
Calcite:	$2\theta_{Cu}$	29.48	43.4	47.68
	d(Å)	3.03	2.08(+/.0.01)	1.91
	counts	606	580	232
Quartz:	$2\theta_{Cu}$	26.6		
	d(Å)	3.35 (+/.0.01)		
	counts	180		

Sample 113:- Siderite

Analysis reveals only small evidence of siderite, plus quartz and calcite

Siderite:-	$2\theta_{Cu}$	32.08		
	d(Å)	Small peak, no d-value		
Quartz:-	$2\theta_{Cu}$	26.71	20.89	50.24
	d(Å)	3.33	4.25	1.81

	counts	1132	352	312
Calcite:-	$2\theta_{Cu}$	39.53		
	d(Å)	2.28		
	counts	322		

Sample 115:- Siderite

Analysis also reveals quartz

Siderite:	$2\theta_{Cu}$	31.76	50.22
	d(Å)	2.81 ($^{+}$/.0.02)	1.82 ($^{+}$/.0.06)
	counts	356	316
Quartz:	$2\theta_{Cu}$	26.69	36.57
	d(Å)	3.34	2.46
	counts	456	356

SAMPLE AS:: POWDERING CALCITE
Upto 66.610
29.571°2θ d=3.02 Calcite
26.320°2θ d=3.35 Quartz
23.471°2θ d=3.79

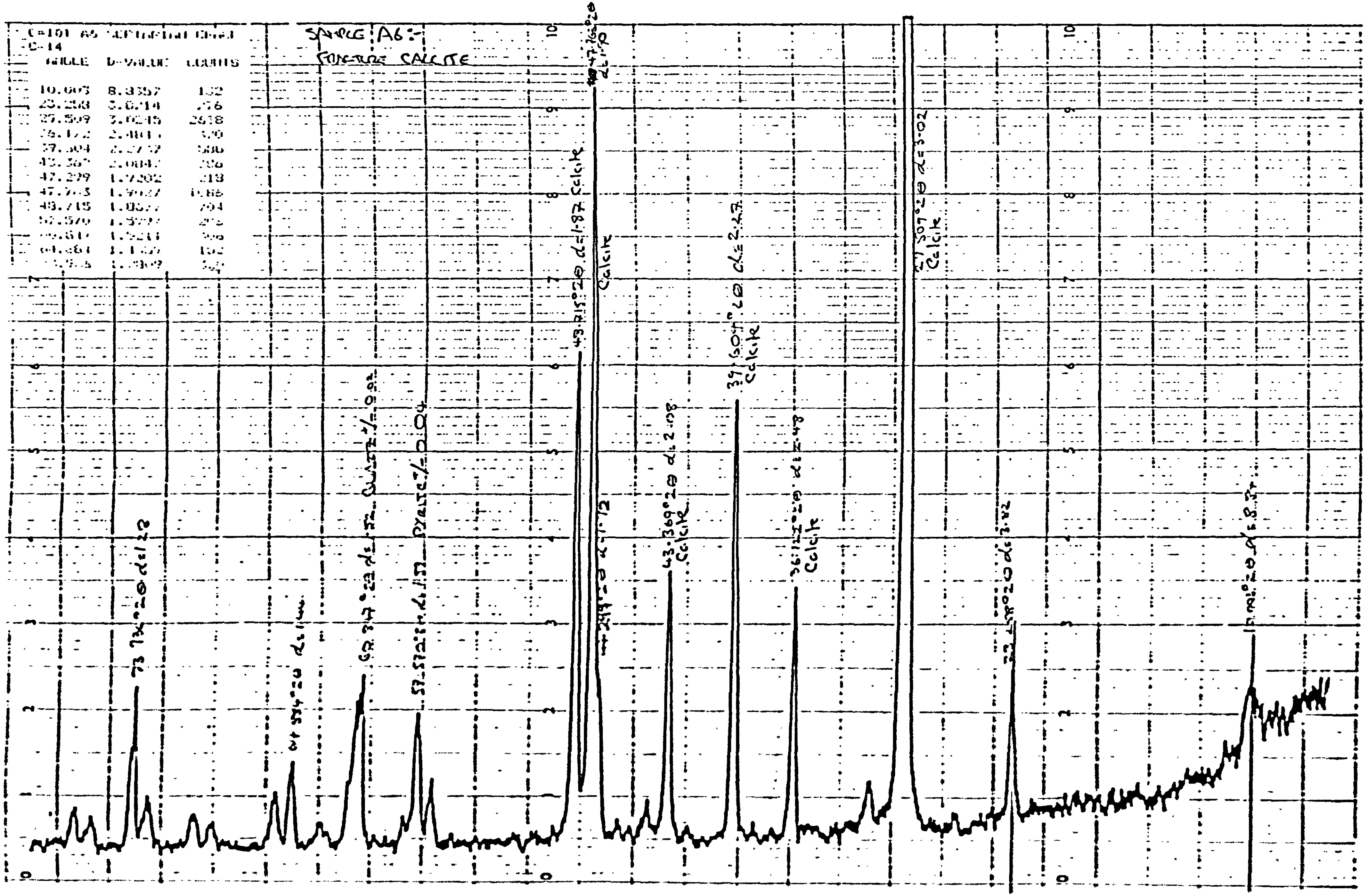
SAMPLE A6:-
FRACTURE CALCITE
C-14
ANGLE D-VALUE COUNTS
10.003 8.3357 132
47.299 1.7202
48.715
73.73°2θ d=1.28
27.507°2θ d=3.02
Calcite
39.504°2θ d=2.27
Calcite
43.369°2θ d=2.08
Calcite
43.715°2θ d=1.87 Calcite
Calcite
Pyrite %= 0.04
Quartz %= 0.92

4

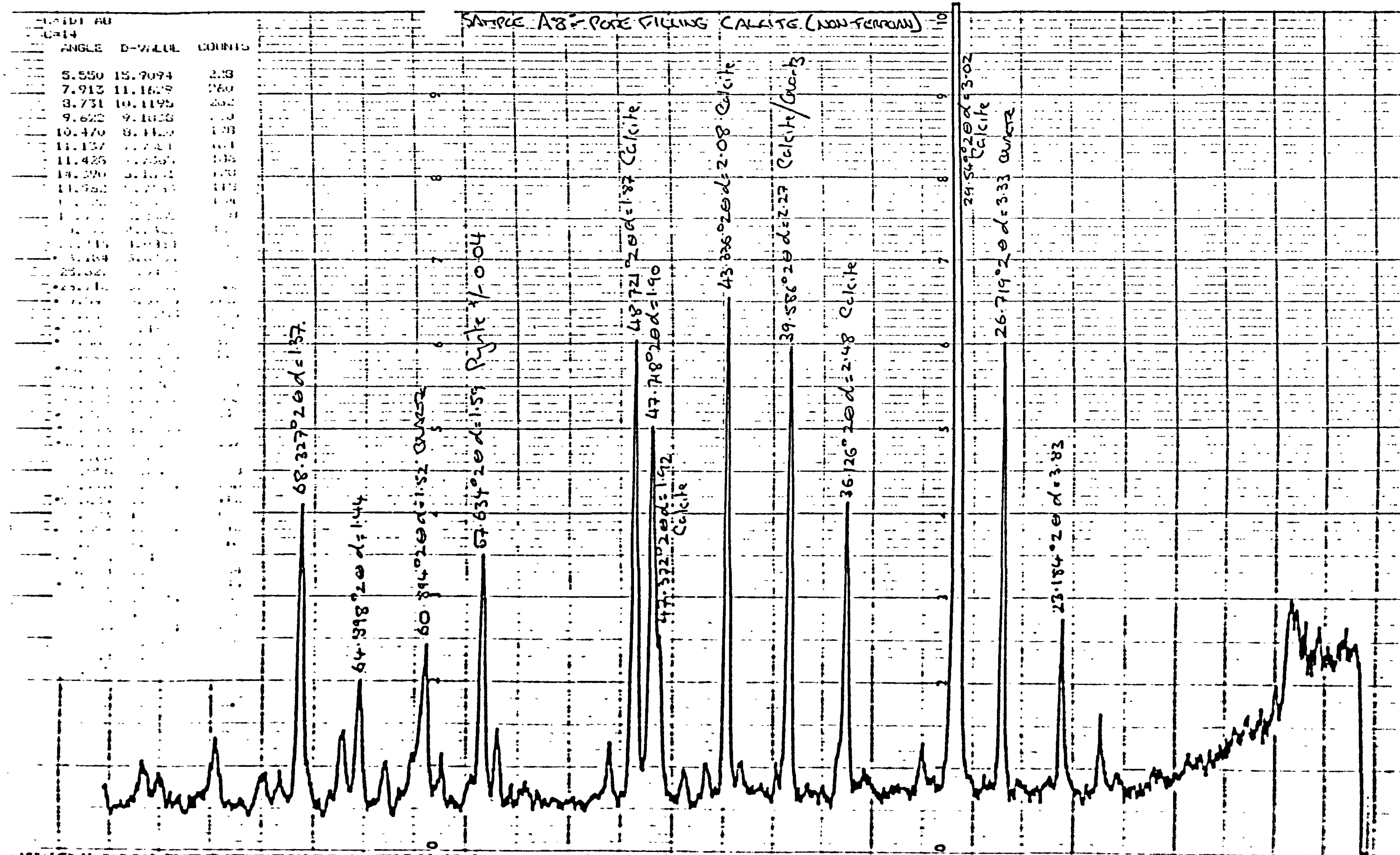
SAMPLE A8: PORE FILLING CALCITE (NON-FERROAN)
ANGLE D-VALUE COUNTS
5.550 15.9094 233
7.913 11.1629 260
68.327°2θ d=1.37
64.998°2θ d=1.44
60.894°2θ d=1.52 QUARTZ
67.634°2θ d=1.57 Pyrite ±/-0.04
48.721°2θ d=1.87 Calcite
47.748°2θ d=1.90
47.522°2θ d=1.92 Calcite
43.336°2θ d=2.08 Calcite
39.586°2θ d=2.27 Calcite/Qtz
36.126°2θ d=2.48 Calcite
29.54°2θ d=3.02 Calcite
26.719°2θ d=3.33 QUARTZ
23.184°2θ d=3.83

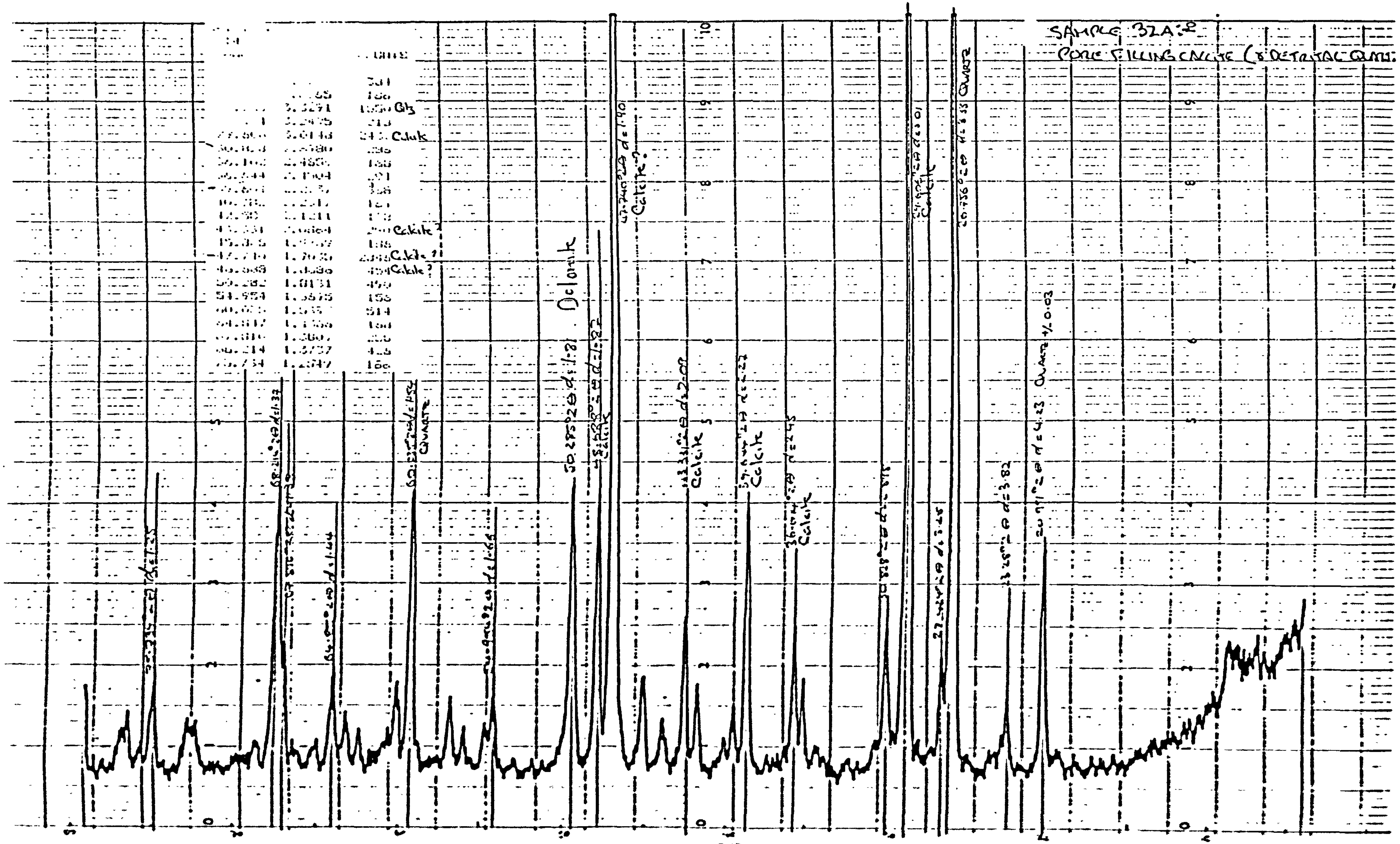
SAMPLE 32A-2
PORE FILLING CALCITE (& DETRITAL QUARTZ)
Dolomite
Calcite
Calcite?
Quartz
Quartz +/- 0.03

L

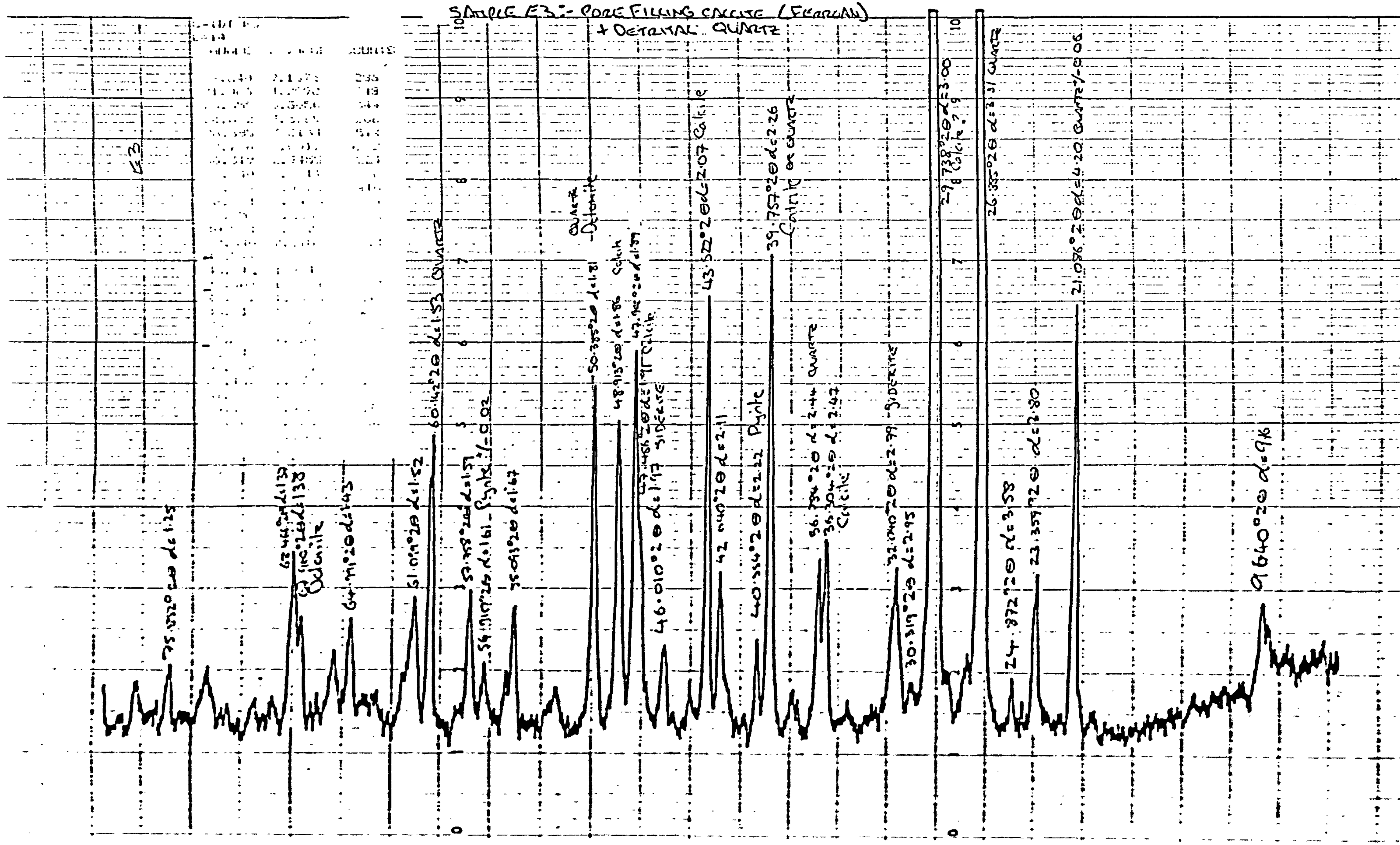
SAMPLE E3:- PORE FILLING CALCITE (FERROAN)
+ DETRITAL QUARTZ
E3
9.640°2θ d=9.16
21.086°2θ d=4.20 QUARTZ ⅟-0.06
23.359°2θ d=3.80
24.872°2θ d=3.58
26.335°2θ d=3.31 QUARTZ
29.738°2θ d=3.00
30.319°2θ d=2.95
32.040°2θ d=2.79 SIDERITE
36.784°2θ d=2.44 QUARTZ
39.757°2θ d=2.26
Calcite or QUARTZ
40.554°2θ d=2.22 Pyrite
42.440°2θ d=2.11
43.522°2θ d=2.07 Calcite
46.010°2θ d=1.97 SIDERITE
48.913°2θ d=1.86 Calcite
50.335°2θ d=1.81
Dolomite
Quartz
55.093°2θ d=1.67
60.142°2θ d=1.53 QUARTZ
61.090°2θ d=1.52
Dolomite
75.550°2θ d=1.25

SAMPLE E43:- PORE FILLING CALCITE (FERROAN) (+ DETRITAL QUARTZ)

L=161 E4
C=14

ANGLE	D-VALUE	COUNTS
5.692	15.5135	214
21.129	4.2012	420
23.379	3.8017	250
26.721	3.3092	5002
29.747	3.0008	1206
32.559	2.7895	226
36.315	2.4598	260
35.791	2.1109	234
39.725	2.2671	472
40.526	2.2241	232
43.452	2.0809	278
47.459	1.9141	21?
47.837	1.8998	475
48.567	1.8422	288
50.407	1.8058	320
57.674	1.5970	222
60.230	1.5352	506
65.010	1.4334	224
67.891	1.3794	254
68.376	1.3708	352
73.495	1.2875	178

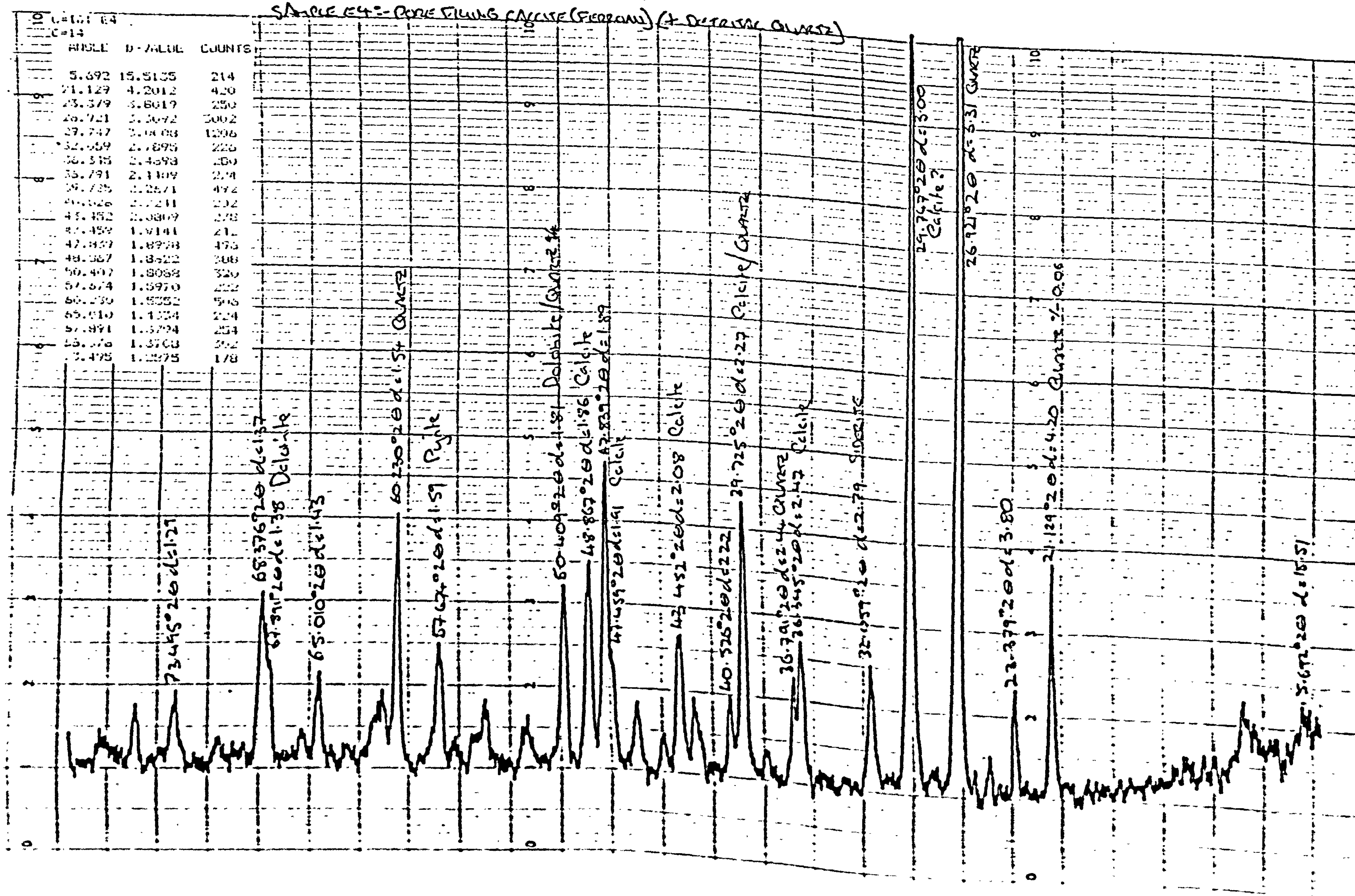

SAMPLE SET 3 - POWDER DIFFRACTOMETER (Cu Kα) (+ Diffracted Quartz)

	d-Å	Counts
5.392	15.5135	214
11.127	7.9512	420
15.579	5.6817	152
17.727	5.0002	1096
20.335	4.3633	200
21.991	4.0378	1096
23.731	3.7461	474
25.455	3.4972	146
27.127	3.2849	1096
28.755	3.1019	1096
30.335	2.9443	1096
31.875	2.8055	1096
33.379	2.6825	1096
34.855	2.5715	1096
36.307	2.4722	1096
37.735	2.3825	1096
39.143	2.3000	1096
40.535	2.2236	1096
41.911	2.1529	1096
43.275	2.0875	1096
44.627	2.0268	1096
45.967	1.9703	1096
47.295	1.9176	1096
48.611	1.8683	1096
49.915	1.8220	1096
51.207	1.7785	1096
52.487	1.7376	1096
53.755	1.6991	1096
55.011	1.6627	1096
56.255	1.6283	1096
57.487	1.5957	1096
58.707	1.5648	1096
59.915	1.5355	1096
61.111	1.5076	1096
62.295	1.4811	1096
63.467	1.4559	1096
64.627	1.4319	1096
65.775	1.4090	1096
66.911	1.3872	1096
68.035	1.3664	1096
69.147	1.3465	1096
70.247	1.3275	1096
71.335	1.3093	1096
72.411	1.2919	1096
73.475	1.2753	1096
74.527	1.2594	1096
75.567	1.2442	1096
76.595	1.2296	1096
77.611	1.2157	1096
78.615	1.2023	1096
79.607	1.1895	1096
80.587	1.1772	1096
81.555	1.1654	1096
82.511	1.1541	1096
83.455	1.1432	1096
84.387	1.1328	1096
85.307	1.1228	1096
86.215	1.1132	1096
87.111	1.1040	1096
87.995	1.0952	1096
88.867	1.0867	1096
89.727	1.0786	1096
90.575	1.0708	1096
91.411	1.0633	1096
92.235	1.0562	1096
93.047	1.0493	1096
93.847	1.0428	1096
94.635	1.0365	1096
95.411	1.0305	1096
96.175	1.0248	1096
96.927	1.0193	1096
97.667	1.0141	1096
98.395	1.0091	1096
99.111	1.0044	1096
99.815	1.0000	1096

$2\theta = 5.392°$ d = 15.5135 Å

$2\theta = 11.127°$ d = 7.9512 Å

$2\theta = 15.579°$ d = 5.6817 Å

$2\theta = 17.727°$ d = 5.0002 Å

$2\theta = 20.335°$ d = 4.3633 Å

$2\theta = 21.991°$ d = 4.0378 Å

$2\theta = 23.731°$ d = 3.7461 Å

$2\theta = 25.455°$ d = 3.4972 Å

$2\theta = 27.127°$ d = 3.2849 Å

$2\theta = 28.755°$ d = 3.1019 Å

$2\theta = 30.335°$ d = 2.9443 Å

$2\theta = 31.875°$ d = 2.8055 Å

$2\theta = 33.379°$ d = 2.6825 Å

$2\theta = 34.855°$ d = 2.5715 Å

$2\theta = 36.307°$ d = 2.4722 Å

$2\theta = 37.735°$ d = 2.3825 Å

$2\theta = 39.143°$ d = 2.3000 Å

$2\theta = 40.535°$ d = 2.2236 Å

$2\theta = 41.911°$ d = 2.1529 Å

$2\theta = 43.275°$ d = 2.0875 Å

$2\theta = 44.627°$ d = 2.0268 Å

$2\theta = 45.967°$ d = 1.9703 Å

$2\theta = 47.295°$ d = 1.9176 Å

$2\theta = 48.611°$ d = 1.8683 Å

$2\theta = 49.915°$ d = 1.8220 Å

$2\theta = 51.207°$ d = 1.7785 Å

$2\theta = 52.487°$ d = 1.7376 Å

$2\theta = 53.755°$ d = 1.6991 Å

$2\theta = 55.011°$ d = 1.6627 Å

$2\theta = 56.255°$ d = 1.6283 Å

$2\theta = 57.487°$ d = 1.5957 Å

$2\theta = 58.707°$ d = 1.5648 Å

$2\theta = 59.915°$ d = 1.5355 Å

$2\theta = 61.111°$ d = 1.5076 Å

$2\theta = 62.295°$ d = 1.4811 Å

$2\theta = 63.467°$ d = 1.4559 Å

$2\theta = 64.627°$ d = 1.4319 Å

$2\theta = 65.775°$ d = 1.4090 Å

$2\theta = 66.911°$ d = 1.3872 Å

$2\theta = 68.035°$ d = 1.3664 Å

$2\theta = 69.147°$ d = 1.3465 Å

$2\theta = 70.247°$ d = 1.3275 Å

$2\theta = 71.335°$ d = 1.3093 Å

$2\theta = 72.411°$ d = 1.2919 Å

$2\theta = 73.475°$ d = 1.2753 Å

$2\theta = 74.527°$ d = 1.2594 Å

$2\theta = 75.567°$ d = 1.2442 Å

$2\theta = 76.595°$ d = 1.2296 Å

$2\theta = 77.611°$ d = 1.2157 Å

$2\theta = 78.615°$ d = 1.2023 Å

$2\theta = 79.607°$ d = 1.1895 Å

$2\theta = 80.587°$ d = 1.1772 Å

$2\theta = 81.555°$ d = 1.1654 Å

$2\theta = 82.511°$ d = 1.1541 Å

$2\theta = 83.455°$ d = 1.1432 Å

$2\theta = 84.387°$ d = 1.1328 Å

$2\theta = 85.307°$ d = 1.1228 Å

$2\theta = 86.215°$ d = 1.1132 Å

$2\theta = 87.111°$ d = 1.1040 Å

$2\theta = 87.995°$ d = 1.0952 Å

$2\theta = 88.867°$ d = 1.0867 Å

$2\theta = 89.727°$ d = 1.0786 Å

$2\theta = 90.575°$ d = 1.0708 Å

$2\theta = 91.411°$ d = 1.0633 Å

$2\theta = 92.235°$ d = 1.0562 Å

$2\theta = 93.047°$ d = 1.0493 Å

$2\theta = 93.847°$ d = 1.0428 Å

$2\theta = 94.635°$ d = 1.0365 Å

$2\theta = 95.411°$ d = 1.0305 Å

$2\theta = 96.175°$ d = 1.0248 Å

$2\theta = 96.927°$ d = 1.0193 Å

$2\theta = 97.667°$ d = 1.0141 Å

$2\theta = 98.395°$ d = 1.0091 Å

$2\theta = 99.111°$ d = 1.0044 Å

$2\theta = 99.815°$ d = 1.0000 Å

SAMPLE 38A POWDER PATTERNS CALCITE CEMENT (4 SAMPLE AVERAGE)

			COUNTS
			224
			570
			785
			306
			318
			164
			330

26.208°2θ d=3.32 Quartz

20.986°2θ d=4.23 Quartz

36.632°2θ d=2.45 Quartz

39.581°2θ d=2.28 Calcite

40.432°2θ d=2.23 Pyrite 1/I₀=0.02

42.502°2θ d=2.12

45.893°2θ d=1.98

50.290°2θ d=1.81 Dolomite/Quartz

55.016°2θ 1/I₀=0.04 Pyrite

60.292°2θ d=1.54 Quartz

64.128°2θ d=1.45

67.658°2θ d=1.38 Dolomite

68.623°2θ d=1.37

73.492°2θ d=1.29

75.665°2θ d=1.26

SAMPLE 40:- PORE FILLING CALCITE (+ DETRITAL QUARTZ + OXID)

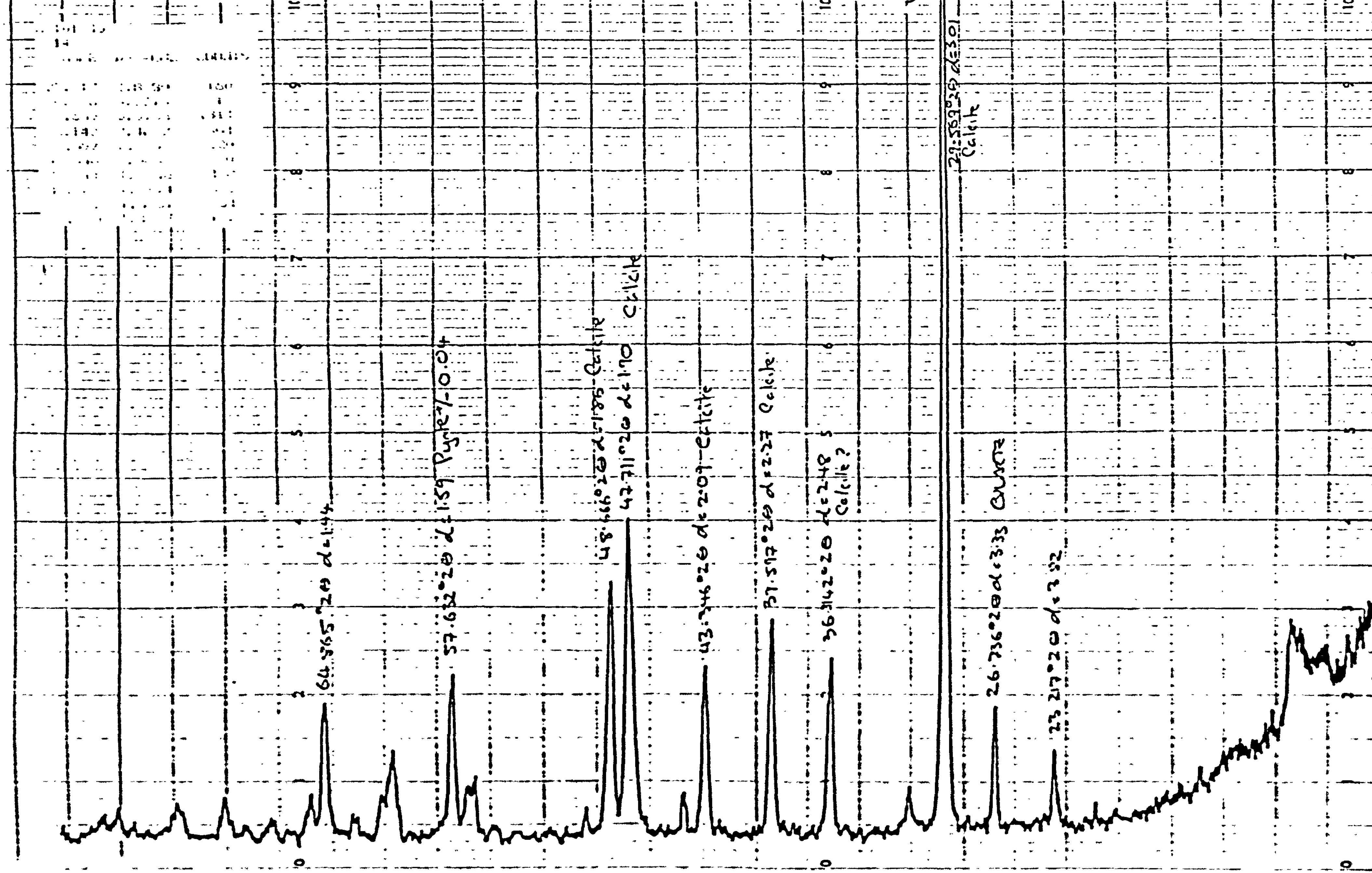

SAMPLE G1:- PORE FILLING CALCITE

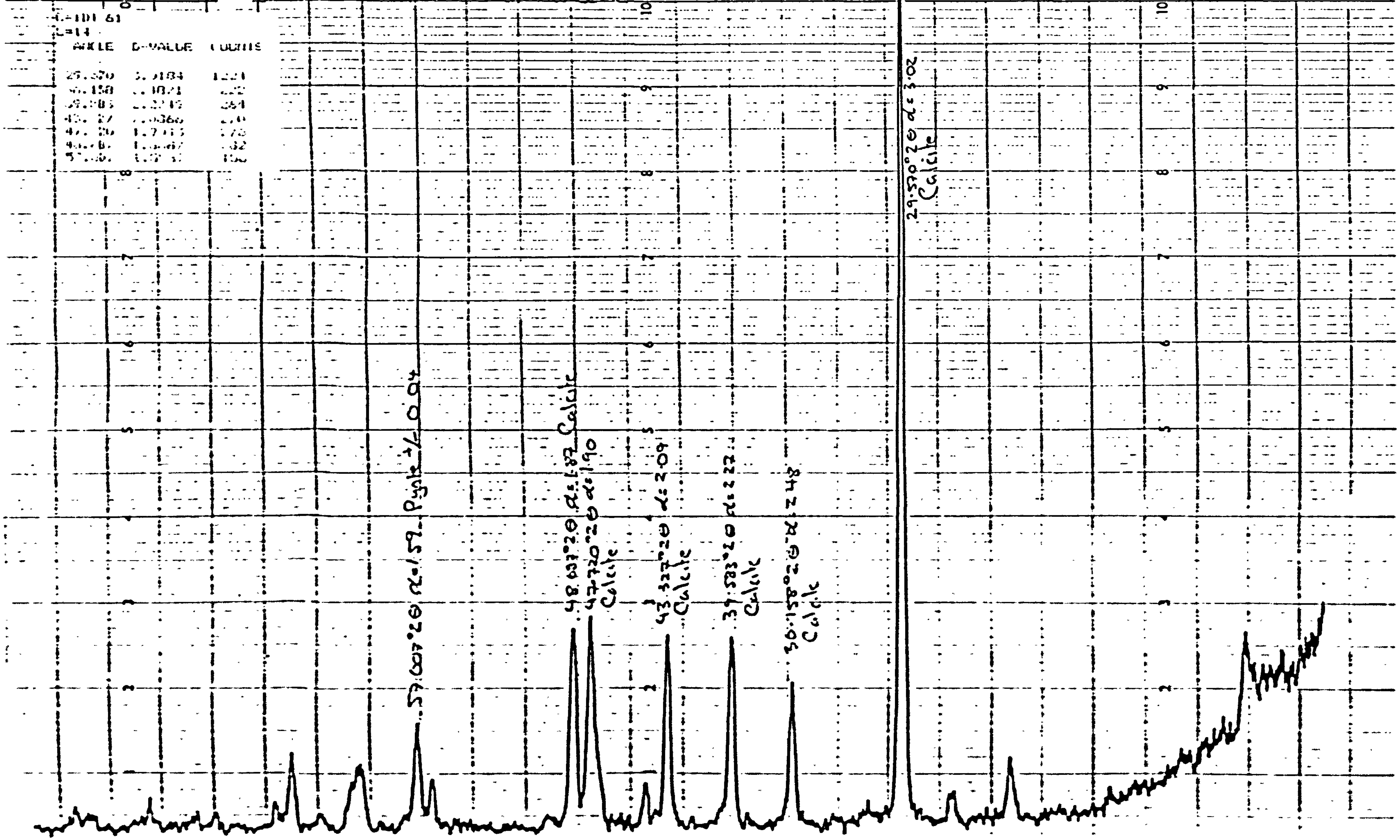

SAMPLE CIO : CORE-FILLING CALCITE
61.019°2θ d=3.52 Quartz
42.683°2θ d=4.92 Calcite
42.610°2θ d=1.91 Calcite
39.536°2θ d=2.28 Calcite
29.458°2θ d=3.03 Calcite

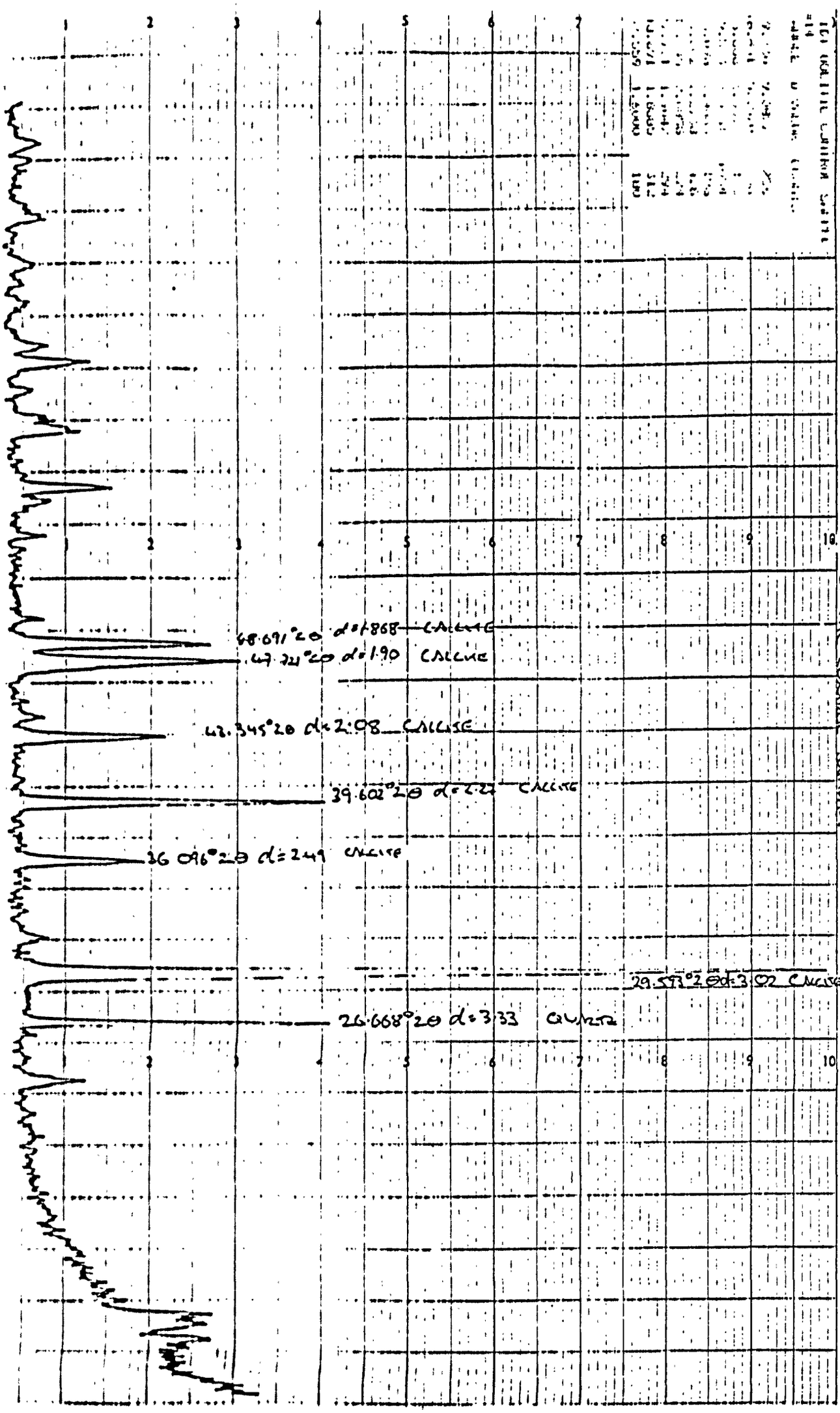
68.091°2θ d=1.868 CALCITE
47.221°2θ d=1.90 CALCITE
42.345°2θ d=2.08 CALCITE
39.602°2θ d=2.22 CALCITE
36.096°2θ d=2.49 CALCITE
29.593°2θ d=3.02 CALCITE
26.668°2θ d=3.33 QUARTZ
OOLITIC COASTAL SANDS.

SAMPLE ICZ7 :- Siderite Rhombs.

49.685°=2θ d=1.91
Calcite

43.4x°=2θ d=2.08
Calcite ?

29.4°=2θ d=3.03
Calcite

R

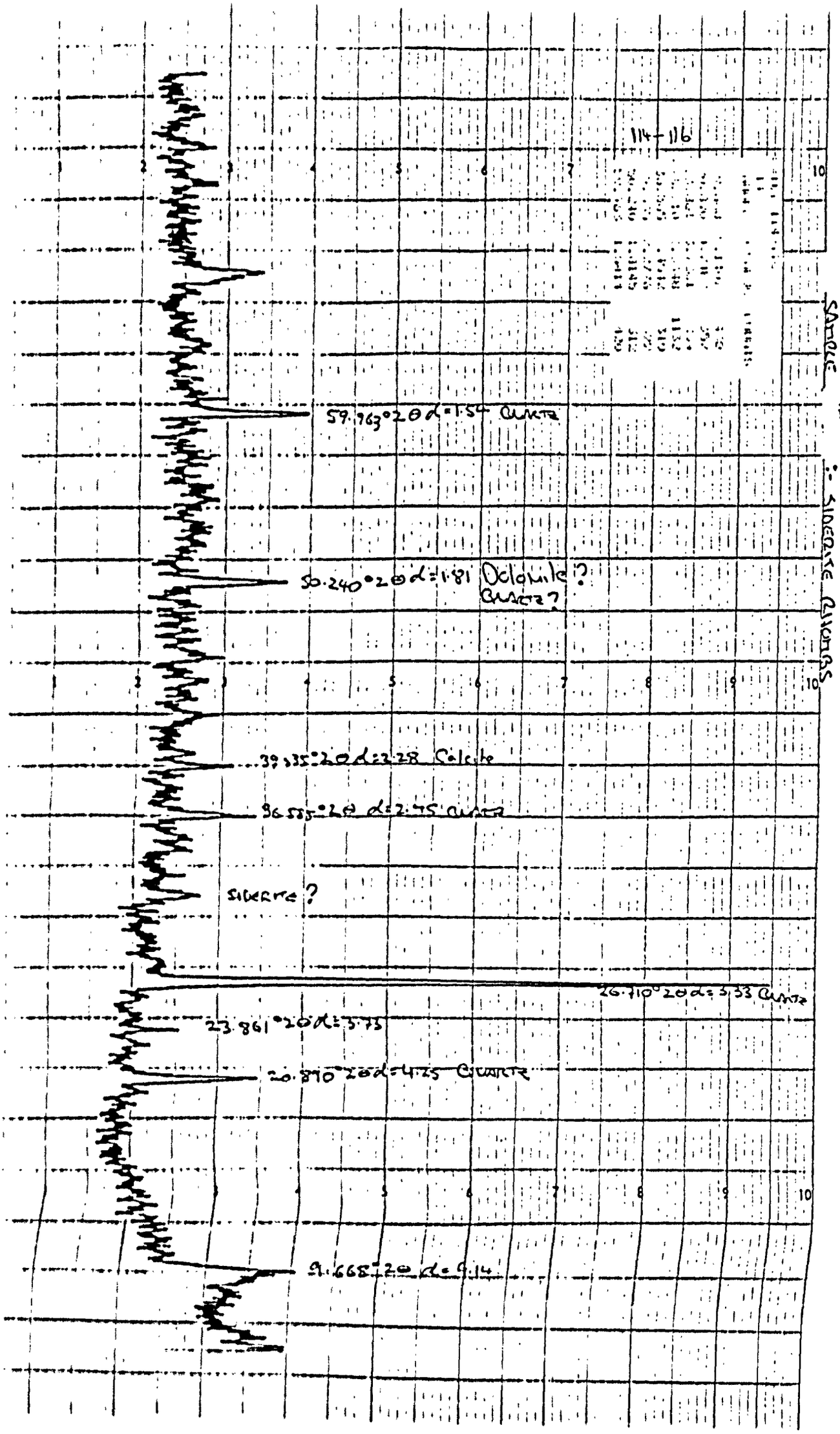
114-116
SAMPLE 12
59.963°2θ d=1.54 Quartz
50.240°2θ d=1.81 Dolomite? Quartz?
39.435°2θ d=2.28 Calcite
36.585°2θ d=2.45 Quartz
Siderite?
26.710°2θ d=3.33 Quartz
23.861°2θ d=3.75
20.870°2θ d=4.25 Quartz
9.668°2θ d=9.14

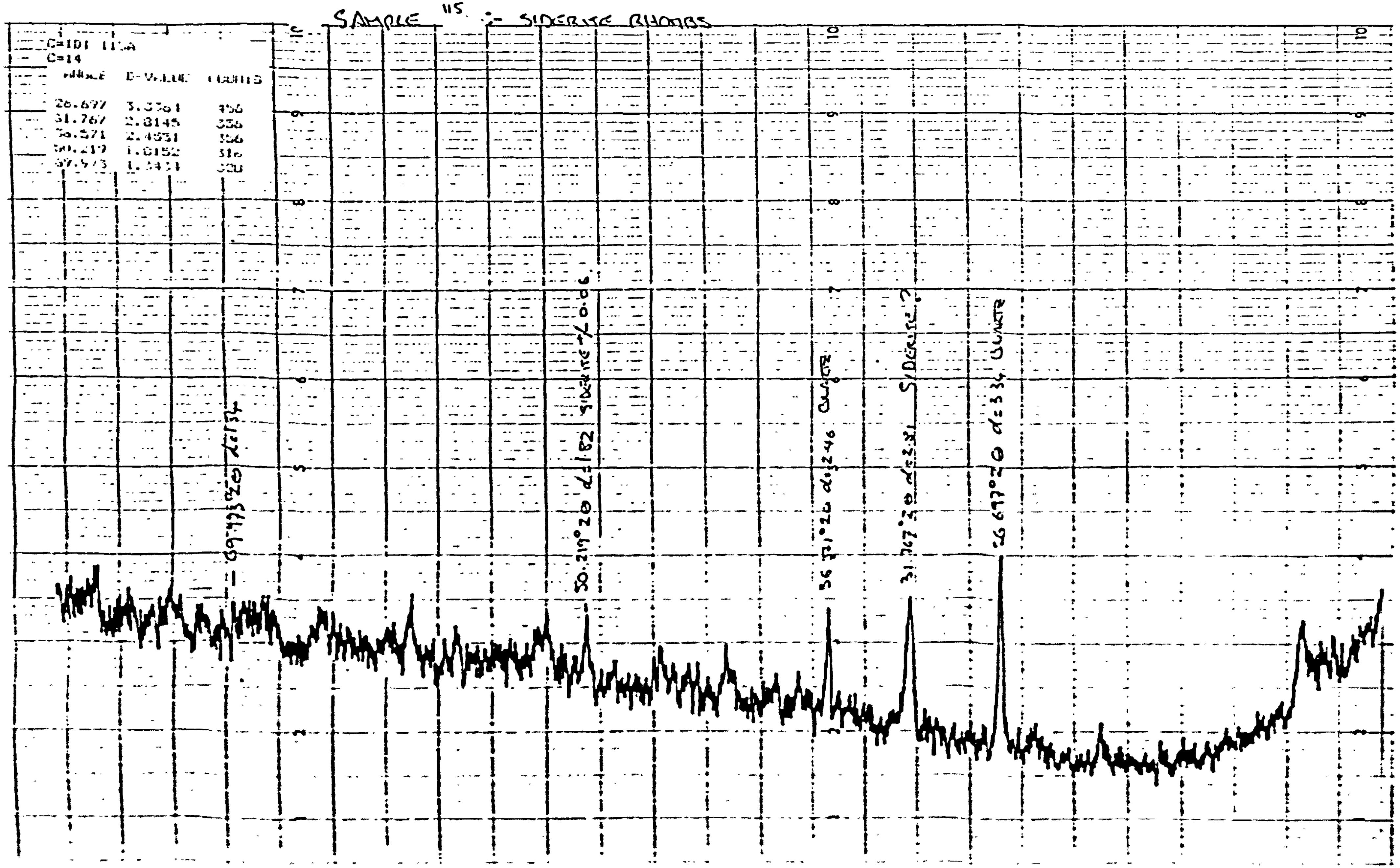
SAMPLE 115 :- SIDERITE RHOMBS
C=IDI 11?A
C=14
ANGLE D-VALUE COUNTS
26.697 3.3361 456
31.767 2.8145 336
36.571 2.4551 356
50.219 1.8152 316
69.973 1.3431 308
26.697°2θ d=3.34 QUARTZ
31.767°2θ d=2.81 SIDERITE ?
36.571°2θ d=2.46 QUARTZ
50.219°2θ d=1.82 SIDERITE +/ 0.06
69.973°2θ d=1.34

A2.2.2: Selected Ericeira Group samples

Sample P14:- Dolomite

Analysis reveals minor quartz

Dolomite:-	$2\theta_{Cu}$	30.93	41.10	50.89	50.26
	d(Å)	2.88	2.19	1.79	1.81
	counts	4170	576	836	502
Quartz:-	$2\theta_{Cu}$	26.74	37.34		
	d(Å)	3.33	2.40		
	counts	446	458		

Sample P17:- Dolomite

Analysis also reveals traces of pyrite

Dolomite:-	$2\theta_{Cu}$	30.79	41.00	50.77	44.80
	d(Å)	2.90	2.19	1.79	2.02
	counts	2572	500	384	322
Pyrite:-	$2\theta_{Cu}$	33.31	37.24		
	d(Å)	2.68	2.41		
	counts	164	250		

Sample P19:- Fracture calcite

Analysis also reveals traces of dolomite

Calcite:-	$2\theta_{Cu}$	29.59	39.62	43.35	47.75
	d(Å)	3.02	2.27	2.08	1.90
	counts	2920	334	290	328
Dolomite:-	$2\theta_{Cu}$	31.01	50.89	44.94	65.83
	d(Å)	2.88	1.79	2.01	1.41
	counts	726	202	200	234

Sample P21:- Dolomite

Analysis reveals minor quartz

Dolomite:-	$2\theta_{Cu}$	30.93	41.10	50.89	50.29
	d(Å)	2.88	2.19	1.79	1.81
	counts	4448	996	602	572
Quartz:-	$2\theta_{Cu}$	26.78	60.06	37.39	
	d(Å)	3.32	1.54	2.40	
	counts	580	426	550	

Sample P38:- Dolomite

Analysis also reveals quartz and traces of pyrite

Dolomite:-	$2\theta_{Cu}$	30.87	41.07	50.82	50.30

	d(Å)	2.89		2.19		1.79		1.81
	counts	4652		754		600		858
Quartz:-	$2\theta_{Cu}$	26.80		21.03		60.06		36.69
	d(Å)	3.32		4.22		1.53		2.44
	counts	3098		1124		478		668
Pyrite:-		$2\theta_{Cu}$	54.99		33.33		37.32	40.40
	d(Å)	1.66		2.68		2.40		2.23
	counts	284		360		534		322

Sample P38G:- Dolomite

Analysis also reveals quartz, and traces of siderite

Dolomite:-	$2\theta_{Cu}$	30.82	41.03	50.82	44.83
	d(Å)	2.89	2.19	1.79	2.01
	counts	1532	462	382	362
Quartz:-	$2\theta_{Cu}$	26.71	20.95	50.19	60.01
	d(Å)	3.33	4.23	1.81	1.54
	counts	1886	326	826	450
Siderite:-	$2\theta_{Cu}$	42.54	45.91		
	d(Å)	2.12	1.97		
	counts	206	394		

Sample P43E:- Calcite

Analysis also reveals quartz, and traces of dolomite and siderite

Calcite:-	$2\theta_{Cu}$	29.55	39.58	43.37	47.73
	d(Å)	3.02	2.27	2.08	1.90
	counts	3020	1132	444	596
Quartz:-	$2\theta_{Cu}$	26.76	20.94	50.24	60.03
	d(Å)	3.33	4.24	1.81	1.54
	counts	8596	2604	1314	894
Dolomite:-	$2\theta_{Cu}$	68.37			
	d(Å)	1.37			
	counts	498			
Siderite:-	$2\theta_{Cu}$	31.63	42.56	45.92	
	d(Å)	2.82	2.12	1.97	
	counts	234	584	376	

Sample P44:- Calcite

Analysis also reveals quartz, and traces of dolomite and siderite

Calcite:-	$2\theta_{Cu}$	29.67	39.70	43.45	47.82
	d(Å)	3.01	2.27	2.08	1.90
	counts	3188	740	416	966
Quartz:-	$2\theta_{Cu}$	26.84	21.08	50.37	60.13
	d(Å)	3.32	4.21	1.81	1.54

	counts	3872	942	558	526
Dolomite:-	$2\theta_{Cu}$	40.48	68.48		
	d(Å)	2.22	1.37		
	counts	414	886		
Siderite:-	$2\theta_{Cu}$	31.73	25.05	42.68	46.03
	d(Å)	2.81	3.55	2.12	1.97
	counts	222	234	396	292

Sample P52C:- Calcite

No other compounds detected

Calcite:-	$2\theta_{Cu}$	29.51	36.10	39.53	43.24
	d(Å)	3.02	2.48	2.27	2.09
	counts	1304	136	154	158

SAMPLE P14
Quartz
Dolomite
Quartz
Dolomite
Calcite
Quartz
Dolomite

SAMPLE P17

U-161 23
L=14
ANGLE D-VALUE COUNTS
23.978 3.708
26.663 3.340
30.793 2.9011 2572
33.310 2.6876
37.242 2.412
41.003 2.17
44.800 2.021
50.778 1.796
DOLOMITE
QUARTZ ?
50.778°2θ d=1.79 DOLOMITE
DOLOMITE
44.800°2θ d=2.02 DOLOMITE
41.003°2θ d=2.19 DOLOMITE
37.242°2θ d=2.41 PYRITE
33.310°2θ d=2.68 PYRITE
30.795°2θ d=2.90 DOLOMITE
26.663°2θ d=3.34 QUARTZ
23.978°2θ d=3.70

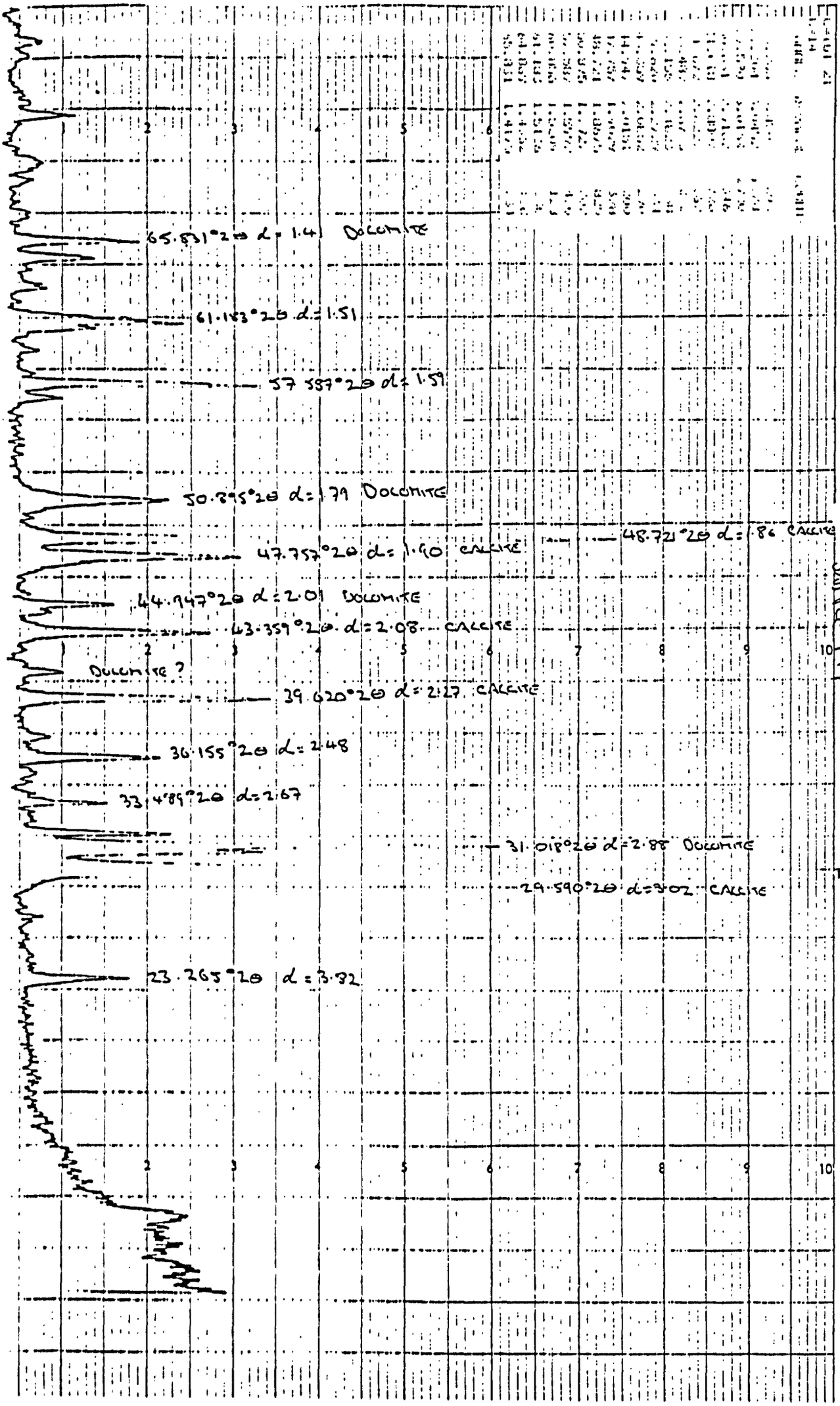
65.831°2θ d = 1.4 Dolomite
61.183°2θ d = 1.51
57.587°2θ d = 1.59
50.895°2θ d = 1.79 Dolomite
48.721°2θ d = 1.86 Calcite
47.757°2θ d = 1.90 Calcite
44.947°2θ d = 2.01 Dolomite
43.359°2θ d = 2.08 Calcite
Dolomite ?
39.620°2θ d = 2.27 Calcite
36.155°2θ d = 2.48
33.489°2θ d = 2.67
31.018°2θ d = 2.88 Dolomite
29.590°2θ d = 3.02 Calcite
23.265°2θ d = 3.82
Sample 019

Sample 12
63.739°2θ d=1.38 Dolomite
63.278°2θ d=1.46
60.060°2θ d=1.54 Qum-12
50.895°2θ d=1.79 Dolomite
50.273°2θ d=1.81 Quartz
44.109°2θ d=2.01 Dolomite
41.109°2θ d=2.19 Dolomite
39.496°2θ d=2.28 Dolomite
37.339°2θ d=2.40 Quartz
32.394°2θ d=2.76 Quartz
30.932°2θ d=2.88 Dolomite
28.739°2θ d=3.09
26.782°2θ d=3.32 Quartz
24.136°2θ d=3.68

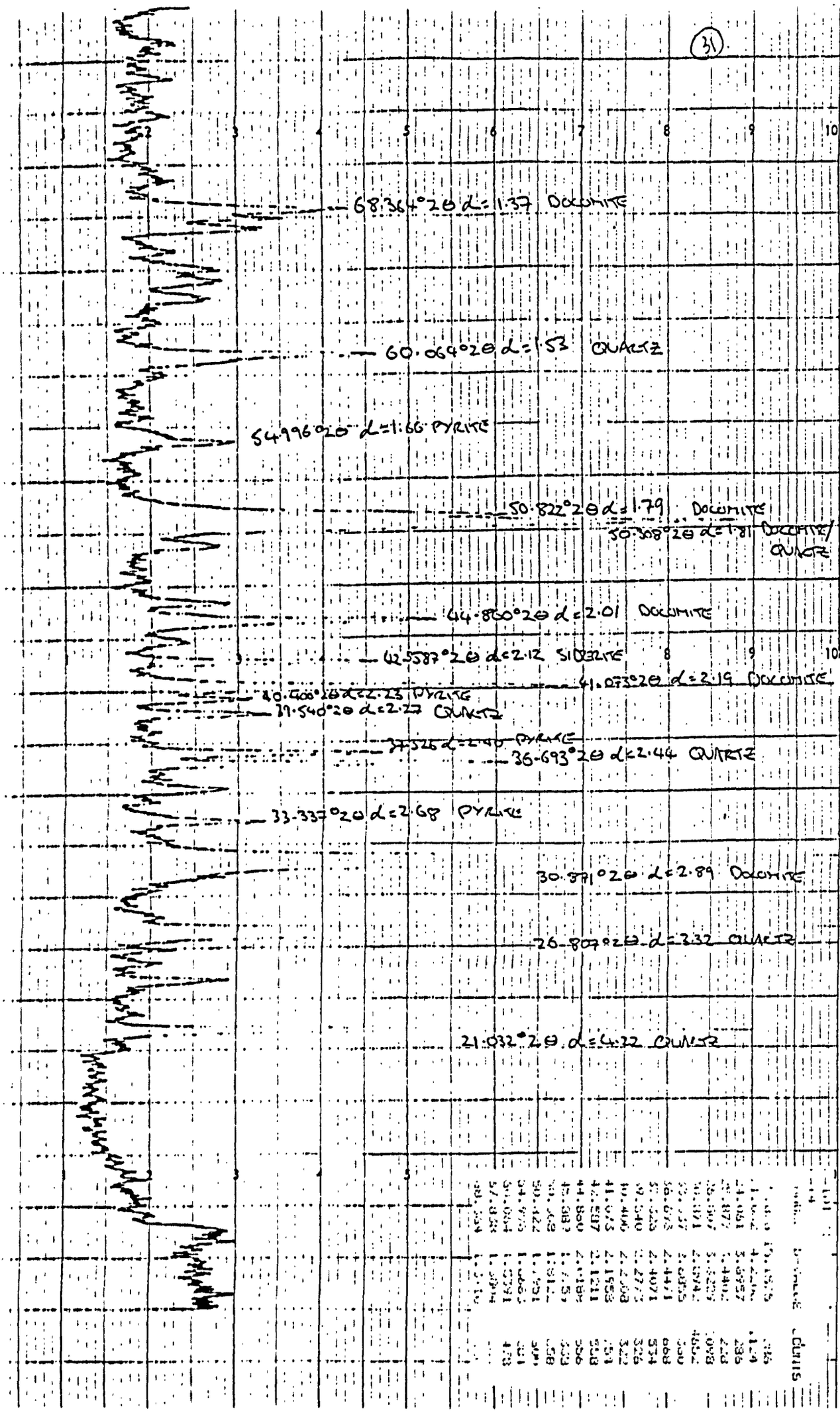
(31)
68.364°2θ d=1.37 DOLOMITE
60.064°2θ d=1.53 QUARTZ
54.996°2θ d=1.66 PYRITE
50.822°2θ d=1.79 DOLOMITE
50.508°2θ d=1.81 DOLOMITE/QUARTZ
44.860°2θ d=2.01 DOLOMITE
42.587°2θ d=2.12 SIDERITE
41.073°2θ d=2.19 DOLOMITE
40.400°2θ d=2.23 PYRITE
39.540°2θ d=2.27 QUARTZ
37.525 d=2.40 PYRITE
36.693°2θ d=2.44 QUARTZ
33.337°2θ d=2.68 PYRITE
30.871°2θ d=2.89 DOLOMITE
26.807°2θ d=3.32 QUARTZ
21.032°2θ d=4.22 QUARTZ
SAMPLE C38-7

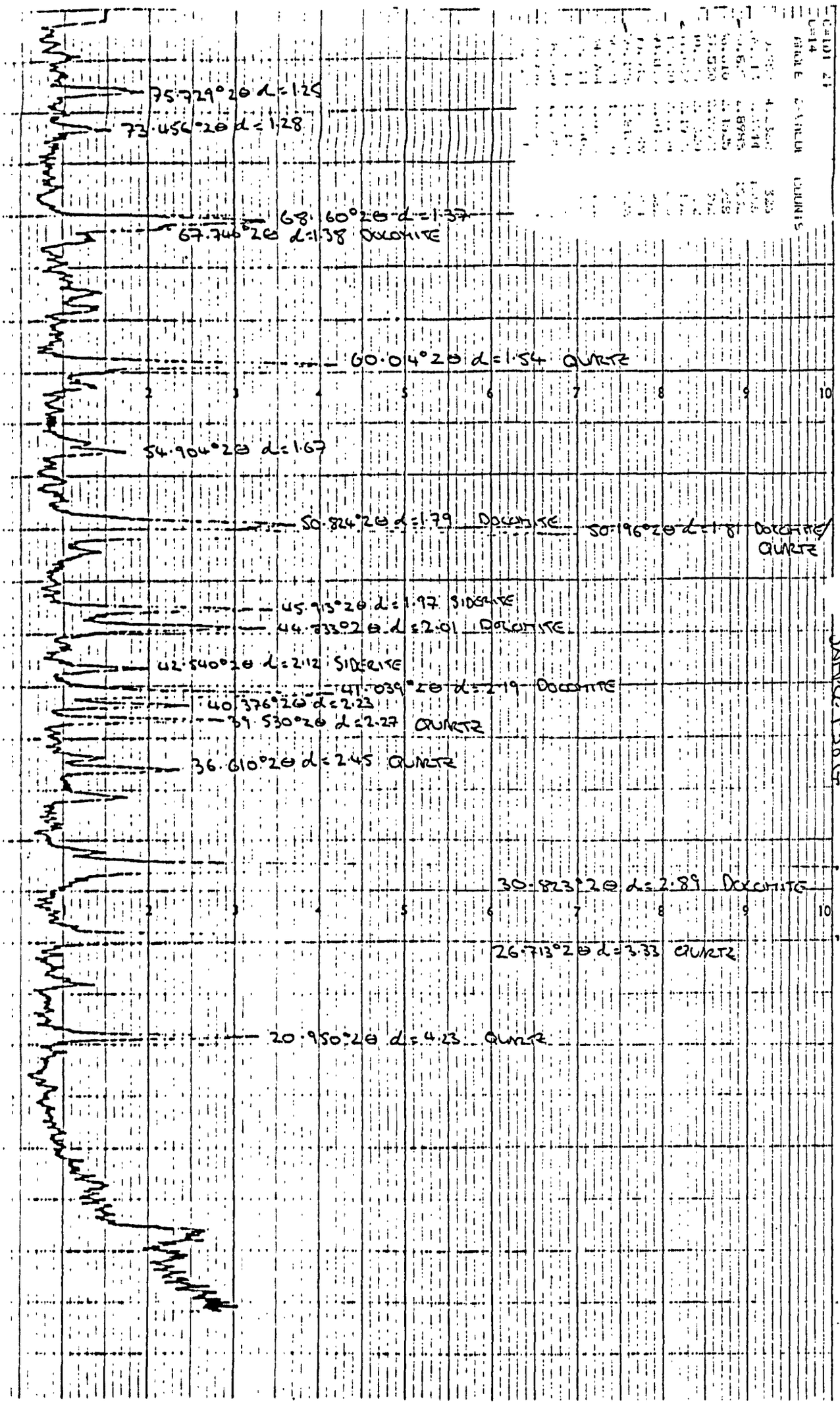
75.729°2θ d=1.25
73.456°2θ d=1.28
68.60°2θ d=1.37
67.746°2θ d=1.38 DOLOMITE
60.04°2θ d=1.54 QUARTZ
54.904°2θ d=1.67
50.824°2θ d=1.79 DOLOMITE
50.196°2θ d=1.81 DOLOMITE/QUARTZ
45.913°2θ d=1.97 SIDERITE
44.833°2θ d=2.01 DOLOMITE
42.540°2θ d=2.12 SIDERITE
41.039°2θ d=2.19 DOLOMITE
40.376°2θ d=2.23
39.530°2θ d=2.27 QUARTZ
36.610°2θ d=2.45 QUARTZ
30.823°2θ d=2.89 DOLOMITE
26.713°2θ d=3.33 QUARTZ
20.950°2θ d=4.23 QUARTZ
SAMPLE P38G

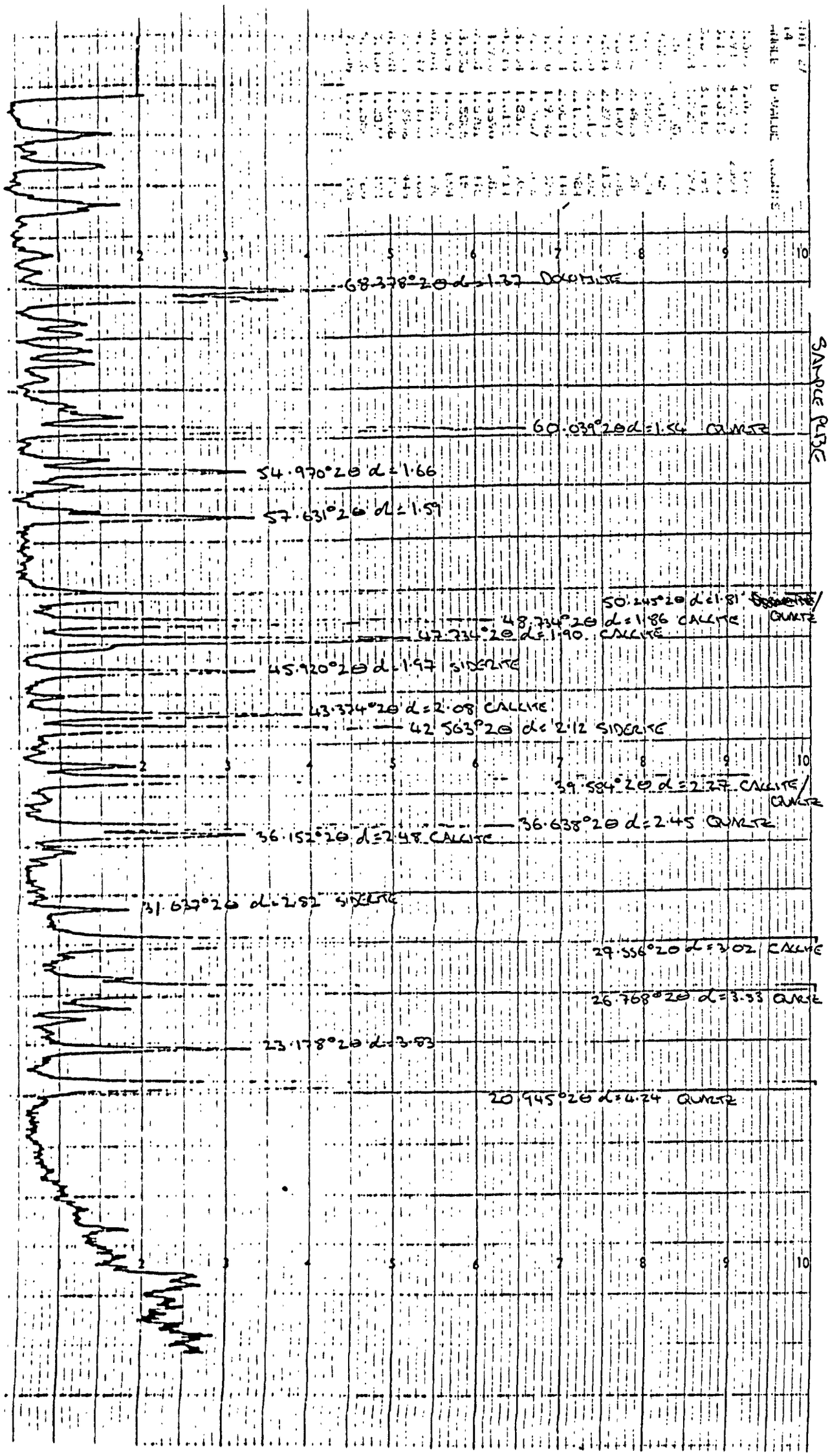
68.378°2θ d=1.37 DOLOMITE
60.039°2θ d=1.54 QUARTZ
SAMPLE PLATE
54.970°2θ d=1.66
57.631°2θ d=1.59
50.245°2θ d=1.81 DOLOMITE/ QUARTZ
48.734°2θ d=1.86 CALCITE
47.734°2θ d=1.90 CALCITE
45.920°2θ d=1.97 SIDERITE
43.374°2θ d=2.08 CALCITE
42.563°2θ d=2.12 SIDERITE
39.584°2θ d=2.27 CALCITE/ QUARTZ
36.638°2θ d=2.45 QUARTZ
36.152°2θ d=2.48 CALCITE
31.627°2θ d=2.82 SIDERITE
29.556°2θ d=3.02 CALCITE
26.768°2θ d=3.33 QUARTZ
23.178°2θ d=3.83
20.945°2θ d=4.24 QUARTZ

SAMPLE C44

68.487°2θ d=1.37 Quartz

64.951°2θ d=1.43

60.139°2θ d=1.54 Quartz

50.332°2θ d=1.81 Quartz/Dolomite

48.830°2θ d=1.86 Calcite

47.821°2θ d=1.901 Calcite

46.033°2θ d=1.97 Silicate

43.450°2θ d=2.08 Calcite

42.678°2θ d=2.12 Silicate

40.486°2θ d=2.22 Dolomite

39.701°2θ d=2.27 Quartz/Calcite

36.784°2θ d=2.44 Quartz

36.246°2θ d=2.48 Calcite

31.937°2θ d=2.81 Silicate

29.673°2θ d=3.01 Calcite

26.842°2θ d=3.32 Quartz

25.054°2θ d=3.55 Biogenic?

21.081°2θ d=4.21 Quartz

2θ

10 9 8 7 6 5 4 3 2

COUNTS

d

SAMPLE (152)
27.917°2θ d=2.02 CALCITE
36.102°2θ d=2.48 CALCITE
39.531°2θ d=2.27 CALCITE
43.243°2θ d=2.09 CALCITE
47.565°2θ d=1.90
48.518°2θ d=1.87 CALCITE
D-VALUE
246
1.64
1.53

Appendix 3: The preparation & isotopic analysis of carbonate cement phases

Isotopic analysis was performed at the Isotope unit of the Post-Graduate Research Institute of Sedimentology, University of Reading by Mike Isaacs. Following, is a brief summary of the preparation and analysis details for carbonate isotopic analysis.

A3.1: *Preparation details*

5-10mg of pure carbonate is weighed into a quartz tube. 4ml of 100% orthophosphoric acid is pipetted into a conical reaction vessel and the sample tube inserted without mixing the contents. The reaction vessel is attached to a pumping manifold and evacuated to degas the acid. After 2-3 hours pumping, the vessels are sealed under vacuum, removed from the manifold and placed in a thermostatically controlled water bath, set to 25.2°C (calcites) or 60°C (dolomites). After thermal equilibrium is reached (1 hour) the carbonate sample is reacted with the acid to form CO_2 gas subsequently used for isotopic analysis. Each sample vessel is kept in the bath overnight to complete the reaction.

The vessel is then returned to the pumping manifold and paired with an evacuated gas tube. A dewar of chilled acetone (-90°C) is placed around the conical vessel (to act as a water vapour cold trap) and liquid nitrogen (-197°C) on the gas tube. The CO_2 gas is then transferred from conical vessel to gas tube by cryogenic distillation, condensing inside the

gas tube below the liquid nitrogen level. Any non-condensable gases are removed by briefly pumping on the frozen CO_2 sample before the tube is sealed, brought to room temperature and taken to a SIRA (Stable Isotope Ratio Analyser) mass spectrometer for analysis. Samples are prepared in batches each containing duplicate internal standards (CAV-1, *Carrara Marble*) of known composition previously calibrated against NBS isotope standards.

A3.2: *Analysis details*

CO_2 gas samples are simultaneously analysed for the stable isotopes $\delta^{13}C$ and $\delta^{18}O$ on a VG Isogas SIRA Series II mass spectrometer. This is a dual inlet, high sensitivity source stable isotope ratio instrument with a split flight tube and 20 port sample manifold. All routine operations are controlled through an IBM PS2/50 PC. Before each analytical run, the mass spectrometer source is tuned to optimise the beams at masses 44, 45 and 46 (CO_2) and the peak shapes checked for quality assurance.

Gas tubes are attached to the manifold ports and samples admitted sequentially to the inlet system for analysis. A CO_2 reference gas, also prepared from the internal standard CAV-1, is kept in the other half of the dual inlet system and the mass ratios 45/44 and 46/44 of the "unknown" samples determined with respect to it, from which uncorrected Delta (‰ PDB) values for $\delta^{13}C$ and $\delta^{18}O$ are derived. The data are subsequently corrected off-line to the results obtained for the internal standards by the Craig method, using a spreadsheet

program developed by Professor Max Coleman.

A3.3: *Sample Results*

Full details of all results are displayed in the following table. For the purpose of data correction, a working assumption of trace mineral phases (i.e. calcite, dolomite or siderite) equal 5% of the major carbonate phase present.

Sample No.	Sample Desc.	Calcite	Dolomite	Siderite	δ^{45}	δ^{46}	δ^{13}	δ^{18}PDB	δ^{18}SMOW
A5	calcite	100	0	0	-31.195	0.799	-31.103	-0.828	30.006
A6	calcite	100	0	0	0.098	-1.679	2.229	-3.524	27.227
A8	calcite	100	0	0	-26.808	0.157	-26.596	-1.748	29.058
32A	calcite	100	0	0	-2.487	-7.386	-0.343	-9.232	21.344
32A (duplicate)	calcite	100	0	0	-2.480	-7.388	-0.336	-9.234	21.341
E3	calcite	100	0	0	-0.538	-4.459	1.642	-6.303	24.362
E4	calcite (dol+sid)	95	2.5	2.5	-0.312	-3.874	1.864	-5.774	24.908
39A	calcite (dol)	95	5	0	-2.272	-3.712	-0.237	-5.602	25.085
40	calcite	100	0	0	-1.472	-0.661	0.727	-2.223	28.568
40 (duplicate)	calcite	100	0	0	-1.412	-0.630	0.790	-2.192	28.601
61	calcite	100	0	0	-2.506	-1.504	-0.351	-3.068	27.698
C10	calcite	100	0	0	0.215	-2.859	2.604	-4.416	26.308
C10(c)	calcite (ooid)	100	0	0	-1.121	-1.732	1.138	-3.292	27.466
C27	siderite	5	0	95	-2.568	-5.052	-0.537	-5.906	24.772
113	siderite	5	0	95	-15.942	-4.990	-14.836	-5.873	24.806
115	siderite	0	0	100	-16.188	0.266	-15.275	-0.660	30.180

Sample No.	Sample Desc.	Calcite	Dolomite	Siderite	δ^{45}	δ^{46}	δ^{13}	δ^{18}PDB	δ^{18}SMOW
P14	dolomite	0	100	0	-3.546	-3.587	-1.632	-4.097	26.636
P17	dolomite	0	100	0	-2.991	-3.768	-1.032	-4.277	26.451
P19	calcite (+ dol)	95	5	0	-4.974	-4.847	-3.087	-6.742	23.910
P21	dolomite	0	100	0	-2.586	-3.270	-0.616	-3.778	26.965
P21 (duplicate)	dolomite	0	100	0	-2.605	-3.371	-0.633	-3.879	26.861
P38	dolomite	0	100	0	-2.890	-3.084	-0.947	-3.593	27.156
P38G	dolomite (+ sid)	0	95	5	-2.675	-3.374	-0.708	-3.902	26.838
P43E	calcite (dol+sid)	95	2.5	2.5	-9.806	-1.399	-8.368	-3.322	27.435
P44	calcite (dol+sid)	95	2.5	2.5	-10.136	-0.912	-8.737	-2.836	27.936
P52C	calcite	100	0	0	-5.010	-3.783	-2.952	-5.351	25.344

Appendix 4: The preparation & analysis of carbonate cement phases under cathodoluminescence

A4.1: *Preparation & analysis details*

Cathodoluminescence (CL) was performed at Cambourne School of Mines, using a "Citl 8200 mk.3" cold cathode luminoscope, which was attached to a "Nikon Labophoto 2" petrographical microscope.

Individual samples were selected to include all carbonate cement phases from both successions. Polished thin sections were prepared for each sample, using an "Epotek 301" fixing cement, which is stable at the temperatures developed by the electron beam. Each sample was positioned on the microscope stage within the vacuum chamber which was then sealed.

Each analysis was conducted at 15-17kv, with a cathode beam current set at 450-460μa. The vacuum was approximately 0.12torr. The cathode current was constantly monitored and kept stable by using the vacuum control.

Photomicrographs were taken using Kodak Tmax or Ilford FP4 35mm black and white print film (ASA 400). For each sample, paired exposures were made, one recording the transmitted light view and the other recording the CL view. Exposure times of between 60

and 150 seconds were estimated for the CL photomicrographs. All photographs were taken using a X4 objective lens. The presence or absence of luminescence in each sample was recorded in terms of nonluminescent, dull luminescent, moderately luminescent or brightly luminescent. The presence of zoning within some carbonate cement phases was recorded in terms of nonzoned, faintly zoned or well zoned.